New Reactions of Titanium Imido and Hydrazido Complexes

Laura C. Stevenson



Thesis submitted to the University of Oxford for the degree of Doctor of Philosophy, November 2015.

The work described in this Thesis was carried out in the Chemistry Research Laboratory, University of Oxford from October 2012 to November 2015 under the supervision of Professor Philip Mountford. All work is my own unless stated to the contrary, and has not previously been submitted for any degree at this or any other university.

Laura C. Stevenson

November 2015

Abstract

Laura C. Stevenson Michaelmas 2015
Worcester College D.Phil. Thesis

This Thesis reports the synthesis and reactions of titanium-nitrogen multiply bonded compounds. Reactions with both acidic and hydridic element-hydrogen bonds are explored along with unsaturated small molecules in general.

Chapter One provides a background on imido and hydrazido complexes, starting with the relevance of the hydrazido ligand to nitrogen fixation. Group 4 alkylidene hydrazide and alkoxyimide complexes are also reviewed. The Chapter focuses in particular on the synthesis, structure, and stoichiometric and catalytic reactions of these complexes with unsaturated substrates.

Chapter Two describes the synthesis of new titanium imido complexes and the reactions with molecules containing N–H or O–H bonds, internal alkynes and nitriles. The analogous reactions of the hydrazido compound Ti($N_2^{iPr}N^{Me}$)($NNPh_2$)(py) are also investigated.

Chapter Three details the reactions of the imido compound Ti($N_2^{iPr}N^{Me}$)(NXyl)(py) with terminal alkynes. Unusual reaction products are described and a full mechanistic study into their formation along with their synthesis and characterisation is presented. In addition, the relevance of these reactions to the catalytic hydrohydrazination of terminal alkynes and diphenylhydrazine with Ti($N_2^{iPr}N^{Me}$)($NNPh_2$)(py) is discussed.

Chapter Four describes the reactivity of the hydrazido compound Ti($N_2^{iPr}N^{Me}$)($NNPh_2$)(py) with a range of silanes and boranes. These reactions are then explored through an in-depth experimental and computational study.

Chapter Five presents full experimental procedures and characterising data for the new complexes reported.

CD Appendix contains CIF files for all new crystallographically characterised complexes

Acknowledgements

First and foremost I would like to thank Professor Philip Mountford for his support, advice, enthusiasm and uttermost excitement for the project. I have learnt a great deal and feel truly honored to have worked with you. Thank you for having faith in me.

I must express my sincerest thanks to all members of the Mountford group past and present. You have made S1 and (mainly) S2 an entertaining and fulfilling place to be. My particular thanks go to Dr Andrew Schwarz for giving me the best possible start, Dr Laura Groom for being ready and willing to discuss everything chemistry and non-chemistry related with a cup of tea in hand. Mr Richard Collins, my comrade from day one, for being an excellent friend and a constant reminder that a positive attitude can get you through almost anything. And, Miss Anastasia Miller, the exceptional Part II student I had the pleasure of supervising, for believing everything I told her. Importantly, I would like to thank all of the above and, in addition, Drs Bryony Core, Liban Saleh, Adam Russell, Junjuda Unruangsri and Miss Lucy Budden for the countless trips to the uni-club and the occasional trips to the PT. Thanks must also go to Mr Richard Collins and Mr Benjamin Clough for the proof reading of this thesis, Dr Matthew Blake for keeping the lab going strong and generally being a great guy and to Miss Simona Mellino for the DFT calculations. Finally, of course, to the Dumbledore of organometallic chemistry, Dr Andrey Protchenko, your wise words and advice have often been literally priceless. Without you all these last three years would have been a whole lot tougher and I will look back on these times with great fondness.

I am hugely indebted to everyone who keeps the CRL running as well as Dr Nick Rees for the help with NMR and Dr Amber Thompson with crystallography.

I must thank all my friends outside of the lab for maintaining my sanity. Especially (almost) Dr Jess Rodgers for the books, food and more recently, squats. I could not have lived here without you.

My greatest thanks go to my biggest fans – my Mum and Dad. I would not be who or where I am without you both and I cannot thank you enough for everything you have done. Also, to my sisters Harriet and Erin, my bestest friends.

Finally to James, for always making me happy. You are the mellowest yellow, the calmest balm and my love.

Contents

	Declaration	i
	Abstract	ii
	Acknowledgements	iii
	Contents	iv
	Abbreviations	viii
	Notes	xiii

Chapter One: Introduction

1.1	General introduction	1
1.2	Nitrogen fixation	2
1.3	Imido ligand	4
1.4	Hydrazido ligand	4
1.4.1	Hydrazido structural features	4
1.5	Group 6 hydrazido complexes	5
1.5.1	Synthesis	5
1.5.2	Stoichiometric reactions	9
1.6	Group 5 hydrazido complexes	10
1.6.1	Synthesis	10
1.7	Group 4 imido and hydrazido complexes	13
1.7.1	Group 4 imido complexes	13
1.7.1.1	Synthesis of titanium imido complexes	13
1.7.1.2	Synthesis of zirconium and hafnium imido complexes	16
1.7.1.3	Structural features	18
1.7.1.4	Stoichiometric reactions	19
1.7.1.5	Catalytic hydroamination	21
1.7.2	Group 4 hydrazido complexes	23
1.7.2.1	Synthesis of titanium hydrazido complexes	23
1.7.2.2	Synthesis of zirconium and hafnium hydrazido complexes	25
1.7.2.3	Structural features	27
1.7.2.4	Stoichiometric reactions involving the $M{=}N_{\alpha}$ bond	29
1.7.2.5	Stoichiometric reactions involving the $N_{\alpha}{-}N_{\beta}$ bond	35
1.7.2.6	Catalytic reactions	39

1.8	Group 4 alkylidene hydrazido complexes	42
1.9	Group 4 alkoxyimido complexes	43
1.10	Summary and objectives	45
1.11	References	45

Chapter Two: Synthesis of diamide-amine supported titanium imido complexes and reactions with N–H and O–H bonds, internal alkynes and nitriles

2.1	Overview	57
2.2	Introduction	57
2.3	Synthesis of new imido compounds	60
2.4	Reaction of Ti($N_2^{iPr}N^{Me}$)(NXyl)(py) (**1**) with N–H bonds	65
2.5	Reaction of Ti($N_2^{iPr}N^{Me}$)($NNPh_2$)(py) (**2.1**) with N–H and O–H bonds	71
2.6	Reaction of Ti($N_2^{iPr}N^{Me}$)(NXyl)(py) (**1**) with internal alkynes	76
2.7	Reaction of Ti($N_2^{iPr}N^{Me}$)(NXyl)(py) (**1**) with nitriles	84
2.8	Reaction of Ti($N_2^{iPr}N^{Me}$)($NNPh_2$)(py) (**2.1**) with nitriles	90
2.9	Proposed mechanism for the reaction of Ti($N_2^{iPr}N^{Me}$)(NXyl)(py) (**1**) and Ti($N_2^{iPr}N^{Me}$)($NNPh_2$)(py) (**2.1**) with nitriles	96
2.10	Conclusion	97
2.11	References	98

Chapter Three: Reactions of Ti($N_2^{iPr}N^{Me}$)(NXyl)(py) with terminal alkynes

3.1	Overview	108
3.2	Introduction	108
3.3	Reaction of Ti($N_2^{iPr}N^{Me}$)(NXyl)(py) (**1**) with electron-withdrawing terminal alkynes	112
3.4	Mechanistic studies on the reaction of Ti($N_2^{iPr}N^{Me}$)(NXyl)(py) (**1**) with electron-withdrawing alkynes	124
3.4.1	Proposed mechanism	124
3.4.2	Kinetic study of the isomerisation of Ti($H_2N_2^{iPr}N^{Me}$)(CCC_6F_5)$_2$(NXyl) (**23**) to Ti($N_2^{iPr}N^{Me}$){N(Xyl)C(H)C(H)(C_6F_5)}(CCC_6F_5) (**24**)	126
3.4.3	Isotope effects	131
3.4.3.1	Pre-equlibrium	131
3.4.3.2	Crossover experiment	133
3.4.3.3	Interpreting the isotope effect for the isomerisation of **23** to **24**	139
3.4.3.4	Independent estimate of the isotope effect	141

3.4.4	Kinetic analysis with HCC-4-$C_6H_4CF_3$	144
3.4.5	Crossover experiments with other alkynes	145
3.5	Solid-state structures of the vinylamide-acetylide compounds	151
3.6	Nitrogen hydrogen/deuterium exchange experiments	155
3.7	Relevance of the reactions of Ti($N_2^{iPr}N^{Me}$)(NXyl)(py) (**1**) with terminal alkynes to the reactions of Ti($N_2^{iPr}N^{Me}$)($NNPh_2$)(py) (**2.5**) with terminal alkynes	156
3.7.1	Kinetic isotope effect measurements	157
3.7.2	Identifying bis(acetylide) intermediates	160
3.7.3	Competition experiments	162
3.7.4	NH/D exchange reactions	162
3.7.5	Hydrohydrazination catalysis	164
3.8	Reaction of Ti($N_2^{iPr}N^{Me}$)(NXyl)(py) (**1**) with other terminal alkynes	166
3.9	Reaction of Ti($N_2^{iPr}N^{Me}$)(NDipp)(py) (**3**) with terminal alkynes	170
3.10	Conclusion	173
3.11	References	175

Chapter Four: Reactions of Ti($N_2^{iPr}N^{Me}$)($NNPh_2$)(py) with silanes and boranes

4.1	Overview	182
4.2	Introduction	182
4.3	Reaction of Ti($N_2^{iPr}N^{Me}$)($NNPh_2$)(py) (**2.1**) with silanes	184
4.4	Mechanism of the reaction of Ti($N_2^{iPr}N^{Me}$)($NNPh_2$)(py) (**2.1**) with silanes	188
4.5	Reaction of Ti($N_2^{iPr}N^{Me}$)($NNPh_2$)(py) (**2.1**) with butylsilane	195
4.6	Reaction of Ti($N_2^{iPr}N^{Me}$)($NNPh_2$)(py) (**2.1**) with boranes	200
4.7	Mechanism of the reaction of Ti($N_2^{iPr}N^{Me}$)($NNPh_2$)(py) (**2.1**) with 9-BBN	203
4.8	Reaction of Ti($N_2^{iPr}N^{Me}$)($NNPh_2$)(py) (**2.1**) of H_2	211
4.9	Reaction of Ti($N_2^{iPr}N^{Me}$){N(H)SiH_2Ph}(NPh_2) (**43**) with silanes	212
4.10	DFT study of the mechanism of Ti($N_2^{iPr}N^{Me}$){N(H)SiH_2Ph}(NPh_2) (**43**) with silanes	217
4.11	Reaction of Ti($N_2^{iPr}N^{Me}$){N(H)SiH_2Ph}(NPh_2) (**43**) with 9-BBN	220
4.12	Reaction of Ti($N_2^{iPr}N^{Me}$)($NNPh_2$)(py) (**2.1**) with pinacolborane and catecholborane	227
4.13	Reaction of Ti(N_2N^{py})($NNPh_2$)(py) (**1.75**) with 9-BBN	231
4.14	Reaction of Ti($N_2^{iPr}N^{Me}$)($NNPh_2$)(py) (**2.1**) with halosilanes	234
4.15	Other reactions	236
4.16	Conclusion	236

4.17 References 238

Chapter Five: Experimental details and characterising data

5.1 General methods and instrumentation 245
5.2 Literature preparations 245
5.3 X-ray collection and processing parameters 247
5.4 Computational details 247
5.5 Experimental details and characterising data for Chapter Two 248
5.6 Experimental details and characterising data for Chapter Three 265
5.7 Experimental details and characterising data for Chapter Four 281
5.8 References 300

Appendix 303
CD Appendix

Abbreviations

General

Å	Ångstrom
Atm	atmosphere(s)
Avg.	average
ca.	*circa*, about
cf.	*confer*, compared to
CSD	Cambridge Structural Database
^{o}	degrees
^{o}C	degrees Celsius
D	day(s)
Fac	facially coordinating
G	grams
H	hour(s)
K	Kelvin
kcal mol^{-1}	kilocalorie(s) per mole
mbar	millibar(s)
Mer	Meridonally coordinating
min	minute(s)
mL	millilitre(s)
mmol	millimole(s)
RT	room temperature
s	second(s)
μ	bridging
μmol	micromole(s)
vs.	versus

Chemical

9-BBN	9-Borabicyclo[3.3.1]nonane
acac	acetylacetonate
Ar	aryl group
Ar'	2,6-$C_6H_3{}^{i}Pr_2$
Ar^{F_5}	C_6F_5

Ar^f	3,5-$C_6H_3(CF_3)_2$
bipy	2,2′-bipyridine
Bu	*n*-butyl
Bu^tpy	di-*tert*-butyl pyridine
CCC^{Bu}-NHC	2-(1,3-bis(N-butylimidazol-2-ylidene)-phenylene
Cp	C_5H_5
Cp*	C_5Me_5
Cy	Cyclohexyl
DIBAL	Diisobutylaluminium hydride
Dipp	2,6-$C_6H_3(CHMe_2)_2$
DMAP	4-dimethylaminopyridine
DME	1,2-dimethoxyethane
dmpe	$Me_2PCH_2CH_2PMe_2$
dpma	*N,N*-di(pyrrolyl-α-methyl)-*N*-methylamine
dppe	$Ph_2PCH_2CH_2PPh_2$
E	generic chalcogen atom
EIE	equilibrium isotope effect(s)
Et	Ethyl
HBCat	1,3,2-benzodioxaborole
H-BHT	HO-2,4,6-$C_6H_3{}^tBu_2Me$
HBPin	4,4,5,5-tetramethyl-1,3,2-dioxaborolane
H_2Me_4taa	tetramethyl dibenzotetraaza[14]annulene
$H_2N_2{}^{PFP}N_{py}$	$MeC(2\text{-}C_5H_4N)(CH_2NHC_6F_5)_2$
$(HN^{Xyl})_2N_{py}$	$MeC(2\text{-}C_5H_4N)(CH_2NXyl)_2)$
$HC(Me_2pz)_3$	tris(3,5-dimethylpyrazolyl)methane
$HC(pz)_3$	tris(pyrazolyl)methane
HIPT	3,5-(2,4,6-$C_6H_2{}^iPr_3)_2C_6H_3$
Hpypyr	2-(2′-pyridyl)-3,5-dimethylpyrrole
H_2Tip	2-((2-thiol-phenylimino)methylene)phenol
^{i}Pr	*iso*-propyl
KIE	kinetic isotope effect(s)
L	a supporting ligand (set)
Me	methyl
Me_2pz	3,5-dimethylpyrazolyl
Me_2Calix	dianion of 1,3-dimethyl ether of *tert*-butyl calix[4]arene

Me_3[6]ane	1,3,5-trimethyltriazacyclohexane
Me_3[9]ane	1,4,7-trimethyltriazacyclononane
Mes	2,4,6-$C_6H_2Me_3$
MOCVD	metal organic chemical vapour deposition
NacNac	[{(Ar)NC(Me)}$_2$CH]
N_2NN'	(2-C_5H_4N)$CH_2N(CH_2CH_2NSiMe_3)_2$
$HN_2^{iPr}N^{Me}$	$MeN(CH_2CH_2N^iPr)(CH_2CH_2NH^iPr)$
N_2N^R	generic diamidoamine ligand
N_2N^{py}	MeC(2-C_5H_4N)$(CH_2NHSiMe_3)_2$
N_2N^{Me}	$MeN(CH_2CH_2NSiMe_3)_2$
N_2N^{Me,C_3}	$MeN(CH_2CH_2CH_2NSiMe_3)_2$
$N_2N^{SiMe_3}$	$Me_3SiN(CH_2CH_2NSiMe_3)_2$
$N_2^{iPr}N^{Me}$	$(MeN(CH_2CH_2N^iPr)_2$
$N_2^{TBS}N_{py}$	MeC(2-C_5H_4N){$CH_2N(Si^tBuMe_2)$}$_2$
$N_2^{TFAP}N_{py}$	MeC(2-C_5H_4N){CH_2NH(2-$C_6F_4NMe_2$)}$_2$
$N^{Xyl}N$	2-(3,5-dimethylphenylamino)pyrrolinato
N_2O	(O-$(CH_2CH_2NSiMe_3)_2$
$N_2^{Ar}O$	(O(2-$C_6H_4NSiMe_3$)$_2$
OTf	$CF_3SO_3^-$
P	generic phosphine ligand
Ph	phenyl
py	pyridine
py′	4-pyrrolidinopyridine
pz	pyrazolyl
R	generic aryl or alkyl
SiP^R_3	Si(*o*-$C_6H_4PR_2$)$_3$
^{t}Bu	*tert*-butyl
^{t}Bu-bipy	4,4′-di-*tert*-butyl-2,2′-bipyridine
THF	tetrahydrofuran
TMP	2,2,6,6-tetramethylpiperidine
Tol	4-C_6H_4Me
TTP	*meso*-tetra-*p*-tolylporphyrinato dianion
X	generic halide
Xyl	2,6-$C_6H_3Me_2$
ZPE	zero point energy

Calculations

DFT	density functional theory
TS	transition state(s)

Mass Spectrometry

EI	electron impact
HR	high-resolution
m/z	mass to charge ratio
MS	mass spectrometry

Nuclear Magnetic Resonance Spectroscopy

$^{13}C\{^{1}H\}$	proton-decoupled ^{13}C
$^{11}B\{^{1}H\}$	proton-decoupled ^{11}B
app.	apparent
br	broad
COSY	correlation spectrocopy
d	doublet
HMBC	heteronuclear multiple bond correlation
HMQC	heteronuclear single quantum correlation
Hz	Hertz
i	*ipso*
J	coupling constant
m	*meta*
m	multiplet
MHz	Megahertz
NMR	nuclear magnetic resonance
NOE	nuclear Overhauser effect
o	*ortho*
p	*para*
ppm	parts per million
q	quartet

ROESY	rotating-frame nuclear Overhauser Effect spectroscopy
s	singlet
sept	septet
t	triplet
VT	variable temperature
δ	chemical shift in ppm

Infrared Spectroscopy

br	broad
FT-IR	fourier transform infrared red
IR	infrared red
cm^{-1}	wavenumber
m	medium
s	strong
w	weak
ν	frequency

Notes

Literature compounds described in in this Thesis are numbered **1.x**, **2.x**, **3.x**, **4.x** according to the Chapter in which they occur. The new compounds described in this Thesis are numbered **1** – **xx**. Density functional theory (DFT) calculated compounds are clearly stated in the text.

X-ray crystallography data was collected, solved and refined by the author with the help and guidance of Prof. Philip Mountford. For compounds **1**, **5**, **16**, **17**, **23**, **24**, **29**, **38**, **43**, and **44,** data was collected by Dr Andrew Schwarz. Molecular drawings were produced by Prof. Philip Mountford.

DFT calculations were performed by Simona Mellino of University of Oxford in collaboration with Dr Eric Clot of Université Montpellier France.

Chapter One

Introduction

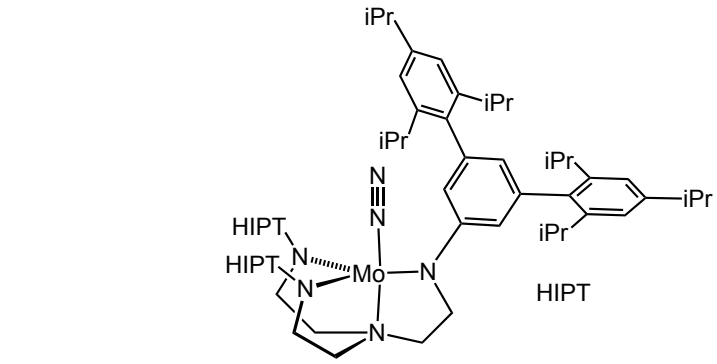
1.1 General Introduction

Transition metal-ligand multiple bonds have been studied in depth over the past four decades. Such compounds have yielded a wide range of structure, bonding and reactivity advances, and in particular, research into transition metal-nitrogen multiple bonds has flourished. This is in part due to their relevance to the catalytic reduction of dinitrogen to ammonia. Intermediates proposed during such catalytic cycles are of particular relevance to this thesis. Namely, the imido and hydrazido ligands, M=NR and $M=NNR_2$ (R = alkyl or aryl). Both ligands have found practical applications in industrial and biological processes, for example, the stoichiometric and catalytic reduction of dinitrogen, olefin polymerisation, MOCVD (Metal-organic Chemical Vapour Deposition) and new catalytic C–N bond forming reactions. With the knowledge that the catalytic reduction of dinitrogen to ammonia by transition metal hydrazido compounds is unlikely to supersede the Haber-Bosch process, recent focus has been on the aforementioned catalytic C–N bond forming reactions targeting complex organo-nitrogen molecules. This area has been dominated by Group 4 hydrazido compounds of which there has also been great interest in their stoichiometric reactions. This Thesis describes a new titanium imido compound along with its novel reactivity with small molecules. Its reactions with alkynes are used to probe the mechanism for hydrohydrazination catalysis, and a range of new transformations of a previously reported hydrazido compound are discussed.

1.2 Nitrogen fixation

Many biomolecules essential to life contain nitrogen.[1] Nitrogen is abundant in the atmosphere as the inert dinitrogen molecule however, most organisms cannot metabolise it due to its stability, and instead, utilise fixed forms such as ammonia or nitrate.[2-6] Nitrogen fixation is therefore necessary to sustaining life on earth. The industrial Haber-Bosch process involves the conversion of dinitrogen and dihydrogen to ammonia over an Fe-based catalyst at 400 ^{o}C and 200 atm, and the Frank-Caro cyanamide process converts dinitrogen to cyanamide using calcium carbide at temperatures of 1000 ^{o}C.[7-10] In comparison, nitrogen fixation by nitrogenase enzymes occur at ambient temperature and pressure. Following the development of techniques for extracting nitrogenases in their active form in the 1960s,[11, 12] numerous investigations into the structure and catalytic function have been reported.[13] However, despite crystallographic structures providing insight into the nature of the active sites, the cores of which contain both iron and sulphur and in most cases molybdenum (FeMo-cofactor), no consensus regarding the mechanism for nitrogen fixation or the mode of N_2 binding has been established.[14-31]

The presence of molybdenum and iron at the active site of several nitrogenase enzymes has inspired work targeting later metal compounds capable of reducing dinitrogen. Various transition metal-dinitrogen complexes have been synthesised, many capable of the stoichiometric transformation into ammonia.[2, 32-36] One notable example was reported by Chatt, who found that $(P)_4M(N_2)L$ (**1.1**, M = Mo or W, P = phosphine ligand, L = a monodentate ligand including N_2) could reduce dinitrogen to ammonia in the presence of electron and proton sources. The proposed mechanism was based on several isolated molybdenum complexes with partially reduced dinitrogen intermediates coordinated, however, catalytic activity was never achieved.[37, 38] Schrock reported the first catalytic reduction of dinitrogen using the sterically crowded tris(amido)amine supported molybdenum compound Mo(HIPTN$_3$N) (**1.2**, HIPT = 3,5-(2,4,6-$C_6H_2{}^{i}Pr_3$)C_6H_3, Figure 1.1), with the bulky pyridinium salt [2,6-$HNC_5H_3Me_2$][$BAr^f{}_4$] (Ar^f = 3,5-$C_6H_3(CF_3)_2$) as a proton source and decamethylchromocene as the electron source.[39-44] Many species in the proposed catalytic cycle were also isolated and characterised, hence a clear picture has emerged on how catalytic reduction occurs at these molybdenum compounds (Figure 1.1).



1.2

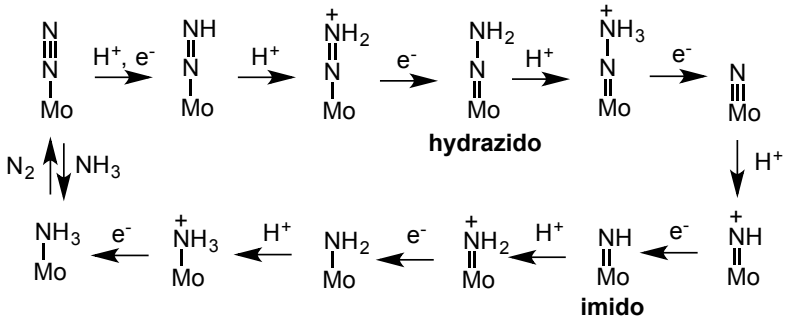


Figure 1.1. Structure of Mo(HIPTN$_3$N) (**1.2**) and the catalytic cycle for the reduction of dinitrogen to ammonia.

Since this discovery, several other molybdenum based catalysts have been reported to catalyse the reduction of dinitrogen to ammonia with greater turnover numbers than the Schrock system.[45-47] A number of iron complexes have also been studied in relation to the reduction of dinitrogen. One of the more notable examples is the use of the tetradentate trisphosphinosilyl supported dinitrogen compounds Fe(SiP$^{R}_{3}$)(N$_2$) (**1.3**, SiP$^{R}_{3}$ = Si(2-C$_6$H$_4$PR$_2$)$_3$ R = Ph or ^{i}Pr) to characterise intermediates bearing partly reduced nitrogen, suggesting that the catalytic reduction of dinitrogen with iron complexes is possible.[48]

Both imido and hydrazido ligands have been idenified as key intermediates in the Schrock and Chatt cycles (highlighted in Figure 1.1). This has driven studies into compounds containing such ligands, initially on later group metals and, over the last 20 years, on earlier metals extending across the periodic table.

1.3 Imido ligand

The imido ligand has been an active area of research in organometallic chemistry for many years and compounds spanning the periodic table have been synthesised. Several reviews have been published.[49-53] The dianionic terminal imido ligand can act as a four-electron donor that is capable of forming a strong triple bond to the metal centre. The M=NR linkage isoelectronic with the terminal oxo group M=O and the $\{NR\}^{2-}$ moiety is isolobal with $\{C_5R_5\}^-$.[54, 55]

1.4 Hydrazido ligand

Transition metal hydrazides occupy a pivotal position on the pathway for both the biological and laboratory based conversion of dinitrogen to ammonia. The chemistry of Group 6 hydrazides has thus been charted extensively, in particularly with regards to models for the biological fixation of dinitrogen. In comparison, more recent work looking at Group 4 hydrazido compounds has evolved around new C–N bond forming reactions.

1.4.1 Hydrazido structural features

Figure 1.1 shows the hydrazido ligand bound "end-on". However, the presence of $N_\beta R_2$ enables hydrazido ligands to bind in a number of different modes to the metal centre, Figure 1.2.[56] The formal charge can be either -1 or -2 depending on the substituents on N_α, both of which can demonstrate additional coordination of N_β (η^2). Hydrazido(2-) ligands can bind to either one or two (μ) metal centres through N_α. Hydrazido ligands described in this Thesis will be primarily four-electron donor monomeric "end-on" bound (η^1-hydrazido(2-)), isoelectronic with the imido ligand.

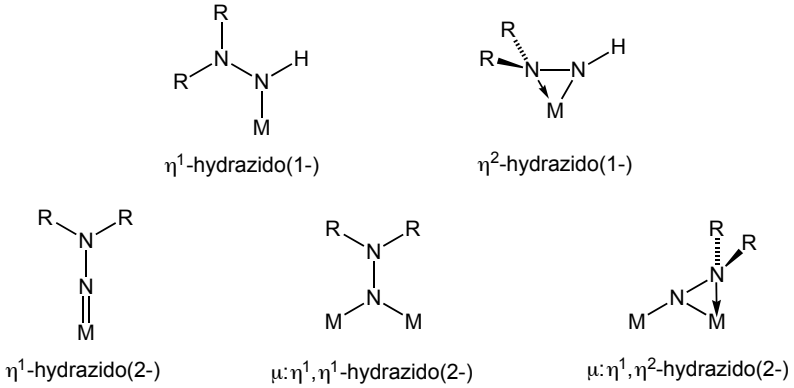


Figure 1.2. Bonding modes of hydrazido ligands.

η^1-hydrazido(2-) ligands can be drawn as an alternate resonance form, this is know as an isodiazene (Figure 1.3). The neutral isodiazene resonance form binds to the metal centre with a dative M←N_α bond and contains a N_α=N_β double bond as a result of the N_α=N_β π^* orbital being unoccupied. The relative contributions of the two resonance forms significantly affects the reactivity of the complexes. Relevant geometric parameters can be used to identify the contribution of each form (M–N_α and N_α–N_β bond lengths and angles subtended at N_β).[56]

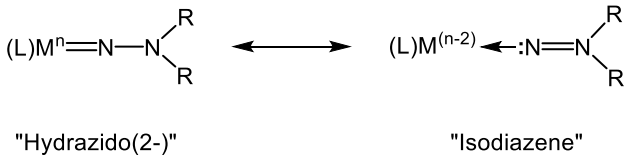


Figure 1.3. The hydrazido(2-) and neutral isodiazene resonance forms.

Mid to late transition metal complexes (Group 6 and later) generally contain a larger contribution from the neutral isodiazene form as a result of their less reducing nature. Due to the nominally dative M←N_α bond, reactivity here is minimal and is instead observed at N_β. Complexes with the earlier metals (in particular Group 4) exist with a much larger contribution from the hydrazido(2-) form. This is apparent from the longer N_α–N_β bonds and M–N_α triple bonds. In principle N_β would be sp^3 hybridised, however this is only observed with alkyl substituted hydrazido complexes as the presence of aryl groups allows for delocalisation of the N_β lone pair and thus a planar geometry. Group 5 hydrazido complexes generally show intermediate behaviour.

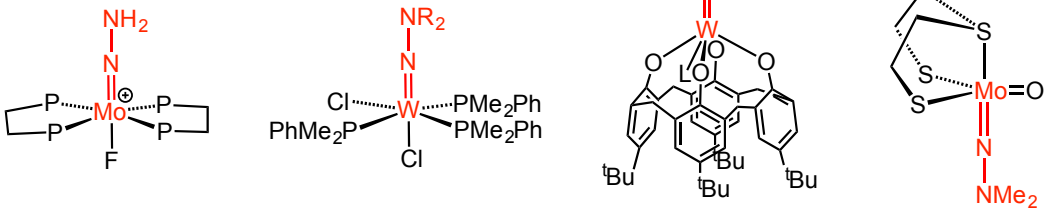
The hydrazido and isodiazene resonance forms can be compared to the Schrock and Fischer carbenes repectively.[56-60] Schrock carbenes (alkylidenes) are found with early transition metals in high oxidation states and are dianionic, much like the hydrazido(2-) ligand. Fischer carbenes are bound to later, less reducing metals and are in general less reactive than their Schrock counterparts.

1.5 Group 6 hydrazido complexes

1.5.1 Synthesis

Due to the relevance of Group 6 hydrazido compounds to nitrogen reduction, much of the early work on terminal hydrazido compounds focussed on the later metals. Hidai and co-workers have contributed significantly to this field, synthesising a wide range of molybdenum and tungsten hydrazido compounds. They described the synthesis of

$[Mo(N_2H_2)(F)(dppe)_2][BF_4]$ (**1.4**, dppe = $Ph_2PCH_2CH_2PPh_2$, Figure 1.4) from the corresponding dinitrogen compound $Mo(N_2)_2(dppe)_2$ and $H[BF_4]$ in 1976,[61] and the tungsten congener $[W(N_2H_2)(F)(dppe)_2][BF_4]$ (**1.5**) was reported two years later.[62] The same methodology was used to synthesise $[W(N_2H_2)(OTf)(dppe)_2][OTf]$ (**1.6**, OTf = $CF_3SO_3^-$) by Fields *et al.* in 1998.[63]



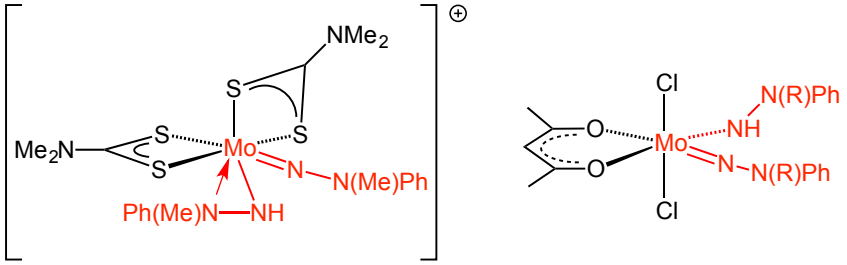
1.4 R = Me (**1.7**) or Ph (**1.8**) **1.9** (L = MeCN) **1.10**

Figure 1.4. Examples of structurally charcterised molybdenum and tungsten η^1-hydrazido(2-) complexes.

Niemoth-Anderson *et al*. reported the reaction of WCl_6 or $MoCl_5$ with alkyl and aryl hydrazines or hydrazine hydrochloride salts to yield the compounds $W(NNRR')Cl_4$ and $Mo(NNRR')Cl_3$ (R = R′ = Me or Ph; R = Ph, R′ = H or Me). These complexes were then reduced in the presence of phosphine ligands to yield compounds such as $W(NNR_2)Cl_2(PMe_2Ph)_3$ (R = Me (**1.7**) or Ph (**1.8**), Figure 1.4).[64] The M–N_α bond distance was found to be shorter for the diaryl hydrazide **1.8** compared to the dialkyl compound **1.7** (1.761(8) *vs*. 1.851(5) Å). The diaryl η^1-hydrazido(2-) tungsten compound $W(NNPh_2)(L)(MeCN)$ ((**1.9**), L = *tert*-butylcalix[4]arene) has also been reported and was synthesied following a simple protonolysis reaction with $W(NNPh_2)(O^tBu)_4$.[65] The same methodology was employed targeting the molybdenum analogue, which resulted in the formation of the dimeric compound $[Mo(NNPh_2)(L)]_2$.

It was reported in 2003 that the reaction of thiolate-supported molybdenum oxide compounds $Mo(O)_2\{X(CH_2CH_2S)_2\}$ (X = O or S) with hydrazines yielded hydrazido(2-) compounds, for example $Mo(NNMe_2)(O)\{S(CH_2CH_2S)_2\}$ (**1.10**, Figure 1.4).[66] Reaction with Me_3SiCl was able to replace the remaining oxide with two choride ligands and in the case of $Mo(NNMe_2)Cl_2\{O(CH_2CH_2S)_2\}$ further reaction with an equivalent of hydrazine yields a bis(hydrazido(2-)) compound. The structurally authenticated molybdenum bis(hydrazido(2-)) species

$Mo(NNPh_2)_2(SCNMe_2)_2$ has also been described, synthesised following reaction of the bis(oxo) compound $MoO_2(S_2CNMe_2)_2$ with hydrazine.[67] Both hydrazido ligands contain linear Mo–N_α–N_β bond angles (169.9(8) °) and Mo–N_α and N_α–N_β bond lengths of 1.910(8) Å and 1.31(1) Å respectively. The relatively long and short Mo–N_α and N_α–N_β bonds indicate a significant isodiazene contribution.[68] The mixed η^2-hydrazido(1-)/η^1-hydrazido(2-) compound $[Mo(NHNMePh)(NNMePh)(S_2CNMe_2)_2][BPh_4]$ (**1.11**, Figure 1.5) was synthesised following reaction of the bis(hydrazido(2-)) compound $Mo(NNMePh)_2(S_2CNMe_2)_2$ with Me_3SiCl.[69] The two Mo–N bond lengths are significantly longer in the η^2-hydrazido(1-) ligand compared to the η^1-hydrazido(2-) ligand, as expected (2.069(8) and 2.175(9) *vs.* 1.75(1) Å).

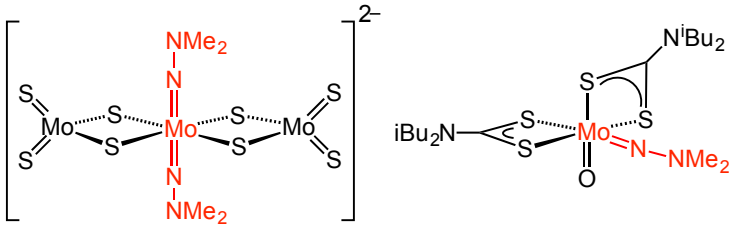


1.11 R = Ph (**1.12a**) or Me (**1.12b**)

Figure 1.5. Examples of structurally characterised mixed hydrazido(1)/hydrazido(2-) complexes.

Examples of mixed η^1-hydrazido(1-)/η^1-hydrazido(2-) compounds were reported by Carillo and Gouzerh in 1994, also resulting from the reaction of the molydenum oxo precursor with hydrazines. Acetylacetonate (acac) was used as the suporting ligand to yield complexs of the type Mo(NHNRR′)(NNRR′)(acac)X_2 (R = R′ = Ph (**1.12a**); R = Ph, R′ = Me (**1.12b**); X = Cl, Br or I, Figure 1.5).[70] When X = Cl both **1.12a** and **1.12b** were structurally characterised and found to contain both hydrazido ligands bound in an "end-on" manner. This differs to what was observed in **1.11** where the hydrazido(1-) ligand is bound in a "side-on" manner, and is suggested to be a result of steric constraints. Nevertheless the hydrazido(1-) and hydrazido(2-) ligands can be easily distinguished. Almost linear Mo=N_α–N_β bond angles of 173.8(2) and 171.9(4) ° were observed for **1.12a** and **1.12b** respectively, as well as short Mo–N_α bond distances of 1.750(2) and 1.752(4) Å. The hydrazide(1-) Mo–N_α distances are significanly longer (1.948(5) and 1.948(2) Å) and the Mo–N_α–N_β bond angles are bent (104.5(4) and 142.9(2) °). The bis(hydrazido(2-)) complexes were easily acessible in both cases by reaction with various phosphorus reagents.

Many of these Group 6 hydrazido compounds exhibit significant isodiazene contribution as demonstrated by the lengthened M–N_α bond distances and shortened N_α–N_β bond distances in comparison to complexes of the early metals (*vide infra*). A rare example of a compound containing "pure" isodiazene ligands is $[Mo_3S_8(NNMe_2)_2]^{2-}$ (**1.13**) shown in Figure 1.6.[71] The MoS_4 groups prevent π-donation between the metal and N_α and thus the M–N_α bond distances are significantly longer than the examples discussed above. For example the comparative dialkyl sulphur ligand supported compound $Mo(NNMe_2)(O)(S_2CN^iBu_2)_2$ (**1.14**, Figure 1.6) has a Mo–N_α bond distance of 1.881(18) Å in comparison to 2.13(1) Å found in **1.13**.[72] The isodiazene form is also apparent from the short N_α–N_β bond distance of 1.16(2) Å in **1.13** compared to 1.390(18) Å in **1.14**. This comparison demonstrates clearly the structural differences between a "pure" isodiazene NNR_2 ligand and one containing contributions from both isodiazene and hydrazido resonance forms.



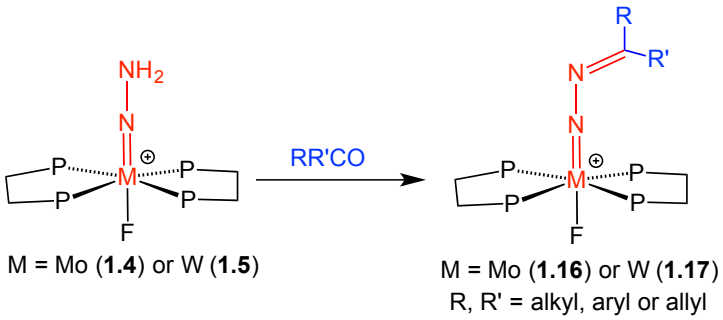
1.13 **1.14**

Figure 1.6. Molecular structures of $[Mo_3S_8(NNMe_2)_2]^{2-}$ (**1.13**) and $Mo(NNMe_2)(O)(S_2CN^iBu_2)_2$ (**1.14**).

Examples of chromium hydrazides are limited. However, Wiberg described the synthesis of the chromium compound $[CpCr\{NN(SiMe_3)_2\}]_2$ (**1.15**) from Cp_2Cr and $Me_3SiNNSiMe_3$ in 1978. A crystal structure was not obtained. However, the compound is thought to be dimeric.[73]

1.5.2 Stoichiometric reactions

Extensive work was put into understanding the mechanisms for the Schrock and Chatt cycles which involve breaking the N_α–N_β bond of the hydrazido intermediates. As a result the stiochiometric reactions of several of these Group 6 hydrazido(2-) compounds have been studied.

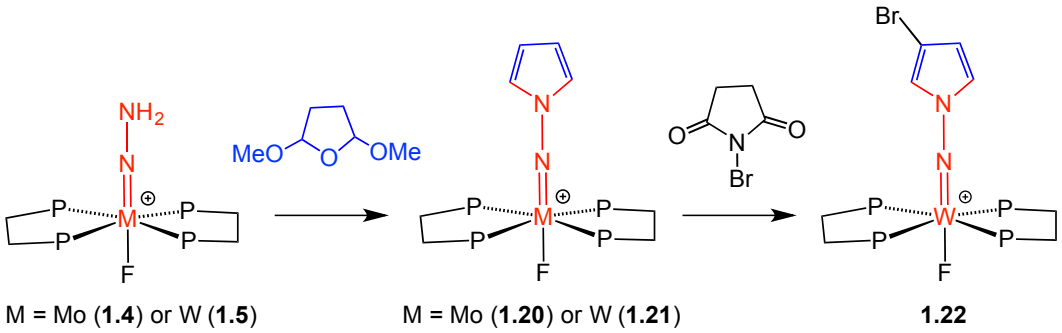


M = Mo (**1.4**) or W (**1.5**)

M = Mo (**1.16**) or W (**1.17**)
R, R' = alkyl, aryl or allyl

Equation 1.1

Hidai found that the unsubstituted hydrazido(2-) compounds $[M(N_2H_2)(F)(dppe)_2][BF_4]$ (M = Mo (**1.4**) or M = W (**1.5**)) react with a range of aldehydes and ketones to yield the diazoalkane complexes $[M(F)(NNCRR')(dppe)_2][BF_4]$ (M = Mo (**1.16**) and M = W (**1.17**), Equation 1.1) as well as several other carbonyl containing molecules to yield the corresponding organo-dinitrogen ligands.[38, 62, 74-76] Reaction with acyl chlorides resulted in substitution at N_β through HCl elimination and reaction of the bromide analogue $[M(N_2H_2)(Br)(dppe)_2][Br]$ (M = Mo or W) gave $[M(Br)\{NN(H)C(O)NHPh\}(dppe)_2][Br]$ (**1.18**, M = Mo or W).[75] It was also shown that the protons attached to N_β could be removed by addition of a base such as KO^tBu to yield dinitrogen complexes, for example the reaction of $[W(N_2H_2)(NCMe)(dppe)_2][OTf]$ (**1.19**) to yield $[W(N_2)(NCMe)(dppe)_2]$.



M = Mo (**1.4**) or W (**1.5**) M = Mo (**1.20**) or W (**1.21**) **1.22**

Scheme 1.1. Reaction of $[Mo(N_2H_2)(F)(dppe)_2][BF_4]$ (**1.4**) and $[W(N_2H_2)(F)(dppe)_2][BF_4]$ (**1.5**) with a furan.

It is apparent that the reactions of Group 6 hydrazido compounds are dominated by transformations involving nucleophilic attack by N_β. This is demonstrated nicely by the addition of oxygen heterocycles such as furans and substituted cyclic acetals to compounds of the type $(L)M{=}NNH_2$, which result in displacement of the oxygen atom to yield nitrogen heterocycles. For example, reaction of $[M(N_2H_2)(F)(dppe)_2][BF_4]$ (M = Mo (**1.4**) or W (**1.5**)) with 2,5-dimethoxytetrahydrofuran resulted in the formation of $[M(NNC_4H_4)(F)(dppe)_2][BF_4]$ (M = Mo (**1.20**) and M = W (**1.21**), Scheme 1.1).[38, 76] Subsequent reaction of **1.21** with an electrophile resulted in *β*-regioselective substitution (compared to *α*-regioselective electrophilic substitution which occurs in free pyrrole) (**1.22**, Scheme 1.1). Reactions involving cleavage of the N–N bond require forcing conditions such as the use of $LiAlH_4$ or concentrated acid.[77]

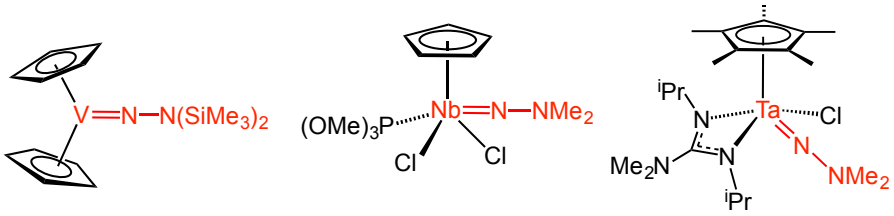
1.6 Group 5 hydrazido complexes

Although nitrogenases containing Fe only, and Fe and V at the active site have been studied[78-81] the number of Group 5 hydrazido compounds that exist is relatively small, especially in comparison to Group 6.

1.6.1 Synthesis

The first Group 5 hydrazido complex, $Cp_2V\{NN(SiMe_3)_2\}$ (**1.23**, Figure 1.7) was reported by Wiberg in 1976 and was synthesised *via* the same synthetic route used to access the chromium analgoue **1.15**.[82] The solid state structure indicates a linear V–N_α–N_β bond angle (180 °), a short V–N_α bond distance (1.666(6) Å) and a long N_α–N_β bond distance (1.369(9) Å) indicating a hydrazido(2-) ligand.[83] Alkyl and aryl substituted vanadium hydrazides of the type $V\{N(CH_2CH_2S)_3\}(NNRR')$ (R = R′ = Me (**1.24**); R = Ph, R′ = Me (**1.25**) or H (**1.26**)) were reported by Sabota *et al. via* reaction

of the oxo compounds with the appropiate hydrazine.[84, 85] In comparison to **1.23**, the dimethyl compound **1.24** exhibits V–N_α and N_α–N_β bond distances longer and shorter respectively (1.681(3) and 1.305(5) Å), implying a greater contribution from the isodiazene resonance form. Further examples of structurally characterised vanadium hydrazido compounds exist, $[V(NNMePh)Cl_2(NH_2NMePh)]Cl$ (**1.27**)[86] was synthesised from the reaction of $VCl_3(MeCN)_3$ with $PhMeNNH_2$ and $(C_9H_{18}NN)_2(OSiMe_3)_2V(\mu\text{-}O)V(O)(OSiMe_3)_2$ (**1.28**) from H_4NVO_3 and amino-2,2,6,6-tetramethylpiperidine.[87] Both complexes exhibit bond distances similar to that of **1.24**. More recently, Banerjee and Odom reported the synthesis of several vanadium hydrazido(2-) compounds where all of the elemental connections found in nitrogenase enzymes, S, N and O are in the same coordination sphere.[88] One of these compounds was structurally characterised, namely $[V(NNMe_2)(TIP)(dmpe)]I$ (**1.29,** H_2TIP = 2-((2-thiol-phenylimino)methylene)phenol, dmpe = $Me_2PCH_2CH_2PMe_2$). The N_α–N_β bond is relatively short (1.293(3) Å) indicating double bond character. The V–$N_\alpha$bond distance (1.698(2) Å) is within the region expected for significant contributions from both the hydrazide and isodiazene resonance forms. In 2013 Hirao *et al.* reported the synthesis and characterisation of dialkyl and diaryl vanadium hydrazido compounds supported by substituted tris(2-hydroxyphenyl)amines from the corresponding oxo compounds.[89]



1.23 **1.33** **1.41**

Figure 1.7. Examples of Group 5 η^1-hydrazido compounds.

The first niobium hydrazido compound was synthesised in 1997 by Green *et al.* Reaction of the tetrachloride complex $CpNbCl_4$ with Me_2NNH_2 and two equivalents of NEt_3 yielded $CpNb(NNMe_2)Cl_2$ (**1.30**).[90] The compounds $(C_5H_4Me)Nb(NNMe_2)Cl_2$ (**1.31**) and $CpNb(NNMePh)Cl_2$ (**1.32**) were also synthesised in an analogous manner. The solid state structure of **1.30** showed it to be dimeric with one η^1-hydrazido ligand and one μ:η^1,η^2-hydrazido ligand. The η^1-hydrazido ligand has Nb–N_α and N_α–N_β bond distances consistent with a dianionic four-electron donor (1.67(2) and 1.38(2) Å respectively). Addition of $P(OMe)_3$ results

in the formation of the monomeric species $CpNb(NNMe_2)Cl_2\{P(OMe)_3\}$ (**1.33**, Figure 1.7) which contains longer and shorter Nb–N_α and N_α–N_β bond distances compared to **1.30** suggesting a larger contribution from the isodiazene resonance form. The sandwich compounds $Cp_2Nb(NNMe_2)Cl$ (**1.34**) and $(C_5H_4Me)_2Nb(NNMe_2)Cl$ (**1.35**) were synthesied by addition of $Li[C_5H_4R]$ (R = H or Me) to **1.30** and **1.31** respectively.[91]

Numerous examples of tantalum η^1-hydrazido compounds have also been reported. The bis(hydrazido) compound $[Ta(NNC_9H_{18})_2Cl_4][NEt_3H]$ (**1.36**) was synthesied by Wilkinson *et al*. in 1997 from $TaCl_5$, along with the niobium analogue from $NbCl_5$.[87] Compound **1.36** has Ta–N_α and N_α–N_β bond distances typical of an isodiazene ligand which is also supported by a planar geometry at N_β. The diphenylhydrazido compounds $M(NNPh_2)(DME)Cl_3$ (M = Ta (**1.37**) and M = Nb (**1.38**), DME = 1,2-dimethoxyethane) were also synthesised from MCl_5 in a Lewis-acid catalysed dehydrohalogenation reaction with diphenylhydrazine.[92, 93] The tantalum complex **1.37** has been shown by Bercaw to be a useful synthon toward a range of tantalum hydrazido compounds supported by anionic ligands. For example both $Cp_2Ta(NNPh_2)Cl$ (**1.39**) and $Ta(N_2N^{Me})(NNPh_2)Cl$ (**1.40**, N_2N^{Me} = $MeN(CH_2CH_2NSiMe_3)_2$) were synthesied from **1.37** *via* salt metathesis reactions. Both compounds **1.37** and **1.40** showed geometric parameters consistent with with a hydrazido(2-) ligand, whereas **1.39** displayed a longer Ta–N_α bond and a non-linear Ta–N_α–N_β angle (167.04(1) ^{o}) characteristic of significant isodiazene contribution.

In 2013 the synthesis of a cyclopentadienyl-guanidinate supported tantalum hydrazide was reported, namely $Cp^*Ta\{(Me_2N)C(N^iPr)_2\}(NNMe_2)(Cl)$ (**1.41**, Figure 1.7) as well as its reduction with KC_8 to yield $Cp^*Ta\{(Me_2N)C(N^iPr)_2\}(NNMe_2)$ (**1.42**).[94] Analysis of the geometric parameters of both stuctures indicate that on reduction the contribution from the hydrazide(2-) resonance form increases. Both compounds react with MeOTf undergoing alkylation at N_β resulting in the following compounds $[Cp^*Ta\{(Me_2N)C(N^iPr)_2\}(NNMe_3)(Cl)][OTf]$ (**1.43**) and $[Cp^*Ta\{(Me_2N)C(N^iPr)_2\}(NNMe_3)][OTf]$ (**1.44**). Compound **1.44** can undergo further reaction with Na/Hg resulting in reductive N_α–N_β bond cleavage forming either $[Cp^*Ta\{(Me_2N)C(N^iPr)_2\}(\mu\text{-}N)]_2$ or $Cp^*Ta\{(Me_2N)C(N^iPr)_2\}(NH)(OTf)$ depending on the reaction conditions.

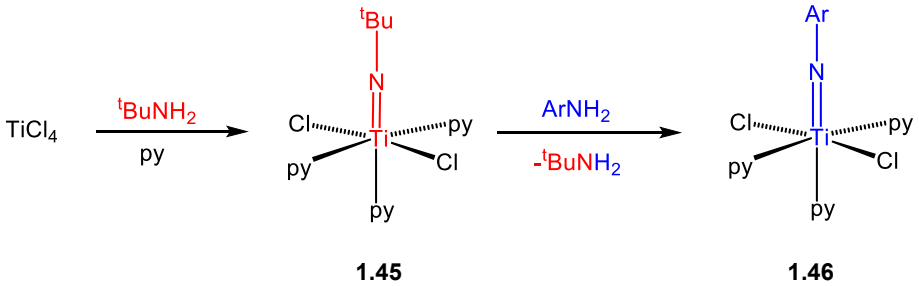
1.7 Group 4 imido and hydrazido complexes

Few examples exist of the reactions of Group 5 and 6 hydrazido compounds, and in all of this chemistry the M=NNR$_2$ functional group reactivity is characterised exclusively by transformations involving the N$_\beta$ atom and/or N$_\alpha$–N$_\beta$ reductive cleavage. This is, in many cases, due to the large contribution from the isodiazene resonance form. In contrast, work over the last 20 years has demonstrated that Group 4 hydrazido compounds display a wealth of stoichiometric and catalytic reactions focussed at the M=N$_\alpha$ bond. These more reducing metals better support the hydrazido(2-) ligand thus resulting in reactive metal-nitrogen triple bonds. Such compounds are also of great interest due to their relation to the dianionic imido ligand M=NR (R = alkyl or aryl) of which great success has also been found with the Group 4 metals. Imido ligands are a well established ligand class and have continued to be of interest due to their practical applications as well as fundamental structure, bonding and reactivity studies. The synthesis and reactivity of both imido and hydrazido compounds will be discussed in this Thesis, therefore a short literature review on the synthesis, structure and reactivity of Group 4 imido compounds is first presented.

1.7.1 Group 4 imido complexes

1.7.1.1 Synthesis of titanium imido complexes

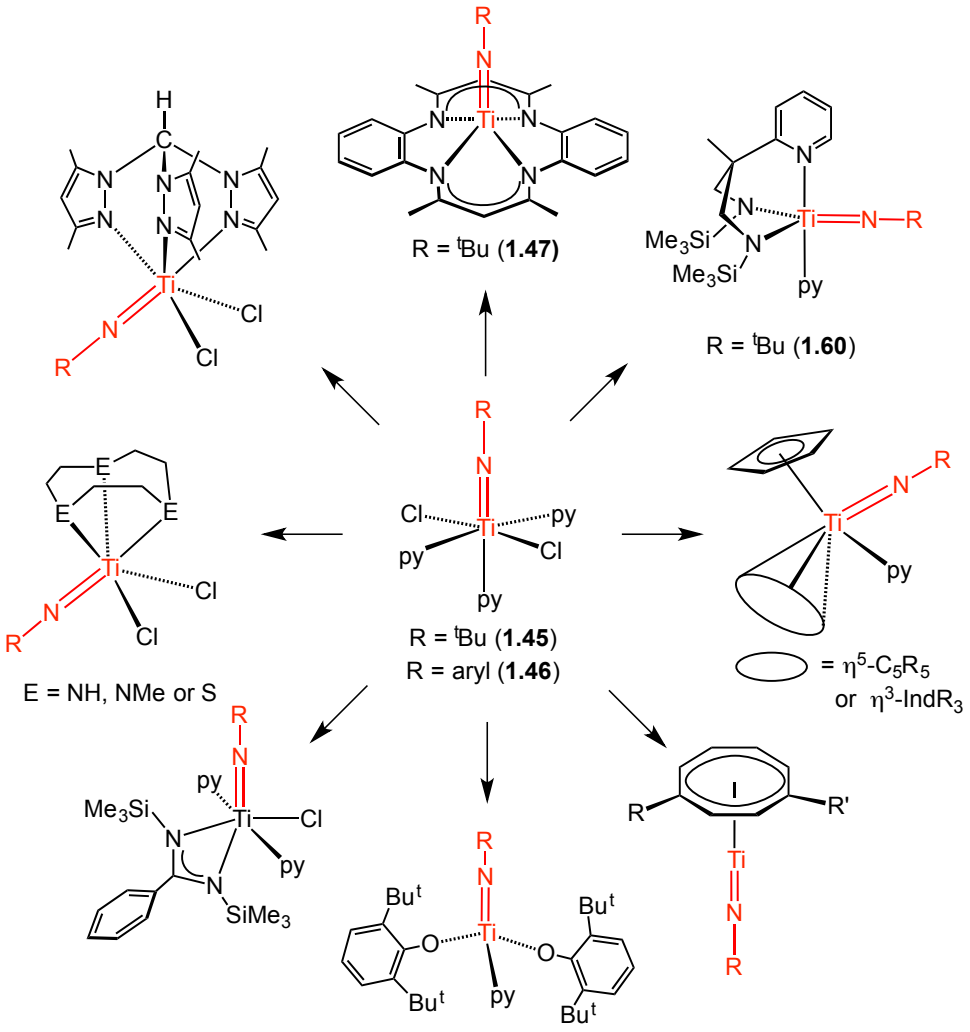
The first structurally authenticated terminal imido titanium compound was reported by Roesky in 1990, Ti{NP(S)Ph$_2$}Cl$_2$(py)$_3$ was synthesised from the reaction of TiCl$_4$ with Ph$_2$P(S)NSiMe$_3$ and Me$_3$SiCl.[95] Later that year the imido compound Ti(NPh)(OAr′)$_2$(py′)$_2$ (py′ = 4-pyrrolidinopyridine) was described following a thermolysis reaction of Ti{η^2-N(Ph)N(Ph)}(OAr′)$_2$(py′)$_2$ or through addition of py′ and PhNH$_2$ to Ti{η^2-N(^{t}Bu)C(CH$_2$Ph)$_2$}(OAr′)$_2$(py′).[96] The transient imido compound Ti(NHSi^{t}Bu$_3$)$_2$(NSi^{t}Bu$_3$) was synthesised from Ti(NHSi^{t}Bu$_3$)$_3$Cl with MeLi.[97] Alternative methods of synthesising imido compounds include the oxidation of Ti^{II} species[98, 99] and reaction of compounds of the type (L)TiCl$_2$ with two equivalents of MNHR (M = Li or K).[100]



1.45 **1.46**

Scheme 1.2. Synthesis of alkyl and aryl titanium imido synthons.

A more general route was published by Mountford *et al*. in 1994, which detailed the high yielding multi-gram synthesis of $Ti(N^tBu)Cl_2(py)_3$ (**1.45**, Scheme 1.2) from $TiCl_4$, $^tBuNH_2$ and pyridine.[101] Arylimido complexes of the type $Ti(NAr)Cl_2(py)_3$ (**1.46**, Examples of Ar = Xyl (2,6-$C_6H_3Me_2$), Tol (4-C_6H_4Me) and Ph, Scheme 1.2) were also obtained by arylamine/*tert*-butylimide exchange reactions with **1.45**.[53, 101-103] The analogous reactions of $TiCl_4$ with $ArNH_2$ and pyridine were unsuccessful. Such tris(pyridine) imido compounds revolutionised research into titanium imido compounds, as they provide verstile entry points into a wide range of compounds following reaction with a variety of lithiated ligands (Scheme 1.3).[53, 100, 103-107]



Scheme 1.3. Examples of various titanium alkyl/arylimido complexes synthesised from $Ti(NR)Cl_2(py)_3$ (R = alkyl (**1.45**) or aryl (**1.46**)).

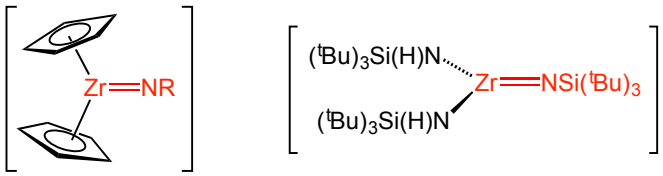
In many cases it is also possible to carry out the arylamine/*tert*-butylimide exchange reaction subsequent to reaction with a lithated ligand. For example, reaction of the tetraazamacrocycle-supported *tert*-butylimido complex $Ti(N^tBu)(Me_4taa)$ (**1.47**, H_2Me_4taa = tetramethyl dibenzotetraaza[14]-annulene) with a range of aryl amines ($ArNH_2$, Ar = Ph, Tol, Xyl, 4-$C_6H_4NO_2$ and 4-$C_6H_4NMe_2$) yielded the corresponding arylimido compounds **1.48** cleanly.[104, 105]

The compound $Ti(NMe_2)_2Cl_2$ (**1.49**) has also proved to be a useful synthetic entry point into titanium imido compounds. Compound **1.49** is synthesised *via* a simple redistribution reaction between $TiCl_4$ and $Ti(NMe_2)_4$ and following protonolysis with the required amine, RNH_2 (R = alkyl or aryl), yields imido complexes of the type

$Ti(NR)(NHMe_2)_2Cl_2$ (R = alkyl (**1.50**) or aryl (**1.51**)).[108] A second protonolysis reaction can then be carried out with a selection of neutral ligands to yield dichloride imido compounds. For example, reaction with $Me_3[9]aneN_3$ ($Me_3[9]aneN_3$ = 1,4,7-trimethyltriazacyclononane) yields the compounds $Ti(NR)(Me_3[9]aneN_3)Cl_2$ (R = alkyl (**1.52**) or aryl (**1.53**)).[109] In some cases the previously described tris(pyridine) imido compounds **1.45** and **1.46** could be synthesised from **1.50** and **1.51** following reaction in neat pyridine at 60 ^oC. This synthetic method allowed access to some previously unknown imido synthons of the type **1.46** and also yielded the first titanium compound to contain a chiral imido ligand, namely, $Ti[N\{S\text{-}(-)\text{-}CH(Me)Ph]Cl_2(py)_3$.[110] The *trans* effect of the imido ligand in compounds of the type **1.45** and **1.46** results in a longer $Ti–N_{pyridine}$ bond distance for the *trans* pyridine ligand. This results in a relatively labile pyridine ligand which can be removed under reduced pressure to form the chloride-bridged dimers $Ti_2(NR)_2Cl_2(\mu\text{-}Cl)(py)_4$ (R = alkyl or aryl).

1.7.1.2 Synthesis of zirconium and hafnium imido complexes

The first zirconium imido compounds were a family of complexes of the type $Cp_2Zr(NR)$ (R = ^{t}Bu (**1.54**) or Xyl (**1.55**), Figure 1.8) described by Bergman in 1988.[111] These transient species were synthesised from thermolysis of the corresponding amido compounds $Cp_2Zr(NHR)(R')$ (R′ = alkyl) and spontaneously dimerised in solution to give dimeric complexes with bridging imido ligands. The THF adduct $Cp_2Zr(N^tBu)(THF)$ (**1.56**) could, however, be isolated, when the thermolyisis was carried out in THF.[112] Dimeric zirconium and hafnium complexes containing bridging imido ligands had been previously observed by Nugent in 1979 *via* the reaction of $M(NMe_2)_4$ (M = Zr or Hf) with $^tBuNH_2$.[113] The larger radius of zirconium and hafnium compared to titanium hinders the synthesis of monomeric terminal imido compounds as more steric protection is required at the reactive metal-nitrogen multiple bond. This same method was used to synthesise other Cp-supported complexes a few years later.[114]



R = ^{t}Bu (**1.54**) or Xyl (**1.55**) **1.57**

Figure 1.8. Early examples of transient zirconium imido compounds.

The transient imide [Zr(NSi^{t}Bu$_3$)(HNSi^{t}Bu$_3$)$_2$] (**1.57**, Figure 1.8) was reported by Wolczanski and co-workers again following a thermolysis procedure, subsequent trapping with THF yielded the isolable compound Zr(NSi^{t}Bu$_3$)(NHSi^{t}Bu$_3$)$_2$(THF).[115] Wigley *et al.* reported the zirconium analogue of the titanium synthon Ti(NAr)Cl$_2$(py)$_3$ (**1.46**), namely Zr(NAr′)Cl$_2$(py)$_3$ (**1.58**, Ar′ = 2,6-C$_6$H$_3$^{i}Pr$_2$) obtained from the reaction of ZrCl$_4$(THF)$_2$ with LiNAr′, Me$_3$SiCl and pyridine but only for this specific imido N-subsitutent.[116] In the absence of pyridine the compound Zr(NAr′)Cl$_2$(THF)$_2$ was formed, this compound was later crystallographically characterised by Mountford and shown to be a dimeric species containing bridging imido ligands.[117] The analogous hafnium compound Hf(NAr′)Cl$_2$(THF)$_2$ was also reported.[116] Attempts were made to access a more versatile zirconium synthon which would allow access to a wider range of imido N-substituents and thus a wider range of compounds. Protonolysis methodoligies based on the reactions of Zr(CH$_2$SiMe$_3$)$_2$Cl$_2$(Et$_2$O)$_2$ and Zr(NMe$_2$)$_2$Cl$_2$(THF)$_2$ with a range of primary alkyl and aryl amines do provide general entry points to dimeric zirconium imido dichloride compounds, however addition of pyridine to such compounds did not result in monomeric compounds and addition of lithiated ligands was not successful.[117]

Compound **1.58** has been shown to be a precursor to other zirconium imido complexes, namely [(η-C$_8$H$_8$)Zr(NAr′)]$_2$ and [(η-C$_5$H$_4$Me)ZrCl(μ-NAr′)]$_2$ and other research groups have used Wigley's compounds for the synthesis of 2,6-diisopropylphenyl imido complexes.[118, 119] Zirconium and hafnium imido compounds can also be synthesised from dichloride precursors. For example, reaction of the macrocycle supported dichloride compound (TTP)MCl$_2$ (M = Zr or Hf, TTP = meso-tetra-p-tolylporphyrinato dianion) with two equivalents of LiNHAr′ yielded M(NAr′)(TTP) (M = Zr (**1.59**) or Hf).[118] Once isolated these compounds react with amines to yield bis(amide) compounds. Mountford *et al.* reported the synthesis of the imido compound Zr(N$_2$NN′)(N^{t}Bu)(py) (N$_2$NN′ = (2-

$C_5H_4N)CH_2N(CH_2CH_2NSiMe_3)_2$) from the dichloride precursor $Zr(N_2NN')Cl_2$ and $LiCH_2SiMe_3$, $^tBuNH_2$ and pyridine. Again addition of a primary amine yielded a bis(amide) compound.[120]

1.7.1.3 Structual features

As part of the on-going research into titanium imido compounds, several studies detailing both experimental and computational studies into the geometric and electronic structures of such compounds have emerged. The details of some of these studies will be discussed here, all compounds mentioned are monomeric with a formal $\sigma^2\pi^4$ metal-nitrogen triple bond. For the following compounds, $Ti(NR)Cl_2(py)_3$ (R = alkyl (**1.45**) or aryl (**1.46**)), $Ti(NR)(NHMe_2)_2Cl_2$ (R = alkyl (**1.50**) or aryl (**1.51**)) and $Ti(NR)(Me_3[9]aneN_3)Cl_2$ (R = alkyl (**1.52**) or aryl (**1.53**)), short Ti–N bond lengths (range 1.672(2) – 1.7420(13) Å) and linear Ti–N–R bond angles (range 164.46(17) – 180 ^{o}) are indicative of such a triple bond.[101, 108, 121, 122] In general, the alkylimido compounds have shorter Ti–N bonds in comparison to their arylimido counterparts (avg. Ti–NR bond length R = alkyl, 1.690(1) Å and R = aryl 1.7183(7) Å). A clear example of this is found in the series of compounds $Ti(NR)(NHMe_2)_2Cl_2$ (R = ^{i}Pr (**1.50a**), Ph (**1.51a**), C_6F_5 (**1.51b**), 2,3,5,6-C_6HCl_4 (**1.51c**), 2-$C_5H_4CF_3$ (**1.51d**) and 2-$C_6H_4{}^t$Bu (**1.51e**))[108] and the series of compounds $Ti(NR)(Me_3[9]ane)Cl_2$ (R = ^{t}Bu (**1.52a**), Xyl (**1.53a**), Ar′ (**1.53b**), Ph (**1.53c**), and C_6F_5 (**1.53d**))[121] where the Ti–N bonds lengths increased in the order R = alkyl < aryl < electron-withdrawing aryl. The Ti–N bond lengthening effect of the electron-withdrawing substituent was also observed in the following series of compounds, $Ti(NR)Cl_2(py)_3$ (R = ^{t}Bu (**1.45**), 4-C_6H_4Me (**1.46a**) and 4-$C_6H_4NO_2$ (**1.46b**)). Compound **1.46b** was found to have a much longer bond length than **1.45** and **1.46a** (1.722(3) *vs.* 1.705(3) and 1.705(4) Å).[101] For this latter series of compounds the higher coordination number and *trans* influence of the pyridine ligand generally result in a longer Ti–N bond distance.

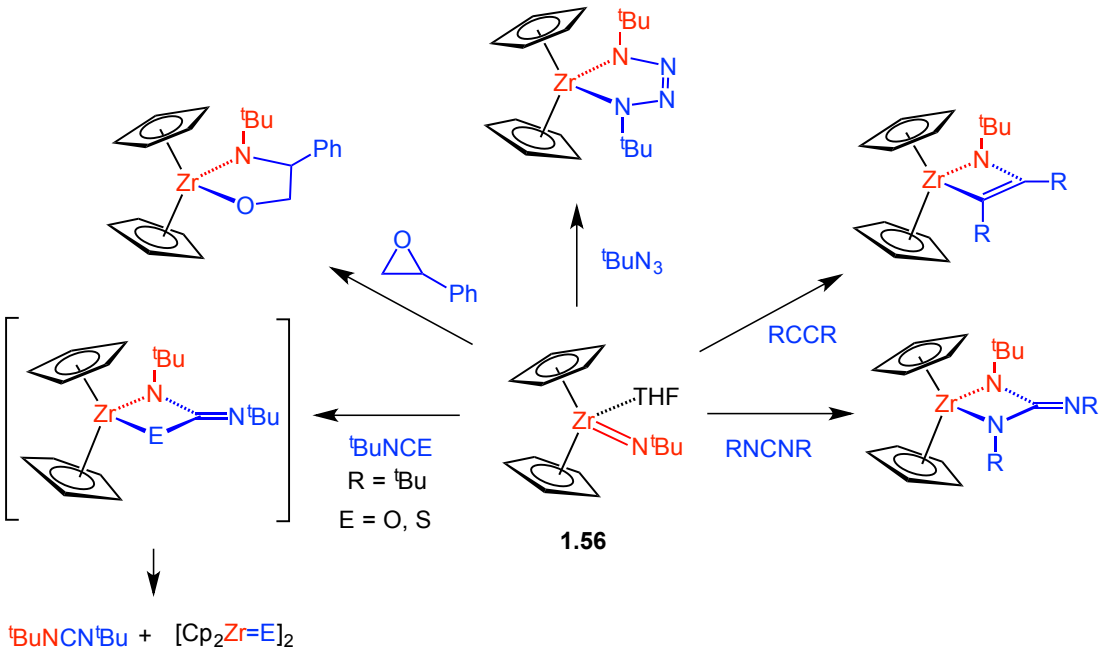
In 2011, a DFT study was carried out in order to better understand the structure and bonding of a range of cyclopentadienyl-amidinate supported imido and hydrazido compounds.[123] The model system $CpTi\{MeC(NMe)_2\}(NR)$ (R = alkyl, aryl or NR_2) was employed and it was found that the Ti=N bond length was significantly shorter when R = Me compared to R = Ph (1.688 *vs*. 1.709 Å) consistent with the experimental results discussed above. When R = Ph, donation from the Ti=N π orbital can occur into the π* orbital of the phenyl ring. Donation from the π orbital of the

phenyl ring into the π* orbital of Ti=N can also occur, both effects lead to a longer Ti=N bond.

As mentioned the *trans* influence of the imido ligand can result in loss of the *trans*-pyridine ligand under vacuum and formation of chloride bridged dimers. In 1999 a computational study investigating this *trans* effect in compounds of the type $Ti(NR)Cl_2(py)_3$ (R = alkyl (**1.45**) or aryl (**1.46**)) was published.[124] They report that although the *trans*-pyridine ligands are longer than the *cis*-pyridine ligands in all cases (in agreement with experimental results) the difference in the *trans* and *cis* Ti–N bond distances does not vary as the R group is varied.

1.7.1.4 Stoichiometric reactions

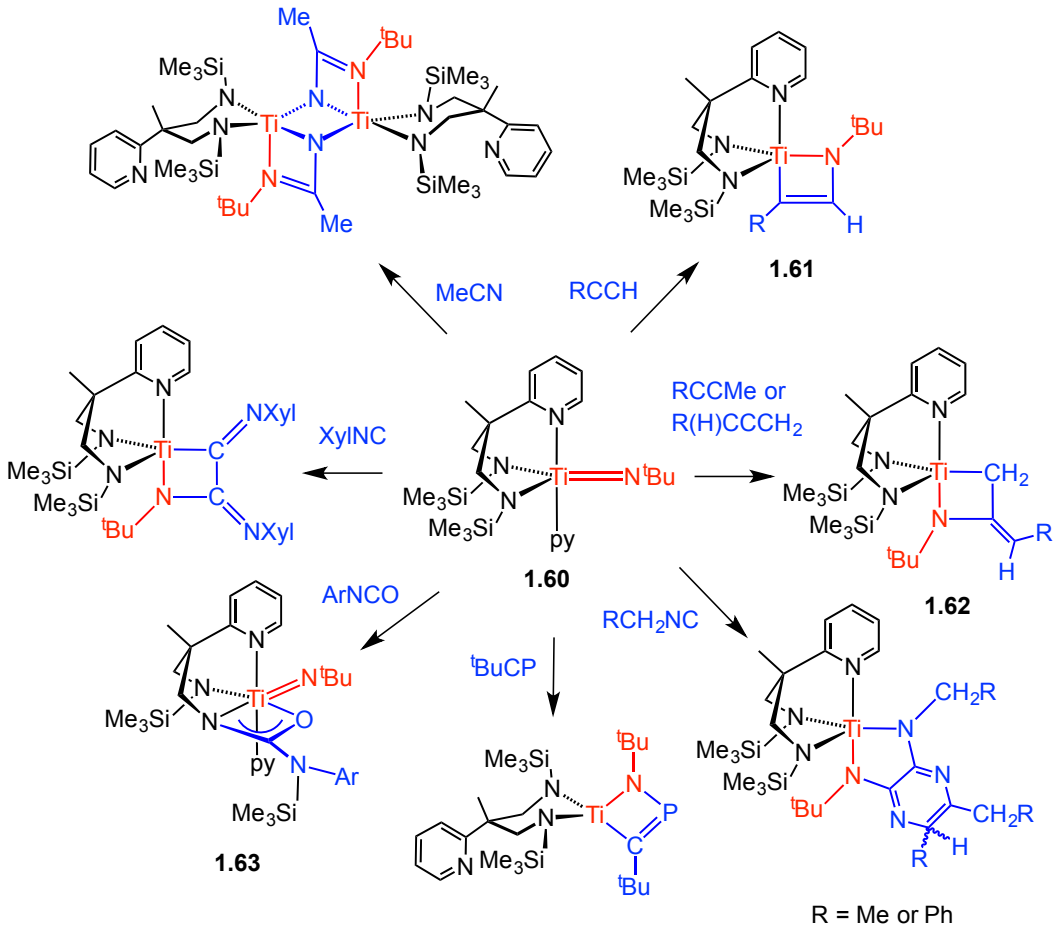
The main point of interest for Group 4 imido compounds is their reactivity at the unsaturated M=NR linkage. The majority of Group 4 imido reaction chemistry involves [2+2] cycloaddition reactions at the imido bond. However, some examples involving C–H activation have also been reported. Bergman's zirconium imide $Cp_2Zr(N^tBu)(THF)$ (**1.56**) displays extensive reaction chemistry with various substrates, some examples are shown in Scheme 1.4.[112, 125-128]



Scheme 1.4. Selected reactions of the zironocene imido compound $Cp_2Zr(N^tBu)(THF)$ (**1.56**).

Many of the reactions of **1.56** were found to be reversible and some reaction products exist in equilibrium with the starting materials. Examples involving the reaction with alkynes, alkenes and allenes in some cases lead to hydroamination of the organic substrates, *vide infra*. Compound **1.56** has also been found to activate sp^2 C–H bonds including those in cyclopentene, norbornene and the Cp ring of various Cp-supported transition metal complexes.[129]

The diamide-amine supported complex Ti(N_2N^{py})(N^tBu)(py) (**1.60**, N_2N^{py} = MeC(2-C_5H_4N)(CH_2NSiMe_3)$_2$) exhibits a particularly rich reaction chemistry and selected transformations are outlined in Scheme 1.5.[100, 103, 130-136] Reaction of **1.60** with terminal alkynes yielded azatitanocyclobutene compounds of the type **1.61**, whereas reaction with internal alkynes or allenes lead to the formation of titanaazetidines **1.62**. Interestingly reaction with isocyanates resulted in insertion into the N_{amide}–Si bond to yield **1.63** containing an intact imido ligand.



Scheme 1.5. Selected reactions of Ti(N_2N^{py})(N^tBu)(py) (**1.60**).

In 2009, Gade and co-workers published the synthesis of the cyclopentadienyl-amidinate compounds Cp*Ti($N^{Xyl}N$)(NAr) (Ar = Xyl (**1.64**) or 2,4,6-$C_6H_2Me_3$ (Mes) (**1.65**), $N^{Xyl}N$ = 2-(3,5-dimethylphenylamino)pyrrolinato) and Cp*Ti($N^{Xyl}N$)(N^tBu)($^tBuNH_2$) (**1.66**), and their reactivity with terminal alkynes. The arylimido compounds **1.64** and **1.65** produced azatitanocyclobutene compounds following cycloaddition reactions, whereas the alkylimido compound **1.66** underwent a C–H activation reaction of the terminal alkyne to yield the acetylide-amide compound Cp*Ti($N^{Xyl}N$)(HN^tBu)(CCAr).[137]

Several other compounds display reactivity with organic molecules. For example, reaction of Zr(NAr′)(TTP) (**1.59**) with isocyanates proceeds *via* a cycloaddition reaction followed by isomerisation and a subsequent extrusion reaction to generate carbodiimides.[138] The comparable compounds Ti(NAr)(Me_4taa) (**1.48**, Ar = Ph, Tol, Xyl, 4-$C_6H_4NO_2$ or 4-$C_6H_4NMe_2$) gave an alternative reaction yielding the κ^2N,N-bound ureate complexes Ti{N(Ar)C(O)N(Ar)}(Me_4taa) which were stable to extrusion and in some cases reversible.[105]

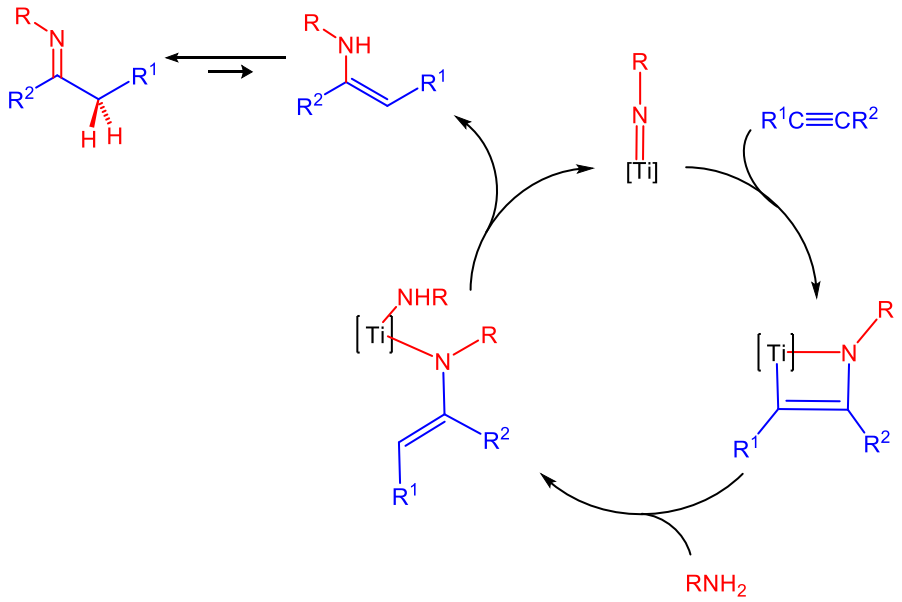
Titanium imido complexes have been shown to be capable of activating H–H and S–H bonds. The compound (η^5-C_5H_3-1,3-$SiMe_3$)$_2$Ti(NPh) and its homologues add H_2 in a 1,2 fashion across the imido bond yielding hydride-amide compounds.[99] The compound Cp_2Ti(N^tBu)(py) reacts with MeSH to yield Cp_2Ti$(SMe)_2$ and with SH_2 to yield the dimer Cp_2Ti(μ-S)$_2$TiCp_2 or the monomer Cp_2Ti$(SH)_2$.[139] The corresponding reaction of Ti(N^tBu)(Me_4taa) with H_2S gave the terminal sulfide compound Ti(Me_4taa)(S).[104]

Another interesting reaction was observed for the cyclopentadienyl-amidinate supported compound Cp*Ti{MeC(N^iPr)$_2$}(NTol) with $PhSiH_2X$ (X = Cl or Br), which gave cleavage of the silicon-halogen bond to yield silylamido-chloride complexes which were unstable in solution.[140]

1.7.1.5 Catalytic hydroamination

Hydroamination is the addition of an N–H bond across an unsaturated C–C bond and is an atom-economical method for the efficient formation of new C–N bonds. Group 4 metals have been widely studied as such catalysts and through a series of mechanistic studies three mechanisms have been established.[129, 141-151] The most commonly found mechanism, the “imide route” proceeds through a [2+2] cycloaddition reaction at the

M=NR bond. Protonolysis with an equivalent of amine then occurs to regenerate the imido catalyst and release the organic amine-alkene which then undergoes tautomerisation to yield the more stable imine isomer (Scheme 1.6).[152-156] Some examples are discussed below.



Scheme 1.6. General hydroamination catalytic cycle.

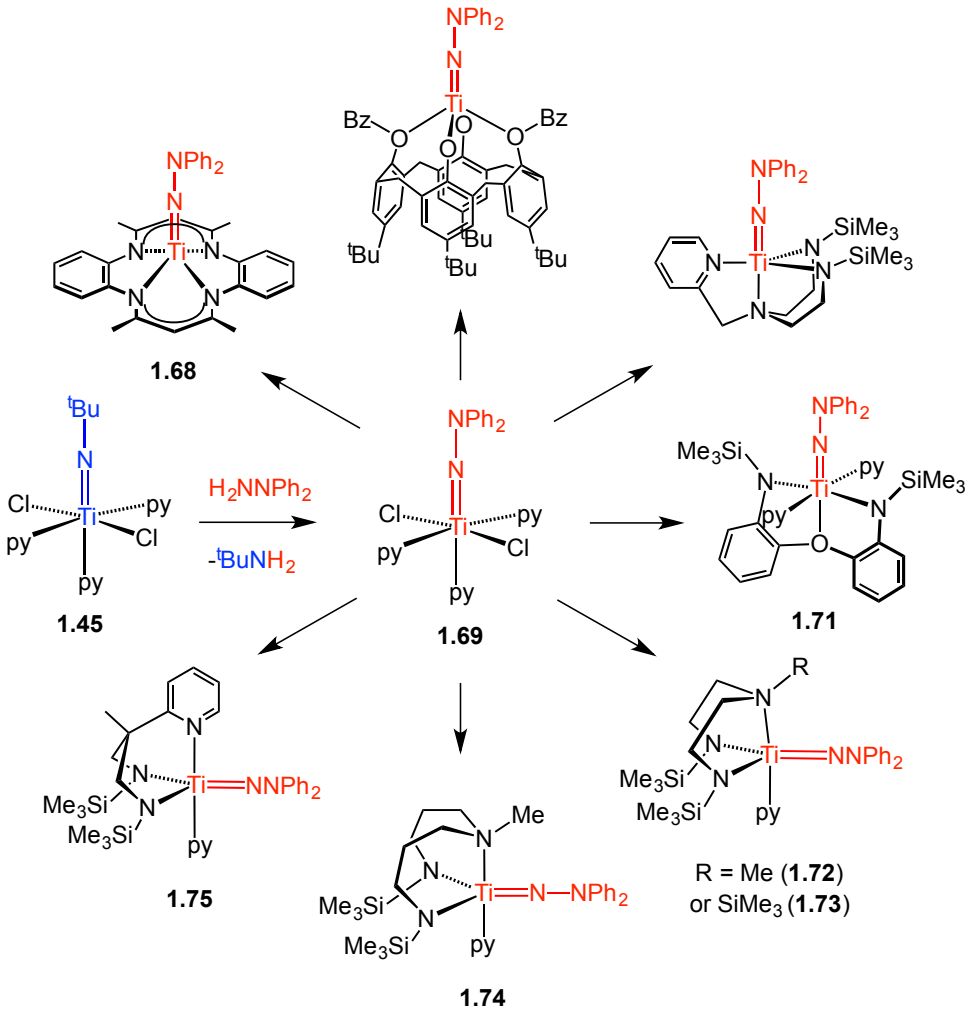
The titanium complexes Cp*Ti($N^{Xyl}N$)(NXyl) (**1.64**) and Cp*Ti($N^{Xyl}N$)($N^{t}Bu$)($^{t}BuNH_2$) (**1.66**) catalyse the hydroamination of both terminal and internal alkynes at 5 mol% catalyst loading however, long reaction times and high temperatures are required (24 h, 105 ^{o}C).[137] The parent compound Cp*Ti($N^{Xyl}N$)Me_2 (**1.67**), from which both **1.64** and **1.66** are synthesised was also found to be an active catalyst (the imido species are generated *in situ*). Both compounds were also shown to catalyse intramolecular hydroamination reactions. Several other titanium catalysts have been reported including $Cp_2Ti(\eta^2\text{-}Me_3SiC_2SiMe_3)$,[146] $Ti(NMe_2)_2$(dpma) (dpma = *N,N*-di(pyrrolyl-α-methyl)-*N*-methylamine),[56] and $Ti(NMe_2)_4$.[157] All three of which are proposed to proceed *via* an imido intermediate synthesised *in situ*. Examples of zirconium and hafnium hydroamination catalysts include Bergman's zirconium complex $Cp_2Zr(NHXyl)_2$[153] and Trate's hafnium complex (CCC^{Bu}-NHC)$Hf(NMe_2)I_2$ (CCC^{Bu}-NHC = 2-(1,3-bis(N-butylimidazol-2-ylidene)-phenylene).[158]

1.7.2 Group 4 hydrazido compounds

1.7.2.1 Synthesis of titanium hydrazido complexes

Although the synthesis of the first monomeric titanium terminal hydrazide was reported in the 1970s following reaction of Cp_2TiCl_2 with two equivalents of 1,2-bis(trimethylsilyl)diazene ($Me_3SiN{=}NSiMe_3$) to yield $Cp_2Ti\{NN(SiMe_3)_2\}$,[73] it was not until 1999 that the next terminal titanium hydrazido compound was reported, $Ti(NNPh_2)(Me_4taa)$ (**1.68**).[105] The synthesis and solid-state structure of $Ti(NNMe_2)(^tBu\text{-}bipy)(dpma)$ (^tBu-bipy = 4,4′-di-*tert*-butyl-2,2′-bipyridine) was described by Odom in 2004.[56] The sucessful synthesis of the diphenylhydrazide analogues of the imido synthons **1.45** and **1.50**, $Ti(NNPh_2)Cl_2(py)_3$ (**1.69**) and $Ti(NNPh_2)Cl_2(NHMe_2)$ (**1.70**) following a hydrazine/*tert*-butylimide exchange methodology allowed access to a huge range of hydrazido complexes.[159]

Compound **1.69** was synthesised from **1.45** and Ph_2NNH_2 (Scheme 1.7) and and **1.70** from $Ti(NMe_2)_2Cl_2$ (**1.49**) and Ph_2NNH_2. Various examples of η^1-hydrazido(2-) complexes synthesised *via* salt metathesis with **1.69** are shown in Scheme 1.7. Attempts to synthesise dimethyl analogues of **1.45** and **1.50** using Me_2NNH_2 resulted in the formation of dimers containing bridging hydrazido ligands. These dimers were found to be inert to protonolysis or salt metathesis, indicating that the hydrazido bridges are not easily cleaved.

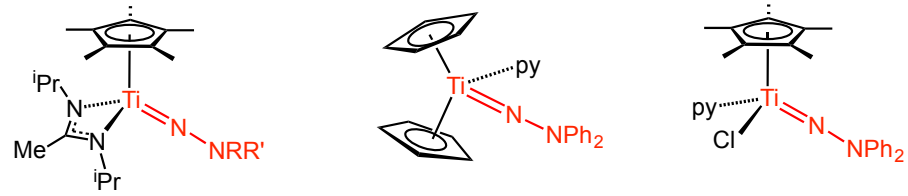


Scheme 1.7. Synthesis of $Ti(NNPh_2)Cl_2(py)_3$ (**1.69**) and examples of titanium hydrazido compounds synthesied from **1.69**.

A ligand set that has been particularly sucessful is the dianionic tridentate nitrogen or oxygen ligands. Compounds **1.71** - **1.75** are examples containing such a supporting ligand set.[160, 161] When the apical donor is an oxygen atom these ligands are capable of binding in a κ^3-*fac* or κ^3-*mer* manner, addition of 2,2'-bipyridine to **1.71** results in a change from κ^3-*mer* to κ^3-*fac* coordination.[162]

However, when the apical donor is nitrogen a κ^3-*fac* coordination mode is observed in all cases. In all the compounds shown in Scheme 1.7 the hydrazido ligand is *cis* to the apical donor atom. However, DFT calculations have shown that the *trans* orientation is electronically more favoured. In most cases steric demands make the *cis* equatorial position more favourable.[161]

The cyclopentadienyl-amidinate ligand set has been the focus of much attention due to the wide range of reactivity observed with the resulting compounds. The complexes $Cp^*Ti\{MeC(N^iPr)_2\}(NNRR')$ (R = R′ = Me (**1.76**) or Ph (**1.77**); R = Me, R′ = Ph (**1.78**), Figure 1.9) were reported by Mountford and co-workers following reaction of the imido compound $Cp^*Ti\{MeC(N^iPr)_2\}(N^tBu)$ with the corresponding hydrazine.[123, 163] Gade also reported the synthesis of the hydrazido analogous of **1.64** and **1.66**, $Cp^*Ti(N^{Xyl}N)(NNRR')(L)$ (R = R′ = Ph (**1.79**) or Me (**1.80**); R = Ph, R′ = Me (**1.81**); L = py or DMAP).[164] Other examples of Cp-supported hydrazido compounds include $Cp_2Ti(NNPh_2)(py)$ (**1.82**) and $Cp^*Ti(NNPh_2)(py)(Cl)$ (**1.83**), both of which are synthesised from the parent imido complex using a hydrazine/*tert*-butylimide exchange reaction.[165]



R = R' = Me (**1.76**) or Ph (**1.77**);
R = Ph, R' = Me (**1.78**)

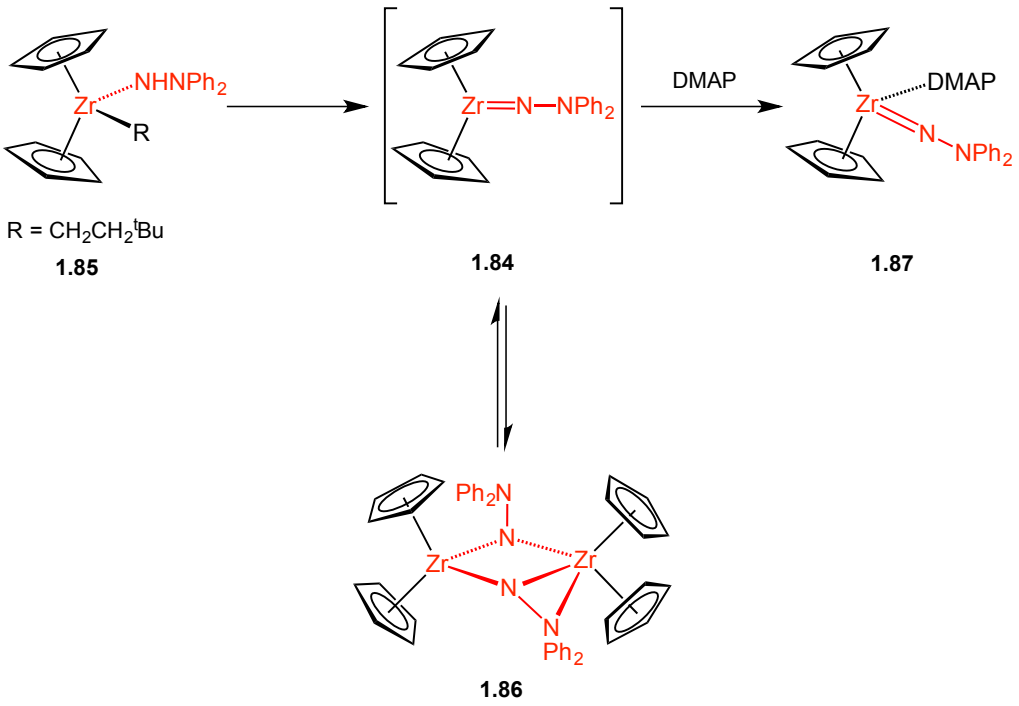
1.82

1.83

Figure 1.9. Examples of titanium hydrazido compounds supported by Cp ligands.

1.7.2.2 Synthesis of zirconium and hafnium hydrazido complexes

The first monomeric terminal hydrazido zirconium compound was synthesised by Bergman in 1991, $Cp_2Zr(NNPh_2)$ (**1.84**) was obtained *via* the thermolysis of $Cp_2Zr(NHNPh_2)(CH_2CH_2{}^tBu)$ (**1.85**).[166] Compound **1.84** dimersises rapidly in solution to yield the bridging μ-η^1:η^2-hydrazido(2-) complex **1.86**. However, in the presence of a stabilising donor ligand such as DMAP (4-dimethylaminopyridine) the monomeric compound $Cp_2Zr(NNPh_2)(DMAP)$ (**1.87**) can be isolated (Scheme 1.8).



Scheme 1.8. Monomeric and dimeric terminal zirconocene hydrazido(2-) complexes.

The diamide-pyridyl supported zirconium hydrazido compound $Zr(N_2^{TBS}N_{py})(NNPh_2)(py)$ (**1.88**, $N_2^{TBS}N_{py}$ = $MeC(2\text{-}C_5H_4N)(CH_2NSiMe_2{}^tBu)_2$) was reported by Gade in 2007 using $Zr(N_2^{TBS}N_{py})Cl_2$ and $LiNHNPh_2$ followed by addition of $LiN(SiMe_3)_2$.[167] The same method was used to synthesise the first hafnium hydrazido compound $Hf(N_2^{TBS}N_{py})(NNPh_2)(py)$ (**1.89**) in 2008.[168] Attempts to synthesise the calixarene-supported zirconium complexes $Zr(NNR_2)(Me_2Calix)$ (R = Me or Ph, Me_2Calix = dianion of 1,3-dimethyl ether of *tert*-butyl calix[4]arene) *via* the same method resulted in the formation of bis(hydrazido(1-)) complexes.[160]

No zirconium hydrazido synthon to which a range of ligands can be added has been reported and often the supporting ligand is introduced to the metal centre prior to the hydrazido ligand. For example $Zr(NMe_2)_4$ has proved to be a useful starting material and addition of the neutral ligand $(HN^{Xyl})_2N_{py}$ ($(HN^{Xyl})_2N_{py}$ = $MeC(2\text{-}C_5H_4N)(CH_2NXyl)_2$) yields the diamide compound $Zr\{(N^{Xyl})_2N_{py}\}(NMe_2)_2$. A second protonolysis reaction can then be carried out with the desired hydrazine $RNNH_2$ (R = C_9H_{10} or $C_{12}H_8$) in the presence of DMAP to yield the hydrazido compounds $Zr\{(N^{Xyl})_2N_{py}\}(NNR)(DMAP)_2$ (R = C_9H_{10} or $C_{12}H_8$).[169] Interestingly, reaction of the protio ligand $H_2N_2{}^{PFP}N_{py}$ ($H_2N_2{}^{PFP}N_{py}$ = $MeC(2\text{-}C_5H_4N)(CH_2N(H)C_6F_5)_2$) bearing electron-withdrawing aryl substituents on the N_{amide} atoms resulted in the formation of

the difluoride compound $Zr(N_2^{TFAP}N_{py})F_2$ (**1.90**, $N_2^{TFAP}N_{py}$ = MeC(2-C_5H_4N){CH_2N(2-$C_6F_4NMe_2$)}$_2$) following reaction with $Zr(NMe_2)_4$ at 90 ^oC. Compound **1.90** results from the exchange of one of the *ortho*-fluorine substituents on both aryl rings by a dimethylamido group orginating from $Zr(NMe_2)_4$. It was still possible to obtain a hydrazido compound from **1.90** *via* reaction with $LiNHNPh_2$ and $LiN(SiMe_3)_2$ and the compound was isolated and cystallographically characterised.[170]

1.7.2.3 Structural features

There have been several studies detailing the structure of titanium hydrazido compounds with particular attention being paid to the effect of the N_β substituents and comparison to related imido systems. Mountford and co-workers described a DFT computational study on the bonding in the hydrazido compound Ti{$HC(pz)_3$}$(NNPh_2)Cl_2$ ($HC(pz)_3$ = tris(pyrazolyl)methane) as a model for Ti{$HC(Me_2pz)_3$}$(NNPh_2)Cl_2$ ($HC(Me_2pz)_3$ = tris(3,5-dimethylpyrazolyl)methane) and Ti{$HC(pz)_3$}$(NMe)Cl_2$ as a model for the imido compound Ti{$HC(pz)_3$}$(N^tBu)Cl_2$.[159] They found that while both imido and hydrazido ligands bind to the metal centre through one σ and two π interactions resulting in a formally triple bond, one of the π interactions in the hydrazido compound is destabilised compared to the other π bond. This manifests itself in a lengthening of the Ti=N bond and differs from the imido compund where the two π interactions are degenerate. However, this study and others clearly demonstrate the isolobal relationship between imido and hydrazido ligands.

For the series of compounds Cp*Ti{$MeC(N^iPr)_2$}(NNRR′) (R = R′ = Me (**1.76**) or Ph (**1.77**); R = Me, R′ = Ph (**1.78**)), each of which were structurally characterised, the short $Ti=N_\alpha$, long N_α–N_β bond distances (1.723(2) – 1.734(2) Å and 1.369(2) – 1.386(2) Å) and linear Ti–N_α–N_β bond angles (159.5(1) – 166.3(2) ^{o}) are consistent with formal Ti≡N triple bonds and N–N single bonds.[123] Thus, the NNR_2 functional group is a η^1-hydrazido(2-) ligand in all cases. When the N_β substituents are aryl groups the nitrogen atom appears planar, consistent with sp^2 hybridisation, this is a result of lone pair delocalisation into at least one of the aryl rings. In comparison, the dimethyl hydrazido compound **1.76** contains a pyramidal N_β atom, as expected. The $Ti=N_\alpha$distances for **1.77** and **1.78** are equivalent within error to the value of 1.738(2) Å found for Ti=N bond in the arylimido compound Cp*Ti{$MeC(N^iPr)_2$}(NXyl)

(**1.91**).[122] Within the series **1.76 - 1.78** the Ti=NR bond distances vary in the order $Ti{=}NNPh_2 \approx Ti{=}NNMePh > Ti{=}NNMe_2$. The homologous series $Ti(Me_2Calix)(NNRR')$ (R = R′ = Me (**1.92**) or Ph (**1.93**); R = Me, R′ = Ph (**1.94**)) has also been structurally charcterised. The $Ti{=}N_\alpha$ distances were found to be the same within error although, all were longer than the Ti=N bond in the corresponding alkylimido compound $Ti(Me_2Calix)(N^tBu)$ (**1.95**).[160] Gade and co-workers also reported a series of compounds with the same set of hydrazido ligands however the additional donor ligand varied between each compound making precise comparisons difficult.[164]

DFT calculations on simplified models of the compounds **1.76 - 1.78** were carried out and the same trend in bond lengths was observed.[123] The reason for the longer Ti=N bond distances for $NNPh_2$ and NNPhMe is better conjugation of the N_β lone pair with the $Ti{=}N_\alpha$ π* antibonding orbital as a result of the planarity at N_β. In line with this, forcing planarity at the N_β atom of the dimethyl hydrazide model results in a lengthening of the $Ti{=}N_\alpha$ bond and shortening of the $N_\alpha{-}N_\beta$ bond. DFT calculations were also carried out on alkyl and arylimido compounds for comparison. The model aryl substituent was -Ph, the Ti=N bond distance was found to be shorter than was observed experimentally for the xylyl imido compound **1.91**. This is presumably caused by the larger steric bulk of the imido substituent in the real compound. The Ti=N bond distance was found to be longer for the aryl substituent compared to the alkyl substituent as a result of the π accepting nature of the phenyl ring, thus allowing donation from the Ti=N π orbital to the π* orbital on Ph. Overall these experimental and DFT results indicate that alkyl imides have the shortest Ti=N bond distances while aryl imides and alkyl or aryl hydrazide Ti=N bond distances are more similar. When comparing the hydrazide systems, the geometry at N_β has the biggest effect on the Ti=N bond distance with a planar geometry resulting in a longer bond. All of the model systems described here show that the Ti=N bond is a formally triple bond containing two principal dπ-pπ molecular orbitals which form or contribute towards the three highest MOs of the complexes.[123]

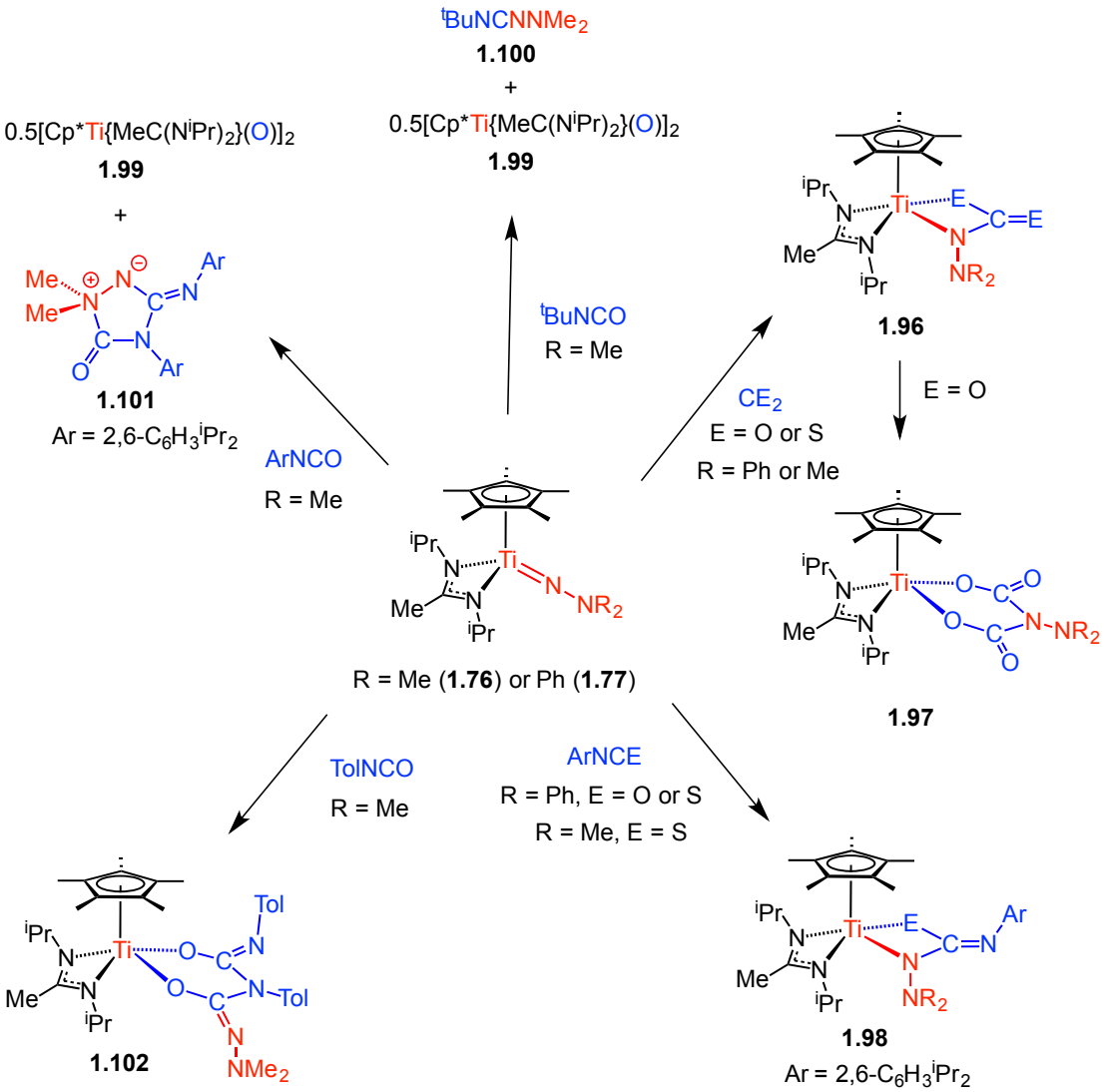
1.7.2.4 Stoichiometric reactions involving the M=N_α bond

Group 4 hydrazido compounds exhibit a wealth of reactivity with small molecules and reaction at the M=N_α multiple bond *via* a [2+2] cycloaddition reaction is now a well established reaction pathway. In many cases the cycloaddition reaction products can be isolated and characterised and then, undergo futher reaction. These secondary reactions, not including N_α–N_β cleavage, include inclusion of a second substrate into the now single M–N_α bond or extrusion of an organic fragment.

The first examples of isolable compounds resulting from [2+2] cycloaddition reactions of a titanium hydrazido compound were the reactions of the macrocycle supported compound Ti(NNPh$_2$)(Me$_4$taa) (**1.68**) with CO_2 or TolNCO. However, neither metallacyclic product was structurally authenticated.[105] The sandwich compound Cp$_2$Ti(NNPh$_2$)(py) (**1.82**, Figure 1.9), with ^{t}BuCP underwent a [2+2] cycloaddition reaction and was one of the first examples of a structurally authenticated cycloaddition product for any metal hydrazide, as well as the first reported reactivity of a hydrazido compound with a phosphaalkyne.[171] Since these early examples the stoichiometric reaction chemistry of Group 4 hydrazides has progressed rapidly and selected examples will be discussed below.

As was found with their imido analogues, the stoichiometric reactions of the cyclopentadienyl-amidinate supported hydrazido compounds Cp*Ti{MeC(N^{i}Pr)$_2$}(NNR$_2$) (R = Me (**1.76**) or Ph (**1.77**)) have been particularly fruitful. Selected reactions and reaction products are shown in Schemes 1.9 and Figure 1.10. With CE_2 (E = S or O) [2+2] cycloaddition reactions occurred, initially yielding compounds of the type **1.96**. When E = O a second insertion occurred into the now single Ti–N_α bond resulting in "double insertion" complexes of the type **1.97**, Scheme 1.9.[123] Reaction of **1.76** and **1.77** with isocyanates gave different reaction products. Reaction of the diphenylhydrazido compound **1.77** yielded isolable cycloaddition products with both alkyl and aryl isocyanates (**1.98**, Scheme 1.9), whereas the dimethylhydrazido compound **1.76** reacted with ArNCO and ^{t}BuNCO to give the oxo dimer [Cp*Ti{MeC(N^{i}Pr)$_2$}(μ-O)]$_2$ (**1.99**) and the organic fragments, ^{t}BuNCNNMe$_2$ (**1.100**), and N(Me)$_2$NC(NAr)N(Ar)C(O) (**1.101**), respectively following extrusion from the inherently unstable cycloaddition intermediates, Scheme 1.9.[123] Interestingly, reaction of **1.76** with two equivalents of TolNCO gave Cp*Ti{MeC(N^{i}Pr)$_2$}{OC(NNMe$_2$)N(Tol)C(NTol)O} (**1.102**) following the same

cycloaddition-extrusion pathway as with RNCO (R = Ar or ^{t}Bu). However, in this case rapid cycloaddition of the extruded organic fragment to (L)Ti=O (instead of dimerisation) formed Cp*Ti{MeC(N^{i}Pr)$_2$}{N(Tol)C(NNMe$_2$)O} (not observed) which then reacts with a second equivalent of TolNCO to give **1.102**.



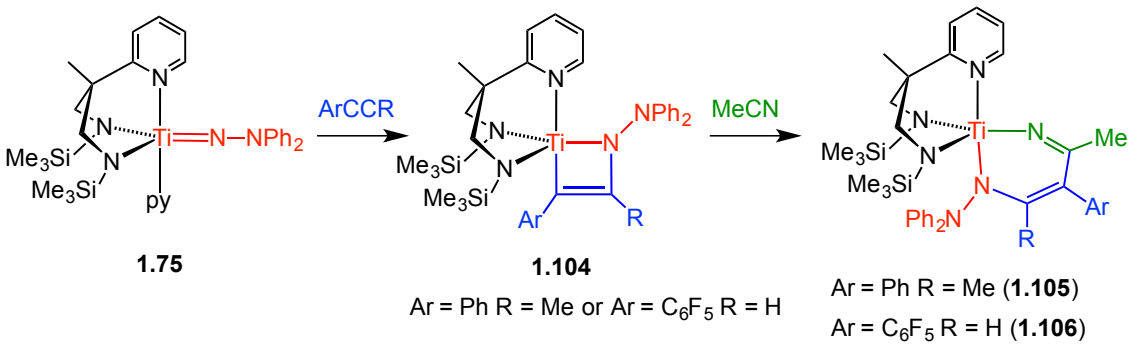
Scheme 1.9. Reaction of Cp*Ti{MeC(N^{i}Pr)$_2$}(NNR$_2$) (R = Me (**1.76**) or Ph (**1.77**)) with unsaturated substrates.

Similar reactivity was observed with the compounds Cp*Ti(N^{Xyl}N)(NNRR′) (R = R′ = Ph (**1.79**) or Me (**1.80**); R = Ph, R′ = Me (**1.81**); L = py or DMAP) and cycloaddition reaction products were obtained with PhNCS and PhNCO. However, in comparison to the reactions of **1.76** and **1.77** where cycloadditions with isocyanates and isothiocyanates were solely formed as the κ^{2}N,E-bound products (E = O or S), here both κ^{2}N,E- and κ^{2}N,N′-bound isomers were observed.[172] Complementary DFT

calculations were later carried out and indicate that although the κ^2N,N′ coordination mode is electronically favoured, in some cases κ^2N,E coordination is preferable for steric reasons.[122, 123, 173] Corresponding reactivity has been observed for the diamide-amine supported compound Ti(N_2N^{Me})($NNPh_2$)(py) (**1.72**) with the bulky 2,6-diisopropylphenyl cyanates ArNCO, ArNCS and ArNCSe. All of which gave κ^2N,E-bound (E = O, S or Se) cycloaddition reaction products, in the case of ArNCO the pyridine ligand is still bound in the reaction product whereas with ArNCS and ArNCSe it is not.[173]

Reactions of zirconium hydrazides with isocyanates and isothiocyanates are also known. Gade reported that the reaction of Zr($N_2^{TBS}N_{py}$)($NNPh_2$)(py) (**1.88**) with MesNCS and PhNCS gave isolable cycloddition reaction products with the new ligand bound in a κ^2N,S-fashion.[174] Cycloaddition reactions of the zirconium compound **1.88** and the analogous hafnium compound **1.89** with alkyl and aryl allenes were also described, proceeding with Markovnikov regioselectivity in both cases, as well as [2+3] cycloaddition reactions with azides.

Compounds **1.76** and **1.77** showed no reaction with alkynes. In comparison, Gade's more open cyclopentadienyl-amidinate supported compound Cp*Ti($N^{Xyl}N$)($NNMe_2$)(DMAP) (**1.80**) reacts with one equivalent of PhCCH to yield Cp*Ti($N^{Xyl}N$){N(NMe_2)C(Ph)(H)} (**1.103**), in which the C(H) carbon is bound to titanium. Calculations show that the other regioisomer with the CAr bound to titanium is electronically favoured. However, the steric bulk of the supporting Cp*-amidinate ligand prevents the alkyne from approaching with this orientation, and in the case of **1.76** and **1.77** from reacting at all. In comparison the diamide-amine supported compound Ti(N_2N^{py})($NNPh_2$)(py) (**1.75**) reacts with both terminal and internal alkynes to give azametallacyclic compounds of the type Ti(N_2N^{py}){N(NPh_2)C(R)C(Ar)}(py) (**1.104**, Ar = phenyl or substituted phenyl; R = H or Me, Scheme 1.10) where the CAr atoms are bound to titanium.



Scheme 1.10. Reaction of $Ti(N_2N^{py})(NNPh_2)(py)$ (**1.75**) with alkynes and nitriles.

Tandem reactions with alkynes and nitriles have also been reported and it was shown that the reaction of **1.75** with a 1:1 mixture of MeCN and PhCCMe or $HCCC_6F_5$ gave the cross-coupled products $Ti(N_2N^{py})\{NC(Me)C(Ph)C(Me)NNPh_2\}$ (**1.105**) and $Ti(N_2N^{py})\{NC(Me)C(C_6F_5)C(H)NNPh_2\}$ (**1.106**) respectively, Scheme 1.10.[173] It is thought that these compounds result from the insertion of MeCN into the Ti–C(Ar) bond of the azatitanacyclobutene compounds of the type **1.104** formed from the reaction of **1.75** with either alkyne. This was the first example of insertion of MeCN into a metallacyclic moiety derived from a hydrazido ligand. A related system has however been described by Odom and Banerjee, they found that an *in situ* generated dimethylhydrazido compound undergoes sequential cycloaddition of ^{n}BuCCH followed by insertion of ^{t}BuNC to form a monoanionic β-diketiminate ligand.[175]

Reactions of Group 4 hydrazides with nitriles are less well established and only more recently have examples been reported. In all cases reaction results in net insertion of the nitrile into the the $Ti{=}N_\alpha$ bond. Examples include the diamide-amine and diamide-ether supported compounds $Ti(N_2N^{py})(NNPh_2)(py)$ (**1.75**), $Ti(N_2N^{Me})(NNPh_2)(py)$ (**1.72**) and $Ti(N_2O)(NNPh_2)(py)_2$ (**1.107**, N_2O = $(O(CH_2CH_2NSiMe_3)_2)$ which react with nitriles bearing electron-withdrawing aryl substituents to yield the compounds $(L)Ti\{NC(Ar^{Fx})NNPh_2\}(py)_n$ (L = N_2N^{py} (**1.108**), N_2N^{Me} (**1.109**) and N_2O (**1.110**); n = 1 or 2, Ar^{Fx} = C_6F_5 or 2,6-$C_6H_3F_2$, Figure 1.10). The electron-withdrawing nature of the nitrile is important in synthesising stable reaction products as reaction of both $Ti(N_2O)(NNPh_2)(py)_2$ (**1.107**) and $Ti(N_2^{Ar}O)(NNPh_2)(py)_2$ (**1.71**, $N_2^{Ar}O$ = $(O(2\text{-}C_6H_4NSiMe_3)_2)$ with PhCN resulted in a mixture of compounds, and reaction of $Ti(N_2N^{py})(NNPh_2)(py)$ (**1.75**) with MeCN resulted in the dimeric compound **1.111** (Figure 1.10). Cycloaddition intermediates are proposed in all cases.

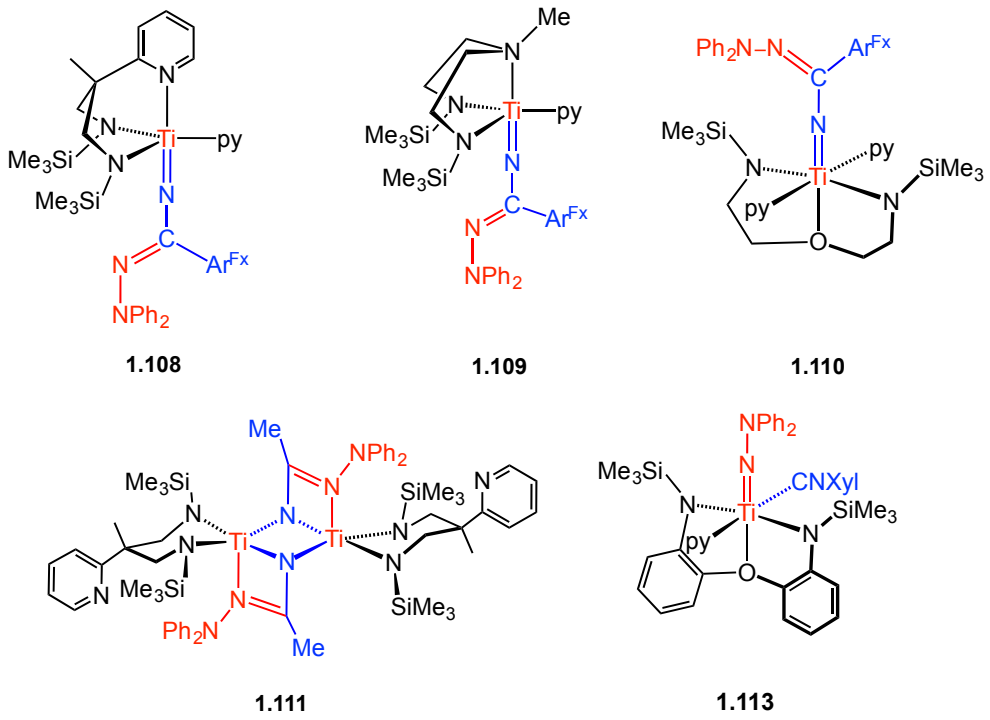


Figure 1.10. Reaction products of titanium hydrazides with nitriles and isonitriles.

Reactions with isonitriles often result in N_α–N_β bond cleavage, *vide infra*, however compounds **1.77** and **1.71** react with with ^{t}BuNC and XylNC, respectively to yield the adducts $Cp^*Ti\{MeC(N^iPr)_2\}(NNMe_2)(CN^tBu)$[176] (**1.112**) and $Ti(N_2^{Ar}O)(NNPh_2)(py)(CNXyl)$ (**1.113**) (Figure 1.10).[162]

As well as the reactivity discussed above, the dimethyl hydrazido compound $Cp^*Ti\{MeC(N^iPr)_2\}(NNMe_2)$ (**1.76**) reacts with a range of silanes. This results in unusual titanium hydride compounds of the type $Cp^*Ti\{MeC(N^iPr)_2\}(H)\{N(NMe_2)SiH_2Ar\}$ (**1.114**, Figure 1.11) from the 1,2-addition of an Si–H bond across the Ti=N_α bond.[140] The analogous reaction products are observed on reaction with the halosilanes $PhSiH_2Cl$ and $PhSiH_2Br$, however Si–Cl/Br 1,2-addition occurs instead, resulting in a titanium halogen bond. Although the diphenylhydrazido compound does not undergo reaction with primary silanes it does react with two equivalents of the chlorosilanes $PhSiH_2Cl$ or PhMeSiHCl forming the dichloride-hydrazido(1-) complexes $Cp^*Ti\{N(NPh_2)SiHRPh\}Cl_2$ (R = H (**1.115**) or Me (**1.116**)) and the silylated amidines **1.117** and **1.118**, Figure 1.11. The κ^2-coordination of the substituted hydrazide ligand is not unexpected and is usually found in titanium hydrazido(1-) compounds.

Coordination of N_β was also observed on reaction with $[Et_3NH][BPh_4]$ in which protonation of the N_α atom occured yielding the compound $[Cp^*Ti\{MeC(N^iPr)_2\}\{\eta^2\text{-}N(H)NMe_2\}][BPh_4]$ (**1.119**, Figure 1.11). Interestingly reaction with alkylating agents MeI, EtBr and CH_2PhBr resulted in alkylation at N_β yielding $[Cp^*Ti\{MeC(N^iPr)_2\}(NNRMe_2)][X]$ (R = Me, X = I (**1.120**); R = CH_2PhBr (**1.121**) or Et (**1.122**), X = Br, Figure 1.11).

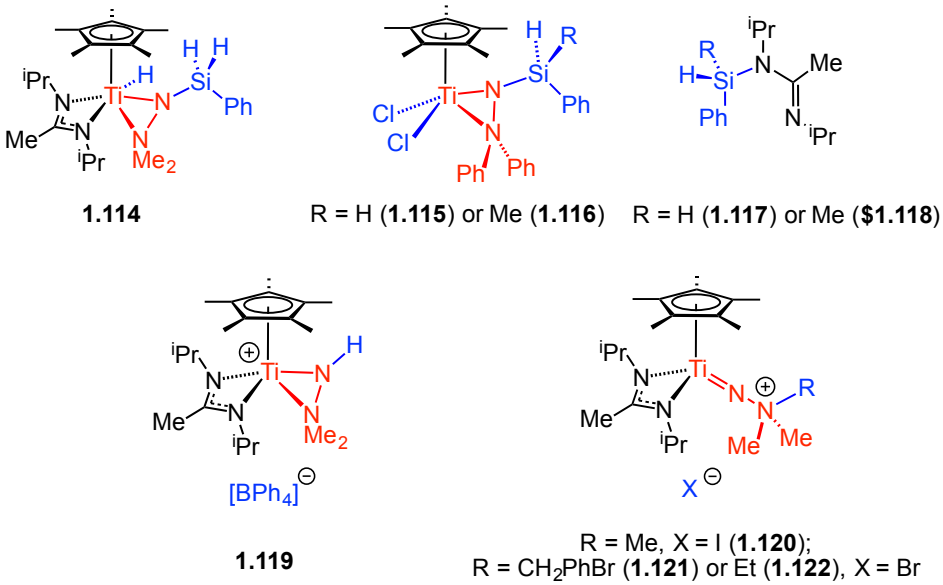
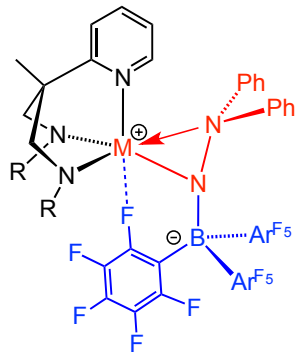


Figure 1.11. Reaction products resulting from the reaction of $Cp^*Ti\{MeC(N^iPr)_2\}(NNMe_2)$ (**1.76**) and $Cp^*Ti\{MeC(N^iPr)_2\}(NNPh_2)$ (**1.77**) with silanes.

Finally, it is known that $B(Ar^{F5})_3$ can be used to remove coordinated pyridine from both hydrazido and imido compounds to generate base-free species.[164] In some cases it has been found that reaction with a second equivalent of $B(Ar^{F5})_3$ can occur yielding η^2-hydrazido(1-) compounds of the type **1.123,** Figure 1.12. These compounds contain a stabilising M···F interaction from one of the aryl groups on $B(Ar^{F5})_3$.[168, 173]



1.123

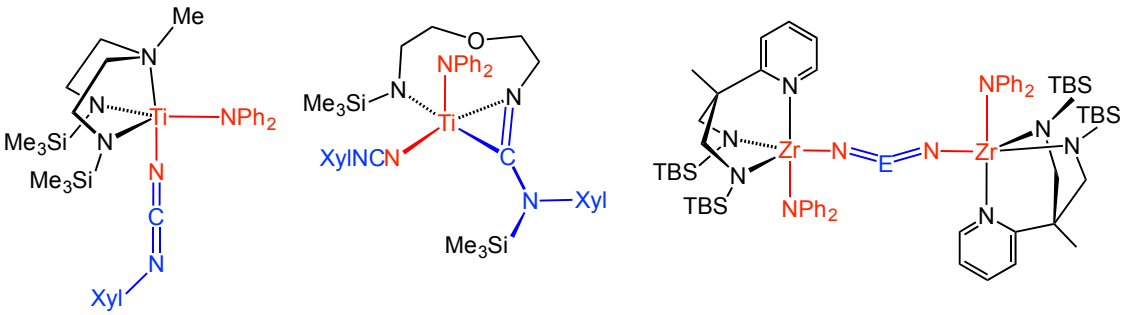
M = Ti or Zr ; R = $SiMe_3$ or $SiMe_2{}^tBu$

Figure 1.12. η^2-hydrazido(1-) compounds

1.7.2.5 Stoichiometric reactions involving N_α–N_β bond cleavage

The presence of the $N_\beta R_2$ substituent on $M{=}N_\alpha N_\beta R_2$ containing compounds allows for N_α–N_β bond cleavage reactions to occur. The potential cleavage of this relatively weak bond is what differentiates these compounds from their imido counterparts. Such reductive cleavage of the N_α–N_β bond has been found to occur with oxidisable substrates such as isonitriles.

For example, the diamide-amine compounds $Ti(N_2N^{py})(NNPh_2)(py)$ (**1.75**) and $Ti(N_2N^{Me})(NNPh_2)(py)$ (**1.72**) both react with one equivalent of XylNC to give the N_α–N_β bond cleavage products $Ti(N_2N^{py})(NPh_2)(NCNXyl)$ (**1.124**) and $Ti(N_2N^{Me})(NPh_2)(NCNXyl)$ (**1.125**, Figure 1.13) respectively.[173] DFT calculations indicate that loss of pyridine, followed by coordination of the isonitrile to yield an adduct occur prior to the formation of a three-membered intermediate which is supported by coordination of N_β. From here, N_α–N_β bond cleavage is facile and results in formation of the final products.[173] This isonitrile insertion reaction had previously been reported for the zirconium compound $Zr(N_2{}^{TBS}N_{py})(NNPh_2)(py)$ (**1.88**) and ^{t}BuNC[167] and was later reported for the reaction of $Ti(N_2O)(NNPh_2)(py)_2$ (**1.107**) with ^{t}BuNC.[162]

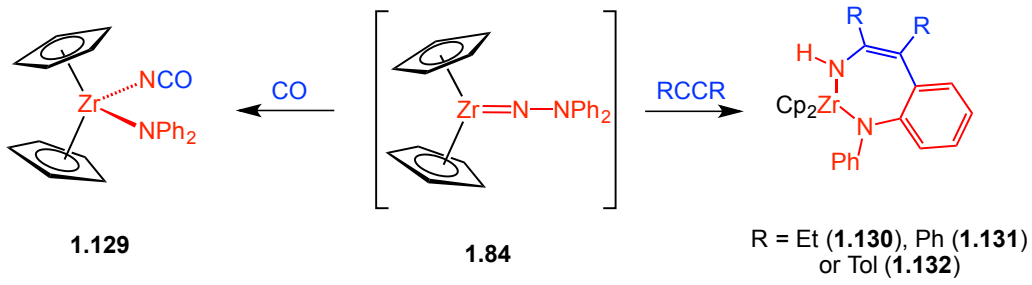


1.125 **1.126** E = S (**1.127**) or Se (**1.128**)

Figure 1.13. N_α–N_β cleavage reaction products of group 4 hydrazido compounds.

$Ti(N_2O)(NNPh_2)(py)_2$ (**1.107**) also reacts with XylNC, however two equivalents are required. The first equivalent results in N_α–N_β bond cleavage as above and the second equivalent reacts with one of the N–$SiMe_3$ ligand bonds yielding **1.126**, Figure 1.13. N_α–N_β bond cleavage reactions are also observed in the reaction of $Zr(N_2{}^{TBS}N_{py})(NNPh_2)(py)$ (**1.88**) with Ph_3PSe or propylene sulphide forming the dimeric compounds $Zr(N_2{}^{TBS}N_{py})(NPh_2)\}_2(\mu\text{-}N_2E)$ (E = S (**1.127**) or Se (**1.128**), Figure 1.13)[167] and more recently the reaction with excess iodine was reported to yield tetraphenyl hydrazine and N_2.[177] Addition of 0.5 equivalents of iodine resulted in the formation of the amide compound $Zr(N_2{}^{TBS}N_{py})(NPh_2)(I)$ and the release of N_2, a radical mechanism is proposed.

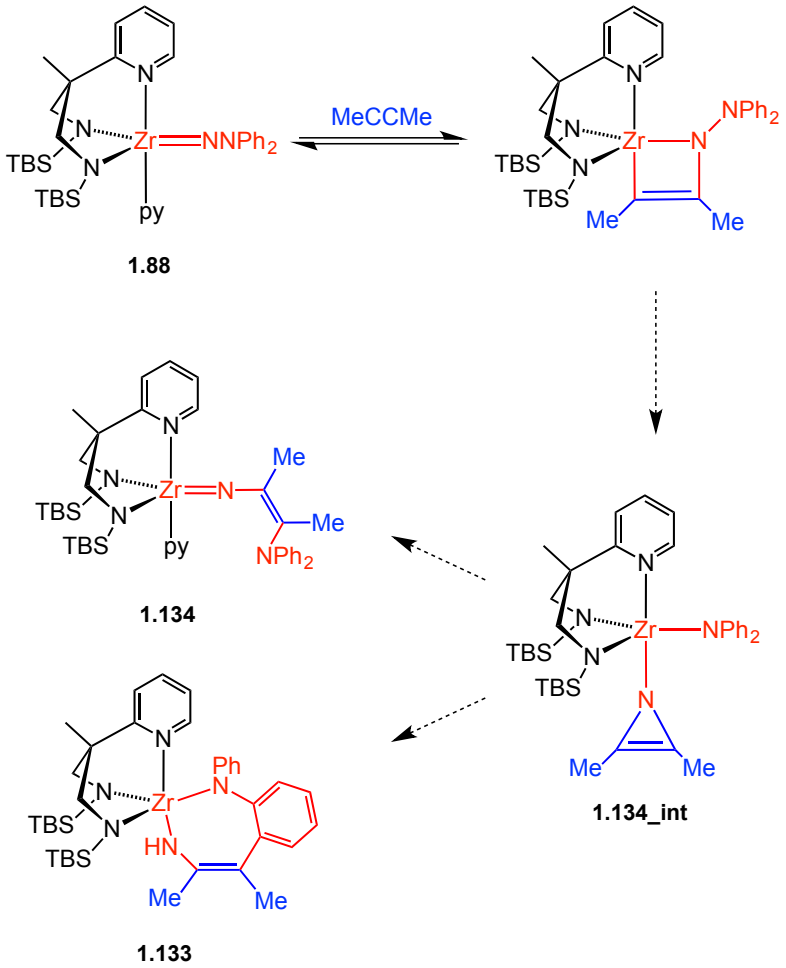
The isonitrile-induced reductive cleavage of the N_α–N_β bond discussed above is reminiscent of an early example of Group 4 hydrazide reactivity reported by Bergman. The compound $Cp_2Zr(NNPh_2)$ (**1.84**) reacts with CO resulting in N_α–N_β bond cleavage and the formation of the mixed amide/metallated isocyanate $Cp_2Zr(NCO)(NPh_2)$ (**1.129**, Scheme 1.11).[166] This compound was also found to react with the symmetrical alkynes RCCR (R = Et, Ph or Tol) yielding the compounds $Cp_2Zr\{N(H)C(R)C(R)$-1,2-$C_6H_4N(Ph)\}$ (R = Et (**1.130**), Ph (**1.131**) and Tol (**1.132**)) containing seven-membered rings resulting from N_α–N_β bond cleavage reactions followed by C–H activation.[166]



1.129 **1.84** R = Et (**1.130**), Ph (**1.131**) or Tol (**1.132**)

Scheme 1.11. Reaction of $Cp_2Zr(NNPh_2)$ (**1.84**) with alkynes and CO.

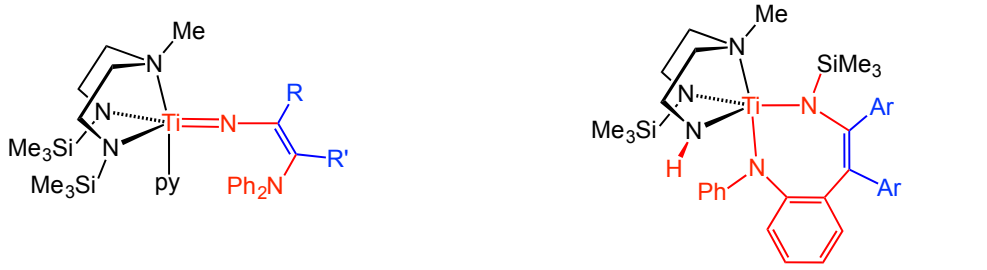
Gade has reported similar reactivity with alkynes; the compound $Zr(N_2^{TBS}N_{py})(NNPh_2)(py)$ (**1.88**) was found to react with a range of internal alkynes yielding the seven-membered cyclic compounds $Zr(N_2^{TBS}N_{py})\{N(Ph)C_6H_4C(R)C(R)N(H)\}$ (**1.133**, R = alkyl or aryl).[178] However, when MeCCMe was used two reaction products were observed in equal amounts, the vinylimido compound $Zr(N_2^{TBS}N_{py})\{NC(Me)C(Me)NPh_2\}(py)$ (**1.134**) was observed as well as the seven-membered cyclic species (Scheme 1.12). DFT calculations were carried out, investigating the formation of these compounds and the N-metallated azirine **1.134_int** was identified as the key intermediate for the formation of both **1.133** and **1.134**. The intermediate **1.134_int** results from a [2+2] cycloaddition reaction followed by an N–N bond cleavage reaction. [178]



Scheme 1.12. Proposed mechanism for the reaction of $Zr(N_2^{TBS}N_{py})(NNPh_2)(py)$ (**1.88**) with MeCCMe.

The cycloaddition reactions of the diamide-amine supported compound $Ti(N_2N^{py})(NNPh_2)(py)$ (**1.75**) with internal and terminal alkynes have been discussed above. When the azametallacylic reaction product $Ti(N_2N^{py})\{N(NPh_2)C(Me)C(Ph)\}$ (**1.104a**) was left to stand in solution for 3 days at room temperature further reaction occurred to yield the vinylimido compound $Ti(N_2N^{py})\{NC(Ph)C(Me)NPh_2\}(py)$ (**1.135**).[171] Similarly reaction of $Ti(N_2N^{Me})(NNPh_2)(py)$ (**1.72**) with a range of internal alkynes resulted in the formation of analogous vinyl imido compounds $Ti(N_2N^{Me})\{NC(R)C(Me)NPh_2\}(py)$ (R = alkyl or aryl (**1.136**, Figure 1.14).[179]

However, when the diaryl alkynes ArCCAr (Ar = Ph or 4-C_6H_4OMe) were used the compounds $Ti\{MeN(CH_2CH_2NSiMe_3)(CH_2CH_2NH)\}\{N(SiMe_3)C(Ar)C(Ar)$-1,2-$C_6H_4N(Ph)\}$ (Ar = Ph (**1.137**) and 4-C_6H_4OMe (**1.138**)) were observed as well as the expected vinyl imido compounds $Ti(N_2N^{Me})\{NC(Ar)C(Ar)NPh_2\}(py)$ (Ar = Ph (**1.139**) or 4-C_6H_4OMe (**1.140**)). These compounds are reminiscent of the compounds **1.130**, **1.131**, **1.132** and **1.133** described above and are thought to form *via* the same mechanism followed by a 1,3-$SiMe_3$ sigmatropic shift, Figure 1.14 .[180]



R = alkyl or aryl R' = Me (**1.136**)

R = R' = Ph (**1.139**) or 4-C_6H_4OMe (**1.140**)

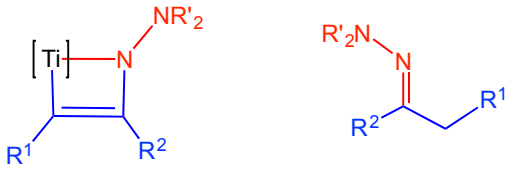
Ar = Ph (**1.37**) or 4-C_6H_4OMe (**1.38**)

Figure 1.14. Reaction products of $Ti(N_2N)(NNPh_2)(py)$ (**1.72**) with alkynes.

1.7.2.6 Catalytic reactions

As many Group 4 imido compounds have been reported to be effective catalysts for the hydroamination of alkynes, naturally a substantial body of work has evolved studying the possible catalytic reactions of terminal Group 4 hydrazido compounds. The corresponding catalytic reaction, namely hydrohydrazination (N–H addition across the alkyne C≡C bond), to form hydrazones has receieved much attention and several examples exist.[56, 141, 146, 152, 164, 181-183] As with hydroamination, hydrohydrazination is postulated to proceed *via* metallacycles of the type **1.141**, these metallacycles can then undergo protonolysis of the Ti–C and Ti–N bonds to form

hydrazones (**1.142**) *via* transient mixed bis(hydrazido(1-)) intermediates (analogous to the mechanism for hydroamination shown in Scheme 1.6).



1.141 **1.142**

Figure 1.15. Metallacyclic intermediates **1.141** and hydrazones **1.142**.

Such catalytic reactions have been typically found to require high temperatures (> 75 ^{o}C) and long reaction times (2 - 75 h) with harsher conditions being employed for internal alkynes. In many cases the active hydrazido catalyst is synthesised *in situ* from the corresponding diamide pre-catalyst (L)Ti(NMe_2)$_2$ on reaction with hydrazine. In 2011 Gade reported that the cyclopentadienyl-amidinate compounds Cp*Ti($N^{Xyl}N$)(NNRR′)(L) (R = R′ = Ph (**1.79**) or Me (**1.80**); R = Ph, R′ = Me (**1.81**); L = py, DMAP or ^{t}BuNH$_2$) were capable of catalysing the hydrohydrazination of a range of alkynes with quantitative conversion (5 mol% catalyst loading) at ambient temperature within 1 h.[164] In some cases further reaction of the hydrazones can occur to catalytically produce other small nitrogen containing molecules. For example indoles[56, 141, 146, 181, 184], pyrroles[141] and tryptamines[185] have been described, these cyclisation reactions often require the addition of an external Lewis base such as $ZnCl_2$.

Furthermore, an iminohydrazination reaction has been developed using the pre-catalysts **1.143** and **1.144** (Figure 1.16), where an alkyne, hydrazine and isocyanide are coupled in a single reaction *via* a titanium hydrazido compound forming a 1,3-iminohydrazone.[175, 183] This has been developed further and the precatalyst $Ti(NMe_2)_2(pypyr)_2$ (**1.145**, Hpypyr = 2-(2′-pyridyl)-3,5-dimethylpyrrole, Figure 1.16) can be used in the multicomponent coupling of alkynes, isonitriles and monosubstituted hydrazines to yield pyrazoles in a single step without the need for an external Lewis acid.[186]

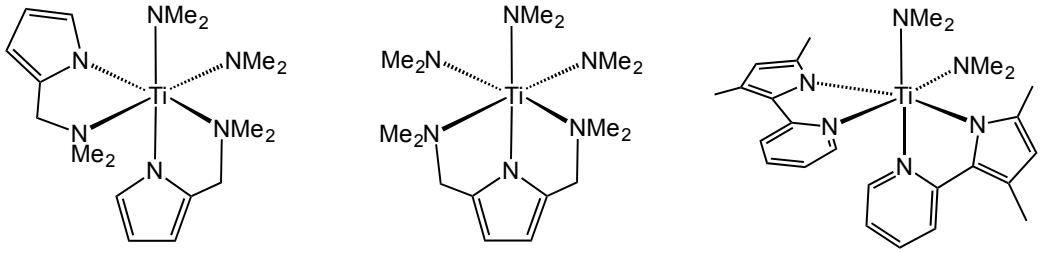
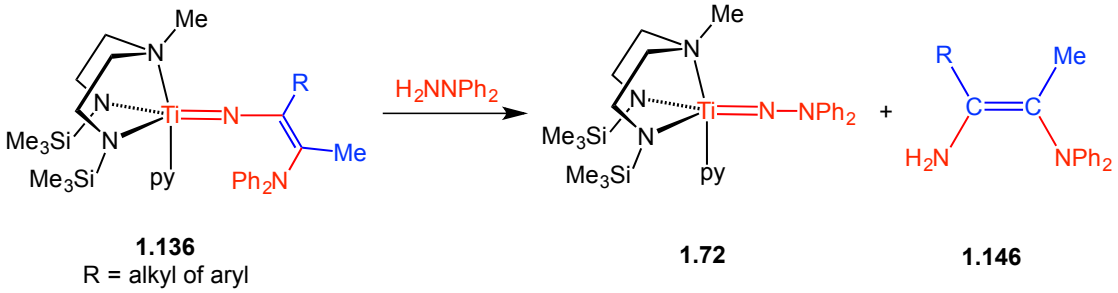


Figure 1.16. Titanium pre-catalysts.

As discussed above the diamide-amine supported titanium hydrazido compound $Ti(N_2N^{Me})(NNPh_2)(py)$ (**1.72**) undergoes N_α–N_β insertion with a range of alkynes to yield vinyl imido compounds of the type **1.136**.[179] Addition of one equivalent of Ph_2NNH_2 to such vinyl imido compounds regenerates the starting hydrazide along with the organic side product $RC(NH_2)C(Me)NPh_2$ (**1.146**, Equation 1.2). This was the first example of this type of transformation of alkynes and hydrazines and the reaction can be carried out catalytically from either **1.72** or **1.136** with the overall result being the 1,2-diamination of alkynes, a previously unknown reaction.



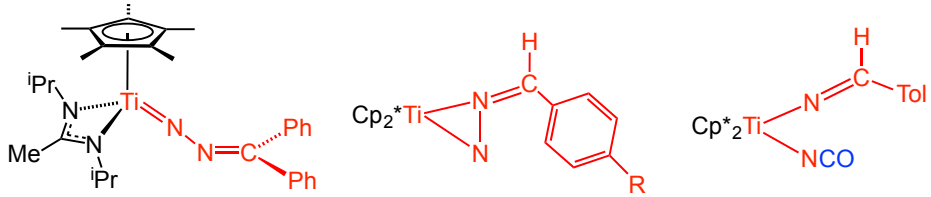
Equation 1.2

Much work has been put into elucidating the full mechanism, which will be discussed further in the introduction to Chapter Three of this Thesis, and extending the scope of

alkynes and hydrazines that can be used.[179, 180, 187] Very recent work has found that replacing the -$SiMe_3$ substituents on the N_{amide} atoms of **1.72** with the less sterically demanding -^{i}Pr substituents resulted in a dramatic switch in the type of catalysis of alkynes and hydrazines, back to the usually found hydrohydrazination.[188] The details of this reaction are introduced later and examined in this Thesis.

1.8 Group 4 alkylidene hydrazido complexes

Alongside the growing area of the synthesis and reactivity of Group 4 imido and hydrazido compounds has been the development of other derivatives. Alkylidene hydrazido compounds, otherwise known as diazoalkane or hydrazonido complexes contain an additional CR_2 subsutituent on N_β and have received some attention. Typically the synthesis of these compounds has required the use of potentially explosive reagents.[189] However, recent work in our group utilised a hydrazone/*tert*-butylimide exchange methodology (much like in the synthesis of many titanium hydrazido compounds) to synthesise the cyclopentadienyl-amidinate supported compound Cp*{$MeC(N^iPr)_2$}($NNCPh_2$) (**1.147**, Figure 1.17).[190]



1.147 **1.148** **1.150**

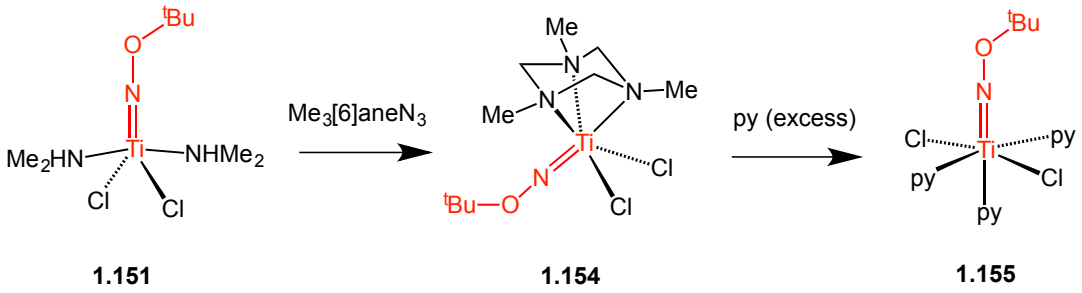
Figure 1.17. Titanium alkylidene hydrazido compounds and reaction product of Cp*$_2$Ti{η^2-NNC(H)Ar} (**1.148**) with CO.

As with Group 4 hydrazido compounds a range of bonding modes are available as well as two possible resonance forms. Although many examples exist with an alkylidene hydrazido ligand bound in a side-on manner, including Bergman's Cp*$_2$Ti{η^2-NNC(H)$SiMe_3$} and Cp*$_2$Ti{η^2-NNC(H)Ar} (**1.148**, Figure 1.17),[191, 192] compounds containing a η^1-alkylidene hydrazido are limited to **1.147** and $Cp_2Ti(NNCPh_2)(PMe_3)$ (**1.149**).[193] Reactivity studies to date are limited, compound **1.148** was found to react with CO resulting in N_α–N_β bond cleavage forming Cp*$_2$Ti{NC(H)Tol}(NCO) (**1.150**, Figure 1.17)[191, 192] reminiscent of the reaction of the zirconium hydrazide $Cp_2Zr(NNPh_2)$ (**1.84**) with CO.[166] A comprehensive study of the reactivity of Cp*{$MeC(N^iPr)_2$}($NNCPh_2$) (**1.147**) with small molecules has been

carried out and in general the reactivity patterns observed mirrored that of the imido and hydrazido analogues.[190]

1.9 Group 4 alkoxyimido complexes

The wide range of Group 4 imido and hydrazido compounds and their vast reactivity observed with small molecules, in particular the catalytic C–N bond forming reactions, has recently prompted work in our group investigating compounds containing other heteroatoms bound to N_α. The majority of this work has centered around the use of oxygen as the heteroatom to yield alkoxyimido compounds, Ti=NOR. The first Group 4 alkoxyimido compounds were synthesised in 2011 by Schwarz, $Ti(NO^tBu)Cl_2(NHMe_2)_2$ (**1.151**) was synthesised from $Ti(NMe_2)_2Cl_2$ (**1.49**) and $^tBuONH_2$ in an analogous fashion to the imido and hydrazido counterparts. Addition of a range of neutral tridentate ligands yielded dichloride compounds, $(L)TiCl_2$, (L = $Me_3[9]aneN_3$ (**1.152**), $HC(Me_2pz)_3$ (**1.153**) and $Me_3[6]aneN_3$ ($Me_3[6]aneN_3$ = trimethyl-1,3,5-triazacyclohexane**, 1.154**)). Addition of an equivalent of $^tBuONH_2$ to $Ti(N^tBu)Cl_2(py)_3$ (**1.45**) did not result in the formation of $Ti(NO^tBu)Cl_2(py)_3$ (**1.155**). However, compound **1.155** could be obtained following addition of an excess of pyridine to **1.154** as shown in Scheme 1.13.

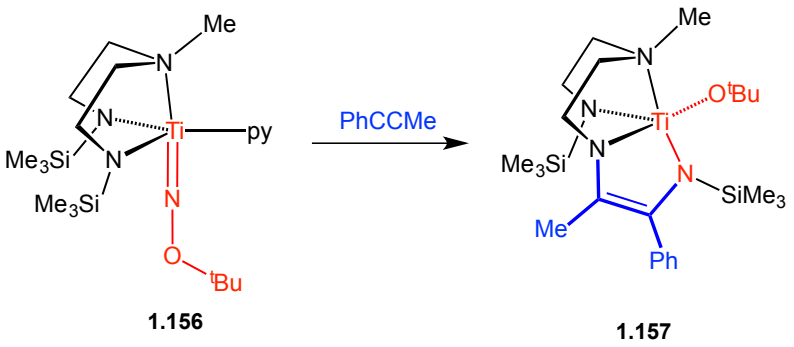


1.151 **1.154** **1.155**

Scheme 1.13. Synthesis of the titanium alkoxyimido synthon $Ti(NO^tBu)Cl_2(py)_3$ (**1.15**).

As was found with the imido and hydrazido analogues, **1.15** proved to be an exceptionally useful synthon and following addition of a range of lithiated ligands several new titanium alkoxyimides were synthesied. Reaction of the alkoxyimido compound $Ti(N_2N^{Me})(NO^tBu)(py)$ (**1.156**) with PhCCMe gave net insertion of the alkyne into one of the Ti–$NSiMe_3$ bonds as well as N–O bond cleavge to yield **1.157**, Equation 1.3. This is in contrast to the analogous hydrazido compound which was a

catalyst for the 1,2-diamination of alkynes. The reactivity of **1.156** shown here shuts down the possibility of an analogous type of catalysis occuring.

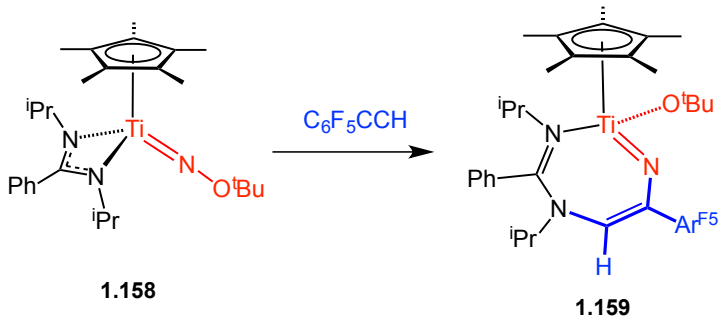


1.156 **1.157**

Equation 1.3

Encouraged by the wide range of reactivity observed with both the imido and hydrazido cyclopentadienyl-amidinate supported compounds and in an attempt to further develop the reaction chemistry of titanium alkoxyimides, Cp*Ti{PhC(N^{i}Pr)$_2$}(NO^{t}Bu) (**1.158**) was synthesied *via* a *tert*-butoxyamine/*tert*-butylimide exchange reaction from the corresponding imido compound. The reactivity of **1.158** with an assortment of unsaturated substrates including CS_2, isocyanates, aldehydes, ketones and nitriles has been described and is the only detailed reactivity study of a Group 4 alkoxyimido compound to date. As was the case with the corresponding alkylidene hydrazido compound **1.147** the reactivity of **1.158** was generally not found to differ dramatically from imides and hydrazides.

Interestingly however, reaction of **1.158** with the terminal alkyne HCCC$_6$F$_5$ only, resulted in the formation of the single product **1.159**, Equation 1.4. Compound **1.159** is proposed to result from an initial [2+2] cycloaddition reaction followed by N–O bond cleavage to give an azirinyl intermediate and this in turn undergoes nucleophilic attack by one of the amidinate nitrogen atoms.



1.158 **1.159**

Equation 1.4

1.10 Summary and objectives

This Chapter has mapped the evolution of Group 4 imido and Groups 4-6 hydrazido compounds, including their synthesis, reactivity patterns, bonding and structure analysis and practical applications. The Group 4 examples are of the greatest relevance to the experimental Chapters of this Thesis. The current direction for Group 4 hydrazido compounds is based around understanding and developing the possible catalytic C–N bond forming reactions, as well as looking into methods of replacing N_β with different heteroatoms and the resultant effects on bonding and reactivity. The former provides the basis for this Thesis.

One aim of this Thesis is to investigate the mechansim for the stoichiometric and catalytic reactions of a previously described hydrazido compound with alkynes. To aid with this, a novel imido compound that reacts in an analogous manner is targeted. Secondly, as both of these compounds yield unusual reaction products with alkynes, their reactivity with other small molecules in particular those containing Si–H or B–H bonds is pursued.

1.11 References

1. S. J. Ferguson, *Curr. Opin. Chem. Biol.*, 1998, **2**, 182.
2. H. P. Jia and E. A. Quadrelli, *Chem. Soc. Rev.*, 2014, **43**, 547.
3. B. A. MacKay and M. D. Fryzuk, *Chem. Rev.*, 2004, **104**, 385.
4. D. E. Canfield, A. N. Glazer and P. G. Falkowski, *Science*, 2010, **330**, 192.
5. Q. Cheng, *J. Integr. Plant Biol.*, 2008, **50**, 786.
6. B. Thamdrup, *Ann. Rev. Ecol. Evol. Syst.*, 2012, **43**, 407.
7. G. Ertl, *Angew. Chem. Int. Ed.*, 2008, **47**, 3524.
8. J. R. Jennings, *Catalytic Ammonina Synthesis. Fundamentals and Practice*, Plenum Press, New York, 1991.
9. F. Haber, *Naturwissenschaften*, 1923, **11**, 339.
10. F. Haber, *Naturwissenschaften*, 1922, **10**, 1041.
11. W. A. Bulen, R. C. Burns and J. R. LeComte, *Biochem. Biophys. Res. Commun.*, 1964, **17**, 265.
12. J. E. Carnahan, L. E. Mortenson, H. F. Mower and J. E. Castle, *Biochem. Biophys. Acta.*, 1960, **44**, 520.
13. B. K. Burgess and D. J. Lowe, *Chem. Rev.*, 1996, **96**, 2983.
14. J. Kim and D. Rees, *Science*, 1992, **257**, 1677.

15. S. B. Jang, L. C. Seefeldt and J. W. Peters, *Biochemistry*, 2000, **39**, 14745.
16. S. B. Jang, L. C. Seefeldt and J. W. Peters, *Biochemistry*, 2000, **39**, 641.
17. P. Strop, P. M. Takahara, H.-J. Chiu, H. C. Angove, B. K. Burgess and D. C. Rees, *Biochemistry*, 2001, **40**, 651.
18. S. Sen, R. Igarashi, A. Smith, M. K. Johnson, L. C. Seefeldt and J. W. Peters, *Biochemistry*, 2004, **43**, 1787.
19. S. Sen, A. Krishnakumar, J. McClead, M. K. Johnson, L. C. Seefeldt, R. K. Szilagyi and J. W. Peters, *J. Inorg. Biochem*, 2006, **100**, 1041.
20. J. W. Peters, M. H. B. Stowell, S. M. Soltis, M. G. Finnegan, M. K. Johnson and D. C. Rees, *Biochemistry*, 1997, **36**, 1181.
21. O. Einsle, F. A. Tezcan, S. L. A. Andrade, B. Schmid, M. Yoshida, J. B. Howard and D. C. Rees, *Science*, 2002, **297**, 1696.
22. B. Schmid, M. W. Ribbe, O. Einsle, M. Yoshida, L. M. Thomas, D. R. Dean, D. C. Rees and B. K. Burgess, *Science*, 2002, **296**, 352.
23. R. Sarma, D. W. Mulder, E. Brecht, R. K. Szilagyi, L. C. Seefeldt, H. Tsuruta and J. W. Peters, *Biochemistry*, 2007, **46**, 14058.
24. R. Sarma, B. M. Barney, S. Keable, D. R. Dean, L. C. Seefeldt and J. W. Peters, *J. Inorg. Biochem*, 2010, **104**, 385.
25. T. Spatzal, M. Aksoyoglu, L. Zhang, S. L. A. Andrade, E. Schleicher, S. Weber, D. C. Rees and O. Einsle, *Science*, 2011, **334**, 940.
26. K. M. Lancaster, M. Roemelt, P. Ettenhuber, Y. Hu, M. W. Ribbe, F. Neese, U. Bergmann and S. DeBeer, *Science*, 2011, **334**, 974.
27. J. A. Wiig, Y. Hu, C. C. Lee and M. W. Ribbe, *Science*, 2012, **337**, 1672.
28. K. M. Lancaster, Y. Hu, U. Bergmann, M. W. Ribbe and S. DeBeer, *J. Am. Chem. Soc.*, 2013, **135**, 610.
29. H. I. Lee, P. M. C. Benton, M. Laryukhin, R. Y. Igarashi, D. R. Dean, L. C. Seefeldt and B. M. Hoffman, *J. Am. Chem. Soc.*, 2003, **125**, 5604.
30. T. C. Yang, N. K. Maeser, M. Laryukhin, H.-I. Lee, D. R. Dean, L. C. Seefeldt and B. M. Hoffman, *J. Am. Chem. Soc.*, 2005, **127**, 12804.
31. D. Lukoyanov, V. Pelmenschikov, N. Maeser, M. Laryukhin, T. C. Yang, L. Noodleman, D. R. Dean, D. A. Case, L. C. Seefeldt and B. M. Hoffman, *Inorg. Chem.*, 2007, **46**, 11437.
32. K. C. MacLeod and P. L. Holland, *Nature Chem.*, 2013, **5**, 559.
33. M. D. Fryzuk, *Chem. Commun.*, 2013, **49**, 4866.

34. Y. Tanabe and Y. Nishibayashi, *Coord. Chem. Rev.*, 2013, **257**, 2551.
35. C. J. M. van der Ham, M. T. M. Koper and D. G. H. Hetterscheid, *Chem. Soc. Rev.*, 2014, **43**, 5183.
36. N. Khoenkhoen, B. de Bruin, J. N. H. Reek and W. I. Dzik, *Eur. J. Inorg. Chem.*, 2015, **2015**, 567.
37. J. Chatt, A. J. Pearman and R. L. Richards, *J. Chem. Soc., Dalton Trans.*, 1977, DOI: 10.1039/DT9770001852, 1852.
38. M. Hidai, *Coord. Chem. Rev.*, 1999, **185-186**, 99.
39. R. R. Schrock, *Angew. Chem. Int. Ed.*, 2008, **47**, 5512.
40. R. R. Schrock, *Acc. Chem. Res.*, 2005, **38**, 955.
41. W. W. Weare, X. Dai, M. J. Byrnes, J. M. Chin, R. R. Schrock and P. Müller, *Proc. Natl. Acad. Sci.*, 2006, **103**, 17099.
42. D. V. Yandulov and R. R. Schrock, *Science*, 2003, 76.
43. D. V. Yandulov and R. R. Schrock, *Inorg. Chem.*, 2005, **44**, 1103.
44. D. V. Yandulov and R. R. Schrock, *J. Am. Chem. Soc.*, 2002, **124**, 6252.
45. K. Arashiba, E. Kinoshita, S. Kuriyama, A. Eizawa, K. Nakajima, H. Tanaka, K. Yoshizawa and Y. Nishibayashi, *J. Am. Chem. Soc.*, 2015, **137**, 5666.
46. K. Arashiba, Y. Miyake and Y. Nishibayashi, *Nature. Chem.*, 2011, **3**, 120.
47. H. Tanaka, A. Sasada, T. Kouno, M. Yuki, Y. Miyake, H. Nakanishi, Y. Nishibayashi and K. Yoshizawa, *J. Am. Chem. Soc.*, 2011, **133**, 3498.
48. Y. Lee, N. P. Mankad and J. C. Peters, *Nature Chem.*, 2010, **2**, 558.
49. W. A. Nugent and B. L. Haymore, *Coord. Chem. Rev.*, 1980, **31**, 123.
50. W. A. Nugent and J. M. Mayer, *Metal-Ligand Multiple Bonds*, Wiley-Interscience, New York, 1988.
51. D. E. Wigley, *Prog. Inorg. Chem.*, 1994, **42**, 239.
52. M. H. Chisholm and I. P. Rothwell, in *Comprehensive Coordination Chemistry*, eds. G. Wilkinson, R. D. Gillard and J. A. McCleverty, Pergamon Press, Oxford, 1987, vol. 2, p. 161.
53. P. Mountford, *Chem. Commun.*, 1997, 2127.
54. D. N. Williams, J. P. Mitchell, A. D. Poole, U. Siemeling, W. Clegg, D. C. R. Hockless, P. A. O'Neil and V. C. Gibson, *J. Chem. Soc., Dalton Trans.*, 1992, 739.
55. D. S. Glueck, J. C. Green, R. I. Michelman and I. N. Wright, *Organometallics*, 1992, **11**, 4221.

56. Y. Li, Y. Shi and A. L. Odom, *J. Am. Chem. Soc.*, 2004, **126**, 1794.
57. J. D. Selby, M. Feliz, A. D. Schwarz, E. Clot and P. Mountford, *Organometallics*, 2011, **30**, 2295.
58. S. Kahlal, J.-Y. Saillard, J.-R. Hamon, C. Manzur and D. Carrillo, *J. Chem. Soc., Dalton Trans.*, 1998, 1229.
59. R. Aumann and E. O. Fischer, *Angew. Chem. Int. Ed.*, 1967, **6**, 879.
60. R. R. Schrock, *Chem. Rev*, 2002, **102**, 145.
61. M. Hidai, T. Kodama, M. Sato, M. Harakawa and Y. Uchida, *Inorg. Chem.*, 1976, **15**, 2694.
62. M. Hidai, Y. Mizobe, M. Sato, T. Kodama and Y. Uchida, *J. Am. Chem. Soc.*, 1978, **100**, 5740.
63. L. D. Field, N. G. Jones and P. Turner, *Organometallics*, 1998, **17**, 2394.
64. J. D. Niemoth-Anderson, J. R. D. Debord, T. Adrian George, C. R. Ross Ii and J. J. Stezowski, *Polyhedron*, 1996, **15**, 4031.
65. C. Redshaw and M. R. Elsegood, *Inorg. Chem.*, 2000, **39**, 5164.
66. Z. Janas, L. B. Jerzykiewicz, R. L. Richards and P. Sobota, *Inorg. Chim. Acta.*, 2003, **350**, 379.
67. M. W. Bishop, J. Chatt, J. R. Dilworth, M. B. Hursthouse and M. Motevalle, *J. Less Common Met.*, 1977, **54**, 487.
68. J. Chatt, B. L. Crichton, J. Dilworth, P. Dahlstrom, R. Gutkoska and J. Zubieta, *Transition Met. Chem.*, 1979, **4**, 271.
69. J. Chatt, J. R. Dilworth, P. L. Dahlstrom and J. Zubieta, *J. Chem. Soc. Chem. Commun.*, 1980, 786.
70. C. Bustos, C. Manzur, D. Carrillo, F. Robert and P. Gouzerh, *Inorg. Chem.*, 1994, **33**, 1427.
71. J. R. Dilworth, J. Zubieta and J. R. Hyde, *J. Am. Chem. Soc.*, 1982, **104**, 365.
72. A. C. Stergiou, S. Bladenopoulou and C. Tsiamis, *Inorg. Chim. Acta.*, 1994, **217**, 61.
73. N. Wiberg, H.-W. Haring, G. Huttner and P. Friedrich, *Chem. Ber.*, 1978, **111**, 2708.
74. T. Aoshima, Y. Mizobe, M. Hidai and J. Tsuchiya, *J. Organomet. Chem.*, 1992, **423**, 39.
75. K. Iwanami, Y. Mizobe, T. Takahashi, T. Kodama, Y. Uchida and M. Hidai, *Bull. Chem. Soc. Jpn.*, 1981, **54**, 1773.

76. M. Hidai, *Chem. Rev.*, 1995, **95**, 1115.
77. P. C. Bevan, J. Chatt, G. J. Leigh and E. G. Leelamani, *J. Organomet. Chem.*, 1977, **139**, C59.
78. E. Krahn, B. Weiss, M. Kröckel, J. Groppe, G. Henkel, S. Cramer, A. Trautwein, K. Schneider and A. Müller, *J. Biol. Inorg. Chem.*, 2002, **7**, 37.
79. S. Siemann, K. Schneider, M. Dröttboom and A. Müller, *Eur. J. Biochem.*, 2002, **269**, 1650.
80. D. Rehder, *Coord. Chem. Rev.*, 1999, **182**, 297.
81. R. R. Eady, *Coord. Chem. Rev.*, 2003, **237**, 23.
82. N. Wiberg, H. W. Häring and O. Schieda, *Angew. Chem. Int. Ed.*, 1976, **15**, 386.
83. M. Veith, *Angew. Chem. Int. Ed.*, 1976, **15**, 387.
84. S. C. Davies, D. L. Hughes, Z. Janas, L. Jerzykiewicz, R. L. Richards, J. Roger Sanders and P. Sobota, *Chem. Commun.*, 1997, 1261.
85. S. C. Davies, D. L. Hughes, Z. Janas, L. B. Jerzykiewicz, R. L. Richards, J. R. Sanders, J. E. Silverston and P. Sobota, *Inorg. Chem.*, 2000, **39**, 3485.
86. J. Bultitude, L. F. Larkworthy, D. C. Povey, G. W. Smith, J. R. Dilworth and G. J. Leigh, *J. Chem. Soc. Chem. Commun.*, 1986, 1748.
87. A. A. Danopoulos, R. S. Hay-Motherwell, G. Wilkinson, T. K. N. Sweet and M. B. Hursthouse, *Polyhedron*, 1997, **16**, 1081.
88. S. Banerjee and A. L. Odom, *Dalton Trans.*, 2008, 2005.
89. T. Moriuchi, K. Ikeuchi and T. Hirao, *Dalton Trans.*, 2013, **42**, 11824.
90. M. L. H. Green, J. T. James, J. F. Saunders and J. Souter, *J. Chem. Soc., Dalton Trans.*, 1997, 1281.
91. M. L. H. Green, J. T. James and A. N. Chernega, *J. Chem. Soc., Dalton Trans.*, 1997, 1719.
92. I. A. Tonks and J. E. Bercaw, *Inorg. Chem.*, 2010, **49**, 4648.
93. I. A. Tonks, A. C. Durrell, H. B. Gray and J. E. Bercaw, *J. Am. Chem. Soc.*, 2012, **134**, 7301.
94. A. J. Keane, P. Y. Zavalij and L. R. Sita, *J. Am. Chem. Soc.*, 2013, **135**, 9580.
95. H. W. Roesky, H. Voelker, M. Witt and M. Noltemeyer, *Angew. Chem. Int. Ed. Engl.*, 1990, **29**, 669.
96. J. E. Hill, R. D. Profilet, P. E. Fanwick and I. P. Rothwell, *Angew. Chem. Int. Ed. Engl.*, 1990, **29**, 664.

97. C. C. Cummins, C. P. Schaller, G. D. Van Duyne, P. T. Wolczanski, A. W. E. Chan and R. Hoffmann, *J. Am. Chem. Soc.*, 1991, **113**, 2985.

98. R. Duchateau, A. J. Williams, S. Gambarotta and M. Y. Chiang, *Inorg. Chem.*, 1991, **30**, 4863.

99. T. E. Hanna, I. Keresztes, E. Lobkovsky, W. H. Bernskoetter and P. J. Chirik, *Organometallics*, 2004, **23**, 3448.

100. N. Hazari and P. Mountford, *Acc. Chem. Res.*, 2005, **38**, 839.

101. A. J. Blake, P. E. Collier, S. C. Dunn, W.-S. Li, P. Mountford and O. V. Shishkin., *J. Chem. Soc., Dalton Trans.*, 1997, 1549.

102. S. C. Dunn, A. S. Batsanov and P. Mountford, *J. Chem. Soc., Chem. Commun.*, 1994, 2007.

103. L. H. Gade and P. Mountford, *Coord. Chem. Rev.*, 2001, **216-217**, 65.

104. D. Swallow, J. M. McInnes and P. Mountford, *J. Chem. Soc., Dalton Trans.*, 1998, 2253.

105. A. J. Blake, J. M. McInnes, P. Mountford, G. I. Nikonov, D. Swallow and D. J. Watkin, *J. Chem. Soc., Dalton Trans.*, 1999, 379.

106. S. C. Dunn, P. Mountford and D. A. Robson, *J. Chem. Soc., Dalton Trans.*, 1997, 293.

107. E. Müller, J. Müller, F. Olbrich, W. Brüser, W. Knapp, D. Abeln and F. T. Edelmann, *Eur. J. Inorg. Chem.*, 1998, **1998**, 87.

108. N. Adams, H. R. Bigmore, T. L. Blundell, C. L. Boyd, S. R. Dubberley, A. J. Sealey, A. R. Cowley, M. E. G. Skinner and P. Mountford, *Inorg. Chem.*, 2005, **44**, 2882.

109. N. Adams, H. J. Arts, P. D. Bolton, D. Cowell, S. R. Dubberley, N. Friederichs, C. Grant, M. Kranenburg, A. J. Sealey, B. Wang, P. J. Wilson, A. R. Cowley, P. Mountford and M. Schröder, *Chem. Commun.*, 2004, 434.

110. C. Lorber, R. Choukroun and L. Vendier, *Eur. J. Inorg. Chem.*, 2006, 4503.

111. P. J. Walsh, F. J. Hollander and R. G. Bergman, *J. Am. Chem. Soc.*, 1988, **110**, 8729.

112. P. J. Walsh, F. J. Hollander and R. G. Bergman, *Organometallics*, 1993, **12**, 3705.

113. W. A. Nugent and R. L. Harlow, *Inorg. Chem.*, 1979, **18**, 2030.

114. R. L. Zuckerman, S. W. Krska and R. G. Bergman, *J. Am. Chem. Soc.*, 2000, **122**, 751.

115. C. C. Cummins, S. M. Baxter and P. T. Wolczanski, *J. Am. Chem. Soc.*, 1988, **110**, 8731.

116. D. J. Arney, M. A. Bruck, S. R. Huber and D. E. Wigley, *Inorg. Chem.*, 1992, **31**, 3749.

117. S. R. Dubberley, S. E. Evans, C. L. Boyd and P. Mountford, *Dalton Trans.*, 2005, 1448.

118. A. J. Blake, P. Mountford, G. I. Nikonov and D. Swallow, *Chem. Commun.*, 1996, 1835.

119. A. J. Blake, P. E. Collier, L. H. Gade, P. Mountford, J. Lloyd, S. M. Pugh, M. Schubart, M. E. G. Skinner and J. M. Trösch, *Inorg. Chem.*, 2001, **40**, 870.

120. M. E. G. Skinner, T. Toupance, D. A. Cowhig, B. R. Tyrrell and P. Mountford, *Organometallics*, 2005, **24**, 5586.

121. N. Adams, H. J. Arts, P. D. Bolton, D. Cowell, S. R. Dubberley, N. Friederichs, C. M. Grant, M. Kranenburg, A. J. Sealey, B. Wang, P. J. Wilson, M. A. Zuideveld, A. J. Blake, M. Schröder and P. Mountford, *Organometallics*, 2006, **25**, 3888.

122. A. E. Guiducci, C. L. Boyd and P. Mountford, *Organometallics*, 2006, **25**, 1167.

123. P. J. Tiong, A. Nova, L. R. Groom, A. D. Schwarz, J. D. Selby, A. D. Schofield, E. Clot and P. Mountford, *Organometallics*, 2011, **30**, 1182.

124. N. Kaltsoyannis and P. Mountford, *J. Chem. Soc., Dalton Trans.*, 1999, 781.

125. K. E. Meyer, P. J. Walsh and R. G. Bergman, *J. Am. Chem. Soc.*, 1995, **117**, 974.

126. S. Y. Lee and R. G. Bergman, *Tetrahedron*, 1995, **51**, 4255.

127. S. Y. Lee and R. G. Bergman, *J. Am. Chem. Soc.*, 1995, **117**, 5877.

128. S. A. Blum, V. A. Rivera, R. T. Ruck, F. E. Michael and R. G. Bergman, *Organometallics*, 2005, **24**, 1647.

129. A. P. Duncan and R. G. Bergman, *Chem. Rec.*, 2002, **2**, 431.

130. D. J. M. Trösch, P. E. Collier, A. Bashall, L. H. Gade, M. McPartlin, P. Mountford and S. Radojevic, *Organometallics*, 2001, **20**, 3308.

131. B. D. Ward, A. Maisse-Francois, P. Mountford and L. H. Gade, *Chem. Commun.*, 2004, 704.

132. N. Vujkovic, J. L. Fillol, B. D. Ward, H. Wadepohl, P. Mountford and L. H. Gade, *Organometallics*, 2008, **27**, 2518.

133. A. Bashall, P. E. Collier, L. H. Gade, M. McPartlin, P. Mountford and D. T. Trösch, *Chem. Commun.*, 1998, 2555.
134. A. Bashall, P. E. Collier, L. H. Gade, M. McPartlin, P. Mountford, S. M. Pugh, S. Radojevic, M. Schubart, I. J. Scowen and D. J. M. Trösch, *Organometallics*, 2000, **19**, 4784.
135. S. M. Pugh, D. J. M. Trösch, D. J. Wilson, A. Bashall, F. G. N. Cloke, L. H. Gade, P. B. Hitchcock, M. McPartlin, J. F. Nixon and P. Mountford, *Organometallics*, 2000, **19**, 3205.
136. B. D. Ward, G. Orde, E. Clot, A. R. Cowley, L. H. Gade and P. Mountford, *Organometallics*, 2005, **24**, 2368.
137. K. Weitershaus, B. D. Ward, R. Kubiak, C. Muller, H. Wadepohl, S. Doye and L. H. Gade, *Dalton Trans.*, 2009, 4586.
138. J. L. Thorman, I. A. Guzei, V. G. Young and L. K. Woo, *Inorg. Chem.*, 1999, **38**, 3814.
139. P. Mountford, *J. Organomet. Chem.*, 1997, **528**, 15.
140. P. J. Tiong, A. Nova, A. D. Schwarz, J. D. Selby, E. Clot and P. Mountford, *Dalton Trans.*, 2012, **41**, 2277.
141. A. L. Odom, *Dalton Trans.*, 2005, 225.
142. S. Doye, *Synlett.*, 2004, 1653.
143. K. C. Hultzsch, *Adv. Synth. Catal.*, 2005, **347**, 367.
144. L. L. Schafer and A. V. Lee, *Eur. J. Inorg. Chem.*, 2007, 2243.
145. T. E. Müller, K. C. Hultzsch, M. Yus, F. Foubelo and M. Tada, *Chem. Rev.*, 2008, **108**, 3795.
146. A. Tillack, H. Jiao, I. Garcia Castro, C. G. Hartung and M. Beller, *Chem. Eur. J.*, 2004, **10**, 2409.
147. B. F. Straub and R. G. Bergman, *Angew. Chem. Int. Ed.*, 2001, **40**, 4632.
148. S. Tobisch, *Dalton Trans.*, 2006, 4277.
149. S. Tobisch, *Chem. Eur. J.*, 2007, **13**, 4884
150. C. Müller, R. Koch and S. Doye, *Chem. Eur. J.*, 2008, **14**, 10430.
151. S. Tobisch, *Chem. Eur. J.*, 2008, **14**, 8590
152. J. S. Johnson and R. G. Bergman, *J. Am. Chem. Soc.*, 2001, **123**, 2923.
153. P. J. Walsh, A. M. Baranger and R. G. Bergman, *J. Am. Chem. Soc.*, 1992, **114**, 1708.

154. A. M. Baranger, P. J. Walsh and R. G. Bergman, *J. Am. Chem. Soc.*, 1993, **115**, 2753.

155. F. Pohlki and S. Doye, *Angew. Chem. Int. Ed.*, 2001, **40**, 2305.

156. L. E. N. Allan, G. J. Clarkson, D. J. Fox, A. L. Gott and P. Scott, *J. Am. Chem. Soc.*, 2010, **132**, 15308.

157. L. Ackermann, R. G. Bergman and R. N. Loy, *J. Am. Chem. Soc.*, 2003, **125**, 11956.

158. J. Cho, T. K. Hollis, E. J. Valente and J. M. Trate, *J. Organomet. Chem.*, 2011, **696**, 373.

159. T. B. Parsons, N. Hazari, A. R. Cowley, J. C. Green and P. Mountford, *Inorg. Chem.*, 2005, **44**, 8442.

160. A. J. Clulow, J. D. Selby, M. G. Cushion, A. D. Schwarz and P. Mountford, *Inorg. Chem.*, 2008, **47**, 12049.

161. J. D. Selby, C. D. Manley, A. D. Schwarz, E. Clot and P. Mountford, *Organometallics*, 2008, **27**, 6479.

162. J. Unruangsri, H. Morgan, A. D. Schwarz, A. D. Schofield and P. Mountford, *Organometallics*, 2013, **32**, 3091.

163. P. J. Tiong, A. D. Schofield, J. D. Selby, A. Nova, E. Clot and P. Mountford, *Chem. Commun.*, 2010, **46**, 85.

164. K. Weitershaus, H. Wadepohl and L. H. Gade, *Organometallics*, 2009, **28**, 3381.

165. J. D. Selby, C. D. Manley, M. Feliz, A. D. Schwarz, E. Clot and P. Mountford, *Chem. Commun.*, 2007, 4937.

166. P. J. Walsh, M. J. Carney and R. G. Bergman, *J. Am. Chem. Soc.*, 1991, **113**, 6343.

167. H. Herrmann, J. L. Fillol, H. Wadepohl and L. H. Gade, *Angew. Chem. Int. Ed.*, 2007, **46**, 8426.

168. H. Herrmann, J. L. Fillol, T. Gehrmann, M. Enders, H. Wadepohl and L. H. Gade, *Chem. Eur. J.*, 2008, **14**, 8131.

169. S. A. Scholl, H. Wadepohl and L. H. Gade, *Organometallics*, 2013, **32**, 937.

170. S. A. Scholl, G. T. Plundrich, H. Wadepohl and L. H. Gade, *Inorg. Chem.*, 2013, **52**, 10158.

171. J. D. Selby, C. Schulten, A. D. Schwarz, A. Stasch, E. Clot, C. Jones and P. Mountford, *Chem.Commun.*, 2008, 5101.

172. K. Weitershaus, J. L. Fillol, H. Wadepohl and L. H. Gade, *Organometallics*, 2009, **28**, 4747.
173. A. D. Schofield, A. Nova, J. D. Selby, A. D. Schwarz, E. Clot and P. Mountford, *Chem. Eur. J.*, 2011, **17**, 265.
174. T. Gehrmann, G. T. Plundrich, H. Wadepohl and L. H. Gade, *Organometallics*, 2012, **31**, 3346.
175. S. Banerjee and A. L. Odom, *Organometallics*, 2006, **25**, 3099.
176. P. J. Tiong, DPhil Thesis, University of Oxford, 2012.
177. T. Gehrmann, J. Lloret-Fillol, H. Herrmann, H. Wadepohl and L. H. Gade, *Organometallics*, 2013, **32**, 3877.
178. T. Gehrmann, S. A. Scholl, J. L. Fillol, H. Wadepohl and L. H. Gade, *Chem. Eur. J.*, 2012, **18**, 3925.
179. A. D. Schofield, A. Nova, J. D. Selby, C. D. Manley, A. D. Schwarz, E. Clot and P. Mountford, *J. Am. Chem. Soc.*, 2010, **132**, 10484.
180. A. D. Schofield, DPhil Thesis, Univeristy of Oxford, 2012.
181. C. Cao, Y. Shi and A. L. Odom, *Org. Lett.*, 2002, **4**, 2853.
182. S. Banerjee, E. Barnea and A. L. Odom, *Organometallics*, 2008, **27**, 1005.
183. S. Banerjee, Y. Shi, C. Cao and A. L. Odom, *J. Organomet. Chem.*, 2005, **690**, 5066.
184. L. Ackermann and R. Born, *Tet. Letts.*, 2004, **45**, 9541.
185. V. Khedkar, A. Tillack, M. Michalik and M. Beller, *Tet. Letts.*, 2004, **45**, 3123.
186. A. A. Dissanayake and A. L. Odom, *Chem. Commun.*, 2012, **48**, 440.
187. L. R. Groom, DPhil Thesis, University of Oxford, 2014.
188. A. D. Schwarz, C. S. Onn and P. Mountford, *Angew. Chem. Int. Ed.*, 2012, **51**, 12298.
189. Y. Mizobe, Y. Ishii and M. Hidai, *Coord. Chem. Rev.*, 1995, **139**, 281.
190. P. J. Tiong, L. R. Groom, E. Clot and P. Mountford, *Chem. Eur. J.*, 2013, **19**, 4198.
191. J. L. Polse, A. W. Kaplan, R. A. Andersen and R. G. Bergman, *J. Am. Chem. Soc.*, 1998, **120**, 6316.
192. A. W. Kaplan, J. L. Polse, G. E. Ball, R. A. Andersen and R. G. Bergman, *J. Am. Chem. Soc.*, 1998, **120**, 11649.

193. L. B. Kool, M. D. Rausch, H. G. Alt, M. Herberhold, A. F. Hill, U. Thewalt and B. Wolf, *J. Chem. Soc., Chem. Commun.*, 1986, 408.

Chapter Two

Synthesis of diamide-amine supported titanium imido complexes and reactions with N–H and O–H bonds, internal alkynes and nitriles

2.1 Overview

This chapter will first describe the synthesis and characterisation of new diamide-amine supported titanium imido complexes. Subsequently the reactions of the new imido compound Ti($N_2^{iPr}N^{Me}$)(NXyl)(py) (**1**) with organic molecules containing N–H bonds are discussed, alongside the comparable reactions of the reported hydrazido compound Ti($N_2^{iPr}N^{Me}$)($NNPh_2$)(py) (**2.1**). Finally the reactivity of **1** and **2.1** with internal alkynes and nitriles will be described.

2.2 Introduction

As described in Chapter One of this Thesis, the synthesis, characterisation and reactivity of Group 4 compounds containing a metal-ligand multiple bond have been studied in considerable depth over the past 20 years.[1-15] The imido ligand (M=NR, formally a $\sigma^2\pi^4$ triple bond in most instances[13, 16-23]) has been the focal point for much of this work and is therefore often used as a bench mark for comparison with other multiply bonded N-donor ligands. The stoichiometric reactions of Group 4 compounds containing such a polar π-donor imido functional group with both saturated and unsaturated substrates has yielded a huge range of reaction products, usually involving a [2+2] cycloaddition reaction with the electrophilic substrates. Similarly the catalytic reactions of such compounds typically involve the imido group as the reaction site, the most well-understood being alkene, allene and alkyne hydroamination.[24-27] The area of Group 4 metal-nitrogen bonds has continued to expand and terminal hydrazide complexes (M=NNR_2) have begun to be explored. Building on early examples by Wiberg[28] and Bergman[29] many reports detailing the structure and reactivity of dialkyl or diarly hydrazido(2-) compounds now exist, in particular for M=Ti[7, 30-54] and M=Zr.[55-68] Group 4 hydrazides have been reported to react in an analogous manner to Group 4 imides in many cases, thus, a range of reaction products resulting from cycloaddition, cycloaddition-insertion, cycloaddition-elimination and NNR_2 groups transfer reactions have been reported.[34, 36, 40-42, 44, 45, 50, 61, 69, 70] However, several examples exist where the reactivity with small molecules differs considerably and reactions resulting in N_α–N_β bond reductive cleavage or insertion with oxidisable substrates such as CO, isonitriles and alkynes have been observed.[7, 29, 36, 44, 46, 54, 55, 65] The catalytic reactions of Group 4 hydrazide compounds have also proved to be fruitful, with many examples of compounds capable of

hydrohydrazination catalysis reported,[31, 37, 42, 50, 52, 71-77] along with the more recently established diamination catalysis.[44] Furthermore, an iminohydrazination reaction has been developed where an alkyne, hydrazine and isocyanide are coupled in a single reaction *via* a titanium hydrazide complex.[32]

A DFT study of the electronic nature of terminal hydrazido and alkylimido complexes found that although the terminal hydrazide ligand binds to the metal centre in a manner analogous to that of terminal imido compounds, one of the Ti=N_α π components is significantly destabilised by the formal lone pair on the N_β atom. This in turn renders the multiple bond more reactive.[33]

Encouraged by the diverse range of chemistry of Group 4 hydrazido compounds, work within our group has recently focussed on replacing the N_β atom of the hydrazide moiety by either an oxygen or a boron atom, giving alkoxyimido and borylimido compounds respectively. A range of titanium alkoxyimides are been synthesised from the precursors $Ti(NO^tBu)Cl_2(NHMe_2)_2$ or $Ti(NO^tBu)Cl_2(py)_3$[78, 79] and a full reactivity study of the Cp*-amidinate supported alkoxyimido compound $Ti\{PhC(N^iPr_2)_2\}(NO^tBu)$ has been carried out.[80] The corresponding borylimido chemisty is in the very early stages of development. However, several compounds of titanium, zirconium and hafnium have been synthesised and some initial experiments suggest that such systems show promise for subsequent reactivity studies.[81, 82]

Unsurprisingly, the choice of supporting ligand has been of exceptional importance in obtaining well behaved imido, hydrazido, alkoxyimido and borylimido complexes that exhibit controlled reactivity. A variety of ligands have been employed successfully. One of the most effective at promoting new chemistry at the multiple bond in Group 4 complexes have been diamide-amine ligands of the type, $RN(CH_2)_nN(SiMe_3))_2$, (R = Me n = 2 (N_2N^{Me}) or n = 3 (N_2N^{Me,C_3}) or R = $SiMe_3$ n = 2 ($N_2N^{SiMe_3}$)), diamide-pyridine ligands of the type $(2\text{-}C_5H_4N)CMe(CH_2SiMe_2R)$ (R = Me (N_2N^{py}) or R = ^{t}Bu ($N_2{}^{TBS}N_{py}$)) and more recently diamide-ether ligands of the type $O(CH_2CH_2SiMe_3)_2$ (N_2O) and $O(2\text{-}C_6H_4NSiMe_3)_2$ ($N_2{}^{Ar}O$).[36, 39, 40, 44-46, 55, 57, 58, 60, 63-65, 83-85] These dianionic chelating ligands provide a well-defined and relatively non-labile environment around the metal centre and been used extensively in early metal transition metal chemistry as well as metal-ligand multiple bond chemistry.[12, 83, 86-92] Structural and DFT studies suggest that the π-donor ability of the N_{amide} atoms of these types of ligands destabilise the M=N_α multiple bond and promote reactivity.[39, 92]

Much success has also been had with Cp* amidinate supported systems and a range of imido compounds with varying N-imido substituents and hydrazides with various N_β substituents have been reported.[48, 49, 51, 93-97] The combination of C_5Me_5 and the amidinate supporting ligand, like with the diamide-amine systems, provide a balance of steric protection and electron donation conducive to promoting reactivity at the M=N bond.

The subsequent reactivity of Ti=N bonds with small molecules is hugely dependent on the choice of ligand set. For example, the cyclopentadienyl-amidinate supported compounds Cp*Ti{MeC(N^{i}Pr)$_2$}(NNR$_2$) (R = Me (**1.76**) and R = Ph (**1.77**)) do not react with alkynes, whereas the more open cyclopentadienyl-amidinate compound Cp*Ti(N^{Xyl}N)(NNMe$_2$)(DMAP) (**1.80**) reacts with PhCCH to yield a metallacycle with a Markovinikov type geometry.[41] Moreover, both **1.80** and Cp*Ti(N^{Xyl}N)(NNPh$_2$)(^{t}BuNH$_2$) (**1.79**) are catalysts for the hydrohydrazination of alkynes (Figure 2.1).

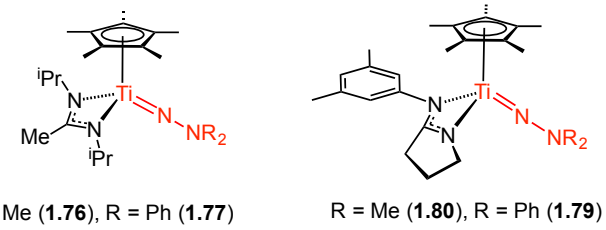


Figure 2.1. Cyclopentadienyl-amidinate supported hydrazido compounds.

Subtle changes in diamide-amine supporting ligands can also lead to differing reactivity. As described in Chapter One, the hydrazido compound Ti(N$_2$N^{Me})(NNPh$_2$)(py) (**1.72**, Figure 2.2) reacts with internal alkynes to yield vinyl imido compounds of the type **2.2** (Figure 2.3). The alkyne has regiospecifically inserted into the N–N bond following a [2+2] cycloaddition reaction and both **1.72** and **2.2** are catalysts for the 1,2-diamination of alkynes.[44]

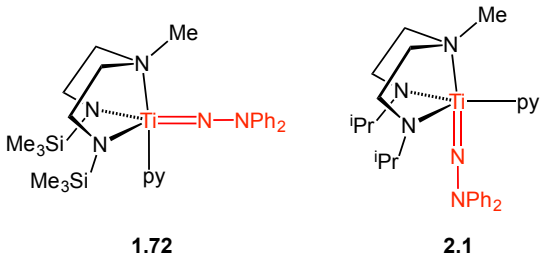
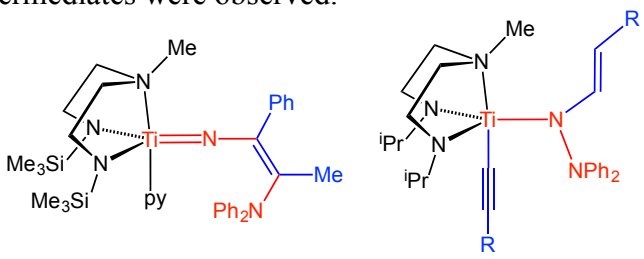


Figure 2.2. Diamide-amine supported hydrazide compounds.

Subsequent to this the hydrazido compound Ti($N_2^{iPr}N^{Me}$)($NNPh_2$)(py) (**2.1**, $N_2^{iPr}N^{Me}$ = ($MeN(CH_2CH_2N^iPr)_2$) was synthesised where the N_{amide}–$SiMe_3$ substituents were replaced with ^{i}Pr groups. The reduced steric bulk on the N_{amide} donor atoms allows the hydrazido ligand to occupy the electronically preferred axial position. Reaction with internal alkynes gave complex mixtures. However, reaction with two equivalents of terminal alkynes yielded the unusual vinylhydrazide-acetylide compounds of the type **2.3**, shown in Figure 2.3. A switch in the type of catalysis was observed and both **2.1** and **2.3** are catalysts for the hydrohydrazination of alkynes.[50] The mechanism was proposed to proceed *via* an azametallacyclobutene species. However, unlike with **1.72**, no such intermediates were observed.



2.2 **2.3**

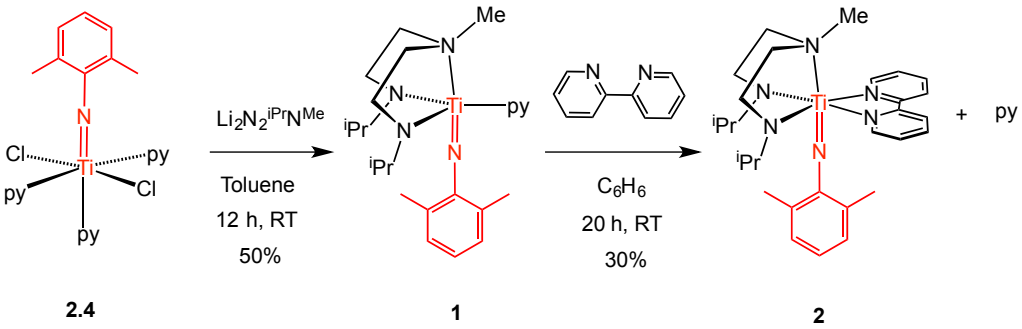
Figure 2.3. Reaction products of diamide-amine supported diphenylhydrazide compounds with alkynes.

As the reactions of the $N_2^{iPr}N^{Me}$ supported hydrazido compound **2.1** with alkynes deviated significantly from that of the well understood compound **1.72**, it was deemed interesting to investigate the reactions of this new hydrazide with other unsaturated substrates. Furthermore, as initial attempts to elucidate the mechanism for the formation of compounds of the type **2.3** were inconclusive, due to their rapid formation from **2.1** (< 5 mins), an imido compound which would react in a similar manner was targeted with the hope of revealing some mechanistic information. These mechanistic studies with alkynes will be described in Chapter Three, but first the synthesis and characterisation of imido compounds supported by $N_2^{iPr}N^{Me}$ will be discussed along with the reactions with other small molecules.

2.3 Synthesis of new imido compounds

The alkylimido compound Ti($N_2^{iPr}N^{Me}$)(N^tBu)(py) was initially targeted *via* reaction of Ti(N^tBu)Cl_2(py)$_3$ (**1.45**) with $Li_2N_2^{iPr}N^{Me}$ which was synthesised according to literature methods.[98] Disappointingly the reaction did not proceed smoothly on the NMR tube scale or on the preparative scale, and only intractable oily mixtures were

obtained. In comparison, reaction with the arylimido precursor $Ti(NXyl)Cl_2(py)_3$ (**2.4**)[99] at -78 °C proceeds cleanly to yield $Ti(N_2{}^{iPr}N^{Me})(NXyl)(py)$ (**1**) in 50% isolated yield (Scheme 2.1). This is a well-established route allowing access to a wide range of hydrazido and imido titanium compounds in multi-gram quantities.



Scheme 2.1. Synthesis of the imido compounds $Ti(N_2{}^{iPr}N^{Me})(NXyl)(py)$ (**1**) and $Ti(N_2{}^{iPr}N^{Me})(NXyl)(bipy)$ (**2**).

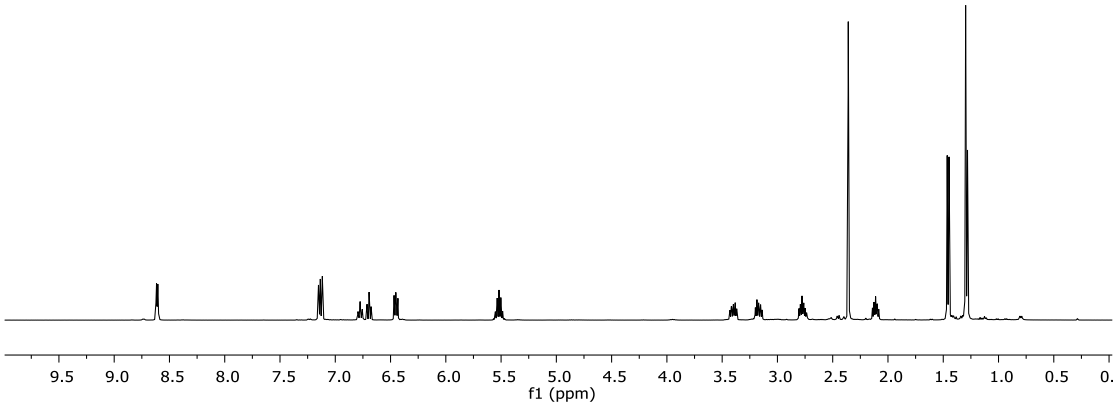


Figure 2.4. ^1H NMR spectrum (400.1 MHz) of $Ti(N_2{}^{iPr}N^{Me})(NXyl)(py)$ (**1**) in C_6D_6 at 25 °C.

The ^1H (Figure 2.4) and ^{13}C NMR spectra of **1** indicate a single isomer with resonances attributable to the NXyl moiety, one coordinated pyridine ligand and a κ^3-*fac*-bound diamide-amine ligand. The $N_2{}^{iPr}N^{Me}$ methylene proton signals appear as four inequivalent multiplet resonances (relative intensity 2H each) at 3.43 - 2.11 ppm and the resonances assigned to the *iso*-propyl substituents are observed as a single septet and a pair of doublets.

Diffraction-quality crystals were grown from a saturated benzene solution at room temperature and the solid-state structure is shown in Figure 2.5 along with selected bond lengths and angles in Table 2.1. Compound **1** has trigonal-bipyramidal geometry

at titanium with the imido ligand occupying the axial position *trans* to the NMe donor and the diamide-amine ligand coordinated facially. The Ti–N_{py} bond length is typical of neutral σ-only interactions with titanium.[100] The short Ti–N_{imide} distance of 1.7581(19) Å and approximately linear Ti–N_{imide}–C_{ipso} angle of 174.59(17) ^{o} establishes sp hybridisation at N_{imide} and a formal $\sigma^2\pi^4$ Ti≡N triple bond. Both N_{amide} atoms are sp^2 hybridised and have an approximately trigonal planar geometry as indicated by the sum of the angles subtended at N(2) and N(3) being *ca.* 360 ^{o}. This is typical for early transition metal complexes[39, 87, 101] and indicates that the lone pairs of electrons are participating in π-bonding interactions with the titanium centre.

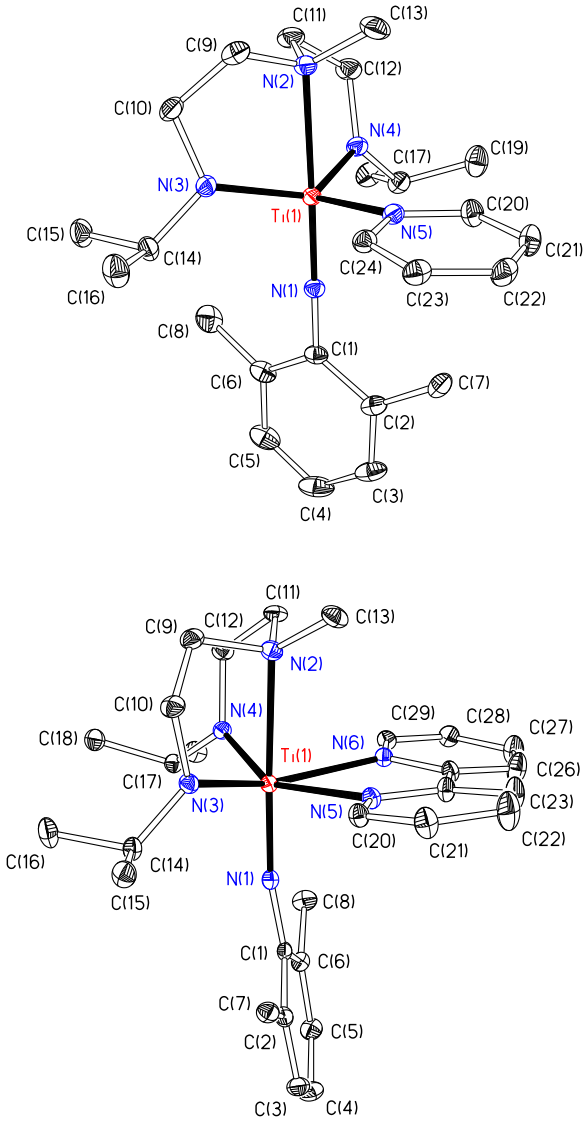


Figure 2.5. Displacement ellipsoid plot (20% probability) of Ti($N_2^{iPr}N^{Me}$)(NXyl)(py) (**1**) (top) and Ti($N_2^{iPr}N^{Me}$)(NXyl)(bipy) (**2**) (bottom). H atoms are omitted for clarity.

Table 2.1. Selected bond distances (Å) and angles (°) for Ti($N_2^{iPr}N^{Me}$)(NXyl)(py) (**1**) and Ti($N_2^{iPr}N^{Me}$)(NXyl)(bipy) (**2**).

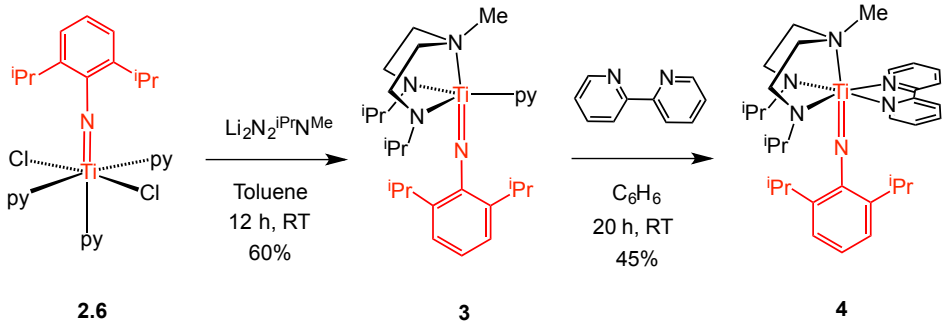
Parameter	**1**	**2**
Ti(1)-N(1)	1.7581(19)	1.770(3)
Ti(1)-N(2)	2.342(2)	2.366(4)
Ti(1)-N(3)	1.970(2)	2.001(4)
Ti(1)-N(4)	1.959(2)	2.016(3)
Ti(1)-N(5)	2.2002(19)	2.308(3)
Ti(1)-N(6)	-	2.330(3)
N(1)-C(1)	1.374(3)	1.382(5)
N(1)-Ti(1)-N(2)	175.48(8)	177.78(14)
N(3)-Ti(1)-N(4)	129.78(8)	106.82(15)
N(3)-Ti(1)-N(5)	107.15(8)	89.56(13)
N(4)-Ti(1)-N(5)	113.24(8)	-
N(4)-Ti(1)-N(6)	-	87.89(13)

The axial position of the imido ligand is unusual, despite it being the electronically preferred orientation. When the multiple bond occupies the equatorial position, competition for π-donation into the same d-orbitals occurs with the lone pairs situated on the N_{amide} atoms.[92] However, this orientation is often preferred as it reduces steric clash between the bulky N_{amide} substituents (usually $SiMe_3$) and the imido/hydrazido ligand.[44, 102, 103] Here, and in **2.1** the sterically less demanding iso-propyl substituents allow the imido and hydrazido ligands to occupy the axial position. This removes the π-donation clash and potentially allows for the formation of an 18-electron compound. This is reflected in the Ti–N_{amide} distances of 1.970(2) and 1.959(2) Å, which are similar to those in **2.1** (1.9795(14) or 1.9726(15) Å). In comparison the compounds Ti(N_2N^{Me})($NNPh_2$)(py) (**1.72**) and Ti(N_2N^{Me})(N^tBu)(py) (**2.5**) which contain equatorially orientated hydrazido and imido ligands have significantly longer Ti–N_{amide} bond distances (2.0136(16) or 2.0033(15) Å and 2.037(2) or 2.023(2) Å) as a result as competitive π-donation with the multiple bond. Nonetheless, there is an inherent ambiguity in the extent of pi-donation in these systems with there often being insufficient metal-based acceptor orbitals of the correct symmetry.

The titanium nitrogen bond in **1** is longer than was found in the analogous hydrazido compound **2.1** (1.7581(19) *vs*. 1.7444(14) Å). Arylimide and hydrazide M=N bond distances are typically very similar due to comparable σ- and π-bonding abilities, as discussed in Chapter One of this Thesis. Therefore, it is proposed that the elongated Ti=N bond is due a larger steric clash between the *ortho*-methyl imido substituents and the N_{amide} substituents than is experienced in **2.1**. This is reflected in the slightly shorter Ti–N_{amide} distances in **1** compared to **2.1**, mentioned above.

Addition of one equivalent of 2,2'-bipyridine to a benzene solution of **1** led to displacement of the equatorial pyridine ligand to form the six-coordinate 2,2'-bipyridyl complex Ti($N_2^{iPr}N^{Me}$)(NXyl)(bipy) (**2**). Diffraction-quality crystals were grown from a saturated benzene solution at room temperature and the solid-state structure is shown in Figure 2.5. Compound **2** adopts a six-coordinate distorted octahedral structure with the bipyridine ligand occupying the equatorial plane, and the imido ligand *trans* to the NMe donor. The Ti–N_{imide} bond length is now 1.770(3) Å, longer than what was observed in **1**. However, along with the almost linear Ti–N_{imide}–C_{ipso} angle of 177.78 °, this is still consistent with a formal triple titanium nitrogen bond. The Ti–N_{amide} and Ti–N_{amine} are also slightly longer than the analogous distances in **1**, as a result of the higher coordination number.

To assist with reactivity studies described later in this Thesis, an arylimido compound with bulkier *ortho* substituents supported by the $N_2^{iPr}N^{Me}$ ligand was also synthesised. The 2,6-diisopropylphenylimido substituent was employed and the compound Ti($N_2^{iPr}N^{Me}$)(NDipp)(py) (**3**) (Dipp = 2,6-$C_6H_3{}^iPr_2$) was isolated as a yellow powder in 60% yield following a salt metathesis reaction with Ti(NDipp)Cl_2(py)$_3$ (**2.6**)[99] (Scheme 2.2).



2.6 **3** **4**

Scheme 2.2. Synthesis of the imido compounds Ti($N_2^{iPr}N^{Me}$)(NDipp)(py) (**3**) and Ti($N_2^{iPr}N^{Me}$)(NDipp)(bipy) (**4**).

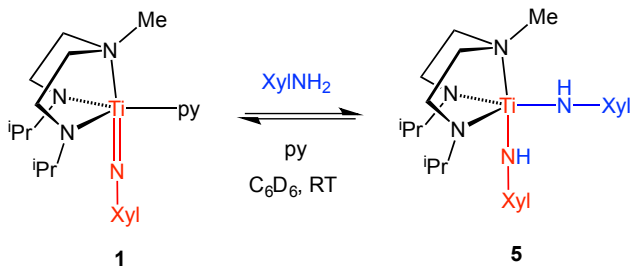
The six-coordinate 2,2'-bipyridyl compound Ti($N_2^{iPr}N^{Me}$)(NDipp)(bipy) (**4**) was also synthesised following substitution of the pyridine ligand (Scheme 2.2). Diffraction-quality crystals could not be obtained; however, the NMR data is fully consistent with C_s symmetric structures depicted. Both **3** and **4** were also characterised by IR spectroscopy and elemental analysis.

Chapter Three of this Thesis will describe the reactions of the imido compound **1** with terminal alkynes as a model for the reactions of the hydrazido compound **2.1**. In the hope that a bulkier imido substituent could provide further mechanistic information the reactions of **3** with terminal alkynes were also probed. However, it was found that the initial reactions of **3** did not differ from that of **1** and thus further reactivity studies were not pursued. Subsequently only the reactions of **1** with other small molecules are described below.

2.4 Reaction of Ti($N_2^{iPr}N^{Me}$)(NXyl)(py) (1) with N–H bonds

The reactions of X–H bonds with Group 4 imido and hydrazido compounds make up a small proportion of reactivity examples. However, these include 1,2-addition of Si–H and H–H bonds to yield hydride compounds,[51, 104] as well as sp^2 and sp C–H bond activation.[10, 53] Reactions with N–H bonds are typically limited to exchange reactions employed to synthesise hydrazides and other M=NR (R = aryl, O^{t}Bu) containing compounds from alkylimides.

When the reaction of **1** with $XylNH_2$ was followed by ^{1}H NMR spectroscopy at room temperature an equilibrium mixture of **1** and the new species Ti($N_2^{iPr}N^{Me}$)$(NHXyl)_2$ (**5**) (*ca*. 50% conversion) was formed (Equation 2.1). Addition of two further equivalents of $XylNH_2$ or, repeated removal of liberated pyridine *in vacuo* led to quantitative conversion. Conversely, addition of excess pyridine or one equivalent of 2,2'-bipyridine, led to complete formation of **1** or **2** respectively. On the preparative scale, **5** was obtained by crystallisation from hexane solution containing excess $XylNH_2$ at room temperature. Diffraction-quality crystals were obtained in the same manner. The solid-state structure is shown in Figure 2.7 and confirms compound **5** is the bis(xylylamide) species shown in Equation 2.1 resulting from transfer of one proton onto the N_{imide} atom of **1**.



Equation 2.1

The ^{1}H NMR spectrum of **5**, shown in Figure 2.6, is fully consistent with the C_s symmetric solid-state structure. Two sets of N(H)Xyl resonances are observed and were assigned through the use of a ^{1}H ROESY NMR experiment. The N–H resonance at 7.65 ppm is attributed to the *cis*-N(H)Xyl (*cis* refers to the position relative to NMe) as a through-space correlation to the NMe signal was observed. Subsequently, the remaining *cis*-N(H)Xyl and *trans*-N(H)Xyl resonances could be distinguished. A medium intensity ν(N–H) band at 3293 cm^{-1} in the IR spectra of **5** is present, although in principle two should be observed. The ^{1}H NMR spectrum of **5-*d*$_2$**, synthesised from **1** and XylND$_2$ is also shown in Figure 2.6, the N–H resonances are no longer observed and the corresponding signals are present in the ^{2}H NMR spectrum.

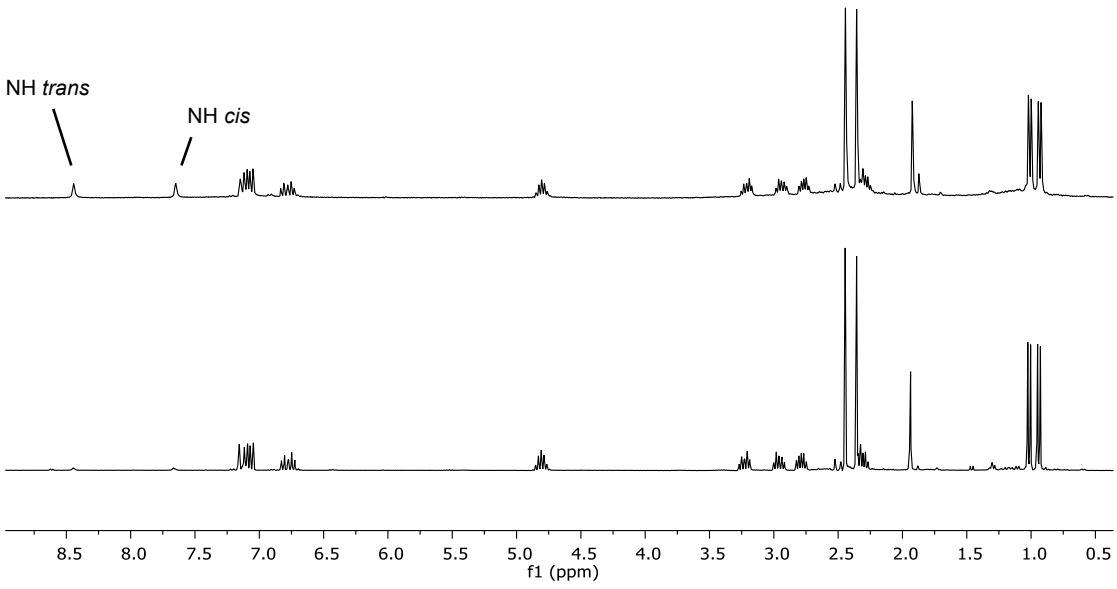


Figure 2.6. Top: ^{1}H NMR spectrum (299.9 MHz) of Ti($N_2^{iPr}N^{Me}$)(NHXyl)$_2$ (**5**) in C_6D_6 at 298 K. Bottom: ^{1}H NMR spectrum (299.9 MHz) of Ti($N_2^{iPr}N^{Me}$)(NDXyl)$_2$ (**5-*d*$_2$**) in C_6D_6 at 298 K.

Compound **5** is a five-coordinate distorted trigonal bipyramidal bis(xylylamide) compound with an N(1)-Ti(1)-N(3) angle of 169.04(3) ^{o}. The diamide-amine ligand is

facially bound occupying one axial and two equatorial sites. The -N(H)Xyl moiety containing the N(2) atom occupies the remaining equatorial position and the neutral NMe donor and remaining N(H)Xyl ligand (containing N(1)) occupy the axial sites. The Ti(1)-N(1) and Ti(1)-N(2) bond distances are within the expected region for titanium amide bonds (1.9884(7) and 1.9704(7) Å),[11, 13, 100] with the slightly shorter bond (Ti(1)-N(2) *cis* to NMe) present in the sterically less encumbered *cis* position. Interestingly the sum of the angles subtended at N(2) (346.4(1) °) deviates significantly from the expected trigonal planar geometry, in comparison the angles subtended at N(1) remains close to 360 ° (353.5(1) °). The space-filling model indicates that N(2) is forced to adopt this geometry due to steric clashes of the Xyl ring. The angles subtended at N(4) and N(5) are approximately 360 ° and the Ti(1)-N(4/5) bond lengths are 1.9579(6) and 1.9476(7) Å respectively, significantly shorter than in **1** reflecting the loss of the imido ligand.

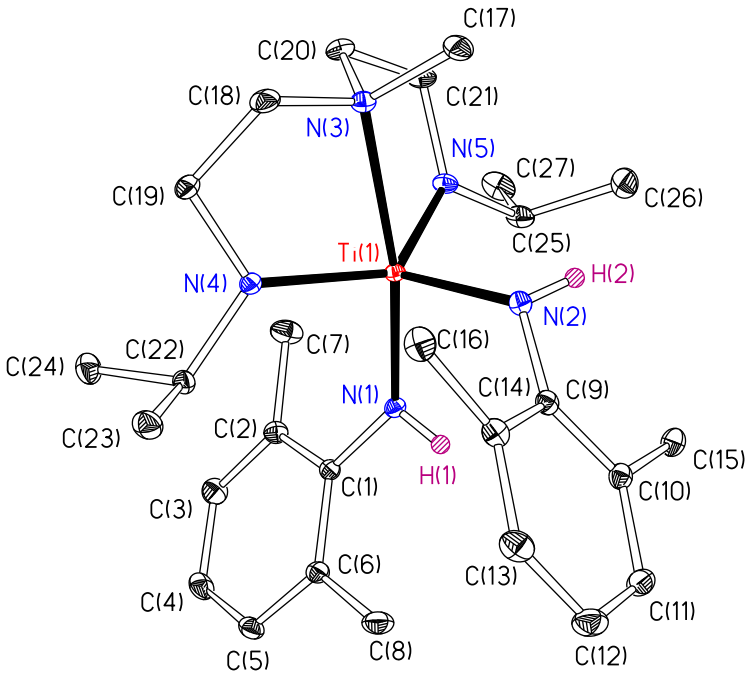


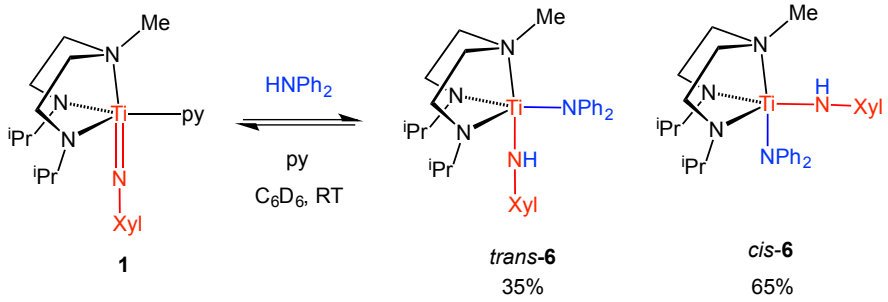
Figure 2.7. Displacement ellipsoid plot (20% probability) of Ti($N_2^{iPr}N^{Me}$)$(NHXyl)_2$ (**5**). Carbon-bound H atoms are omitted for clarity.

Table 2.2. Selected bond distances (Å) and angles (°) for Ti($N_2^{iPr}N^{Me}$)(NHXyl)$_2$ (**5**).

Ti(1)-N(1)	1.9884(7)	N(1)-Ti(1)-N(2)	95.23(3)
Ti(1)-N(2)	1.9704(7)	N(1)-Ti(1)-N(4)	96.51(3)
Ti(1)-N(3)	2.3054(7)	N(1)-Ti(1)-N(5)	103.50(3)
Ti(1)-N(4)	1.9579(6)	N(2)-Ti(1)-N(3)	95.53(3)
Ti(1)-N(5)	1.9476(7)	N(2)-Ti(1)-N(4)	117.71(3)
N(1)-C(1)	1.4012(10)	N(2)-Ti(1)-N(5)	105.79(3)
N(2)-C(9)	1.4060(10)	N(4)-Ti(1)-N(5)	129.81(3)
N(1)-H(1)	0.866(12)	Ti(1)-N(1)-C(1)	139.92(6)
N(2)-H(2)	0.867(12)	Ti(1)-N(2)-C(9)	128.17(5)
		Ti(1)-N(1)-H(1)	104.3(7)
		Ti(1)-N(2)-H(2)	106.2(8)
		H(1)-N(1)-C(1)	109.3(7)
		H(2)-N(2)-C(9)	112.0(7)

The secondary amine, Ph_2NH reacts in a similar manner with **1** resulting in a 1:4 equilibrium mixture of the imido compound **1** and the new species Ti($N_2^{iPr}N^{Me}$)(NHXyl)(NPh_2) (**6**) (Equation 2.2). Removal of the solvent and liberated pyridine *in vacuo* and redissolving the mixture in C_6D_6 results in > 95% conversion to **6**. Again addition of 2,2'-bipyridine to a mixture of **1** and **6** gives slow conversion to the six-coordinate imido compound **2**, demonstrating the reversibility of the N–H addition across the Ti–N_{imide} bond. Crystallisation from a saturated solution in benzene gave a small number of diffraction-quality crystals shown to be *trans*-Ti($N_2^{iPr}N^{Me}$)(NHXyl)(NPh_2) (*trans*-**6**, *trans* refers to relative position of N(H)Xyl and NMe). The molecular structure is shown in Figure 2.8, selected bond distances and angles are shown in Table 2.3 and will be discussed below. Compound **6** exists as a mixture of two isomers in a 2:1 ratio according to NMR integration. The isomers were assigned in solution through the use of a ^{1}H ROESY NMR experiment. An NOE between the NH resonance of the major isomer and the NMe signal of the major isomer, indicates that *cis*-Ti($N_2^{iPr}N^{Me}$)(NHXyl)(NPh_2) (*cis*-**6**) is the major isomer in solution. Moreover, the chemical shift of the NH proton in *cis*-**6** is similar to the *cis*-NH proton in **5** (7.83 and 7.65 ppm respectively) and the NH resonance attributed to

trans-Ti($N_2^{iPr}N^{Me}$)(NHXyl)(NPh_2) (*trans*-**6**) has a similar chemical shift to the *trans*-NH proton in **5** (8.34 and 8.45 ppm respectively), consistent with this isomer assignment. The ν(N–H) band is observed at 3260 cm^{-1} in the IR spectrum of **6**.



Equation 2.2

Compound **6** contains a five-coordinate titanium centre with a trigonal bipyramidal geometry. In addition to the *fac*-coordinated $N_2^{iPr}N^{Me}$ ligand (occupying one axial and two equatorial sites) there is an equatorially positioned NPh_2 group and a N(H)Xyl ligand *trans* to the NMe donor. The Ti(1)-N(4/5) bonds (1.9568(4) and 1.9596(4) Å) are shorter than in **1** (1.970(2) and 1.959(2) Å) and are similar to those in **5**, reflecting the absence of the strongly π-donating NXyl ligand. The Ti(1)-N(1) bond is very similar to the comparable bond in **5** (1.9854(4) *vs.* 1.9884(7) Å) and the Ti(1)-N(2) bond (2.0019(3) Å) is longer due to the bulky nature of the phenyl substituents. However, it is still within the usual range for titanium amide complexes and all four N_{amide} atoms have a trigonal planar geometry and sp^2 hybridization. The N(2)-C_{ipso} distances differ significantly, (1.4037(5) and 1.4382(6) Å) indicating delocalisation of the lone pair on N(2) into just one of the phenyl rings.

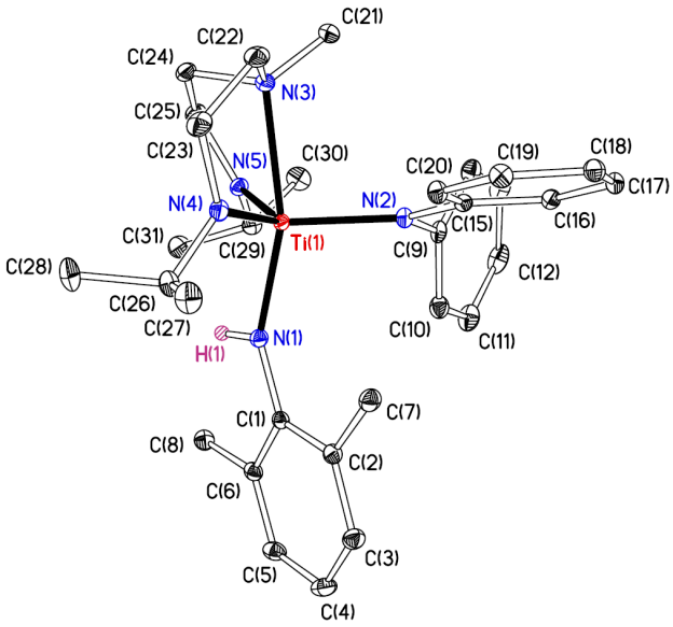


Figure 2.8 Displacement ellipsoid plot (20% probability) of Ti($N_2^{iPr}N^{Me}$)(NHXyl)(NPh_2) (*trans*-**6**). Carbon-bound H atoms are omitted for clarity.

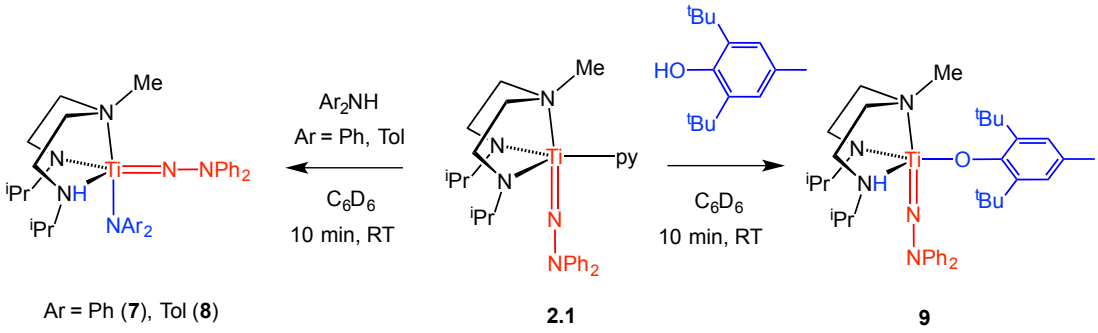
Table 2.3. Selected bond distances (Å) and angles (°) for Ti($N_2^{iPr}N^{Me}$)(NHXyl)(NPh_2) (*trans*-**6**).

Ti(1)-N(1)	1.9854(4)	N(1)-Ti(1)-N(2)	103.881(14)
Ti(1)-N(2)	2.0019(3)	N(1)-Ti(1)-N(4)	99.747(16)
Ti(1)-N(3)	2.2735(4)	N(1)-Ti(1)-N(5)	93.119(16)
Ti(1)-N(4)	1.9568(4)	N(2)-Ti(1)-N(3)	93.918(14)
Ti(1)-N(5)	1.9596(4)	N(2)-Ti(1)-N(4)	113.883(15)
N(1)-C(1)	1.3944(6)	N(2)-Ti(1)-N(5)	115.934(15)
N(2)-C(9)	1.4382(6)	N(4)-Ti(1)-N(5)	123.306(15)
N(2)-C(15)	1.4037(5)	Ti(1)-N(1)-C(1)	148.94(3)
N(1)-H(1)	0.875(7)	Ti(1)-N(2)-C(9)	111.51(3)
		Ti(1)-N(1)-H(1)	102.3(4)
		H(1)-N(1)-C(1)	108.3(4)
		Ti(1)-N(2)-C(15)	133.32(3)
		C(9)-N(2)-C(15)	115.17(3)

Transfer of protons from an external proton source onto a N_{imide} atom is common method for the synthesis of hydrazido compounds, and usually involves the transfer of two protons. The transfer of one proton to form bis(amide) compounds observed here is unusual and has previously only been seen with zirconium imido compounds.[105-107]

2.5 Reaction of Ti($N_2^{iPr}N^{Me}$)($NNPh_2$)(py) (2.1) with N–H and O–H bonds

Unfortunately reaction of the hydrazido compound Ti($N_2^{iPr}N^{Me}$)($NNPh_2$)(py) (**2.1**) with one equivalent of $XylNH_2$ yielded a complicated ^{1}H NMR spectrum in which no one compound could be distinguished. On standing at room temperature for 12 hours resonances associated with protio-ligand ($H_2N_2^{iPr}N^{Me}$) were observed. In contrast, addition of Ph_2NH gave immediate formation of Ti($HN_2^{iPr}N^{Me}$)($NNPh_2$)(NPh_2) (**7,** $HN_2^{iPr}N^{Me}$ = $MeN(CH_2CH_2N^iPr)(CH_2CH_2NH^iPr)$) where one of the N_{amide} atoms of the supporting ligand has been protonated and the hydrazido ligand remains intact (Scheme 2.3).



Scheme 2.3. Reaction of Ti($N_2^{iPr}N^{Me}$)($NNPh_2$)(py) (**2.1**) with N–H and O–H bonds.

The ^{1}H NMR spectrum of **7** is consistent with a single isomer C_1 symmetric product and characteristic inequivalent *iso*-propyl and methylene groups on the $N_2^{iPr}N^{Me}$ ligand are observed giving four doublets and eight multiplets respectively. The N(H)C<u>H</u>Me_2 resonance at 3.37 ppm is a doublet of septets due to three bond coupling to N–H as well as the methyl protons ($^3J_{CH\text{-}NH}$ = 5.7 Hz, $^3J_{CH\text{-}CH_3}$= 6.5 Hz). This resonance is significantly more shielded than the NC<u>H</u>Me_2 signal (4.42 ppm) and the corresponding signal in **2.1**. The fine structure of the N(<u>H</u>)CHMe_2 resonance at 2.13 ppm was not observed due to its broad nature however coupling to N(H)C<u>H</u>Me_2 was apparent form the 2D ^{1}H COSY NMR spectrum. The N<u>H</u> resonances in compounds **6** and **5** are considerably more deshielded (range 7.65 - 8.45 ppm) consistent with the formation of a different type of reaction product here. Addition of 2,2'-bipyridine

gave slow formation of the known hydrazido compound Ti($N_2^{iPr}N^{Me}$)($NNPh_2$)(bipy) (**2.7**)[108] containing the bidentate ligand and liberated Ph_2NH.

On a preparative scale, **7** was isolated as a pale brown powder in 72% yield and a very weak ν(N–H) band was observed at 3236 cm^{-1} in the solid-state nujol IR spectrum. Unfortunately, all attempts to grow diffraction-quality crystals were unsuccessful due to the instability of **7** in solution. On standing over several hours in C_6D_6 $H_2N_2^{iPr}N^{Me}$ was observed possibly due to a redistribution reaction. A ^{1}H ROESY NMR experiment to determine whether the hydrazido ligand occupies the axial or equatorial position was not possible due to overlapping NPh_2 and $NNPh_2$ aromatic resonances that could not be distinguished. To aid with isomer assignment the reaction of **2.1** with Tol_2NH was carried out on an NMR tube scale. This gave the analogous reaction product Ti($HN_2^{iPr}N^{Me}$)($NNPh_2$)($NTol_2$) (**8**) with distinguishable -$NTol_2$ and -$NNPh_2$ aromatic signals. A through-space correlation between the *o*-Ph resonance of the hydrazido ligand and the NMe resonance in the ^{1}H ROESY spectrum suggests the hydrazido ligand occupies the equatorial position. This is surprising as it places the titanium-nitrogen multiple bond in the electronically disfavoured position and the NAr_2 ligand in the sterically more demanding position. The monoanionic diamine-amide supporting ligand may create a different steric and electronic environment around the metal centre causing electronic and steric preferences to differ.

With the hope of synthesising a more crystalline reaction product, **2.1** was mixed with one equivalent of H-BHT (H-BHT = HO-2,4,6-$C_6H_3{}^tBu_2Me$). Quantitative formation of the hydrazido compound Ti($HN_2^{iPr}N^{Me}$)($NNPh_2$)(BHT) (**9**) was observed on the NMR tube scale and a red powder was obtained in 49% yield on a preparative scale (Scheme 2.3). The ^{1}H and ^{13}C NMR data are consistent with a C_1 symmetric structure, analogous to that of **7** and **8** and the NH resonance is observed in the same region (2.25 - 1.94 ppm, overlapping with methylene protons). Interestingly the NH proton does not demonstrate through-bond coupling to the methine proton (N(H)C<u>H</u>Me_2), and both methine resonances appear as septets. However the N(H)C<u>H</u>Me_2 resonance appears significantly upfield of the NC<u>H</u>Me_2 proton (3.90 *vs.* 5.77 ppm), like in **7** and **8**. Two distinct ^{t}Bu resonances are observed each of relative intensity 9H, as well as two aromatic singlets each of relative intensity 1H due to restricted rotation about the Ti–O bond. Diffraction-quality crystals were grown from a saturated benzene solution confirming the connectivity shown in Scheme 2.3. Interestingly addition of an

equivalent of 2,2'-bipyridine to **9** gave no reaction, unlike with **7** and **8**, probably due to the oxophilicity of titanium. Subsequently the reaction of **1** with H-BHT was carried out on the NMR tube scale. Disappointingly, a complicated ^{1}H NMR spectrum was obtained from which no one species could be identified. This is postulated to be due to competitive protonation of the N_{imide} and N_{amide} atoms.

The molecular structure and selected bond lengths and angles are given in Figure 2.9 and Table 2.4. Compound **9** contains a five-coordinate titanium centre with approximately trigonal bipyramidal geometry. The hydrazido ligand occupies the axial position *trans* to the NMe donor and the three equatorial positions are occupied by the BHT(1-) ligand and both the $^{iPr}N_{amide}$(1-) and $^{iPr}NH_{amine}$ atoms of the $HN_2{}^{iPr}N^{Me}$ supporting ligand. The Ti(1)-N(1) bond distance is the same with error to that in **2.1** which, along with almost linear Ti(1)-N(1)-N(2) angle of 178.85(9) ^{o}, confirms the hydrazido ligand remains intact. The long Ti(1)-N(5) distance of 2.2601(10) Å along with the trigonal pyramidal geometry at N(5) are consistent with a neutral amine donor. In comparison the Ti(1)-N(4) distance of 1.9727(10) Å remains similar to the Ti–N_{amide} bond distances in **2.1** and the trigonal planar geometry is maintained. Finally it is noted that the Ti(1)-N(3) and Ti(1)-O(1) bond distances lies within the expected range for such bonds.[100]

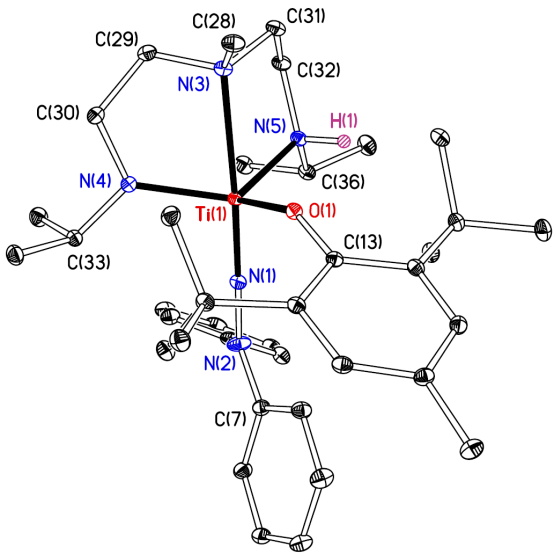


Figure 2.9. Displacement ellipsoid plot (20% probability) of $Ti(HN_2^{iPr}N^{Me})(NNPh_2)(BHT)$ (**9**)**.** Carbon-bound H atoms are omitted for clarity.

Table 2.4 Selected bond distances (Å) and angles (°) for $Ti(HN_2^{iPr}N^{Me})(NNPh_2)(BHT)$ (**9**).

Ti(1)-N(1)	1.7453(10)	Ti(1)-N(1)-N(2)	178.85(9)
Ti(1)-O(1)	1.9257(8)	Ti(1)-O(1)-C(13)	148.19(7)
Ti(1)-N(3)	2.4424(10)	O(1)-Ti(1)-N(4)	122.57(4)
Ti(1)-N(4)	1.9729(10)	O(1)-Ti(1)-N(5)	108.82(3)
Ti(1)-N(5)	2.2604(10)	N(4)-Ti(1)-N(5)	118.24(4)
N(1)-N(2)	1.3600(14)	N(1)-Ti(1)-N(3)	167.75(4)

The solid state IR spectrum displays two ν(N–H) bands at 3278 and 3247 cm^{-1}, in contrast the solution phase (benzene) IR spectrum contains just one ν(N–H) band at 3250 cm^{-1}. This is postulated to be due to two geometric isomers in the solid state of which only one molecular structure was obtained.

As discussed the reaction of imido compounds with proton sources typically results in two protons transfers to yield a new multiply bonded ligand, in some cases a single protonation can occur yielding an amide ligand. Interestingly the Group 6 imido compound $W(N_2N^{py})(NPh)Me_2$ reacts with $[PhMe_2NH][BAr^F{}_4]$ to give the N_2N^{py}-

protonated product $[W(HN_2N^{py})(NPh)Me_2][BAr^F{}_4]$ containing a monoanionic unsymmetrical supporting ligand as described above.[92]

In comparison, examples of the reactions of hydrazido compounds with proton sources are limited. Two examples of the protonation of Group 4 hydrazide(2-) have reported. Odom described the N_β-protonated compound $[Ti(dpma)(^tBu\text{-}bipy)(NNH_2Ph)]^+$ from the reaction of the hydrazide precursor with HOTf. However, it was not structurally authenticated.[35] The N_α-protonated compound $[Cp^*Ti\{MeC(N^iPr)_2\}\{N(NMe_2)H\}]^+$ was described by Mountford following the reaction of $Cp^*Ti\{MeC(N^iPr)_2\}(NNMe_2)$ with $[Et_3NH][BPh_4]$.[51] A number of other Group 4 hydrazide (1-) complexes possessing either a κ^1- or κ^2-N(NRR′)H ligand have been reported.[31, 47, 56, 109-111] However none were prepared from protonation of a hydrazide(2-) ligand. Many N_α- and N_β-protonated Group 6 hydrazide complexes have been described[112-114] and both experimental and DFT studies suggest that protonation at N_β can be preferred but rapid 1,2-proton shift can occur to yield N_α-protonated compounds.[115-117]

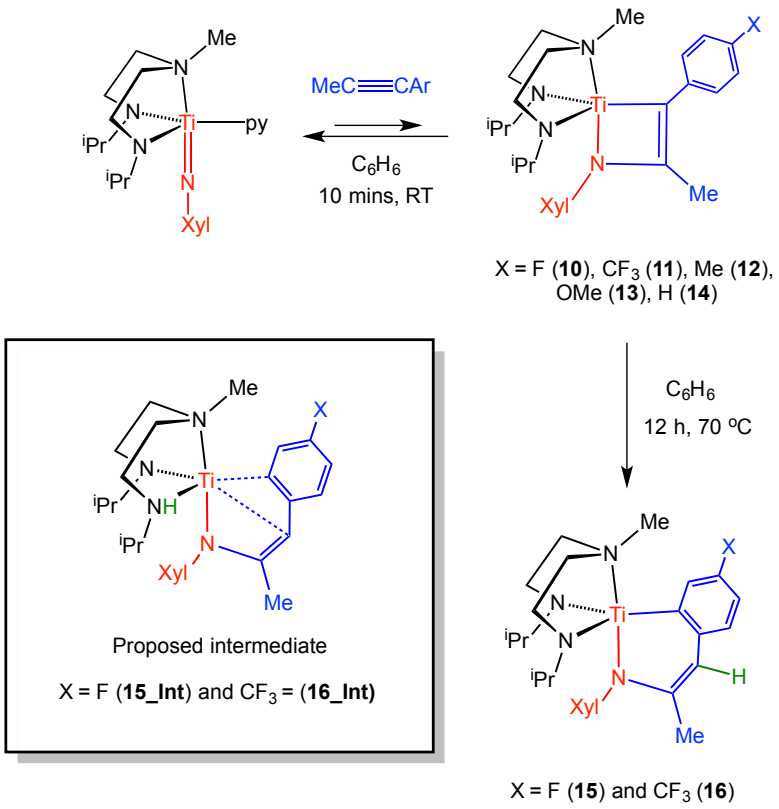
Here protonation of an N_{amide} atom has occurred rather than at the hydrazido ligand. This type of protonation has been observed before on a diamide-amine supported titanium complex, but not in a controlled manner. When the imido compound $Ti(N_2N^{Me})(N^tBu)(py)$ (**2.5**) was reacted with Ph_2NNH_2 only 35% conversion to the desired hydrazide compound $Ti(N_2N^{Me})(NNPh_2)(py)$ (**1.72**) was observed due to concomitant protonation of the N_{amide} atoms of the ligand releasing protio-ligand (compound **1.72** could be synthesised cleanly from $Ti(NNPh_2)Cl_2(py)_3$ (**1.69**) and $Li_2N_2N^{Me}$).[39] However here, more electron-releasing N_{amide} substituents (^{i}Pr compared to $SiMe_3$) result in more basic N_{amide} atoms, which, along with their smaller size allow protonation to occur exclusively at this site.

The differing sites of protonation of **1** and **2.1** are probably due to a delicate balance of basicity and π-donor ability. A shorter Ti=N bond in **2.1** leads to longer Ti–N_{amide} bonds and thus more basic N_{amide} atoms. Moreover, preferential protonation of the N_{imide} atom rather than N_{amide} in **1** and N_{amide} over $N_{hydrazide}$ in **2.1** is consistent with decreased acidity of aniline compared to hydrazine.[118, 119]

2.6 Reaction of Ti($N_2^{iPr}N^{Me}$)(NXyl)(py) (1) with internal alkynes

As mentioned in the introduction to this Thesis, reactions of Group 4 imides and hydrazides with alkynes has been a topic of growing interest for the past 20 years.[9-14, 24-27, 29, 31, 32, 34, 36, 37, 40, 42, 44, 50, 62, 66, 68, 71, 72, 74-76, 120-128] The reactions of **1** and **2.1** with terminal alkynes will be discussed in detail in the next chapter of this Thesis and the reactions with internal alkynes below.

The imido compound Ti($N_2^{iPr}N^{Me}$)(NXyl)(py) (**1**) reacts with the internal alkynes MeCC-4-C_6H_4X (X = F, CF_3, Me, OMe, H), to yield equilibrium mixtures of **1** and the azatitanocyclobutene complexes Ti($N_2^{iPr}N^{Me}$){N(2,6-$C_6H_3Me_2$)C(Me)C(4-C_6H_4X)} (X = F (**10**), CF_3 (**11**), Me (**12**), OMe (**13**), H (**14**)) (Scheme 2.4). The imido ligand has undergone a formal [2+2] cycloaddition. The formation of such metallacyclic species is well documented in both imido and hydrazido chemistry as stoichiometric reaction products as well as intermediates in catalytic cycles.[10, 12, 13, 44, 71, 106, 120, 121, 125, 126, 129, 130] Conversion to the metallacyclic products could be increased *via* repeated removal of the liberated pyridine *in vacuo* and redissolving in benzene. However, eventually this leads to decomposition of the compounds. Similarly an excess of alkyne could be used to increase the conversion. With MeCC-4-C_6H_4X (X = Me, OMe, H) using one equivalent gives just 15 - 20% conversion, increasing this to three to five equivalents gives between 40 and 55% conversion to **12** - **14** following removal of the liberated pyridine. Higher conversion was not possible without decomposition of the reaction mixture. Similarly, reaction with one equivalent of MeCC-4-C_6H_4X (X = F, CF_3) and removal of the liberated pyridine yielded **10** and **11** in 30 and 70% conversion respectively, achieving higher conversion was here hindered due to the onward reaction of **10** and **11** (*vide infra*). Thus, **10** - **14**, were characterised *in situ* as mixtures with **1** by NMR spectroscopy. Addition of excess pyridine to a solution containing an equilibrium mixture of **10** - **12** and **1** results in complete conversion to **1** and free MeCC-4-C_6H_4X (X = F, CF_3, Me) indicative of a reversible reaction.



Scheme 2.4. Reaction of Ti($N_2^{iPr}N^{Me}$)(NXyl)(py) (**1**) with internal alkynes

The azatitanacyclobutene species exist exclusively as anti-Markovnikov *trans* isomers. The anti-Markovnikov nature results from the regiochemistry of the cycloaddition reaction which places the ArC bound to Ti and the MeC bound to N. This regiochemistry has been observed in several crystallographically characterised azatitanacyclobutene complexes,[44, 120, 126] and the NMR data obtained here are fully consistent with this regiochemistry. The ArC=CMe and ArC=CMe resonances appear in the characteristic regions of 201.3 - 206.7 ppm and 167.34 - 167.9 ppm respectively in the ^{13}C NMR spectrum, and a through-bond correlations between the titanium bound carbon atom and *ortho*-aromatic protons was observed in all cases. Recently Gade *et al*. reported the synthesis and X-ray structure of the first Markovnikov cycloaddition product of an imidotitanium complex with a terminal alkyne.[53] The *trans* assignment refers to the *trans* arrangement of the Ti–N bond of the metallacycle to the NMe donor. 2D NOE experiments were carried out in order to confirm this assignment but were inconclusive.

Heating an equilibrium mixture of the imido species **1** and **10** or **11** at 70 ^{o}C gave a greater proportion of the metallacyclic species. However, in both cases irreversible formation of a third compound was also observed. Resonances attributed to the new compounds were observed prior to complete conversion of **1** to **10** or **11** even at room temperature. Heating the solutions for 16 hours at 70 ^{o}C resulted in quantitative conversion on the NMR tube scale. No new compounds were observed when **12**, **13** or **14** were heated at 70 ^{o}C for several hours. Crystalline red powders were isolated on a preparative scale in 30% yield following precipitation from a hexane solution. The low yields are attributed to the compounds high solubility. Diffraction-quality crystals were grown from concentrated hexane solutions at room temperature in both cases, allowing the compounds to be identified as Ti($N_2^{iPr}N^{Me}$){N(2,6-$C_6H_3Me_2$)C(Me)C(H)C(C_6H_3F)} (**15**) and Ti($N_2^{iPr}N^{Me}$){N(2,6-$C_6H_3Me_2$)C(Me)C(H)C($C_6H_3CF_3$)} (**16**) (Scheme 2.4). The solid-state structures are shown in Figure 2.9 and selected bond distances and angles in Table 2.5.

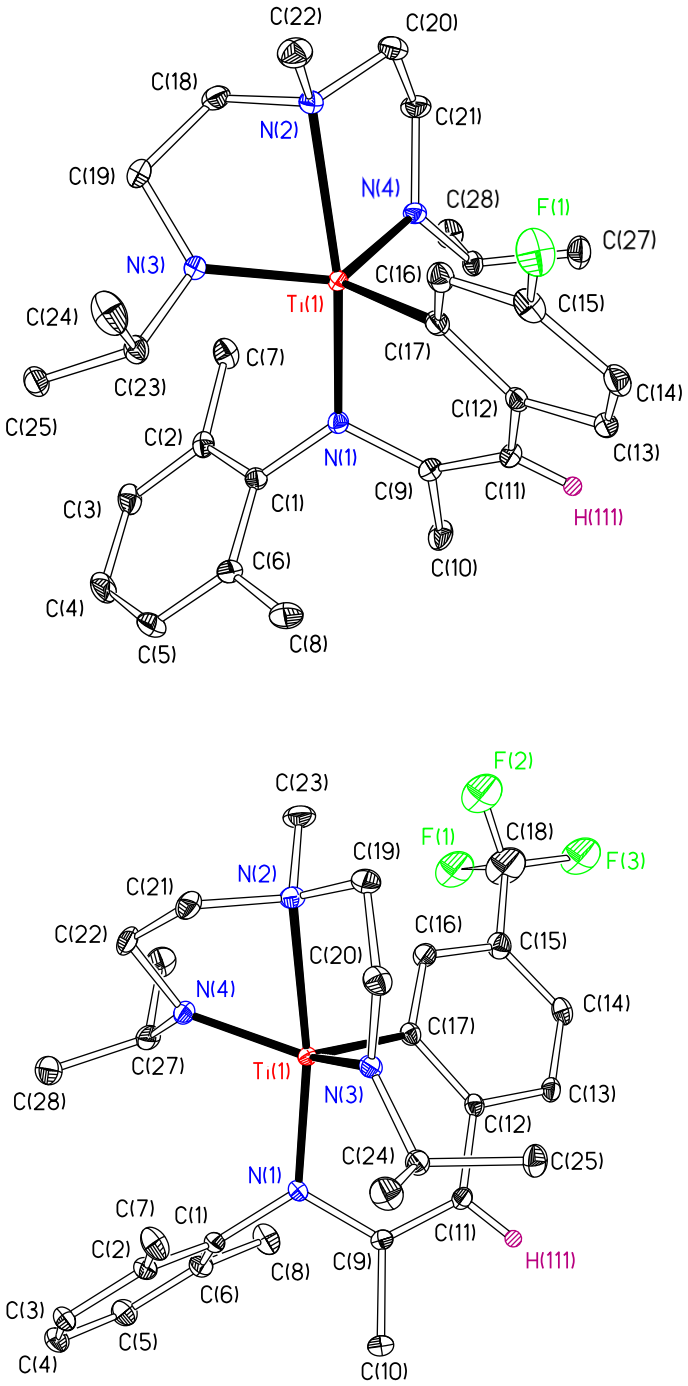


Figure 2.9. Displacement ellipsoid plot (20% probability) of Ti($N_2^{iPr}N^{Me}$){N(2,6-$C_6H_3Me_2$)C(Me)C(H)C(C_6H_3F)} (**15**) (top) and Ti($N_2^{iPr}N^{Me}$){N(2,6-$C_6H_3Me_2$)C(Me)C(H)C($C_6H_3CF_3$)} (**16**) (bottom). H atoms except H(111) are omitted for clarity.

Table 2.5. Selected bond distances and angles for Ti($N_2^{iPr}N^{Me}$){N(2,6-$C_6H_3Me_2$)C(Me)C(H)C(C_6H_3F)} (**15**) and Ti($N_2^{iPr}N^{Me}$){N(2,6-$C_6H_3Me_2$)C(Me)C(H)C($C_6H_3CF_3$)} (**16**).

Parameter	**15**	**16**
Ti(1)-N(1)	1.9800(18)	1.9845(17)
Ti(1)-N(2)	2.3365(19)	2.3450(18)
Ti(1)-N(3)	1.930(2)	1.9606(17)
Ti(1)-N(4)	1.9605(19)	1.9247(18)
Ti(1)-C(17)	2.119(2)	2.123(2)
N(1)-C(1)	1.429(3)	1.435(2)
N(1)-C(9)	1.403(3)	1.398(3)
C(9)-C(10)	1.511(3)	1.512(3)
C(9)-C(11)	1.354(3)	1.361(3)
C(11)-C(12)	1.447(3)	1.450(3)
C(12)-C(17)	1.421(3)	1.416(3)
C(12)-C(13)	1.413(3)	1.415(3)
C(13)-C(14)	1.381(4)	1.375(3)
C(14)-C(15)	1.378(4)	1.393(3)
C(15)-C(16)	1.375(3)	1.394(3)
C(16)-C(17)	1.409(3)	1.407(3)
N(1)-Ti(1)-C(17)	90.76(8)	90.62(8)
N(1)-Ti(1)-N(3)	99.60(8)	101.83(7)
N(1)-Ti(1)-N(4)	102.69(8)	100.21(7)
C(17)-Ti(1)-N(3)	111.95(9)	109.10(8)
C(17)-Ti(1)-N(4)	109.84(9)	114.07(8)
C(17)-C(12)-C(11)	122.8(2)	122.86(18)
C(11)-C(9)-N(1)	123.2(2)	123.64(19)
C(9)-N(1)-Ti(1)	116.62(14)	117.03(13)

Compounds **15** and **16** are *ortho*-metallated vinylamide species with the vinylamide moiety and *ortho*-metallated aromatic ring contained within the same six-membered ring. The amide moiety is *trans* to the NMe donor and the titanium carbon bond to the C_6H_3X ring occupies the equatorial position *cis* to the NMe donor in both cases. The diamide-amine ligands occupy the remaining axial sites and two equatorial sites giving five-coordinate distorted trigonal bipyramidal complexes. The orientation of the -NXyl moiety *trans* to NMe is consistent with the assignment of **10** and **11** as the *trans* isomers.

The Ti(1)-N(1) bond distances of 1.9800(18) and 1.9845(17) Å for **15** and **16** are typical of amide(1-) interactions and are similar in length to some titanium vinylamide compounds discussed in the next chapter. The N(1)-C(9) bond distances of 1.403(3) and 1.398(3) Å for **15** and **16** are within the expected region for nitrogen-carbon single bonds, however, show a slight reduction in comparison to other carbon-nitrogen single bonds within the same compounds (for example, N(3)-C(19) and N(3)-C(23) are 1.456(3) Å and 1.474(3) Å respectively in **15**), suggesting a small amount of delocalisation of the N(1) lone pair into the vinyl moiety. The C(9)-C(11) bond lengths of 1.354(3) and 1.361(3) Å are indicative of double bonds and thus both **15** and **16** are well described by the valence bond representations shown in Scheme 2.4.

The Ti(1)-C(1) bond distances of 2.119(2) and 2.123(2) Å for **15** and **16** are consistent with σ-interactions of titanium with a sp^2 aromatic carbon atom.[100] For example, the compound $\{(C_5H_4)SiMe_2(N^tBu)\}Ti\{(o\text{-}C_6H_4)C(Ph)=C(Ph)\}$ contains a titanium-carbon bond to an aromatic ring with a vinyl substituent and has the distance 2.081(7) Å.[131] Similarly, the compound $[\{o\text{-}C_6H_4(CH=N\text{-}2,6\text{-}C_6H_3{}^iPr)\}TiCl_3]$ contains a Ti–Ar bond within a metallacycle and was found to be 2.109(2) Å.[132] The Ti(1)-N(3) and Ti(1)-N(4) bond distances are shorter than the comparable distances in the starting imido compound due to increased $N_{2p(\pi)} \rightarrow Ti_{3d(\pi)}$ interactions (av. 1.9440(37) *vs.* 1.965(3) Å).

The mechanism for the formation of **15** and **16** is proposed to proceed *via* transfer of an *o*-aromatic proton onto an N_{amide} atom of the supporting ligand to yield intermediates depicted as **15_Int** and **16_Int,** shown in Scheme 2.4. Intermediates **15_Int** and **16_Int** contain partially formed bonds between the C=C atoms, and *o*-aromatic carbon atoms to titanium. Subsequent intramolecular hydrogen transfer to

C=C leads to Ti–$C_{aromatic}$ bond formation and the creation of a six-membered ring. An electron-withdrawing aryl substituent will render the *o*-aromatic protons more acidic allowing this transformation only when X = F or CF_3.

The room temperature ^{1}H and ^{13}C NMR spectra of **15** indicate that the compound possesses C_s symmetry in solution. A sharp doublet at 1.01 ppm is attributed to the 'outside' CHMe$_2$ protons (attached to C(24) and C(37)) and the broad doublet at 0.66 ppm to the 'inside' CHMe$_2$ protons (attached to C(25) and C(28)), confirmed by ^{1}H ROESY NMR experiments. On cooling a sample of **15** to -60 ^{o}C in toluene-d_8, the $N_2^{iPr}N^{Me}$ ligand *iso*-propyl resonances decoalesed into four doublets (three overlapping) due to diastereotopic CHMe$_2$ groups and two broad multiplets (CHMe$_2$) which could be identified as septets at -80 ^{o}C, consistent with a C_1 symmetric compound (Figure 2.10).

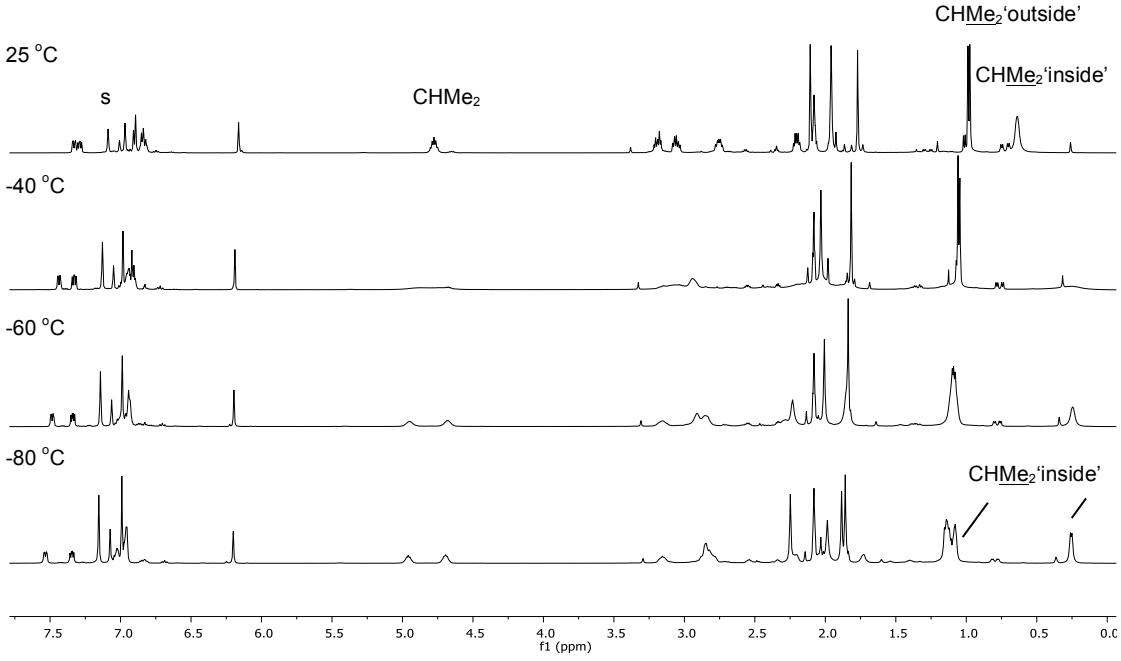


Figure 2.10. ^{1}H NMR spectra (499.9 MHz) of Ti($N_2^{iPr}N^{Me}$){N(2,6-$C_6H_3Me_2$)C(Me)C(H)C(C_6H_3F)} (**15**) in toluene-d_8 at 25 ^{o}C, -40 ^{o}C, -60 ^{o}C and -80 ^{o}C. 's' denotes residual protio solvent.

In the solid-state structure of **15** the xylyl ring points out of the vertical {N(1),N(2),C(17),Ti(1)} plane. Subsequently the N(1)-C(9) bond and ensuing metallacycle point into the plane. This results in an asymmetric compound with the xylyl ring close to the 'inside' methyl C(25) but far away from the 'inside' methyl

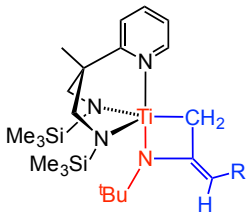
C(28) consistent with the ^{1}H NMR spectra obtained at low temperature. One of the CH$\underline{Me}_2$ doublets is significantly more shielded than the other three (0.31 *vs.* 1.13 - 1.18 ppm). This resonance is assigned to the protons attached to C(25), the centre of the xylyl ring in the solid-state structure of **15** is 2.744 Å away from C(25) and thus the protons experience a shielding ring current effect. The large chemical shift difference between the 'inside' $CHMe_2$ at -80 ^{o}C accounts for the broad signal at room temperature. A ^{13}C NMR spectra was recorded at -80 ^{o}C, four C$\underline{H}Me_2$, two C$\underline{H}Me_2$ and four CH_2 resonances were observed due to the $N_2^{iPr}N^{Me}$ ligand, fully consistent with a C_1 symmetric compound.

At room temperature a fluxional process allowing the xylyl ring to be positioned into the vertical plane close to C(28) can occur and a time averaged NMR spectra of the two conformers is observed. At -80 ^{o}C a spin saturation exchange was observed between the two C$\underline{H}Me_2$ resonances and the two 'inside' CH$\underline{Me}_2$ resonances indicating that conformational exchange is still occurring.

Compound **16** has comparable ^{1}H and ^{13}C NMR spectra to **15** at room temperature and at -80 ^{o}C suggesting the same fluxional conformation change is taking place. A minor set of signals were observed in the ^{1}H NMR spectra of **16** making up < 10% of the total, this is presumed to be a result of an isomer where by the NXyl amide moiety is *cis* to the NMe donor placing the Ti–C bond in the axial position. Many of the resonances overlap with the major isomer and no ^{13}C resonances could be identified corresponding to this isomer, thus full characterisation was not possible.

Azametallacyclobutenes of Group 4 are key intermediates in a range stoichiometric and catalytic C–N and C–C coupling reactions,[10, 106, 122, 125, 133] thus, their onward reaction either intermolecularly or intramolecularly is of interest. For example, the catalytic hydroamination of alkynes involves reaction of a metallacycle with an equivalent of primary amine to release the organic enamine,[73, 106, 133, 134] and catalytic iminoamination and carboamination of alkynes involve the insertion of an isocyanide or imine into the reactive M-C bond of a azametallacyclobutene intermediate.[121, 135-138] The azametallacyclobutene compound Ti($N_2^{Xyl}N^{py}$){κ^2-N(^{t}Bu)CH=CPh} ($N_2^{Xyl}N^{py}$ = MeC(2-C_5H_4N)($CH_2NXyl)_2$) undergoes several stoichiometric reactions including insertion of a chalogen atom to yield five-membered rings[139] and reaction with a second equivalent of alkyne to yield stable azatitanacyclohexadiene compounds.[130] No reaction with of the azatitanocyclobutuene compounds **10** - **14** was observed with

a second equivalent of alkyne. The imido compound Ti(N_2N^{py})(N^tBu)(py) (**1.60**) reacts with internal alkynes to also yield four-membered azatitanacycles but with the alkene bond outside of the four-membered ring (Figure 2.11).



1.62

Figure 2.11. Azatitanacycle obtained from the reaction of Ti(N_2N^{py})(N^tBu)(py) (**1.60**) with internal alkynes.

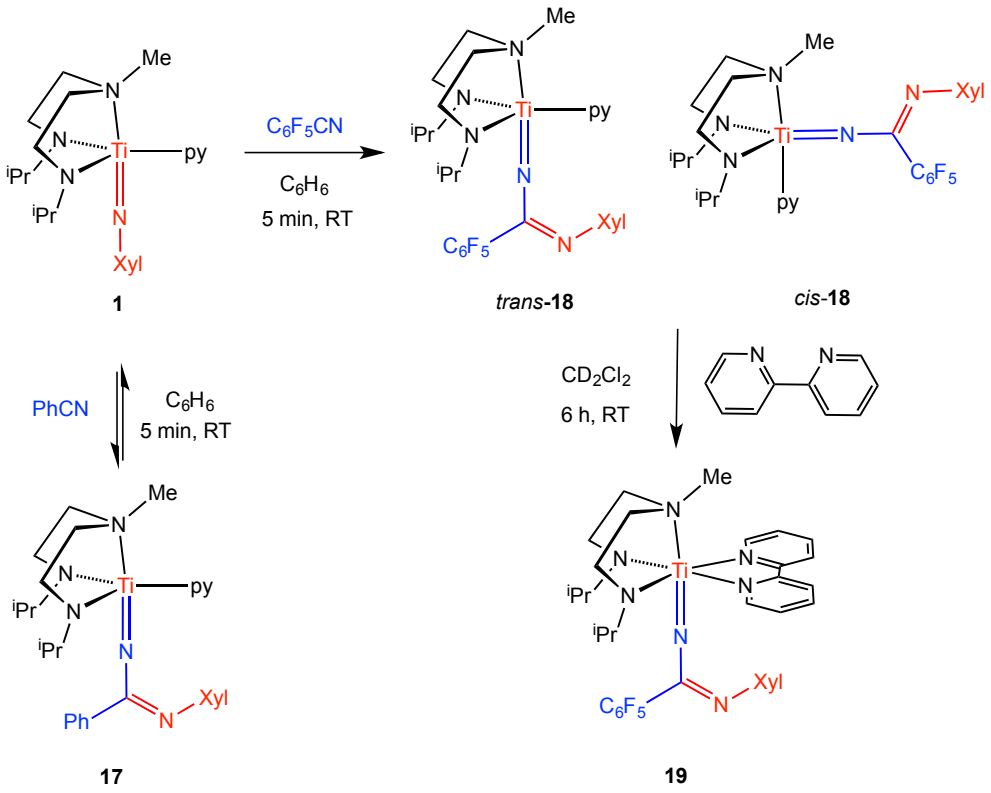
Proposed to be the result of a cycloaddition reaction between π-bonded allene ligand and an imido ligand following an initial C–H activation reaction and subsequent H atom transfer.[84] Therefore, although this intramolecular reaction is unprecedented in the reactions of azatitanocyclobutene species, unusual reactivity has been observed with internal alkynes before as well as subsequent reactivity at the Ti–C bond.

2.7 Reaction of Ti($N_2^{iPr}N^{Me}$)(NXyl)(py) (1) with nitriles

The reactions of transition metal nitrides,[140, 141] alkylidenes[121, 142-145] and alkylidynes[146-151] with nitriles are well established, the corresponding reactivity with transition metal imides is less well developed. In 2000 the reaction of the diamide-amine supported imido compound Ti(N_2N^{py})(N^tBu)(py) (**1.60**) with MeCN was reported to proceed *via* a cycloaddition reaction at the imido bond followed by a self-trapping dimerisation reaction to yield the dimeric complex (N_2N^{py})$_2$Ti$_2${μ-NC(Me)(N^tBu)}$_2$ (Scheme 1.5, Chapter One).[91] This compound was the first example of a doubly deprotonated μ-η^2-N-monosubstituted amidinate ligand. Subsequently, reactivity studies of titanium hydrazido, alkylidene hydrazido and alkoxyimido compounds have included organic nitriles. The hydrazido compound Ti(N_2N^{py})($NNPh_2$)(py) (**1.75**) reacts with MeCN to give an analogous dimeric species, in contrast Ti(N_2N^{Me})($NNPh_2$)(py) (**1.72**) gave mixtures with MeCN or PhCN.[46] However, both compounds along with the diamide-ether supported compounds **1.70** and **1.107** react with fluorinated benzonitriles to give net Ti=N insertion products of the type (L)Ti{NC(Ar)$NNPh_2$}(py)$_n$ (n = 1 or 2) containing hydrazonamide ligands.[54] The same Ti=N insertion was observed with the alkoxyimido compound

Cp*Ti{PhC(N^{i}Pr)$_2$}(NO^{t}Bu) (**1.158**) to yield compounds containing a new class of *tert*-butoxybenzimidamide ligands.[80] The new *tert*-butoxybenzimidamide functionality reacts with a further two equivalents of C_6F_5CN across the Ti=N bond to yield six-membered rings. Comparable "double insertion" reaction products were observed with the alkylidene hydrazido compound **1.147**.[152] Double nitrile insertion reactions have also been reported with the transient oxo and sulfido complexes Cp*$_2$Zr(E) (E = O or S).[3] Recently, reaction of a scandium imido compound with PhCN has been described to proceed *via* a [2+2] cycloaddition reaction at the multiple bond followed by a C–H activation reaction of the ligand yielding a N-monosubstituted monoanionic amidinate ligand.[153] Encouraged by the unusual reaction products of **1** and **2.1** with alkynes it was hoped to observe some novel reactivity with nitriles.

The reactions of the imido compound **1** with organic nitriles are summarised in Scheme 2.5. Disappointingly, reaction with MeCN resulted in a mixture of compounds. However, the insertion products Ti($N_2^{iPr}N^{Me}$)(NC(Ar)NXyl)(py) (Ar = Ph (**17**)), C_6F_5 (**18**)) were obtained from reaction with PhCN and C_6F_5CN respectively. Compounds **17** and **18** were isolated as yellow powders on a preparative scale and characterised by NMR and IR spectroscopy and elemental analysis, all of which are consistent with the addition of one equivalent of ArCN to **1**. The connectivity shown in Scheme 2.5 was confirmed by X-ray diffraction for **17** (*vide infra*). Full characterisation by NMR spectroscopy was carried out in CD_2Cl_2 in both cases due to low solubility in C_6D_6. However, the compounds were found to have limited stability in both CD_2Cl_2 and C_6D_6 and unidentified resonances were observed after several hours at room temperature. On dissolving a small amount of **17** in C_6D_6 an equilibrium was established and a 1:1 mixture of **1** and **17** was observed as well as liberated PhCN. In comparison pure **18** (*cis* and *trans*) shows no tendency to dissociate in solution, this is consistent with previously described examples of the reactions of titanium imides and hydrazides with nitriles where electron-withdrawing aryl groups have been reported to stabilise addition products.[46, 54, 80, 152] No reaction occurred with further equivalents of nitrile in either case.



Scheme 2.5. Reactions of Ti($N_2^{iPr}N^{Me}$)(NXyl)(py) (**1**) with organic nitriles.

Compound **18** exists as a mixture of two isomers in a 3:2 ratio according to NMR integration (^{1}H NMR spectrum shown in Figure 2.12). This is due to the ability of the amidinate(2-) ligand to occupy either the equatorial site *cis* to the NMe donor (*cis*-**18**) or the axial site *trans* to the NMe donor (*trans*-**18**). Spin saturation transfer measurements showed exchange on the NMR timescale between the isomers indicating facile *cis*/*trans* isomerisation, however, preventing meaningful NOE measurements and assignment of the isomers.

On addition of one equivalent of 2,2'-bipyridine to *cis*-**18** and *trans*-**18** on the NMR tube scale, quantitative conversion to Ti($N_2^{iPr}N^{Me}$)(NC(C_6F_5)NXyl)(bipy) (**19**) was observed after six hours, along with the release of pyridine (Scheme 2.5). Compound **19** was also found to be unstable in solution and decomposed over four hours, thus preventing characterisation by X-ray crystallography. However, the ^{1}H (Figure 2.12), ^{13}C and ^{19}F NMR spectra are consistent with a single isomer of a C_s-symmetric, six-coordinate complex containing a bidentate 2,2'-bipyridine ligand in the equatorial positions and the amidinate ligand in the axial position. Analogous reactions have been described for the hydrazido compound Ti(N_2N^{Me})($NNPh_2$)(py) which exists with $-NNPh_2$ in the *cis* position exclusively and, the alkoxyimido compound

$Ti(N_2N^{Me})(NO^tBu)(bipy)$ which exists a mixture of *cis* and *trans* isomers. On addition of 2,2'bipyridine the single isomer compounds $Ti(N_2N^{Me})(NNPh_2)(bipy)$ and $Ti(N_2N^{Me})(NO^tBu)(bipy)$ are formed containing the hydrazido and alkoxyimido ligands in the *trans* position.[78, 154]

The chemical shift of the N<u>Me</u> resonance is postulated to be diagnostic in determining whether the titanium nitrogen multiple bond is *cis* or *trans* to it. The signal being more shielded when *trans* to the electron rich multiple bond. The hydrazido compound $Ti(N_2^{iPr}N^{Me})(NNPh_2)(py)$ (**2.1**) exists as a mixture of *cis* and *trans* isomers with the NMe resonances observed at 2.49 and 1.28 ppm respectively. The NMe signal in the 2,2'-bipyridine analogue $Ti(N_2^{iPr}N^{Me})(NNPh_2)(bipy)$ (which exists exclusively as the *trans* isomer) is observed at 1.07 ppm, consistent with this. Therefore, the major isomer of **18** has been assigned as the *trans* isomer. The NMe resonance appears at 1.48 ppm compared to 1.88 ppm for the minor isomer and is also more similar to the analogous resonance in **19** (1.22 ppm, Figure 2.12). Similarly the major isomer C<u>H</u>Me_2 resonance is comparable to the analogous resonance in **19** (5.30 and 4.86 ppm) whereas the minor *cis* isomer C<u>H</u>Me_2 resonance appears at 3.73 ppm, again consistent with the major isomer being more structurally similar to **19**.

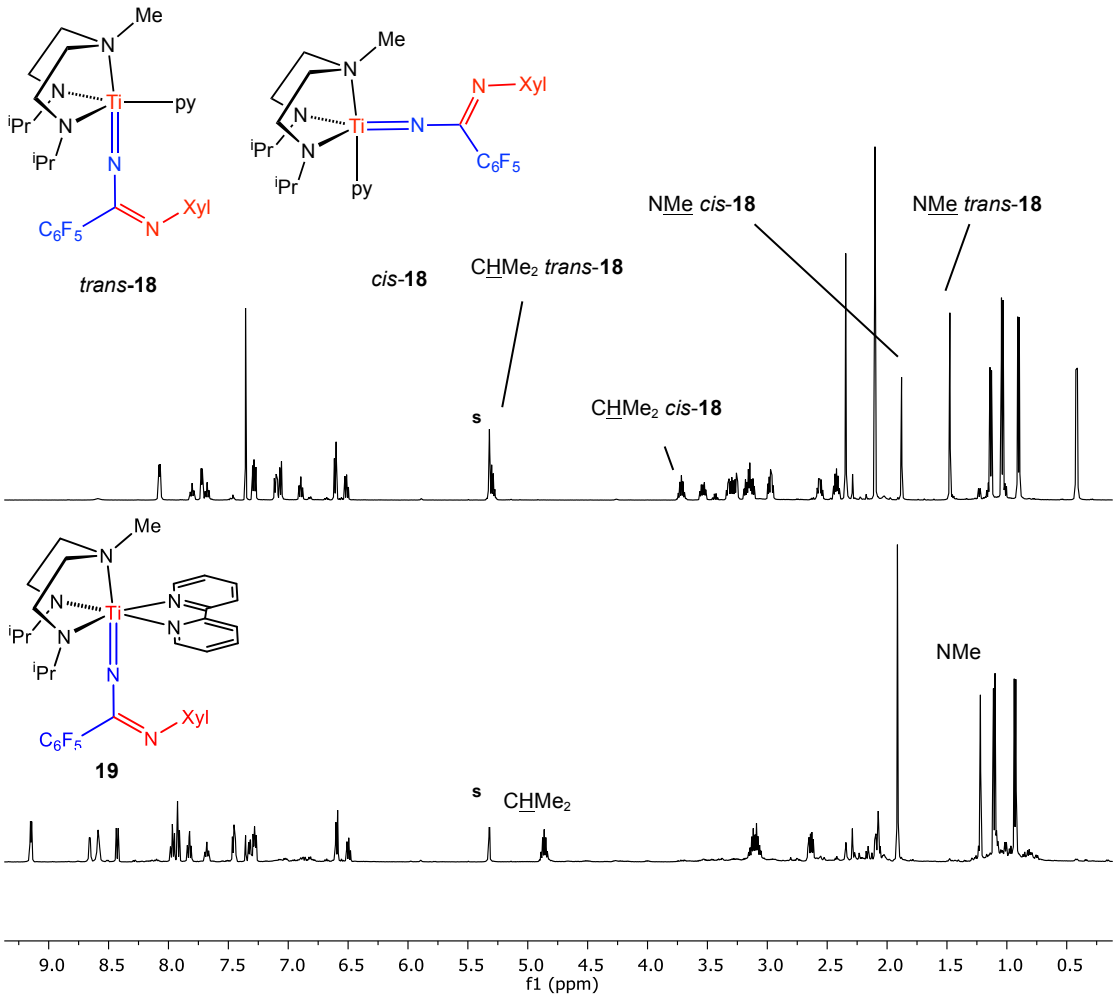


Figure 2.12. Top: ^{1}H NMR spectrum (500.3 MHz, 298K) of Ti($N_2^{iPr}N^{Me}$)(NC(C_6F_5)NXyl)(py) (**18**) in CD_2Cl_2. Bottom: ^{1}H NMR spectrum (500.3 MHz, 298K) of Ti($N_2^{iPr}N^{Me}$)(NC(C_6F_5)NXyl)(bipy) (**19**) in CD_2Cl_2. "s" denotes residual protio-solvent.

Diffraction-quality crystals of **17** were obtained by slow cooling of a saturated benzene solution from 70 °C to room temperature. The molecular structure is shown in Figure 2.13 along with selected distances and angles in Table 2.6. Ti($N_2^{iPr}N^{Me}$){NC(Ph)NXyl}(py) (**17**) is a five-coordinate N-monosubstituted amidinate(2-) complex resulting from the net insertion of one equivalent PhCN into the Ti=N triple bond of **1**. The amidinate(2-) ligand lies in the axial position *trans* to the NMe donor and the pyridine ligand occupies the equatorial site. This is the same orientation of multiple bond and neutral donor observed in **1**. The Ti(1)-N(1) bond length (1.7751(14) Å) is longer than in **1** (1.7581(19) Å), suggesting diminished Ti=N multiple bonding character; however along with the almost linear angle subtended at

N(1) (168.44(14) °), is still consistent with sp hybridisation at N(1) and a formal Ti≡N triple bond. Associated molecular structures of hydrazonamides (L)Ti{NC(Ar)NNPh$_2$}(py)$_n$ (n = 1 or 2) also show longer Ti=N bond lengths when compared to the parent hydrazido compounds (L)Ti(NNPh$_2$)(py)$_n$. The distances within the NC(Ph)NXyl ligand are consistent with the valence bond representations in Scheme 2.5. The N(1)-C(1) (1.339(2) Å) and N(2)-C(1) (1.295(3) Å) distances are consistent with C–N single and C=N double bonds respectively suggesting limited delocalisation across the Ti=NC(Ph)NXyl fragment.[155] The sum of the angles subtended at C(1) is 359.96(29) ° indicating sp^2 hybridisation and a trigonal planar environment. Both the Ti(1)-N(3) and Ti(1)-N(6) bond lengths (2.3531(15) and 2.1818(15) Å respectively) are typical of neutral nitrogen σ-only interactions with titanium, with the Ti(1)-N(3) bond length being longer as a result of the *trans*-labilising effect of the multiple bond. The Ti–N$_{amide}$ distances are the same within error to what was observed in **1** (av. 1.9617(21) *vs.* 1.965(3) Å). Interestingly, the pyridine donor ligand is orientated directly above the xylyl moiety in the same plane. This results in some relatively close contacts between the ring carbon (C(28)···C(10) = 3.713 Å and C(31)···C(13) = 3.569 Å) as a result of π-stacking between the rings.

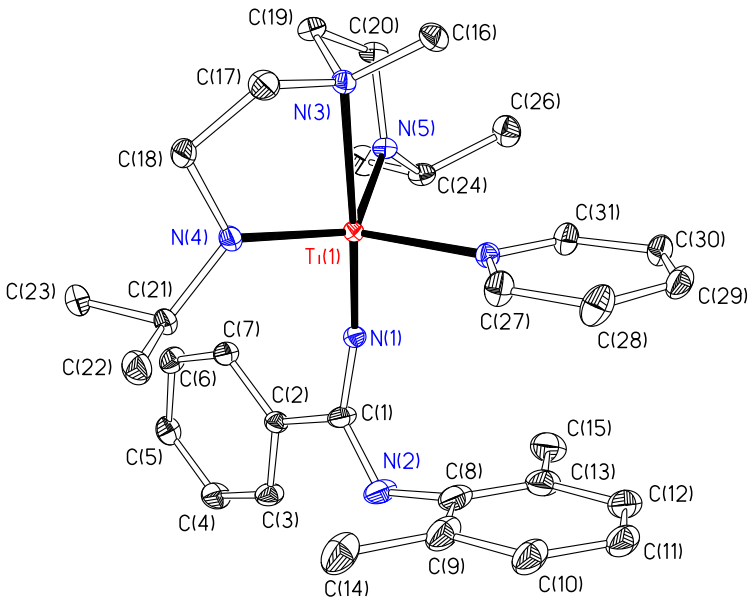


Figure 2.13. Displacement ellipsoid plot (20% probability) of Ti(N$_2$^{iPr}N^{Me}){NC(Ph)NXyl}(py) (**17**). H atoms are omitted for clarity.

Table 2.6. Selected bond distances (Å) and angles (°) for $Ti(N_2^{iPr}N^{Me})\{NC(Ph)NXyl\}(py)\}$ (**17**).

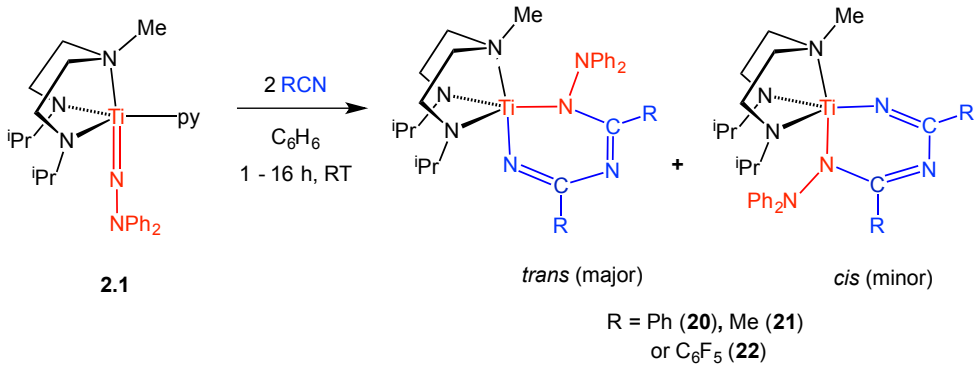
Ti(1)-N(1)	1.7751(14)	Ti(1)-N(1)-C(1)	168.44(14)
Ti(1)-N(3)	2.3531(15)	N(3)-Ti(1)-N(4)	76.26(6)
Ti(1)-N(4)	1.9652(14)	N(3)-Ti(1)-N(5)	77.16(6)
Ti(1)-N(5)	1.9582(15)	N(3)-Ti(1)-N(6)	86.80(5)
Ti(1)-N(6)	2.1818(15)	N(4)-Ti(1)-N(5)	126.79(7)
N(1)-C(1)	1.339(2)	N(5)-Ti(1)-N(6)	105.07(6)
C(1)-N(2)	1.295(3)	N(4)-Ti(1)-N(6)	118.39(6)
C(1)-C(2)	1.511(2)	N(1)-C(1)-C(2)	117.23(15)
N(2)-C(8)	1.418(3)	C(2)-C(1)-N(2)	115.62(17)
		N(1)-C(1)-N(2)	127.11(18)

Compounds **17** and **18** are unusual in that they contain a N-monosubstituted monodentate non-bridging doubly deprotonated amidinate ligand, in contrast to N,N'-disubstituted amidinates $RC(NR')_2$ which are well established versatile, monoanionic ligands in main group-, transition- and lanthanide-metal chemistry.[156, 157] Structurally authenticated titanium compounds containing similar ligands result from the aforementioned reactions of alkoxyimido and hydrazido compounds with nitriles. The hydrazonamide ligands formed from **1.72** were found to contain a longer Ti=N bond when electron-withdrawing substituents on the nitrile were employed. The solid-state structure of **18** was not obtained so a direct comparison could not be made. However, a longer titanium-nitrogen atom in **18** in comparison to **17** may explain the reduced preference for the electronically favoured axial position as the multiple bond character is reduced.

2.8 Reaction of $Ti(N_2^{iPr}N^{Me})(NNPh_2)(py)$ (2.1) with nitriles

Reaction of the hydrazido compound $Ti(N_2^{iPr}N^{Me})(NNPh_2)(py)$ (**2.1**) with internal alkynes has already been reported to yield unidenitified mixtures.[50] However, reaction of **2.1** with nitriles had not yet been investigated. Reaction of **2.1** with one or two equivalents of RCN (R = Ph, C_6F_5, Me) yielded the metallacyclic complexes $Ti(N_2^{iPr}N^{Me})\{N(NPh_2)C(R)NC(R)N\}$ (R = Ph (**20**), R = Me (**21**) and R = C_6F_5 (**22**)),

incorporating two equivalents of the nitrile coupled in a head to tail manner across the Ti=N bond, as established by X-ray crystallography for R = Ph and R = Me (Equation 2.3). No evidence was found for a 1:1 reaction product or intermediates when the reactions were followed by ^{1}H NMR spectroscopy in all cases. In the case of C_6F_5CN conversion reached 100% after just one hour whereas with PhCN and MeCN the reaction only reached completion after 16 hours at room temperature.



2.1

Equation 2.3

No reaction occurred when an equivalent of 2,2'-bipyridine was added to a solution of **20**, similarly addition of C_6F_5CN to solution containing **20** did not result in the formation of **22**, consistent with irreversible formation of **20**. The solid-state structures of **20** and **21** are shown in Figure 2.14, in both cases the -$NNPh_2$ moiety is *cis* to the NMe donor. This orientation is maintained in solution as determined by ^{1}H ROESY NMR experiments which indicated through-space correlations between the *o*-$NNPh_2$ of the hydrazido moiety and the NMe resonances of the supporting ligand in both cases. Both compounds have a minor isomer making up 20% of the total according to NMR integration; this is attributed to an orientation with the $NNPh_2$ moiety in the *trans* position.

In the ^{1}H NMR spectra of **20** three sets of phenyl signals are observed in a 2:1:1 ratio due to the hydrazido phenyl substituents and the two inequivalent inserted nitrile moieties. A through-space correlation in the ^{1}H ROESY NMR spectrum was observed between the *iso*-propyl methine substituent of the supporting ligand and one of the inserted nitrile *o*-Ph resonances. Thus allowing this signal to be assigned as the protons attached to C(26) and C(22) (nitrile in the *trans* position, N(4)-C(20)-C(21)) and hence all remaining aromatic resonances to be assigned. Similarly, compound **21**

was fully assigned with the aid of through-space correlations observed between the *o*-$NNPh_2$ protons and the adjacent Me moiety in the ^{1}H ROESY NMR spectrum.

No solid-state structure was obtained for **22** but on the basis of analytical data and the structures of **20** and **21** the major isomer has also been assigned as the *cis* isomer with the minor *trans* isomer making up 20% of the total. The ^{19}F NMR spectra demonstrates two sets of signals (2:2:1) resulting from the inequivalent -C_6F_5 rings. A ^{19}F COSY experiment and ^{19}F-^{13}C HSQC experiment were used to correlate the ^{19}F resonances to each other and to the ^{13}C resonances.

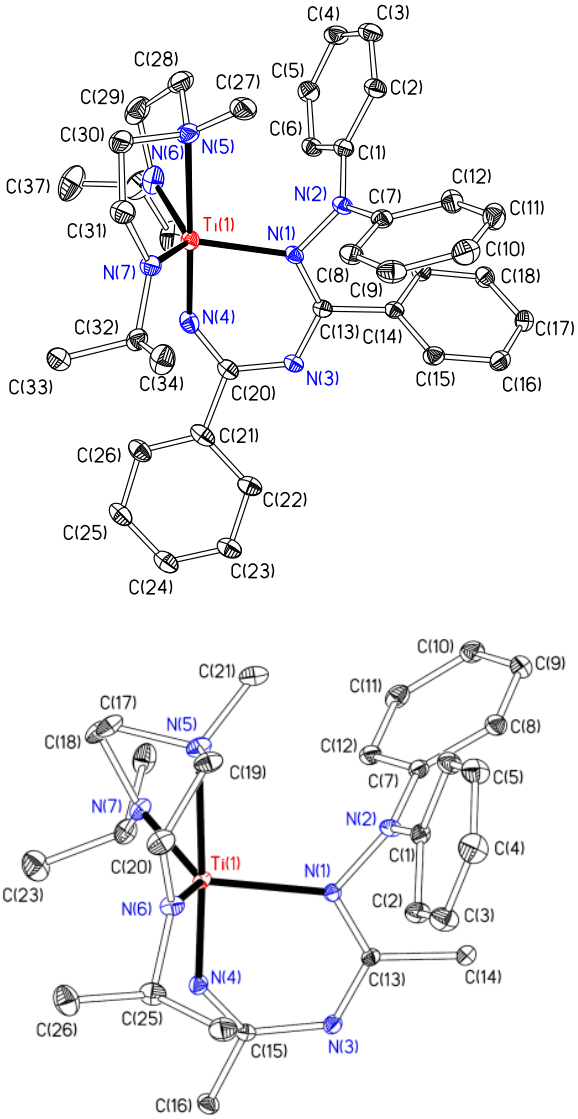


Figure 2.14. Top: displacement ellipsoid plot (20% probability) of $Ti(N_2^{iPr}N^{Me})\{N(NPh_2)C(Ph)NC(Ph)N\}$ (**20**) H atoms are omitted for clarity. Bottom: $Ti(N_2^{iPr}N^{Me})\{N(NPh_2)C(Me)NC(Me)N\}$ (**21**) H atoms other independent molecule are omitted for clarity.

Table 2.7. Selected bond lengths (Å) and angles (°) for $Ti(N_2^{iPr}N^{Me})\{N(NPh_2)C(R)NC(R)N\}$ R = Ph (**20**) and R= Me (**21**).

Parameter	**20**	**21**
Ti(1)-N(1)	2.1323(15)	2.115(2)
Ti(1)-N(4)	1.8423(17)	1.844(2)
Ti(1)-N(5)	2.3749(18)	2.339(2)
Ti(1)-N(6)	1.943(2)	1.936(2)
Ti(1)-N(7)	1.9438(16)	1.942(2)
N(1)-N(2)	1.432(2)	1.434(3)
N(1)-C(13)	1.356(2)	1.355(3)
C(13)-N(3)	1.322(2)	1.327(3)
N(3)-C(20)/(15)	1.368(2)	1.376(3)
C(20)/(15)-N(4)	1.289(3)	1.280(3)
C(13)-C(14)	1.506(2)	1.515(4)
C(20)/(15)-C(21)/C(16)	1.493(3)	1.509(3)
N(4)-Ti(1)-N(6)	106.80(9)	104.25(10)
N(4)-Ti(1)-N(7)	98.97(7)	101.71(10)
N(1)-Ti(1)-N(6)	113.33(7)	115.28(9)
N(1)-Ti(1)-N(7)	116.70(7)	113.12(9)
Ti(1)-N(1)-C(13)	126.55(12)	127.37(17)
N(1)-C(13)-N(3)	127.02(17)	126.4(2)
N(3)-C(20)/(15)-N(4)	123.66(17)	124.1(2)
C(20)/(15)-N(4)-Ti(1)	139.95(14)	139.8(2)
Ti(1)-N(1)-N(2)	121.44(11)	119.39(15)
N(2)-N(1)-C(13)	126.55(12)	113.2(2)
N(1)-C(13)-C(14)	120.31(15)	119.5(2)
C(14)-C(13)-N(3)	112.62(15)	114.1(2)
N(3)-C(20)/(15)-C(21)/(16)	114.90(18)	114.9(2)
C(21)/(16)-C(20)/(15)-N(4)	121.44(18)	121.0(2)

The solid-state structures of **20** and **21** are shown in Figure 2.14. They exist as five-coordinate compounds with approximately trigonal bipyramidal geometry at the titanium centre. The tridentante diamide-amine ligands occupy two equatorial and one axial position *fac*-coordinated in a κ^3-N manner. The Ti–N_{amide} distances are shorter than in **2.1** in both cases (av. 1.9434(26) (**20**), 1.939(3) (**21**) *vs.* 1.9761(21) Å (**2.1**)) indicating better $N_{2p(\pi)} \rightarrow Ti_{3d(\pi)}$ donation. The Ti(1)-N(1) (2.1323(15) and 2.115(2) Å) and Ti(1)-N(4) (1.8423(17) and 1.844(2) Å) are all longer than Ti–N_α in **2.1** and the N(1)-N(2) bond lengths (1.432(2) and 1.434(3) Å) are significantly lengthened from 1.371(2) Å in **2.1** indicative of a loss of multiple bonding character. Interestingly the Ti(1)-N(4) bond distances are significantly shorter than the Ti(1)-N(1) bond distances, the shorter Ti(1)-N(4) bonds are consistent with a ketimide-type ligand (–N=CRR') and the longer Ti(1)-N(4) bonds are more similar to a –N(R)–C(R)=N type ligand. [100, 129, 158]

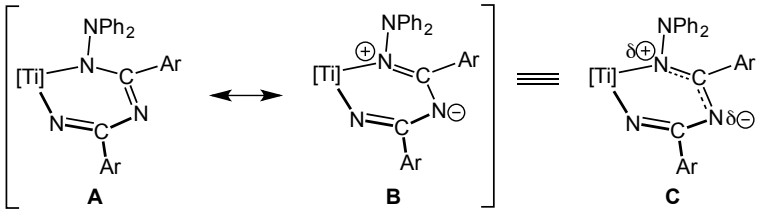


Figure 2.15 Resonance contributions to the bonding in Ti($N_2^{iPr}N^{Me}$){N(NPh_2)C(Ph)NC(Ph)N} R= Ph (**20**), Me (**21**) and C_6F_5 (**22**).

The central Ti, C and N atoms of the metallacycles are approximately co-planar, implying effective π-conjugation. However, there is significant asymmetry within the metallacycles. The nitrogen-carbon bond lengths within the inserted nitrile moiety *trans* to the N^{Me} donor are consistent with single and double bonds (N(3)-C(20/15) 1.368(2) and 1.376(3) Å, N(4)-C(20/15) 1.289(3) and 1.280(3) Å). In comparison, the carbon-nitrogen bond lengths within the central inserted nitrile are more similar to each other (N(1)-C(13) 1.356(2) and 1.355(3) Å, N(3)-C(13) 1.322(2) and 1.327(3) Å). The difference in the single and double bond distances (Δ_{N-C}) is a useful parameter to calculate for discussion and for comparison with previously reported compounds. For **20** the differences are calculated to be Δ_{N-C} = 0.034(4) Å for the central nitrile and Δ_{N-C} = 0.079(5) Å for the *trans* nitrile. The effect is more enhanced in **21**, Δ_{N-C} = 0.028(4) (central) and Δ_{N-C} = 0.096(4) (*trans*). These observations

suggest contributions from both **A** and **B** resonance forms to the bonding in **20** and **21**, leading to the net description of **C** (Figure 2.15).

Compounds containing analogues six-membered metallacycles were mentioned above, namely Cp*Ti{MeC(N^{i}Pr)$_2$}{N(NCPh$_2$)C(Ar^{F5})NC(Ar^{F5})N} (**2.8**) and Cp*Ti{PhC(N^{i}Pr)$_2$}{N(C{Ar^{F5}}NO^{t}Bu)C(Ar^{F5})NC(Ar^{F5})N} (**2.9**) resulting from the reactions of Cp*Ti{MeC(N^{i}Pr)$_2$}(NNCPh$_2$) (**1.147**) and Cp*Ti{PhC(N^{i}Pr)$_2$}(NO^{t}Bu) (**1.158**) with nitriles, respectively. The structural parameters within the six-membered rings are similar in both cases and both **2.8** and **2.9** showed asymmetry within the metallacycle ($\Delta_{N\text{-}C}$ = 0.080(7) and 0.014(7) for **2.8** and $\Delta_{N\text{-}C}$ = 0.118(3) Å and $\Delta_{N\text{-}C}$ = 0.050(3) Å for **2.9**). Compounds **20**, **21** and **22** are the first examples of such compounds derived from a hydrazido species. Other diamide-amine supported hydrazides undergo insertion of one equivalent of nitrile, the insertion of a second equivalent can be attributed to a sterically less demanding environment around the Ti=N bond in **2.1** and intermediates along the reaction pathway.

The reaction of **1.75** with one equivalent of a nitrile and one equivalent of an alkyne resulted in sequential coupling giving exclusive formation of cross-coupled products.[46] Analogous reactions were attempted here. The reaction of **2.1** with HCCTol and PhCN or MeCN (1:2:2) gave almost exclusive formation (90%) of the known alkyne reaction product, Ti(N$_2$^{iPr}N^{Me}){N(NPh$_2$)C(H)C(H)Tol)}(CCTol). In comparison, reaction of **2.1** with HCCTol and C$_6$F$_5$CN (1:2:2) gave **22** as the major product (85%), consistent with more stable reaction products when electron-withdrawing substituents are employed on the nitrile. This has been investigated for the reaction of **1.72** with nitriles. DFT calculations showed that increased fluorination of the nitrile substrate both lowered the activation barrier to the intermediate metallacycles Ti(N$_2$N^{py}){N(NPh$_2$)C(Ar)N} (*vide infra*) and increased the thermodynamic stability of the final products Ti(N$_2$N^{py}){NC(ArF$_x$)NNPh$_2$}(py) by stabilising the electron rich Ti=NC(Ar)NNPh$_2$ group.

2.9 Proposed mechanism for the reaction of Ti($N_2^{iPr}N^{Me}$)(NXyl)(py) (1) and Ti($N_2^{iPr}N^{Me}$)($NNPh_2$)(py) (2.1) with nitriles

Figure 2.16 shows potential pathways for the formation of compounds **18** - **22**. As in the reactions with internal alkynes, the mechanism begins with loss of pyridine to form an intermediate with a vacant coordination site for nitrile binding. Following coordination of an equivalent of nitrile, a [2+2] cycloaddition reaction across the Ti=N_α bond of **1** or **2.1** can occur to give azametallacyclobutene intermediates of type **D**, such intermediates have precedent in both titanium imido and hydrazido chemistry.[46, 91] This intermediate could then undergo ring-opening through dissociation of the original Ti–N bond to form intermediates of type **E** followed by trapping with pyridine to form a five coordinate species. This is where the reaction of **1** with nitriles stops and the amidinate(2-) complexes **18** and **17** were isolated. For the hydrazide case a subsequent [2+2] cycloaddition across the Ti=N bond of the corresponding hydrazonamide complex, **E**, followed by isomerisation of the four-membered metallacycle to yield a more stable six-membered metallacycle would give **G**. Alternatively insertion of a second equivalent of RCN into the Ti–NCAr bond of the **D** would lead directly to **G**.

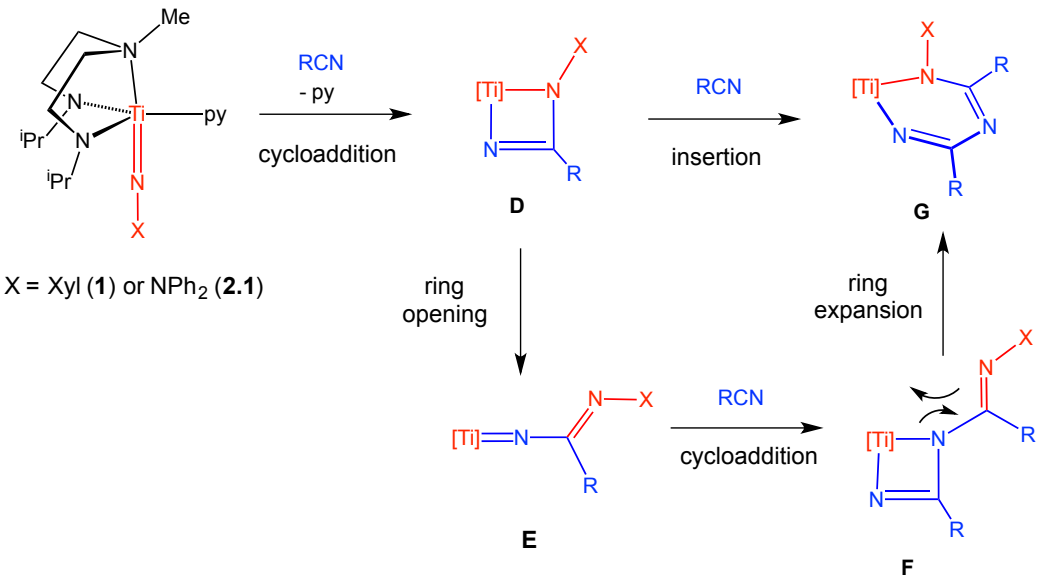


Figure 2.16. Proposed mechanism for reaction of Ti($N_2^{iPr}N^{Me}$)(NXyl)(py) (**1**) and Ti($N_2^{iPr}N^{Me}$)($NNPh_2$)(py) (**2.1**) with nitriles.

2.10 Conclusion

This Chapter has described the synthesis and characterisation of four new imido compounds supported by the iso-propyl substituted diamide-amine ligand $N_2^{iPr}N^{Me}$. Both xylylimido compounds $Ti(N_2^{iPr}N^{Me})(NXyl)(py)$ (**1**) and $Ti(N_2^{iPr}N^{Me})(NXyl)(bipy)$ (**2**) were structurally authenticated and the imido ligand found to occupy the electronically preferred axial position *trans* to the NMe donor, as was found in the analogous hydrazido compound $Ti(N_2^{iPr}N^{Me})(NNPh_2)(py)$ (**2.1**). Reaction of **1** with primary and secondary amines gave diamide compounds following transfer of a proton onto the imido ligand, In contrast the hydrazide species **2.1** yielded compounds containing monoanionic diamine-amide ligands due to protonation of one of the N_{amide} atoms. This type of compound was structurally authenticated following the reaction of **2.1** with BHT. Comparative reactions are limited as Group 4 imido and hydrazido reactivity studies have typically focussed on C–N bond forming reactions. The motivation for investigating such reactivity here is linked to reactions described in the subsequent Chapters of this Thesis.

The reactivity of compound **1** with internal alkynes is discussed and found to yield the expected azatitanacyclobutene species following a [2+2] cycloaddition reaction. When electron-withdrawing substituents are employed a subsequent intramolecular reaction occurs to yield *ortho*-metallated vinylamide species. The reaction products could not be compared to those with **2.1** as it has previously been reported that unidentified mixtures were obtained with internal alkynes.

The reactions of both **1** and **2.1** with nitriles are reported and compounds resulting from the insertion of one and two equivalents respectively into the Ti=N bonds are described. This is a novel transformation of titanium imides with nitriles. The insertion of a second equivalent with **2.1** to yield compounds **20** - **22**, differs from the reaction of **1.72** with nitriles, which yielded hydrazonamide compounds due to the insertion of just one equivalent of a nitrile. However, it is proposed to follow the same reaction pathway.

Overall the novel imido compound **1** appears to be less reactive than the analogous hydrazide compound **2.1**. This results in controlled reactions with internal alkynes yielding isolable products and reaction with just one equivalent of a nitrile in comparison to two equivalents observed with **2.1**. The differing sites of protonation of

1 and **2.1** indicate a marked difference in electronics, with the hydrazido compound containing more basic N_{amide} atoms as a result of a shorter Ti=N bond as well as a more reactive multiple bond.

2.11 References

1. M. J. Carney, P. J. Walsh, F. J. Hollander and R. G. Bergman, *J. Am. Chem. Soc.*, 1989, **111**, 8751.
2. M. J. Carney, P. J. Walsh and R. G. Bergman, *J. Am. Chem. Soc.*, 1990, **112**, 6426.
3. M. J. Carney, P. J. Walsh, F. J. Hollander and R. G. Bergman, *Organometallics*, 1992, **11**, 761.
4. M. R. Smith, P. T. Matsunaga and R. A. Andersen, *J. Am. Chem. Soc.*, 1993, **115**, 7049.
5. J. L. Polse, R. A. Andersen and R. G. Bergman, *J. Am. Chem. Soc.*, 1995, **117**, 5393.
6. W. A. Howard, T. M. Trnka, M. Waters and G. Parkin, *J. Organomet. Chem.*, 1997, **528**, 95.
7. A. J. Blake, J. M. McInnes, P. Mountford, G. I. Nikonov, D. Swallow and D. J. Watkin, *J. Chem. Soc., Dalton Trans.*, 1999, 379.
8. I. Pappas and P. J. Chirik, *Angew. Chem. Int. Ed.*, 2014, **53**, 6241.
9. D. E. Wigley, *Prog. Inorg. Chem.*, 1994, **42**, 239.
10. A. P. Duncan and R. G. Bergman, *Chem. Rec.*, 2002, **2**, 431.
11. P. Mountford, *Chem. Commun.*, 1997, 2127.
12. L. H. Gade and P. Mountford, *Coord. Chem. Rev.*, 2001, **216-217**, 65.
13. N. Hazari and P. Mountford, *Acc. Chem. Res.*, 2005, **38**, 839.
14. A. R. Fout, U. J. Kilgore and D. J. Mindiola, *Chem. Eur. J.*, 2007, **13**, 9428.
15. C. M. Kozak and P. Mountford, *Angew. Chem. Int. Ed.*, 2004, **43**, 1186
16. T. R. Cundari, *J. Am. Chem. Soc.*, 1992, **114**, 7879.
17. Z. Lin and M. B. Hall, *Coord. Chem. Rev.*, 1993, **123**, 149.
18. P. Mountford and D. Swallow, *J. Chem. Soc., Chem. Commun.*, 1995, 2357.
19. N. Kaltsoyannis and P. Mountford, *J. Chem. Soc., Dalton Trans.*, 1999, 781.
20. T. R. Cundari, *Chem. Rev.*, 2000, **100**, 807.
21. A. D. Schwarz, A. J. Nielson, N. Kaltsoyannis and P. Mountford, *Chem. Sci.*, 2012, **3**, 819.

22. S. C. Dunn, N. Hazari, N. M. Jones, A. G. Moody, A. J. Blake, A. R. Cowley, J. C. Green and P. Mountford, *Chem. Eur. J.*, 2005, **11**, 2111.
23. For ease of representation the Ti−NX (X = R, OR) moieties are all drawn as "Ti=N", although in most cases the Ti−N linkage is best considered to be a triple bond
24. I. Bytschkov and S. Doye, *Eur. J. Org. Chem.*, 2003, 935.
25. S. Doye, *Synlett.*, 2004, 1653.
26. L. L. Schafer and A. V. Lee, *Eur. J. Inorg. Chem.*, 2007, 2243.
27. T. E. Müller, K. C. Hultzsch, M. Yus, F. Foubelo and M. Tada, *Chem. Rev.*, 2008, **108**, 3795.
28. N. Wiberg, H.-W. Haring, G. Huttner and P. Friedrich, *Chem. Ber.*, 1978, **111**, 2708.
29. P. J. Walsh, M. J. Carney and R. G. Bergman, *J. Am. Chem. Soc.*, 1991, **113**, 6343.
30. J. L. Thorman and L. K. Woo, *Inorg. Chem.*, 2000, **39**, 1301.
31. Y. Li, Y. Shi and A. L. Odom, *J. Am. Chem. Soc.*, 2004, **126**, 1794.
32. S. Banerjee, Y. Shi, C. Cao and A. L. Odom, *J. Organomet. Chem.*, 2005, **690**, 5066.
33. T. B. Parsons, N. Hazari, A. R. Cowley, J. C. Green and P. Mountford, *Inorg. Chem.*, 2005, **44**, 8442.
34. S. Banerjee and A. L. Odom, *Organometallics*, 2006, **25**, 3099.
35. S. Patel, Y. Li and A. L. Odom, *Inorg. Chem.*, 2007, **46**, 6373.
36. J. D. Selby, C. D. Manley, M. Feliz, A. D. Schwarz, E. Clot and P. Mountford, *Chem. Commun.*, 2007, 4937.
37. S. Banerjee, E. Barnea and A. L. Odom, *Organometallics*, 2008, **27**, 1005.
38. A. J. Clulow, J. D. Selby, M. G. Cushion, A. D. Schwarz and P. Mountford, *Inorg. Chem.*, 2008, **47**, 12049.
39. J. D. Selby, C. D. Manley, A. D. Schwarz, E. Clot and P. Mountford, *Organometallics*, 2008, **27**, 6479.
40. J. D. Selby, C. Schulten, A. D. Schwarz, A. Stasch, E. Clot, C. Jones and P. Mountford, *Chem.Commun.*, 2008, 5101.
41. K. Weitershaus, J. L. Fillol, H. Wadepohl and L. H. Gade, *Organometallics*, 2009, **28**, 4747.

42. K. Weitershaus, H. Wadepohl and L. H. Gade, *Organometallics*, 2009, **28**, 3381.
43. T. Janssen, R. Severin, M. Diekmann, M. Friedemann, D. Haase, Saak, W., S. Doye and R. Beckhaus, *Organometallics*, 2010, **29**, 1806.
44. A. D. Schofield, A. Nova, J. D. Selby, C. D. Manley, A. D. Schwarz, E. Clot and P. Mountford, *J. Am. Chem. Soc.*, 2010, **132**, 10484.
45. P. J. Tiong, A. D. Schofield, J. D. Selby, A. Nova, E. Clot and P. Mountford, *Chem. Commun.*, 2010, **46**, 85.
46. A. D. Schofield, A. Nova, J. D. Selby, A. D. Schwarz, E. Clot and P. Mountford, *Chem. Eur. J.*, 2011, **17**, 265.
47. J. D. Selby, M. Feliz, A. D. Schwarz, E. Clot and P. Mountford, *Organometallics*, 2011, **30**, 2295.
48. P. J. Tiong, A. Nova, E. Clot and P. Mountford, *Chem. Commun.*, 2011, **47**, 3147.
49. P. J. Tiong, A. Nova, L. R. Groom, A. D. Schwarz, J. D. Selby, A. D. Schofield, E. Clot and P. Mountford, *Organometallics*, 2011, **30**, 1182.
50. A. D. Schwarz, C. S. Onn and P. Mountford, *Angew. Chem. Int. Ed.*, 2012, **51**, 12298.
51. P. J. Tiong, A. Nova, A. D. Schwarz, J. D. Selby, E. Clot and P. Mountford, *Dalton Trans.*, 2012, **41**, 2277.
52. P. D. Schweizer, H. Wadepohl and L. H. Gade, *Organometallics*, 2013, **32**, 3697.
53. K. Weitershaus, B. D. Ward, R. Kubiak, C. Muller, H. Wadepohl, S. Doye and L. H. Gade, *Dalton Trans.*, 2009, 4586.
54. J. Unruangsri, H. Morgan, A. D. Schwarz, A. D. Schofield and P. Mountford, *Organometallics*, 2013, **32**, 3091.
55. H. Herrmann, J. L. Fillol, H. Wadepohl and L. H. Gade, *Angew. Chem. Int. Ed.*, 2007, **46**, 8426.
56. H. Herrmann, J. L. Fillol, T. Gehrmann, M. Enders, H. Wadepohl and L. H. Gade, *Chem. Eur. J.*, 2008, **14**, 8131.
57. H. Herrmann, J. L. Fillol, H. Wadepohl and L. H. Gade, *Organometallics*, 2008, **27**, 172.
58. H. Herrmann, T. Gehrmann, H. Wadepohl and L. H. Gade, *Dalton Trans.*, 2008, 6231.

59. H. Herrmann, H. Wadepohl and L. H. Gade, *Dalton Trans.*, 2008, 2111.
60. T. Gehrmann, J. L. Fillol, H. Wadepohl and L. H. Gade, *Angew. Chem. Int. Ed.*, 2009, **48**, 2152.
61. R. F. Munha, L. F. Veiros, M. T. Duarte, M. D. Fryzuk and A. M. Martins, *Dalton Trans.*, 2009, 7494.
62. T. Gehrmann, J. L. Fillol, S. A. Scholl, H. Wadepohl and L. H. Gade, *Angew. Chem. Int. Ed.*, 2011, **50**, 5757.
63. T. Gehrmann, J. L. Fillol, H. Wadepohl and L. H. Gade, *Organometallics*, 2012, **31**, 4504.
64. T. Gehrmann, M. Kruck, H. Wadepohl and L. H. Gade, *Chem. Commun.*, 2012, **48**, 2397.
65. T. Gehrmann, G. T. Plundrich, H. Wadepohl and L. H. Gade, *Organometallics*, 2012, **31**, 3346.
66. T. Gehrmann, S. A. Scholl, J. L. Fillol, H. Wadepohl and L. H. Gade, *Chem. Eur. J.*, 2012, **18**, 3925.
67. S. A. Scholl, G. T. Plundrich, H. Wadepohl and L. H. Gade, *Inorg. Chem.*, 2013, **52**, 10158.
68. S. A. Scholl, H. Wadepohl and L. H. Gade, *Organometallics*, 2013, **32**, 937.
69. A. J. Blake, J. M. McInnes, P. Mountford, G. I. Nikonov, D. Swallow and D. J. Watkin, *J. Chem. Soc., Dalton Trans.*, 1999, 379.
70. T. Gehrmann, J. L. Fillol, H. Wadepohl and L. H. Gade, *Organometallics*, 2010, **29**, 28.
71. A. L. Odom, *Dalton Trans.*, 2005, 225.
72. C. Cao, Y. Shi and A. L. Odom, *Org. Lett.*, 2002, **4**, 2853.
73. J. S. Johnson and R. G. Bergman, *J. Am. Chem. Soc.*, 2001, **123**, 2923.
74. A. Tillack, H. Jiao, I. Garcia Castro, C. G. Hartung and M. Beller, *Chem. Eur. J.*, 2004, **10**, 2409.
75. L. Ackermann and R. Born, *Tet. Letts.*, 2004, **45**, 9541.
76. V. Khedkar, A. Tillack, M. Michalik and M. Beller, *Tet. Letts.*, 2004, **45**, 3123.
77. K. Weitershaus, H. Wadepohl and L. H. Gade, *Organometallics*, 2009, **28**, 4898.
78. A. D. Schwarz, A. Nova, E. Clot and P. Mountford, *Inorg. Chem.*, 2011, **50**, 12155.

79. A. D. Schwarz, A. Nova, E. Clot and P. Mountford, *Chem. Commun.*, 2011, **47**, 4926.
80. L. R. Groom, A. D. Schwarz, A. Nova, E. Clot and P. Mountford, *Organometallics*, 2013, **32**, 7520.
81. B. Clough, unpublished work.
82. B. Xie, unpublished work.
83. A. J. Blake, P. E. Collier, L. H. Gade, M. McPartlin, P. Mountford, M. Schubart and I. J. Scowen, *Chem. Commun.*, 1997, 1555.
84. A. Bashall, P. E. Collier, L. H. Gade, M. McPartlin, P. Mountford and D. T. Trösch, *Chem. Commun.*, 1998, 2555.
85. P. E. Collier, S. M. Pugh, H. S. C. Clark, J. B. Love, A. J. Blake, F. G. N. Cloke and P. Mountford, *Inorg. Chem.*, 2000, **39**, 2001.
86. S. Friedrich, M. Schubart, L. H. Gade, I. J. Scowen, A. J. Edwards and M. McPartlin, *Chem. Ber.-Recueil*, 1997, **130**, 1751.
87. L. H. Gade, *Chem. Commun.*, 2000, 173.
88. A. Bashall, P. E. Collier, L. H. Gade, M. McPartlin, P. Mountford, S. M. Pugh, S. Radojevic, M. Schubart, I. J. Scowen and D. J. M. Trösch, *Organometallics*, 2000, **19**, 4784.
89. A. J. Blake, P. E. Collier, L. H. Gade, P. Mountford, J. Lloyd, S. M. Pugh, M. Schubart, M. E. G. Skinner and J. M. Trösch, *Inorg. Chem.*, 2001, **40**, 870.
90. D. J. M. Trösch, P. E. Collier, A. Bashall, L. H. Gade, M. McPartlin, P. Mountford and S. Radojevic, *Organometallics*, 2001, **20**, 3308.
91. S. M. Pugh, D. J. M. Trösch, D. J. Wilson, A. Bashall, F. G. N. Cloke, L. H. Gade, P. B. Hitchcock, M. McPartlin, J. F. Nixon and P. Mountford, *Organometallics*, 2000, **19**, 3205.
92. B. D. Ward, G. Orde, E. Clot, A. R. Cowley, L. H. Gade and P. Mountford, *Organometallics*, 2004, **23**, 4444.
93. A. E. Guiducci, C. L. Boyd and P. Mountford, *Organometallics*, 2006, **25**, 1167.
94. C. L. Boyd, A. E. Guiducci, S. R. Dubberley, B. R. Tyrrell and P. Mountford, *J. Chem. Soc., Dalton Trans.*, 2002, 4175.
95. A. E. Guiducci, C. L. Boyd, E. Clot and P. Mountford, *Dalton Trans.*, 2009, 5960.

96. C. L. Boyd, E. Clot, A. E. Guiducci and P. Mountford, *Organometallics*, 2005, **24**, 2347.

97. A. E. Guiducci, A. R. Cowley, M. E. G. Skinner and P. Mountford, *J. Chem. Soc., Dalton Trans.*, 2001, 1392.

98. J.-L. Fauré, H. Gornitzka, R. Réau, D. Stalke and G. Bertrand, *Eur. J. Inorg. Chem.*, 1999, 2295.

99. A. J. Blake, P. E. Collier, S. C. Dunn, W.-S. Li, P. Mountford and O. V. Shishkin., *J. Chem. Soc., Dalton Trans.*, 1997, 1549.

100. D. A. Fletcher, R. F. McMeeking and D. Parkin, *J. Chem. Inf. Comput. Sci.*, 1996, **36**, 746 (The UK Chemical Database Service: CSD version 5.36 updated May 2015).

101. R. Kempe, *Angew. Chem., Int. Ed. Eng.*, 2000, **39**, 468.

102. C. Manley, Part II Thesis, University of Oxford, 2007.

103. H. Morgan, Part II Thesis, University of Oxford, 2011.

104. T. E. Hanna, I. Keresztes, E. Lobkovsky, W. H. Bernskoetter and P. J. Chirik, *Organometallics*, 2004, **23**, 3448.

105. A. J. Blake, P. Mountford, G. I. Nikonov and D. Swallow, *Chem. Commun.*, 1996, 1835.

106. P. J. Walsh, A. M. Baranger and R. G. Bergman, *J. Am. Chem. Soc.*, 1992, **114**, 1708.

107. M. E. G. Skinner, T. Toupance, D. A. Cowhig, B. R. Tyrrell and P. Mountford, *Organometallics*, 2005, **24**, 5586.

108. C. S. Onn, Part II Thesis, University of Oxford, 2012.

109. I. A. Latham, G. J. Leigh, G. Huttner and I. Jibril, *J. Chem. Soc., Dalton Trans.*, 1986, 385.

110. D. L. Hughes, G. J. Leigh and D. G. Walker, *J. Chem. Soc., Dalton Trans.*, 1989, 1413.

111. D. L. Hughes, M. Jimenez-Tenorio, G. J. Leigh and D. G. Walker, *J. Chem. Soc., Dalton Trans.*, 1989, 2389.

112. T. Takahashi, Y. Mizobe, M. Sato, Y. Uchida and M. Hidai, *J. Am. Chem. Soc.*, 1979, **101**, 3405.

113. J. R. Dilworth, R. A. Henderson, P. Dahlstrom, T. Nicholson and J. A. Zubieta, *J. Chem. Soc., Dalton Trans.*, 1987, 529.

114. A. Galindo, A. Hills, D. L. Hughes, R. L. Richards, M. Hughes and J. Mason, *J. Chem. Soc., Dalton Trans.*, 1990, 283.

115. A. Dreher, K. Mersmann, C. Nather, I. Ivanovic-Burmazovic, R. van Eldik and F. Tuczek, *Inorg. Chem.*, 2009, **48**, 2078.

116. S. Schenk, B. Le Guennic, B. Kirchner and M. Reiher, *Inorg. Chem.*, 2008, **47**, 3634.

117. A. K. Guha and A. K. Phukan, *Inorg. Chem.*, 2011, **50**, 8826.

118. F. G. Bordwell and D. J. Algrim, *J. Am. Chem. Soc.*, 1988, **110**, 2964.

119. Y. Zhao, F. G. Bordwell, J.-P. Cheng and D. Wang, *J. Am. Chem. Soc.*, 1997, **119**, 9125.

120. H. Wang, H. Chan and Z. Xie, *Organometallics*, 2005, **24**, 3772.

121. F. Basuli, H. Aneetha, J. C. Huffman and D. J. Mindiola, *J. Am. Chem. Soc.*, 2005, **127**, 17992.

122. P. L. McGrane, M. Jensen and T. Livinghouse, *J. Am. Chem. Soc.*, 1992, **114**, 5459.

123. P. L. McGrane and T. Livinghouse, *J. Am. Chem. Soc.*, 1993, **115**, 11485.

124. J. L. Bennett and P. T. Wolczanski, *J. Am. Chem. Soc.*, 1997, **119**, 10696.

125. J. L. Polse, R. A. Andersen and R. G. Bergman, *J. Am. Chem. Soc.*, 1998, **120**, 13405.

126. B. D. Ward, A. Maisse-Francois, P. Mountford and L. H. Gade, *Chem. Commun.*, 2004, 704.

127. G. Zhao, F. Basuli, U. J. Kilgore, H. Fan, H. Aneetha, J. C. Huffman, G. Wu and D. J. Mindiola, *J. Am. Chem. Soc.*, 2006, **128**, 13575.

128. A. A. Dissanayake and A. L. Odom, *Chem. Commun.*, 2012, **48**, 440.

129. P. D. Bolton, M. Feliz, A. H. Cowley, E. Clot and P. Mountford, *Organometallics*, 2008, **27**, 6096.

130. N. Vujkovic, B. D. Ward, A. Maisse-Francois, H. Wadepohl, P. Mountford and L. H. Gade, *Organometallics*, 2007, **26**, 5522.

131. S. M. Nettles and J. L. Petersen, *J. Organomet. Chem.*, 2007, **692**, 4654.

132. D. Zhao, W. Gao, Y. Mu and L. Ye, *Chem. - Eur. J.*, 2010, **16**, 4394.

133. A. M. Baranger, P. J. Walsh and R. G. Bergman, *J. Am. Chem. Soc.*, 1993, **115**, 2753.

134. L. E. N. Allan, G. J. Clarkson, D. J. Fox, A. L. Gott and P. Scott, *J. Am. Chem. Soc.*, 2010, **132**, 15308.

135. C. Cao, Y. Shi and A. L. Odom, *J. Am. Chem. Soc.*, 2003, **125**, 2880.
136. R. T. Ruck, R. L. Zuckerman, S. W. Krska and R. G. Bergman, *Angew. Chem. Int. Ed.*, 2004, **43**, 5372.
137. R. T. Ruck and R. G. Bergman, *Organometallics*, 2004, **23**, 2231.
138. H. Aneetha, F. Basuli, J. Bollinger, J. C. Huffman and D. J. Mindiola, *Organometallics*, 2006, **25**, 2402.
139. N. Vujkovic, J. L. Fillol, B. D. Ward, H. Wadepohl, P. Mountford and L. H. Gade, *Organometallics*, 2008, **27**, 2518.
140. M. H. Chisholm, E. E. Delbridge, A. R. Kidwell and K. B. Quinlan, *Chem. Commun.*, 2003, 126.
141. R. L. Gdula, M. J. A. Johnson and N. W. Ockwig, *Inorg. Chem.*, 2005, **44**, 9140.
142. C. D. Wood, S. J. McLain and R. R. Schrock, *J. Am. Chem. Soc.*, 1979, **101**, 3210.
143. R. R. Schrock and J. D. Fellmann, *J. Am. Chem. Soc.*, 1978, **100**, 3359.
144. K. M. Doxsee, J. B. Farahi and H. Hope, *J. Am. Chem. Soc.*, 1991, **113**, 8889.
145. B. Hessen, J.-K. F. Buijink, A. Meetsma, J. Teuben, G. Helgesson, M. Hakansson, S. Jagner and A. L. Spek, *Organometallics*, 1993, **12**, 2268.
146. M. L. Listemann and R. R. Schrock, *Organometallics*, 1985, **4**, 74.
147. J. H. Freudenberger and R. R. Schrock, *Organometallics*, 1986, **5**, 398.
148. M. H. Chisholm, K. Folting, M. L. Lynn, D. B. Tiedtke, F. Lemoigno and O. Eisenstein, *Chem. Eur. J.*, 1999, **5**, 2318.
149. A. M. Geyer, R. L. Gdula, E. S. Wiedner and M. J. A. Johnson, *J. Am. Chem. Soc.*, 2007, **129**, 3800.
150. B. C. Bailey, A. R. Fout, H. Fan, J. Tomaszewski, J. C. Huffman, J. B. Gary, M. J. A. Johnson and D. J. Mindiola, *J. Am. Chem. Soc.*, 2007, **129**, 2234.
151. A. M. Geyer, E. S. Wiedner, J. B. Gary, R. L. Gdula, N. C. Kuhlmann, M. J. A. Johnson, B. D. Dunietz and J. W. Kampf, *J. Am. Chem. Soc.*, 2008, **130**, 8984.
152. P. J. Tiong, L. R. Groom, E. Clot and P. Mountford, *Chem. Eur. J.*, 2013, **19**, 4198.
153. J. Chu, E. Lu, Z. Liu, Y. Chen, X. Leng and H. Song, *Angew. Chem.* , 2011, **123**, 7819.
154. A. D. Schofield, DPhil Thesis, Univeristy of Oxford, 2012.

155. F. H. Allen, O. Kennard, D. G. Watson, L. Brammer, A. G. Orpen and R. Taylor, *J. Chem. Soc., Perkin Trans. 2*, 1987, S1.

156. F. T. Edelmann, *Coord. Chem. Rev.*, 1994, **137**, 403.

157. J. Barker and M. Kilner, *Coord. Chem. Rev.*, 1994, **133**, 219.

158. M. J. Ferreira and A. M. Martin, *Coord. Chem. Rev.*, 2006, **250**, 118.

Chapter Three

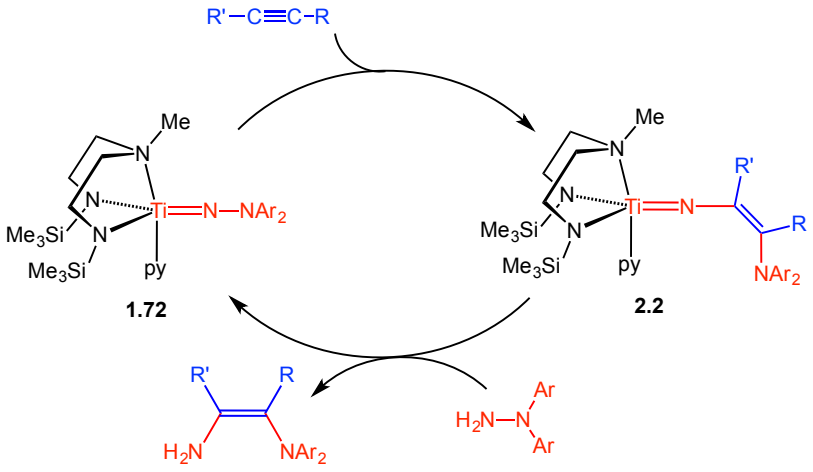
Reactions of Ti($N_2^{iPr}N^{Me}$)(NXyl)(py) with terminal alkynes

3.1 Overview

This Chapter describes the reactions of the new titanium imido compound Ti($N_2^{iPr}N^{Me}$)(NXyl)(py) (**1**) with terminal alkynes. The synthesis and characterisation of the reaction products are discussed, along with a full mechanistic study including labelling experiments and kinetic analysis. Finally, the relevance of these experiments to the reactions of Ti($N_2^{iPr}N^{Me}$)($NNPh_2$)(py) (**2.1**) with terminal alkynes is presented.

3.2 Introduction

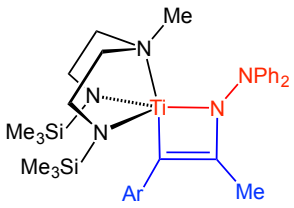
As was introduced in Chapter One of this Thesis, Group 4 imido and hydrazido compounds display a broad range of reactivity with small unsaturated molecules.[1-21] A topic of growing interest is the reactions with alkynes, which have produced a range of new C–N bond forming reactions following reaction at the unsaturated bond. In the case of terminal alkynes, there is also the possibility of competitive 1,2-C–H bond activation across the M=N bond.[22-24] Catalytic C–N bond forming reactions with alkynes have been of particular interest and include hydroamination, hydrohydrazination and iminohydrohydrazination,[6, 11, 25-39] all of which result in the net addition of an N–H bond across an unsaturated C–C bond. More recently, the 1,2-diamination of alkynes and hydrazines has been reported with Ti(N_2N^{Me})($NNPh_2$)(py) (**1.72**).[8, 12] This is a novel transformation and involves the addition of the N–N bond of N,N'-diarylhydrazines across the triple bond of internal alkynes (Scheme 3.1).



R = Me, R' = Ph, 4-C_6H_4OMe, 4-$C_6H_4{}^tBu$, 4-$C_6H_4CF_3$ or Me; R = R' = 4-$C_6H_4CF_3$
Ar = Ph, 4-C_6H_4OMe or 4-$C_6H_4{}^tBu$;

Scheme 3.1. Catalytic cycle for the 1,2-diamination of various internal alkynes with diarylhydrazines using Ti(N_2N^{Me})($NNAr_2$)(py).

The stoichiometric reactions of **1.72** with internal alkynes yield vinylimido compounds of the type $Ti(N_2N^{Me})\{NC(R)C(Me)NPh_2\}(py)$ (**2.2**, R = Me, Ph, Tol, 4-$C_6H_4{}^tBu$, 4-C_6H_4OMe, 4-$C_6H_4CF_3$), which are also active catalysts (Scheme 3.1). Experimental and computational results have established the mechanism for their formation. A [2+2] cycloaddition reaction occurs between the alkyne and $Ti{=}N_\alpha$ to yield a metallacyclic species (**1.145**) shown in Figure 3.1. Metallacyclic species were observed during the low temperature reactions of **1.72** with electron-withdrawing internal alkynes and have been isolated for the closely related diamide-pyridyl hydrazido compound $Ti(N_2N^{py})(NNPh_2)(py)$ (**1.75**) with terminal alkynes.



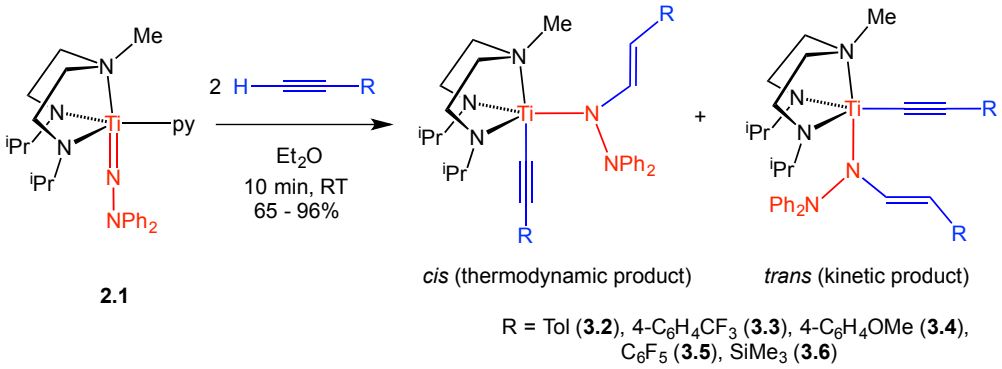
1.145

Figure 3.1. Metallacyclic intermediate formed from the reaction of $Ti(N_2N^{Me})(NNPh_2)(py)$ (**1.72**) with internal alkynes.

Coordination of N_β to titanium brings about a conformational change in the 4-membered ring and facilitates nucleophilic attack of the π density located on C_{Ti} into the N_α–N_β σ* orbital inducing N_α–N_β bond cleavage and C_{Ti}–N_α bond formation. Lastly, nucleophilic attack by N_β on C_{Me} followed by C–C bond formation ultimately yields the vinylimido complexes.[12, 40] Two successive hydrogen transfers from diarylhydrazine to the vinylimido ligand complete the catalytic cycle and regenerate **1.72**, releasing the organic diaminoalkene product (Scheme 3.1).[41] The catalysis was carried at 10 mol% catalyst loading and the organic products were isolated.

It was found that non-productive side reactions of **1.72** with both Ph_2NNH_2 and the diaminoalkene products occur, resulting in formation of protio ligand ($MeN\{CH_2CH_2N(H)SiMe_3\}_2$), and therefore a loss of catalyst activity.[41] Work carried out in our group since has shown that ligand modification can circumvent these decomposition reactions. Replacing the $SiMe_3$ groups on the N_{amide} atoms with substituted phenyl groups bearing a wide range of substituents gave more robust catalysts, although the reactions require heating at 70 °C to achieve appreciable conversion.[42]

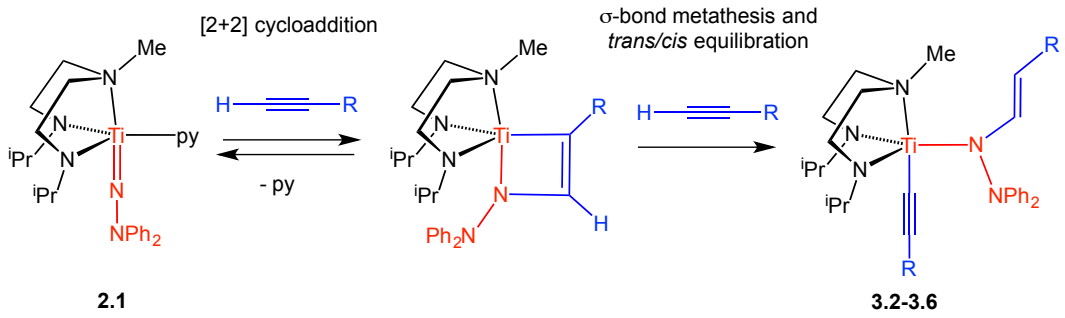
As part of developing the chemistry of compounds of the type **1.72** and its homologues by modification of the N_{amide} substituents, the closely related ligand $H_2N_2^{iPr}N^{Me}$ (**3.1**, $H_2N_2^{iPr}N^{Me}$ = $MeN(CH_2CH_2NH^iPr)_2$) containing the sterically less demanding isopropyl substituents was prepared. Preparation follows a simple condensation reaction of $MeN(CH_2CH_2NH_2)_2$ with acetone followed by reduction with $LiAlH_4$, subsequent lithiation of **3.1** and reaction with $Ti(NNPh_2)Cl_2(py)_3$ (**1.69**) yielded the new hydrazido compound $Ti(N_2^{iPr}N^{Me})(NNPh_2)(py)$ (**2.1**).[32] Reaction of **2.1** with the internal alkynes PhCCMe or MeCCMe gave unidentified mixtures, among which no single species could be identified. However, $Ti(N_2^{iPr}N^{Me})(NNPh_2)(py)$ (**2.1**) reacts with a range of terminal alkynes forming the vinylhydrazide-acetylide compounds $Ti(N_2^{iPr}N^{Me})\{N(NPh_2)C(H)C(H)(R)\}(CCR)$ (R = Tol (**3.2**), 4-$C_6H_4CF_3$ (**3.3**), 4-C_6H_4OMe (**3.4**), C_6F_5 (**3.5**), $SiMe_3$ (**3.6**)), Equation 3.1.



Equation 3.1

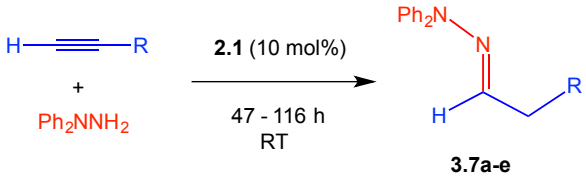
The *cis* isomer (*cis* refers to the *cis* orientation of the vinylhydrazide ligand and NMe donor) was the major isomer observed at room temperature in all cases. When the reaction of **2.1** and HCC-4-C_6H_4Me was followed from -70 ^oC the first formed product was the *trans* isomer, which then converted predominantly to the *cis* isomer as room temperature was approached. No other intermediates were observed. The *cis* isomer may be thermodynamically favoured on steric grounds as it places the bulky -$N(NPh_2)C(H)C(H)(Ar)$ moiety away from the isopropyl substituents. The formation of these compounds was rapid and the reactions were complete within minutes. The reactions are irreversible and proposed to proceed *via* a [2 + 2] cycloaddition reaction followed by a σ-bond metathesis to yield the final products

(Scheme 3.2). A similar mechanism has been proposed by Fryzuk for the reaction of a zirconium dinitrogen compound with terminal alkynes.[43]



Scheme 3.2. Proposed mechanism for the formation of vinylhydrazide-acetylide compounds.

Some preliminary results showed that both **2.1** and **3.2** - **3.6** are catalysts for the hydrohydrazination of terminal alkynes with Ph_2NNH_2. This reactivity contrasts remarkably with that of **1.72**. The product of catalysis is specific for the formation of the anti-Markovnikov hydrazones, Equation 3.2. The catalysis was slow at room temperature, requiring 47 - 116 hours to reach conversion > 90% and an order of magnitude slower when $HCCC_6F_5$ was used. However, these slow reactions are not untypical of titanium catalysed hydrohydrazination carried out at room temperature,[29, 31, 34] with the exception of a more recently reported system by Gade.[10]



R = Tol (**a**), 4-$C_6H_4CF_3$ (**b**), 4-C_6H_4OMe (**c**), C_6F_5 (**d**), $SiMe_3$ (**e**)

Equation 3.2

The catalysis is independent of alkyne concentration and no significant kinetic isotope effect was found when using DCCTol (KIE = 1.1(1)). A much more significant isotope effect of 3.7(2) was observed when Ph_2NND_2 was used suggesting that the turnover-limiting step is protonation of the vinylhydrazide-acetylide species to yield the organic hydrazone.

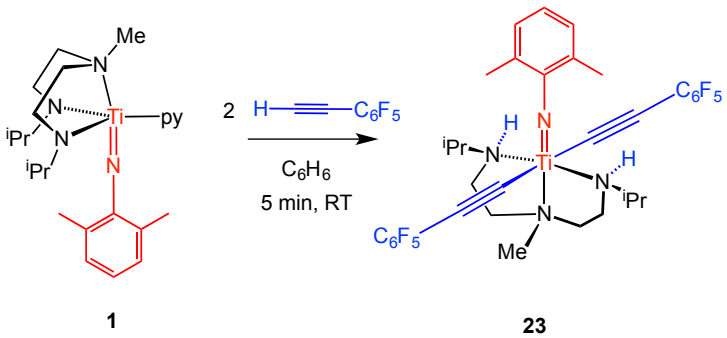
Although titanium azametallacylcobutene complexes derived from imido or hydrazido compounds are known, and there are many examples of inserting unsaturated

substrates into the M–C bond,[6, 20, 44-46] this was the first example of a σ-bond metathesis at this stage. A similar type of intermediate containing both hydrazido(1-) (or amido) and a vinylhydrazido(1-) (or vinylamido) moieties is often employed in hydrohydrazination (and hydroamination) catalytic cycles following protonolysis of the M–C bond of a metallacycle. Therefore compounds **3.2 - 3.6** represented the first isolated models of this vinylhydrazido(1-) moiety.

Since the reactions of the **2.1** with terminal alkynes yielded such unusual products, it was hoped that further studies could provide more information with regards to the mechanism for their formation and the subsequent catalytic cycle. However, as mentioned above, the reactions of **2.1** with terminal alkynes are complete within minutes and no intermediates were observed at low temperature. Therefore, interested in understanding this chemistry further, reaction of the analogous imido compound Ti($N_2^{iPr}N^{Me}$)(NXyl)(py) (**1**), described in Chapter Two of this Thesis, with terminal alkynes will now be discussed.

3.3 Reaction of Ti($N_2^{iPr}N^{Me}$)(NXyl)(py) (1) with electron-withdrawing terminal alkynes

Reaction of Ti($N_2^{iPr}N^{Me}$)(NXyl)(py) (**1**) with two equivalents of $HCCC_6F_5$ gave the unusual bis(acetylide) species Ti($H_2N_2^{iPr}N^{Me}$)(CCC_6F_5)$_2$(NXyl) (**23**), in which both the N_{amide} atoms have been protonated and the imido ligand remains intact (Equation 3.3). The reaction was quantitative when carried out on the NMR tube scale and **23** was isolated in 60% yield on a preparative scale. Diffraction-quality crystals were grown from a saturated toluene solution at -30 °C. The solid-state structure is shown in Figure 3.2 with selected bond lengths and angles listed in Table 3.1.



1 **23**

Equation 3.3

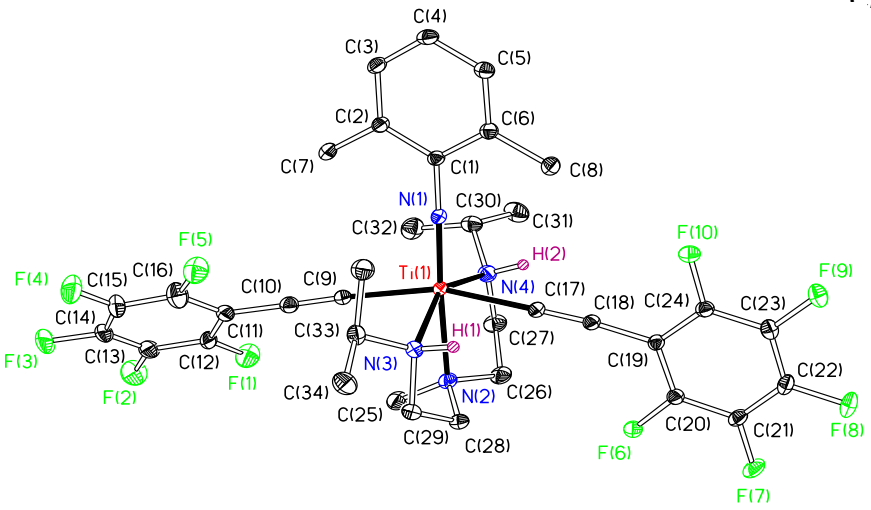


Figure 3.2. Displacement ellipsoid plot (25% probability) of $Ti(H_2N_2^{iPr}N^{Me})(CCC_6F_5)_2(NXyl)$ (**23**)**.** Carbon-bound H atoms are omitted for clarity.

Table 3.1. Selected bond distances (Å) and angles (°) for $Ti(H_2N_2^{iPr}N^{Me})(CCC_6F_5)_2(NXyl)$ (**23**).

Ti(1)-N(1)	1.7327(10)	N(1)-Ti(1)-N(2)	173.36(5)
Ti(1)-N(2)	2.3897(11)	N(1)-Ti(1)-N(3)	108.14(4)
Ti(1)-N(3)	2.2787(11)	N(1)-Ti(1)-N(4)	97.12(5)
Ti(1)-N(4)	2.2252(12)	N(3)-Ti(1)-N(4)	151.22(4)
Ti(1)-C(9)	2.2098(13)	N(2)-Ti(1)-N(3)	78.35(4)
Ti(1)-C(17)	2.2182(13)	N(2)-Ti(1)-N(4)	76.25(4)
C(9)-C(10)	1.1979(19)	Ti(1)-N(1)-C(1)	177.79(9)
C(17)-C(18)	1.2132(18)	N(1)-Ti(1)-C(9)	98.41(5)
C(10)-C(11)	1.4237(19)	N(1)-Ti(1)-C(17)	96.85(5)
C(18)-C(19)	1.4278(17)	N(2)-Ti(1)-C(9)	83.33(4)
		N(2)-Ti(1)-C(17)	82.69(4)
		N(3)-Ti(1)-C(9)	84.84(4)
		N(3)-Ti(1)-C(17)	80.70(4)
		N(4)-Ti(1)-C(9)	105.29(5)
		N(4)-Ti(1)-C(17)	82.85(5)

Compound **23** has an approximately octahedral geometry around the titanium centre, with the neutral tridentate ligand coordinated meridonally, the two acetylide ligands mutually *trans* and the NMe donor *trans* to the imido moiety. The Ti–N(H) bond distances are now typical of neutral σ-only interactions (2.2787(11) and 2.2252(12) Å compared to 1.970(2) and 1.959(2) Å in **1**). The Ti–N_{imide} bond is significantly shortened compared to **1** (1.7327(10) *vs.* 1.7581(19) Å), as the N_{amide} donor atoms are now protonated they can no longer compete with the imido ligand for the π-acceptor orbitals on titanium. This allows for better π-donation from the imido ligand, and a shorter Ti–N_{imide} bond, despite the higher coordination number. Both of the ^{i}Pr substituents are positioned on the same side of the {N(1), N(2), N(3), N(4)} plane, thus the compound does not possess C_2 symmetry and the two acetylide ligands are in chemically different environments.

Compound **23** is the first example of a Group 4 bis(acetylide) compound not supported by a cyclopentadienyl ligand. The Ti–C bond lengths (2.2098(13) and 2.2182(13) Å) are slightly longer than the distances in the titanium bis(acetylide) compound $(C_5H_4SiMe_3)_2Ti(CCSiMe_3)_2$ (2.124(5) and 2.103(5) Å).[47]

Interestingly, there are some relatively close intermolecular contacts between -C_6F_5 ring carbons of adjacent molecules in the crystal lattice, shown in Figure 3.3. The aromatic ring containing atoms C(19) - C(24), which lies in the same plane as the xylyl imido substituent, perpendicular to the {N(1), N(2), N(3), N(4)} plane (the ring containing atoms C(11) - C(16) is twisted significantly out of this plane) is orientated in an offset face-to-face manner with the same perfluorophenyl aromatic ring on one adjacent molecule. This π-stacking is finite and does not propagate to form chains. The close contacts exist between C(19)···C(23A), C(20)···C(24A) and C(21)···C(24A) and are measured to be 3.332, 3.450 and 3.562 Å, respectively. Such π-stacking type interactions are well known in general for fluorinated aryl rings including between the N-substituents of titanium imido compounds.[48-55]

Another intermolecular short contact exists between H(1) and F(8) of the adjacent molecule, also shown in Figure 3.3. The ability of a C–F bond to act as a hydrogen-bond acceptor is somewhat disputed in the literature.[56-63] Dunitz and Taylor examined this in a survey of crystal structures from the Cambridge Structural Database and Protein Data Bank and they used the criterion of < 2.3 Å to identify such interactions.[59] A review published in 2015 by Paquin *et al.* outlines other criteria for

weak hydrogen bonds, for example a X–H···F angle close to 180 ° and a lengthening of the X–H bond on formation of a hydrogen bond.[64] The H(1)···F(8) distance of 2.267 Å and N(3)-H(1)···F(8) angle of 156.8 ° suggests that a weak hydrogen bond exists. An analogous interaction is not observed on the other side of the molecule. However, no significant lengthening of the N(3)-H(1) bond is observed in comparison to N(4)-H(2) and the two bond distances are the same within error (1.954(18) and 1.931(18) Å for N(3)-H(1) and N(4)-H(2) respectively). The ν(N–H) band lies at 3232 cm^{-1} in the solid-state IR spectrum and there is a slight broadening of the peak possibly due to inequivalent N–H environments. A solution phase IR spectrum was recorded in benzene and the N–H peak and is very slightly red-shifted to 3236 cm^{-1}. This could be indicative of the loss of the weak N–H···F interaction in solution resulting in a stronger N–H bond. However, it is equally likely to simply reflect the change in medium. In 2005 Mountford and co-workers described several titanium compounds containing N–H···Cl hydrogen bonds in the solid-state, which exhibited much larger ν(N–H) red shifts (20 - 60 cm^{-1}) when recorded in solution.[54]

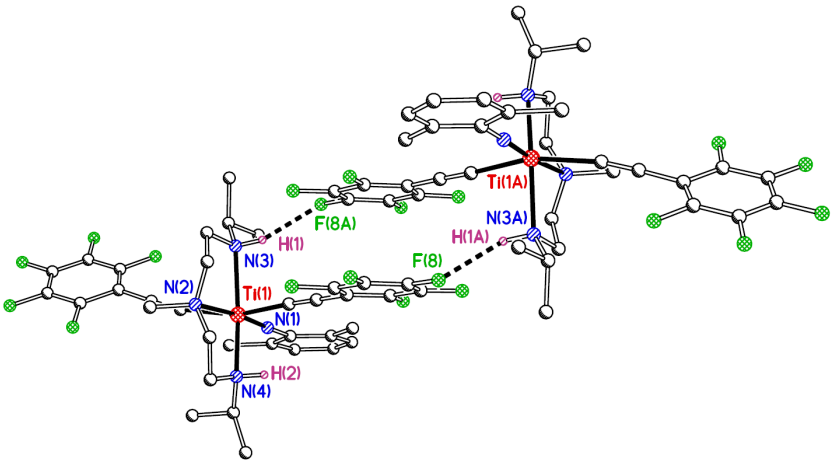


Figure 3.3. Pairwise arrangement of molecules of Ti($H_2N_2^{iPr}N^{Me}$)(CCC_6F_5)$_2$(NXyl) (**23**) in the solid state. C-bound H atoms omitted. Atoms drawn as spheres of arbitrary radius. Atoms carrying the suffix 'A' are related to their counterparts by the symmetry operator [–*x*, 1-*y*, 1-*z*].

A band at 2089 cm^{-1} in the Nujol mull and solution phase infrared spectra is attributed to ν(C≡C) consistent with Cp-supported titanium and zirconium acetylide ligands frequencies reported in the literature.[24, 65] Addition of two equivalents of $DCCC_6F_5$ to **1** gave **23-*d*$_2$** where the deuterium atoms reside exclusively on the amide nitrogen

atoms as identified from ^{1}H and ^{2}H NMR spectra. The ν(N–H) band is absent in the IR spectrum of **23-*d*$_2$** and the ν(N–D) band is found at 2406 cm^{-1}, in reasonable agreement with the prediction made by the harmonic oscillator model (2285 cm^{-1}).

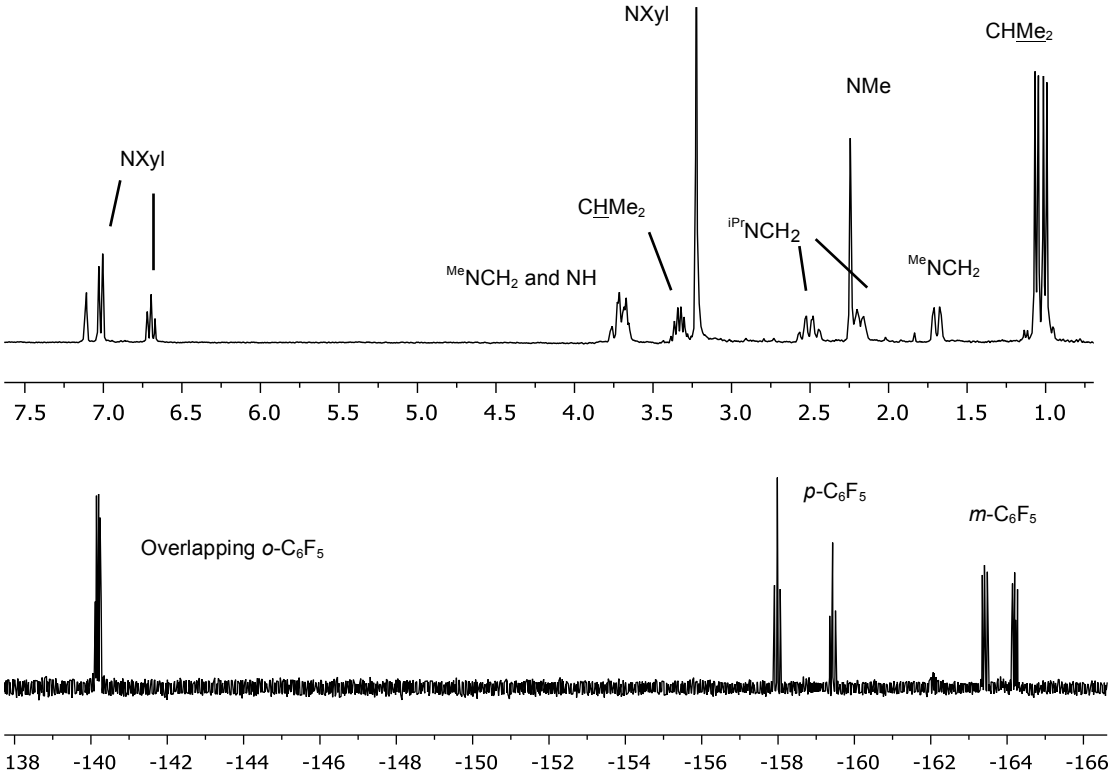


Figure 3.4. Top: ^{1}H NMR spectrum (299.9 MHz) of Ti($H_2N_2^{iPr}N^{Me}$)(CCC_6F_5)$_2$(NXyl) (**23**) in C_6D_6 at 298 K. Bottom: ^{19}F NMR spectrum (282.1 MHz) of Ti($H_2N_2^{iPr}N^{Me}$)(CCC_6F_5)$_2$(NXyl) (**23**) in C_6D_6 at 298 K.

The solution ^{1}H and ^{19}F NMR spectra of **23** are shown in Figure 3.4 and are fully consistent with the C_s symmetric solid-state structure. Two sets of signals are observed in the ^{19}F NMR spectrum indicating that the two fluorinated rings are in different environments, *vide supra*. The C<u>H</u>Me$_2$ resonance has undergone a significant upfield shift compared to **1** (3.37 *vs.* 5.52 ppm) and is a doublet of septets due to three bond coupling to both CH<u>Me$_2$</u> and NH. The NC_6H_3<u>Me$_2$</u> signal appears more downfield compared to **1** at 3.27 ppm (2.36 ppm in **1**) and the pair of doublets at 1.03 and 1.11 ppm are attributed to the CH<u>Me$_2$</u> protons. The multiplet at 3.84 - 3.66 ppm has relative intensity 4H as one $^{Me}NCH_2$ and NH resonances overlap. The relative intensity is reduced to 2H in **23-*d*$_2$**.

Interestingly, the multiplet pattern resulting from the diastereotopic CH_2 methylene protons is quite distinctive compared to complexes of the corresponding $N_2^{iPr}N^{Me}$

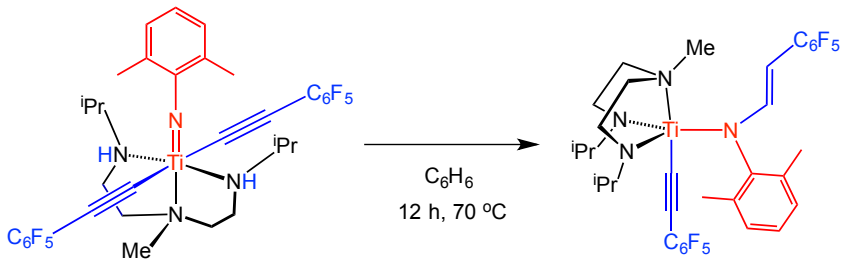
dianionic ligand. When the diamide-amine ligand is dianionic and bound in a κ^3-*fac* manner, four almost identical multiplets are observed due to two and three bonding coupling, the two $^{iPr}NC\underline{H}_2$ resonances appearing downfield of the $^{Me}NC\underline{H}_2$ resonances in all cases.

In the ^{1}H NMR spectrum of **23** four multiplets are also observed for the methylene protons. One of the $^{Me}NC\underline{H}_2$ resonances is the most downfield at 3.84 - 3.66 ppm, followed by the two multiplets resulting from the $^{iPr}NC\underline{H}_2$ at 2.55 ppm and 2.24 ppm and the most upfield resulting from the remaining $^{Me}NC\underline{H}_2$ proton at 1.73 ppm. The multiplets are no longer identical due to the meridional arrangement of the now neutral ligand. The $^{Me}NC\underline{H}_2$ resonance at 1.73 ppm is a broad doublet with a ^2J coupling constant of 12.6 Hz. The ^{1}H-^{1}H COSY NMR spectra indicates a three bond coupling to both of the $^{iPr}NC\underline{H}_2$ protons. However, this fine structure is not observed in the ^{1}H NMR spectra. Similarly the $^{iPr}NC\underline{H}_2$ resonances have a different appearance due to the additional coupling to N–H.

Several examples report the synthesis of Group 4 acetylide compounds *via* C–H activation of a terminal alkyne. These reactions usually involve transfer of the proton to the X atom of a Ti–X multiple bond (X = N or O).[23, 24, 65-67] The addition of phenylacetylene to a scandium imido compound has also been reported resulting in acetylide-amido compound.[68] The analogous reaction also occurs with the tantalum imido compound $[Cp^*_2Ta(N^tBu)(THF)][B(C_6F_5)_4]$.[69] Some magnesium alkynyl complexes have been synthesised *via* protonation of a bound amide[70, 71] and a similar reaction has been reported with an iridium amido compound with phenylacetylene.[72] Thus, the formation of **23** is not wholly unusual, but was, however, unexpected. Furthermore, the possibility that initial H transfer to the N_{imide} atom occurs prior to transfer onto the N_{amide} atoms cannot be ruled out. The reactions of **1** with $XylNH_2$ and Ph_2NH were described in Chapter Two and both resulted in transfer of the H atom onto the N_{imide} atom.

Heating a benzene solution of **23** at 70 ^oC for 12 hours resulted in isomerisation to the vinylamide(1-)-acetylide(1-) complex $Ti(N_2{}^{iPr}N^{Me})\{N(Xyl)C(H)C(H)C_6F_5\}(CCC_6F_5)$ (**24**) (Equation 3.4). No other intermediates were observed. This compound is the vinylamido analogue of **3.5**, the compound observed when the $N_2{}^{iPr}N^{Me}$ supported hydrazido compound **2.1** was reacted with two equivalents of $HCCC_6F_5$. Heating **23-*d*$_2$** results in the formation of **24-*d*$_2$** where the mutually coupled doublets at 8.35 and

4.64 ppm resulting from the vinyl protons in the ^{1}H NMR spectrum are no longer present and the expected resonances are observed in the ^{2}H NMR spectrum. Compound **24** can be synthesised directly from **1** without isolating **23**. Addition of $DCCC_6F_5$ to a solution of **24** does not result in any isotope scrambling suggesting that the formation of **24** is irreversible. The solid-state structure of **24** is shown in Figure 3.5. However, the structural details will be discussed later in the Chapter alongside analogous compounds**.**



23 **24**

Equation 3.4

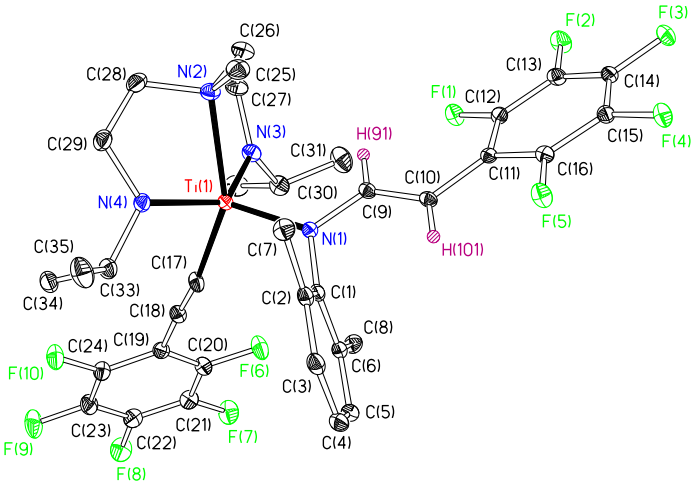
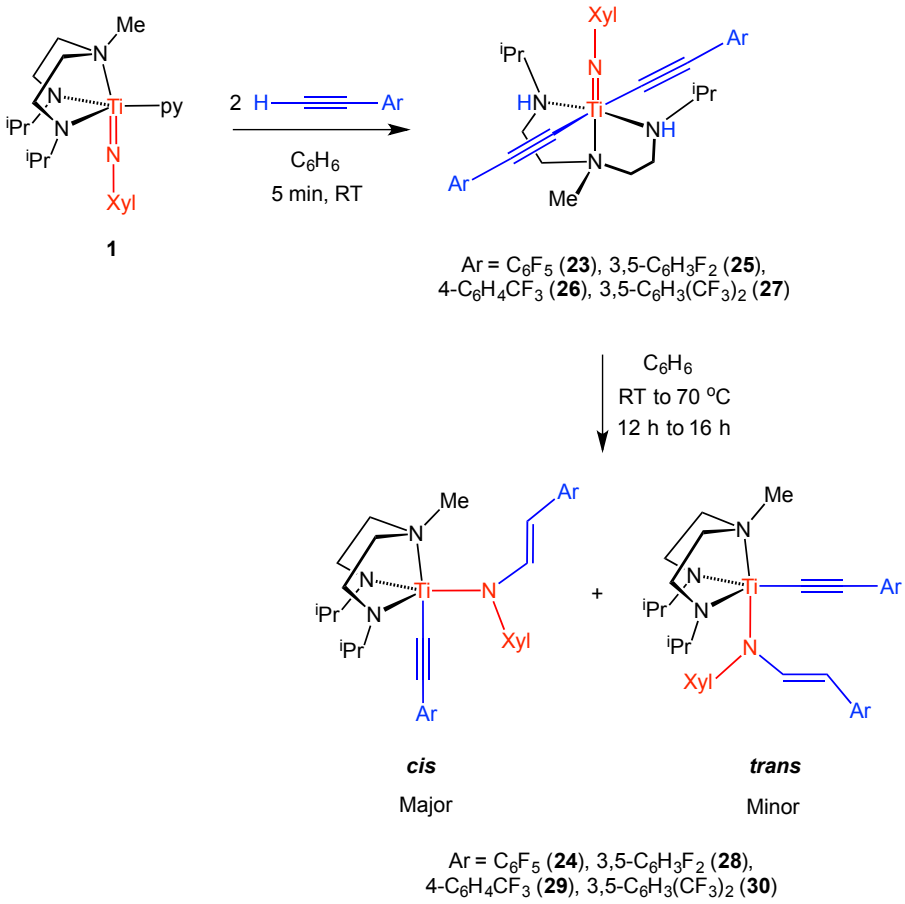


Figure 3.5. Displacement ellipsoid plot (20% probability) of $Ti(N_2^{iPr}N^{Me})\{N(Xyl)C(H)C(H)(C_6F_5)\}(CCC_6F_5)$ (**24**). H atoms except H(91) and H(101) and the other crystallographically independent molecule are omitted for clarity.

Reaction of $Ti(N_2^{iPr}N^{Me})(NXyl)(py)$ (**1**) with two equivalents of HCCAr where Ar = 3,5-$C_6H_3F_2$, 4-$C_6H_4CF_3$ or 3,5-$C_6H_3(CF_3)_2$ resulted in the formation of analogous bis(acetylide) compounds $Ti(H_2N_2^{iPr}N^{Me})(CCAr)_2(NXyl)$ (Ar = 3,5-$C_6H_3F_2$ (**25**), 4-$C_6H_4CF_3$ (**26**) and 3,5-$C_6H_3(CF_3)_2$ (**27**)) followed by isomerisation to vinylamide-

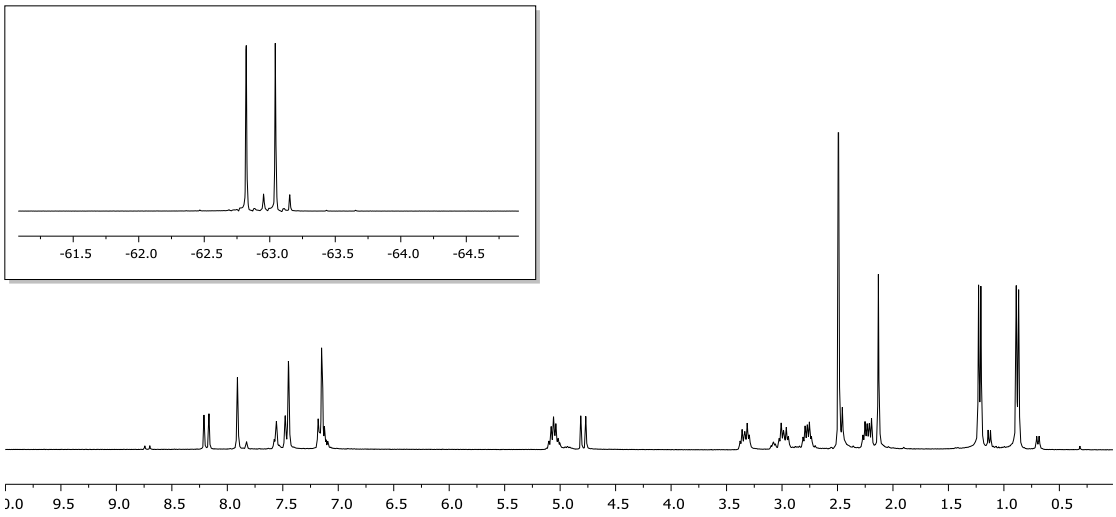
acetylide compounds Ti($N_2^{iPr}N^{Me}$){N(Xyl)C(H)C(H)Ar}(CCAr) (Ar = 3,5-$C_6H_3F_2$ (**28**), 4-$C_6H_4CF_3$ (**29**) and 3,5-$C_6H_3(CF_3)_2$ (**30**)) (Scheme 3.3).



Scheme 3.3. Reaction of Ti($N_2^{iPr}N^{Me}$)(NXyl)(py) (**1**) with electron-withdrawing terminal aryl alkynes.

Compounds **25** - **27** form immediately at room temperature, and within five minutes begin to rearrange to the corresponding vinylamide-acetylide complexes. After ten hours at room temperature isomerisation was complete. Compounds **28** - **30** were synthesised on a preparative scale and characterised by ^{1}H, ^{13}C, ^{19}F NMR and IR spectroscopy, elemental analysis and in the case of **30**, X-ray crystallography (the solid-state structure will be discussed later). The ^{1}H NMR spectrum of **30** is shown by way of example in Figure 3.6. The mutually coupled doublets at 8.19 and 4.79 ppm are attributed to the vinylic protons TiNC(H) and TiNC(H)C(H) respectively. The ^{19}F NMR spectrum displays two singlets consistent with two aryl environments. The minor resonances are a result of the *trans* isomer. The ^{1}H NMR spectra of compounds

28 and **29** are comparable and all spectra are fully consistent with the connectivity shown in Scheme 3.3.



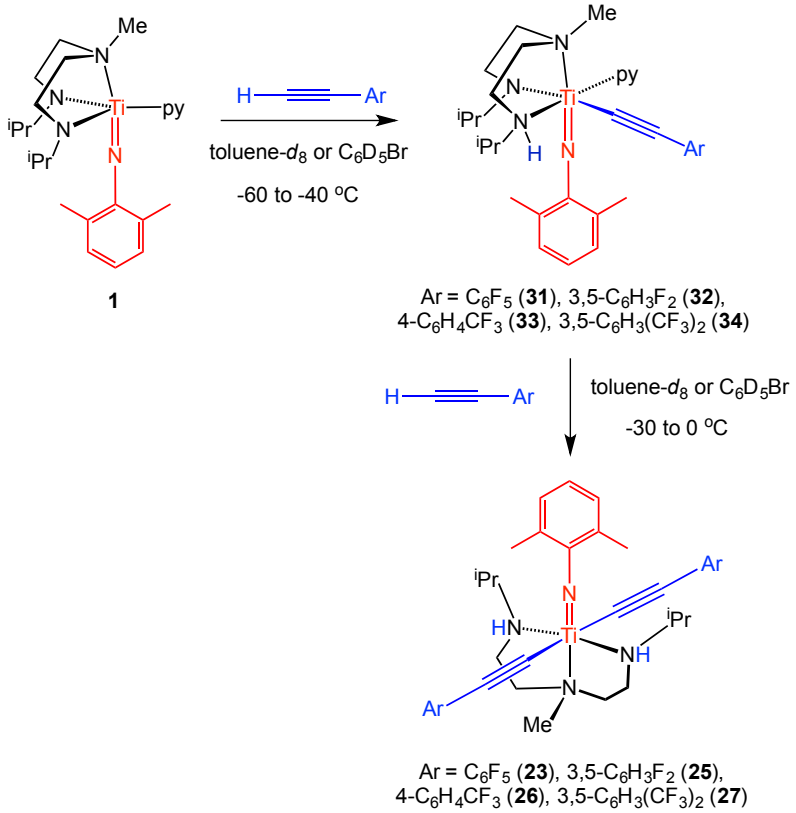
Figures 3.6. ^{1}H NMR spectrum (299.9 MHz) of Ti($N_2^{iPr}N^{Me}$){N(Xyl)C(H)C(H)-3,5-$C_6H_3(CF_3)_2$}(CC-3,5-$C_6H_3(CF_3)_2$) (**30**) in C_6D_6 at 298 K. Inset : corresponding ^{19}F NMR spectrum (282.1 MHz, 298 K, C_6D_6).

As the isomerisation reactions occur readily at room temperature it was not possible to isolate the bis(acetylide) intermediates on a preparative scale. Thus ^{1}H, ^{19}F and ^{13}C NMR spectra of **25**, **26** and **27** were obtained at low temperature by carrying out the reactions at -40 ^{o}C, and then warming to between -10 and 0 ^{o}C, allowing full conversion to the bis(acetylide) compounds, but slowing down the isomerisation. The chemical shifts observed in the ^{13}C NMR spectra associated with the acetylide ligands are distinctive, and in all three cases two resonances are observed between 144.5 - 157.7 and 106.3 - 114.2 ppm resulting from the Ti<u>C</u> and TiC<u>C</u> environments respectively. These signals are in the same region as observed in **23** (Ti<u>C</u>C = 166.4 and 164.0 ppm and TiC<u>C</u> = 97.5 and 95.7 ppm).

Resonances attributable to the NH protons are observed and in all cases the C<u>H</u>Me_2 resonances are shifted significantly upfield and appear in the region of 3.31 - 3.36 ppm. This upfield shift of the methine proton when the N_{amide} atom is protonated has been observed in several compounds described in the Chapter Two. The NC_6H_3<u>Me_2</u> resonances experience an upfield shift and the CH<u>Me_2</u> signals experience a downfield shift analogous to what was observed in **23**. The expected diagnostic pattern of methylene signals is apparent. The similarity in the ^{1}H and ^{13}C NMR spectra and the

presence of two fluorine environments resulting from the inequivalent acetylide ligands in all three compounds confirms the assignment of compounds **25** - **27** as the bis(acetylide) compounds shown in Schemes 3.3 and 3.4.

In order to observe the first addition of alkyne to **1** prior to the formation of **23, 24** - **27** the reaction of **1** with two equivalents of alkyne was followed from -78 °C. Intermediates were observed at -60 °C when using $HCCC_6F_5$ and at -40 °C when using HCC-3,5-$C_6H_3(CF_3)_2$, HCC-3,5-$C_6H_3F_2$ and HCC-4-$C_6H_4CF_3$ and are proposed to be the 6-coordinate species Ti($HN_2^{iPr}N^{Me}$)(CCAr)(NXyl)(py) (Ar = C_6F_6 (**31**), 3,5-$C_6H_3F_2$ (**32**), 4-$C_6H_4CF_3$ (**33**) and 3,5-$C_6H_3(CF_3)_2$ (**34**)) (Scheme 3.4). On warming, the second addition of alkyne was observed; with $HCCC_6F_5$ this reached completion as -30 °C was approached, and with the other alkynes as 0 °C was approached. On warming to room temperature (or heating with $HCCC_6F_5$) isomerisation to the vinylamide-acetylide compounds followed.



Scheme 3.4. Reaction of Ti($N_2^{iPr}N^{Me}$)(NXyl)(py) (**1**) with electron-withdrawing terminal aryl alkynes from low temperature.

Figure 3.7 shows representative ^{1}H NMR spectra of the subsequent steps for the reaction of **1** with HCC-3,5-$C_6H_3F_2$. The bottom spectrum is the ^{1}H NMR spectrum of **1** in toluene-d_8 prior to the addition of any alkyne at low temperature. The ^{1}H NMR spectrum resulting from the first addition of alkyne yielding the mono(acetylide) species **32** was recorded at -40 ^{o}C and is shown above that of **1**. The ^{1}H NMR spectrum of the bis(acetylide) species **25** is shown next resulting from the addition of a second equivalent of alkyne. The ^{1}H NMR spectrum of the vinylamide-acetylide species **28** is shown at the top, and was recorded once the isomerisation from **25** was complete.

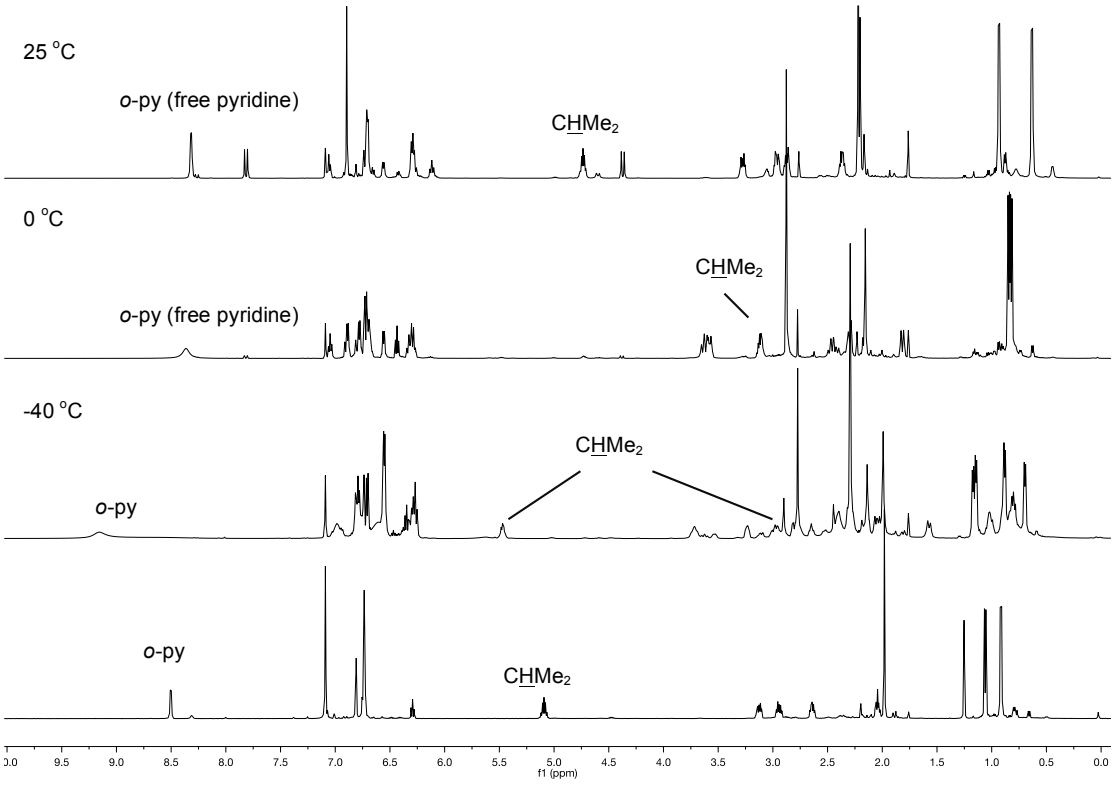


Figure 3.7. ^{1}H NMR spectra (499.9 MHz, toluene-d_8) of Ti($N_2^{iPr}N^{Me}$)(NXyl)(py) (**1**) at 298 K (bottom), Ti($HN_2^{iPr}N^{Me}$)(CC-3,5-$C_6H_3F_2$)(NXyl)(py) (**32**) at 233 K (second), Ti($H_2N_2^{iPr}N^{Me}$)(CC-3,5-$C_6H_3F_2$)$_2$(NXyl) (**25**) at 273 K (third) and Ti($N_2^{iPr}N^{Me}$){N(Xyl)C(H)C(H)-3,5-$C_6H_3F_2$}(CC-3,5-$C_6H_3F_2$) (**28**) at 298 K (top).

Intermediates **31** - **34** are C_1 symmetric in solution due to the unsymmetrical nature of the ligand and inequivalent equatorial ligands. Four doublets are observed for the CH$\underline{\text{Me}}_2$ protons and two for the C$\underline{\text{H}}$Me$_2$ protons. The two methine resonances are observed between 5.97 - 5.72 ppm and 3.06 - 2.62 ppm, the more upfield resulting from NHC$\underline{\text{H}}$Me$_2$. Interestingly the pyridine ligand appears to be coordinating to

titanium in all cases, as indicated by the downfield chemical shifts compared to free pyridine (Figure 3.7). Only one set of resonances are observed in the ^{19}F NMR spectra consistent with just one acetylide ligand environment. These mono(acetylide) intermediates are proposed to be six-coordinate complexes with the imido ligand in the axial position, as in the starting imido compound. The acetylide ligand *cis* to the N–H bond (expected from C–H addition across Ti–N) and the pyridine ligand occupying the remaining coordination site *trans* to the now amine donor. It is possible that the NH^{i}Pr donor is no longer coordinated to titanium. 1D and 2D ^{1}H NOE NMR experiments were carried out in an attempt to probe the arrangement of ligands, however no useful correlations were observed. The ^{13}C NMR spectra indicate only one resonance for Ti<u>C</u>C and one for TiC<u>C</u>, again consistent with just one acetylide ligand. Four signals are observed as a result of the methylene carbon atoms, four from the CH<u>Me</u>$_2$ carbons and two from the CH<u>Me</u>$_2$, carbons consistent with unsymmetrical ligand backbones.

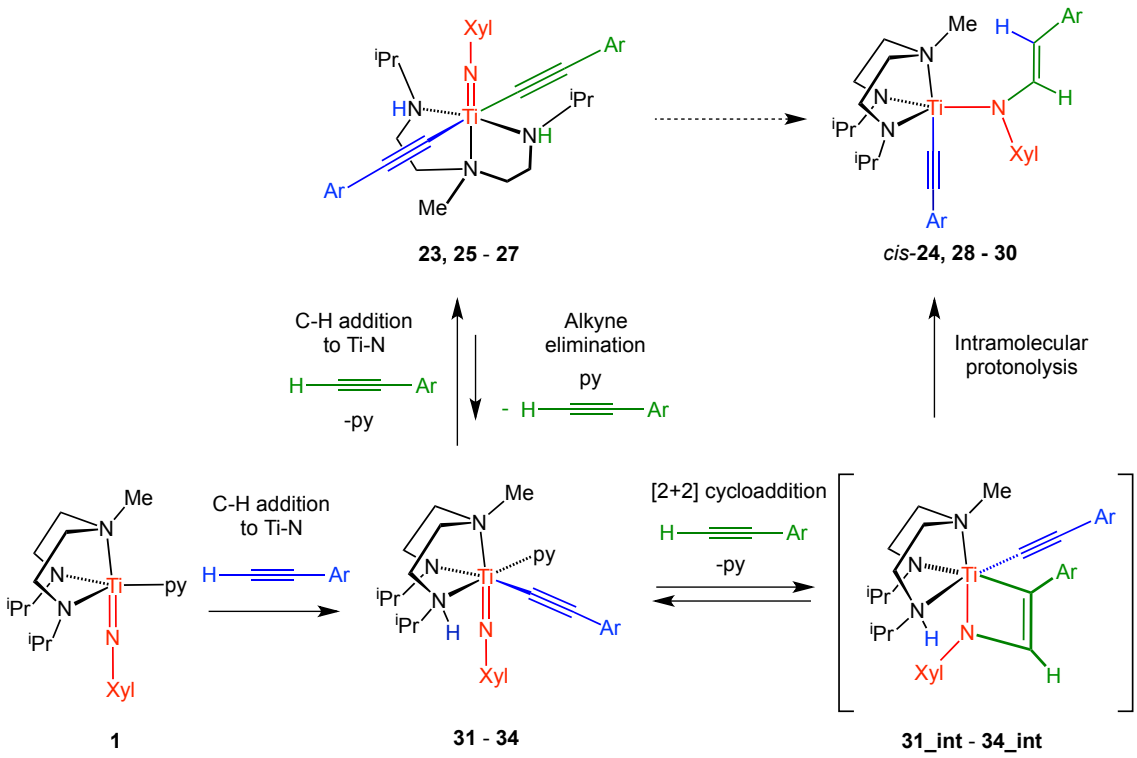
The mono(acetylide) compounds **31** - **34** are proposed to contain the acetylide and the NH^{i}Pr ligands in a *cis* orientation. In the solid-state structure of **23** only one acetylide ligand remains *cis* to a N–H, therefore the second alkyne addition must have an associated low energy rearrangement allowing the two acetylide ligands to become trans to each other.

The reaction of Ti($N_2^{iPr}N^{Me}$)($NNPh_2$)(py) (**2.1**) with Ph_2NH or H-BHT was described in Chapter Two. The reaction products **7** and **9** also contain a monoanionic ligand due to protonation of a N_{amide} atom. Compound **9** was structurally authenticated and the new N–H bond is *cis* to the BHT ligand. Such compounds are isolable models of the mono(acetylide) species described above, and demonstrate that in some cases formal H^+ addition to the Ti–N_{amide} bond is favourable. Compounds **7** and **9** do not containing a pyridine ligand unlike compounds **31** - **34** most likely due to the increased steric bulk of the new –NPh_2 and –BHT ligands in comparison to an acetylide ligand.

3.4 Mechanistic studies on the reaction of Ti($N_2^{iPr}N^{Me}$)(NXyl)(py) (1) with electron-withdrawing terminal alkynes

3.4.1 Proposed mechanism

The proposed mechanism for the formation of bis(acetylide) compounds **23, 25 - 27** and their subsequent isomerisation to the vinylamide-acetylide compounds **24, 28 - 30** is shown in Scheme 3.5. Two C–H σ-bond metathesis reactions at the Ti–N_{amide} bonds of **1** result in formation of the bis(acetylide) products **23, 25 - 27** *via* mono(acetylide) intermediates **31 - 34**. An equivalent of alkyne can then eliminate to reform the mono(acetylide). This alkyne addition-elimination is reversible and the mono and bis(acetylide) species are in rapid equilibrium in solution. Alternatively, instead of re-adding the free alkyne, an irreversible [2+2] cycloaddition reaction can occur yielding the 6-coordinate azatitanocyclobutene-acetylide intermediates **31_int - 34_int** (not observed) followed by intramolecular protonolysis from the remaining N–H to Ti–C. This gives the vinylamide-acetylide compounds with the vinylamide ligand *trans* to the NMe donor (not observed). Rapid isomerisation to the *cis* isomer then occurs and the *cis* isomer is the major product in all cases. When the reactions of Ti($N_2^{iPr}N^{Me}$)($NNPh_2$)(py) (**2.1**) with terminal alkynes were followed from low temperature the *trans* isomer was observed as the first formed product and rapid isomerisation occurred above 0 ^oC. However here, reaction temperatures above 0 ^oC are required for the reaction to occur at all, therefore the *trans* isomer is not observed as the first formed product as *trans*/*cis* isomerisation occurs readily at the reaction temperature. The *trans* orientation of the vinyl protons is consistent with replacing the Ti–C bond of a metallacycle with a new C–H bond. For example, Fryzuk reported the reaction of a zirconium dinitrogen compound with two equivalents of PhCCH proceeded *via* a [2+2] cycloaddition reaction followed by protonation of the metallacycle to yield a new vinyl moiety with a *trans* arrangement.[43]



Scheme 3.5. Proposed reaction mechanism for the reaction of Ti($N_2^{iPr}N^{Me}$)(NXyl)(py) (**1**) with electron withdrawing terminal aryl alkynes.

The bis(acetylide) compound **23** is evidently kinetically more stable than **25 - 27** as it can be isolated at room temperature prior to isomerisation. It has been reported that relative M–X bond enthalpies correlate with the H–X bond enthalpies.[73-76] Furthermore, it has been experimentally observed that the M–C bond energies increase more rapidly with changes in substituent than the corresponding C–H bond, therefore the difference in M–C bond strengths is larger than the corresponding difference in C–H bond strengths. Thus, there is a thermodynamic preference to break the stronger C–H bond.[77] DFT calculations have been used to validate these trends by predicting changes in relative bond enthalpies with varying substituents.[78] Such calculations were found to be in particularly good agreement with a experimental report by Wolzanski who published correlations between Ti–C and H–C bond enthalpies for Ti(R)$(silox)_2(NHSi^tBu_3)$.[79, 80]

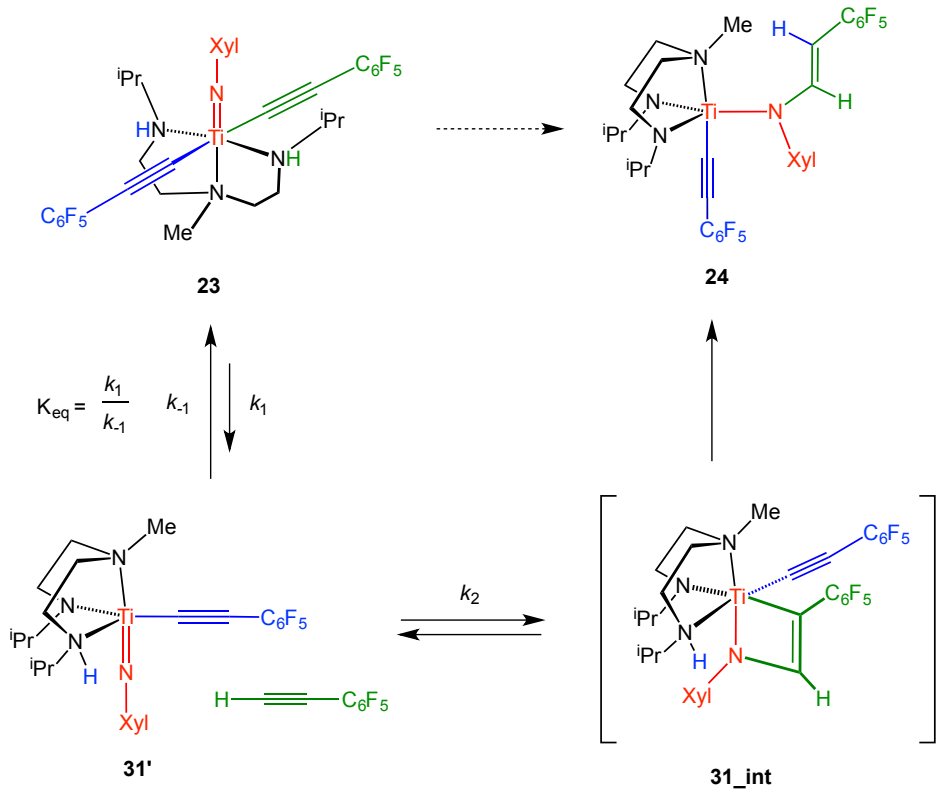
The C–H stretching frequency of terminal alkynes can be used as a guide for C–H bond strength and thus M–C bond strength. Thin film IR spectra were obtained for the following alkynes $HCCC_6F_6$, HCC-4-$C_6H_4CF_3$ and HCC-4-C_6H_4Me, and the C–H stretching mode was observed at 3310, 3306 and 3291 cm^{-1}, respectively. Stronger H–C bonds, and therefore stronger M–C bonds result when electron-withdrawing

substituents are employed with the strongest bond found for the -C_6F_5 substituent. $HCCC_6F_5$ also contains the most acidic C–H bond, despite it being the strongest. This is a consequence of the more electron-withdrawing aryl group and thus a more polar H–C bond and a more stable conjugate base, due to a stabilising inductive effect as well as delocalisation of the negative charge.

The differing bond strengths and acidities are likely to contribute towards the formation of **31** and **23** at a lower temperature than was observed for **32** - **34** and **25** - **27**. However, although the trend in H–C and therefore M–C bond strength is in line with the observed stability of bis(acetylide) compounds, meaning that stronger Ti–C bonds are formed when $HCCC_6F_5$ is employed thus making elimination of an alkyne less favourable. The difference in ν(C–H) stretches is very small and the relative Ti–C bond strengths are unlikely to be solely responsible for the large difference in stability between bis(acetylide) species. This suggests that a later step in the isomerisation not involving Ti–C bond formation or cleavage is important for a low energy isomerisation.

3.4.2 Kinetic study of the isomerisation of Ti($H_2N_2^{iPr}N^{Me}$)(CCC_6F_5)$_2$(NXyl) (23) to Ti($N_2^{iPr}N^{Me}$){N(Xyl)C(H)C(H)(C_6F_5)}(CCC_6F_5) (24)

Since Ti($H_2N_2^{iPr}N^{Me}$)(CCC_6F_5)$_2$(NXyl) (**23**) can be isolated, the isomerisation reaction to Ti($N_2^{iPr}N^{Me}$){N(Xyl)C(H)C(H)(C_6F_5)}(CCC_6F_5) (**24**) could be interrogated without concern for the role of pyridine. The rate of isomerisation to **24** was studied using ^{1}H NMR spectroscopy by following the decay of **23** by integration over several hours. Carrying out the reaction in the presence of an internal siloxane standard demonstrated that the isomerisation was quantitative on the NMR tube scale. The rate constant for the elimination of an equivalent of alkyne from **23** to form **31′** (**31′** represents the pyridine-free intermediate) and the reverse reaction to form **23** from **31′** are denoted "k_1" and "k_{-1}", respectively. The overall rate constant for the alternative cycloaddition reaction followed by intramolecular protonolysis of **31′** with alkyne is denoted "k_2" (Scheme 3.6).



Scheme 3.6. Mechanism for the formation of $Ti(N_2{}^{iPr}N^{Me})\{N(Xyl)C(H)C(H)C_6F_5\}(CCC_6F_5)$ (**24**) from $Ti(H_2N_2{}^{iPr}N^{Me})(CCC_6F_5)_2(NXyl)$ (**23**).

As none of the mono(acetylide) species **31′** is observed during the course of reaction, a steady-state approximation was applied to this intermediate in order to obtain a rate equation (Equations 3.5 - 3.9). The final form of the rate equation is shown in Equation 3.9. The approximation $k_{-1} >> k_2$, Equation 3.7, has been used because complete formation of the bis(acetylide) species occurs prior to a slow isomerisation requiring elevated temperatures. The observed rate constant (k_{obs}) is a combination of the equilibrium constant (K_{eq}) between **23** and **31′** and the secondary k_2 value.

$$\frac{d[\mathbf{31'}]}{dt} = k_1[\mathbf{23}] - k_{-1}[\mathbf{31'}][\text{alkyne}] - k_2[\mathbf{31'}][\text{alkyne}] = 0 \quad (3.5)$$

$$[\mathbf{31'}] = \frac{k_1[\mathbf{23}]}{k_{-1}[\text{alkyne}] + k_2[\text{alkyne}]} \quad (3.6)$$

$$\frac{d[\mathbf{24}]}{dt} = k_2[\mathbf{31'}][\text{alkyne}] \quad (3.7)$$

$$= \frac{k_1 k_2[\mathbf{23}]}{k_{-1} + k_2}$$

$$\frac{d[\mathbf{24}]}{dt} = \frac{k_1 k_2[\mathbf{23}]}{k_{-1}} \quad (\text{if } k_{-1} >> k_2)$$

$$K_{eq} = \frac{k_1}{k_{-1}} \quad (3.8)$$

$$-\frac{d[\mathbf{23}]}{dt} = \frac{d[\mathbf{24}]}{dt} = K_{eq}k_2[\mathbf{23}] = k_{obs}[\mathbf{23}] \quad (3.9)$$

The isomerisation of **23** to **24** in toluene-d_8 was monitored in the temperature range 60 - 83 ^oC. By way of example, a plot showing the decay of **23** and growth of **24** at 75 ^oC is shown in Figure A1 of the Appendix. The reaction followed first order kinetics over this temperature range as judged by linear semilogarithmic plots of $\ln([\mathbf{23}]_t/[\mathbf{23}]_0)$ *vs.* time (Figure 3.8). The reaction was monitored over 13 hours and the plots of 68 - 83 ^oC are shown to at least 85% conversion (approximately three half-lives). However, reaction at 60 and 65 ^oC only reached 35% and 55% conversion, respectively, during this time. To check that accurate rate constants were still being obtained the reaction was monitored at 60 ^oC for 44 hours allowing the reaction to reach 85% conversion; the rate constant obtained was similar (1.23(2) x 10^{-5} *vs.* 0.99(1) x 10^{-5} s^{-1}). The rate is independent of excess alkyne with the rate constants being found to be approximately the same when the isomerisation was monitored in the presence of two or six extra equivalents of $HCCC_6F_5$ at 70 ^oC (6.18(1) x10^{-5}, 6.15(1) x 10^{-5} and 5.99(2) x 10^{-5} s^{-1} for zero, two and six equivalents of alkyne respectively). Similarly, k_{obs} was found to be independent of the concentration of **23** and reactions monitored at double and triple

the concentration at 75 ^{o}C showed no systematic variation (9.33(2) x10^{-5}, 11.45(1) x 10^{-5} and 10.52(2) x 10^{-5} s^{-1} for standard, double and triple the concentration respectively). The reaction was monitored in the presence of an equivalent of pyridine (**23** made *in situ* from **1** and $HCCC_6F_5$) at 70 ^{o}C which also had no effect on the observed rate constant (6.44(1) x 10^{-5} *vs.* 6.18(1) x 10^{-5} s^{-1}), showing that the expected trapping of **31′** by pyridine (forming **31**) does not inhibit the overall transformation of **23** to **24**.

An Eyring analysis of the rate constants, k_{obs}, was carried out giving the activation parameters $\Delta H^{\ddagger}$ = 29.1(2.2) kcal mol^{-1} and $\Delta S^{\ddagger}$ = 6(6) cal mol^{-1} K^{-1} ($\Delta G_{298}^{\ddagger}$ = 27.3(2.2) kcal mol^{-1}) (Figure 3.8). The free energy of activation ($\Delta G^{\ddagger}$) is consistent for a reaction that requires elevated temperature to proceed. The overall entropy of activation is effectively zero, at first sight this suggests a reaction pathway where both dissociatively and associatively activated steps play a role in k_{obs} as implied by the proposed mechanism. The isomerisation of **23-*d*$_2$** to **24-*d*$_2$** was also monitored in the same manner at 70, 75 and 83 ^{o}C, the rate constants were found to be 4.17(1) x $10^{-5,}$ 7.05(1) x 10^{-5} and 13.56(5) x 10^{-5} s^{-1} (in comparison to 6.18(1) x 10^{-5} s^{-1}, 9.33(2) x10^{-5} and 19.69(8) x 10^{-5} s^{-1} for **23**) giving a small kinetic isotope effect of 1.4(1) at all recorded temperatures. Kinetic isotope effects for reactions involving C–H/N–H bond breaking reactions are usually larger. For example there are several reports of zirconium, titanium and tantalum compounds undergoing abstraction of a N-H atom by another ligand to yield an organic product, in a similar manner to the k_1 step proposed above.[81-88] Large kinetic isotope effects were reported in all cases (4.6 - 14.1) and are often proposed to be a result of transition states where the transfer of H is relatively linear. Generally smaller kinetic isotope effects in the region 2.5 – 3.5 are expected for proton transfers occurring by non-linear transition states,[32, 41, 89-92] although smaller values have been reported.[93, 94] The small isotope effect observed here for the isomerisation of **23** to **24** may suggest the presence of isotope-sensitive equlibria rather than a KIE for one step. An equilibrium isotope effect of 1.28 for a similar reaction was described by Bergman and will be discussed in detail later[65] and inverse equilibrium isotope effects of the order 0.3 - 0.8 have been reported for alkane elimination reactions.[95-97]

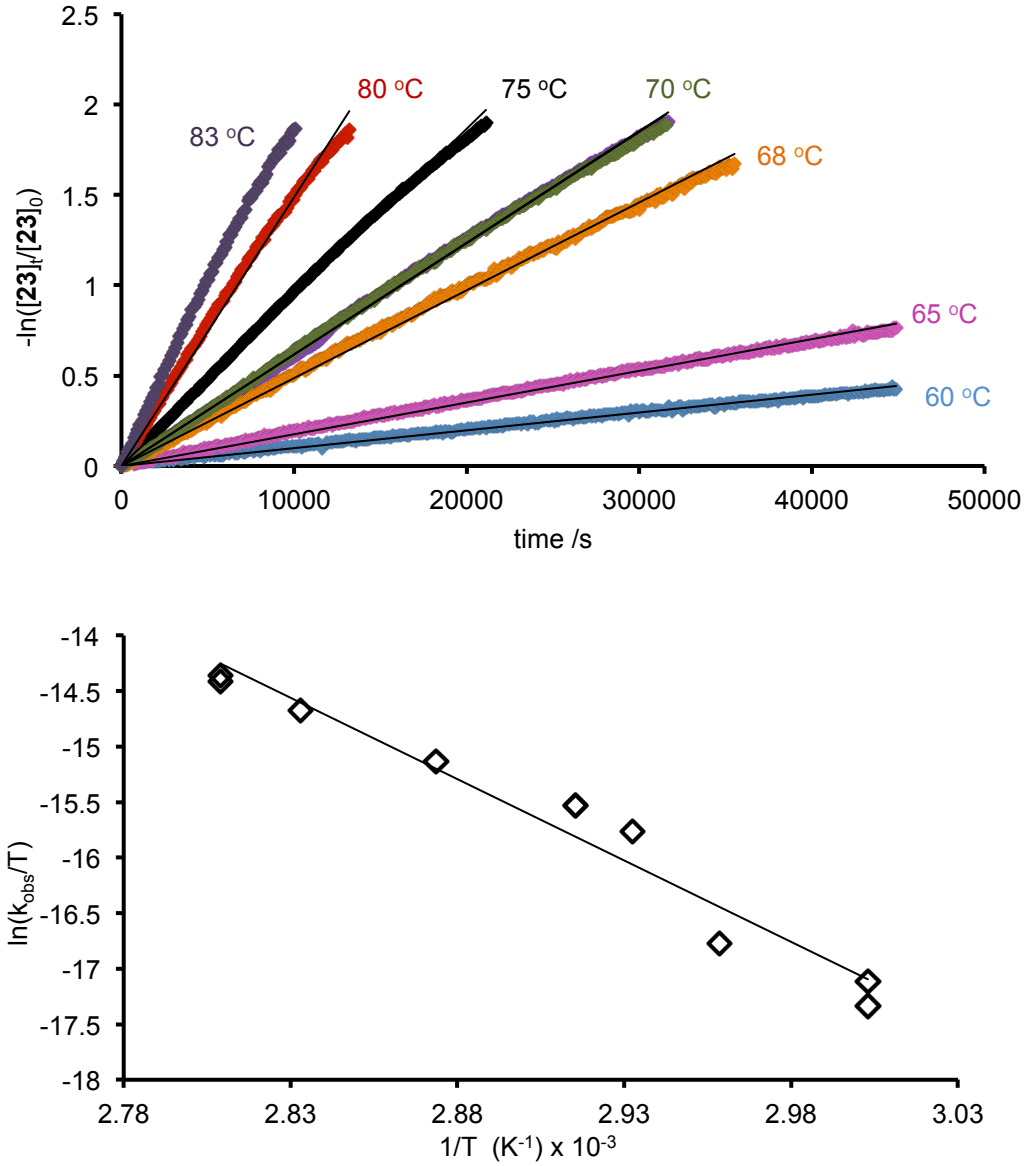
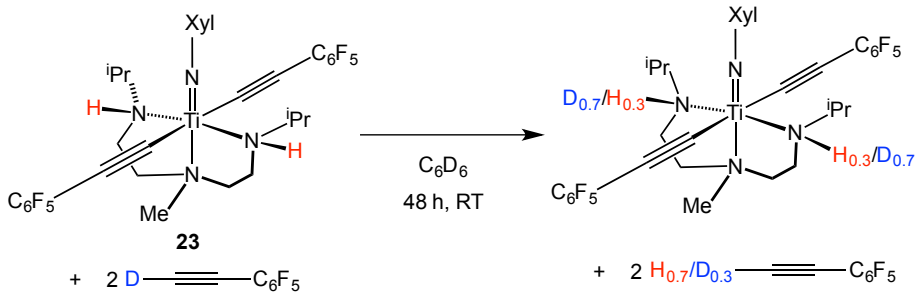


Figure 3.8. Top: first order semi-logarithmic plots for the isomerisation of $Ti(H_2N_2^{iPr}N^{Me})(CCC_6F_5)_2(NXyl)$ (**23**) in toluene-d_8. (avg. r^2 = 0.994, range 0.983-0.999). Bottom: Eyring plot for the isomerisation of $Ti(H_2N_2^{iPr}N^{Me})(CCC_6F_5)_2(NXyl)$ (**23**) in toluene-d_8. Activation parameters derived from linear regression analysis (r^2 = 0.957): $\Delta H^{\ddagger}$ = 29.1(2.2) kcal mol^{-1}; $\Delta S^{\ddagger}$ = 6(6) cal mol^{-1} K^{-1}; $\Delta G_{298}^{\ddagger}$ = 27.3(2.2) kcal mol^{-1}. Note that the experiments at 333, 343 and 356 K were repeated in duplicate (points at 1/T = 3.03 x10^{-3}, 2.92 x 10^{-3} and 2.81 x 10^{-3} K^{-1}).

3.4.3 Isotope effects

3.4.3.1 Pre-equilibrium

Isotope-sensitive equilibria occurring prior to the rate-determining step in a multi-step reaction can result in a observed isotope effect for the overall reaction.[98] The following experiment was used to probe the presence of such equlibria in this system. On reaction of Ti($H_2N_2^{iPr}N^{Me}$)(CCC_6F_5)$_2$(NXyl) (**23**) with two equivalents of $DCCC_6F_5$, a reduction in the relative intensity of the N–H resonances of **23** along with the appearance of the alkyne C–H resonance at 2.83 ppm was seen in the ^{1}H NMR spectrum, indicating incorporation of deuterium into the N–H positions (Equation 3.10). After just 10 minutes the relative intensity of the N–H resonance had reduced to 80% of its original value, the intensity continued to decrease over time and after 5 hours was measured to be 40%. On standing for 48 hours at room temperature the relative intensity of the N–H resonance indicates that only 30% carries a hydrogen atom, meaning that 70% of the $^{iPr}N_{amine}$ atoms are carrying a deuterium atom. The **23-*d*$_1$**, **23-*d*$_2$** and **23** isotopomers could not be distinguished. The increase in relative intensity of the alkyne C–H resonance is not complimentary. This discrepancy is due to the unusually long relaxation time of the C–H terminal alkyne proton, which was independently measured to be T_1 = 80 s. Therefore, a ^{1}H NMR spectrum was recorded with d_1 = 500 s, allowing sufficient time for the C–H proton to relax and an accurate integration obtained. The C–H resonance now indicates that 70% of the free alkyne in solution exists as the protio form. This equilibration occurs without rearrangement to the final vinylamide-acetylide product.



Equation 3.10

Incorporation of deuterium into the N–H positions is possible due to the rapid equilibrium between the bis(acetylide) species **23** and the mono(acetylide) species **31′**. Following elimination of an equivalent of $HCCC_6F_5$ from **23** addition of either

$HCCC_6F_5$ or $DCCC_6F_5$ can occur. Further evidence of a different alkyne (to the one that has eliminated) adding to a mono(acetylide) intermediate will be described later. All isotopomers of the bis(acetylide) and mono(acetylide) compounds are in equilibrium in solution. No mono(acetylide) species is observed, indicating that the equilibrium sits almost entirely on the side of the bis(acetylide) compound.

The non-statistical distribution of H and D across **23** and the free alkyne following equilibration implies the presence of an equilibrium isotope effect (EIE). Equilibrium isotope effects are usually understood in terms of zero point energy (ZPE). In particular, isotopomers with deuterium located in the site with the highest vibrational frequency are the most stable. This is the result of the difference is zero point energies increasing with vibrational frequency and thus deuterium populating the site which has the greatest ZPE stabilisation i.e. deuterium prefers to reside in the stronger bond.[99, 100]

The preference for deuterium to reside on the N atoms rather than hydrogen indicates that there is a larger ZPE difference between N–D and C–D than N–H and C–H. This would be the expected result if N–H is stronger than C–H. The stretching frequencies are 3232 (Nujol mull) and 3310 cm^{-1} (thin film) for **23** and $HCCC_6F_5$ respectively suggesting that actually the $C_{(sp)}$–H (sp) alkyne bond is stronger than the $N_{(sp3)}$–H amine bond. However, the stretching frequencies of the corresponding N–D and C–D bonds were found to be 2406 (Nujol mull) and 2599 cm^{-1} (neat), thus the difference in zero point energies is larger for NH/ND than for CH/CD ($\Delta\upsilon$ = 826 cm^{-1} vs. $\Delta\upsilon$ = 711 cm^{-1}) despite N–H being the weaker bond. This means that $\Delta\upsilon$ (NH,CH) < $\Delta\upsilon$ (ND,CD) and deuterium populates the site with the greatest ZPE stabilisation. There are reported examples where ZPE interpretations are not sufficient in explaining the observed EIEs as a consequence of there being other isotopically sensitive frequency modes which, when combined, result in a greater ZPE stabilisation for the apparently weaker bond (by comparing just the stretching frequency).[99, 101] This may be the case here and **23** may have some vibrations weakly coupled to that of N–H resulting in a larger ZPE difference.

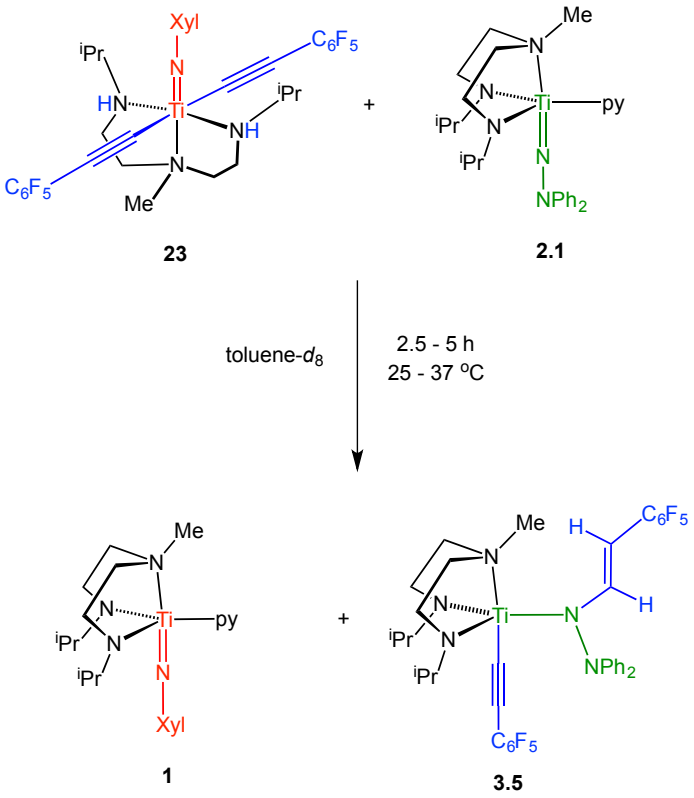
This experiment is important as it demonstrates a stronger preference for deuterium to reside on N_{amine} as opposed to the C–D bond of the free alkyne compared to hydrogen. This has implications for the overall isomerisation reaction of **23** to **24**. The first step

in the mechanism is the reversible elimination of an equivalent of alkyne from **23** to form **31′**, the position of this equilibrium will be altered on substitution of hydrogen for deuterium, as deuterium has a stronger preference to reside in the N–D bond. Therefore, K_{eq} will decrease for the equilibrium between **23-*d*$_2$** and **31′-*d*$_1$** compared to that for **23** to **31′** and a normal equilibrium isotope effect would be expected.

This phenomenon has implications for understanding the overall kinetic isotope effect observed for the isomerisation of **23** to **24**. The facile incorporation of deuterium into the N_{amine} positions at room temperature suggests that alkyne elimination from **23** is facile and thus not rate-determining in the isomerisation of **23** to **24**. Therefore **31′** is the species that undergoes the rate-determining step and hence knowledge of the EIE between **23** and **31′** is important. On substitution of H for D K_{eq} will decrease thus reducing the concentration of **31′** in solution. Therefore slowing the overall reaction. Measurement of K_{eq} could not be obtained by traditional methods of monitoring the ratio of two species in solution over a temperature range, as at room temperature no mono(acetylide) is observed in solution and on heating isomerisation would occur.

3.4.3.2 Crossover experiment

A second important observation was that reaction of Ti($H_2N_2^{iPr}N^{Me}$)(CCC_6F_5)$_2$(NXyl) (**23**) with the hydrazido compound Ti($N_2^{iPr}N^{Me}$)($NNPh_2$)(py) (**2.1**) gave quantitative conversion to the known imido compound Ti($N_2^{iPr}N^{Me}$)(NXyl)(py) (**1**) and the known vinylhydrazide-acetylide compound Ti($N_2^{iPr}N^{Me}$){N(NPh_2)C(H)C(H)(C_6F_5)}(CCC_6F_5) (**3.5**) (Equation 3.11).



Equation 3.11

This crossover experiment demonstrates that addition of both equivalents of alkyne across the titanium-nitrogen bonds of **1** are reversible in the presence of an alkyne trap. The reaction was monitored in toluene-d_8 by ^{1}H NMR spectroscopy in the temperature range 25 - 37 ^{o}C, and the decay of **23** measured by integration. The reaction followed first order kinetics as judged by linear semilogarithmic plots of $\ln([\mathbf{23}]_t/[\mathbf{23}]_0)$ *vs.* time. An Eyring analysis of the rate constants, k_{obs}, was carried out giving the activation parameters $\Delta H^{\ddagger}$ = 16(1) kcal mol^{-1} and $\Delta S^{\ddagger}$ = -20(4) cal mol^{-1} K^{-1} ($\Delta G_{298}^{\ddagger}$ = 22.4(1.2) kcal mol^{-1}) (Figure 3.9). The negative entropy of activation is surprising and is thought to be due to the second alkyne elimination being base-assisted. Coordination of a pyridine ligand prior to elimination could result in a negative entropy of activation.

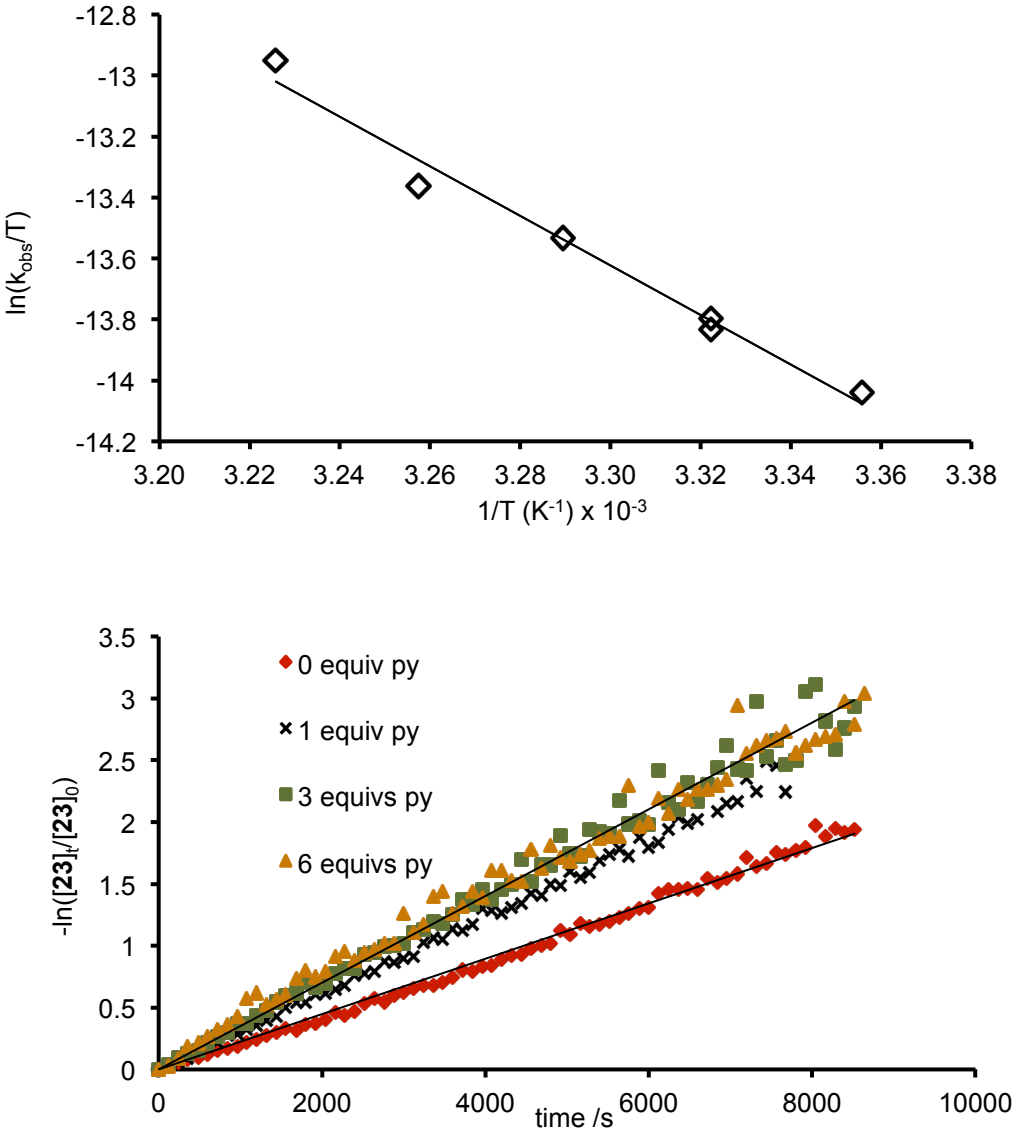
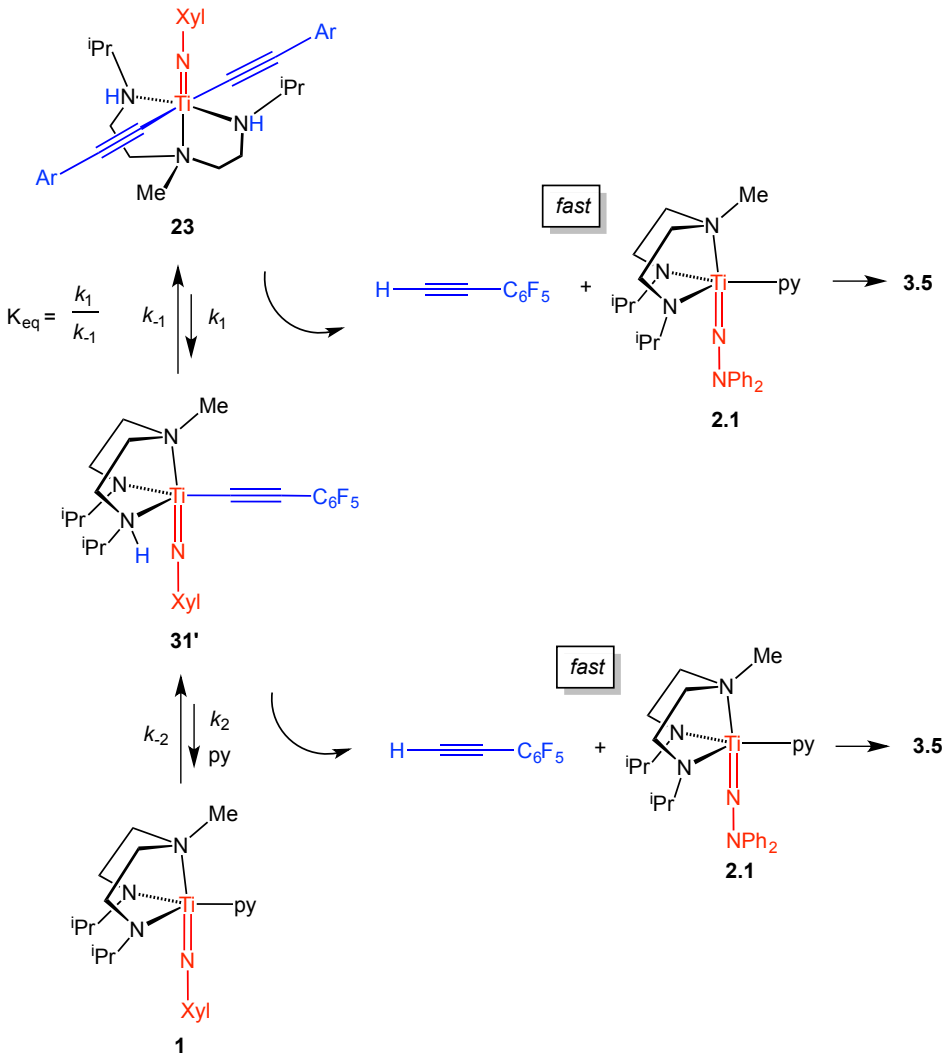


Figure 3.9. Top: Eyring plot for the reaction of Ti($H_2N_2^{iPr}N^{Me}$)(CCC_6F_6)$_2$(NXyl) (**23**) with Ti($N_2^{iPr}N^{Me}$)($NNPh_2$)(py) (**2.1**) in toluene-d_8. Activation parameters derived from linear regression analysis (r^2 = 0.981): $\Delta H^{\ddagger}$ = 16(1) kcal mol^{-1}; $\Delta S^{\ddagger}$ = -20(4) cal mol^{-1} K^{-1}; $\Delta G_{298}^{\ddagger}$ = 22.4(1.2) kcal mol^{-1}. Bottom: First order semi-log plots for the reaction of Ti($H_2N_2^{iPr}N^{Me}$)(CCC_6F_6)$_2$(NXyl) (**23**) with Ti($N_2^{iPr}N^{Me}$)($NNPh_2$)(py) (**2.1**) in toluene-d_8 with the number of equivalents of pyridine indicated at 298 K. 0 equivs of pyridine (r^2 = 0.982) k_{obs} = 23.2(2) x 10^{-5} s^{-1}, 1 equiv of pyridine (r^2 = 0.994) k_{obs} = 31.3(3) x 10^{-5} s^{-1}, 3 equivs of pyridine (r^2 = 0.985) k_{obs} = 35.2(3) x 10^{-5} s^{-1}, 6 equivs of pyridine (r^2 = 0.981) k_{obs} = 35.1(3) x 10^{-5} s^{-1}. Note that the experiment at 301 K was repeated in duplicate (point at 1/T = 3.32 x10^{-3} K^{-1}).

The rate constant was comparable (22.7(1) x10^{-5} *vs.* 23.8(2) x 10^{-5} s^{-1}) when an extra equivalent of **2.1** was used, suggesting that the activation parameters obtained reflect the two subsequent alkyne elimination reactions to reform the imido compound **1**. This is expected as the reaction of **2.1** with terminal alkynes is rapid and complete within minutes. This allows the kinetic treatment shown in Equations 3.12 - 3.15. The first step is the same in the isomerisation of **23** to **24**, thus elimination of an equivalent of alkyne to form the mono(acetylide) intermediate **31′** is denoted by the same rate constant "k_1" (the reverse reaction by "k_{-1}", Scheme 3.7).

The rate of formation of **1** can be written as shown in Equation 3.12 assuming that the reverse reaction to reform **31′** from **1** is negligible as eliminated alkyne is irreversible scavenged by **2.1**. Applying a steady-state approximation to **31′** (Equation 3.13) results in the rate equation shown in Equation 3.14. Again as the concentration of alkyne is essentially zero because it is immediately scavenged by **2.1**, the approximation k_{-1}[alkyne] << k_2[py] can be applied. The rate equation now has the form shown in Equation 3.15 where k_{obs} is effectively the rate constant for elimination of alkyne from **23** (k_1). However, there is no excess pyridine in the system meaning that the concentration of pyridine throughout the reaction is not large as **2.1** is the only source.

Therefore, the rate of reaction was monitored in the presence of one, three and six extra equivalents of pyridine at 298 K. With one extra equivalent a small increase in the rate constant was observed from 23.8(2) x 10^{-5} s^{-1} to 31.3(2) x 10^{-5} s^{-1}. However, on increasing this to three equivalents of pyridine only a small increase to 35.2(3) x 10^{-5} s^{-1} was observed and on using six equivalents of pyridine no further increase was observed (35.1(3) x 10^{-5} s^{-1}) (Figure 3.9). Thus the reaction is almost at saturation as the increase in rate constant on addition of pyridine is small. This allows the value of k_1 to be estimated to be between 23.8(2) x 10^{-5} and 35.2(3) x 10^{-5} s^{-1}.



Scheme 3.7. Mechanism for the formation of Ti($N_2^{iPr}N^{Me}$)(NXyl)(py) (**1**) from Ti($N_2H_2^{iPr}N^{Me}$)(CCC_6F_5)$_2$(NXyl) (**23**).

$$\frac{d[\mathbf{1}]}{dt} = k_2[\mathbf{31'}][py] \tag{3.12}$$

$$[\mathbf{31'}] = \frac{k_1[\mathbf{23}]}{k_{-1}[alkyne] + k_2[py]} \tag{3.13}$$

$$\frac{d[\mathbf{1}]}{dt} = \frac{k_1 k_2[\mathbf{23}][py]}{k_{-1}[alkyne] + k_2[py]} \tag{3.14}$$

$$\frac{d[\mathbf{1}]}{dt} = k_1[\mathbf{23}] = k_{obs}[\mathbf{23}] \quad \text{if} \quad k_{-1}[alkyne] << k_2[py] \tag{3.15}$$

The same reaction with **23-d_2** was monitored at 298 K and a kinetic isotope effect of 3.4(1) was observed (k_{obs} = 6.99(3) x 10^{-5} s^{-1}). This is a larger value in comparison to what was observed for the isomerisation of **23** to **24** and is consistent with a reaction involving abstraction of a proton from a metal bound nitrogen atom, as occurs in both the k_1 and k_2 steps to reform the imido compound **1**. Comparable examples include the reaction of compounds of the type (^{t}Bu$_3$SiNH)$_3$ZrR (R = Me, CH_2Ph or Ph) in C_6D_6 to yield compounds of the type (^{t}BuSiND)$_3$ZrC_6D_5 and RH *via* a rate-determining 1,2-elimination to yield an imido intermediate. When R = Me a kinetic isotope effect of 6.27(9) was obtained and when R = Ph the smaller value of 4.6(4) was obtained.[81, 85] Smaller KIE values have been reported for rate-determining N–H bond breaking reactions in catalytic reactions. Scott and co-workers described KIEs between 2.5 – 3.0 for the transfer of N–H protons and the formation of an imido intermediate.[90] Similarly the turnover limiting step in the hydrohydrazination catalytic cycle of **2.1** was proposed to be transfer of N–H protons of free hydrazine to the vinylhydrazide-acetylide intermediate as a KIE of 3.7(2) was obtained when Ph_2NND_2 was employed.[32] A close comparison can be drawn to a system described by Andersen and Bergman; they reported a KIE of 3.77(28) for the conversion of Cp*$_2$Ti(OH)(CCPh) to the transient titanium oxo-species Cp*$_2$Ti=O and HCCPh followed by a cycloaddition reaction.[65]

Importantly, as only a small increase in k_{obs} was observed in the presence of excess pyridine, the KIE observed here can be used as an approximate value for the KIE of k_1, the elimination of an equivalent of alkyne from **23**. Knowledge of this value provides a greater insight into the mechanism for the isomerisation of **23** to **24** and interpretation of the observed isotope effect will now be discussed further.

3.4.3.3 Interpreting the isotope effect for the isomerisation of 23 to 24

Significantly, the above crossover reaction of **23** with **2.1** proceeds readily at 25 ^{o}C and is complete after just 5 hours. When the temperature is raised to 37 ^{o}C the reaction time is reduced to 2.5 hours. The rate constant at this temperature was found to be 73.7(4) x 10^{-5} s^{-1}. In comparison 60 ^{o}C was the lowest temperature at which the isomerisation of **23** to **24** was monitored; at this temperature approximately 44 hours were required for the reaction to reach 85% completion and the rate constant obtained was an order of magnitude smaller (1.23(1) x 10^{-5} s^{-1}). Similarly the reaction of **23** with $DCCC_6F_5$ occurs readily at room temperature resulting in incorporation of deuterium into **23** following alkyne elimination and addition.

The first step in all of these reactions is elimination of one equivalent of $HCCC_6F_5$ from the bis(acetylide) **23**. The ease with which the crossover and exchange experiments occur strongly suggest that alkyne elimination from **23** to reform **31** (or **31′** or **1**) is facile. Thus, as postulated, alkyne elimination (k_1) is not the rate-determining step in the isomerisation of **23** to **24** and a reaction within the "k_2" step is.

As discussed above the isotope effect for the isomerisation of **23** to **24** is 1.4(1). The observed isotope effect is the ratio of the k_{obs} values. Based on the derived rate equation (Equation 3.9) the ratio of the k_{obs} values can be considered as a ratio of the equilibrium constants multiplied by the ratio of the k_2 values (Equation 3.16).

$$\text{Rate} = K_{eq}k_2[\mathbf{23}] = k_{obs}[\mathbf{23}] \qquad (3.9)$$

$$\text{KIE} = \frac{k_{obs(H)}}{k_{obs(D)}} = \frac{K_{eq(H)}}{K_{eq(D)}} \times \frac{k_{2(H)}}{k_{2(D)}} \qquad (3.16)$$

The overall isotope effect in multi-step reactions is the composite of the isotope effects for forward and backwards steps up to and including the rate-determining steps. Therefore, although k_1 is not rate-determining, knowledge of the equilibrium isotope effect for the pre-equilibrium occurring prior to the rate-determining k_2 step is essential in correctly interpreting the overall isotope effect. The two steps that follow alkyne elimination are represented by k_2. A [2+2] cycloaddition reaction involving no C–H or N–H bond breaking, followed by an intramolecular protonolysis reaction where an N–H bond in broken and a C–H bond is formed. As mentioned, kinetic

isotope effects for reactions involving proton transfer are typically large. Thus, the former [2+2] cycloaddition reaction is proposed to be the rate-determining step, and further evidence for this will be described later. As no bond breaking occurs in this step there will be no associated isotope effect and $k_{2(H)} \approx k_{2(D)}$. Therefore, the observed isotope effect is the result of the equilibrium isotope effect between **23** and **31′**. On substitution of H for D the concentration of the species undergoing the rate-determining step (**31′**) is reduced as a result of K_{eq} decreasing, therefore a small normal isotope effect is observed despite the rate-determining step having no associated KIE.

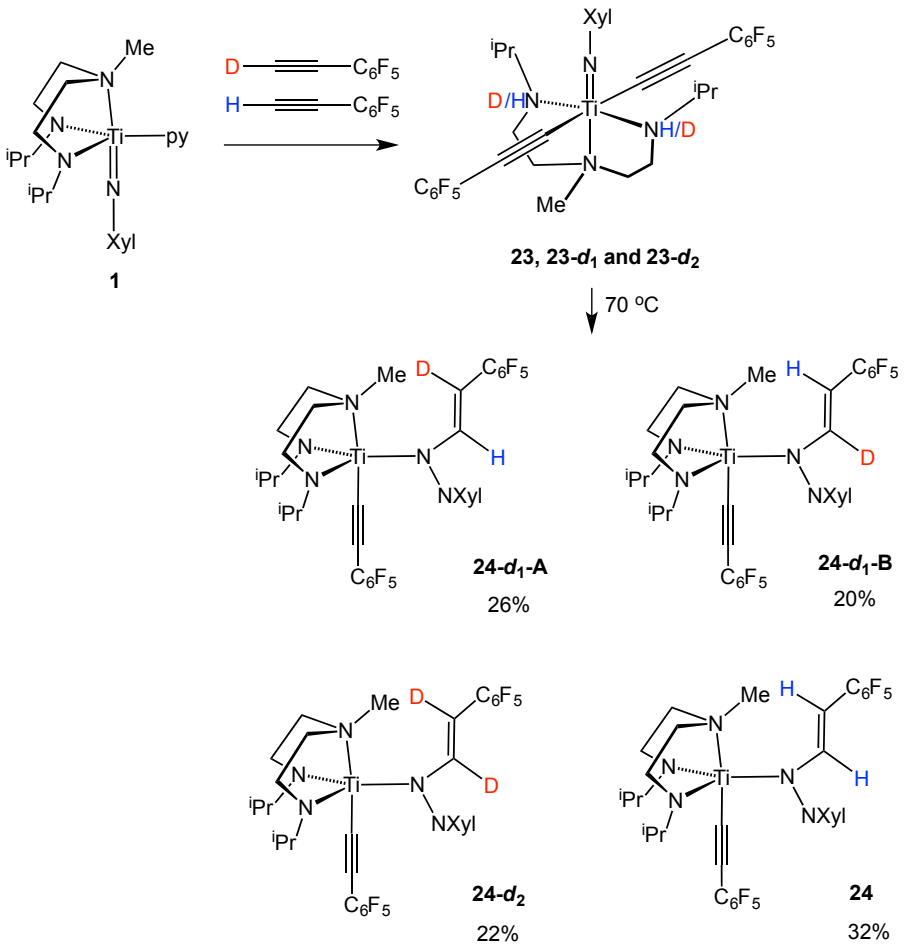
A negative entropy of activation would be expected from such a rate-determining step. However, as discussed earlier, in the absence of pyridine the entropy of activation is negligible ($\Delta S^{\ddagger}$ = 6(6) cal mol^{-1} K^{-1}). It is possible that once an equivalent of alkyne has eliminated from **23** it does not leave the reaction sphere and the same alkyne undergoes cycloaddition, meaning the reaction occurs in essentially an intramolecular (or inner-sphere type) manner, although, later results will demonstrate that this is not always the case.

Examples of equilibrium isotope effects include the intramolecular exchange between $(C_5Me_4H)_2Zr(ND^tBu)H$ and $(C_5Me_4H)_2Zr(NH^tBu)D$ which has a K_{eq} value of 0.41 as a result of deuterium preferring to reside in the stronger N–D bond.[102] A similar experiment was reported by Bullock who described the addition of hydrogen to a cationic manganese compound, resulting in new Mn–H and N–H bonds. When HD was employed the deuterium was preferentially found in the N position and the hydrogen on Mn. However, both sites were in rapid equilibrium and the equilibrium isotope effect was estimated to be in the range 0.13 - 0.23 at -20 ^{o}C.[103] Since metal hydride bonds are weaker there is a stronger preference for deuterium to reside in the stronger N–D bonds, hence the effect is more enhanced in comparison to the value obtained here. The closest comparable example is a reaction described by Bergman and Andersen.[65] They report the [2+2] cycloaddition reactions of the titanium oxo compound $Cp^*_2Ti(O)(py)$ with terminal alkynes to yield metallacycles. Thermolysis of these metallacycles at 45 - 100 ^{o}C results in conversion to hydroxoacetylide compounds of the type $Cp^*_2Ti(OH)(CCR)$. Mechanistic studies were carried out including the kinetics of the rearrangement and the mechanism was proposed to follow a facile cycloreversion followed by proton transfer and Ti–C bond formation.

As the reaction was reversible and both species were observed in solution, a direct measurement of the equilibrium isotope effect between the metallacycle and acetylide species was possible. They were also able to obtain a kinetic isotope effect for the formation of the acetylide species from the metallacycle. The equilibrium isotope effect was found to be 0.781(14) as deuterium favours the higher frequency bond (O–H) and thus the equilibrium shifts further to the hydroxoacetylide species on substitution of H for D. As the hydroxoacetylide species is defined as the product the observed EIE is inverse, in comparison, the bis(acetylide) compound **23** is defined as the starting material and thus a normal EIE for the elimination of an alkyne is obtained. When both equilibriums are defined in the same direction the values are comparable (1.4(1) *vs.* 1.28 (1/0.781)). An equilibrium isotope effect is the ratio of the forward and reverse kinetic isotope effects. The crossover experiment of **23** with **2.1** allowed an approximate value for the KIE of k_1 (the forward reaction) to be obtained thus the approximate KIE for k_{-1} is 2.4(2). This is similar to the KIE that Bergman described (2.94(6)) and is in the region expected for a C–H bond breaking reaction.

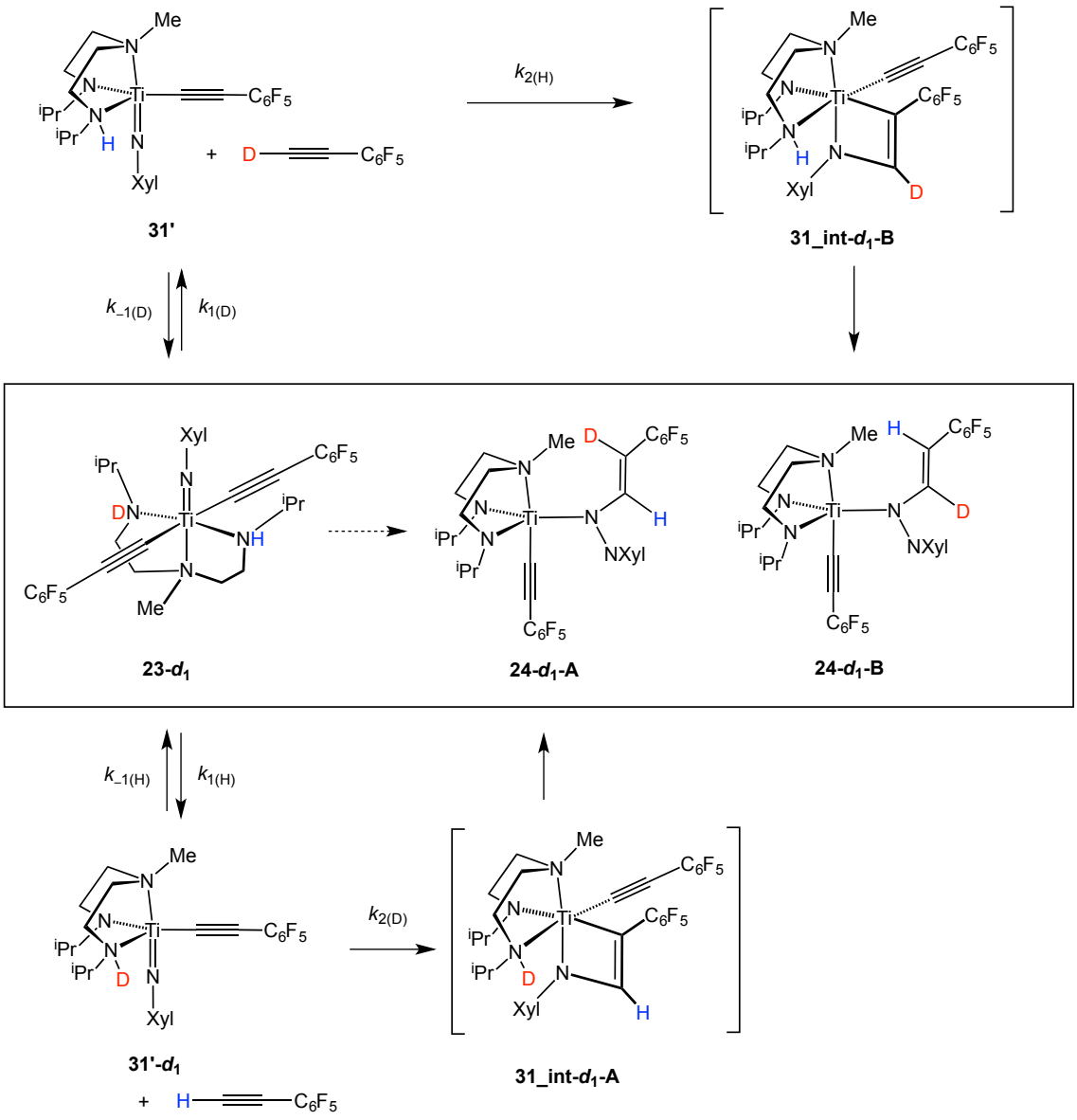
3.4.3.4 Independent estimate of the isotope effect

The observed isotope effect could also be obtained from an independent reaction. Reaction of Ti($N_2^{iPr}N^{Me}$)(NXyl)(py) (**1**) with a mixture of one equivalent of $HCCC_6F_5$ and one equivalent of $DCCC_6F_5$ results in the immediate formation of all four isotopomers of **23**, although they could not be distinguished. On heating at 70 ^oC isomerisation occurs and the d_0-, d_1- and d_2-labelled vinylamide-acetylide isotopomers were observed in a non-statistical distribution (Scheme 3.8). The two d_1- isotopomers are distinguished with the labels A and B. The isotopomer **24-d_1-A** refers to the deuterium atom in the TiNC(H)C(D) position and the isotopmer **24-d_1-B** with the deuterium atom in the TiNC(D)C(H) position.



Scheme 3.8 The isotopomers formed from the reaction of Ti($N_2^{iPr}N^{Me}$)(NXyl)(py) (**1**) with one equivalent of $HCCC_6F_5$ and one equivalent of $DCCC_6F_5$.

Assuming that following alkyne elimination from **23**, cycloaddition at the same titanium centre occurs, since the amount of mono(acetylide) and free alkyne present at any one time is very small ($k_{-1} >> k_1$), the isotopomers labelled **24-*d*$_1$-A** and **24-*d*$_1$-B** must arise from the same first formed bis(acetylide) isotopomer **23-*d*$_1$** (Scheme 3.8 and 3.9). Isotopomer **24-*d*$_1$-A** is formed when $HCCC_6F_5$ eliminates and undergoes cycloaddition leaving N–D to undergo intramolecular protonolysis. Similarly **24-*d*$_1$-B** is formed when $DCCC_6F_5$ eliminates first (Scheme 3.9). The rate laws for the formation of **24-*d*$_1$-A** and **24-*d*$_1$-B** from **23-*d*$_1$** are shown in Equations 3.17 and 3.19 respectively. The observed rate constants can be written as a combination of $K_{eq(H/D)}$ and $k_{2(H/D)}$ values as shown in Equations 3.18 and 3.20.



Scheme 3.9. Mechanism for the formation of **24-d_1-A** and **24-d_1-B** from the mono-deuterated isotopomer **23-d_1**.

$$\frac{d[\mathbf{24}\text{-}\boldsymbol{d_1}\text{-}\mathbf{A}]}{dt} = \frac{k_{1(H)}k_{2(D)}[\mathbf{23}\text{-}\boldsymbol{d_1}]}{k_{-1(H)}} = k_{obs(A)}[\mathbf{23}\text{-}\boldsymbol{d_1}] \quad (3.17)$$

$$k_{obs(A)} = \frac{k_{1(H)}}{k_{-1(H)}} \times k_{2(D)} = K_{eq(H)}k_{2(D)} \quad (3.18)$$

$$\frac{d[\mathbf{24}\text{-}\boldsymbol{d_1}\text{-}\mathbf{B}]}{dt} = \frac{k_{1(D)}k_{2(H)}[\mathbf{23}\text{-}\boldsymbol{d_1}]}{k_{-1(D)}} = k_{obs(B)}[\mathbf{23}\text{-}\boldsymbol{d_1}] \quad (3.19)$$

$$k_{obs(B)} = \frac{k_{1(D)}}{k_{-1(D)}} \times k_{2(H)} = K_{eq(D)}k_{2(H)} \quad (3.20)$$

$$\frac{\%\mathbf{24}\text{-}\boldsymbol{d_1}\text{-}\mathbf{A}}{\%\mathbf{24}\text{-}\boldsymbol{d_1}\text{-}\mathbf{B}} = \frac{k_{obs(A)}}{k_{obs(B)}} = \frac{K_{eq(H)}}{K_{eq(D)}} \times \frac{k_{2(D)}}{k_{2(H)}} \quad (3.21)$$

Assuming irreversible formation of **24-*d*$_0$**, **-*d*$_1$** and **-*d*$_2$** the ratio of **24-*d*$_1$-A** and **24-*d*$_1$-B** can be used to compare the two k_{obs} values (Equation 3.21). The value obtained from Equation 3.21 (%**24-*d*$_1$-A**/%**24-*d*$_1$-B** = 26/20 = 1.3) is very similar to the isotope effect observed from the isomerisation of **23** (1.4(1)). As speculated k_2 has no associated primary kinetic isotope effect and the value of 1.3 is consistent with this. If $k_{2(H)} \approx k_{2(D)}$ then Equation 3.21 is the same as Equation 3.16 since $k_{2(H)}/k_{2(D)} \approx k_{2(D)}/k_{2(H)} \approx 1$. Hence the distribution of isotopomers is a consequence of the equilibrium isotope effect between **23** and **31′**.

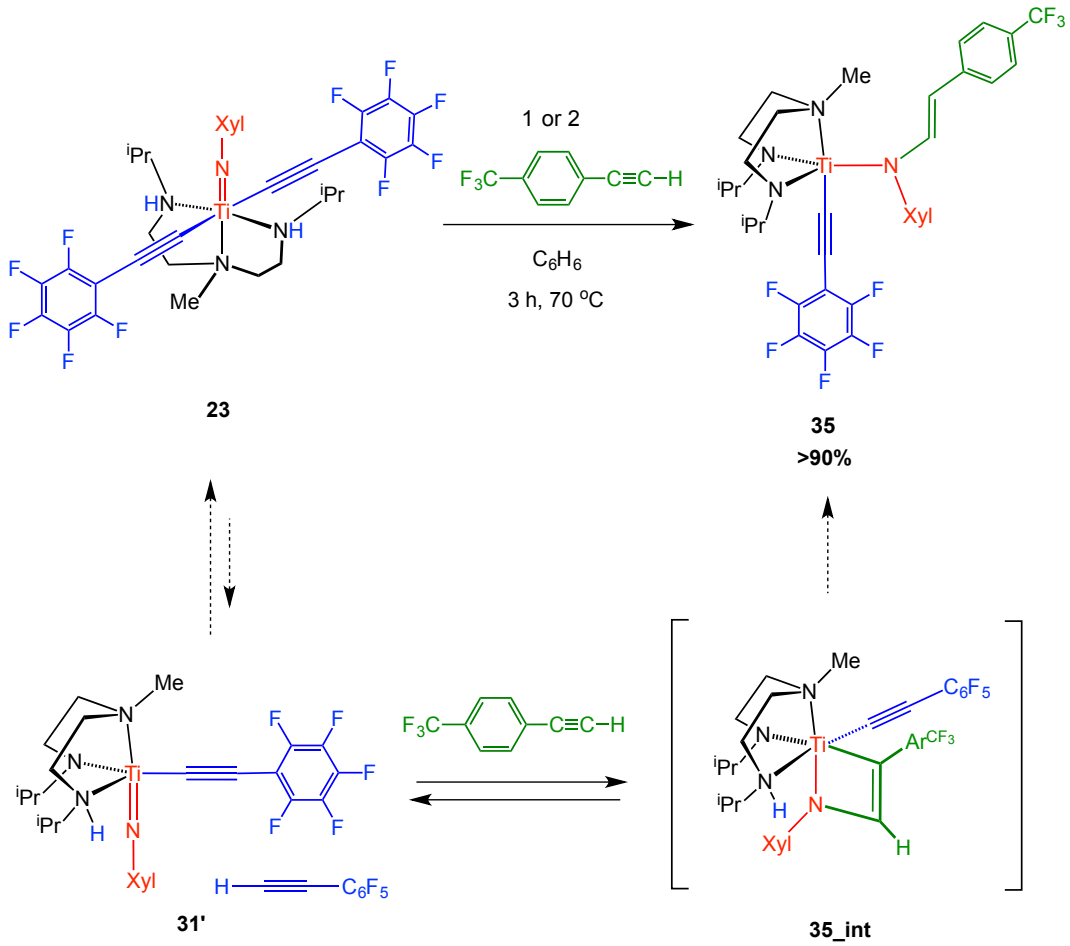
3.4.4 Kinetics analysis with HCC-4-$C_6H_4CF_3$

As the bis(acetylide) compounds synthesised from the other alkynes could not be isolated a full kinetic analysis was not carried out. However, the isomerisation of Ti($H_2N_2^{iPr}N^{Me}$)(CC-4-$C_6H_4CF_3$)$_2$(NXyl) (**26**) (made *in situ* from **1**) to Ti($N_2^{iPr}N^{Me}$){N(Xyl)C(H)C(H)-4-$C_6H_4CF_3$}(CC-4-$C_6H_4CF_3$) (**29**) was monitored by ^{1}H NMR spectroscopy and the decay of **26** measured by integration. The reaction was again 1st order in **26** and the rate constant was extracted from semilogarithmic plots of ln([**26**]$_t$/[**26**]$_0$) *vs.* time. The rate constant at 25 ^{o}C (6.51(2) x 10^{-5} s^{-1}) is much larger than the rate constant obtained for the isomerisation of **23** to **24** at the lowest recorded temperature (60 ^{o}C, 1.228(5) x 10^{-5} s^{-1}). The reaction of **1** with two equivalents of DCC-4-$C_6H_4CF_3$ was also followed, and the isotope effect was found to be 1.8(1).

Similarly the reaction of **1** with one equivalent of HCC-4-$C_6H_4CF_3$ and 1 equivalent of DCC-4-$C_6H_4CF_3$ yielded all four isotopomers of **29** in a non-statistical distribution. The ratio of the **29-*d*$_1$-A** and **29-*d*$_1$-B** isotopomers can again be used to compare the k_{obs} values and this also equals 1.8. The larger isotope effect is not fully understood, but could be a result of a more facile cycloaddition reaction (*vide infra*).

3.4.5 Crossover experiments with other alkynes

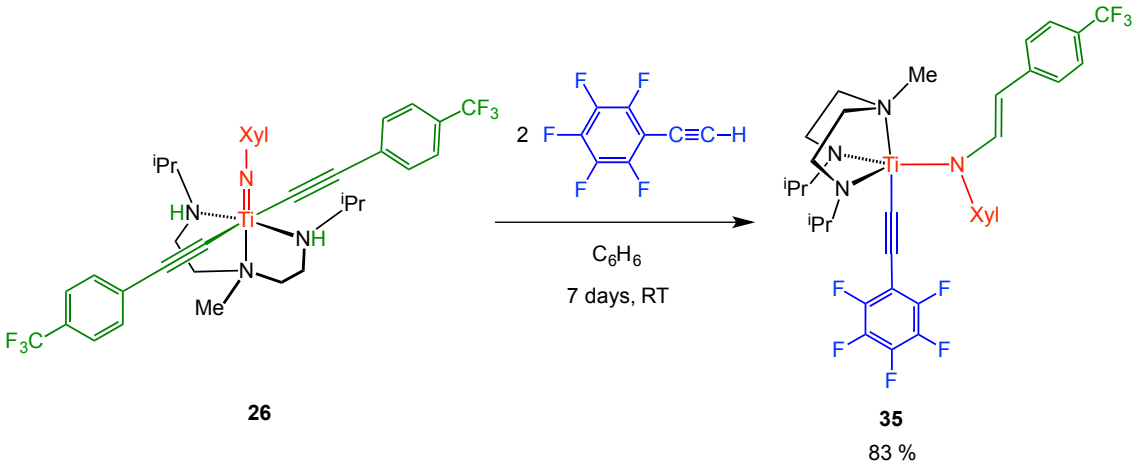
Interestingly, reaction of the bis(acetylide) compound **23** with two equivalents of HCC-4-$C_6H_4CF_3$ leads to almost exclusive formation (96%) of the crossover product Ti($N_2^{iPr}N^{Me}$)(CCC_6F_5){N(Xyl)C(H)C(H)(-4-$C_6H_4CF_3$)} (**35**) after heating for three hours at 70 ^oC (Scheme 3.10). Reaction of **23** with just one equivalent of HCC-4-$C_6H_4CF_3$ also yields **35** as the major product when heated at 70 ^oC or left at room temperature (90%, 3 hours and 98%, 14 days respectively). Compound **35** was isolated on a preparative scale and diffraction-quality crystals were obtained from a benzene solution at 4 ^oC. The solid-state structure is shown in Figure 3.12 and the structural details will be discussed later alongside analogous compounds. Following elimination of $HCCC_6F_5$ from **23** the mono(acetylide) intermediate **31** has a choice of alkynes with which it can react. Here the HCC-4-$C_6H_4CF_3$ alkyne has undergone the [2+2] cycloaddition reaction followed by intramolecular protonolysis, rather than the eliminated $HCCC_6F_5$ alkyne, with > 90% selectivity (Scheme 3.10). Compound **35** was also the major product following reaction of the imido compound **1** with one equivalent of $HCCC_6F_5$ and one equivalent of HCC-4-$C_6H_4CF_3$.



Scheme 3.10. Mechanism for the formation of Ti($N_2^{iPr}N^{Me}$))\{N(Xyl)C(H)C(H)(-4-$C_6H_4CF_3$)\}(CCC_6F_5) (**35**).

Since Ti($H_2N_2^{iPr}N^{Me}$)(CC-4-$C_6H_4CF_3$)$_2$(NXyl) (**26**) could not be isolated the comparable experiment with $HCCC_6F_5$ was not possible. Instead, **26** was made *in situ* and two equivalents of $HCCC_6F_5$ were added immediately (Equation 3.22). After 1.5 hours at room temperature the reaction mixture contained a mixture of bis(acetylide) compounds, when left at room temperature for longer, vinylamide-acetylide complexes began to form. After 7 days at room temperature the mixture contained **35** (83%), **29** (4%) and **23** (13%). The vinylamide-acetylide complex **35** with the -C_6F_5 moiety in the acetylide position and -4-$C_6H_4CF_3$ moiety the vinylamide position is again the favoured product. Therefore, once one HCC-4-$C_6H_4CF_3$ has eliminated from **26**, a σ-bond metathesis with $HCCC_6F_5$ occurs faster than any cycloaddition reactions resulting in the formation of mixed bis(acetylide) species. Preferential elimination of HCC-4-$C_6H_4CF_3$ then occurs and thus the situation is the same as when starting from **23** and adding HCC-4-$C_6H_4CF_3$. The small amount of **29** observed may have formed

before any of $HCCC_6F_5$ alkyne was added and the remaining **23** indicates that the reaction has not yet reached completion. However, the major product is clear.



Equation 3.22

Reaction of **23** with two equivalents of DCC-4-$C_6H_4CF_3$ was carried out on an NMR tube scale and scrambling in positions H_a and H_b of **35** was observed (Figure 3.10). The appearance of deuterium in the H_a position as well as the H_b position suggests that both DCC-4-$C_6H_4CF_3$ and $HCCC_6F_5$ (eliminated from **23**) take part in a pre-equilibrium (between mono(acetylide) and bis(acetylide) compounds) allowing scrambling of the Ti-N(H/D) positions as well as both alkynes in solution prior to a cycloaddition reaction.

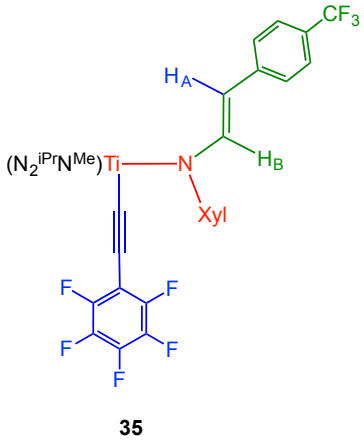


Figure 3.10. Position labelling of $Ti(N_2^{iPr}N^{Me})\{N(Xyl)C(H)C(H)C_6H_4CF_3\}(CCC_6F_5)$ (**35**).

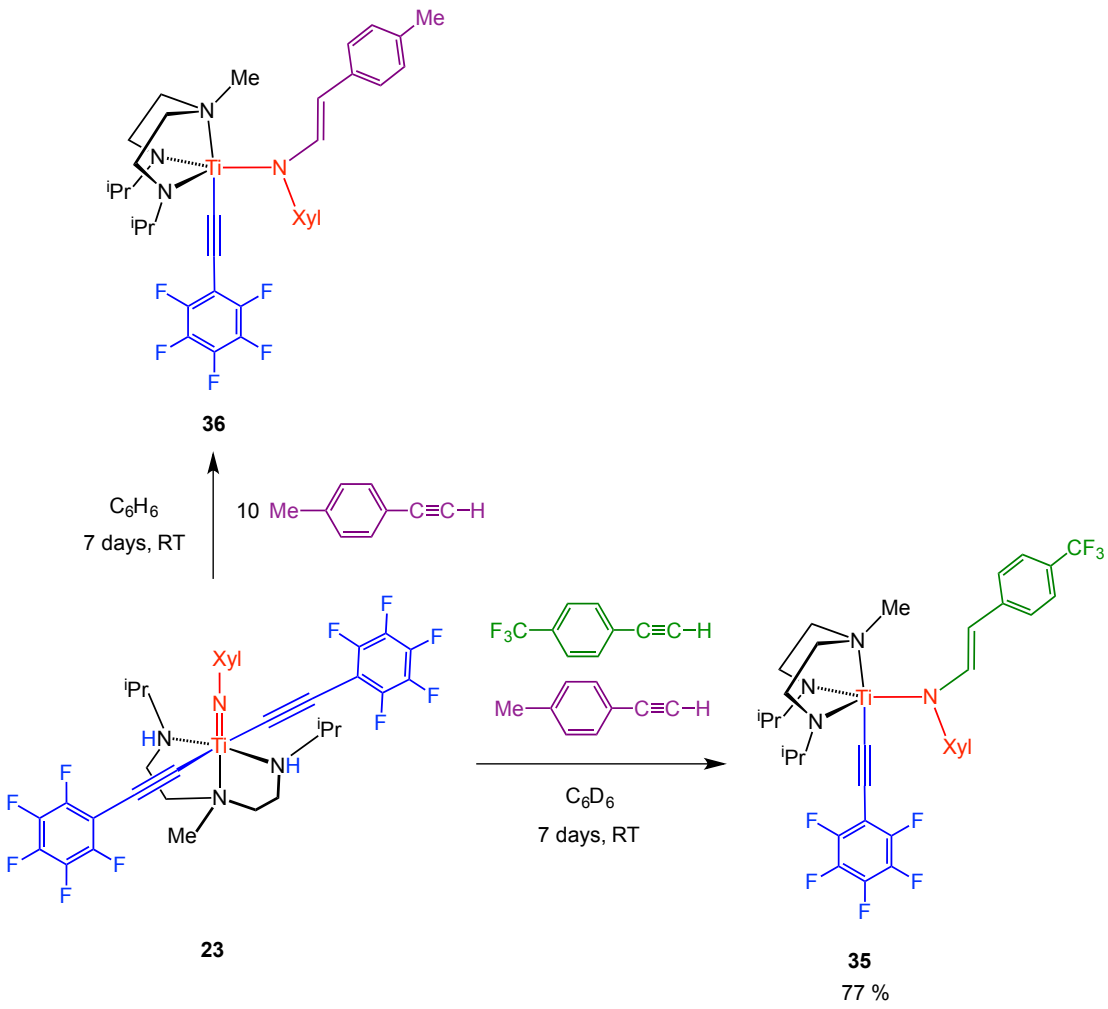
The preference for the $HCCC_6F_5$ alkyne to occupy the acetylide position is partly due to stronger Ti–C_{ac} bonds and less basic Ti–$\underline{C}_{ac}$ atoms making elimination of $HCCC_6F_5$ less favourable due to the more electron-withdrawing nature of the aryl ring. The HCC-4-$C_6H_4CF_3$ alkyne occupies the vinyl position preferentially due to a more facile

cycloaddition reaction (*vide infra*). When $HCCC_6F_5$ eliminates from **23**, **31** will be in the presence of an excess of HCC-4-$C_6H_4CF_3$, which could also contribute to the selectivity. However, the formation of **35** from **26** suggests that HCC-4-$C_6H_4CF_3$ will preferentially undergo the cycloaddition reaction even when it is not in excess. The formation of **35** from **26** is interesting as it indicates that both alkynes can eliminate from a bis(acetylide).

The formation of **35** from **23** requires heating at 70 ^oC for three hours for completion, in comparison the isomerisation of **23** to **24** is only 50% complete after three hours at 70 ^oC and requires 12 hours to reach completion. This is consistent with a facile elimination of $HCCC_6F_5$ from **23** followed by a rate-determining cycloaddition reaction which is slower with $HCCC_6F_5$.

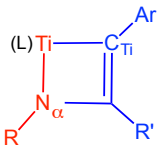
In an attempt to understand why the cycloaddition step proceeds more readily with HCC-4-$C_6H_4CF_3$ compared to $HCCC_6F_5$ the following experiments were carried out. $Ti(H_2N_2^{iPr}N^{Me})(CCC_6F_5)_2(NXyl)$ (**23**) was mixed with one equivalent of the more electron-rich terminal aryl alkyne HCC-4-C_6H_4Me on the NMR tube scale. At room temperature the reaction proceeded very slowly and on heating at 70 ^oC a mixture of **24** and the mixed vinylamide-acetylide compound $Ti(N_2^{iPr}N^{Me})\{N(Xyl)C(H)C(H)C_6H_4Me\}(CCC_6F_5)$ (**36**) was observed. When 10 equivalents of HCC-4-C_6H_4Me were used and the reaction left for 7 days at room temperature quantitative formation of the crossover product **36** was observed (Scheme 3.11). The excess alkyne could be removed under reduced pressure and **36** was synthesised on a preparative scale and fully characterised by NMR and IR spectroscopy, mass spectrometry and elemental analysis.

A competition reaction was then carried out in which reaction of **23** with one equivalent of HCC-4-C_6H_4Me and one equivalent of HCC-4-$C_6H_4CF_3$ gives a mixture of vinylamide-acetylide species over several days at room temperature. $Ti(N_2^{iPr}N^{Me})\{N(Xyl)C(H)C(H)C_6H_4CF_3\}(CCC_6F_5)$ (**35**) is the major product (77%) and small amounts of both $Ti(N_2^{iPr}N^{Me})\{N(Xyl)C(H)C(H)C_6H_4Me\}(CCC_6F_5)$ (**36**) (15%) and $Ti(N_2^{iPr}N^{Me})\{N(Xyl)C(H)C(H)C_6F_5\}(C_6F_5)$ (**24**) (7%) were also observed (Scheme 3.11). The formation of **35** as the major product in this reaction along with the longer reaction time and higher number of alkyne equivalents required to synthesis **36** independently, indicate that the cycloaddition reaction proceeds more readily with HCC-4-$C_6H_4CF_3$.



Scheme 3.11. Reaction of $Ti(H_2N_2{}^{iPr}N^{Me})(CCC_6F_5)_2(NXyl)$ (**23**) with HCC-4-C_6H_4Me and competition reaction with HCC-4-C_6H_4Me and HCC-4-$C_6H_4CF_3$.

The electron-withdrawing and donating properties of aryl alkynes have been reported to affect both the stability of azatitanacyclobutene intermediates and their onward reactivity. As previously discussed, the hydrazido compound $Ti(N_2N^{Me})(NNPh_2)(py)$ (**1.72**) reacts with internal alkynes to yield azatitanacyclobutene intermediates followed by insertion of the alkyne into the N–N bond to yield vinylimido compounds. Experimental and DFT studies found that electron-withdrawing substituents on ArCCR yielded more thermodynamically stable cycloaddition complexes. Electron-withdrawing aryl groups bound to C_{Ti} help to lower the energy of both the π_{cc} and π^*_{cc} orbitals reducing the unfavourable overlap between the lone pair on N_α and π_{cc} whilst increasing the favourable overlap between the empty π^*_{cc} orbital and lone pair on N_α (Figure 3.11).



L = N_2N^{Me} R = NPh_2 R' =Me

L = $HN_2^{iPr}N^{Me}$ R = Xyl R' =H

Figure 3.11. Azatitanacyclobutene intermediates.

The subsequent reaction step to yield the vinylimido compounds involves the nucleophilic attack of C_{Ti} on N_{α}. More electron-donating aryl groups increase the nucleophilicity of C_{Ti} and therefore accelerate the reaction. As this step was found to be rate-determining the overall reaction was thus promoted by electron-donating substituents on the aryl group of the alkyne.[12]

Comparisons can be drawn with this system. Cycloaddition reactions of the mono(acetylide) will yield more stable azatitanacyclobutene intermediates with alkynes containing electron-withdrawing aryl substituents. The subsequent intramolecular protonolysis of C_{Ti} by Ti–NH will be more facile when the C_{Ti} atom is more basic, and will therefore be promoted by electron-donating aryl substituents. As the cycloaddition reaction of the mono(acetylide) **31** occurs almost exclusively with HCC-4-$C_6H_4CF_3$ instead of HCC-4-C_6H_4Me the electronic preference for a stable metallacycle is apparent. This is in line with a rate-determining cycloaddition reaction followed by a facile intramolecular protonolysis.

However, this analysis is not consistent with a slower cycloaddition reaction with $HCCC_6F_5$. Reaction with this alkyne should form the most thermodynamically stable azatitanacyclobutene intermediate; this difference is attributed to steric effects. Substituents on the *ortho*- and *meta*- positions as well as the *para*- mean that a larger steric clash is experienced on trying to undergo the cycloaddition reaction thus making it energetically more difficult.

3.5 Solid-state structures of vinylamide-acetylide compounds

The solid-state structures of the vinylamide-acetylide compounds which have been crystallographically characterised will now be discussed. The X-ray structure of the mixed product Ti($N_2^{iPr}N^{Me}$){N(Xyl)C(H)C(H)$C_6H_4CF_3$}(CCC_6F_5) (**35**) is shown in Figure 3.12 along with that of Ti($N_2^{iPr}N^{Me}$){N(Xyl)C(H)C(H)-3,5-$C_6H_3(CF_3)_2$}(CC-3,5-$C_6H_3(CF_3)_2$) (**30**). The structure of Ti($N_2^{iPr}N^{Me}$){N(Xyl)C(H)C(H)C_6F_5}(CCC_6F_5) (**24**) is shown in Figure 3.5, earlier in this Chapter and will be discussed alongside **35** and **30**. The analogous bond distances and angles of the published vinylhydrazide-acetylide compound Ti($N_2^{iPr}N^{Me}$){N(NPh_2)C(H)C(H)-4-C_6H_4Me}(CC-4-C_6H_4Me) (**3.2**) are also shown for comparison.

Compounds **35, 30** and **24** are five-coordinate η^1-titanium vinylamide(1-)-acetylide(1-) complexes with the diamide-amine ligand bound in a κ^3-*fac*-manner occupying one axial and two equatorial sites. The geometry at Ti(1) is distorted from trigonal bipyramidal especially in the axial plane with a N(2)–Ti(1)–C_{ac}(1) angle of 148.28(7), 148.49(11) and 149.20(9) ^{o} for **35, 30** and **24** respectively. However, the equatorial nitrogen atoms N(1), N(3) and N(4) are effectively co-planar with the sum of the angles subtended at Ti(1) equating to 356.15(11), 356.28(19) and 355.24 (16) ^{o} for **35, 30** and **24** respectively. The remaining axial site is occupied by an acetylide ligand.

The Ti(1)–C_{ac}(1) bond lengths are slightly shorter than the titanium acetylide bond lengths found in the solid-state structure of **23** (2.1231(19) , 2.117(3) and 2.140(2) Å for **35, 30** and **24** respectively, compared to 2.2098(13) and 2.2182(13) Å in **23**). This is a result of both the lower coordination number and orientation *trans* to a neutral amine donor as opposed to another acetylide(1-) ligand. There is little difference to the corresponding titanium acetylide bond in the vinylhydrazide(1-) compound **3.2** (2.1079(14) Å) and thus no apparent trend in bond length to electron-withdrawing properties of the aryl substituents. These values are also in good agreement with examples of Cp* supported titanium acetylide bond lengths reported by Bergman *et al*.[24, 65] The alkyne and alkene bond lengths in all three compounds are within the expected ranges for such multiple bonds and are very similar to the comparable bond lengths in **3.2**.

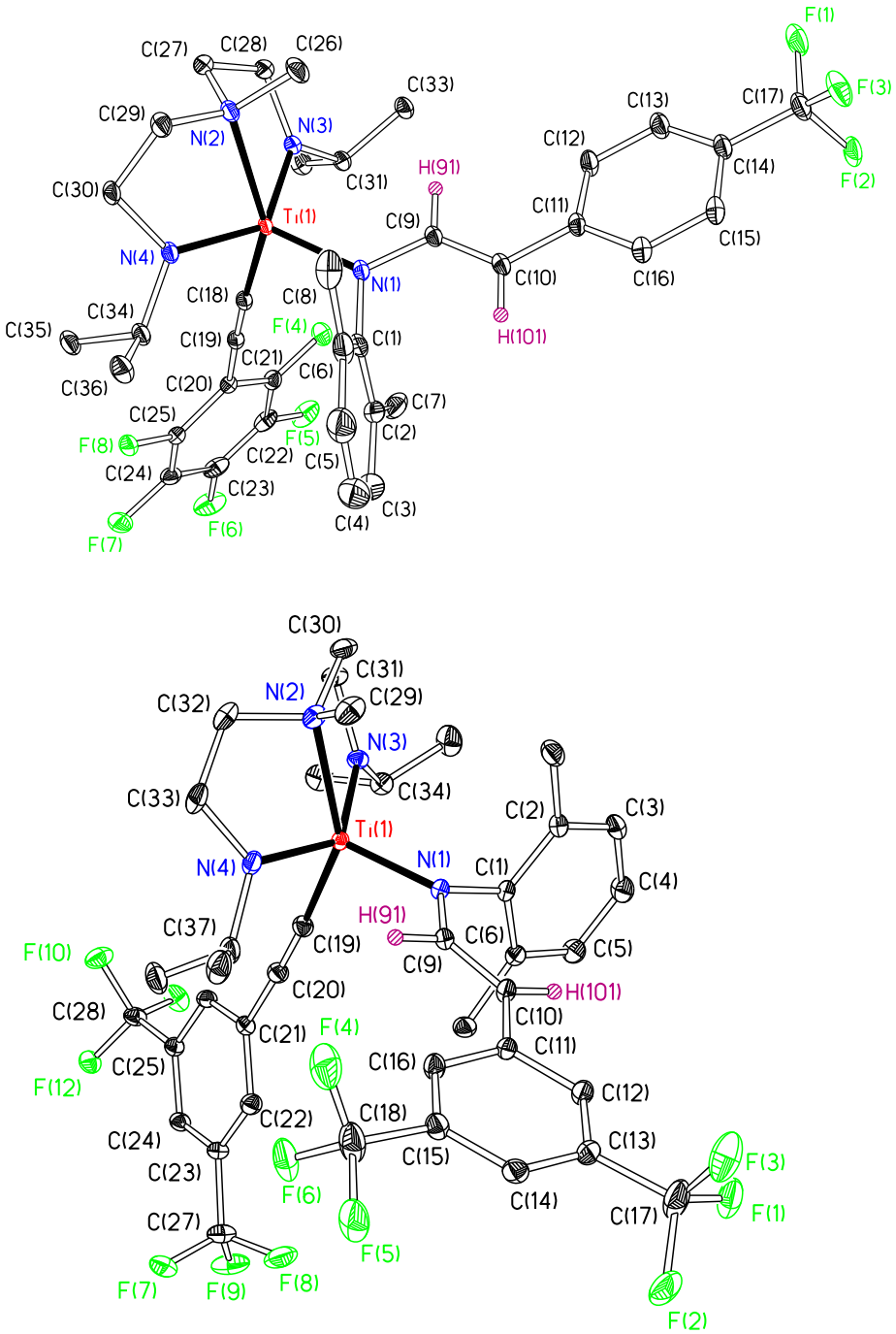


Figure 3.12. Top: displacement ellipsoid plot (20% probability) of Ti($N_2^{iPr}N^{Me}$){N(Xyl)C(H)C(H)$C_6H_4CF_3$}(CCC_6F_5) (**35**). H atoms except H(91) and H(101) and the other independent molecule are omitted for clarity. Bottom: displacement ellipsoid plot (20% probability) of Ti($N_2^{iPr}N^{Me}$){N(Xyl)C(H)C(H)-3,5-$C_6H_3(CF_3)_2$}(CC-3,5-$C_6H_3(CF_3)_2$) (**30**). H atoms except H(91) and H(101) are omitted for clarity.

Table 3.2. Selected bond distances (Å) and angles (°) for **35, 30**, **24** and **3.2**.

Parameter	35	30	24	3.2
Ti(1)-N(1)	1.9714(16)	1.922(2)	1.988(19)	1.9775(11)
Ti(1)-N(2)	2.3197(16)	2.298(3)	2.296(2)	2.2993(12)
Ti(1)-N(3)	1.9230(16)	1.922(3)	1.931(2)	1.9221(12)
Ti(1)-N(4)	1.9298(15)	1.881(3)	1.925(2)	1.9262(12)
Ti(1)-$C_{ac}(1)$[a]	2.1231(19)	2.117(3)	2.140(2)	2.1079(14)
N(1)-C(9)	1.387(2)	1.382(4)	1.383(3)	1.3864(17)
C(9)-C(10)	1.340(3)	1.317(4)	1.354(3)	1.346(2)
C(10)-C(11)	1.463(2)	1.455(4)	1.462(3)	1.4678(19)
N(1)-C(1)	1.434(3)	1.418(4)	1.434(3)	-
$C_{ac}(1)$-$C_{ac}(2)$[a,b]	1.207(3)	1.202(5)	1.207(4)	1.215(2)
$C_{ac}(2)$-$C_{ac}(3)$[b,c]	1.429(3)	1.425(5)	1.427(4)	1.4356(19)
N(1)-Ti(1)-N(2)	109.84(6)	110.05(10)	103.53(8)	108.01(5)
N(101)-Ti(101)-N(102)	-	-	108.75(8)	-
N(1)-Ti(1)-$C_{ac}(1)$[a]	101.84(7)	101.40(12)	107.15(9)	103.12(5)
N(101)-Ti(101)-$C_{ac}(101)$[d]	-	-	103.66(9)	-
N(1)-Ti(1)-N(3)	108.83(6)	113.25(11)	107.07(9)	106.06(5)
N(1)-Ti(1)-N(4)	113.90(7)	109.81(11)	116.42(8)	113.48(5)
N(3)-Ti(1)-N(4)	133.42(7)	133.22(11)	131.75(10)	135.46(5)
N(2)-Ti(1)-N(3)	73.77(7)	74.63(11)	74.96(9)	75.05(5)
N(2)-Ti(1)-N(4)	75.09(6)	74.26(12)	75.51(8)	73.93(5)
N(2)-Ti(1)-$C_{ac}(1)$[a]	148.28(7)	148.49(11)	149.20(9)	148.77(5)
N(102)-Ti(101)-$C_{ac}(101)$[d]	-	-	147.56(10)	-
$C_{ac}(1)$-$C_{ac}(2)$-$C_{ac}(3)$[a,b,c]	178.10(19)	177.0(4)	176.2(3)	178.27(15)
Ti(1)-N(1)-C(9)	125.44(13)	121.91(19)	120.93(15)	128.1(1)
Ti(1)-N(1)-C(1)	119.62(12)	118.56(18)	123.69(4)	-
N(1)-C(9)-C(10)	126.11(18)	128.7(3)	126.4(2)	128.7(1)
C(1)-N(1)-C(9)	114.93(16)	118.2(2)	115.39(18)	116.42(11)
C(9)-C(10)-C(11)	125.21(19)	125.5(3)	125.7(2)	123.8(1)
N(3,4)-Ti(1)-N(1)-C(9)[e]	13.2	3.0	28.5	14.6
N(103)-Ti(101)-N(101)-C(109)[f]	-	-	16.4	-

[a] "$C_{ac}(1)$" = C(18) **35**, C(19) **30**, C(17) **24**. [b] "$C_{ac}(2)$" = C(19) **35**, C(20) **30**, C(18) **24**. [c] "$C_{ac}(3)$" = C(20) **35**, C(21) **30**, C(19) **24**. [d] "$C_{ac}(101)$" = C(117) **24**. [e] Torsion angle for this linkage. [f] Torsion angle for the other independent molecule of **24**

The Ti(1)-N(1) bond distances are within the region expected for amide(1-) ligands. N(1) is planar in all cases with the angles subtended calculated to be 359.99(29), 358.67(33), and 360.01(46) ^{o} for **35, 30** and **24** respectively. The lone pair located on N(1) can donate into either a π-acceptor orbital on Ti or, the π* orbital of the C=C bond, the latter resulting in delocalisation into the vinyl moiety. The Ti(1)-N(1) bond distance in **30** is significantly shorter than in **35** and **24** (1.922(2) Å compared to 1.9714(16) and 1.988(19) Å) suggesting more donation into the titanium π-acceptor orbital.

The N(4)-Ti(1)-N(1)-C(9) torsion angle in **30** is just 3.0 ^{o}, meaning that the lone pair located on N(1) is well positioned for a π-bonding interaction with titanium. In comparison, the N(3)-Ti(1)-N(1)-C(9) torsion angles in **35** and **24** are 13.2 and 28.5 ^{o} respectively. Thus the lone pairs on the N(1) atoms are rotated out of the axial plane and are not as well aligned for a π-bonding interaction with titanium, resulting in longer Ti(1)-N(1) bonds. Delocalisation into the vinyl moiety is reduced in **30** as a result of preferential donation into the titanium π-acceptor orbital. This is apparent when comparing the alkene C(9)-C(10) bond distances, which is significantly shorter in **30** compared to **35** and **23** (1.317(4) Å compared to 1.340(3) (**35**) and 1.354(3) Å **24**) due to reduced donation into the C=C π* orbital.

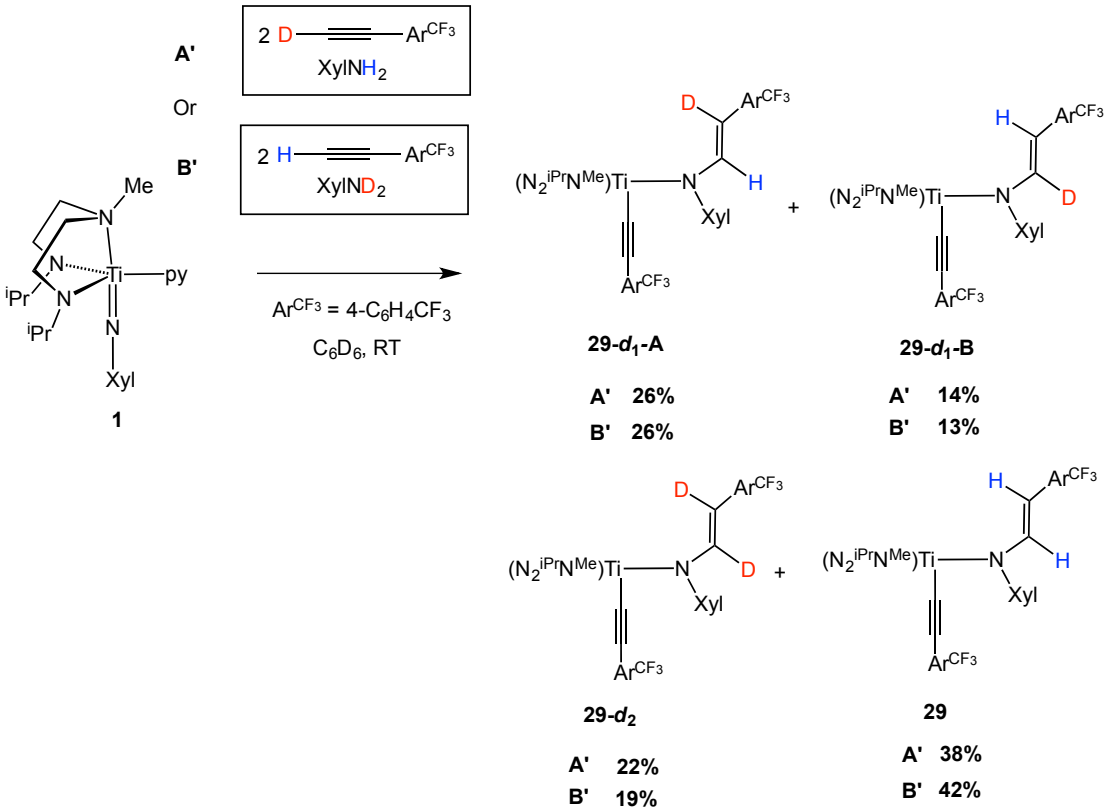
The bond distances to the $N_2^{iPr}N^{Me}$ ligands are with within the expected ranges for amide and amine bonding to titanium. Interestingly the Ti–N_{amide} bond distances are shorter than for **1** (range 1.881(3) - 1.931(2) Å compared to 1.970(2) and 1.959(2) Å). This is a consequence of more electron-deficient titanium centres when no metal-ligand multiple bonds are present thus allowing better π-donation from the lone pairs located on the N_{amide} atoms.

For both **35** and **24** there are two independent molecules in the unit cell. For **35** all the bond distances and angles are very similar in the two molecules, therefore are only listed for the molecule shown in Figure 3.12. For **24** all the bond distances are very similar, however, the corresponding N(3)-Ti(1)-N(1)-C(9) torsion angle, N(103)-Ti(101)-N(101)-C(109) is quite different (16.4 ^{o}). The angles subtended at titanium in the axial plane are very similar in both molecules, 359.88(15) ^{o} and 359.97(16) ^{o}, however the contributing angles differ between the two molecules. For the molecule which is shown in Figure 3.5 the N(1)-Ti(1)-N(2) angle is 103.53(8) ^{o} the corresponding N(101)-Ti(101)-N(102) angle is 108.75(8) ^{o} similarly the N(1)-Ti(1)-

C(17) is 107.15(9) and N(101)-Ti(101)-C(117) is 103.66(9) °. The angles for the molecule not shown in Figure 3.12 are more similar to the corresponding angles in **30** and **35** and this arrangement results in the smaller torsion angle more similar to that in **35**. Other angles observed in the independent molecule of **24** are very similar and have therefore not been included in Table 3.2.

3.6 Nitrogen hydrogen/deuterium exchange experiments

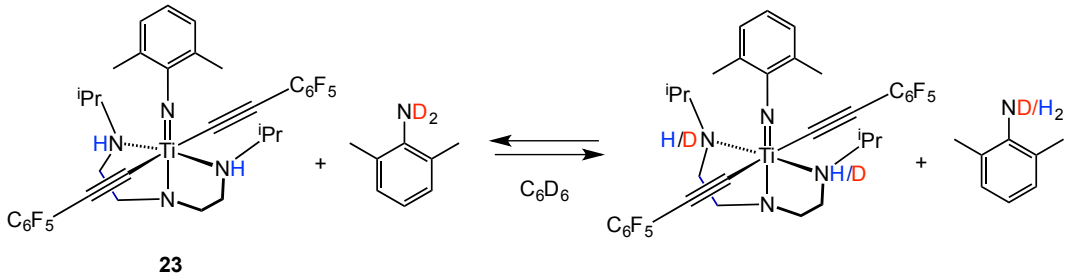
To aid understanding of the mechanism of hydrohydrazination of alkynes using **2.1** (discussed in the next section) further H/D exchange experiments were carried out. Reaction of Ti($N_2^{iPr}N^{Me}$)(NXyl)(py) (**1**) with two equivalents of HCC-4-$C_6H_4CF_3$ in the presence of one equivalent of $XylND_2$ results in all four possible isotopomers **29**, formed in the distribution shown in Equation 3.23. The same distribution was observed when deutero-alkyne and protio-aniline were used. Direct exchange between the Ti–NH of the ligand in the mono(acetylide) and bis(acetylide) intermediates and the ND of the aniline (or vice versa) results in scrambling of both vinyl positions.



Equation 3.23

The H/D exchange occurring between the complexed neutral triamine ligand $H_2N_2^{iPr}N^{Me}$ (**3.1**) and the free amine was directly observed by following a mixture of

23 with one equivalent of $XylND_2$ by ^1H and ^2H NMR spectroscopy (Equation 3.24). After five hours at room temperature the resonance for $XylNH_2$ and/or XylNHD was observed. This continued to grow in intensity when left at room temperature for three days, after which time the relative intensities indicated that approximately 70% of the hydrogen remained on the Ti–N atoms and the free aniline contains approximately 70% deuterium. No conversion to **24** was observed on this timescale but on heating at 70 ^oC for several hours isomerisation to **24** occurred and H and D were present in both vinyl positions.

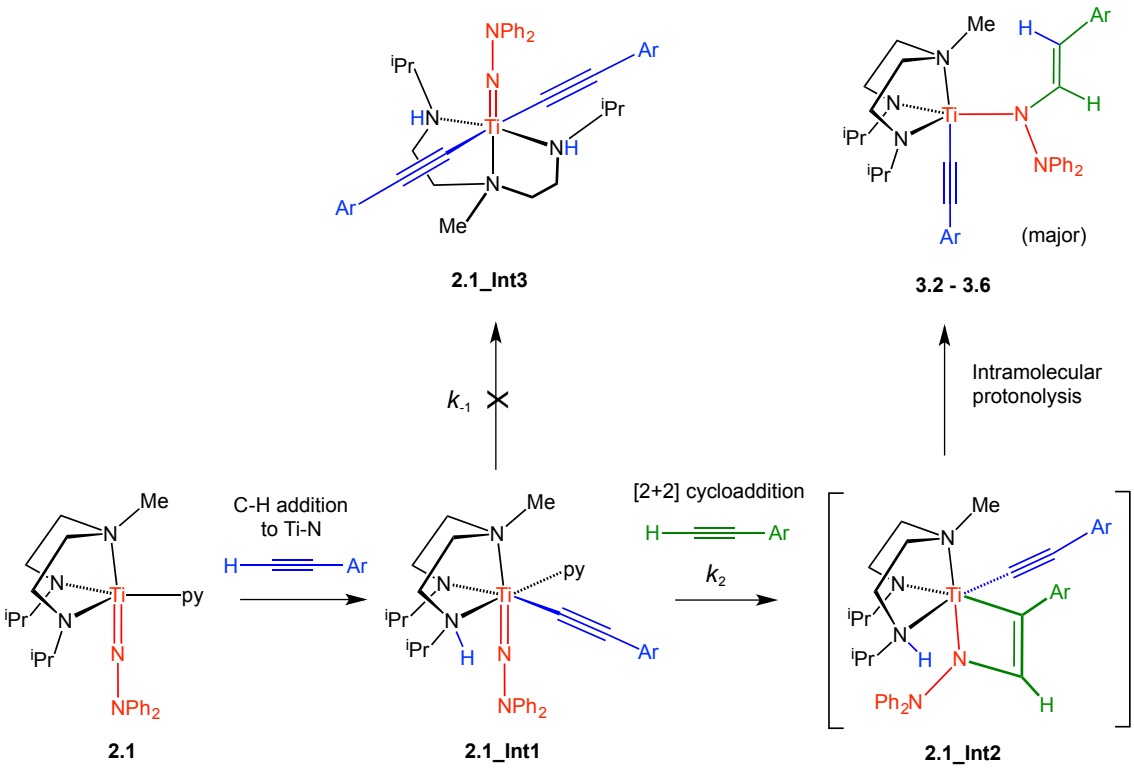


23

Equation 3.24

3.7 Relevance of the reactions of Ti($N_2^{iPr}N^{Me}$)(NXyl)(py) (1) with terminal alkynes to the reactions of Ti($N_2^{iPr}N^{Me}$)($NNPh_2$)(py) (2.1) with terminal alkynes

The stoichiometric and catalytic reactions of the hydrazido compound Ti($N_2^{iPr}N^{Me}$)($NNPh_2$)(py) (**2.1**) with terminal alkynes have been published[32] and were discussed in the introduction to this Chapter. The 1:2 stoichiometric reaction products are vinylhydrazide-acetylide compounds, which, along with **2.1** are catalysts for the hydrohydrazination of terminal alkynes. No intermediates were observed at room temperature or when the reaction of **2.1** with HCC-4-C_6H_4Me was followed from low temperature. The mechanism was proposed to proceed *via* a [2+2] cycloaddition reaction followed by a σ-bond metathesis reaction with the second equivalent of alkyne (Scheme 3.2). However, intermediates observed at room and low temperature in the reactions of the corresponding imido compound **1**, with alkynes and subsequent mechanistic investigations discussed above, suggest that an alternative mechanism is in operation.



Scheme 3.12. Mechanism for the reaction of Ti($N_2^{iPr}N^{Me}$)($NNPh_2$)(py) (**2.1**) with terminal alkynes.

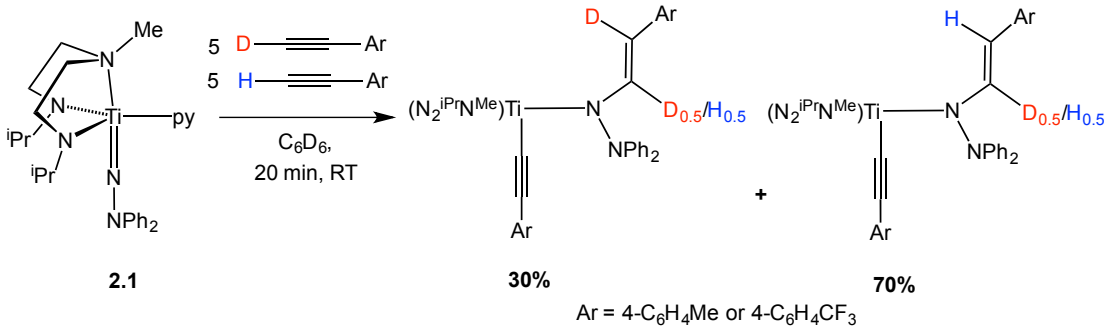
The proposed alternative mechanism is shown in Scheme 3.12 and follows the same pathway as the reaction of **1** with terminal alkynes. Addition of one equivalent of alkyne to **2.1** yields the mono(acetylide) intermediates (**2.1_Int1**), this is immediately followed by a [2+2] cycloaddition reaction at the hydrazido ligand to yield azatitanocyclobutene intermediates (**2.1_Int2**). Subsequent intramolecular protonolysis and *trans* to *cis* isomerisation then occurs to yield the final thermodynamic products (**3.2 - 3.6**). Formation of the kinetic bis(acetylide) products does not occur. Thus, $k_2 >> k_{-1}$, which is in contrast to reaction with the imido compound **1** where $k_2 << k_{-1}$ and complete formation of the bis(acetylide) compounds was observed before isomerisation. This is attributed to a more reactive hydrazide multiple bond which preferentially undergoes reaction rather than a second C–H addition.

3.7.1 Kinetic isotope effect measurements

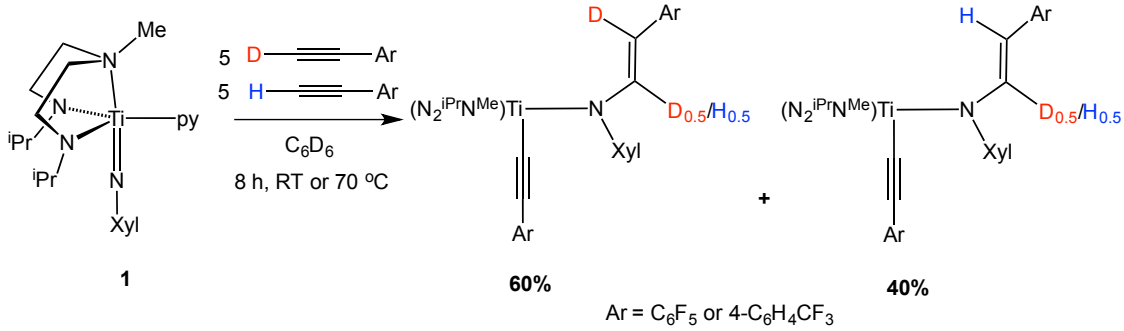
As the reactions of Ti($N_2^{iPr}N^{Me}$)($NNPh_2$)(py) (**2.1**) with alkynes are complete within minutes it was not possible to carry out a full kinetic study for comparison with **1**.

Therefore, competition reactions were carried out to assess the kinetic isotope effect. Reaction of **2.1** with HCC-4-C_6H_4Me and DCC-4-C_6H_4Me (1:5:5) resulted in the formation of all four isotopomers of Ti($N_2^{iPr}N^{Me}$){N(NPh_2)C(H)C(H)-4-C_6H_4Me}(CC-4-C_6H_4Me) (**3.2**) (Equation 3.25). The TiNC(H/D)C(H/D) position contained significantly higher incorporation of H (70:30% H:D on the basis of ^1H and ^2H spectroscopic analysis). The distribution of H and D in this position reflects what occurs in the first step of the mechanism, since the proton that undergoes the initial C–H activation, is ultimately transferred to this position. Therefore a kinetic isotope effect of 2.4(1) was obtained for the σ-bond metathesis reaction to form **2.1_Int1**. This assumes that the final intramolecular protonolysis to form **3.5** is facile (as was found in the reactions of **1** with alkynes). In comparison the TiNC(H/D) position contained equal amounts of H and D (50:50%, H:D); this result implies that there is no preference for H over D alkyne in forming the metallacyle as no C–H/D bonds are broken or formed consistent with the proposed mechanism.

The effect is less pronounced in the reaction of **2.1** with HCC-4-$C_6H_4CF_3$ and DCC-4-$C_6H_4CF_3$ (1:5:5). The TiNC(H/D)C(H/D) position contained 65:35%, H:D (KIE = 1.9) and the TiNC(H/D) position contained almost equal H and D. The same analysis could not carried out with $HCCC_6F_5$ as the vinyl doublet that results from the TiNC(H)C(H) proton overlaps with the methine ligand resonance preventing accurate integration. The KIEs of 1.9 and 2.4 are in the region expected for such a C–H bond breaking reaction, as mentioned the KIE for the formation of the titanium hydroxoacetylide species $Cp^*_2Ti(OH)(CCPh)$ is 2.94(6). The values are also comparable to the conversion of Mg{κ^2N-HC($Me_2pz)_3$}{N($SiHMe_2)_2$}$_2$ to the zwitterionic mono(amide) compound Mg{C($Me_2pz)_3$}{N($SiHMe_2)_2$} and HN($SiHMe_2)_2$ as a result of addition of the apical C–H bond of the ligand across the Mg–N_{amide} bond, in a similar manner to what occurs here. A kinetic isotope effect of 1.91(2) was obtained consistent with a C–H bond cleavage during the rate limiting step.[94] The KIE for the addition of an equivalent of $HCCC_6F_5$ to the monoacetylide intermediate **31′** (k_{-1}, Scheme 3.6) was earlier estimated to be 2.4(2), the values obtained here for a very similar reaction are in good agreement.



Equation 3.25



Equation 3.26

In comparison, reaction of the imido compound **1** with HCC-4-$C_6H_4CF_3$ and DCC-4-$C_6H_4CF_3$ (1:5:5) exhibited a preference for D over H in the TiNC(H/D)C(H/D) position (40:60%, H:D) (Equation 3.26). Even though preferential breaking of the C–H bonds will occur initially to form the mono- and bis(acetylide) species, once HCC-4-$C_6H_4CF_3$ has eliminated from the bis(acetylide) to form the mono(acetylide) either HCC-4-$C_6H_4CF_3$ or DCC-4-$C_6H_4CF_3$ can re-add prior to the slow k_2 step. Rapid equilibration between the two will lead to accumulation of deuterium in the N_{amine} positions. This translates to more D in the TiNC(H/D)C(H/D) vinyl position. Reaction of **1** with $HCCC_6F_5$ and $DCCC_6F_5$ (1:5:5) resulted in approximately the same distribution in both positions (Equation 3.26). No selectivity was observed in the TiNC(H/D) position again consistent with a [2+2] cycloaddition reaction in which no C–H/D bonds are broken. This demonstrates how the distribution of isotopomers differs when a reversible second alkyne addition to yield a bis(acetylide) compound occurs. Thus, the preference of H over D in the reactions of **2.1** is consistent with the addition of one equivalent of alkyne followed immediately by the cycloaddition

avoiding the equilibration effect. If the k_2 step were slower (like in the imide case) and equilibration occurred then D would accumulate in the N_{amine} position.

3.7.2 Identifying bis(acetylide) intermediates

The reaction of **2.1** with two equivalents of $HCCC_6F_5$ was revisited with the hope of identifying some intermediates now the ^{1}H NMR spectra of both the mono(acetylide) and bis(acetylide) compounds formed from the imido complex **1** are well understood. A ^{1}H NMR spectrum recorded within five minutes of mixing at room temperature indicated an 85:15% mixture of the expected vinylhydrazide-acetylide compound **3.5** and the bis(acetylide) compound $Ti(H_2N_2{}^{iPr}N^{Me})(CCC_6F_5)_2(NNPh_2)$ (**2.1_Int3-C_6F_5**). The ^{1}H NMR spectra of the analogous compound $Ti(H_2N_2{}^{iPr}N^{Me})(CCC_6F_5)_2(NXyl)$ (**23**) and the mixture of **3.5** and **2.1_Int3-C_6F_5** are shown in Figure 3.13 in the region of 0.5 - 4.0 ppm. The resonances resulting from the bis(acetylide) species **2.1_Int3-C_6F_5** are labelled with an asterisk.

The ^{1}H NMR spectra of **2.1_Int3-C_6F_5** and **23** are very similar. The meridonal arrangement of the neutral tris(amine) ligand in such compounds synthesised from **1** results in diagnostic multiplet resonances corresponding to the diastereotopic methylene protons. The same pattern is observed here and the distinctive multiplet at 1.67 ppm shows a clear similarity to the analogous resonance in **23**. The resonance resulting from the C<u>H</u>Me_2 methine is a doublet of septets due to coupling to CH<u>Me_2</u> and the N–H proton, as in **23**. Similarly, two sets of C_6F_5 resonances are observed in the ^{19}F NMR spectrum, consistent with a bis(acetylide) compound. After 1.5 hours at room temperature **2.1_Int3-C_6F_5** is present in < 5% and on standing overnight all of **2.1_Int3-C_6F_5** converted to **3.5**. Due to the low concentration and short lifetime of **2.1_Int3-C_6F_5** a ^{13}C NMR spectrum and the corresponding 2D NMR experiments could not be recorded. Compound **2.1_Int3-C_6F_5** was not observed in a higher percentage when the reaction was carried out and followed from -78 ^{o}C and no other intermediates were identified.

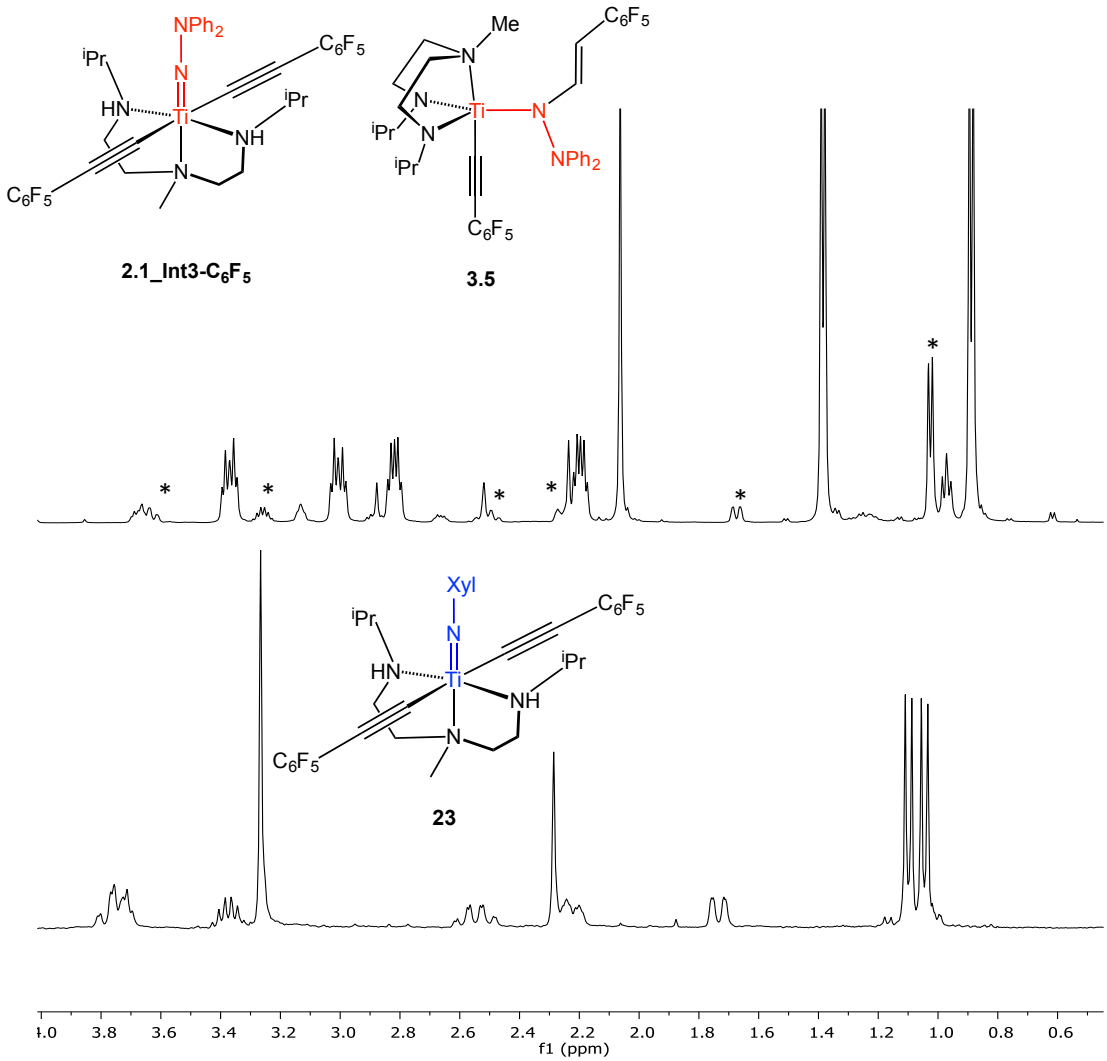


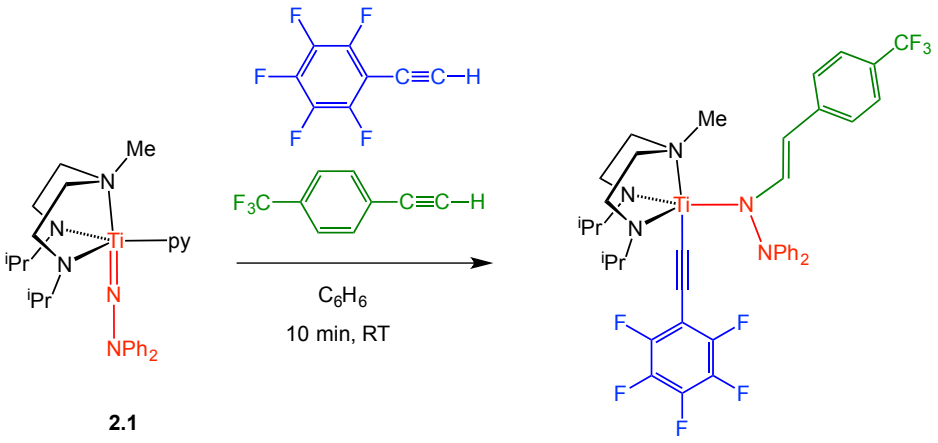
Figure 3.13. Top: ^{1}H NMR spectrum (499.9 MHz, 298 K) of $Ti(N_2^{iPr}N^{Me})\{N(NPh_2)C(H)C(H)C_6F_5\}(CCC_6F_5)$ (**3.5**) and $Ti(H_2N_2^{iPr}N^{Me})(CCC_6F_5)_2(NNPh_2)$ (**2.1_Int3-C_6F_5**) from 0.5 - 4 ppm in C_6D_6. Resonances labelled "*" correspond to **2.1_Int3-C_6F_5**. Bottom: ^{1}H NMR spectrum (499.9 MHz, 298 K) of $Ti(H_2N_2^{iPr}N^{Me})(CCC_6F_5)_2(NXyl)$ (**23**) from 0.5 - 4 ppm in C_6D_6.

The small amount of **2.1_Int3-C_6F_5** observed indicates that following formation of the mono(acetylide) (**2.1_Int1-C_6F_5**) a minor amount undergoes a second alkyne addition to yield the bis(acetylide) intermediate **2.1_Int1-C_6F_5**. The slow isomerisation of **2.1_Int3-C_6F_5** to **3.5** suggests that the reaction from **2.1** is unlikely to be proceeding *via* this intermediate. It also implies that elimination of an alkyne from **2.1_Int3-C_6F_5** to reform **2.1_Int1-C_6F_5** is difficult and the subsequent cycloaddition

reaction is much faster. Intermediates of the type **2.1_Int3** were not observed in the reaction of **2.1** with HCC-4-$C_6H_4CF_3$ or HCC-4-C_6H_4Me presumably due to less acidic C–H bonds, weaker Ti–C bonds and more facile [2+2] cycloaddition reactions.

3.7.3 Competition experiments

It was found that reaction of **2.1** with one equivalent of HCC-4-$C_6H_4CF_3$ and one equivalent of $HCCC_6F_5$ resulted in formation of the mixed vinylhydrazide-acetylide compound $Ti(N_2{}^{iPr}N^{Me})\{N(NPh_2)C(H)C(H)C_6H_4CF_3)\}(CCC_6F_5)$ (**37**) with 75% selectivity on the NMR tube scale (Equation 3.27). Compound **37** was not synthesised on a preparative scale and the NMR spectra were assigned by analogy.



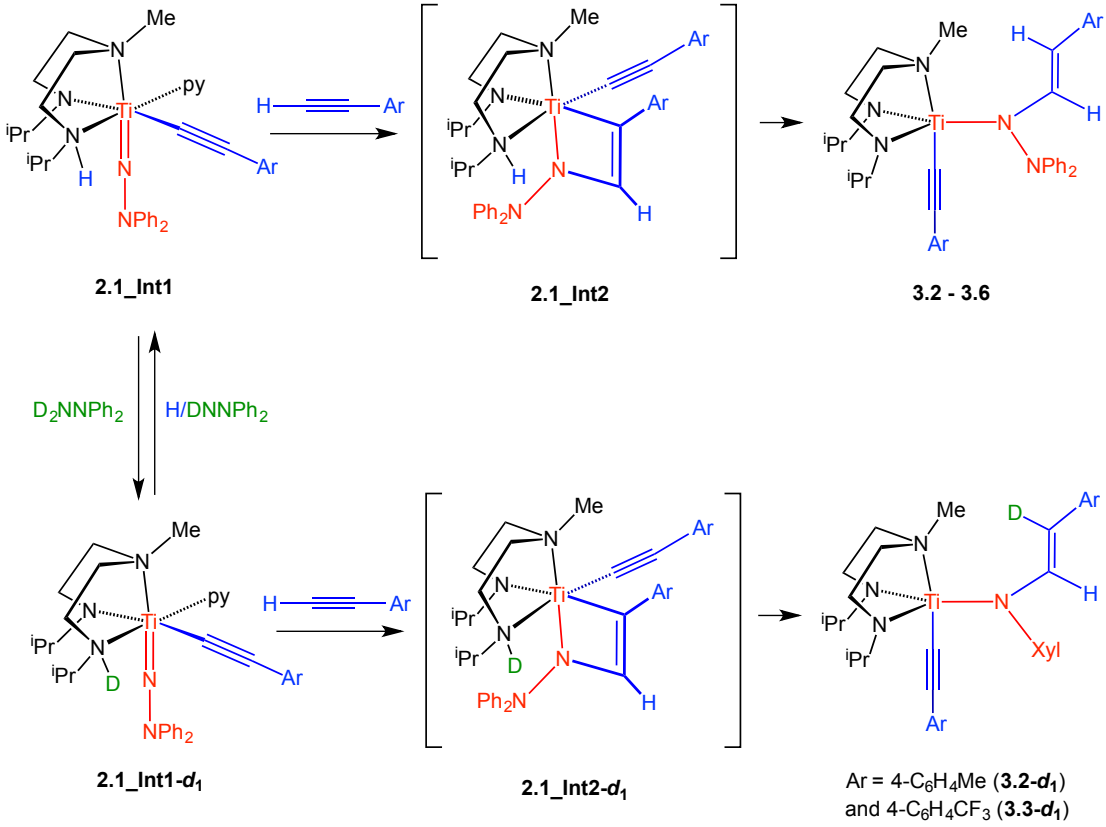
Equation 3.27

The compounds $Ti(N_2{}^{iPr}N^{Me})\{N(NPh_2)C(H)C(H)C_6H_4CF_3)\}(CCC_6H_4CF_3)$ (**3.3**) and $Ti(N_2{}^{iPr}N^{Me})\{N(NPh_2)C(H)C(H)C_6H_4C_6F_5)\}(CCC_6F_5)$ (**3.5**) were also observed in 16% and 9% yields respectively. Formation of compound **37** is consistent with the proposed mechanism. The $HCCC_6F_5$ alkyne undergoes C–H addition as it contains the most acidic C–H bond and the resultant acetylide ligand has the strongest Ti–C bond. Then, the subsequent cycloaddition reaction occurs preferentially with HCC-4-$C_6H_4CF_3$ for steric reasons.

3.7.4 NH/D exchange reactions

Direct exchange between Ti–NH bonds and N–D bonds of a free amine was described above. The same phenomenon was observed in the reaction of **2.1** with two equivalents of HCCAr (Ar = 4-C_6H_4Me or 4-$C_6H_4CF_3$) in the presence of D_2NNPh_2,

or *vice versa* (DCCAr (Ar = 4-C_6H_4Me or 4-$C_6H_4CF_3$) and Ph_2NNH_2). Reaction of **2.1** with one equivalent of HCCAr yields mono(acetylide) intermediates **2.1_Int1** which contains a Ti–NH bond (not observed). Direct exchange can occur with D_2NNPh_2 to yield **2.1_Int1-*d*$_1$** which, following cycloaddition with HCCAr, will transfer the D atom into the TiNC(H)C(H) position yielding **3.2-*d*$_1$** and **3.3-*d*$_1$** (Scheme 3.13).

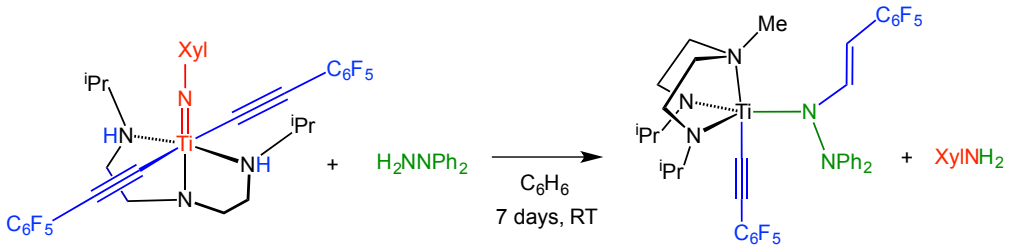


Scheme 3.13. Mechanism for the reaction of Ti($N_2^{iPr}N^{Me}$)($NNPh_2$)(py) (**2.1**) with HCCAr in the presence of D_2NNPh_2.

No deuterium incorporation was observed on the TiNC(H)C(H) position. This implies that only one alkyne C–H addition is occurring and it is irreversible, thus preventing scrambling of the free alkyne in solution prior to cycloaddition. No mono(acetylide) intermediates were observed implying that the NH/D exchange reactions are exceptionally facile and occur very quickly at room temperature. No isotope scrambling between HCCAr and D_2NNPh_2 occurred when tested independently or when **3.2** was mixed with D_2NNPh_2 (prior to their onward reaction which does not start until 40 minutes after mixing). These observations differ to the analogous reactions of **1** which undergoes a reversible second alkyne addition, allowing

scrambling into both vinyl positions of the final product (Equation 3.23). Importantly, these observations are inconsistent with initially proposed mechanism for the reaction of **2.1** with internal alkynes. A cycloaddition reaction followed by a σ-bond metathesis would not account for the incorporation of deuterium into the TiNC(H)C(H) position.

Interestingly, reaction of **23** with Ph_2NNH_2 gave quantitative conversion to $Ti(N_2^{iPr}N^{Me})\{N(NPh_2)C(H)C(H)(C_6F_5)\}(CCC_6F_5)$ (**3.5**) and free $XylNH_2$ (Equation 3.28).



23 **3.5**

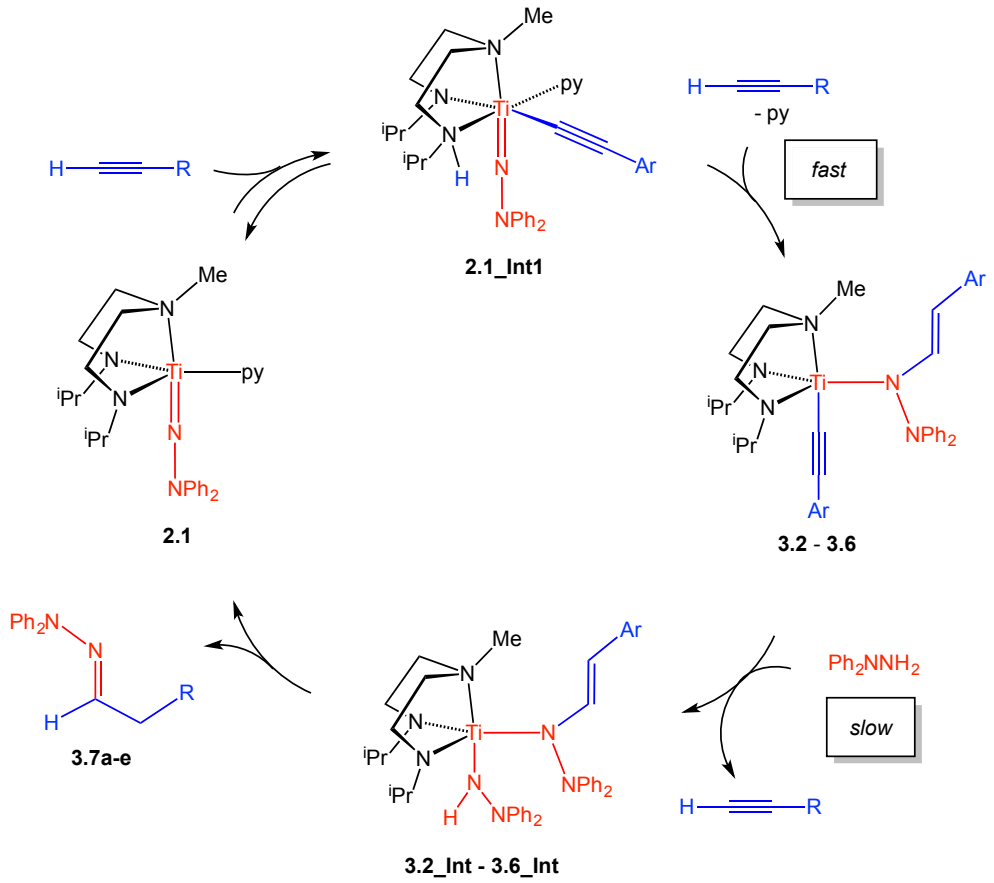
Equation 3.28

When an equivalent of alkyne eliminates from **23** there is a vacant coordination site at which $XylNH_2/Ph_2NNH_2$ exchange can occur. It is also possible that exchange could occur with **23**. However, no **2.1_Int3-C_6F_5** was observed over the course of the reaction suggesting that this is unlikely. Moreover, it has been reported that amine/imide exchange reactions at six-coordinate titanium compounds are very slow.[55] Transfer of protons to the imido moiety is unsurprising, as described in Chapter one of this Thesis amine/hydrazine exchange methodology is used to synthesise several hydrazido compounds. Subsequent cycloaddition and intramolecular protonolysis with the hydrazido mono(acetylide) intermediate will be fast yielding **3.5**.

3.7.5 Hydrohydrazination catalysis

Based on the mechanism for the formation of vinylhydrazide-acetylide compounds along with already published results, a new mechanism for hydrohydrazination catalysis with **2.1** can be proposed (Scheme 3.14). Formation of the vinylhydrazide-acetylide species **3.2** - **3.6**, followed by protonation of the acetylide ligand with Ph_2NNH_2 yields bis(hydrazido(1-)) intermediates **3.2_Int** - **3.6_Int** which are not observed. Compound **3.2** has been shown to release the acetylide ligand before the hydrazone in the presence of the more acidic proton source XylOH.[32] This is followed

by intramolecular protonolysis to regenerate the hydrazido compound **2.1** and liberate the organic hydrazone products **3.7a-e**. It is important to note that when the catalysis with **2.1** was carried out with HCC-4-C_6H_4Me and D_2NNPh_2 (1:10:10) the first formed intermediate **3.2** contains both hydrogen and deuterium in the TiNC(H)C(H) position, consistent with Scheme 3.14. As the catalysis progresses, the amount of deuterium in this position increases due to the excess of Ph_2NND_2 in the system.



Scheme 3.14. Hydrohydrazination catalytic cycle.

In comparison to that of **2.1**, reaction of **1** with HCC-4-$C_6H_4CF_3$ and $XylNH_2$ (1:10:10) gave only the stoichiometric vinylamide-acetylide reaction product **29**. No subsequent reaction with aniline or alkyne occurred and hence catalytic hydroamination does not occur. However, reaction of **1** with HCC-4-$C_6H_4CF_3$ and Ph_2NNH_2 (1:10:10) resulted in the slow formation of the hydrazone organic product **3.7b** (as well as one equivalent of the organic product expected from **29**). The rate of catalysis is slower compared to that of **2.1** under identical conditions and had only reached 15% conversion compared to 43% with **2.1** after 20 hours at room temperature. Compound **29** reacts slowly with Ph_2NNH_2 and after 48 hours at room

temperature 10% of the titanium is still **29** thus, the concentration of active catalyst is lower. So although **1** has provided an excellent model for the stoichiometric reactions of **2.1** with alkynes, it is a less good model for catalysis.

3.8 Reaction of Ti($N_2^{iPr}N^{Me}$)(NXyl)(py) (1) with other terminal alkynes

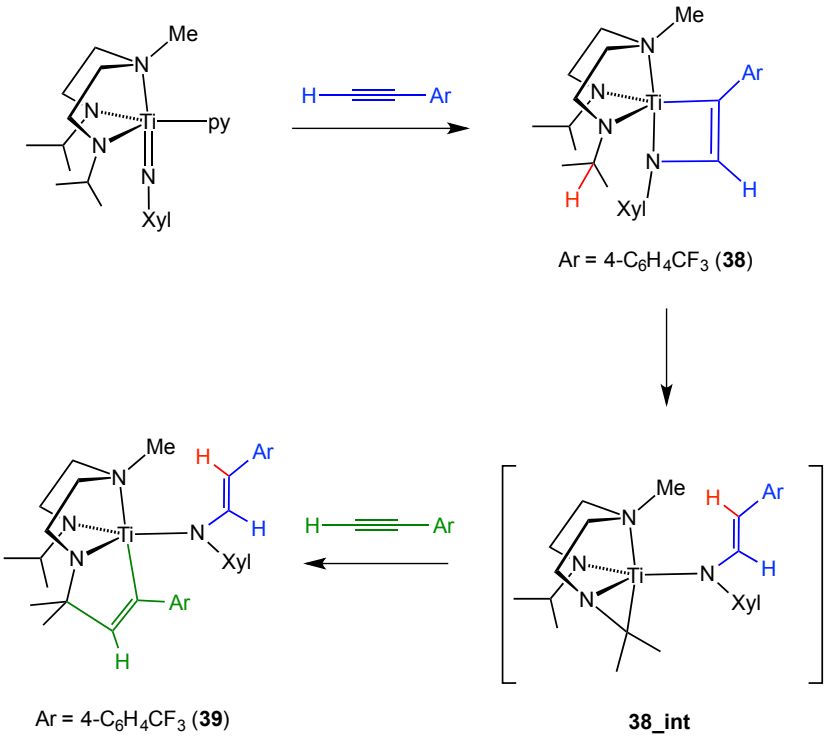
The above discussion refers to electron-withdrawing terminal alkynes only, this is in contrast to the reactions of **2.1** with terminal alkynes which proceed to form the analogous vinylhydrazide-acetylide compounds with a range of both electron-withdrawing and electron-donating substituents on the aryl ring.

Reaction of Ti($N_2^{iPr}N^{Me}$)(NXyl)(py) (**1**) with two equivalents of HCC-4-C_6H_4Me gave a mixture of compounds. A singlet at 9.93 ppm in the ^{1}H NMR spectrum was observed, typical of an azametallacyclobutene species as well as resonances reminiscent of the bis(acetylide) compounds discussed above. After standing at room temperature for 36 hours two sets of vinylic doublets were observed along with several other unknown resonances. A similar mixture of products was observed when **1** was mixed with two equivalents of HCC-4-C_6H_4OMe. Attempts to separate the compounds or vary the reaction conditions were not successful and reaction with one equivalent of HCC-4-C_6H_4Me or HCC-4-C_6H_4OMe did not result in the formation of one compound.

On reaction with two equivalents HCC-4-$C_6H_4CF_3$ at room temperature, **1** undergoes two C–H additions to form Ti($H_2N_2^{iPr}N^{Me}$)(CC-4-$C_6H_4CF_3$)$_2$(NXyl) (**26**) followed by isomerisation to yield Ti($N_2^{iPr}N^{Me}$){N(Xyl)C(H)C(H)-4-$C_6H_4CF_3$}(CC-4-$C_6H_4CF_3$) (**29**). It was noticed that carrying out this reaction at 70 ^{o}C gave a different outcome. A 1:2 mixture of **1** and HCC-4-$C_6H_4CF_3$ was mixed at room temperature, heated to 70 ^{o}C and then monitored by ^{1}H and ^{19}F NMR spectroscopy. After five minutes three distinct compounds were observed. Approximately 50% of the species reacted as expected and yielded **29**. A singlet at 9.71 ppm suggests that the metallacyclic species Ti($N_2^{iPr}N^{Me}$){N(Xyl)C(H)C($C_6H_4CF_3$)} (**38**) is present (35%), and a signal in the ^{19}F NMR spectrum was observed at -61.6 ppm. Many examples of this type of compounds with terminal alkynes have been reported before and the resonances observed here are fully consistent with such compounds.[12, 104, 105]

The third species (15%) has two mutually coupled doublets at 4.85 and 8.34 ppm, very similar to the vinylic doublets observed in **29**. After 30 minutes at 70 ^{o}C the

solution contained approximately a 3:2 mixture of **29** and the unidentified compound. None of the metallacyclic species **38** remained. Decomposition of the unknown compound occurred with further heating. However, if the solution was rapidly cooled to room temperature after being at 70 °C for 30 minutes, the mixture was not altered over several days.



Scheme 3.15. Alternative reaction pathway for the reaction of Ti($N_2^{iPr}N^{Me}$)(NXyl)(py) (**1**) with terminal alkynes.

The third compound is believed to be Ti{$N^{iPr}N^{Me}$NCMe$_2$C(H)C$C_6H_4CF_3$)}{N(2,6-$C_6H_3Me_2$)C(H)C(H)$C_6H_4CF_3$} (**39,** Scheme 3.15). Following a [2+2] cycloaddition reaction to yield the metallacyclic species **38**, ligand activation occurs and one of the isopropyl methine protons undergoes addition across the Ti–C bond resulting in the titanaziridine intermediate **38_int**, which contains the same vinylamide moiety as **29**. Following this, insertion of the second equivalent of alkyne into the Ti–C bond occurs giving **39**, which contains a five-membered ring. Titanaziridine complexes are known and have been invoked as intermediates in many Ti-mediated cross coupling reactions.[106] There are a few examples of isolated titanaaziridines, for example Sattler *et al.* reported the synthesis the titanaziridine compound $Cp_2Ti\{\eta$-N(Ph)C(Ph)$\}(PMe_3)$ and the subsequent reaction with 1-octyne which proceeds *via* insertion into the Ti–C bond to yield the analogous five-membered ring compound.[107]

Reaction of metallaaziridines with unsaturated small molecules to yield four- and five-membered rings has also been reported for many zirconium, tantalum and niobium complexes.[108-113]

It was not possible to separate **39** from **29** and attempts at altering reaction conditions to synthesise **39** as the sole product were not successful. Therefore, **39** has been characterised by ^{1}H, ^{13}C and ^{19}F NMR spectroscopy as a mixture with **29** and is fully consistent with the proposed structure.

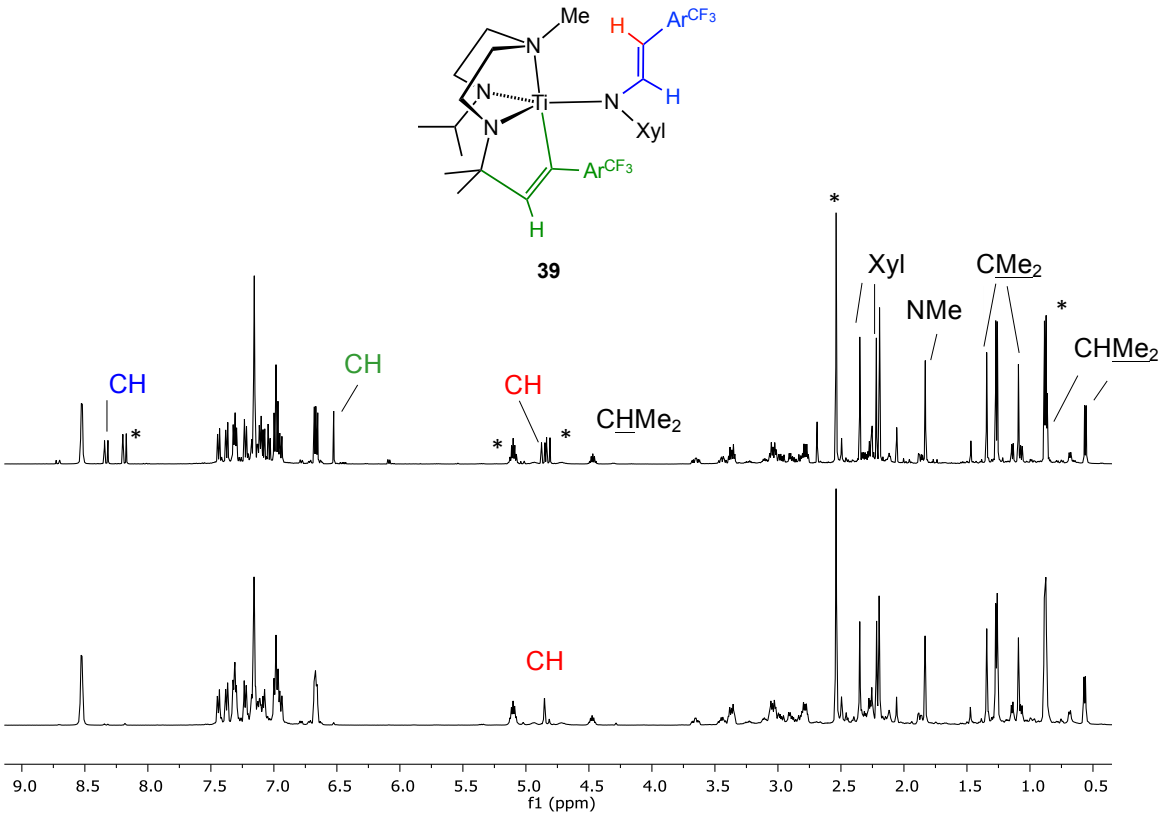


Figure 3.14. Top: ^{1}H NMR spectrum (499.9 MHz, 298 K) of Ti{N^{iPr}N^{Me}NCMe$_2$C(H)CC$_6$H$_4$CF$_3$)}{N(2,6-C$_6$H$_3$Me$_2$)C(H)C(H)C$_6$H$_4$CF$_3$} (**39**) in C$_6$D$_6$. Resonances labelled "*" correspond to **29**. Bottom: ^{1}H NMR spectrum (499.9 MHz, 298 K) of Ti{N^{iPr}N^{Me}NCMe$_2$C(D)CC$_6$H$_4$CF$_3$)}{N(2,6-C$_6$H$_3$Me$_2$)C(D)C(H)C$_6$H$_4$CF$_3$} (**39-*d*$_2$**) in C$_6$D$_6$.

The ^{1}H NMR spectrum of the mixture is shown in Figure 3.14, all resonances attributed to **39** are labelled (except for aromatic and methylene signals) and peaks associated with **29** are marked with an asterisk. The singlet at 6.70 ppm is assigned as the C–H of the alkyne moiety inserted into the Ti–C bond (labelled green). A ^{1}H-^{13}C HMBC experiment revealed a coupling from this proton to a quaternary carbon resonance at 198.1 ppm and a quaternary carbon resonance at 67.1 ppm, resulting

from the Ti–C and the CMe_2 atoms respectively. The very downfield resonance of Ti–C is typical for titanium-bound carbon atoms. The CMe_2 resonance also demonstrates correlations to two singlets in the ^{1}H NMR spectrum each of relative intensity 3H and have thus been assigned as the CMe_2 protons. The singlet nature of these signals is consistent with the loss of the methine proton from this group. Furthermore, the ^{1}H-^{13}C HMBC revealed a longer range coupling between the CMe_2 protons and the C–H of the inserted alkyne contained within the five-membered ring. The other half of the ligand backbone and the vinylamide moiety result in ^{1}H and ^{13}C chemical shifts very similar to those observed for **29**. In the ^{19}F NMR spectrum, two resonances are observed at -61.3 and -61.5 ppm, similar to the resonance observed for the -CF_3 group in the vinylamide moiety of **29**.

The ^{1}H NMR spectrum obtained when the reaction was repeated with two equivalents of DCC-4-$C_6H_4CF_3$ is also shown in Figure 3.14. The singlet at 6.70 ppm and the doublet at 8.51 ppm are absent showing that both of these hydrogen atoms are derived from the alkyne (the expected resonances are present in the ^{2}H NMR spectrum). The TiNC(H)C(H) resonance at 5.04 ppm still has relative intensity of 1H, however is a singlet due to deuteration of the TiNC(H) position. This is consistent with this proton (labelled red) originating as $CHMe_2$. Subsequently, the reaction of the hydrazido compound **2.1** with HCC-4-$C_6H_4CF_3$ was carried and immediately heated, however no other intermediates were observed. The occurrence of this alternative mechanism at high temperature implies that [2+2] cycloaddition reactions with terminal alkynes can occur at the Ti=N bond of **1** (and possibly **2.1**) however, require more energy. Thus, at room temperature reactions involving the facile C–H addition across the Ti–N_{amide} bonds occur exclusively.

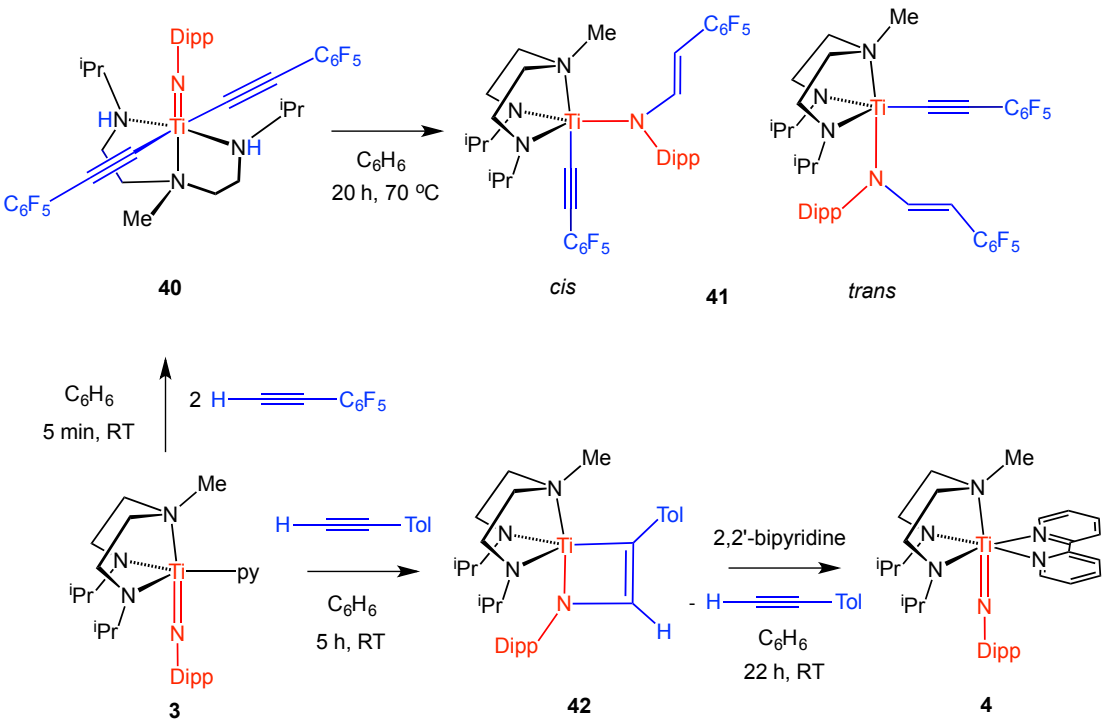
This competing pathway is the reason why the reactions of **1** with HCC-4-C_6H_4Me and HCC-4-C_6H_4OMe do not yield single reaction products. In the ^{1}H NMR spectra of both reaction mixtures, signals thought to be associated with both the vinylamide-acetylide and aziridine alkyne insertion product are observed following resonances that are reminiscent of metallacyclic and bis(acetylide) compounds. However neither of the reaction pathways appears to proceed as smoothly; this is most likely due to the less stable nature of the metallacycles when employing these electron-rich alkynes.

There are several reported examples of competing C–H activation and [2+2] cycloaddition reactions of compounds containing multiple bonds with alkynes. The

C–H activation reactions typically occur by transfer of the C–H proton onto the Ti–X atom of a multiple bond. Bergman reported the reversible [2+2] cycloaddition reactions of a titanium oxo species, which on heating underwent rearrangement to hydroxoacetylide compounds, *via* cycloreversion followed by proton transfer and formation of a titanium acetylide carbon bond.[65] Similarly, Bercaw described the reaction of a tantalum imido compound with propyne, which proceeded to a mixture of cycloaddition and C–H activation products. They found that using a more acidic alkyne resulted in exclusive formation of the C–H activation product.[69] Bergman later published a paper discussing the reaction of the titanium imido compound Cp^*_2TiNPh which yielded a metallacyclic product on reaction with propyne but C–H activation with phenylacetylene. They state that the preference is likely steric in origin as the metallacyclic product with phenylacetylene would be very sterically congested.[24] Finally, Gade *et al* report on the reactions of both alkyl and aryl half sandwich titanium imido compounds, the former of which was found to undergo C–H activation with alkynes and the latter cycloaddition reactions.[23] It is important to note that C–H bond activation reactions of transiently generated imido compounds have been studied extensively by Wolczanski and others in recent years.[81, 86] Although these examples provide clear similarities, the C–H bond activation reactions all take place at the multiple bond, as well as the cycloaddition reactions. Therefore they are different to the reactions of **1** with terminal alkynes which initially leave the multiple bond intact.

3.9 Reaction of Ti($N_2^{iPr}N^{Me}$)(NDipp)(py) (3) with terminal alkynes

As the reactions of the imido compound **1** with terminal alkynes provided excellent insight into how the reactions of **2.1** with terminal alkynes proceed and allowed a more controlled mechanistic study to be carried out. It was decided to probe the alkyne reactions of the imido compound Ti($N_2^{iPr}N^{Me}$)(NDipp)(py) (**3**) containing the Dipp substituent, to see if the larger steric bulk would allow isolation of intermediates that were previously only observed at low temperature or just postulated. The reactions of **3** with some terminal alkynes are summarised in Scheme 3.16.



Scheme 3.16. Reaction of Ti($N_2^{iPr}N^{Me}$)(NDipp)(py) (**3**) with terminal aryl alkynes.

Reaction of **3** with two equivalents of $HCCC_6F_5$ gave the bis(acetylide) compound Ti($H_2N_2^{iPr}N^{Me}$)(CCC_6F_5)$_2$(NDipp) (**40**). Heating this compound with or without the liberated pyridine present, at 70 °C for 20 hours results in quantitative conversion to the vinylamide-acetylide compound Ti($N_2^{iPr}N^{Me}$){N(Dipp)C(H)C(H)C_6F_5}(CCC_6F_5) (**41**), no other intermediates were observed. In all the analogous vinylamide-acetylide compounds synthesised from **1** the *cis* isomer is the major, or only, isomer observed. However, here, the *cis* and *trans* isomers are present in equal amounts. Many of the resonances in the ^{1}H NMR spectrum associated with one of the isomers are either very broad or not observed, similarly in the ^{13}C NMR spectrum only one set of $N_2^{iPr}N^{Me}$ peaks are observed. The broad and in many cases overlapping signals prevent isomer assignment *via* through space ^{1}H NMR spectroscopy correlation experiments.

The position of the resonances resulting from the alkene protons (TiNC(H)C(H)) can be used to assign the *cis* and *trans* isomers by comparison to the analogous compounds synthesised from **1**. The doublets resulting from TiNC(H)C(H) protons appear further downfield in the minor *trans* isomer compared to the major *cis* isomer (4.98 and 8.95 ppm (*trans*) *vs*. 4.61 and 8.31 ppm (*cis*) for

$Ti(N_2^{iPr}N^{Me})(CCC_6F_5)(NXyl)C(H)C(H)C_6F_5)$ (**24**) and 5.0 and 8.75 ppm (*trans*) *vs*. 4.82 and 8.18 (*cis*) for $Ti(N_2^{iPr}N^{Me})(CC(3,5\text{-}C_6H_3(CF_3)_2)\{N(Xyl)C(H)C(H)(3,5\text{-}C_6H_3(CF_3)_2\}$ (**30**)). Here one set of signals appears at 4.59 and 8.43 ppm and the other at 5.05 and 9.02 ppm. Thus, the more downfield resonances are assigned as the *trans* isomer and the upfield resonances as the *cis* isomer. All of the ^1H and ^{13}C signals assigned as the *cis* isomer are distinct. Many of the signals associated with the *trans* isomer are broad and cannot be identified. This could be due to restricted rotation of the vinylamide group when it is in the more sterically encumbered *trans* position close to the ^{i}Pr groups.

A sample of **41** in toluene-d_8 was gradually heated up to 80 ^oC and monitored in situ by NMR spectroscopy. At 80 ^oC many of the signals for *cis* isomer became broad, and the ratio of the two isomers changed to approximately 1:2 *cis* to *trans*. On returning to room temperature the ratio returned to 1:1. On cooling the sample down to -80 ^oC many of the signals associated with both isomers decoalesed and a spectrum consistent with two C_1 symmetric compounds was observed. Twelve $CH\underline{Me}_2$ signals were observed and eight $C\underline{H}Me_2$. This is due to restricted rotation of the vinylamide ligand of both isomers at lower temperature resulting in a loss of C_s symmetry. Many of the signals were overlapping resulting in a complicated spectrum, therefore full characterisation by NMR spectroscopy was not carried out at -80 ^oC. ^1H, ^{13}C and ^{19}F NMR spectra of **41** were recorded at 298 K and all resonances attributed to the *cis* isomer are reported as well as distinct resonances resulting from the *trans* isomer. An NMR tube scale reaction of **3** with 2 equivalents of HCC-4-$C_6H_4CF_3$ was also carried out and proceeded to form a bis(acetylide) compound which subsequently isomerised to the vinylamide-acetylide compound.

Reaction of **3** with one equivalent of HCC-4-C_6H_4Me gave reversible formation of the metallacyclic compound $Ti(N_2^{iPr}N^{Me})\{N(Dipp)C(H)C(4\text{-}C_6H_4Me)\}$ (**42**) over the course of five hours which was characterised by NMR and IR spectroscopy and elemental analysis. Only one regioisomer of **42** was observed and has been assigned as the anti-Markovnikov isomer with the $Ar\underline{C}$ bound to Ti on the basis of NMR spectroscopy. This regiochemistry has been observed in several crystallographically characterised azatitanacyclobutene complexes and calculations have shown that it is the electronically preferred regioisomer.[12, 105, 114] Addition of one equivalent of 2,2'-bipyridine to **42** gave a cycloreversion reaction yielding the imido compound **4** and

liberated alkyne. Addition of a second equivalent of HCC-4-C_6H_4Me resulted in the slow formation of several unidentified species at room temperature over several hours.

The bulky ^{i}Pr groups in the *ortho* position of the aryl imido moiety in **3** have little effect on the reactivity in comparison to **1**. Although the metallacyclic species **42** could be isolated from the reaction with HCC-4-C_6H_4Me, whereas with **1**, similar species could not be; subsequent reactivity of this compound did not proceed smoothly and did therefore not provide any extra information.

3.10 Conclusion

This Chapter details the reactions of Ti($N_2^{iPr}N^{Me}$)(NXyl)(py) (**1**) with terminal alkynes. Reaction with electron-withdrawing terminal aryl alkynes proceed *via* two subsequent σ-bond metathesis reactions to first yield mono(acetylide) compounds of the type Ti($HN_2^{iPr}N^{Me}$)(CCAr)(NXyl)(py) (**31 - 34**), which have been characterised by NMR spectroscopy at low temperature. Addition of the second equivalent yields bis(acetylide) compounds of the type Ti($H_2N_2^{iPr}N^{Me}$)$(CCAr)_2$(NXyl) (**23, 25 - 27**) with a meridonal arrangement of the now neutral ligand. When Ar = C_6F_5 this compound has been isolated, and in the other cases the compounds have been characterised by NMR spectroscopy at low temperature.

Isomerisation to vinylamide-acetylide compounds of the type Ti($N_2^{iPr}N^{Me}$){N(Xyl)C(H)C(H)Ar}(CCAr) (**24, 28 - 30**) occurs on standing at room temperature or on heating at 70 ^{o}C. These are the analogous reaction products of the reaction of Ti($N_2^{iPr}N^{Me}$)$(NNPh_2)$(py) (**2.1**) with terminal alkynes.

An isomerisation mechanism is proposed. Elimination of one equivalent of an alkyne from a bis(acetylide) species results in the formation of a mono(acetylide) species which can undergo a [2+2] cycloaddition reaction at the titanium-nitrogen multiple bond with the eliminated alkyne. Intramolecular protonolysis of the remaining N–H to the titanium bound carbon atom can then occur resulting in the formation of the final products. A full kinetic analysis was carried out on the isomerisation of **23** to **24** and the activation parameters were extracted from an Eyring plot. The observed isotope effect of 1.4(1) is a result of the equilibrium isotope effect of the pre-equilibrium between the bis(acetylide) and mono(acetylide) compounds prior to the rate-determining cycloaddition step, which has no associated kinetic isotope effect.

The distribution of isotopomers in the reaction of **1** with $HCCC_6F_5$ and $DCCC_6F_5$ (1:1:1) is consistent with this analysis. The two isotopomers **24-*d*$_1$-A** and **24-*d*$_2$-B** result from the same first formed intermediate **23-*d*$_1$** and are observed in the ratio expected if the distribution was controlled by the relative $K_{eq(H)}$ and $K_{eq(D)}$ values and is independent of the relative $k_{2(H)}$ and $k_{2(D)}$ values as $k_{2(H)} = k_{2(D)}$.

Mixed vinylamide-acetylide compounds can be synthesised from the reaction of the bis(acetylide) compound **23** with one equivalent of HCC-4-$C_6H_4CF_3$ or 10 equivs of HCC-4-C_6H_4Me. These compounds result from preferential cycloaddition with the sterically smaller alkyne as well as stronger Ti–C bonds with more electron-withdrawing alkynes. Competition reactions indicate that the formation of the metallacycle is important and not the subsequent protonolysis, as a clear preference for the more electron-withdrawing alkyne is observed.

Facile NH/ND exchange reactions are demonstrated between the N–H of a free organic species with Ti–N–H bonds. This direct exchange explains the scrambling observed in the reaction of **2.1** with alkynes in the presence of Ph_2NND_2.

The same mechanism is proposed for the reaction of **2.1** with terminal alkynes. However, a second alkyne addition does not occur and bis(acetylide) species are not formed (except when Ar = C_6F_5). The KIEs of 2.4(1) and 1.9(1) extracted from competition experiments are consistent with a C–H bond breaking reaction to form a mono(acetylide) species. The faster reaction of **2.1** with alkynes compared to **1** is attributed to more basic Ti–N_{amide} atoms and a more reactive Ti=N multiple bond. Based on these experiments a new catalytic cycle for the hydrohydrazination of terminal alkynes with diphenylhydrazine is proposed.

An alternative reaction mechanism with HCC-4-$C_6H_4CF_3$ is observed and proposed to occur *via* a [2+2] cycloaddition reaction followed by ligand activation. A product of this reaction pathway is characterised by NMR spectroscopy. Competing reaction pathways are the reason why single reaction products could not be isolated from the reactions **1** with non-electron-withdrawing alkynes. Finally the reactions of the bulkier imido compound Ti($N_2^{iPr}N^{Me}$)(NDipp)(py) (**3**) with alkynes has been presented, the reactions of **3** with electron-withdrawing terminal alkynes did not differ from that of **1**. However, a metallacyclic species was isolated from the reaction with HCC-4-C_6H_4Me.

3.11 References

1. D. E. Wigley, *Prog. Inorg. Chem.*, 1994, **42**, 239.
2. P. Mountford, *Chem. Commun.*, 1997, 2127.
3. L. H. Gade and P. Mountford, *Coord. Chem. Rev.*, 2001, **216-217**, 65.
4. P. D. Bolton and P. Mountford, *Adv. Synth. Catal.*, 2005, **347**, 355.
5. N. Hazari and P. Mountford, *Acc. Chem. Res.*, 2005, **38**, 839.
6. A. L. Odom, *Dalton Trans.*, 2005, 225.
7. A. R. Fout, U. J. Kilgore and D. J. Mindiola, *Chem. Eur. J.*, 2007, **13**, 9428.
8. J. D. Selby, C. D. Manley, M. Feliz, A. D. Schwarz, E. Clot and P. Mountford, *Chem. Commun.*, 2007, 4937.
9. J. D. Selby, C. Schulten, A. D. Schwarz, A. Stasch, E. Clot, C. Jones and P. Mountford, *Chem.Commun.*, 2008, 5101.
10. K. Weitershaus, J. L. Fillol, H. Wadepohl and L. H. Gade, *Organometallics*, 2009, **28**, 4747.
11. K. Weitershaus, H. Wadepohl and L. H. Gade, *Organometallics*, 2009, **28**, 3381.
12. A. D. Schofield, A. Nova, J. D. Selby, C. D. Manley, A. D. Schwarz, E. Clot and P. Mountford, *J. Am. Chem. Soc.*, 2010, **132**, 10484.
13. P. J. Tiong, A. D. Schofield, J. D. Selby, A. Nova, E. Clot and P. Mountford, *Chem. Commun.*, 2010, **46**, 85.
14. R. F. Munha, L. F. Veiros, M. T. Duarte, M. D. Fryzuk and A. M. Martins, *Dalton Trans.*, 2009, 7494.
15. A. J. Blake, J. M. McInnes, P. Mountford, G. I. Nikonov, D. Swallow and D. J. Watkin, *J. Chem. Soc., Dalton Trans.*, 1999, 379.
16. T. Gehrmann, J. L. Fillol, H. Wadepohl and L. H. Gade, *Organometallics*, 2010, **29**, 28.
17. T. Gehrmann, G. T. Plundrich, H. Wadepohl and L. H. Gade, *Organometallics*, 2012, **31**, 3346.
18. H. Herrmann, J. L. Fillol, H. Wadepohl and L. H. Gade, *Angew. Chem. Int. Ed.*, 2007, **46**, 8426.
19. J. Unruangsri, H. Morgan, A. D. Schwarz, A. D. Schofield and P. Mountford, *Organometallics*, 2013, **32**, 3091.
20. A. D. Schofield, A. Nova, J. D. Selby, A. D. Schwarz, E. Clot and P. Mountford, *Chem. Eur. J.*, 2011, **17**, 265.

21. P. J. Walsh, M. J. Carney and R. G. Bergman, *J. Am. Chem. Soc.*, 1991, **113**, 6343.
22. J. L. Polse, A. W. Kaplan, R. A. Andersen and R. G. Bergman, *J. Am. Chem. Soc.*, 1998, **120**, 6316.
23. K. Weitershaus, B. D. Ward, R. Kubiak, C. Muller, H. Wadepohl, S. Doye and L. H. Gade, *Dalton Trans.*, 2009, 4586.
24. J. L. Polse, R. A. Andersen and R. G. Bergman, *J. Am. Chem. Soc.*, 1998, **120**, 13405.
25. I. Bytschkov and S. Doye, *Eur. J. Org. Chem.*, 2003, 935.
26. S. Doye, *Synlett.*, 2004, 1653.
27. L. L. Schafer and A. V. Lee, *Eur. J. Inorg. Chem.*, 2007, 2243.
28. T. E. Müller, K. C. Hultzsch, M. Yus, F. Foubelo and M. Tada, *Chem. Rev.*, 2008, **108**, 3795.
29. Y. Li, Y. Shi and A. L. Odom, *J. Am. Chem. Soc.*, 2004, **126**, 1794.
30. S. Banerjee, Y. Shi, C. Cao and A. L. Odom, *J. Organomet. Chem.*, 2005, **690**, 5066.
31. S. Banerjee, E. Barnea and A. L. Odom, *Organometallics*, 2008, **27**, 1005.
32. A. D. Schwarz, C. S. Onn and P. Mountford, *Angew. Chem. Int. Ed.*, 2012, **51**, 12298.
33. P. D. Schweizer, H. Wadepohl and L. H. Gade, *Organometallics*, 2013, **32**, 3697.
34. C. Cao, Y. Shi and A. L. Odom, *Org. Lett.*, 2002, **4**, 2853.
35. J. S. Johnson and R. G. Bergman, *J. Am. Chem. Soc.*, 2001, **123**, 2923.
36. A. Tillack, H. Jiao, I. Garcia Castro, C. G. Hartung and M. Beller, *Chem. Eur. J.*, 2004, **10**, 2409.
37. L. Ackermann and R. Born, *Tet. Letts.*, 2004, **45**, 9541.
38. V. Khedkar, A. Tillack, M. Michalik and M. Beller, *Tet. Letts.*, 2004, **45**, 3123.
39. K. Weitershaus, H. Wadepohl and L. H. Gade, *Organometallics*, 2009, **28**, 4898.
40. A. D. Schofield, DPhil Thesis, Univeristy of Oxford, 2012.
41. L. R. Groom, DPhil Thesis, University of Oxford, 2014.
42. A. D. Schwarz and M. Oishi, personal communication.

43. L. Morello, J. B. Love, B. O. Patrick and M. D. Fryzuk, *J. Am. Chem. Soc.*, 2004, **126**, 9480.
44. A. P. Duncan and R. G. Bergman, *Chem. Rec.*, 2002, **2**, 431.
45. S. Banerjee and A. L. Odom, *Organometallics*, 2006, **25**, 3099.
46. A. A. Dissanayake and A. L. Odom, *Chem. Commun.*, 2012, **48**, 440.
47. H. Lang, M. Herres and L. Zsolnai, *Organometallics*, 1993, **12**, 5008.
48. M. D. Blanchard, R. P. Hughes, T. E. Concolino and A. L. Rheingold, *Chem. Mater.*, 2000, **12**, 1604.
49. S. Lorenzo, G. R. Lewis and I. Dance, *New J. Chem.*, 2000, **24**, 295.
50. P. A. Deck, C. E. Kroll, W. G. Hollis and F. R. Fronczek, *J. Organomet. Chem.*, 2001, **637-639**, 107.
51. P. A. Deck, M. J. Lane, J. L. Montgomery, C. Slebodnick and F. R. Fronczek, *Organometallics*, 2000, **19**, 1013.
52. G. S. Hair, A. H. Cowley, J. D. Gorden, J. N. Jones, R. A. Jones and C. L. B. Macdonald, *Chem. Commun.*, 2003, 424.
53. N. Adams, A. R. Cowley, S. R. Dubberley, A. J. Sealey, M. E. G. Skinner and P. Mountford, *Chem. Commun.*, 2001, 2738.
54. N. Adams, H. R. Bigmore, T. L. Blundell, C. L. Boyd, S. R. Dubberley, A. J. Sealey, A. R. Cowley, M. E. G. Skinner and P. Mountford, *Inorg. Chem.*, 2005, **44**, 2882.
55. N. Adams, H. J. Arts, P. D. Bolton, D. Cowell, S. R. Dubberley, N. Friederichs, C. M. Grant, M. Kranenburg, A. J. Sealey, B. Wang, P. J. Wilson, M. A. Zuideveld, A. J. Blake, M. Schröder and P. Mountford, *Organometallics*, 2006, **25**, 3888.
56. P. Murray-Rust, W. C. Stallings, C. T. Monti, R. K. Preston and J. P. Glusker, *J. Am. Chem. Soc.*, 1983, **105**, 3206.
57. L. Shimoni and J. Glusker, *Struc. Chem.*, 1994, **5**, 383.
58. J. A. K. Howard, V. J. Hoy, D. O'Hagan and G. T. Smith, *Tetrahedron*, 1996, **52**, 12613.
59. J. D. Dunitz and R. Taylor, *Chem. Eur. J.*, 1997, **3**, 89.
60. G. R. Desiraju, *Acc. Chem. Res*, 2002, **35**, 565.
61. D. O'Hagan, *Chem. Soc. Rev.*, 2008, **37**, 308.
62. H.-J. Schneider, *Chem. Sci.*, 2012, **3**, 1381.

63. J. R. Loader, S. Libri, A. J. H. M. Meijer, R. N. Perutz and L. Brammer, *CrystEngComm.*, 2014, **16**, 9711.
64. P. A. Champagne, J. Desroches and J.-F. Paquin, *Synthesis*, 2015, **47**, 306.
65. J. L. Polse, R. A. Andersen and R. G. Bergman, *J. Am. Chem. Soc.*, 1995, **117**, 5393.
66. P. J. Walsh, F. J. Hollander and R. G. Bergman, *J. Organomet. Chem.*, 1992, **428**, 13.
67. H. M. Hoyt and R. G. Bergman, *Angew. Chem. Int. Ed.*, 2007, **46**, 5580.
68. T. Chu, W. E. Piers, J. L. Dutton and M. Parvez, *Organometallics*, 2013, **32**, 1159.
69. R. E. Blake, D. M. Antonelli, L. M. Henling, W. P. Schaefer, K. I. Hardcastle and J. E. Bercaw, *Organometallics*, 1998, **17**, 718.
70. I. L. Fedushkin, N. M. Khvoinova, A. A. Skatova and G. K. Fukin, *Angew. Chem. Int. Ed.*, 2003, **42**, 5223.
71. K.-C. Yang, C.-C. Chang, J.-Y. Huang, C.-C. Lin, G.-H. Lee, Y. Wang and M. Y. Chiang, *J. Organomet. Chem.*, 2002, **648**, 176.
72. K. Murata, H. Konishi, M. Ito and T. Ikariya, *Organometallics*, 2002, **21**, 253.
73. H. E. Bryndza, L. K. Fong, R. A. Paciello, W. Tam and J. E. Bercaw, *J. Am. Chem. Soc.*, 1987, **109**, 1444.
74. P. L. Holland, R. A. Andersen, R. G. Bergman, J. Huang and S. P. Nolan, *J. Am. Chem. Soc.*, 1997, **119**, 12800.
75. P. L. Holland, R. A. Andersen and R. G. Bergman, *Comments Inorg. Chem.*, 1999, **21**, 115.
76. L. E. Schock and T. J. Marks, *J. Am. Chem. Soc.*, 1988, **110**, 7701.
77. D. D. Wick and W. D. Jones, *Organometallics*, 1999, **18**, 495.
78. E. Clot, C. Mégret, O. Eisenstein and R. N. Perutz, *J. Am. Chem. Soc.*, 2006, **128**, 8350.
79. J. L. Bennett and P. T. Wolczanski, *J. Am. Chem. Soc.*, 1994, **116**, 2179.
80. J. L. Bennett and P. T. Wolczanski, *J. Am. Chem. Soc.*, 1997, **119**, 10696.
81. C. C. Cummins, S. M. Baxter and P. T. Wolczanski, *J. Am. Chem. Soc.*, 1988, **110**, 8731.
82. L. M. Slaughter, P. T. Wolczanski, T. R. Klinckman and T. R. Cundari, *J. Am. Chem. Soc.*, 2000, **122**, 7953.
83. C. P. Schaller and P. T. Wolczanski, *Inorg. Chem.*, 1993, **32**, 131.

84. C. P. Schaller, J. B. Bonanno and P. T. Wolczanski, *J. Am. Chem. Soc.*, 1994, **116**, 4133.
85. C. P. Schaller, C. C. Cummins and P. T. Wolczanski, *J. Am. Chem. Soc.*, 1996, **118**, 591.
86. J. L. Bennett and P. T. Wolczanski, *J. Am. Chem. Soc.*, 1997, **119**, 10696.
87. C. C. Cummins, C. P. Schaller, G. D. Van Duyne, P. T. Wolczanski, A. W. E. Chan and R. Hoffmann, *J. Am. Chem. Soc.*, 1991, **113**, 2985.
88. J. K. C. Abbott, L. Li and Z.-L. Xue, *J. Am. Chem. Soc.*, 2009, **131**, 8246.
89. T. H. Lowry and K. S. Richardson, *Mechanism and Theory in Organic Chemistry*, Harper and Row, New York, 1987.
90. L. E. N. Allan, G. J. Clarkson, D. J. Fox, A. L. Gott and P. Scott, *J. Am. Chem. Soc.*, 2010, **132**, 15308.
91. K. Manna, A. Ellern and A. D. Sadow, *Chem. Commun.*, 2010, **46**, 339.
92. A. L. Reznichenko and K. C. Hultzsch, *Organometallics*, 2010, **29**, 24.
93. A. L. Reznichenko and K. C. Hultzsch, *J. Am. Chem. Soc.*, 2012, **134**, 3300.
94. M. G. Cushion, J. Meyer, A. Heath, A. D. Schwarz, I. Fernández, F. Breher and P. Mountford, *Organometallics*, 2010, **29**, 1174.
95. W. D. Jones, *Acc. Chem. Res*, 2003, **36**, 140.
96. K. E. Janak, D. G. Churchill and G. Parkin, *Chem. Commun.*, 2003, 22.
97. T. O. Northcutt, D. D. Wick, A. J. Vetter and W. D. Jones, *J. Am. Chem. Soc.*, 2001, **123**, 7257.
98. E. M. Simmons and J. F. Hartwig, *Angew. Chem. Int. Ed.*, 2012, **51**, 3066.
99. T. Hascall, D. Rabinovich, V. J. Murphy, M. D. Beachy, R. A. Friesner and G. Parkin, *J. Am. Chem. Soc.*, 1999, **121**, 11402.
100. G. Parkin, *Acc. Chem. Res.*, 2009, **42**, 315.
101. D. Rabinovich and G. Parkin, *J. Am. Chem. Soc.*, 1993, **115**, 353.
102. H. E. Toomey, D. Pun, L. F. Veiros and P. J. Chirik, *Organometallics*, 2008, **27**, 872.
103. E. B. Hulley, K. D. Welch, A. M. Appel, D. L. DuBois and R. M. Bullock, *J. Am. Chem. Soc.*, 2013, **135**, 11736.
104. N. Vujkovic, B. D. Ward, A. Maisse-Francois, H. Wadepohl, P. Mountford and L. H. Gade, *Organometallics*, 2007, **26**, 5522.
105. B. D. Ward, A. Maisse-Francois, P. Mountford and L. H. Gade, *Chem. Commun.*, 2004, 704.

106. H. A. Reichard and G. C. Micalizio, *Chem. Sci.*, 2011, **2**, 573.
107. L. Li, K. E. Kristian, A. Han, J. R. Norton and W. Sattler, *Organometallics*, 2012, **31**, 8218.
108. M. V. Galakhov, M. Gómez, P. Gómez-Sal and P. Velasco, *Organometallics*, 2005, **24**, 848.
109. M. V. Galakhov, M. Gomez, G. Jimenez, P. Royo, M. A. Pellinghelli and A. Tiripicchio, *Organometallics*, 1995, **14**, 2843.
110. K. E. Kristian, M. Iimura, S. A. Cummings, J. R. Norton, K. E. Janak and K. Pang, *Organometallics*, 2009, **28**, 493.
111. J. M. P. Lauzon and L. L. Schafer, *Dalton Trans.*, 2012, **41**, 11539.
112. J. S. Figueroa, N. A. Piro, D. J. Mindiola, M. G. Fickes and C. C. Cummins, *Organometallics*, 2010, **29**, 5215.
113. M. V. Galakhov, M. Gómez, P. Gómez-Sal and P. Velasco, *Organometallics*, 2005, **24**, 3552.
114. H. Wang, H. Chan and Z. Xie, *Organometallics*, 2005, **24**, 3772.

Chapter Four

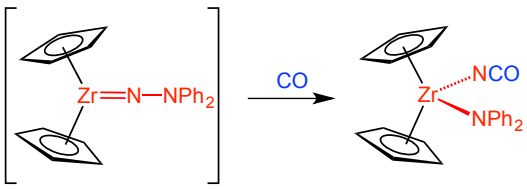
Reactions of $Ti(N_2^{iPr}N^{Me})(NNPh_2)(py)$ with silanes and boranes

4.1 Overview

This Chapter describes the reactions of the hydrazido compound $Ti(N_2^{iPr}N^{Me})(NNPh_2)(py)$ (**2.1**) with the Si–H and B–H bonds of silanes and boranes. The synthesis and characterisation of the reaction products are described, along with a combined experimental and DFT mechanistic study. The onward reaction of one isolated silylamido reaction product with further equivalents of silanes and boranes is also investigated. Part of this work has been published.[1]

4.2 Introduction

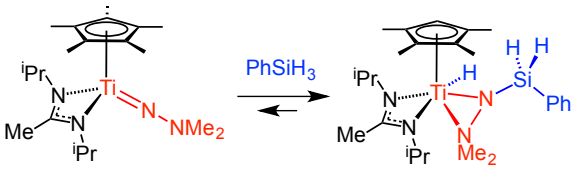
As mentioned in previous Chapters, Group 4 imido and hydrazido compounds exhibit a range of reactivity with small molecules. Focus over the last 5 – 8 years has been on the latter, and a variety of addition and insertion reactions of the $Ti{=}N_\alpha$ multiple bond with unsaturated substrates have been reported.[2-17] While some aspects of this chemistry are reminiscent of that of the related and better-established Group 4 imides,[18-20] a distinctive aspect of Group 4 hydrazido (and the related alkoxyimides (L)Ti=NOR[21]) is the typically facile reductive cleavage of the N_α–N_β bond. This can occur with oxidisable substrates such as CO (Equation 4.1),[2] isocyanides,[6, 14] and alkynes to from new N-element functional groups and/or organic products.[9, 11, 12]



1.84 **1.129**

Equation 4.1

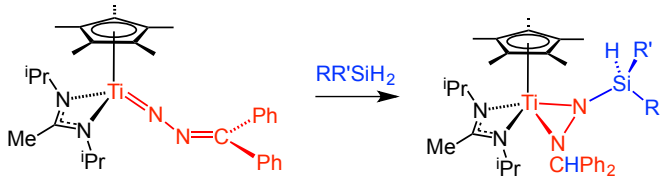
Despite this recent activity, the reactions of terminal Group 4 $M{=}NNR_2$ functional groups with small molecules containing hydridic element hydrogen bonds remains underexplored. Although there is precedent for Si–H addition to metal heteroatom multiple bonds in general,[18-20, 22, 23] only one example of the reaction of Group 4 hydrazides with the Si–H bond of silanes has been reported to date. This is the reversible 1,2-addition (without N_α–N_β cleavage) to the $Ti{=}N_\alpha$ multiple bond of $Cp^*Ti\{MeC(N^iPr)_2\}(NNMe_2)$ (**1.76**) shown in Equation 4.2.[24] The corresponding diphenylhydrazide compound $Cp^*Ti\{MeC(N^iPr)_2\}(NNPh_2)$ (**1.77**) showed no reactivity with silanes. Neither **1.76** of **1.77** reacted with H_2.



1.76 **1.114**

Equation 4.2

Comparable reactivity has also been reported with titanium alkylidene hydrazide complexes. Bergman described the reaction of $Cp^*_2Ti\{NNC(H)Tol\}$ with Ph_2SiH_2 and $PhSiH_3$, yielding the analogous hydride-alkylidene hydrazide compounds $Cp^*_2Ti(H)\{N(SiR_3)(NC(H)Tol\}$.[25] Similarly, reaction of the cyclopentadienyl-amidinate supported compound $Cp^*Ti\{MeC(N^iPr)_2\}(NNCPh_2)$ (**1.147**) with both primary and secondary silanes gives $Cp^*Ti\{MeC(N^iPr)_2\}\{N(R'RSiH)N(CHPh_2)\}$ *via* Si–H bond activation (Equation 4.3).[26]



1.147

Equation 4.3

No reactions of hydrazide compounds with primary or secondary boranes are known, although boranes without a B–H bond form Lewis adducts with the Ti=$\underline{N}_\alpha$ atom of certain hydrazides.[14] Very recently Chen and co-workers described the first structurally authenticated example of the 1,2-addition of a B–H bond of a transition-metal imide.[27] The resulting hydride species was trapped with a second equivalent of borane to yield an organohydroborate ligand.

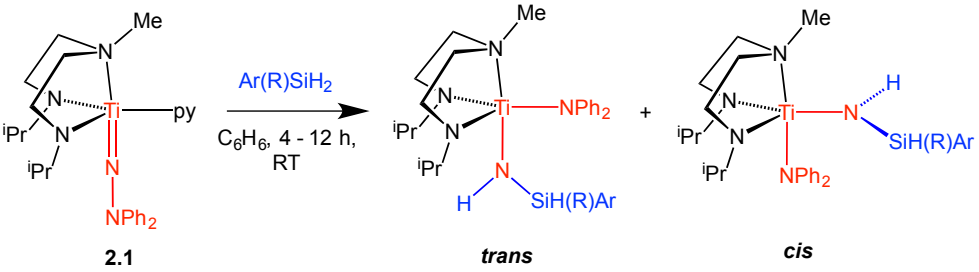
Of further relevance to the work described in this Chapter are the E–H bond activation, and in some cases N–N bond cleavage reactions, of early transition-metal-bound N_2 with Si–H[28-30] and B–H[31-33] bonds of silanes and boranes. These proceed via bimetallic intermediates in all instances. The subsequent N–N bond breaking reactions (formally silyl- or borylimido ligands) are sometimes accompanied by ancillary ligand degradation (especially in the case of Group 5 borane reaction

products) and are typically assisted (in Group 4) by addition of a reducing agent such as CO.

In the previous Chapters of this Thesis the reactions of the imido compound Ti($N_2^{iPr}N^{Me}$)(NXyl)(py) (**1**) and the hydrazido compound Ti($N_2^{iPr}N^{Me}$)($NNPh_2$)(py) (**2.1**) with a variety of small molecules were described. Setting this chemistry apart from the many literature examples is the involvement of the N_{amide} atom of the supporting ligand. The ability of the supporting ligand to accept a proton has led to range of unusual reactivity products from N–H, O–H and C–H activation. Encouraged by the small yet interesting literature precedent for the reactions of Group 4 hydrazido compounds with the Si–H bond of silanes and the propensity for **1** and **2.1** to activate element hydrogen bonds, the reactions with silanes and boranes were explored. DFT calculations described in this Chapter were performed by Simona Mellino at The University of Oxford in collaboration with Dr Eric Clot at Université Montpellier.

4.3 Reaction of Ti($N_2^{iPr}N^{Me}$)($NNPh_2$)(py) (2.1) with silanes

Reaction of Ti($N_2^{iPr}N^{Me}$)($NNPh_2$)(py) (**2.1**) with $PhSiH_3$ at room temperature gave quantitative conversion to the diamide compound Ti($N_2^{iPr}N^{Me}$){N(H)SiH_2Ph}(NPh_2) (**43**), which exists as two isomers denoted ***trans*-43** and ***cis*-43** in a 40:60% ratio according to NMR integration (*trans* and *cis* refer to the relative orientations of the -N(H)SiH_2Ph ligand and NMe donor, Equation 4.4). The isomers were assigned with the aid of a ^{1}H ROESY NMR experiment in which an NOE between the NMe resonance in ***cis*-43** was observed to both the NH and SiH_2 resonances. In comparison ***trans*-43** exhibited a correlation between the NMe resonance and the *o*-NPh_2 resonance.



2.1 ***trans*** ***cis***

R = H, Ar = Ph (**43**), 3,5-$C_6H_3(CF_3)_2$ (**44**) or 4-C_6H_4OMe (**45**)

R = Ph, Ar = Ph (**46**)

Equation 4.4

On the preparative scale **43** was isolated on 90% yield as a dark red sticky solid which was characterised by NMR and IR spectroscopy and elemental analysis. The ^{1}H NMR spectrum is consistent with a C_s symmetric structure with two doublets and one septet due to the $CHMe_2$ substituents and four multiplets due the diasterotopic methylene protons for each of the isomers. Doublets at 5.22 and 5.51 ppm are assigned as the SiH_2 protons for the *cis* and *trans* isomers respectively. Both exhibit a coupling constant of 4.6 Hz due to three-bond coupling to the NH protons, assigned as the broad triplets at 5.65 and 5.88 ppm for the *cis* and *trans* isomers respectively.

To confirm the spectroscopic assignment of NH and SiH_2 the deuterated compound $Ti(N_2^{iPr}N^{Me})\{N(D)SiD_2Ph\}(NPh_2)$ (**43-*d*$_3$**) was prepared from **2.1** and $PhSiD_3$. The mutually coupled SiH_2 and NH resonances were absent in the ^{1}H NMR spectrum and corresponding signals were observed in the ^{2}H NMR spectrum. A ^{29}Si-^{1}H gradient HMBC experiment revealed a one-bond interaction between the doublet at 5.22 ppm and a ^{29}Si resonance at -32.0 ppm ($^{1}J_{Si-H}$ = 203 Hz), likewise between the doublet at 5.51 ppm and a ^{29}Si resonance at -32.5 ppm ($^{1}J_{Si-H}$ = 202 Hz). When followed by ^{1}H NMR spectroscopy in toluene-d_8 from -78 ^{o}C to room temperature the reaction started to occur at *ca*. -10 ^{o}C, initially forming only ***trans*-43**, establishing this as the kinetic product. On warming to *ca*. 10 ^{o}C the *cis* isomer started to appear, and after several hours at room temperature the thermodynamic equilibrium was established. Similar isomerisations have been noted elsewhere with this type of supporting ligand.[14] Spin saturation transfer measurements at 70 ^{o}C obtained from a ^{1}H ROESY NMR experiment showed exchange on the NMR timescale between the isomers, consistent with a facile isomerisation. No exchange on the NMR timescale was observed at room temperature.

Reaction of $Ti(N_2^{iPr}N^{Me})(NNPh_2)(py)$ (**2.1**) also proceeds smoothly with the substituted primary aryl silanes 3,5-$C_6H_3(CF_3)_2SiH_3$ and 4-$C_6H_4OMeSiH_3$ to yield the analogous products $Ti(N_2^{iPr}N^{Me})\{N(H)SiH_2(3,5\text{-}C_6H_3(CF_3)_2)\}(NPh_2)$ (**44**) and $Ti(N_2^{iPr}N^{Me})\{N(H)SiH_2(4\text{-}C_6H_4OMe)\}(NPh_2)$ (**45**) (Equation 4.4). Both **44** and **45** exists as a mixture of *cis* and *trans* isomers assigned with aid of ^{1}H ROESY NMR experiments. Interestingly, ***trans*-44** is the major isomer (65:35%) where as ***cis*-45** is the major isomer as was observed with **43**. Characteristic mutually coupled SiH_2 and NH resonances were present, with the *cis* isomer resonances appearing upfield of the *trans* isomer resonances in both cases. A ^{29}Si-^{1}H gradient HMBC NMR experiment

revealed one bond coupling between the SiH_2 resonances to just one signal at -34.7 ppm in the ^{29}Si NMR spectrum of **44** due to overlapping *cis* and *trans* resonances. Two resonances were observed in the ^{29}Si NMR spectrum of **45** at -32.4 and -32.7 ppm for the *cis* and *trans* isomers respectively.

The ν(Si–H) bands lie between 2101 and 2111 cm^{-1} and the ν(N–H) bands appear between 3390 and 3395 cm^{-1} in the IR spectra of **43** - **45**. These bands were absent in the IR spectrum of **43-*d*$_3$** with corresponding bands observed at 1499 and 2359 cm^{-1}, in reasonable agreement with the predictions made by the harmonic oscillator model (1512 and 2477 cm^{-1}). Unfortunately, **43** - **45** were isolated as sticky solids and all attempts to grow diffraction-quality crystals were unsuccessful.

Reaction with Ph_2SiH_2 gave the analogous reaction product, namely $Ti(N_2^{iPr}N^{Me})\{N(H)SiHPh_2\}(NPh_2)$ (**46**), which likewise exists as a mixture of *cis* and *trans* isomers (50:50% ratio). The reaction proceeds quantitatively on the NMR tube scale and compound **46** was isolated as an orange powder in 40% yield on the preparative scale. Diffraction-quality crystals were grown from a saturated solution in benzene at room temperature and confirm the connectivity shown in Equation 4.4. The solid-state structure of ***trans*-46** is shown in Figure 4.1 and selected bond distances and angles in Table 4.1. The ^{1}H, ^{13}C and ^{29}Si NMR spectra are comparable to those described above for compounds **43** - **45** with a scalar coupling constant of 7.1 Hz observed for the mutually coupled doublets due to the NH (6.13 and 6.30 ppm, *cis* and *trans*) and SiH (5.75 and 5.95 ppm, *cis* and *trans*) resonances. One ν(Si–H) bands was observed at 2089 cm^{-1} and one ν(N–H) band at 3317 cm^{-1}. No reaction was observed between **2.1** with Mes_2SiH_2, Ph_3SiH or Et_3SiH, presumably due to the larger steric bulk. Likewise, no reactivity was observed between the imido compound $Ti(N_2^{iPr}N^{Me})(NXyl)(py)$ (**1**) and any of the above silanes.

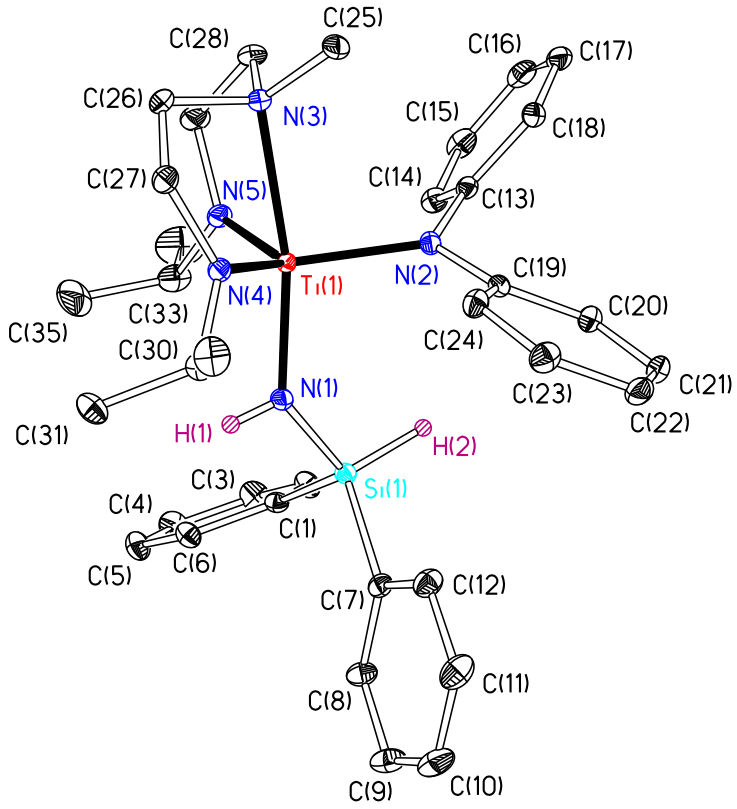


Figure 4.1. Displacement ellipsoid plot (20% probability) of $Ti(N_2^{iPr}N^{Me})\{N(H)SiHPh_2\}(NPh_2)$ (***trans*-46**). Carbon-bound H atoms are omitted for clarity.

Table 4.1. Selected bond distances (Å) and angles for $Ti(N_2^{iPr}N^{Me})\{N(H)SiHPh_2\}(NPh_2)$ (***trans*-46**).

Ti(1)-N(1)	1.9307(9)	N(1)-Ti(1)-N(3)	168.21(4)
Ti(1)-N(2)	2.0115(9)	N(2)-Ti(1)-N(4)	120.43(4)
Ti(1)-N(3)	2.2867(9)	N(2)-Ti(1)-N(5)	113.19(4)
Ti(1)-N(4)	1.9518(9)	N(4)-Ti(1)-N(5)	120.32(4)
Ti(1)-N(5)	1.9405(9)	Ti(1)-N(1)-Si(1)	135.57(6)
N(1)-Si(1)	1.7180(16)	Si(1)-N(1)-H(1)	112.3(11)
		H(1)-N(1)-Ti(1)	111.3(11)

Compound ***trans*-46** is five-coordinate distorted trigonal bipyramidal complex with a N(1)-Ti(1)-N(3) angle of 168.24 °. The diamide-amine ligand is bound facially occupying one axial and two equatorial sites. Complete cleavage of the N_α–N_β bond has resulted in the formation of the new NPh_2 and $N(H)SiHPh_2$ ligands (each having an N atom in a formal -3 oxidation state compared to -2 in **2.1**) positioned *cis* and *trans*, respectively, to the NMe moiety of $N_2^{iPr}N^{Me}$. The Ti(1)-N(1) distance of 1.9307(9) Å is within the region expected for a titanium amide bond. The sum of the angles subtended at N(1) is *ca.* 360 ° indicating significant donation of the lone pair located on N(1) into titanium π-acceptor orbitals. The Ti(1)-N(2) bond distance is slightly longer (2.0115(9) Å), as expected for a secondary amide and is consistent with the distance of 2.0019(3) Å found for the same ligand in compound **6**, described in Chapter Two.

4.4 Mechanism of the reaction of Ti($N_2^{iPr}N^{Me}$)($NNPh_2$)(py) (2.1) with silanes

The formation of the compounds Ti($N_2^{iPr}N^{Me}$){N(H)SiH(R)Ar}(NPh_2) (R = H, Ar = Ph (**43**), 3,5-$C_6H_3(CF_3)_2$ (**44**) or 4-C_6H_4OMe (**45**); R = Ph, Ar = Ph (**46**)) represents the first reductive cleavage of a hydrazide or related N–N bond by a silane at a single metal centre, with net insertion of the N_α atom of Ti($N_2^{iPr}N^{Me}$)($NNPh_2$)(py) (**2.1**) into a silane Si–H bond. Further experiments and DFT calculations were carried out to probe the mechanism.

The full mechanism for the reaction of **2.1** with $PhSiH_3$ was calculated by DFT (Figure 4.2). Two related pathways for the formation of **43** were found, starting from the different isomers of **2.1** ($NNPh_2$ *cis* or *trans* to NMe). The lowest energy pathway leads to the experimentally observed kinetic product ***trans*-43** which may then isomerise readily to the thermodynamic equilibrium mixture of *cis* and *trans* isomers. As is well established for the reactions of many diamide-amine supported imido and hydrazido analogues of **2.1**, the reaction proceeds *via* loss of pyridine to form the four-coordinate **Int1** with a barrier of 17.5 kcal mol^{-1}. The 1,2-addition of Si–H to the Ti=N_α bond of **Int1** proceeds in a facile manner *via* **Int2** (relative G = 13.3 kcal mol^{-1}). The adduct **Int2** features the necessary interactions between Ti and H (1.873 Å) as well as donation of the lone pair situated on N_α into a σ* Si–H orbital resulting in a hypervalent Si atom. However, the Si–N distance is quite long (2.579 Å) and only minimal lengthening of the Ti=N_α bond was observed (1.756 *vs*. 1.729 Å) suggesting $PhSiH_3$ is weakly bound. Breaking of the Si–H bond is accompanied by N_β chelation

to yield the silylhydrazido-hydride species **Int3**. **Int3** is the analogous species found in the reactions of Cp*Ti{MeC(N^{i}Pr)$_2$}(NNMe$_2$) (**1.76**) with silanes, DFT studies on this system found that β-NMe$_2$ played a key role in these reactions providing stabilisation from both a kinetic and thermodynamic point of view. The additional stabilisation gained upon coordination of N$_\beta$ is not available to imido compounds, which may explain the lack of reaction with Ti(N$_2^{iPr}$N^{Me})(NXyl)(py) (**1**). The barrier from this species, namely irreversible hydride transfer to N$_\alpha$ and a highly exergonic reductive N$_\alpha$–N$_\beta$ bond cleavage, to give the final product at -58.7 kcal mol^{-1} is readily accessible ($\Delta G^{\ddagger}$ = 17.3 kcal mol^{-1}). The alternative pathway starting from the *trans* isomer of **2.1**, is almost identical, but the final transition state (analogous to **TS2**) has $\Delta G^{\ddagger}$ = 25.2 kcal mol^{-1} and is therefore not competitive. The full mechanism was also calculated for the reaction of **2.1** with PhSiD$_3$ and the corresponding energies are given in parentheses in Figure 4.2. The final product is 0.7 kcal mol^{-1} lower in energy and **TS2** is 0.2 kcal mol^{-1} higher in energy.

The highest points located on the lowest energy reaction pathway are pyridine loss to form **Int1** ($\Delta G^{\ddagger}$ = 17.5 kcal mol^{-1}) and hydride transfer and N–N bond cleavage to yield the final product ***cis*-43** ($\Delta G^{\ddagger}$ = 17.3 kcal mol^{-1}). These barriers are very close in energy and calculations indicate that they contribute 58 and 42% to the overall rate, respectively. The kinetic isotope effect of 1.16 was calculated, reflecting the contribution of the isotope sensitive hydride transfer to the overall rate. By arbitrarily decreasing the relative G of **Int1** to 18.0 kcal mol^{-1} (from 19.7 kcal mol^{-1}) and allowing the hydride transfer to dominate the rate, the calculated isotope effect is 1.33. Furthermore, by removing the pyridine dissociation barrier completely the maximum possible KIE for the hydride transfer step was calculated to be 1.37. This demonstrates the sensitivity of the calculated KIE to small changes in the calculations and the upper limit that might be expected.

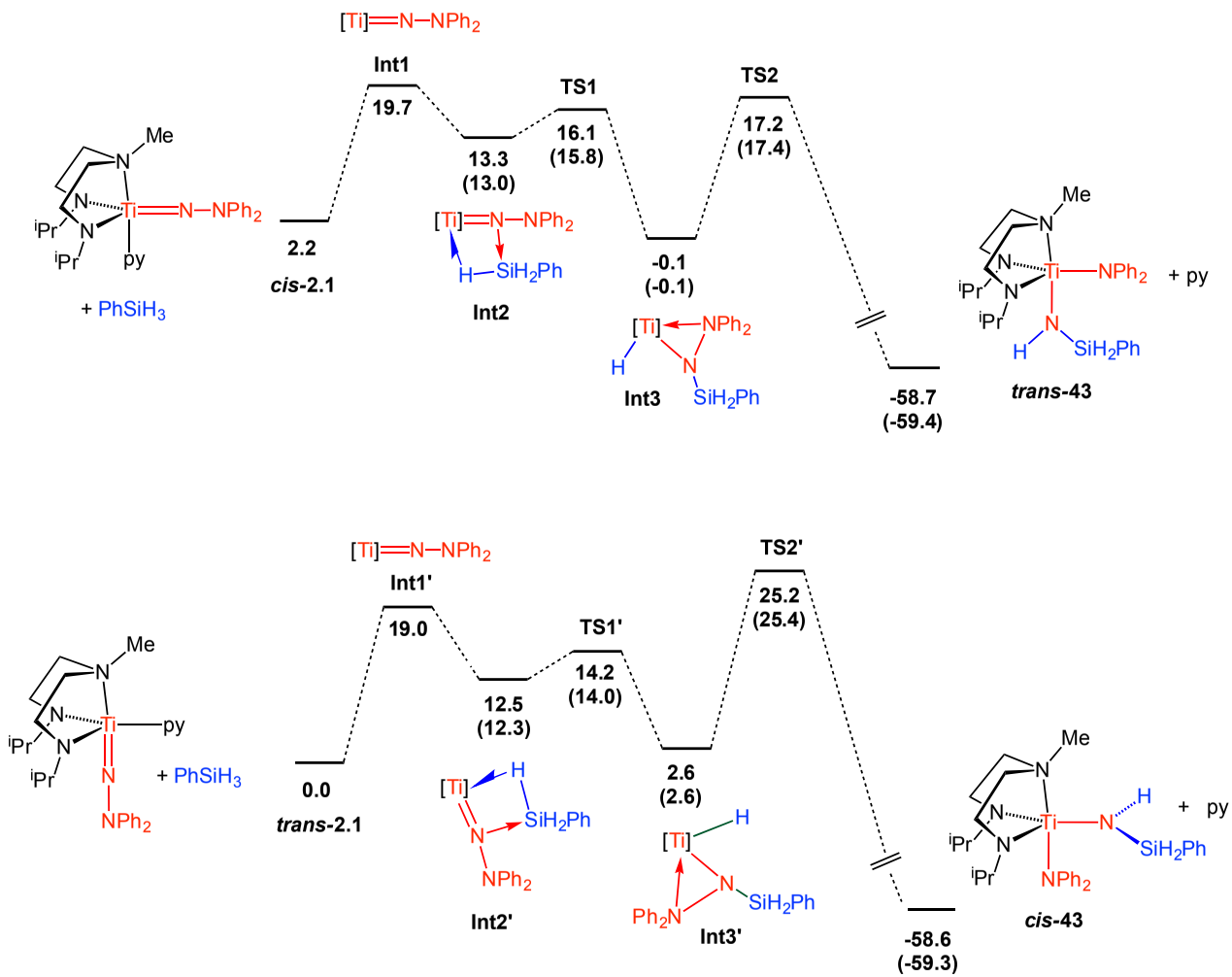


Figure 4.2. DFT mechanism for the reaction of **2.1** with $PhSiH_3$ forming **43** and pyridine. Gibbs free energies (kcal mol^{-1}, T = 298 K) for minima, maxima and transition states (labelled **TSx**) are shown in bold relative to **2.1** and $PhSiH_3$. [Ti] represents $Ti(N_2{}^{iPr}N^{Me})$. The corresponding values for the reactions with $PhSiD_3$ leading to **43-*d*$_3$** are given in parentheses.

The reaction of $Ti(N_2^{iPr}N^{Me})(NNPh_2)(py)$ (**2.1**) and $PhSiH_3$ (1:1 ratio) in C_6D_6 at room temperature was monitored by ^1H NMR spectroscopy and the evolution of $Ti(N_2^{iPr}N^{Me})\{N(H)SiH_2Ph\}(NPh_2)$ (**43**) measured by integration over a period of time. The reaction was initially very fast reaching 55% conversion in eight minutes and then slowing down significantly, requiring approximately four hours to reach completion. This is attributed to the build up of pyridine during the course of the reaction. Therefore, the reaction was carried out in the presence of excess pyridine (five equivalents) in order to assess the rate of reaction at constant pyridine concentration. As expected, a significant decrease in the rate of reaction was observed, consistent with pyridine dissociation contributing to the rate-determining step. However, some minor side reactions occurred and several unidentified resonances were observed preventing a full analysis. Therefore, to assess the rate of reaction without needing to take into account the build up of pyridine the initial rates method was used to effectively calculate the rate, d[**43**]/d*t* at time = 0, t_0. Previous work in our group has successfully used this method to analyse the kinetics of the catalytic diamination of hydrazines with internal alkynes with amide supported titanium compounds.[34]

The graph of [**43**] *vs.* time for the stoichiometric reaction at 298 K gave the non-linear plot shown in Figure 4.3. Graphical software (Origin) was used to fit a curve to all of the data points, thus describing the evolution of product throughout the kinetic study (Equation 4.5, 'y_0', 'A_n' and 'B_n' are empirical constants). The curve was then differentiated to obtain an equation for the gradient, and the gradient calculated at time = 0 s (Equation 4.6). This allows the initial rate of reaction to be calculated (12.44(5) x 10^{-5} mol dm^{-3} s^{-1}, the identical value was found on repeating the experiment). The same reaction was carried with D_3SiPh and the initial rate found to be 8.80(1) x 10^{-5} and 9.26(3) x 10^{-5} mol dm^{-3} s^{-1} on repeat. This gives a kinetic isotope effect between 1.34 and 1.41.

$$[\mathbf{43}] = y_0 + A_1 e^{-t/B_1} + A_2 e^{-t/B_2} \qquad (4.5)$$

$$\frac{d[\mathbf{43}]}{dt} = -\frac{A_1 e^{-t/B_1}}{B_1} - \frac{A_2 e^{-t/B_2}}{B_2} \qquad \left(\frac{d[\mathbf{43}]}{dt}\right)_{t=0} = -\frac{A_1}{B_1} - \frac{A_2}{B_2} \qquad (4.6)$$

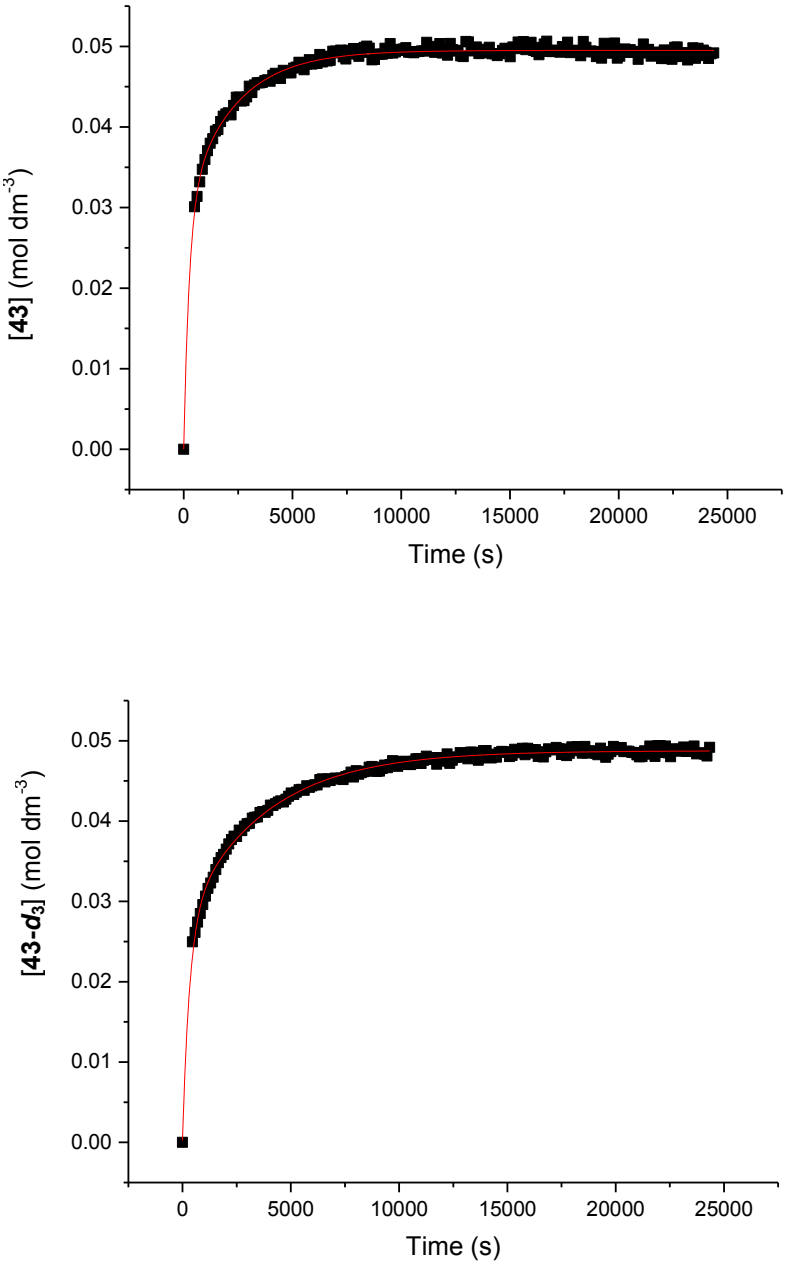
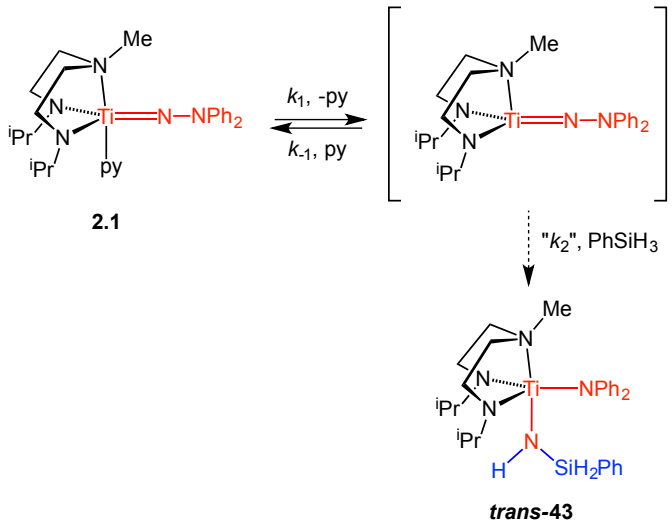


Figure 4.3. Top: plot of [Ti($N_2^{iPr}N^{Me}$){N(H)SiH_2Ph}(NPh_2)] ([**43**]) *vs.* time plotted in Origin. The best-fit line (r^2 = 0.9946) shown gave A_1 = -0.0297(9), B_1 = 257(19), A_2 = -0.0197(7) and B_2 = 2211(76) giving an initial rate of 12.44(5) x 10^{-5} mol dm^{-3} s^{-1}. Bottom: plot of [Ti($N_2^{iPr}N^{Me}$){N(D)SiD_2Ph}(NPh_2)] ([**43-*d*$_3$**]) *vs.* time plotted in Origin. The best-fit line (r^2 = 0.9891) shown gave A_1 = -0.0323(8), B_1 = 371(24), A_2 = -0.0181(7) and B_2 = 3147(113) giving an initial rate of 9.26(3) x 10^{-5} mol dm^{-3} s^{-1}.

An alternative method of measuring the kinetic isotope effect was also carried out. Reaction of **2.1** with an excess of both $PhSiH_3$ and $PhSiD_3$ (1:5:5) allowed calculation of the KIE from the ratio of the two isotopomers **43** and **43-*d*$_3$**. This experiment had to be carried out at -10 ^oC to suppress a silane exchange reaction, which will be discussed later. After 18 hours at -10 ^oC the solution contained approximately 58% **43** and 42% **43-*d*$_3$** as determined from integration of the $Si\underline{H}_2$ resonances against the $C\underline{H}Me_2$ resonances, establishing a KIE of 1.38 in excellent agreement with the initial rates method. Such values are comparable to values found for Si–H addition to Ti=S and Ti=O bonds.[22, 23] Moreover, they are in relatively good agreement with the calculated kinetic isotope effect discussed above. The experimentally observed larger values may suggest that the barrier for pyridine dissociation has been slightly overestimated in calculations.

Experimentally these observations can also be explained by the mechanism and associated rate law detailed in Scheme 4.1 and Equation 4.7. The loss of pyridine forming a reactive pyridine-free intermediate in the first step of the reaction is supported by the DFT analysis and puts this intermediate 17.5 kcal mol^{-1} higher in energy than the starting complex. This is followed by a series of reaction steps, denoted *"k_2"* in Scheme 4.1, including the second rate-limiting step which, from DFT analysis, is proposed to be the hydride transfer step ($\Delta G^{\ddagger}$ = 17.3 kcal mol^{-1}). As no component of the reaction is present in excess the rate law cannot be simplified and both a kinetic isotope effect and inhibition by pyridine are expected.



Scheme 4.1. Experimentally implicated steps in the reaction of **2.1** with $PhSiH_3$.

$$\text{Rate} = \frac{k_1 k_2[\mathbf{2.1}][PhSiH_3]}{k_{-1}[py] + k_2[PhSiH_3]} \qquad (4.7)$$

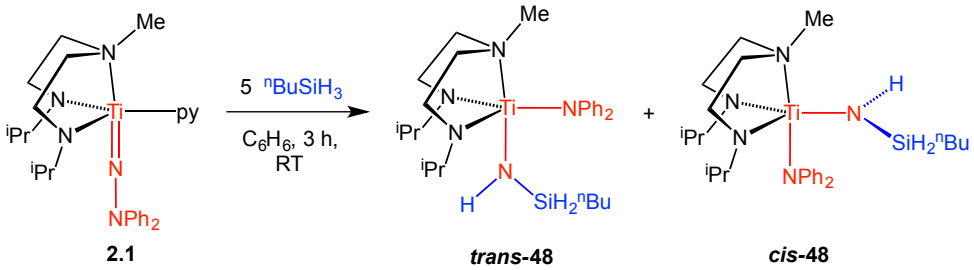
As a further test of Equation 4.7 the DMAP analogue of **2.1** namely $Ti(N_2{}^{iPr}N^{Me})(NNPh_2)(DMAP)$ (**47**) was used instead of **2.1** under otherwise identical reaction conditions. According to Equation 4.7 and Scheme 4.1, the stronger σ donor properties of DMAP compared to pyridine should result in a slower rate of ligand dissociation, k_1, leading to an overall decrease in the rate of reaction. Accordingly the reaction was monitored by ^{1}H NMR spectroscopy and was found to be approximately 100 times slower than with $Ti(N_2N^{Me})(NNPh_2)(py)$ (**2.1**). After *ca.* six hours at room temperature the reaction had reached 30% conversion. In comparison, the reaction of $Ti(N_2{}^{iPr}N^{Me})(NNPh_2)(py)$ (**2.1**) reached 30% conversion in three minutes. However, as was found with an excess of pyridine the reaction did not proceed smoothly, this is proposed to be a consequence of DMAP reacting with intermediates along the reaction pathway and thus prevented further analysis.

This decrease in rate with **47** is supported by calculations, the energy of *cis*-$Ti(N_2{}^{iPr}N^{Me})(NNPh_2)(DMAP)$ (**47**) was calculated to be -1.1 kcal mol^{-1} compared to *cis*-**2.1** at 2.2 kcal mol^{-1} (relative to **Int1** at 19.7 kcal mol^{-1}). Thus, the rate of formation of **43** was calculated to be approximately 90 times slower with the DMAP compound. Overall the experimental results are in good agreement with the DFT

calculations, with both pyridine dissociation and hydride cleavage contributing to the rate.

4.5 Reaction of Ti($N_2^{iPr}N^{Me}$)($NNPh_2$)(py) (2.1) with butylsilane

Initially Ti($N_2^{iPr}N^{Me}$)($NNPh_2$)(py) (**2.1**) reacts with one equivalent of $^{n}BuSiH_3$ in an analogous manner to that above. Resonances attributable to the compound Ti($N_2^{iPr}N^{Me}$){N(H)$SiH_2{}^{n}Bu$}(NPh_2) (**48**) were observed after three hours at room temperature. However, on the NMR tube scale, conversion to **48** did not exceed 70%. This may suggest an equilibrium as was found in the reaction of **1.76** with $^{n}BuSiH_3$. On standing for several days a new set of resonances were observed along with a decrease in intensity of those of **48**. Again the reaction did not reach completion and after several weeks the solution contained a mixture of compounds along with Ph_2NH.

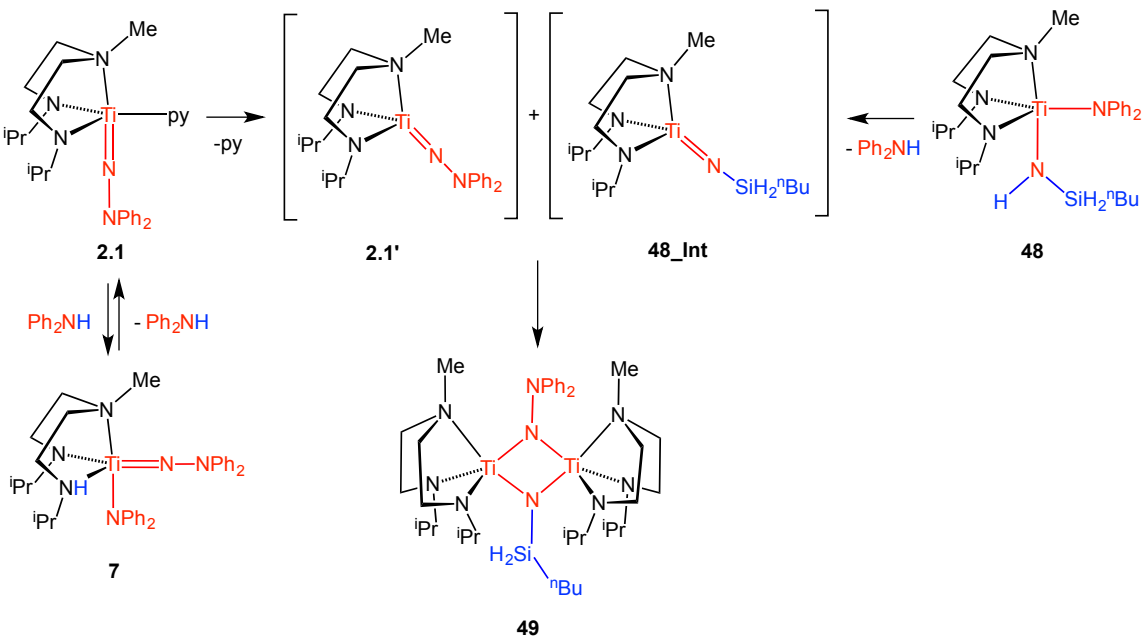


Equation 4.8

The secondary reaction was avoided by using five equivalents of $^{n}BuSiH_3$, converting all of **2.1** and yielding exclusively **48** after three hours at room temperature (Equation 4.8). Following removal of the excess silane under vacuum **48** was fully characterised by NMR and IR spectroscopy and elemental analysis. Compound **48** exists as a 60:40% mixture of *cis* and *trans* isomers as assigned with the aid of a ^{1}H ROESY NMR experiment. Diagnostic NH resonances are observed at 5.69 and 5.97 ppm as broad triplets (*cis* and *trans*). The SiH_2 protons undergo an additional three-bond coupling to the α-^{n}Bu methylene protons and therefore appear as doublet of triplets at 4.71 and 4.99 ppm (*cis* and *trans*). Resonances in the ^{29}Si NMR spectrum are observed at -26.1 and -26.6 ppm for the *cis* and *trans* isomers respectively. The ν(Si–H) band lies at 2092 cm^{-1} and the ν(N–H) band appears at 3317 cm^{-1}, in good agreement with the values obtained for compounds **43** - **46**.

The product of the major side reaction mentioned above was established as the dimeric compound $Ti_2(N_2^{iPr}N^{Me})_2$(μ-$NNPh_2$)(μ-$NSiH_2{}^{n}Bu$) (**49**) following reaction of **48** (made *in situ*) with **2.1** (Scheme 4.2). The reaction was slow and only reached

completion after four weeks at room temperature. During this time the compound $Ti(HN_2^{iPr}N^{Me})(NNPh_2)(NPh_2)$ (**7**), described in Chapter Two, was observed. When the reaction had finished, no **7** remained and one equivalent of Ph_2NH was present. These observations and the formation of **49** can be explained with the aid of Scheme 4.2. Elimination of an equivalent of Ph_2NH from **48** yields the reactive four-coordinate imido species (**48_Int**, not observed) which reacts with **2.1** following liberation of pyridine to yield **49** containing a bridging silylimido and a bridging hydrazido ligand. The formation of **7** accounts for the slow progression of the reaction, liberated Ph_2NH reacts with **2.1** at a rate competitive to dimerisation thus removing **2.1** from the system. Since the formation of **7** is reversible, the thermodynamic product **49** is the sole reaction product after four weeks at room temperature. As established the reactions of **2.1** with silanes are inhibited by the build up of pyridine, this allows for dimerisation to occur competitively towards the end of the reaction accounting for the presence of **49** when just one equivalent of $^{n}BuSiH_3$ is used.



Scheme 4.2. Reaction of $Ti(N_2^{iPr}N^{Me})(NNPh_2)(py)$ (**2.1**) with $Ti(N_2^{iPr}N^{Me})\{N(H)SiH_2{}^{n}Bu\}(NPh_2)$ (**48**).

The reaction was carried out on a preparative scale and the dimer $Ti_2(N_2^{iPr}N^{Me})_2(\mu\text{-}NNPh_2)(\mu\text{-}NSiH_2{}^{n}Bu)$ (**49**) was isolated following crystallisation from the benzene reaction solution as confirmed by X-ray diffraction. The solid-state structure of **49** is shown in Figure 4.4 and selected bond distances and angles in Table 4.2. No reaction

was observed between the phenylsilylamido compound **43** and **2.1** when tested independently possibly due to less facile elimination of Ph_2NH.

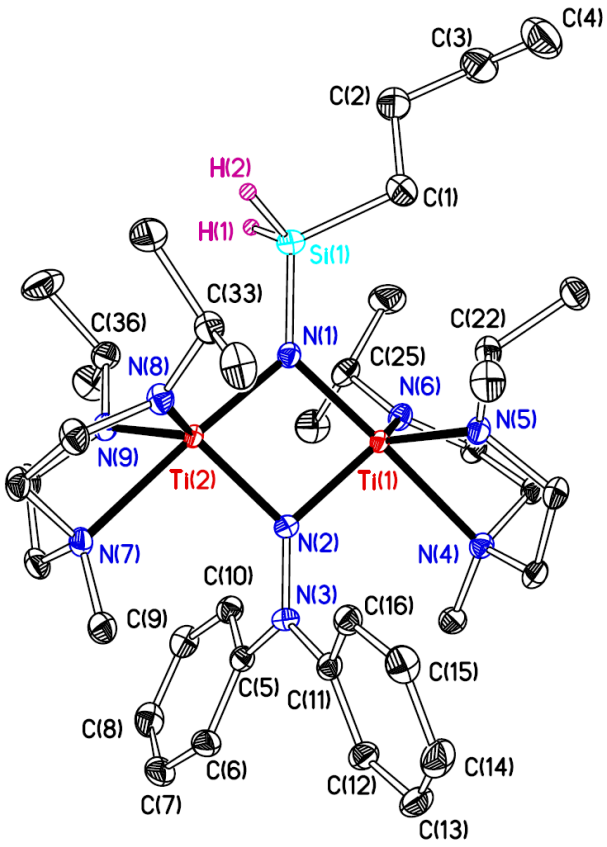


Figure 4.4. Displacement ellipsoid plot (20% probability) of $Ti_2(N_2{}^{iPr}N^{Me})_2(NNPh_2)(NSiH_2{}^{n}Bu)$ (**49**). H atoms are omitted for clarity.

Table 4.2. Selected bond distances (Å) and angles for $Ti_2(N_2^{iPr}N^{Me})_2(NNPh_2)(NSiH_2{}^nBu)$ (**49**).

Ti(1)-N(1)	1.9363(11)	N(1)-Ti(1)-N(2)	83.06(4)
Ti(2)-N(1)	1.9372(11)	N(1)-Ti(2)-N(2)	82.65(5)
Ti(1)-N(2)	1.9655(11)	Ti(1)-N(1)-Ti(2)	98.35(5)
Ti(2)-N(2)	1.9804(11)	Ti(1)-N(2)-Ti(2)	95.94(5)
Ti(1)-N(4)	2.3426(11)	N(2)-Ti(1)-N(5)	114.49(5)
Ti(1)-N(5)	1.9620(11)	N(2)-Ti(1)-N(6)	119.35(5)
Ti(1)-N(6)	1.9792(11)	N(5)-Ti(1)-N(6)	120.52(5)
Ti(2)-N(7)	2.3452(11)	N(1)-Ti(1)-N(4)	175.92(4)
Ti(2)-N(8)	1.9718(11)	N(2)-Ti(2)-N(8)	120.43(5)
Ti(2)-N(9)	1.9647(11)	N(2)-Ti(2)-N(9)	114.91(5)
N(2)-N(3)	1.3958(15)	N(8)-Ti(2)-N(9)	119.10(5)
N(3)-C(5)	1.4055(17)	N(1)-Ti(2)-N(7)	175.83(4)
N(3)-C(11)	1.4093(17)		
N(1)-Si(1)	1.7341(11)		
Si(1)-H(1)	1.38(2)		
Si(1)-H(2)	1.36(2)		
Si(1)-C(1)	1.8769(17)		

Compound **49** contains two five-coordinate titanium centres linked by a μ-$NNPh_2$ ligand and a μ-NSi^nBu ligand with the remainder of each metals coordination sphere comprising of a diamide-amine ligand bound in a κ^3-*fac*-manner. Both titanium atoms have an approximately trigonal bipyramidal geometry with the equatorial nitrogen atoms (N(2), N(5), N(6) and N(2), N(8), N(9)) effectively co-planar and the sum of the angles subtended at Ti(1) and Ti(2) found to be 354.36(9) and 354.44(9) ^{o} respectively. The Ti(1)···Ti(2) distance of 2.931 Å is not unusually short for a binuclear titanium (IV) complex and similar distances have been reported.[35-37] The central Ti_2N_2 ring is planar and has more acute N-Ti-N angles than that at N (83.06(4) and 82.65(5) ^{o} *vs.* 98.35(5) and 95.94(5) ^{o}).

The bridging hydrazide ligand is bound in a symmetrical μ-η^1:η^1 -manner, bridging only through N_α. The Ti(1)-N(2) and Ti(2)-N(2) bond lengths are significantly shorter than the hydrazido ligand found in **2.1** (1.9655(11) and 1.9804(11) Å *vs*. 1.7444(14) Å) due to the bridging nature of the ligand, and are similar to reported values for μ-η^1:η^1 bound hydrazide ligands of titanium.[38, 39] Bridging hydrazido ligands are often bound in a μ-η^1:η^2 manner with addition N_β donation to one of the metal centres, this was not observed here most likely due to steric reasons.[3, 38, 40, 41] The bridging silylimido imido ligand has significantly shorter bonds to titanium (1.9363(11) and 1.9372(11) Å) but are consistent with reported values for Group 4 bridging imido and bridging silylimido ligands.[42, 43] Thus, the central region of the complex is symmetric with trigonal planar bridging nitrogen atoms. The bond lengths to the diamide-amine ligands are within the expected regions and are almost identical on the two sides of the molecule.

The ^{1}H NMR spectrum of **49** is shown in Figure 4.5 and is fully consistent with the solid-state structure. Only one set of resonances are observed for the iso-propyl substituents and four doublets for the methylene protons indicating that the compound contains C_{2v} symmetry in solution. The SiH_2 protons are observed as a triplet at 5.25 ppm with a one-bond correlation ($^1J_{Si\text{-}H}$ = 193 Hz) to a signal at -44.5 ppm in the ^{29}Si NMR spectrum. Two distinct ν(Si-H) bands appear at 2110 and 2082 cm^{-1} in the IR spectrum due to the symmetric and antisymmetric combinations.

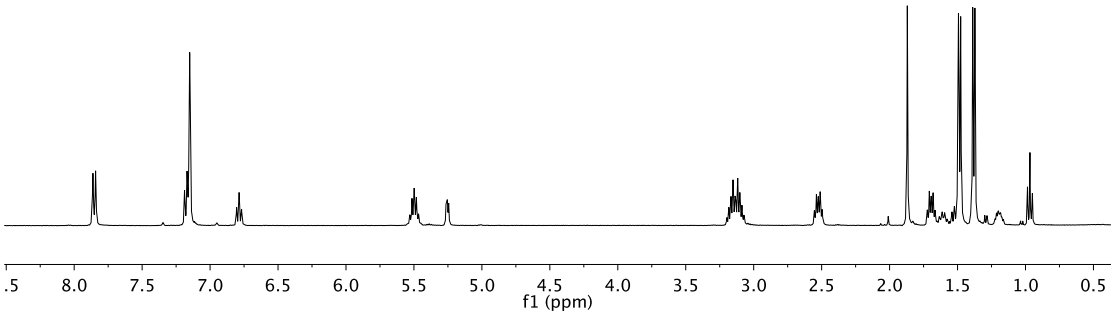
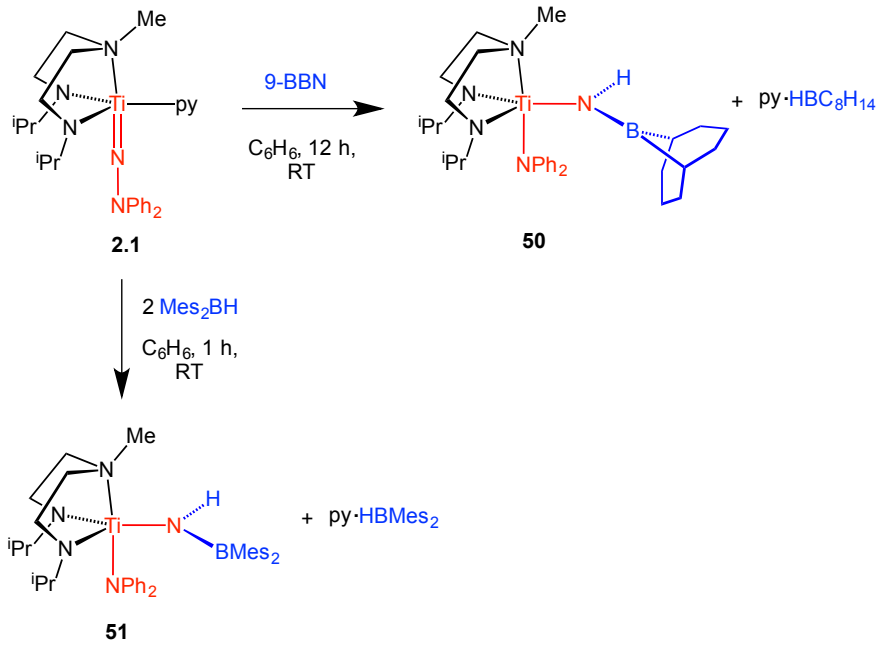


Figure 4.5. ^{1}H NMR spectrum (400.1 MHz) of $Ti_2(N_2^{iPr}N^{Me})_2(NNPh_2)(NSiH_2{}^nBu)$ (**49**) in C_6D_6 at 25 ^oC.

4.6 Reaction of Ti($N_2^{iPr}N^{Me}$)($NNPh_2$)(py) (2.1) with boranes

The unprecedented reactions of **2.1** with silanes prompted us to explore the corresponding reactions with boranes. As shown in Scheme 4.3 reaction of **2.1** with one equivalent of 9-BBN dimer gave clean conversion to the borylamide compound Ti($N_2^{iPr}N^{Me}$){N(H)BC_8H_{14}}(NPh_2) (**50**) together with py·HBC_8H_{14}. In solution **50** exists predominantly as the *cis* isomer (3:1 ratio *cis*/*trans*) illustrated which was characterised by X-ray crystallography. Separation from py·HBC_8H_{14} was achieved on the preparative scale following repeated recrystallisation from benzene leaving **50** as orange crystals. The solid-state structure is shown in Figure 4.6 and selected bond distances and angles in Table 4.3. The ^{1}H and ^{13}C NMR spectra are fully consistent with the solid-state structure and a signal at 54.4 Hz was observed in the ^{11}B{^{1}H} NMR spectrum. In an attempt to identify an intermediate species, the reaction between **2.1** and 9-BBN was followed from -70 ^{o}C to room temperature in toluene-d_8. No intermediates were observed and the emergence of **50** was not observed until room temperature was approached. The analogous reaction with the imido compound Ti($N_2^{iPr}N^{Me}$)(NXyl)(py) (**1**) yielded a mixture of compounds from which only py·HBC_8H_{14} could be identified.



Scheme 4.3. Reaction of Ti($N_2^{iPr}N^{Me}$)($NNPh_2$)(py) (**2.1**) with 9-BBN and $HBMes_2$.

The analogous reaction product Ti($N_2^{iPr}N^{Me}$){N(H)$BMes_2$}(NPh_2) (**51**) along with py·$HBMes_2$ was obtained following reaction with two equivalents of Mes_2BH which

also exists as a mixture of *cis* and *trans* isomers (85:15%). The reaction was complete after just one hour at room temperature and py·$HBMes_2$ was removed by repeating washing with hexane to afford **51** as a red powder. Diffraction-quality crystals were grown from a saturated benzene solution at room temperature and the solid-state structure is shown in Figure 4.6 along with selected bond distances and angles in Table 4.3. Overall, the N_α atom of **2.1** has inserted into the B–H bond of the boranes with concomitant reductive cleavage of the N_α–N_β bond. These reactions are also the first of this type for a single metal centre.

Compounds **50** and **51** both contain a five-coordinate titanium centre with approximately trigonal bipyramidal geometry and the diamide-amine ligands bound in a κ^3-*fac* manner. The borylamide moiety occupies the equatorial position *cis* to the NMe donor and the NPh_2 ligand occupies the remaining coordination site, in both cases. The Ti(1)-N(1) bond distances of 1.9693(15) and 1.9954(18) Å for **50** and **51** are typical of amide(1-) interactions with a longer bond found in **51** due to the large steric bulk of the Mes substituents. Both N(1) atoms have approximately planar geometry with angle subtended about N(1) calculated to be 359.82(26) and 358.14(30) ^{o} respectively. However, the borylamide moiety is significantly twisted out of the equatorial plane, with a N(4)/(5)-Ti(1)-B(1)-H(1) torsion angle of 30.1 and 67.6 ^{o} for **50** and **51** respectively, indicating that the lone pair on N(1) is not well positioned for a π-bonding interaction with titanium. The large steric bulk of the two Mes substituents compared to the bicyclic -C_8H_{14} moiety cause the borylamide moiety to twist further out of the equatorial plane. The N(1)-B(1) bond distances of 1.405(3) and 1.409(3) Å for **50** and **51** are typical of species of the type R_2N–BR'_2 which have significant N=B double bond character *via* $N_{2p}\rightarrow B_{2p}$ π donation.[44]

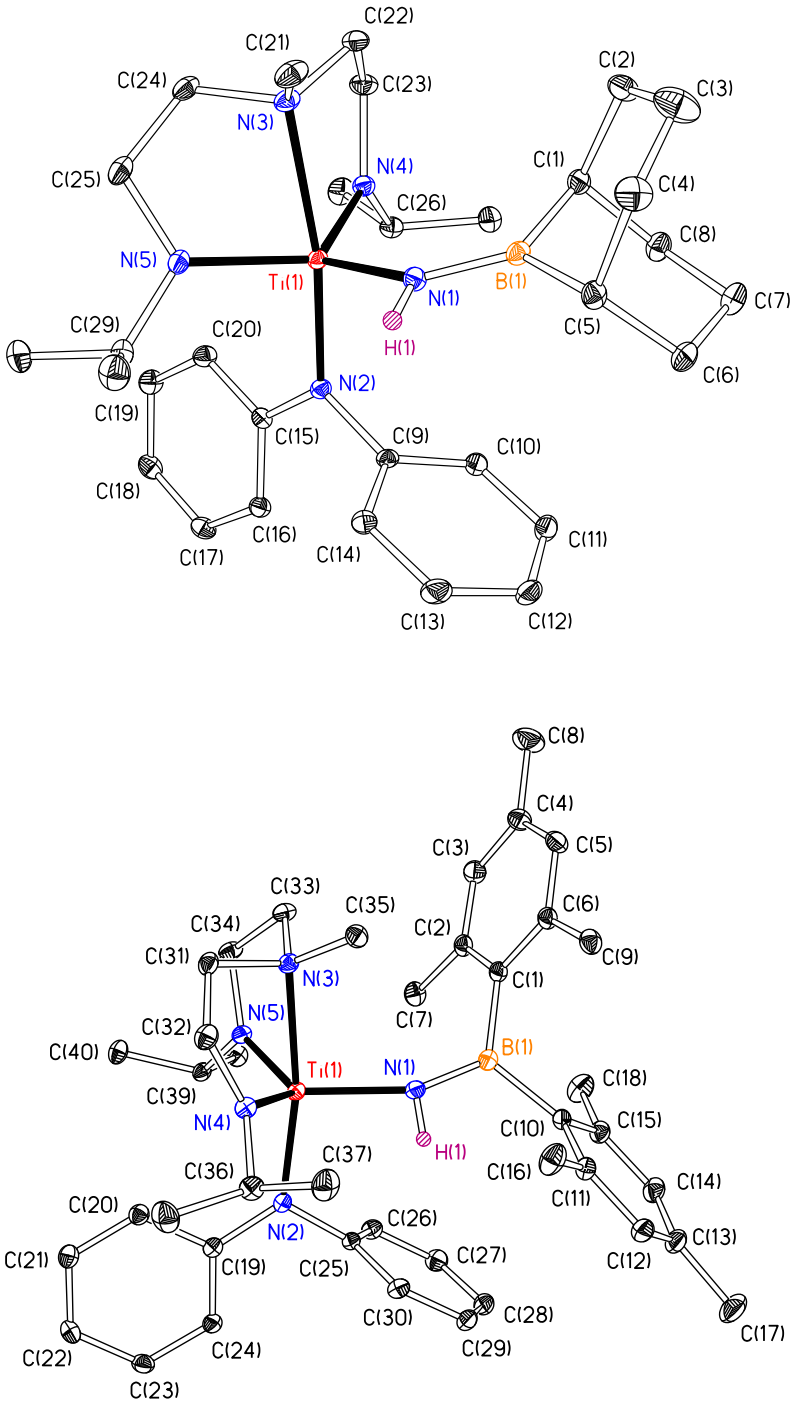


Figure 4.6. Displacement ellipsoid plots (20% probability) of $Ti(N_2^{iPr}N^{Me})\{N(H)BC_8H_{14}\}(NPh_2)$ (**50**) (top) and $Ti(N_2^{iPr}N^{Me})\{N(H)BMes_2\}(NPh_2)$ (**51**) (bottom). Carbon-bound H atoms are omitted for clarity.

Table 4.3. Selected bond distances (Å) and angles (°) for $Ti(N_2^{iPr}N^{Me})\{N(H)BC_8H_{14}\}(NPh_2)$ (**50**) and $Ti(N_2^{iPr}N^{Me})\{N(H)BC_8H_{14}\}(NPh_2)$ (**51**).

Parameter	**50**	**51**
Ti(1)-N(1)	1.9693(15)	1.9954(18)
Ti(1)-N(2)	1.9979(15)	2.0124(18)
Ti(1)-N(3)	2.2767(16)	2.2664(18)
Ti(1)-N(4)	1.9446(16)	1.9457(17)
Ti(1)-N(5)	1.9525(16)	1.9436(17)
N(1)-B(1)	1.405(3)	1.409(3)
N(1)-H(1)	0.92(3)	0.86(3)
N(1)-Ti(1)-N(4)	115.03(7)	114.79(8)
N(1)-Ti(1)-N(5)	114.66(7)	118.54(8)
N(4)-Ti(1)-N(5)	123.20(7)	120.37(7)
N(2)-Ti(1)-N(3)	169.28(6)	169.42(7)
Ti(1)-N(1)-B(1)	136.42(14)	154.34(16)
Ti(1)-N(1)-H(1)	114.5(16)	97.9(18)
B(1)-N(1)-H(1)	108.9(16)	105.9(18)
N(4)/(5)-Ti(1)-B(1)-H(1)	30.12	67.65

4.7 Mechanism of the reaction of $Ti(N_2^{iPr}N^{Me})(NNPh_2)(py)$ (2.1) with 9-BBN

DFT calculations indicate an analogous mechanism to that for $PhSiH_3$. The full pathway from the *cis* isomer of **2.1** with 9-BBN monomer is shown in Figure 4.7. Again dissociation of pyridine is followed by the formation of an adduct (**Int2_B**), prior to 1,2-B–H addition. The increased acceptor ability of boron compared to silicon results in a stronger adduct. This is evident from the short B–N distance of 1.586 Å which is similar in value to the calculated B–N distance in the final product (1.414 Å), a significant lengthening of the $Ti{=}N_\alpha$ bond from 1.729 to 1.843 Å and a decrease in the $Ti{=}N{-}NPh_2$ angle from 165.8 to 151.8 °. Thus, as expected **Int2_B** is lower in energy than the silicon adduct **Int2**. Similarly, the intermediate resulting from B–H addition (**Int3_B**) is lower in energy than the corresponding silicon intermediate (**Int3**) although the barrier is slightly higher (5.9 *vs.* 2.8 kcal mol^{-1}). This is consistent

with a stronger B–H (than Si–H) bond requiring more energy to break.[45] The lower energy of **Int3_B** is likely due to the formation of a strong B–N bond. The final hydride transfer step to yield **50** has an associated barrier of 20.3 kcal mol^{-1} making this the rate-limiting step in the reaction sequence. The low energy of **Int3_B** and high barrier to form **50** suggest that **Int3_B** should be experimentally observed. As this is not the case this may suggest that the barrier has been overestimated. Both dissociation of 9-BBN dimer and reaction of the second equivalent of 9-BBN monomer with pyridine have not been included in the calculations. The free energies were found to be 20.1 and -9.8 kcal mol^{-1} respectively and this will be returned to later. The bond lengths and angles in the DFT structure of **50** are in good agreement with the real values.

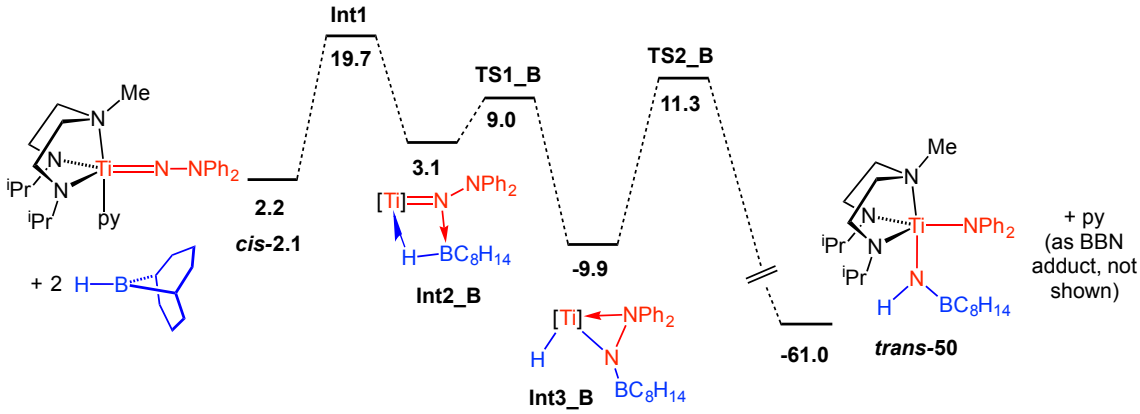


Figure 4.7. DFT mechanism for the reaction of **2.1** with 9-BBN monomer forming **50** and pyridine. Gibbs free energies (kcal mol^{-1}, T = 298 K) for minima, maxima and transition states (labelled **TSx_B**) are shown in bold relative to **2.1** and 9-BBN monomer. [Ti] represents Ti($N_2^{iPr}N^{Me}$). ΔG for adduct formation has been excluded.

The reaction of Ti($N_2^{iPr}N^{Me}$)($NNPh_2$)(py) (**2.1**) and 9-BBN dimer (1:1 ratio) in C_6D_6 at room temperature was monitored by ^{1}H NMR spectroscopy and the evolution of Ti($N_2^{iPr}N^{Me}$){N(H)BC_8H_{14}}(NPh_2) (**43**) measured by integration over a period of time. At the end of the reaction some loss of Ti was observed, evident from the relative intensities of the *o*-pyridine resonance of py·HBC_8H_{14} and methine resonances of **50**. The initial rates methods was therefore used to effectively calculate the rate, d[**50**]/d*t* at time = 0, t_0. The graph of [**50**] *vs.* time for the stoichiometric reaction at 298 K gave a non-linear plot (Figure A2, Appendix). The equation of the

curve takes the form as given in Equation 4.9, differentiation of the curve, as detailed in Equation 4.10, gives the rate of reaction (1.28(3) x 10^{-5} mol dm^{-3} s^{-1}) at t_0. As expected, due to the larger barrier, this is approximately ten times slower than the reaction with $PhSiH_3$. The reaction was found to be zero-order in **2.1** with an initial rate of 1.09(1) x 10^{-5} mol dm^{-3} s^{-1} obtained when two equivalents of **2.1** were used. Interestingly, when the reaction was monitored with the DMAP analogue of **2.1** (**47**) only a marginal decrease in the initial rate was observed (1.02(1) x 10^{-5} mol dm^{-3} s^{-1}) suggesting a rate-determining step after (or before) formation of the base-free intermediate.

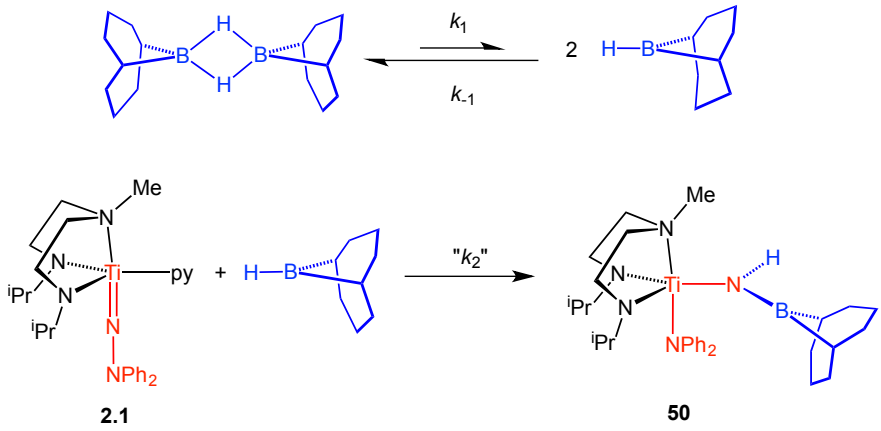
$$[\mathbf{50}] = y_0 + A_1 e^{-t/B_1} \tag{4.9}$$

$$\frac{d[\mathbf{50}]}{dt} = - \frac{A_1 e^{-t/B_1}}{B_1} \qquad \left(\frac{d[\mathbf{50}]}{dt}\right)_{t=0} = - \frac{A_1}{B_1} \tag{4.10}$$

The DFT mechanism described above was calculated for the reaction of **2.1** with 9-BBN monomer. However, 9-BBN exists exclusively as a dimer in non-donor solvents according to kinetic studies on the hydroboration of alkenes with 9-BBN.[46] Dissociation of 9-BBN dimer has been reported to proceed with a rate constant of 1.5 x 10^{-4} s^{-1} and with an estimated barrier of 22.6 kcal mol^{-1}, in benzene at room temperature.[46-48] Attempts to locate the transition state for 9-BBN dimer dissociation using DFT were unsuccessful. However, as mentioned the Gibbs free energy of reaction was calculated to be 20.1 kcal mol^{-1}.

By artificially adding an additional barrier of 22.6 kcal mol^{-1} (to the DFT mechanism) prior to reaction of **Int1** with 9-BBN monomer, to account for 9-BBN dimer dissociation, the effect on the overall mechanism can be considered. Dissociation of 9-BBN dimer would contribute 91% to the overall rate, with the hydride transfer from **Int3_B** to ***trans*-50** making up the remaining 9%. This is in contrast to the reaction of **2.1** with 9-BBN monomer in which formation of ***trans*-50** from **Int3_B** is solely rate-limiting. The reported barrier for 9-BBN dissociation of 22.6 kcal mol^{-1} is close in value to the highest calculated barrier of 20.3 kcal mol^{-1} for the reaction of **2.1** with 9-BBN monomer. Both values are likely to have associated errors and therefore based on this information, the rate-limiting step cannot be distinguished.

Kinetic treatment has been applied extensively to the hydroboration of alkenes with 9-BBN.[46] It has been established that the reaction proceeds through prior dissociation of 9-BBN dimer into the monomer, followed by reaction of the monomer with the alkenes.[46, 47, 49, 50] This is in contrast to earlier studies with disiamylborane, $(Sia_2BH)_2$ where direct reaction of $(Sia_2BH)_2$ with alkenes was proposed.[51] Under such kinetic regime there are two limiting cases. Hydroboration with reactive alkenes demonstrate a first-order dependence on 9-BBN dimer due to rate-limiting dimer dissociation. In comparison, hydroboration with unreactive alkenes demonstrate a half-order dependence on 9-BBN due to a rate limiting B–H addition. The same kinetic treatment can be applied here and is outlined in Scheme 4.4 and Equations 4.11 - 4.13. The full derivation of Equations 4.11 – 4.13 is shown in the Appendix.



Scheme 4.4. Dissociation of 9-BBN dimer to 9-BBN monomer followed by reaction with $Ti(N_2^{iPr}N^{Me})(NNPh_2)(py)$ (**2.1**).

$$\text{Rate} = \frac{k_1 k_2[\mathbf{2.1}][\text{9-BBN dimer}]}{k_{-1}[\text{9-BBN}] + k_2[\mathbf{2.1}]} \qquad (4.11)$$

$$\text{Rate} = k_1[\text{9-BBN dimer}] \quad (\text{if } k_{-1}[\text{9-BBN}] << k_2[\mathbf{2.1}]) \qquad (4.12)$$

$$\text{Rate} = \left[\frac{k_1}{k_{-1}}\right]^{1/2} k_2[\mathbf{2.1}][\text{9-BBN dimer}]^{1/2} \quad (\text{if } k_{-1}[\text{9-BBN}] >> k_2[\mathbf{2.1}]) \qquad (4.13)$$

The rate constant "k_2" is used to denote all the reaction steps in the reaction of **2.1** with 9-BBN monomer. It is known from the DFT calculations that the final step within this is much higher in energy than the other steps therefore, k_2 essentially refers

to the hydride transfer step. Note that the reaction of the 'other' equivalent of 9-BBN monomer, with displaced pyridine is assumed to be fast and non-rate-limiting.

Applying a steady-state approximation to 9-BBN monomer leads to the rate equation shown in Equation 4.11. The approximation k_{-1}[9-BBN] << k_2[**2.1**] can be applied when the k_2 step is fast, in hydroboration kinetics this is the case with reactive alkenes. This leads to the rate equation shown in Equation 4.12 and the rate will show a first-order dependence on 9-BBN dimer. Alternatively, if the k_2 step is slower than 9-BBN dimer dissociation, the rate equation can be written as shown in Equation 4.13. The rate of reaction will show a half-order dependence on 9-BBN dimer and a first-order dependence on **2.1**. Therefore, by establishing the dependence of the rate on 9-BBN dimer concentration, at constant Ti concentration, it should be possible to determine whether 9-BBN dimer dissociation or hydride transfer, is rate-limiting.

As mentioned a zero-order dependence on **2.1** was observed, which suggests that Equation 4.12 is applicable here. When the reaction between **2.1** and 9-BBN dimer (1 - 4 equivalents, 0.05 - 0.20 mol dm^{-3}, Figure A2, Appendix) was monitored at 298 K in C_6D_6 the evolution of **50** followed a similar behaviour as detailed above and therefore initial rates in each case were obtained using the initial rates method (initial rate = 2.9(1) x 10^{-5}, 5.7(2) x 10^{-5} and 7.1(4) x 10^{-5} mol dm^{-3} s^{-1} for two, three and four equivalents of 9-BBN dimer respectively). As shown in Figure 4.8, the initial rates scale linearly with $[\text{9-BBN dimer}]_0$ (top plot) consistent with Equation 4.12. This allows the rate constant k_1 = 3.5(2) x 10^{-4} s^{-1} to be extracted from the gradient, which corresponds to a free energy of activation of 22.2 kcal mol^{-1}. Importantly the initial rates do not scale linearly with $[\text{9-BBN dimer}]_0^{0.5}$ (middle plot) and thus Equation 4.13 does not apply.

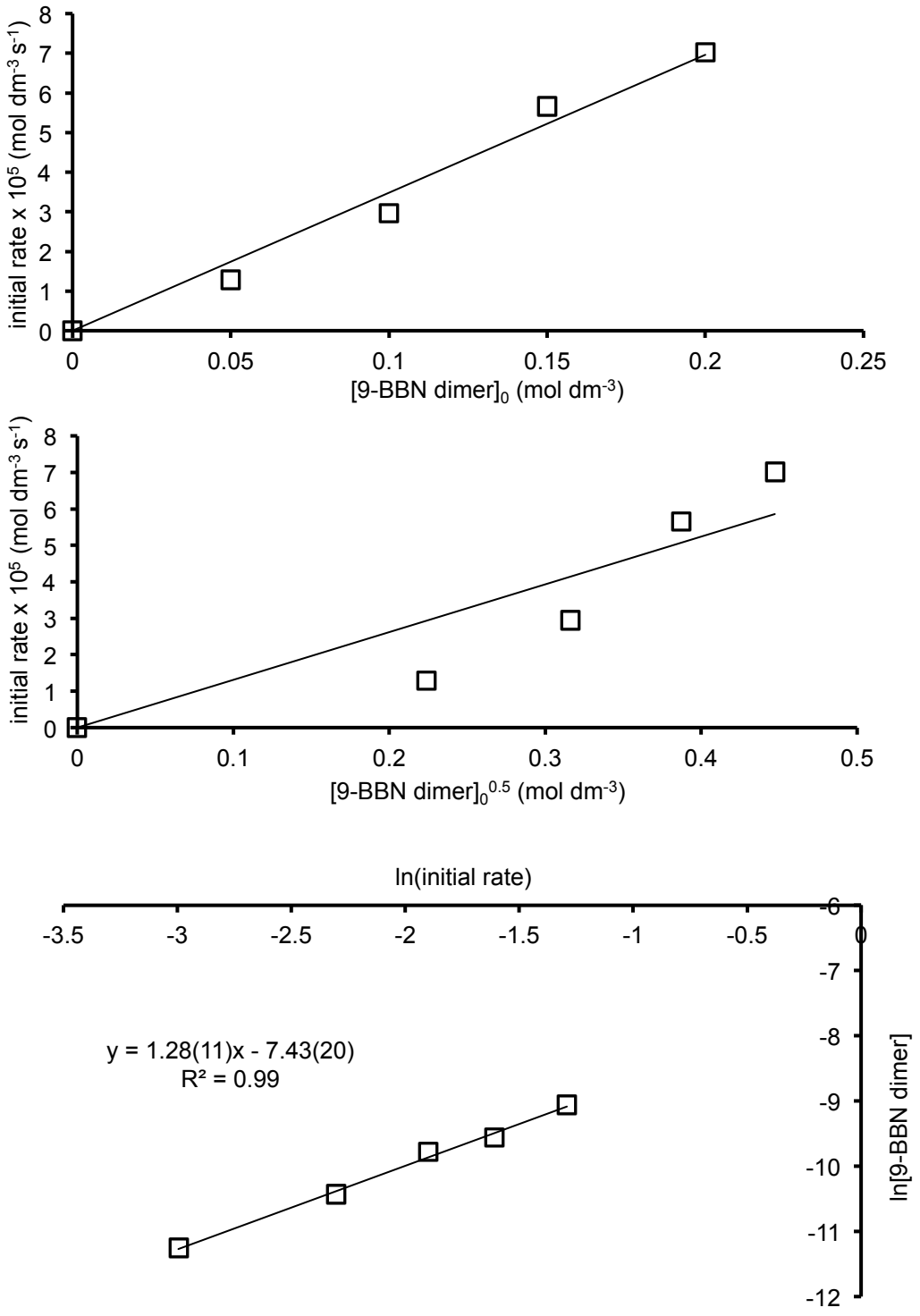


Figure 4.8. Top: plot of initial rate *vs*. $[9\text{-BBN dimer}]_0$ for the reaction of $Ti(N_2^{iPr}N^{Me})(NNPh_2)(py)$ (**2.1**) with 9-BBN dimer, $r^2 = 0.9804$. Middle: plot of initial rate *vs*. $[9\text{-BBN dimer}]_0^{0.5}$ for the reaction of $Ti(N_2^{iPr}N^{Me})(NNPh_2)(py)$ (**2.1**) with 9-BBN dimer, $r^2 = 0.8318$. $[Ti]_0 = 0.05$ mol dm^{-3}. Bottom: logarithmic plot of ln(initial rate) *vs*. ln[9-BBN dimer].

In order to obtain the exact order of the dependence on 9-BBN dimer concentration the logarithmic plot shown in Figure 4.8 was used (bottom plot). Both Equations 4.12 and 4.13 can be written in the general form shown in Equation 4.14 at constant Ti concentration. Therefore, the order of the reaction in 9-BBN dimer can be obtained from the gradient of the logarithmic plot (Equation 4.15).

$$\text{initial rate} = k_{obs}[\text{9-BBN dimer}]^n \tag{4.14}$$

$$\ln(\text{initial rate}) = n \ln([\text{9-BBN dimer}]) + \ln(k_{obs}) \tag{4.15}$$

As can be seen in Figure 4.8 the gradient is 1.28(11), this is closer to one than a half, also indicating a first-order dependence on 9-BBN dimer due to rate-limiting 9-BBN dimer dissociation, consistent with Equation 4.12. From the intercept, k_1 was calculated to be 5.9(7) x 10^{-4} s^{-1}, which corresponds to a free energy of activation of 21.8(1) kcal mol^{-1} (calculated using the Eyring equation).

According to Equation 4.12 the decay of 9-BBN dimer over time should follow first-order kinetics. However, due to broad overlapping resonances in the ^{1}H NMR spectrum it was not possible to obtain an accurate integration of 9-BBN dimer over the course of the reaction. As soon as 9-BBN monomer is formed it will react immediately with **2.1**, therefore the decay of **2.1** should also follow the same first-order kinetics (although this does not mean a first-order relationship between **2.1** and the rate). As expected the reaction of **2.1** with one equivalent of 9-BBN dimer shows first-order kinetics as judged by a semi-logarithmic plot of $\ln([\mathbf{2.1}]_t/[\mathbf{2.1}]_0)$ *vs.* time. From this plot k_1 was found to be 2.28(3) x 10^{-4} s^{-1}, which corresponds to a free energy of activation of 22.4(1) kcal mol^{-1}. It is also possible to estimate k_1 values from the initial rates at varying 9-BBN dimer equivalents. These were found to be in the range 2.6 - 3.7 x 10^{-4} s^{-1}.

Therefore, based on the above kinetics analysis the reaction of **2.1** with 9-BBN proceeds *via* rate-limiting 9-BBN dimer dissociation followed by facile reaction of 9-BBN monomer with base-free **2.1**. This is evident from the observed first-order dependence on the rate on 9-BBN dimer. The rate constant for 9-BBN dimer dissociation (k_1) can be estimated to be between 2.3 and 5.9 x 10^{-4} s^{-1}, which corresponds to a free energy of activation of 21.8(1) - 22.4(1) kcal mol^{-1}. These values are in excellent agreement with the values reported in the literature (k_1 = 1.5 x 10^{-4} s^{-1}

and $\Delta G^{\ddagger}$ = 22.6 kcal mol^{-1}) and crucially are higher in energy than the calculated barrier for hydride transfer.

As mentioned above, the reaction of **2.1** with Mes_2BH proceeds more quickly than with 9-BBN, reaching 100% conversion after one hour. Mes_2BH is a dimer in the solid state but exists as an equilibrium mixture of monomer and dimer in a benzene solution. This is consistent with a fast reaction of **2.1** with monomer boranes. A kinetic or DFT analysis of this reaction has not been carried out.

The reductive transformation of a terminal (L)M=NNR_2 functional group to the corresponding silylamido and borylamido ligands described here and in Section 4.3 are unprecedented. In this context, it is important to note the recent reports of the Si–H and B–H bond addition to the terminal N atom of the vanadium(+5) nitride (DippNacNac)V(N)($NTol_2$) forming V(+3) silyl- and borylamido products with net two-electron reduction of the metal.[52] These reactions (like their iridium[53] (Si–H) and osmium[54] (B–Ph) nitride addition precedents) are mechanistically distinct from those reported here which involve N–N bond cleavage with overall one-electron reduction of the hydrazide $N_{\alpha,\beta}$ atoms as opposed to the metal centre.

4.8 Reaction of Ti($N_2^{iPr}N^{Me}$)($NNPh_2$)(py) (2.1) with H_2

The 1,2-addition of dihydrogen to metal-ligand multiple bonds has been reported for several Group 4 complexes.[23, 55, 56] Unfortunately no reaction was observed between Ti($N_2^{iPr}N^{Me}$)($NNPh_2$)(py) (**2.1**) and H_2 under 2-3 atm. The DFT mechanism was nevertheless calculated and is shown in Figure 4.9.

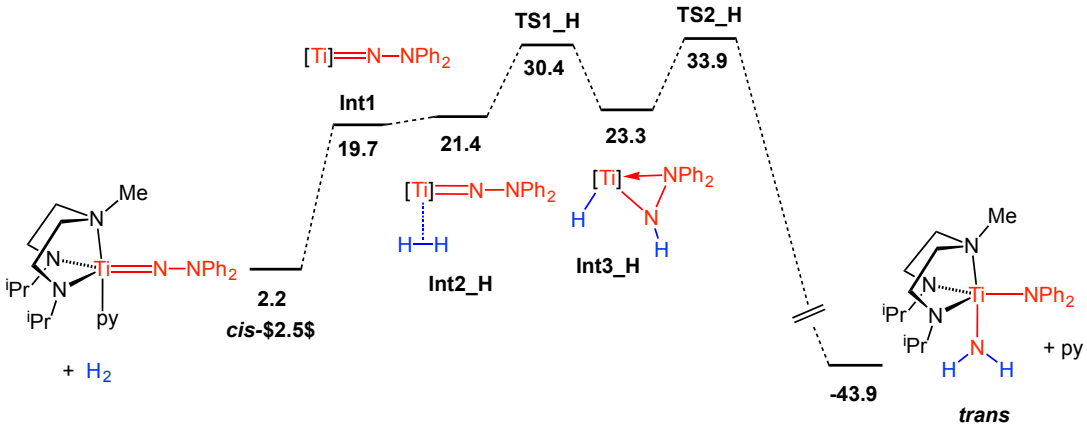
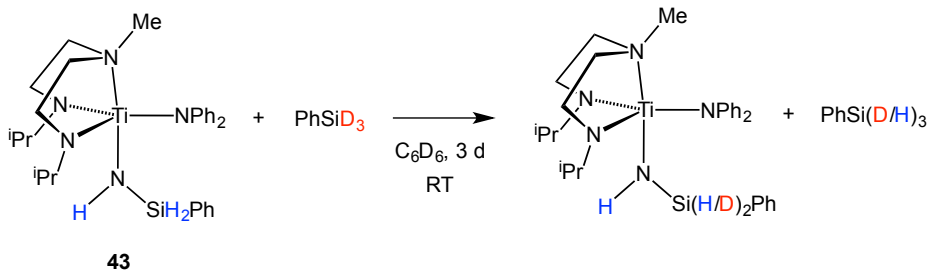


Figure 4.9. DFT mechanism for the reaction of **2.1** with H_2. Gibbs free energies (kcal mol^{-1}, T = 298 K) for minima, maxima and transition states (labelled **TSx_H**) are shown in bold relative to **2.1** and H_2. [Ti] represents Ti($N_2^{iPr}N^{Me}$).

The final products are low in energy indicating that the reaction is thermodynamically feasible. Following formation of the pyridine free species **Int1** the formation of the adduct **Int2_H** is slightly uphill. The relative G of **Int2_H** is higher in energy than the analogous intermediates found with $PhSiH_3$ and 9-BBN. This is attributed to the lack of acceptor ability of H_2, resulting in reduced stabilisation. The 1,2-addition step is also uphill as the formation of one N–H bond and one Ti–H bond is not enough to compensate for the energy required to break the very strong H–H bond. As the intermediates are high in energy the corresponding transition states are also high in energy leading to a kinetically inaccessible reaction pathway. These observations are in line with what has been reported for the hydrazido compound Cp*Ti{$MeC(N^iPr)_2$}($NNMe_2$) (**1.76**), which also showed no reactivity with H_2.

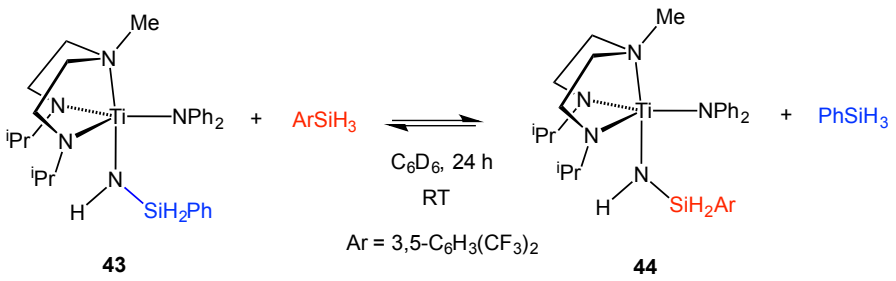
4.9 Reaction of $Ti(N_2^{iPr}N^{Me})\{N(H)SiH_2Ph\}(NPh_2)$ (43) with silanes

Interestingly, reaction of $Ti(N_2^{iPr}N^{Me})\{N(H)SiH_2Ph\}(NPh_2)$ (**43**) with one equivalent of $PhSiD_3$ led to slow incorporation of deuterium into the Si–H sites exclusively. Similarly a multiplet at 4.21 ppm in the ^1H NMR spectrum indicated the presence of hydrogen in free phenylsilane (Equation 4.16). After 24 hours at room temperature there was *ca.* 30% incorporation of D into **43** as judged by integration. On standing for a further two days the SiH_2 resonance of **43** decreased further and a statistical distribution of H and D across the Si–H sites of free silane and **43** was reached. At first sight this appears to suggest reversible formation of **43**. However, during this time no deuterium was incorporated into the N–H site of **43** as established by ^1H and ^2H NMR spectroscopy. To confirm the formation of **43** from **2.1** is irreversible, **43** was mixed with two equivalents of HCC-4-C_6H_4Me which would react immediately with any **2.1**. No reaction occurred at room temperature or on heating at 70 ^oC indicating that the formation of **43** is irreversible



Equation 4.16

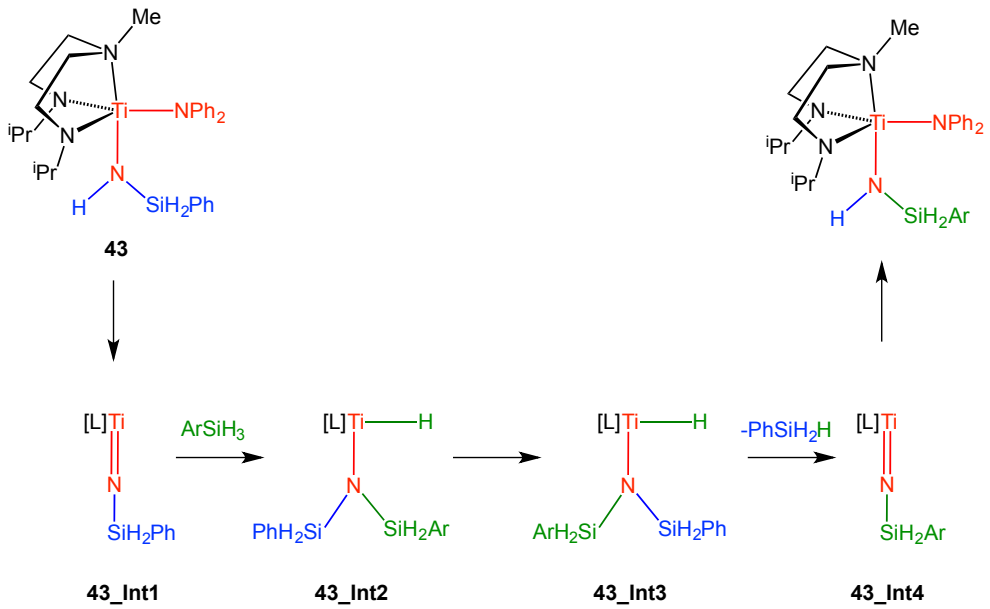
As a control, $PhSiD_3$ and $PhSiH_3$ were mixed in C_6D_6 and left to stand for several days at room temperature. During this time no exchange of the Si–H and Si–D sites occurred. It is therefore unlikely that direct Si–H/D exchange between the on-metal Si–H bonds and off-metal Si–D bonds could account for the above observation. As the substituent on the Si atom in **43** and free silane is the same (Ph), it is not possible to establish from the above experiment whether exchange of the whole SiH_2Ph group is occurring rather than just Si–H/D exchange.



Equation 4.17

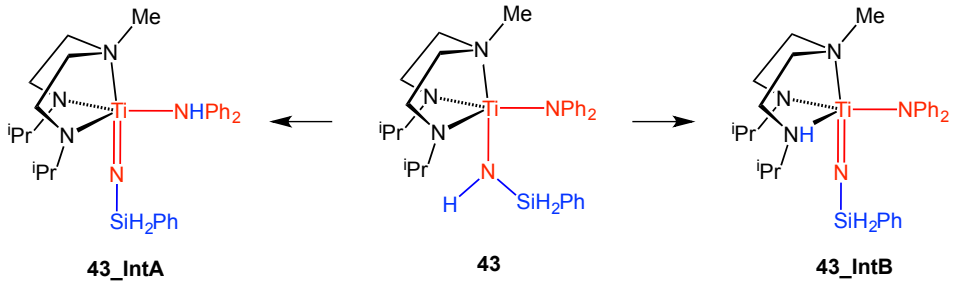
Addition of 3,5-$C_6H_3(CF_3)_2SiH_3$ (one equivalent) to a solution of **43** formed an equilibrium mixture of **44** and **43** (80:20%) after 24 hours at room temperature (Equation 4.17). Addition of further equivalents of 3,5-$C_6H_3(CF_3)_2SiH_3$ gives complete conversion to **44** and $PhSiH_3$. Each compound exists as two isomers in the same ratio as their independent synthesis consistent with facile *cis*/*trans* isomerisation. The analogous reaction occurs with 4-$C_6H_4(OMe)SiH_3$ and Ph_2SiH_2 both reaching equilibrium mixtures of 55:45% (**43**:**45**) and 80:20% (**43**:**46**) respectively after six days at room temperature. Therefore, the reaction of **43** with silanes can result in exchange of the SiH_2Ph amide substituent whilst leaving the remainder of the compound unchanged. This also accounts for the H/D exchange reaction shown in Equation 4.16.

The proposed mechanism for this exchange reaction is shown in Scheme 4.5. Following formation of an imido intermediate **43_Int1** from **43** (*vide infra*), 1,2-addition of Si–H to the Ti=N bond to yield the bis(silyl)amide-hydride species **43_Int2** can occur. Rotation about the Ti–N bond places the original silyl substituent (labelled blue) close to the Ti–H bond (**43_Int3**), subsequent 1,2-elimination reforms an imido intermediate now with the new silylamide substituent (labelled green, **43_Int4**). No intermediates were observed during the course of any of the exchange reactions.



Scheme 4.5. Proposed mechanism for the reaction of $Ti(N_2^{iPr}N^{Me})\{N(H)SiH_2Ph\}(NPh_2)$ (**43**) with silanes.

The formation of an imido intermediate of the type **43_Int1** from **43** could occur in two ways. Transfer of the Ti–N(H)SiH_2Ph proton to the –NPh_2 ligand would yield **43_IntA** shown in Scheme 4.6. Alternatively, transfer of the Ti–N(H)SiH_2Ph proton to one of the Ti–N_{amide} atoms of the supporting ligand would yield **43_IntB**. Both intermediates contain an imido ligand capable of reacting in the manner described above. Neither **43_IntA** or **43_IntB** were observed experimentally.



Scheme 4.6. Two possible mechanisms for the formation of an imido intermediate from **43**.

The reaction of $Ti(N_2^{iPr}N^{Me})(NHXyl)(NPh_2)$ (**6**) with 2,2'-bipyrdine, described in Chapter Two, led to the elimination of Ph_2NH and formation of an imido bond. Addition of 2,2'-bipyrdine to **43** gave no reaction, suggesting transfer of the Ti–N(H)SiH_2Ph proton to the NPh_2 ligand to form **43_IntA** is unlikely.

Compound **43** was mixed with an equivalent of Tol_2NH on the NMR tube scale as a probe for the formation of **43_IntA** from **43**. If **43_IntA** is readily accessible then exchange between the weakly bound neutral ligand -$NHPh_2$ and the sterically and electronically similar Tol_2NH would occur. For example, addition of an equivalent of pyridine-d_5 to the imido compound Ti($N_2^{iPr}N^{Me}$)(NXyl)(py) (**1**) results in immediate scrambling of pyridine and pyridine-d_5 over the bound and free sites. However, no reaction occurred at room temperature over 24 hours. On heating at 70 ^oC for two hours a new set of resonances where observed along with Ph_2NH, heating for a further 22 hours did not increase the conversion and the two species were present in a 1:1 ratio. The new species exists as a mixture of two isomers and has been tentatively assigned as Ti($N_2^{iPr}N^{Me}$){N(H)SiH_2Ph}($NTol_2$) (**52**) containing the $NTol_2$ ligand. The observation of **52** may indicate that **43_IntA** is accessible at high temperature. However, it is equally likely that **52** is the result of direct exchange between Ti–NPh_2 with Tol_2NH in a similar manner to many protonolysis reactions.

Importantly, when the reaction of **43** with 3,5-$C_6H_3(CF_3)_2SiH_3$ was carried out in the presence of an equivalent of Tol_2NH no incorporation of $NTol_2$ into either **43** or **44** was observed. Taking these observations together, the reaction of **43** with silanes is unlikely to proceed *via* **43_IntA** and is thought to instead undergo transfer of the Ti–N(H)SiH_2Ph proton to one of the Ti–N_{amide} atoms to yield **43_IntB**. The reactivity of Ti($N_2^{iPr}N^{Me}$)($NNPh_2$)(py) (**2.1**) and Ti($N_2^{iPr}N^{Me}$)(NXyl)(py) (**1**) described in Chapter Two and Three has centred around the ability of the N_{amide} atoms of the supporting ligand to accept a proton, often resulting in unexpected reactivity products. Thus far in the reactions of **2.1** with silanes and boranes this phenomenon has not be observed, most likely as the reactive element hydrogen bonds are hydridic. Therefore, transfer of this acidic proton to the supporting ligand is in line with much of what has been previously described.

When the reaction between **43** and an excess of 3,5-$C_6H_3(CF_3)_2SiH_3$ (10 or 20 equivalents) was followed at 25 ^oC in C_6D_6 the decay of **43** followed well-behaved pseudo first-order kinetics with respect to Ti as illustrated in Figure 4.10. No change in the observed rate constant, obtained from linear logarithmic plots, was observed when using 20 equivalents (12.7(1) x 10^{-5} s^{-1} *vs.* 12.5(1) x 10^{-5} s^{-1} for 10 equivalents) of silane indicating that under these conditions the rate is independent of silane concentration. The analogous reaction of **43-*d*$_3$** was followed and the observed rate

constant of 2.24(1) x 10^{-5} s^{-1} was obtained. This gives a kinetic isotope effect of 5.6(1) consistent with rate-limiting hydrogen transfer to form the imido intermediate **43_IntB**. Several examples of kinetic isotope effects of this magnitude due to N–H abstraction to yield an imido intermediate have been reported,[57, 58] often as part of a catalytic cycle.[59, 60] For example, Sadow and co-workers found a KIE of 5.4 for the hydroamination of aminoalkenes with a zirconium catalyst due to turnover limiting α-abstraction to form an imido intermediate.[61]

In an attempt to isolate the KIE due to N–H transfer and confirm that Si–H bond breaking/forming does not contribute to the rate determining step, the partially labelled N–D compound Ti($N_2^{iPr}N^{Me}$){N(D)SiH_2Ph}(NPh_2) (**43-*d*$_1$**) was targeted. As mentioned, the reaction of Ti($N_2^{iPr}N^{Me}$){N(H)SiH_2Ph}(NPh_2) (**43**) with $PhSiD_3$ yielded a statistical distribution of H and D across both Si positions. As expected reaction of Ti($N_2^{iPr}N^{Me}$){N(D)SiD_2Ph}(NPh_2) (**43-*d*$_3$**) with one equivalent of $PhSiH_3$ results in approximately 50% incorporation of hydrogen into the Si positions. Attempts to increase the hydrogen incorporation by using extra equivalents of $PhSiH_3$ or leaving for a longer period of time were unsuccessful and resulted in gradual decomposition of the compound. Thus, following removal of the free silane under vacuum the reaction of **43** containing exclusively deuterium in the N position and approximately 1:1 ratio of H and D in the Si position (this refers to a mixture of SiH_2, SiHD and SiD_2 compounds which could not be distinguished) with an excess of 3,5-$C_6H_3(CF_3)_2SiH_3$ (10 equivalents) was followed and the observed rate constant extracted. The rate constant of 2.30(1) x 10^{-5} s^{-1} was obtained and is comparable to that found with **43-*d*$_3$**, consistent with rate-limiting N–D transfer. If a Si–H/D bond breaking reaction were rate-limiting then an increase in the rate of reaction compared to value found for **43-*d*$_3$** would be expected.

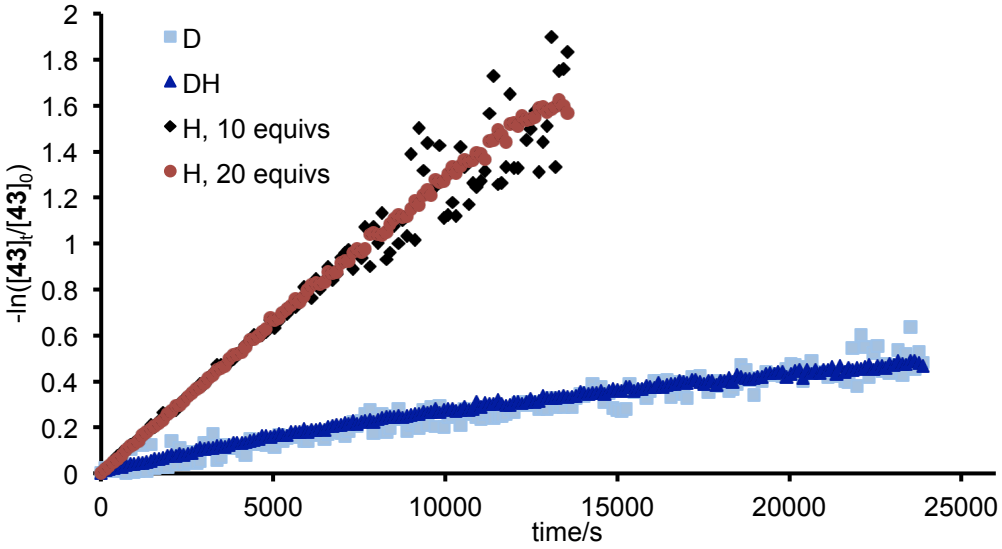


Figure 4.10. First-order semi-logarithmic plots for the reaction of Ti($N_2^{iPr}N^{Me}$){N(H)SiH_2Ph}(NPh_2) (**43**), Ti($N_2^{iPr}N^{Me}$){N(D)SiD_2Ph}(NPh_2) (**43-*d*$_3$**) and Ti($N_2^{iPr}N^{Me}$){N(H)SiHDPh}(NPh_2) with excess 3,5-$C_6H_3(CF_3)_2SiH_3$. (avg. r^2 = 0.947, range 0.917 – 0.996.

The reaction of **43-*d*$_3$** with just one equivalent of 3,5-$C_6H_3(CF_3)_2SiH_3$ was monitored. When the mixture contained approximately a 1:1 mixture of **43** and **44**, hydrogen and deuterium had randomised over all of the Si sites. After the slow H transfer step to yield the imido intermediate **43_IntB**, facile Si–H addition with 3,5-$C_6H_3(CF_3)_2SiH_3$ can occur followed by rotation and elimination of $PhSiD_2H$ as outlined in Scheme 4.5. If these addition and elimination reactions are fast and reversible, then reaction with the Si–H or Si–D bonds of either free silane could occur prior to the H transfer step to reform **43** or **44**. This would account for the scrambling of H and D across the system and would also mask a KIE due to Si–H bond breaking further confirming that the above KIE is due to N–H transfer.

4.10 DFT study of the mechanism of reaction of Ti($N_2^{iPr}N^{Me}$){N(H)SiH_2Ph}(NPh_2) (43) with silanes

It was hoped to gain further insight into the mechanism with the aid of DFT calculations. The main results are presented in Figures 4.11 and 4.12. The two possible pathways for the formation of an imido intermediate were calculated. Path A (Figure 4.11) involves transfer of the Ti–N(H) atom to the NPh_2 ligand. This was calculated for both isomers of **43**. The energies of the intermediates ***trans*-43_IntA** and ***cis*-43_IntA** indicate that they are relatively stable. However, the barriers to reach these intermediates are high ($\Delta G^{\ddagger}$ = 25.5 and 32.2 kcal mol^{-1} for the *trans* and *cis*

isomers respectively). It is possible that the barrier could be lowered by participation of $PhSiH_3$ in some manner. Removal of the $NHPh_2$ ligand from both isomers gives the four-coordinate **IntA** in which the multiple bond occupies a position intermediate between the axial and equatorial positions. Weak donation of the neutral ligand makes this a facile process. However, loss of the $NHPh_2$ ligand results in reduced stabilisation and **IntA** is higher in energy.

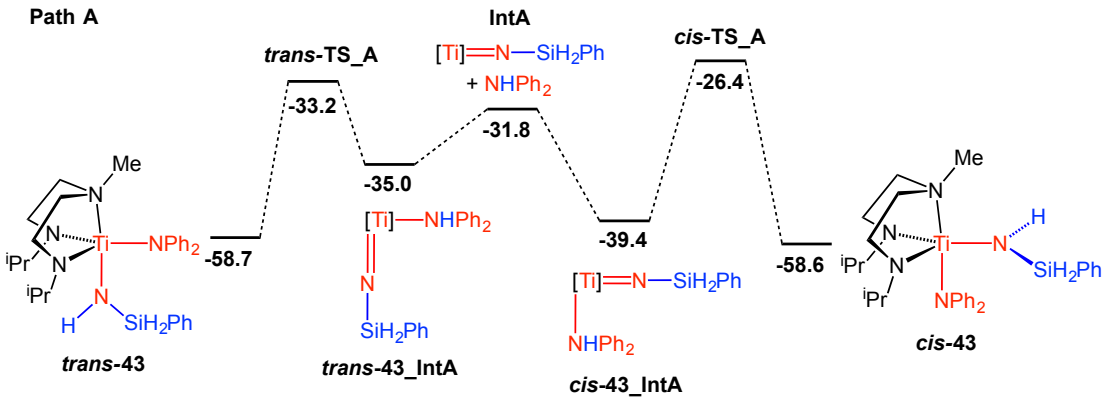


Figure 4.11. DFT mechanism for the formation of an imido intermediates from **43**. Gibbs free energies (kcal mol^{-1}, T = 298 K) for minima, maxima and transition states (labelled **TS_x**) are shown in bold relative to **2.1**. [Ti] represents $Ti(N_2^{iPr}N^{Me})$.

Path B (Figure 4.12) involves migration of the Ti–N(H) atom to one of the $Ti–N_{amide}$ atoms of the supporting ligand, the pathway is calculated for both isomers and they are shown in separate schemes. Again the imido intermediates are quite low in energy but the energy required to overcome the barriers are high ($\Delta G^{\ddagger}$ = 29.3 and 33.7 kcal mol^{-1} for the *trans* and *cis* isomers respectively), inconsistent with a reaction that occurs at room temperature. The possibility of migration of the H atom to the NMe donor of the supporting ligand was not explored due to the lower basicity of this nitrogen atom.

As Path B is in better agreement with experimental results, the energy of the bis(silyl)amide-hydride intermediate (denoted **50_Int2** in Scheme 4.5) resulting from Si–H addition across the imido bond was calculated for both isomers. Both ***trans*-43_Int2** and ***cis*-43_Int2** are low in energy (-41.1 and -38.5 kcal mol^{-1} respectively). However, the transitions states were not well defined and therefore the barrier to reach these intermediates could not be established. The energy of the bis(silyl)amide-

hydride intermediate formed with 3,5-$C_6H_3(CF_3)_2SiH_3$ were also calculated and the energies are shown in brackets. They are lower in energy than the corresponding $PhSiH_3$ intermediates, most likely due to the electron-withdrawing groups conferring some stabilisation to these electron-rich species.

The stability of all the intermediates described above suggests that Pathway B is thermodynamically feasible. However, much difficulty was had locating the transition states and it is possible that an alternative H-migration assisted mechanism is in operation.

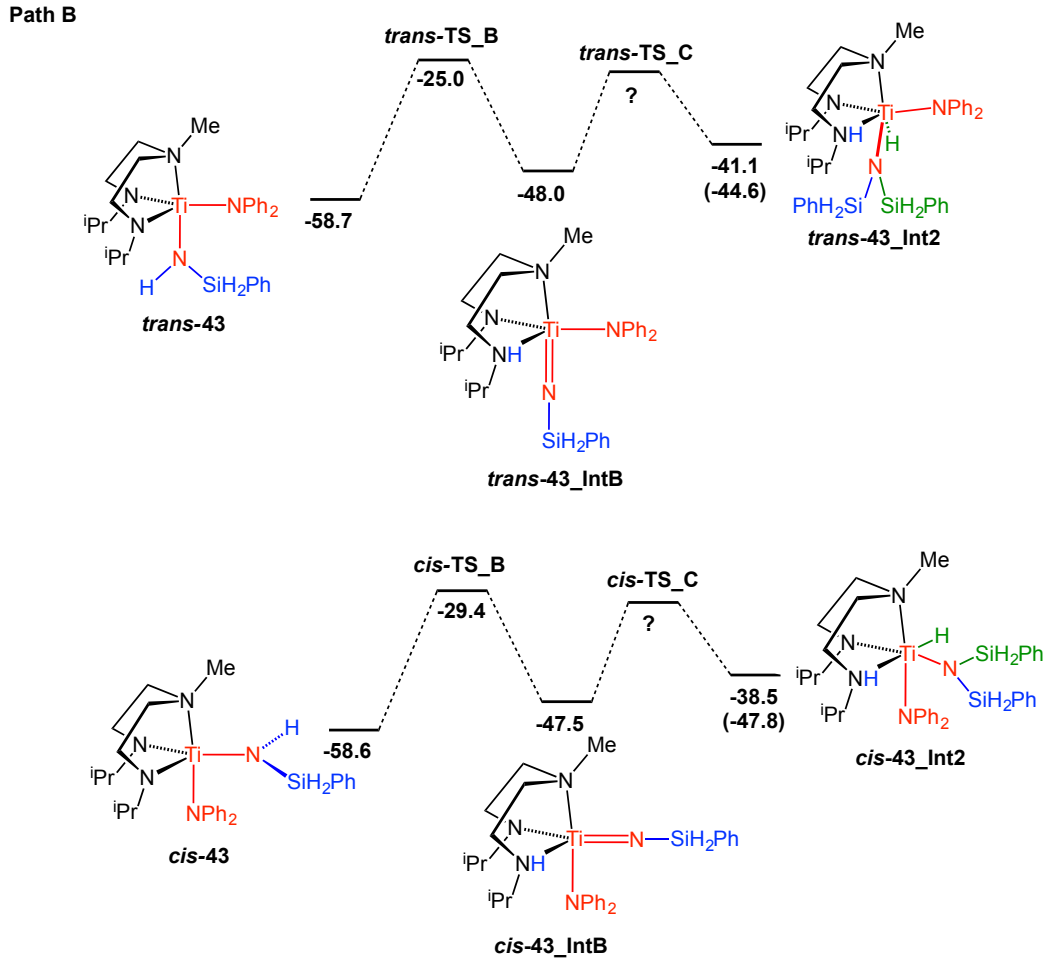


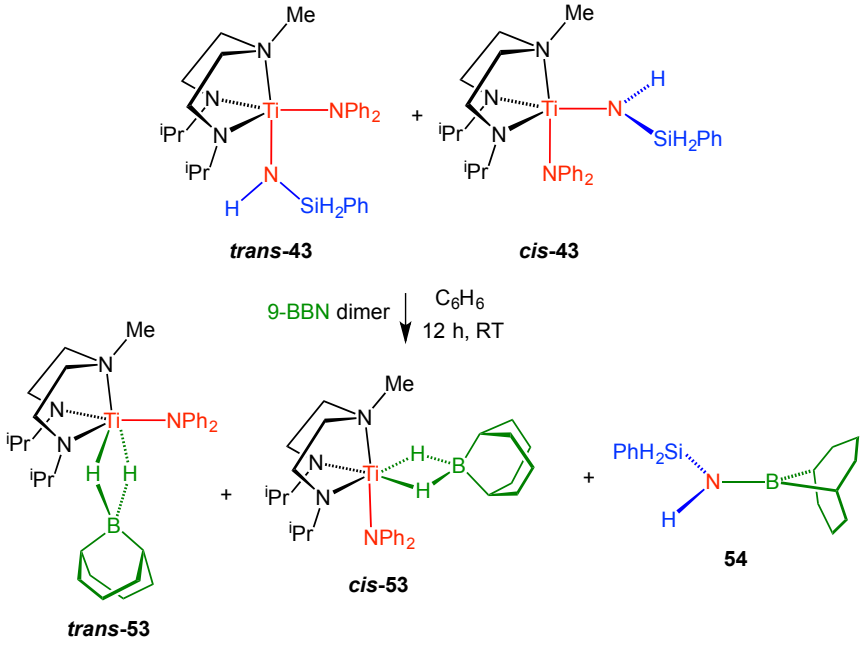
Figure 4.12. DFT mechanism for the formation of imido intermediates from **43** and subsequent reaction with $PhSiH_3$ or 3,5-$(CF_3)_2C_6H_3SiH_3$. Gibbs free energies (kcal mol^{-1}, T = 298 K) for minima, maxima and transition states (labelled **TS_x**) are shown in bold relative to **2.1**. [Ti] represents $Ti(N_2{}^{iPr}N^{Me})$.

Titanium amides have been reported to undergo Ti–N/Si–H exchange with silanes.[62-64] This would not account for the observed reactivity here. However, an analogous N–Si/Si–H exchange might. This possibility was tested by DFT calculations and

intermediates were found to be high in energy. Moreover, such a mechanism would not account for the observed isotope effect.

4.11 Reaction of Ti($N_2^{iPr}N^{Me}$){N(H)SiH_2Ph}(NPh_2) (43) with 9-BBN

Encouraged by the unusual silane exchange reaction described above, the reaction of Ti($N_2^{iPr}N^{Me}$){N(H)SiH_2Ph}(NPh_2) (**43**) with 9-BBN was followed by ^{1}H NMR spectroscopy. **43** consumed one equivalent of 9-BBN dimer forming two new products Ti($N_2^{iPr}N^{Me}$){(μ-H)$_2$BC_8H_{14}}(NPh_2) (**53**, confirmed by X-ray crystallography) and the silylaminoborane Ph_2NSiN(H)BC_8H_{14} (**54**, Equation 4.18).



Equation 4.18

The reaction was quantitative when followed by ^{1}H NMR spectroscopy in C_6D_6, but the isolated yields are modest owing to the difficult separation of **53** and **54**. Compound **53** exists as a mixture of *cis* and *trans* isomers in a 1:1 ratio. The bridging hydrides are observed in the ^{1}H{^{11}B} NMR spectrum as broad singlets at 2.32 and 0.40 ppm. However, due to overlapping resonances it was not possible to assign the bridging hydride signals to the *cis* and *trans* isomers. Two broad signals are observed at 15.3 and 18.4 ppm in the ^{11}B NMR spectrum, which became significantly sharper upon decoupling to the ^{1}H nucleus. The solid-state structure of **53** is shown in Figure 4.13 along with selected bond distances and angles on Table 4.4.

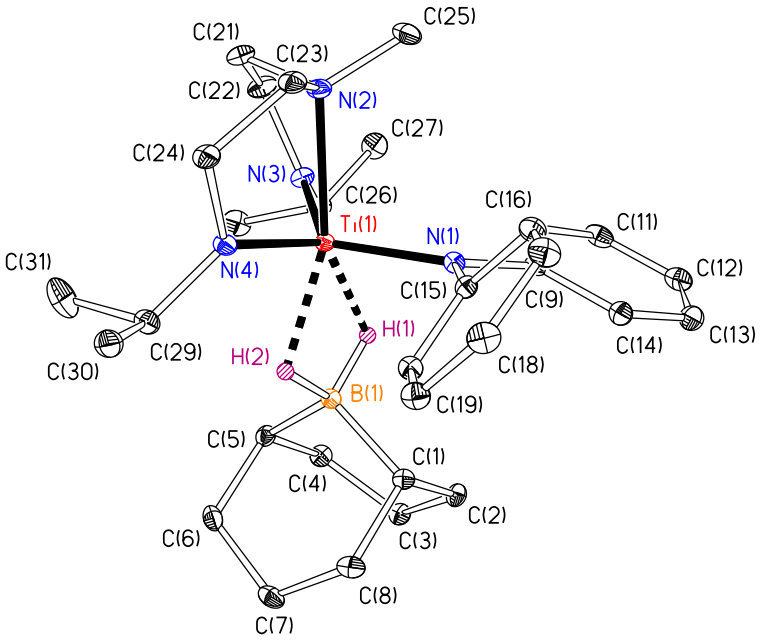


Figure 4.13. Displacement ellipsoid plots (20% probability) of Ti($N_2^{iPr}N^{Me}$){(μ-H)$_2$BC_8H_{14}}(NPh_2) (**53**). Carbon-bound H atoms are omitted for clarity.

Table 4.4. Selected bond distances (Å) and angles for Ti($N_2^{iPr}N^{Me}$){(μ-H)$_2$BC_8H_{14}}(NPh_2) (**53**).

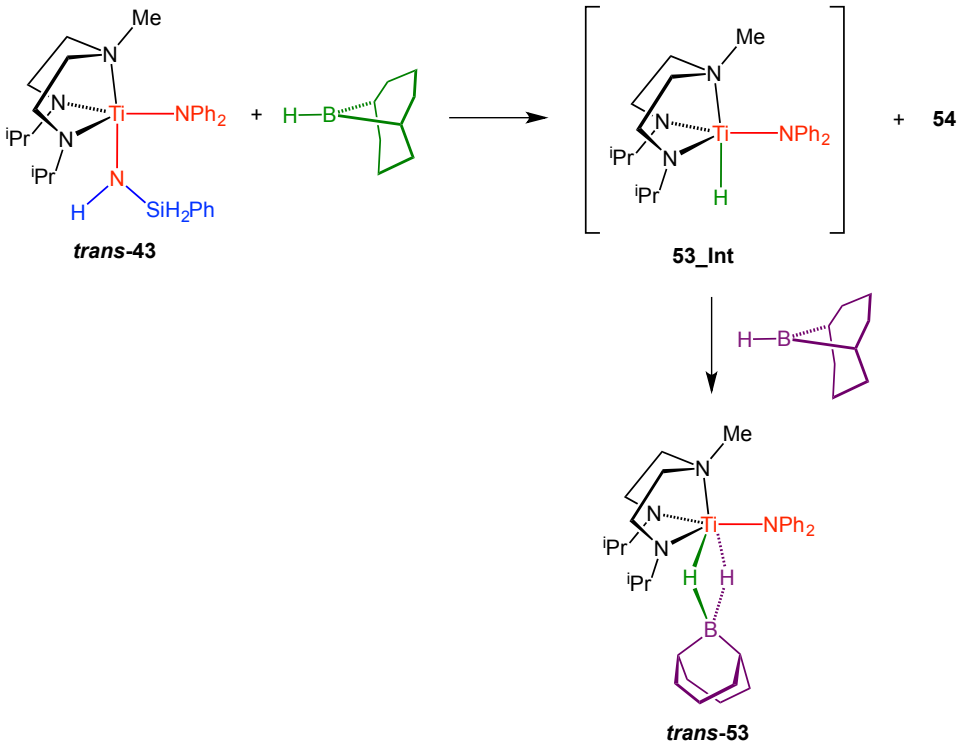
Ti(1)-N(1)	1.9926(6)	N(1)-Ti(1)-N(3)	125.28(2)
Ti(1)-H(1)	1.960(11)	N(1)-Ti(2)-N(4)	108.37(3)
Ti(1)-H(2)	1.914(11)	N(3)-Ti(1)-N(4)	120.66(3)
Ti(1)-N(2)	2.2229(6)	H(1)-Ti(1)-H(2)	56.7(5)
Ti(1)-N(3)	1.9703(6)	H(1)-B(1)-H(2)	101.1(8)
Ti(1)-N(4)	1.9556(6)		
B(1)-H(1)	1.116(10)		
B(1)-H(2)	1.263(12)		

Compound ***trans*-53** contains a facially bound diamide-amine ligand occupying one axial and two of the equatorial sites. The NPh_2 ligand occupies the remaining equatorial site and the 9-BBN hydroborate ligand is bound *trans* to the NMe donor resulting in a pseudo five-coordinate compound. The Ti(1)-N(1) bond distance of 1.9926(6) Å is within the expected region for a titanium amide bond and is similar to distances found for the NPh_2 ligand described earlier. The $(\mu\text{-H})_2BC_8H_{14}$ moiety coordinates to the metal through two bridging hydrides. In contrast to the majority of literature examples containing a $(\mu\text{-H})_2BC_8H_{14}$ ligand,[65-68] there are no agostic interactions between the C_α–H bonds and the metal centre, as indicated by the long M–$H_{C\alpha}$ distances of 3.609 and 3.558 Å. The Ti–B distance of 2.461 Å is similar to Ti–B distances found in organohydroborate Ti complexes without any agostic interactions such as $Cp_2Ti\{(\mu\text{-H})_2BC_8H_{14}\}$ (2.428(2) Å)[69] and $Cp^*Ti\{(\mu\text{-H})_2BC_8H_{14}\}_2(THF)$ (2.458(2) and 2.444(2) Å).[66] The Ti–H bond distances differ slightly, (Ti(1)-H(1) 1.960(11) Å and Ti(1)-H(2) 1.914(11) Å) as do the B–H bond distances (B(1)-H(1) 1.116(10) Å and B(1)-H(2) 1.263(12) Å). Thus the hydrogen atoms are not symmetrically disposed about the titanium and boron atoms and Ti(1)-H(2) contains more hydride character than Ti(1)-H(1). Nevertheless the distances are in good agreement with titanium organohydroborate species reported in the literature.[66, 67, 69, 70] The four membered ring B(1)-H(1)-H(2)-Ti(1) is planar with a small H(1)-Ti(1)-H(2) angle of 56.7(5) ^{o} and large H(1)-B(1)-H(2) angle of 101.1(8) ^{o} again consistent with reported values.

On scale up, **54** was isolated by sublimation as a white solid, which was characterised by NMR and IR spectroscopy and high resolution EI mass spectrometry. The IR spectrum showed bands in the expected regions for ν(Si-H) and ν(N-H) at 2149 and 3376 cm^{-1} respectively. Resonances attributable to the Ph moiety are observed along with a doublet at 5.05 ppm due to the Si–H protons. The N–H signal is broad and the fine structure cannot be distinguished. The signals resulting from the BC_8H_{14} moiety are overlapping in the ^1H NMR spectrum. However, the presence of two B–C signals in the ^{13}C NMR spectrum is indicative of restricted rotation about the N–B bond due to $N_{2p}\rightarrow B_{2p}$ π donation.

The proposed mechanism for the reaction of **43** with 9-BBN is shown in Scheme 4.7. A σ-bond metathesis at the Ti–N(H) bond with the B–H bond of 9-BBN (drawn as the monomer for simplicity) results in elimination of the silylaminoborane **54** and

formation of a transient titanium hydride species **53_Int** (not observed). It is possible that this step is aided by initial coordination of 9-BBN to the Lewis basic amide group. This short-lived metal hydride is then trapped by reaction with a second equivalent of 9-BBN monomer giving **53**.



Scheme 4.7. Proposed mechanism for the reaction of $Ti(N_2^{iPr}N^{Me})\{N(H)SiH_2Ph\}(NPh_2)$ (**43**) with 9-BBN.

There are several examples of this type of transmetallation reaction in the literature, and in many cases the resulting hydride species is trapped by a second equivalent of borane. In 2011, Noth reported the preparation of $(ArO)_3Ti\{(\mu\text{-}H)_2BC_8H_{14}\}$ (ArO = 2,6-$C_6H_3{}^iPr_2$) from the reaction of $(ArO)_3TiMe$ with 9-BBN dimer along with the formation of $MeBC_8H_{14}$.[67] Similarly Hill and co-workers found that reaction of a magnesium alkoxide compound with HBPin yielded a magnesium hydride and pinacolborate ester.[71] Furthermore, the reaction of an amine tris(phenolate) supported titanium alkoxide with BH_3 has been described to yield a metal borohydride species following BH_3 coordination followed by elimination of mono-alkoxyborane and trapping of the hydride with a second equivalent of BH_3.[72] Similar reactions between BH_3.THF and metal chloride complexes have been shown to proceed with the loss of BH_2Cl.[73] Organohydroborate complexes are more typically prepared *via* a salt

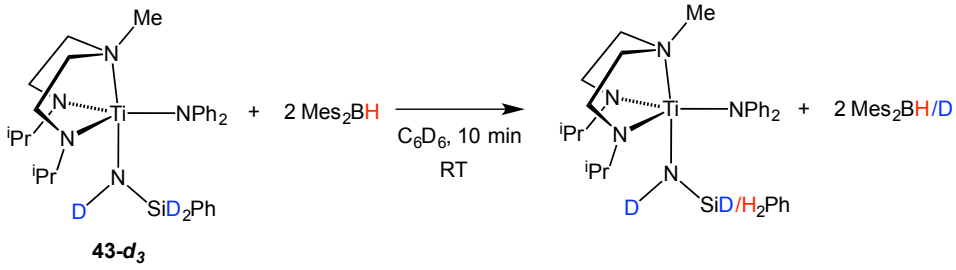
metathesis reaction between a metal chloride and alkali salt of the organoborate or an addition reaction between a metal hydride and alkylborane.[74-77]

When the reaction between **43** and an excess of 9-BBN dimer (10 equivalents) was followed at 25 ^{o}C in C_6D_6 the decay of **43** followed pseudo first-order kinetics with respect to Ti as judged by a linear semi-logarithmic plot of $\ln([\mathbf{43}]_t/[\mathbf{43}]_0)$ *vs.* time. The reaction reached 85% conversion after approximately 1.5 hours and the rate constant of 36.8(1) x 10^{-5} s^{-1} was obtained. The analogous reaction of **43-*d*$_3$** was followed and the observed rate constant of 30.9(6) x 10^{-5} s^{-1} was extracted. In both cases the data obtained was quite scattered, and thus the above values should be taken as an approximate guide. Nevertheless, it is clear that there is a negligible kinetic isotope effect, consistent with the proposed mechanism.

It was postulated that an alternative mechanism involving the formation of an imido intermediate from **43** *via* transfer of the Ti–N(H) atom to Ti–N_{amide}, as was found in the silane exchange reactions described above, could be in operation. However, the lack of a KIE and the overall faster reaction indicate that this is unlikely (reaction of **43** with excess 3,5-$(CF_3)_2C_6H_3SiH_3$ at the same Ti concentration required approximately four hours to reach 85% conversion). It is also noted, that the reaction proceeds more slowly than the reaction of **2.1** with excess 9-BBN at the same Ti concentration. As described previously the rate-limiting step in this reaction was found to be 9-BBN dimer dissociation. Thus, in the reaction of **43** with 9-BBN one of the steps following 9-BBN dimer dissociation is thought to be rate-limiting. It was hoped to carry out further kinetic analysis on this system. However, unfortunately the data obtained was very scattered making meaningful conclusions difficult and it was not pursued further.

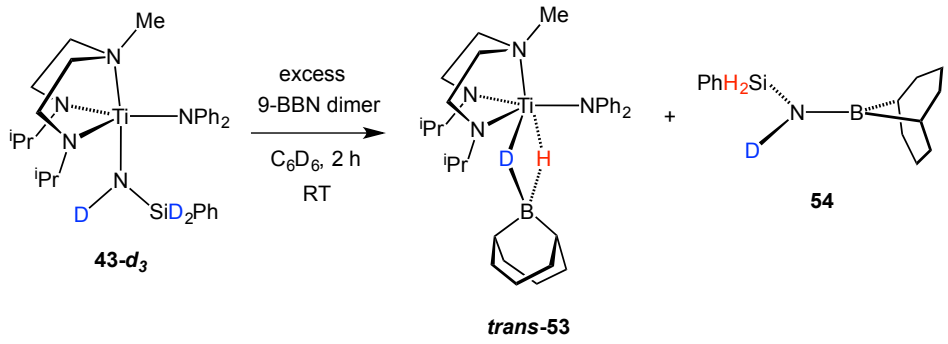
It was noticed in the reaction of **43-*d*$_3$** with excess 9-BBN, that there was significant hydrogen incorporation into the Si–D positions of **43-*d*$_3$** almost immediately after mixing. When the reaction had proceeded 30%, the unreacted **43** contained > 90% hydrogen in the Si positions. No scrambling into the N–D site occurred. When followed by ^{2}H NMR spectroscopy a resonance corresponding to DBC_8H_{14} (9-BBN-*d*$_1$) was observed within 10 minutes of mixing. Importantly, no borylamide **50** or free silane was observed, confirming that just H/D exchange and not a reaction analogous to the silane exchange described above is in operation.

This scrambling is due to direct Si–D/B–H exchange between **43-*d*$_3$** and 9-BBN in solution. Facile off-metal Si–H/B–H exchange has been reported in the literature.[78] When $PhSiD_3$ is mixed with 1.5 equivalents of 9-BBN dimer in C_6D_6 H/D exchange occurred readily and a statistical distribution was reached over all sites after just one hour at room temperature. As a test of on-metal Si–H/B–H exchange, **43-*d*$_3$** was mixed with Mes_2BH (**43** does not react with Mes_2BH when tested independently). After just ten minutes > 50% of the Si positions in **43** contained a hydrogen atom, clearly demonstrating a facile H/D exchange (Equation 4.19). This type of exchange would mask a kinetic isotope effect due to Si–D bond breaking with **43-*d*$_3$** due to the excess of hydrogen in the system. However, a mechanism involving Si–H/D bond breaking is unlikely.



Equation 4.19

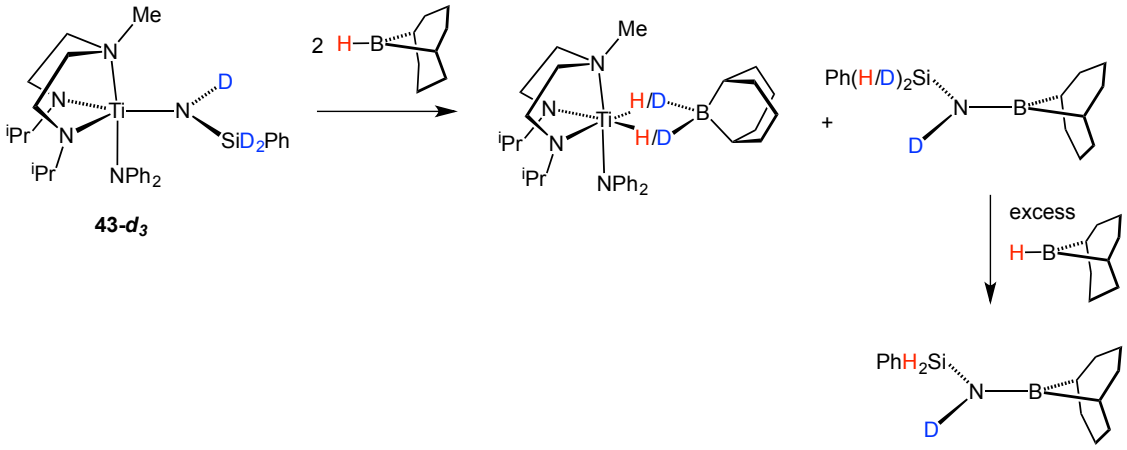
The final products in the reaction of **43-*d*$_3$** with ten equivalents of 9-BBN dimer are as shown in Equation 4.20. **54** contains exclusively hydrogen in the Si positions, due to exchange with the excess 9-BBN, and exclusively deuterium in the N position.



Equation 4.20

Interestingly, despite the excess of 9-BBN in the system there is significant 9-BBN-d_1 (approximately 50%) incorporation into the bridging hydride position of **53**. 9-BBN-

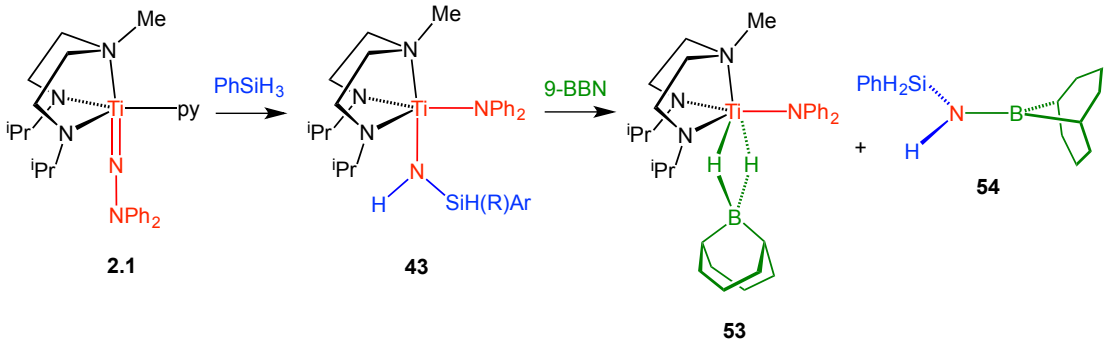
d_1 is present in the system due to exchange of 9-BBN with **43-*d*$_3$**. Its presence in **53** can be been attributed to the preference for deuterium to populate the site with the strongest bond. Both **53** and 9-BBN dimer contain bridging hydrides, the Ti–H bonds will be weaker than the B–H bonds making the B–H bonds in **53** stronger than in free 9-BBN dimer. This is evident from the shorter B–H bonds in **53** compared to 9-BBN dimer (avg. 1.190(2) for **53** *vs*. 1.251(15)).[79, 80]



Scheme 4.8. Reaction of **43-*d*$_3$** with 9-BBN.

As exchange between $PhSiH_3$ and 9-BBN and, **43** and 9-BBN are so facile it follows that exchange between **54** and 9-BBN would also be possible. To test this the reaction of **43-*d*$_3$** with one equivalent of 9-BBN dimer was carried out. As expected, scrambling occurred and hydrogen and deuterium was observed in an approximately statistical distribution across the Si site of **54** and the B site of **53**. Once the reaction had reached completion an excess of 9-BBN was added to the mixture. After three hours **54** contained exclusively hydrogen in the Si position, demonstrating that facile exchange can also occur between **54** and 9-BBN (Scheme 4.8). During the course of the 1:1 reaction and on addition of excess 9-BBN no scrambling of the N–D position of **43** or **54** was observed. Therefore, H/D exchange can occur between both starting material and product, and 9-BBN resulting in scrambling of the Si and B sites.

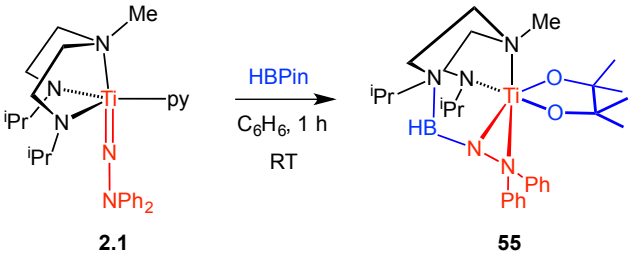
The overall sequential reaction of **2.1** first with $PhSiH_3$ to yield **43** followed by reaction with 9-BBN to yield **53** and **54** has resulted in total extrusion of N_α from the $Ti{=}NNPh_2$ linkage and formation of three different element-nitrogen bonds solely by reaction with Si–H and B–H bonds (Scheme 4.9).



Scheme 4.9. Subsequent reaction of $Ti(N_2^{iPr}N^{Me})(NNPh_2)(py)$ (**2.1**) with $PhSiH_3$ and 9-BBN.

4.12 Reaction of $Ti(N_2^{iPr}N^{Me})(NNPh_2)(py)$ (2.1) with pinacolborane and catecholborane

In contrast to the reactions of the hydrazido compound **2.1** with silanes and boranes described so far, reaction with one equivalent of pinacolborane (HBPin) proceeds smoothly at room temperature to yield $Ti\{N(Me)(CH_2CH_2N^iPr)(CH_2CH_2N(^iPr)B(H)NNPh_2)\}\{OC(Me)_2C(Me_2)O\}$ (**55**) (Equation 4.21).



Equation 4.21

When monitored by ^1H NMR spectroscopy in C_6D_6 at room temperature conversion was quantitative and no intermediates were observed. Diffraction-quality crystals of **55** were obtained from a saturated benzene solution at room temperature, unambiguously confirming the connectivity shown in Equation 4.21. The molecular structure of **55** is shown in Figure 4.14 along with selected bond lengths and angles in

Table 4.6. The NMR spectra and other data are fully consistent with the solid-state structure.

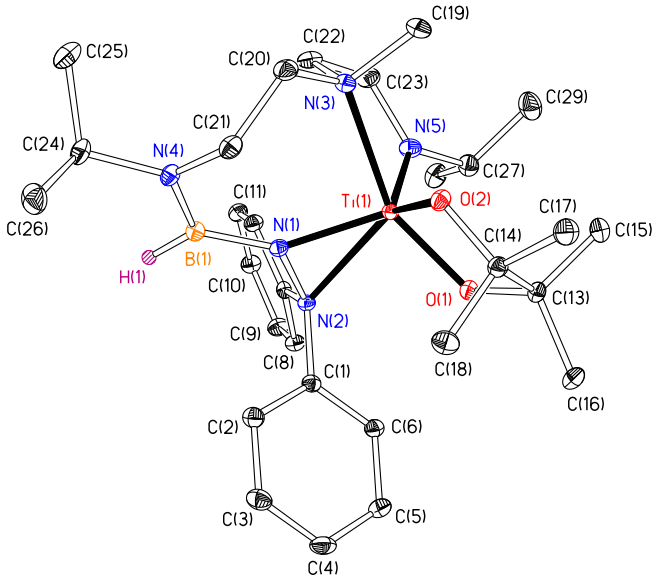


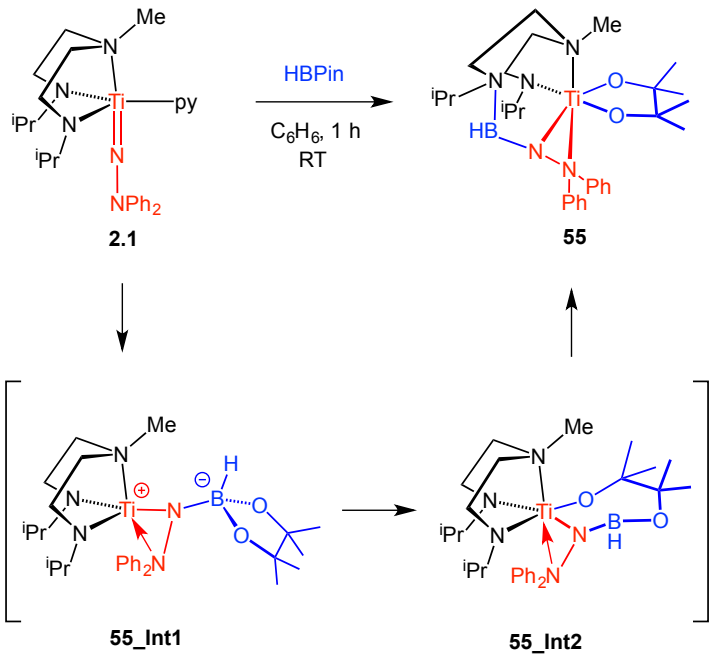
Figure 4.14. Displacement ellipsoid plots (20% probability) of Ti{N(Me)($CH_2CH_2N^iPr$)($CH_2CH_2N(^iPr)B(H)NNPh_2$)}{$OC(Me)_2C(Me_2)O$} (**55**). Carbon-bound H atoms are omitted for clarity.

Table 4.6. Selected bond distances (Å) and angles for Ti{N(Me)($CH_2CH_2N^iPr$)($CH_2CH_2N(^iPr)B(H)NNPh_2$)}{$OC(Me)_2C(Me_2)O$} (**55**).

Ti(1)-N(1)	1.9601(9)	N(1)-Ti(1)-N(2)	37.51(3)
Ti(1)-N(2)	2.3524(8)	N(1)-Ti(1)-N(3)	88.77(3)
Ti(1)-N(3)	2.3136(9)	N(3)-Ti(1)-N(5)	76.84(4)
Ti(1)-N(5)	1.9313(9)	N(3)-Ti(1)-O(1)	152.29(3)
Ti(1)-O(1)	1.8690(7)	N(3)-Ti(1)-O(2)	77.52(3)
Ti(1)-O(2)	1.8942(7)	N(1)-Ti(1)-N(5)	110.11(4)
N(1)-N(2)	1.4353(11)	N(1)-Ti(1)-O(2)	115.47(4)
N(1)-B(1)	1.4257(15)	O(2)-Ti(1)-N(5)	126.43(4)
N(4)-B(1)	1.4099(14)	O(1)-Ti(1)-O(2)	81.62(3)
B(1)-H(1)	1.102(15)		

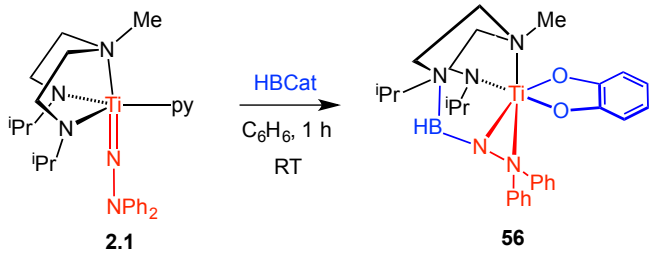
Compound **55** contains a six-coordinate titanium centre with a diolate ligand and a new N(Me)($CH_2CH_2N^iPr$)($CH_2CH_2N(^iPr)B(H)NNPh_2$) group. The substituted hydrazide ligand is κ^2-coordinated as is usually found for titanium hydrazido(1-) complexes,[3, 15, 38, 81-88] which is maintained in solution as shown by inequivalent phenyl groups. The Ti(1)-N(1) and N(1)-N(2) distances of 1.9601(9) and 1.4353(11) Å are significantly lengthened to those of 1.7444(14) and 1.371(2) Å, respectively, in **2.1**. These values lie at the longer end of the ranges previously found for κ^2-coordinated hydrazido(1-) complexes (Ti–N_α: 1.832 - 2.005 Å; N_α–N_β: 1.236 - 1.458 Å)[44] and are consistent with disruption of the Ti–N_α triple bond and a change from sp hybridisation at N(1) in **2.1** to sp^2 in **55**. The Ti(1)-N(2) distances (2.3524(8) Å) is only slightly longer that the NMe neutral donor of the supporting ligand (2.3136(9) Å) and is within the usual range. The short N(4)-B(1) bond distance of 1.4099(14) Å suggests significant N=B double bond character *via* $N_{2p}\rightarrow B_{2p}$ π donation as was observed in compounds **50** and **51**, the N(1)-B(1) bond distances is slightly longer (1.4257(15) Å) presumably due significant $N_{2p}\rightarrow Ti_{3d}$ π donation. The diolate ligand is κ^2-coordinated with a bite angle of 81.62(3) ^{o} and Ti–O bond distances of 1.8690(7) and 1.8942(7), similar in value to titanium diolate ligands reported in the literature.[89-92]

A plausible mechanism for formation of **55** is given in Scheme 4.10. Group 4 hydrazides M($N_2^RN^{py}$)($NNPh_2$)(py) are known to readily form zwitterionic N_α-adducts of the type M($N_2^RN^{py}$){η^2-N(NPh_2)B(Ar^{F5})$_3$} (**1.123**; $N_2^RN^{py}$ = (2-NC_5H_4)CMe(CH_2NR)$_2$; M = Ti, R = $SiMe_3$; M = Zr or Hf, R = $SiMe_2{}^tBu$, Figure 1.12, Chapter One) with B(Ar^{F5})$_3$. Borane coordination to N_α of **2.1** generates an analogous zwitterionic intermediate with coordination of N_β to the formally cationic metal centre, depicted as **55_Int1**. Subsequent cleavage of one B–O bond relieves the electron deficient titanium centre to yield the intermediate **55_Int2**. Finally, nucleophilic attack by an amide nitrogen (N^{iPr}) on the boron atom and cleavage of the remaining B–O bond gives compounds **55**. There have been several examples throughout this thesis demonstrating how the nucleophilicity of the N_{amide} atoms can result in their involvement in the reactions with small molecules, as is found here.



Scheme 4.10. Plausible mechanism for the reaction of Ti($N_2^{iPr}N^{Me}$)($NNPh_2$)(py) (**2.1**) with HBPin.

Reaction of **2.1** with catecholborane (HBCat) proceeded in an analogous manner yielding Ti{N(Me)($CH_2CH_2N^iPr$)($CH_2CH_2N(^iPr)B(H)NNPh_2$)}{$O_2C_6H_4$} (**56**) (Equation 4.22). Compound **56** demonstrated limited stability in solution preventing characterisation by X-ray crystallography. However, the NMR data obtained were in good agreement with the proposed structure and the compound was also characterised by elemental analysis and infrared and mass spectrometry.



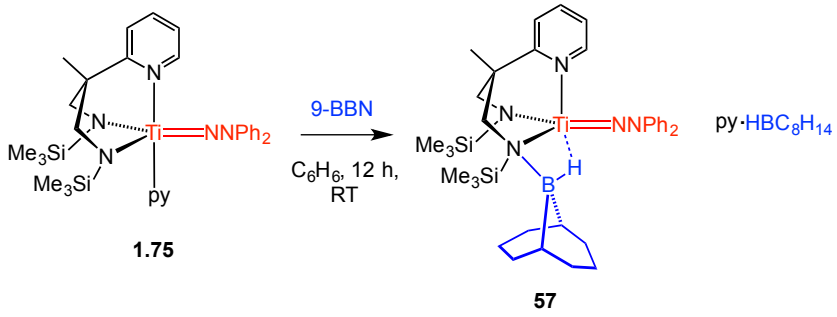
Equation 4.22

Both HBPin and HBCat have been used extensively in synthetic chemistry, in particular as reducing or hydroborating agents.[93-99] The B–O bonds are stronger than the corresponding B–H bonds.[100] Thus, reactions involving cleavage of the B–O bonds are almost unknown and just two structurally characterised compounds resulting from such a reaction have been reported. Marks described an organolanthanide-catalysed pyridine dearomatisation process using pinacolborane

including a deactivation pathway due to B–O bond cleavage.[101] Furthermore, in 2014 Chen and co-workers described the reactions of a scandium phosphinidene compound with boranes, giving B–O bond cleavage with both HBPin and HBCat and B–H cleavage with 9-BBN, proposed to be a result of the strong oxophilicity of the scandium ion.[102] In an analogous manner, the driving force behind the reactions of **2.1** with HBPin and HBCat is thought to be the formation of strong Ti–O bonds.

4.13 Reaction of Ti(N_2N^{py})($NNPh_2$)(py) (1.75) with 9-BBN

As the reactions of **2.1** with a range of organic silanes and boranes have led to a range of unprecedented transformations, the analogous reactions with the hydrazido compounds Ti(N_2N^{Me})($NNPh_2$)(py) (**1.72**) Ti(N_2N^{py})($NNPh_2$)(py) (**1.75**) were attempted. In both cases no reaction was observed with $PhSiH_3$ at room temperature and unidentified mixtures were obtained on heating at 70 °C. Similarly, Ti(N_2N^{Me})($NNPh_2$)(py) (**1.72**) with 9-BBN gave slow conversion to several species of which only py·HBC_8H_{14} could be identified. However, mixing Ti(N_2N^{py})($NNPh_2$)(py) (**1.75**) with one equivalent of 9-BBN dimer gave slow conversion to the adduct Ti{N_2N^{py}-(HBC_8H_{14})}($NNPh_2$) (**57**) where the B atom of 9-BBN is coordinated to one of the N_{amide} atoms and the boron bound hydrogen atom to titanium (Equation 4.23). The reaction was quantitative on the NMR tube scale however **57** was only isolated in 30% yield on scale up due to difficultly in separating from py·HBC_8H_{14}. Single crystals were grown from a saturated benzene solution at room temperature and the solid-state structure is shown in Figure 4.15 along with selected bond distances and angles in Table 4.7.



Equation 4.23

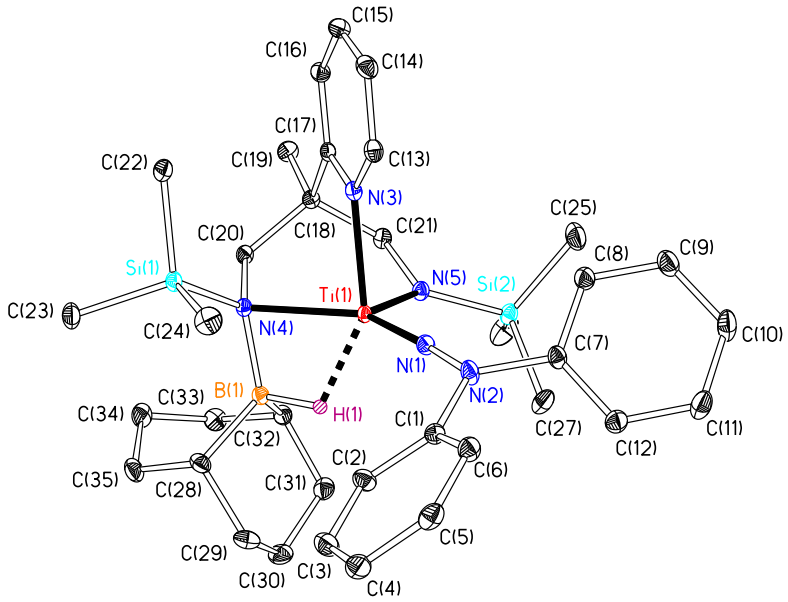


Figure 4.15. Displacement ellipsoid plots (20% probability) of Ti{N_2N^{py}-HBC_8H_{14})}($NNPh_2$) (**57**). Carbon-bound H atoms are omitted for clarity.

Table 4.7. Selected bond distances (Å) and angles for Ti{N_2N^{py}-(HBC_8H_{14})}($NNPh_2$) (**57**).

Ti(1)-N(1)	1.7453(10)	N(1)-Ti(1)-N(4)	140.36(4)
Ti(1)-N(3)	2.1354(10)	N(1)-Ti(1)-N(5)	112.83(5)
Ti(1)-N(4)	2.1818(10)	N(4)-Ti(1)-N(5)	106.29(4)
Ti(1)-N(5)	1.9233(10)	N(1)-Ti(1)-H(1)	95.1(5)
Ti(1)-H(1)	1.798(14)	N(4)-Ti(1)-H(1)	66.3(5)
N(1)-N(2)	1.3565(14)	N(5)-Ti(1)-H(1)	107.8(5)
N(4)-B(1)	1.6045(16)	N(3)-Ti(1)-H(1)	149.5(5)
B(1)-H(1)	1.251(15)	Ti(1)-N(1)-N(2)	174.61(9)

Compound **57** contains a distorted trigonal bipyramidal titanium centre with a κ^3N-bound N_2N^{py} ligand occupying one axial and two equatorial coordination sites. The remaining equatorial site is occupied by a hydrazido(2-) ligand. The Ti(1)-H(1) bond is positioned in the remaining axial position, although significantly distorted with a small N(4)-Ti(1)-H(1) angle of 66.3(5) ^{o} and a large N(5)-Ti(1)-H(1) angle of 107.8(5) ^{o}. The Ti(1)-N(1) bond distance is similar to that in **1.75** which, along with

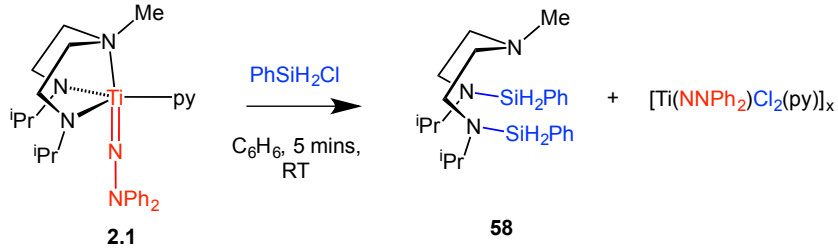
the almost linear Ti(1)-N(1)-N(2) of 174.61(9) ^{o} confirms the hydrazido ligand remains in intact. The Ti(1)-N(4) bond distance is significantly longer than that of Ti(1)-N(5) (2.1818(10) *vs.* 1.9233(10) Å) consistent with reduced $N_{2p} \rightarrow Ti_{3d}$ π donation from N(4). The B(1)-H(1) bond distance of 1.251(15) Å is the same within error to the bridging B–H bonds in 9-BBN dimer[79, 80], indicative of a bridging interaction as a significantly shorter bond would be expected for a terminal B–H bond. Titanium hydrides have been reported to be in the region 1.56 – 1.64 Å,[24, 25] longer distances are found for titanium hydride interactions due to titanium bound nitrogen adducts with boranes (1.84(10) – 2.01(3) Å). [103-106] Thus, the Ti(1)-H(1) distance of 1.798(14) Å suggests significant interaction between the two atoms. Recent work in our group has found addition of several boranes to the cyclopentadienyl-amidinate imido supported compound Cp*Ti{MeC(N^{i}Pr)$_2$}(NTol) yields adducts at the imido nitrogen atom, Ti–H bonds lengths of 1.914(13) and 2.009(13) Å were found.[107] Finally it is noted that the N(4)-B(1) distance of 1.6045(16) Å is within the reported range for nitrogen adducts of 9-BBN[31, 108, 109] and is longer than the N–B bond in compound **50** reflecting the adduct nature of the bond.

A band at 1764 cm^{-1} was observed due to the B-H-Ti unit, typical for a bridging hydride and close to values reported for both titanium and zirconium amidoborane complexes containing a B-H-M connectivity.[104, 106, 110] The ^{1}H, ^{13}C and ^{11}B NMR data are fully consistent with the solid-state structure and the resonance attributable to B–H–Ti was observed as a singlet at 3.96 ppm in the ^{1}H{^{11}B} NMR spectrum.

No onward reaction of **57** was observed. However, the characterisation of an adduct with 9-BBN may indicate that a similar species could be formed in the reaction of **2.1** with 9-BBN at either N_{amide} of the supporting ligand or N_{α} of the hydrazide ligand (as predicted by DFT) prior to B–H bond cleavage.

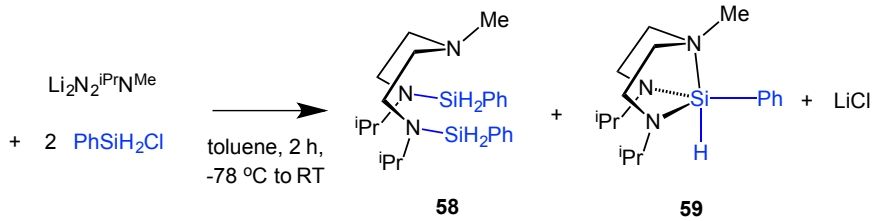
4.14 Reaction of Ti($N_2^{iPr}N^{Me}$)($NNPh_2$)(py) (2.1) with halosilanes

An NMR tube scale reaction of **2.1** with two equivalents of $PhSiH_2Cl$ gave immediate formation of a pale brown precipitate. The $N_2^{iPr}N^{Me}$ ligand peaks in the ^1H NMR spectrum were observed as two triplets for the methylene protons and a single doublet and septet for the *iso*-propyl substituents, indicating a loss of diastereotopic environments. It was proposed that Si–Cl addition across both Ti–N_{amide} bonds had occurred, as shown in Equation 4.24, to yield the organic species **58** and an insoluble Ti species with bridging hydrazide and chloride ligands. However, on the preparative scale the reaction did not proceed smoothly and no one species could be isolated.



Equation 4.24

In an attempt to synthesise **58** independently, $Li_2N_2^{iPr}N^{Me}$ was reacted with two equivalents of $PhSiH_2Cl$. Following extraction into hexane and removal of the solvent under vacuum the ^1H NMR spectrum revealed a mixture of two species in an approximately 1:1 ratio. One species was identified as **58** observed in the above reaction. This was confirmed by mass spectrometry and with the aid of a ^{29}Si-^1H gradient HMBC experiment which revealed correlations between $^{iPr}NCH_2$ methylene protons and the *o*-C_6H_5 protons to the ^{29}Si resonance at -29.9 Hz. The other species was identified by X-ray crystallography to be the five-coordinate silicon species **60** (Equation 4.25).



Equation 4.25

Attempts to separate the mixture were unsuccessful and diffraction-quality crystals of **59** were obtained from a saturated solution of the mixture in hexane at room

temperature. A broad singlet at 5.03 ppm was observed in the ^{1}H NMR spectrum due to SiH along with a set of diamide-amine ligand peaks with a multiplet pattern expected from κ^{3}-*fac* coordination. A signal at -54.2 ppm in the ^{29}Si NMR spectrum demonstrated correlations to both the C<u>H</u>Me$_2$ and ^{iPr}NC<u>H</u>$_2$ protons as well as the *o*-C_6H_5 signal.

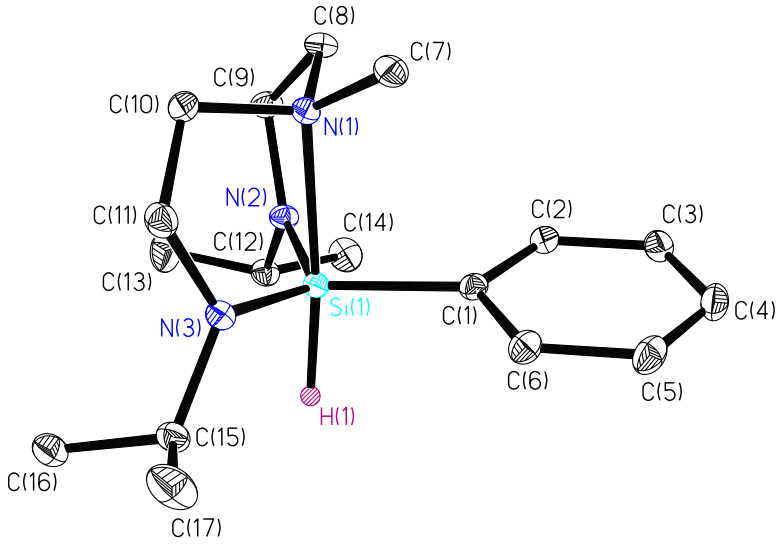


Figure 4.16. Displacement ellipsoid plots (25% probability) of Si($N_2^{iPr}N^{Me}$)(H)(Ph) (**59**). Carbon-bound H atoms are omitted for clarity.

Table 4.7. Selected bond distances (Å) and angles for Si($N_2^{iPr}N^{Me}$)(H)(Ph) (**59**).

Si(1)-N(1)	2.1969(9)	C(1)-Si(1)-N(2)	114.20(4)
Si(1)-N(2)	1.7432(9)	C(1)-Si(1)-N(3)	116.17(4)
Si(1)-N(3)	1.7486(9)	N(2)-Si(1)-N(3)	126.01(4)
Si(1)-H(1)	1.473(12)	N(1)-Si(1)-H(1)	174.1(5)
Si(1)-C(1)	1.9036(10)		

Compound **59** contains a five-coordinate silicon centre with trigonal bipyramidal geometry. The bond lengths to silicon are unremarkable and a similar in value to several known pentacoordinate azametallatranes.[111-114] The equatorial Si–N bonds (Si(1)-N(2)/N(3)) distances of 1.7432(9) and 1.7486(9) Å fall with the precedented region, as does the longer axial Si(1)-N(1) bond of 2.1969(9) Å. The mechanism for

the formation of **59** is unclear but may involve LiH elimination following a single salt metathesis reaction on just one side of $Li_2N_2^{iPr}N^{Me}$.

The compound Cp*Ti{MeC(N^iPr)$_2$}($NNMe_2$) (**1.76**) has been reported to react smoothly with halosilanes as well as silanes to yield 1,2-addition products containing a hydrazide(1-) ligand.[15] However, reaction at the Ti–N_{amide} bonds rather than the Ti=N multiple bond has been a common theme throughout this thesis resulting in a variety of unusual reaction products. As the reaction of **2.1** with $PhSiH_2Cl$ did not proceed cleanly and due to the difficulty in separating the products when synthesised independently the reactions of **2.1** with halosilanes was not pursued further.

4.15 Other reactions

The reactions of Ti($N_2^{iPr}N^{Me}$)($NNPh_2$)(py) (**2.1**) and Ti($N_2^{iPr}N^{Me}$)(NXyl)(py) (**1**) with several other molecules containing element hydrogen bonds were also attempted. These include ^{t}BuSH, PhC(O)Me, $CyPH_2$ (Cy = cyclohexyl), $PhPH_2$, DIBAL-H (diisobutylaluminium hydride), $TMPAlH_2$ (TMP = 2,2,6,6-tetramethylpiperidine) and Mes_2SnH_2. In most cases a mixture of species were observed of which no one could be isolated or identified. No reaction was observed with $CyPH_2$ and some evidence was obtained for a dehydrogenative coupling reaction with Mes_2SnH_2. However, the results were not reproducible or well behaved and were therefore not pursued further.

4.16 Conclusion

The reaction of Ti($N_2^{iPr}N^{Me}$)($NNPh_2$)(py) (**2.1**) with a range of silanes and boranes described in this Chapter provide the first examples of Si–H and B–H induced reductive cleavage of a hydrazide N–N bond. The mechanism has been interrogated by both DFT and experimental techniques and found to proceed *via* E–H (E = addition across the Ti=N bond to yield a silyl or borylhyrazido-hydride intermediates. Transfer of the hydride to N_α accompanied by N–N bond cleavage yields the final products. For the reaction with $PhSiH_3$, dissociation of pyridine from **2.1** and the hydride-transfer step have similar barriers and therefore both contribute to the overall rate. For the reaction with 9-BBN dimer, dissociation of 9-BBN dimer prior to reaction with **2.1** was found to be rate-limiting.

The silyl and borylamido products were isolated and in the case of Ti($N_2^{iPr}N^{Me}$){N(H)$SiHPh_2$}(NPh_2) (**46**), Ti($N_2^{iPr}N^{Me}$){N(H)BC_8H_{14}}(NPh_2) (**50**) and Ti($N_2^{iPr}N^{Me}$){N(H)$BMes_2$}(NPh_2) (**51**) were structurally characterised. The reaction

of **2.1** with $^{n}BuSiH_3$ proceeds in an analogous manner when an excess of silane is used. The resulting silylamido compound **48** can then undergo reaction with **2.1** following elimination of Ph_2NH to yield the dimer **48** with bridging hydrazido and silylimido ligands.

The silylamido compound $Ti(N_2^{iPr}N^{Me})\{N(H)SiH_2Ph\}(NPh_2)$ (**43**) can undergo further reaction with both silanes and boranes. The subsequent reaction with silanes is proposed to proceed *via* an imido intermediate following transfer of the Ti–$N(H)SiH_2Ph$ hydrogen atom to one of the $Ti–N_{amide}$ atoms. Si–H addition to the newly formed imido bond yields a bis(silyl)amide compound which then can undergo rotation, followed by elimination of either silane to reform an imido intermediate. This process can occur reversibly allowing the silyl group to be readily exchanged. Experimental data is fully consistent with this mechanism. However, it was not possible to locate all of the transition states by DFT. The subsequent reaction of **43** with 9-BBN follows a different path and gives the organohydroborate species $Ti(N_2^{iPr}N^{Me})\{(\mu\text{-}H)_2BC_8H_{14}\}(NPh_2)$ (**53**) along with the silylaminoborane compound $Ph_2NSiN(H)BC_8H_{14}$ (**54**). A Ti–N/B–H σ-bond metathesis reaction accounts for the formation of these products and such a reaction has literature precedence.

Interestingly HBPin and HBCat give different reaction products with **2.1** yielding titanium diolate complexes due to B–O bond cleavage. The oxophilicity of titanium is thought to be the driving force behind this reactivity. In attempt to build on these new reactions, the analogous reactions of silanes and boranes with the hydrazido compounds $Ti(N_2N^{Me})(NNPh_2)(py)$ (**1.72**) and $Ti(N_2N^{py})(NNPh_2)(py)$ (**1.75**) were attempted. Just one product was isolated, namely the adduct $Ti\{N_2N^{py}\text{-}(9\text{-}BBN)\}(NNPh_2)$ (**56**). The formation of an adduct at the $Ti–N_{amide}$ may be an indication that previously described reactions also proceed *via* such an adduct.

The reaction of **2.1** with a chlorosilane resulted in reaction at the $Ti–N_{amide}$ bonds and transfer of the diamide-amine ligand to silicon. Unfortunately the new organic product could not be isolated and attempts to synthesise it independently gave the five-coordinate silicon compound **59** alongside the desired species.

4.17 References

1. L. C. Stevenson, S. Mellino, E. Clot and P. Mountford, *J. Am. Chem. Soc.*, 2015, **137**, 10140.
2. P. J. Walsh, M. J. Carney and R. G. Bergman, *J. Am. Chem. Soc.*, 1991, **113**, 6343.
3. Y. Li, Y. Shi and A. L. Odom, *J. Am. Chem. Soc.*, 2004, **126**, 1794.
4. S. Banerjee and A. L. Odom, *Organometallics*, 2006, **25**, 3099.
5. A. A. Dissanayake and A. L. Odom, *Chem. Commun.*, 2012, **48**, 440.
6. H. Herrmann, J. L. Fillol, H. Wadepohl and L. H. Gade, *Angew. Chem. Int. Ed.*, 2007, **46**, 8426.
7. T. Gehrmann, J. L. Fillol, H. Wadepohl and L. H. Gade, *Angew. Chem. Int. Ed.*, 2009, **48**, 2152.
8. T. Gehrmann, M. Kruck, H. Wadepohl and L. H. Gade, *Chem. Commun.*, 2012, **48**, 2397.
9. T. Gehrmann, S. A. Scholl, J. L. Fillol, H. Wadepohl and L. H. Gade, *Chem. Eur. J.*, 2012, **18**, 3925.
10. A. J. Blake, J. M. McInnes, P. Mountford, G. I. Nikonov, D. Swallow and D. J. Watkin, *J. Chem. Soc., Dalton Trans.*, 1999, 379.
11. J. D. Selby, C. D. Manley, M. Feliz, A. D. Schwarz, E. Clot and P. Mountford, *Chem. Commun.*, 2007, 4937.
12. A. D. Schofield, A. Nova, J. D. Selby, C. D. Manley, A. D. Schwarz, E. Clot and P. Mountford, *J. Am. Chem. Soc.*, 2010, **132**, 10484.
13. P. J. Tiong, A. D. Schofield, J. D. Selby, A. Nova, E. Clot and P. Mountford, *Chem. Commun.*, 2010, **46**, 85.
14. A. D. Schofield, A. Nova, J. D. Selby, A. D. Schwarz, E. Clot and P. Mountford, *Chem. Eur. J.*, 2011, **17**, 265.
15. P. J. Tiong, A. Nova, E. Clot and P. Mountford, *Chem. Commun.*, 2011, **47**, 3147.
16. A. D. Schwarz, C. S. Onn and P. Mountford, *Angew. Chem. Int. Ed.*, 2012, **51**, 12298.
17. J. Unruangsri, H. Morgan, A. D. Schwarz, A. D. Schofield and P. Mountford, *Organometallics*, 2013, **32**, 3091.
18. A. P. Duncan and R. G. Bergman, *Chem. Rec.*, 2002, **2**, 431.
19. N. Hazari and P. Mountford, *Acc. Chem. Res.*, 2005, **38**, 839.

20. A. R. Fout, U. J. Kilgore and D. J. Mindiola, *Chem. Eur. J.*, 2007, **13**, 9428.
21. A. D. Schwarz, A. Nova, E. Clot and P. Mountford, *Chem. Commun.*, 2011, **47**, 4926.
22. Z. K. Sweeny, J. L. Polse, R. G. Bergman and R. A. Andersen, *Organometallics*, 1999, **18**, 5502.
23. T. E. Hanna, E. Lobkovsky and P. J. Chirik, *Inorg. Chem.*, 2007, **46**, 2359.
24. P. J. Tiong, A. Nova, A. D. Schwarz, J. D. Selby, E. Clot and P. Mountford, *Dalton Trans.*, 2012, **41**, 2277.
25. A. W. Kaplan, J. L. Polse, G. E. Ball, R. A. Andersen and R. G. Bergman, *J. Am. Chem. Soc.*, 1998, **120**, 11649.
26. P. J. Tiong, L. R. Groom, E. Clot and P. Mountford, *Chem. Eur. J.*, 2013, **19**, 4198.
27. J. Chu, X. Han, C. E. Kefalidis, J. Zhou, L. Maron, X. Leng and Y. Chen, *J. Am. Chem. Soc.*, 2014, **136**, 10894.
28. B. A. MacKay, R. F. Munha and M. D. Fryzuk, *J. Am. Chem. Soc.*, 2006, **128**, 9472.
29. S. P. Semproni, E. Lobkovsky and P. J. Chirik, *J. Am. Chem. Soc.*, 2011, **133**, 10406.
30. M. Hirotsu, P. P. Fontaine, A. Epshteyn and L. R. Sita, *J. Am. Chem. Soc.*, 2007, **129**, 9284.
31. M. D. Fryzuk, B. A. MacKay, S. A. Johnson and B. O. Patrick, *Angew. Chem. Int. Ed.*, 2002, **41**, 3709.
32. B. A. MacKay, S. A. Johnson, B. O. Patrick and M. D. Fryzuk, *Can. J. Chem.*, 2005, **83**, 315.
33. S. P. Semproni and P. J. Chirik, *Eur. J. Inorg. Chem.*, 2013, **2013**, 3907.
34. L. R. Groom, DPhil Thesis, University of Oxford, 2014.
35. S. C. Dunn, N. Hazari, N. M. Jones, A. G. Moody, A. J. Blake, A. R. Cowley, J. C. Green and P. Mountford, *Chem. Eur. J.*, 2005, **11**, 2111.
36. D. L. Thorn, W. A. Nugent and R. L. Harlow, *J. Am. Chem. Soc.*, 1981, **103**, 357.
37. S. Gambarotta, C. Floriani, A. Chiesi-Villa and C. Guastini, *J. Am. Chem. Soc.*, 1983, **105**, 7295.
38. J. D. Selby, M. Feliz, A. D. Schwarz, E. Clot and P. Mountford, *Organometallics*, 2011, **30**, 2295.

39. D. L. Hughes, I. A. Latham and G. J. Leigh, *J. Chem. Soc., Dalton Trans.*, 1986, 393.
40. S. Banerjee, Y. Shi, C. Cao and A. L. Odom, *J. Organomet. Chem.*, 2005, **690**, 5066.
41. T. B. Parsons, N. Hazari, A. R. Cowley, J. C. Green and P. Mountford, *Inorg. Chem.*, 2005, **44**, 8442.
42. C. Lorber, *Coord. Chem. Rev.*, 2015.
43. S. D. Cosham, A. L. Johnson, K. C. Molloy and A. J. Kingsley, *Inorg. Chem.*, 2011, **50**, 12053.
44. D. A. Fletcher, R. F. McMeeking and D. Parkin, *J. Chem. Inf. Comput. Sci.*, 1996, **36**, 746 (The UK Chemical Database Service: CSD version 5.36 updated May 2015).
45. J. E. Huheey, E. A. Keiter and R. L. Keiter, *Inorganic Chemistry : Principles of Structure and Reactivity*, HarperCollins, New York, 4th edn., 1993.
46. H. C. Brown, J. Chandrasekharam and K. K. Wang, *Pure Appl. Chem.*, 1983, **55**, 1387.
47. J. Chandrasekharan and H. C. Brown, *J. Org. Chem*, 1985, **50**, 518.
48. D. J. Parks, W. E. Piers and G. P. A. Yap, *Organometallics*, 1998, **17**, 5492.
49. K. K. Wang and H. C. Brown, *J. Org. Chem*, 1980, **45**, 5303.
50. H. C. Brown, C. G. Scouten and K. K. Wang, *J. Org. Chem*, 1979, **44**, 2589.
51. H. C. Brown and A. W. Moerikofer, *J. Am. Chem. Soc.*, 1961, **83**, 3417.
52. R. Thompson, B. L. Tran, S. Ghosh, C.-H. Chen, M. Pink, X. Gao, P. J. Carroll, M.-H. Baik and D. J. Mindiola, *Inorg. Chem.*, 2015, **54**, 3068.
53. D. Sieh, J. Schoffel and P. Burger, *Dalton Trans.*, 2011, **40**, 9512.
54. T. J. Crevier and J. M. Mayer, *Angew. Chem. Int. Ed.*, 1998, **37**, 1891.
55. T. E. Hanna, I. Keresztes, E. Lobkovsky, W. H. Bernskoetter and P. J. Chirik, *Organometallics*, 2004, **23**, 3448.
56. J. L. Polse, R. A. Andersen and R. G. Bergman, *J. Am. Chem. Soc.*, 1998, **120**, 13405.
57. C. C. Cummins, S. M. Baxter and P. T. Wolczanski, *J. Am. Chem. Soc.*, 1988, **110**, 8731.
58. C. P. Schaller, C. C. Cummins and P. T. Wolczanski, *J. Am. Chem. Soc.*, 1996, **118**, 591.
59. A. L. Reznichenko and K. C. Hultzsch, *Organometallics*, 2010, **29**, 24.

60. L. E. N. Allan, G. J. Clarkson, D. J. Fox, A. L. Gott and P. Scott, *J. Am. Chem. Soc.*, 2010, **132**, 15308.
61. K. Manna, A. Ellern and A. D. Sadow, *Chem. Commun.*, 2010, **46**, 339.
62. X. Liu, Z. i. Wu, H. Cai, Y. Yang, T. Chen, C. E. Vallet, R. A. Zuhr, D. B. Beach, Z.-H. Peng, Y.-D. Wu, T. E. Concolino, A. L. Rheingold and Z. Xue, *J. Am. Chem. Soc.*, 2001, **123**, 8011.
63. J. Y. Corey, *Chem. Rev.*, 2011, **111**, 863.
64. J. Y. Corey and J. Braddock-Wilking, *Chem. Rev.*, 1999, **99**, 175.
65. X. Chen, S. Lim, C. E. Plečnik, S. Liu, B. Du, E. A. Meyers and S. G. Shore, *Inorg. Chem.*, 2004, **43**, 692.
66. E. J. M. Hamilton, J. S. Park, X. Chen, S. Liu, M. R. Sturgeon, E. A. Meyers and S. G. Shore, *Organometallics*, 2009, **28**, 3973.
67. J. Knizek and H. Nöth, *Eur. J. Inorg. Chem.*, 2011, **2011**, 1888.
68. A. G. M. Barrett, M. R. Crimmin, M. S. Hill, P. B. Hitchcock and P. A. Procopiou, *Organometallics*, 2007, **26**, 4076.
69. F.-C. Liu, C. E. Plečnik, S. Liu, J. Liu, E. A. Meyers and S. G. Shore, *J. Organomet. Chem.*, 2001, **627**, 109.
70. E. Ding, B. Du, F.-C. Liu, S. Liu, E. A. Meyers and S. G. Shore, *Inorg. Chem.*, 2005, **44**, 4871.
71. M. Arrowsmith, T. J. Hadlington, M. S. Hill and G. Kociok-Kohn, *Chem. Commun.*, 2012, **48**, 4567.
72. A. L. Johnson, M. G. Davidson and M. F. Mahon, *Dalton Trans.*, 2007, 5405.
73. T. P. Fehlner, *Organometallics*, 2000, **19**, 2643.
74. H. C. Brown, B. Singaram and C. P. Mathew, *J. Org. Chem*, 1981, **46**, 2712.
75. D. Baudry, A. Dormond, B. Lachot, M. Visseaux and G. Zucchi, *J. Organomet. Chem.*, 1997, **547**, 157.
76. D. Barbier-Baudry, A. Dormond and M. Visseaux, *J. Organomet. Chem.*, 2000, **609**, 21.
77. W. J. Evans, J. M. Perotti and J. W. Ziller, *Inorg. Chem.*, 2005, **44**, 5820.
78. G. I. Nikonov, S. F. Vyboishchikov and O. G. Shirobokov, *J. Am. Chem. Soc.*, 2012, **134**, 5488.
79. K. Essalah, J.-C. Barthelat, V. Montiel, S. Lachaize, B. Donnadieu, B. Chaudret and S. Sabo-Etienne, *J. Organomet. Chem.*, 2003, **680**, 182.
80. D. J. Brauer and C. Kruger, *Acta. Cryst.*, 1973, **B29**, 1684.

81. K. Weitershaus, J. L. Fillol, H. Wadepohl and L. H. Gade, *Organometallics*, 2009, **28**, 4747.
82. I. A. Latham, G. J. Leigh, G. Huttner and I. Jibril, *J. Chem. Soc., Dalton Trans.*, 1986, 385.
83. R. Hemmer, U. Thewalt, D. L. Hughes, G. J. Leigh and D. G. Walker, *J. Organomet. Chem.*, 1987, **323**, C29.
84. D. L. Hughes, G. J. Leigh and D. G. Walker, *J. Chem. Soc., Dalton Trans.*, 1989, 1413.
85. D. L. Hughes, M. Jimenez-Tenorio, G. J. Leigh and D. G. Walker, *J. Chem. Soc., Dalton Trans.*, 1989, 2389.
86. B. Goetze, J. Knizek, H. Noth and W. Schnick, *Eur. J. Inorg. Chem.*, 2000, 1849.
87. J.-S. M. Lehn and D. M. Hoffman, *Inorg. Chim. Acta*, 2003, **345**, 327.
88. J. M. Pietryga, J. N. Jones, C. L. B. Macdonald, J. A. Moore and A. H. Cowley, *Polyhedron*, 2006, **25**, 259.
89. T. Kemmitt, G. J. Gainsford, N. I. Al-Salim, H. Robson-Marsden and D. V. Sevastyanov, *Aust. J. Chem.*, 2003, **56**, 1147.
90. D. Wang, R. Yu, N. Kumada and N. Kinomura, *Chem. Mater.*, 1999, **11**, 2008.
91. S. M. Damo, K.-C. Lam, A. Rheingold and M. A. Walters, *Inorganic Chemistry*, 2000, **39**, 1635.
92. A. C. Jones, P. A. Williams, J. F. Bickley, A. Steiner, H. O. Davies, T. J. Leedham, A. Awaluddin, M. E. Pemble and G. W. Critchlow, *J. Mater. Chem.*, 2001, **11**, 1428.
93. C. M. Crudden, Y. B. Hleba and A. C. Chen, *J. Am. Chem. Soc.*, 2004, **126**, 9200.
94. S. Pereira and M. Srebnik, *Tet. Letts.*, 1996, **37**, 3283.
95. R. R. Huddleston, D. F. Cauble and M. J. Krische, *J. Org. Chem*, 2003, **68**, 11.
96. I. P. Query, P. A. Squier, E. M. Larson, N. A. Isley and T. B. Clark, *J. Org. Chem*, 2011, **76**, 6452.
97. S. Pereira and M. Srebnik, *Organometallics*, 1995, **14**, 3127.
98. D. Männig and H. Nöth, *Angew. Chem. Int. Ed.*, 1985, **24**, 878.
99. S. Pereira and M. Srebnik, *J. Am. Chem. Soc.*, 1996, **118**, 909.
100. Y. R. Luo, *Comprehensive Handbook of Chemical Bond Energies*, CRC Press, FL, 2007.

101. A. S. Dudnik, V. L. Weidner, A. Motta, M. Delferro and T. J. Marks, *Nat. Chem.*, 2014, **6**, 1100.
102. W. Wang, Y. Lv, X. Gou, X. Leng and Y. Chen, *Chin. J. Chem.*, 2014, **32**, 752.
103. G. Dell'Amico, F. Marchetti and C. Floriani, *J. Chem. Soc. Dalton. Trans.*, 1982, 2197.
104. H. Helten, B. Dutta, J. R. Vance, M. E. Sloan, M. F. Haddow, S. Sproules, D. Collison, G. R. Whittell, G. C. Lloyd-Jones and I. Manners, *Angew. Chem. Int. Ed.*, 2013, **52**, 437.
105. D. J. Wolstenholme, K. T. Traboulsee, A. Decken and G. S. McGrady, *Organometallics*, 2010, **29**, 5769.
106. P. Binger, F. Sandmeyer and C. Krueger, *Organometallics*, 1995, **14**, 2969.
107. S. Mellino, unpublished work.
108. C. Das Neves Gomes, E. Blondiaux, P. Thuéry and T. Cantat, *Chem. - Eur. J.*, 2014, **20**, 7098.
109. B. Bentivegna, C. I. Mariani, J. R. Smith, S. Ma, A. L. Rheingold and T. J. Brunker, *Organometallics*, 2014, **33**, 2820.
110. T. D. Forster, H. M. Tuononen, M. Parvez and R. Roesler, *J. Am. Chem. Soc.*, 2009, **131**, 6689.
111. A. A. Macharashvili, V. E. Shklover, Y. T. Struchkov, A. Lapsiņa, G. Zelčāns and E. Lukevics, *J. Organomet. Chem.*, 1988, **349**, 23.
112. J. Woning and J. G. Verkade, *Organometallics*, 1991, **10**, 2259.
113. J. Woning, L. M. Daniels and J. G. Verkade, *J. Am. Chem. Soc.*, 1990, **112**, 4601.
114. P. L. Shutov, S. S. Karlov, K. Harms, D. A. Tyurin, M. V. Zabalov, A. V. Churakov, J. A. K. Howard, J. Lorberth and G. S. Zaitseva, *J. Mol. Struct.*, 2004, **689**, 261.

Chapter Five

Experimental details and characterising data

5.1 General methods and instrumentation

All manipulations were carried out using standard Schlenk line or dry-box techniques under an atmosphere of argon or dinitrogen. Solvents were either degassed by sparging with dinitrogen and dried by passing through a column of the appropriate drying agent[1] or refluxed over sodium (toluene), potassium (THF) or Na/K alloy (Et_2O) and distilled. Deuterated solvents were dried over sodium (C_6D_6 and toluene-d_8), potassium (THF-d_8), CaH_2 (C_6D_5Br) or P_2O_5 ($CDCl_3$ and CD_2Cl_2) distilled under reduced pressure and stored under argon in Teflon valve ampoules. Unless otherwise stated NMR samples were prepared under dinitrogen in 5 mm Wilmad 507-PP tubes fitted with J. Young Teflon valves. ^{1}H, $^{13}C\{^{1}H\}$, ^{11}B, $^{11}B\{^{1}H\}$, ^{19}F, ^{119}Sn, ^{29}Si and ^{2}H spectra were recorded on Bruker Ascend 400, Varian Mercury-VX 300, Bruker Avance III 500 NMR or on a Bruker AVC 500 spectrometer fitted with a ^{13}C cryoprobe. ^{1}H and $^{13}C\{^{1}H\}$ and spectra were referenced internally to residual protio-solvent (^{1}H) or solvent (^{13}C) resonances, and are reported relative to tetramethylsilane (δ = 0 ppm). ^{2}H NMR spectra were referenced to the natural abundance deuterium resonance of the protio solvent. ^{19}F, ^{11}B, ^{29}Si and ^{119}Sn were referenced externally to $CFCl_3$, $Et_2O{\cdot}BF_3$, $SiMe_4$ and $SnMe_4$ respectively. Assignments were confirmed as necessary with the use of two dimensional ^{1}H-^{1}H, ^{13}C-^{1}H, ^{19}F-^{19}F, ^{13}C-^{19}F and ^{1}H-^{29}Si NMR correlation experiments. Chemical shifts are quoted in δ (ppm) and coupling constants in Hz. IR spectra were recorded on a Thermo Scientific Nicolet iS5 FTIR spectrometer and samples prepared in a dry-box using NaCl plates as a Nujol mull or as a thin film. The data are quoted in wavenumbers (cm^{-1}). Mass spectra were recorded by the mass spectrometry service of Oxford University's Department of Chemistry. Elemental analyses were carried out by the Elemental Analysis Service at the London Metropolitan University.

5.2 Literature preparations

$Ti(NNPh_2)Cl_2(py)_3$ (**1.69**),[2] $H_2N_2^{iPr}N^{Me}$ (**3.1**),[3] $Li_2N_2^{iPr}N^{Me}$,[3] $Ti(N_2^{iPr}N^{Me})(NNPh_2)(py)$ (**2.1**),[4] $Ti(N_2^{iPr}N^{Me})(NNPh_2)(bipy)$ (**2.7**),[4] $Ti(NXyl)Cl_2(py)_3$ (**2.4**),[5] $Ti(NDipp)Cl_2(py)_3$ (**2.6**),[5] $HBMes_2$,[6] Mes_2SiCl_2,[7] Mes_2SnH_2,[8] $TMPAlH_2$,[9] $HCCC_6F_5$,[10, 11] $DCCC_6H_4CF_3$[12] were synthesised according to published procedures. Mes_2SiH_2 was synthesised according to a modified published procedure below.[13]

Mes_2SiH_2. To a stirred THF (10 mL) solution of Mes_2SiCl_2 (2.4 g, 7.11 mmol) at 0 °C was added a THF solution (10 mL) of $LiAlH_4$ (1.1 g, 28.4 mmol). The reaction mixture was allowed to warm to RT and stirred for 48 hours. The reaction was quenched with ethyl acetate (10 mL) and left to stir for 30 mins. The volatiles were removed under reduced pressure and the resultant solid extracted with toluene (2 x 10 mL). The combined organics were reduced to a third and the solution cooled to 0 °C resulting in precipitation of a white solid which was collected by filtration, washed with pentane and dried *in vacuo*. Yield: 1.5 g (80%). ^1H and ^{13}C NMR spectra were consistent with literature values.[13]

$Ti(N_2N^{py})(NNPh_2)(py)$ (**1.75**) was kindly donated by Dr Daniel Schofield. $PhSiD_3$, 4-$C_6H_4OMeSiH_3$, 3,5-$C_6H_3(CF_3)_2SiH_3$, $PhClSiH_2$ were kindly provided by Dr Pei Jen Tiong. MeCC-4-$C_6H_4CF_3$ and $Ti(N_2N^{Me})(NNPh_2)(py)$ (**1.72**) were kindly donated by Dr Laura Groom. $DCCC_6H_4Me$ was kindly donated by Dr Andrew Schwarz.

1,1-diphenylhydrazine was obtained from Sigma-Aldrich as the hydrogen chloride salt, from which the free hydrazine was obtained by basification, drying and removal of residual solvent, followed by distillation under inert atmospheric conditions. Deuteration of the 2,6-dimethylaniline forming D_2NXyl and of $HCCC_6F_5$ forming $DCCC_6F_5$ was carried out as detailed below. All other reagents were purchased from commercial suppliers and (for liquid reagents) degassed before use, unless specified otherwise. $PhSiH_3$, $Ar^{F_5}CN$, PhCCMe and HCCTol, H_2NXyl were dried over CaH_2 and distilled before use.

Procedure for deuteration of H_2NXyl. Air sensitive techniques were used throughout. To H_2NXyl (4g, 38.2 mmol) was added D_2O (20 mL) and the resulting mixture was stirred rapidly for 12 hours. The solution was allowed to settle. The top layer (D_2NXyl) was then decanted away, dried over CaH_2 and distilled. Yield: 2.8 mL (70%). ^1H NMR analysis indicated ≥98% deuteration.

Procedure for deuteration of $HCCC_6F_5$. To a stirred CH_2Cl_2 (5 mL) solution of $HCCC_6F_5$ (1.0 g, 5.21 mmol) was added D_2O (30 mL) and NaOD (40 % solution in D_2O, 0.020 mL, 0.27 mmol). The resultant mixture was left to stir for 3 days and then quenched with DCl (45 % solution in D_2O, 0.028 mL). The 2 layers were then separated and the aqueous layer was extracted with CH_2Cl_2 (2 x 10 mL). The combined organic layers were dried over Na_2SO_4 and then CH_2Cl_2 was removed

under reduced pressure. Yield: 0.8 g (79%). ^{1}H NMR analysis indicated ≥98% deuteration.

5.3 X-ray data collection and processing parameters

Crystals were mounted on glass fibers using perfluoropolyether oil and cooled rapidly in a stream of cold N_2 using an Oxford Cryosystems Cryostream unit. Diffraction data were measured using either an Enraf-Nonius KappaCCD or Agilent Technologies Supernova diffractometer using Mo-K_α or Cu-K_α radiation, respectively. As appropriate, absorption and decay corrections were applied to the data and equivalent reflections merged.[14, 15] The structures were solved with SIR92[16] or Superflip,[17] and further refinements and all other crystallographic calculations were performed using the CRYSTALS program suite.[18] Other details of the structure solution and refinements are given in the Supporting Information (CIF data – see CD Appendix).

5.4 Computational details

DFT calculations described in this Thesis were performed by Simona Mellino at The University of Oxford in collaboration with Dr Eric Clot at Université Montpellier. Geometry optimisations have been performed with the Gaussian09 package[19] at the B3PW91 level of hybrid density functional theory,[20, 21] with inclusion of Grimme's D3(bj) correction[22, 23] in the optimisation process. The titanium atom was represented by the relativistic effective core potential (RECP) from the Stuttgart group and the associated basis sets,[24] augmented by an f polarization function.[25] The remaining atoms (C, H, N, Si, B) were represented by a svp basis set.[26] The solvent (benzene) influence was taken into consideration through single point calculations on the gas-phase optimized geometry with SCRF calculations within the SMD model.[27] For the SCRF calculations the atoms were treated with a def2-tzvp basis set.[28] Influence of the dispersion forces was also considered by computing the D3(BJ) corrections as described by Grimme.[22, 23] All energies reported in the present work are Gibbs free energies obtained by summing the SMD energy, the gas-phase Gibbs contribution at 298 K and the D3(BJ) correction.

5.5 Experimental details and characterising data for Chapter Two

Ti($N_2^{iPr}N^{Me}$)(NXyl)(py) (1). To a stirred mixture of Ti(NXyl)Cl_2(py)$_3$ (**2.4**, 3.00 g, 6.31 mmol) and $Li_2N_2^{iPr}N^{Me}$ (1.35 g, 6.31 mmol), cooled to -78 °C, was added toluene (40 mL). The reaction was allowed to warm to RT. After 14 hours the volatiles were removed under reduced pressure and the dark brown crude was extracted in toluene (4 x 20 mL). The solution was concentrated by a third. The resulting powder was isolated by filtration and dried *in vacuo* affording **1** as an orange powder. Yield: 1.40 g (50 %). Diffraction-quality crystals were grown from a saturated benzene solution at RT. ^{1}H NMR (C_6D_6, 299.9 MHz, 298 K): δ 8.61 (2 H, d, ^3J = 4.9 Hz, *o*-C_5H_5N), 7.14 (2 H, d, ^3J = 7.8 Hz, *m*-$C_6H_3Me_2$), 6.77 (1 H, t, ^3J = 7.5 Hz, *p*-C_5H_5N), 6.72 (1 H, t, ^3J = 7.3 Hz, *p*-$C_6H_3Me_2$), 6.43 (2 H, m, *m*-C_5H_5N), 5.52 (2 H, app. sept., app. ^3J = 6.0 Hz, C<u>H</u>Me_2), 3.43 (2 H, m, ^{iPr}NC<u>H_2</u>) 3.18 (2 H, m, ^{iPr}NC<u>H_2</u>), 2.78 (2 H, m, ^{Me}NC<u>H_2</u>), 2.37 (6 H, s, C_6H_3<u>Me_2</u>), 2.11 (2 H, m, ^{Me}NC<u>H_2</u>), 1.46 (6 H, d, ^3J = 6.5 Hz, CH<u>Me_2</u>), 1.29 (6 H, d, ^3J = 6.5 Hz, CH<u>Me_2</u>), 1.29 (3 H, s, NMe) ppm.^{13}C{^{1}H} NMR (C_6D_6, 75.4 MHz, 298 K): δ 157.7 (*i*-$C_6H_3Me_2$), 149.0 (*o*-C_5H_5N), 137.5 (*p*-C_5H_5N), 130.7 (*o*-$C_6H_3Me_2$), 127.2 (*m*-$C_6H_3Me_2$), 123.7 (*m*-C_5H_5N), 115.9 (*p*-$C_6H_3Me_2$), 58.9 (<u>C</u>HMe_2), 56.8 (^{Me}NC<u>H_2</u>), 45.9 (^{iPr}NC<u>H_2</u>), 42.7 (NMe), 22.9 (CH<u>Me_2</u>), 22.5 (CH<u>Me_2</u>), 19.7 (NC_6H_3<u>Me_2</u>) ppm. IR (NaCl plates, Nujol mull, cm^{-1}): 1600 (w), 1583 (w), 1405 (m), 1351 (m), 1319 (m), 1306 (m), 1259 (w), 1153 (w), 1091 (w), 1069 (m), 1041 (w), 1030 (w), 997 (w), 821 (m), 754 (w), 702 (w). EI-MS: *m/z* = 445 [M]$^+$ (25%). Anal. found (calcd. for $C_{24}H_{39}N_5Ti$): C, 64.56 (64.71); H, 8.91 (8.82); N, 15.61 (15.72)%.

Ti($N_2^{iPr}N^{Me}$)(NXyl)(2,2'-bipyridine) (2). To a solution of Ti($N_2^{iPr}N^{Me}$)(NXyl))(py) (**1**, 0.150 g, 0.337 mmol) in benzene (2 mL) was added a solution of 2,2'-bipyridine (0.052 g, 0.337 mmol) in benzene (2 mL) at RT. Over the course of 20 h a red precipitate formed. The supernatant was decanted and the dark red solid washed with pentane (2 × 2 mL) and dried *in vacuo* affording **2**. Yield: 0.050 g (30 %). Dark red diffraction-quality crystals of **2** were obtained from a saturated benzene solution at RT. ^{1}H NMR (C_6D_6, 299.9 MHz, 298 K): δ 9.69 (2 H, d, ^3J =5.1 Hz, 6-NC_5H_4), 8.08 (2 H, d, ^3J =7.8 Hz, 3-NC_5H_4), 7.97 (2 H, app. t, app. ^3J = 7.5 Hz, 4-NC_5H_4), 7.48 (2 H, app. t, app. ^3J = 6.0 Hz, 5-NC_5H_4), 6.52 (2 H, d, ^3J = 7.2 Hz, *m*-$C_6H_3Me_2$), 6.10 (1 H, t, ^3J = 7.2 Hz, *p*-$C_6H_3Me_2$), 5.38 (2 H, app. sept., app. ^3J = 6.3 Hz, C<u>H</u>Me_2), 3.31-3.16 (4H, overlapping 2 x m, ^{iPr}NC<u>H_2</u> and ^{iPr}NC<u>H_2</u>), 2.69 (2 H, m, ^{Me}NC<u>H_2</u>), 2.11 (2

H, m, $^{Me}NCH_2$), 1.82 (6 H, s, $C_6H_3Me_2$), 1.33 (6 H, d, ^3J = 6.3 Hz, $CHMe_2$), 1.29 (6 H, d, ^3J = 6.3 Hz, $CHMe_2$), 1.28 (3 H, s, NMe) ppm. $^{13}C\{^1H\}$ NMR (C_6D_6, 75.4 MHz, 298 K): δ 157.6 (*i*-$C_6H_3Me_2$), 154.9 (6-NC_5H_4), 153.5 (2-NC_6H_4), 139.1 (4-NC_6H_4) 133.0 (*o*-$C_6H_3Me_2$), 127.1 (*m*-$C_6H_3Me_2$), 125.1 (5-NC_5H_4), 120.7 (3-NC_5H_4), 114.2 (*p*-$C_6H_3Me_2$), 59.3 ($CHMe_2$), 58.5 ($^{Me}NCH_2$), 44.9 ($^{iPr}NCH_2$), 43.7 (NMe), 23.7 ($CHMe_2$), 21.9 ($CHMe_2$), 19.6 ($C_6H_3Me_2$) ppm. IR (NaCl plates, Nujol mull, cm^{-1}): 1595 (w), 1301 (m), 1260 (s), 1151 (m), 1093 (m), 1016 (m), 800 (s). EI-MS: *m/z* = 366 $[M - C_{10}H_8N_2]^+$ (25 %). Anal. found (calcd. for $C_{29}H_{42}N_6Ti$): C, 66.72 (66.66); H, 8.25 (8.10); N, 15.99 (16.08)%.

Ti($N_2^{iPr}N^{Me}$)(NDipp)(py) (3). To a stirred mixture of Ti{N(2,6-$C_6H_3(CHMe_2)_2$)}$Cl_2(py)_3$ (**2.6**, 1.00 g, 1.88 mmol) and $Li_2N_2^{iPr}N^{Me}$ (0.401 g, 1.88 mmol), cooled to -78 °C, was added toluene (20 mL). The reaction was allowed to warm to RT. After 2 hours the volatiles were removed under reduced pressure and the dark orange crude was extracted in benzene (2 x 20 mL). The volatiles were removed under reduced pressure and the remaining solid was washed with hexane and dried *in vacuo* affording **3** as a yellow powder. Yield: 0.600 g (64 %). ^1H NMR (C_6D_6, 400.1 MHz, 298 K): δ 8.65 (2 H, d, ^3J = 5.0 Hz, *o*-C_5H_5N), 7.16 (2 H, d, ^3J = 7.4 Hz, *m*-$C_6H_3(CHMe_2)_2$), 6.87 (1 H, t, ^3J = 7.4 Hz, *p*-$C_6H_3(CHMe_2)_2$), 6.81 (1 H, t, ^3J = 7.8 Hz, *p*-C_5H_5N), 6.48 (2 H, app. t, app. ^3J = 7.8 Hz, *m*-C_5H_5N), 5.67 (2 H, app. sept., app. ^3J = 6.5 Hz, $CHMe_2$), 3.97 (2 H, sept., ^3J = 7.4 Hz, $C_6H_3(CHMe_2)_2$), 3.39 (2 H, m, $^{iPr}NCH_2$), 3.16 (2 H, m, $^{iPr}NCH_2$), 2.75 (2 H, m, $^{Me}NCH_2$), 2.09 (2 H, m, $^{Me}NCH_2$), 1.44 (6 H, d, ^3J = 6.5 Hz, $CHMe_2$), 1.32 (6 H, d, ^3J = 6.5 Hz, $CHMe_2$), 1.25 (12 H, d, ^3J = 7.4 Hz, $C_6H_3(CHMe_2)_2$), 1.21 (3 H, s, NMe) ppm. $^{13}C\{^1H\}$ NMR (C_6D_6, 100.6 MHz, 298 K): δ 154.6 (*i*-$C_6H_3(CHMe_2)_2$), 149.1 (*o*-C_5H_5N), 142.1 (*o*-$C_6H_3(CHMe_2)_2$), 137.5 (*p*-C_5H_5N), 123.7 (*m*-C_5H_5N), 122.1 (*m*-$C_6H_3(CHMe_2)_2$), 117.0 (*p*-$C_6H_3(CHMe_2)_2$), 58.4 ($CHMe_2$), 56.7 ($^{Me}NCH_2$), 45.4 ($^{Me}NCH_2$), 42.6 (NMe), 27.2 ($C_6H_3(CHMe_2)_2$), 24.5 ($C_6H_3(CHMe_2)_2$), 23.5 ($CHMe_2$), 22.4 ($CHMe_2$) ppm. IR (NaCl plates, Nujol mull, cm^{-1}): 1583 (w), 1573 (w), 1568 (w), 1542 (m), 1340 (w), 1261 (m), 1151 (w), 668 (s). Anal. found (calcd. for $C_{28}H_{47}N_5Ti$): C, 66.87 (67.05); H, 9.35 (9.45); N, 13.81 (13.96)%.

Ti($N_2^{iPr}N^{Me}$)(NDipp)(bipy) (4). To a stirred solution of Ti($N_2^{iPr}N^{Me}$)(NDipp)(py) (**3**, 0.118 g, 0.235 mmol) in benzene (2 mL) was added a solution of 2,2'-bipyridine (0.037 g, 0.235mmol) in benzene (2 mL) at RT. Over the course of 20 h a dark green

precipitate formed. The supernatant was decanted and the dark green solid washed with cold pentane (2 × 2 mL) and dried *in vacuo* affording **4**. Yield 0.060 g (45 %). ^{1}H NMR (C_6D_6, 400.1 MHz, 298 K): δ 9.75 (2 H, d, ^{3}J = 5.4 Hz, 6-NC_5H_4), 7.05-7.01 (4 H, overlapping 2 x m, 3-NC_5H_4 and *m*-$C_6H_3(CHMe_2)_2$), 6.94 (2 H, td, ^{3}J = 7.6 Hz, ^{4}J = 1.8 Hz, 3-NC_5H_4), 6.75 (1 H, t, ^{3}J = 7.4 Hz, *p*-$C_6H_3(CHMe_2)_2$), 6.69 (2 H, m, 4-NC_5H_4), 5.74 (2 H, app. sept., app. ^{3}J = 6.5 Hz, C<u>H</u>Me_2), 4.20 (2 H, sept., ^{3}J = 6.9 Hz, $C_6H_3(C\underline{H}Me_2)_2$), 3.38 (2 H, m, $^{iPr}NC\underline{H}_2$), 3.23 (2 H, m, $^{iPr}NC\underline{H}_2$), 2.55 (2 H, m, $^{Me}NC\underline{H}_2$), 1.87 (2 H, m, $^{Me}NC\underline{H}_2$), 1.69 (6 H, d, ^{3}J = 6.5 Hz, CH<u>Me</u>$_2$), 1.55 (6 H, d, ^{3}J = 6.5 Hz, CH<u>Me</u>$_2$), 1.00 (12 H, d, ^{3}J = 6.9 Hz, $C_6H_3(CH\underline{Me}_2)_2$), 0.92 (3 H, s, NMe) ppm. $^{13}C\{^{1}H\}$ NMR (C_6D_6, 100.6 MHz, 298 K): δ 154.7 (overlapping 6-NC_5H_4 and *i*-$C_6H_3(CHMe_2)_2$), 152.9 (2-NC_5H_4), 144.0 (*o*-$C_6H_3(CHMe_2)_2$), 127.8 (4-NC_5H_4), 124.4 (5-NC_5H_4), 123.9 (*m*-$C_6H_3(CHMe_2)_2$), 119.8 (3-NC_5H_4), 116.7 (*p*-$C_6H_3(CHMe_2)_2$), 58.6 ($^{Me}N\underline{C}H_2$), 58.6 (<u>C</u>HMe_2), 45.2 ($^{iPr}N\underline{C}H_2$), 43.4 (NMe), 26.7 ($C_6H_3(\underline{C}HMe_2)_2$), 25.3 ($C_6H_3(CH\underline{Me}_2)_2$), 23.7 (CH<u>Me</u>$_2$), 22.7 (CH<u>Me</u>$_2$) ppm. IR (NaCl plates, Nujol mull, cm^{-1}): 1600 (w), 1334 (w), 1276 (w), 1260 (m), 1154 (m), 1079 (m), 1021 (m), 886 (w), 797 (m), 755 (s). Anal. found (calcd. for $C_{33}H_{50}N_6Ti$): C, 68.36 (68.50); H, 8.80 (8.71); N, 14.50 (14.52)%.

Ti($N_2^{iPr}N^{Me}$)(NHXyl)$_2$ (5). To a stirred solution of Ti($N_2^{iPr}N^{Me}$)(NXyl)(py) (**1**, 0.290 g, 0.651 mmol) in benzene was added a solution of 2,6-dimethylaniline (0.212 mL, 1.30 mmol) in benzene (3 mL). After stirring for 2 hours at RT the volatiles were removed under reduced pressure. Hexane was added (10 mL) and the solution was left at -30 °C. Red diffraction-quality crystals of **5** were obtained from this hexane solution by filtration. Yield: 0.050 g (16 %). ^{1}H NMR (C_6D_6, 299.9 MHz, 298 K): δ 8.45 (1 H, s, axial NH), 7.65 (1 H, s, equatorial NH), 7.11 (2 H, d, ^{3}J = 7.1 Hz, equatorial *m*-$C_6H_3Me_2$), 7.06 (2 H, d, ^{3}J = 7.4 Hz, axial *m*-$C_6H_3Me_2$), 6.81 (1 H, t, ^{3}J = 7.1 Hz, equatorial *p*-$C_6H_3Me_2$), 6.76 (1 H, t, ^{3}J = 7.4 Hz, axial *p*-$C_6H_3Me_2$), 4.81 (2 H, app. sept., app. ^{3}J = 6.0 Hz, C<u>H</u>Me_2), 3.21 (2 H, m, $^{iPr}NC\underline{H}_2$), 2.94 (2 H, m, $^{iPr}NC\underline{H}_2$), 2.77 (2 H, m, $^{Me}NC\underline{H}_2$), 2.45 (6 H, s, equatorial $C_6H_3\underline{Me}_2$), 2.36 (6 H, s, axial $C_6H_3\underline{Me}_2$), 2.29 (2 H, m, $^{Me}NC\underline{H}_2$), 1.93 (3 H, s, NMe), 1.01 (6 H, d, ^{3}J = 6.0 Hz, CH<u>Me</u>$_2$), 0.94 (6 H, d, ^{3}J = 6.0 Hz, CH<u>Me</u>$_2$) ppm. ^{13}C NMR (C_6D_6, 75.4 MHz, 298 K): δ 153.7 (equatorial *i*-$C_6H_3Me_2$), 152.9 (axial *i*-$C_6H_3Me_2$), 129.1 (axial *m*-$C_6H_3Me_2$), 128.9 (equatorial *m*-$C_6H_3Me_2$), 125.5 (axial *o*-$C_6H_3Me_2$), 124.7 (equatorial *o*-$C_6H_3Me_2$), 119.0 (axial *p*-$C_6H_3Me_2$), 118.8 (equatorial *p*-$C_6H_3Me_2$), 57.2 (<u>C</u>HMe_2),

56.5 (^{Me}N<u>C</u>H$_2$), 47.0 (^{iPr}N<u>C</u>H$_2$), 45.2 (NMe), 21.8 (CH<u>Me</u>$_2$) 21.1 (CH<u>Me</u>$_2$) 20.8 (equatorial C$_6$H$_3$<u>Me</u>$_2$), 20.3 (axial C$_6$H$_3$<u>Me</u>$_2$) ppm. IR (NaCl plates, Nujol mull, cm^{-1}): 3583 (w, ν(N-H)), 3293 (w, ν(N-H)), 1590 (w), 1260 (m), 1098 (m), 1021 (m), 799 (m), 753 (w). Anal. found (calcd. for C$_{27}$H$_{45}$N$_5$Ti): C, 66.46 (66.51); H, 9.40 (9.30); N, 14.28 (14.36)%.

Ti(N$_2^{iPr}$N^{Me})(NHXyl)(NPh$_2$) (6). To a solution of Ti(N$_2^{iPr}$N^{Me})(NXyl)(py) (**1**, 0.133 g, 0.299 mmol) in benzene (3 mL) was added a solution of diphenylamine (0.051 g, 0.299 mmol) in benzene (2 mL) all at RT. After 1 h the volatiles were removed under reduced pressure to afford dark orange sticky solid which was then redissolved in benzene (2 mL), left to stir for 15 mins and the volatiles removed under reduced pressure. The resultant orange oil was triturated with hexane (2 mL) and filtered, yielding **6** as an orange powder which was then dried *in vacuo*. Yield: 0.052 g (35 %). The ^{1}H NMR spectrum indicated an approximately 65:35% mixture of the *cis* and *trans* isomers. Diffraction-quality crystals of **6** were obtained from a saturated benzene solution at RT.

Major isomer (cis): ^{1}H NMR (C$_6$D$_6$, 400.1 MHz, 298 K): δ 7.83 (1 H, br. s, NH), 7.13-7.12 (8 H, overlapping 2 x m, *o*-C$_6$H$_5$ and *m*-C$_6$H$_5$), 6.91 (2 H, d, ^3J = 7.4 Hz, *m*-C$_6$H$_3$Me$_2$), 6.81 (2 H, m, *p*-C$_6$H$_5$)), 6.68 (1 H, d, ^3J = 7.4 Hz, *p*-C$_6$H$_3$Me$_2$), 5.07 (2 H, app. sept., app. ^3J = 6.5 Hz, C<u>H</u>Me$_2$), 3.39 (2 H, m, ^{iPr}NC<u>H</u>$_2$), 3.0 (2 H, m, ^{iPr}NC<u>H</u>$_2$), 2.97 (2 H, m, ^{Me}NC<u>H</u>$_2$), 2.29 (2 H, m, ^{Me}NC<u>H</u>$_2$), 2.15 (6 H, s, C$_6$H$_3$<u>Me</u>$_2$), 1.85 (3 H, s, NMe), 1.11 (6 H, d, ^3J = 6.5 Hz, CH<u>Me</u>$_2$), 0.95 (6 H, d, ^3J = 6.5 Hz, CH<u>Me</u>$_2$) ppm. ^{13}C{^{1}H} NMR (C$_6$D$_6$, 100.6 MHz, 298 K): δ 155.8 (*i*-C$_6$H$_5$), 153.0 (*i*-C$_6$H$_3$Me$_2$), 128.7 (*m*-C$_6$H$_5$), 128.4 (*m*-C$_6$H$_3$Me$_2$), 124.9 (*o*-C$_6$H$_3$Me$_2$), 123.3 (*o*-NC$_6$H$_5$), 121.3 (*p*-NC$_6$H$_5$), 119.1 (*p*-C$_6$H$_3$Me$_2$), 56.3 (^{Me}N<u>C</u>H$_2$), 56.1 (<u>C</u>HMe$_2$), 46.9 (^{iPr}N<u>C</u>H$_2$), 45.8 (NMe), 23.3 (CH<u>Me</u>$_2$), 20.7 (CH<u>Me</u>$_2$), 20.6 (C$_6$H$_3$<u>Me</u>$_2$) ppm.

Minor isomer (trans):^{1}H NMR (C$_6$D$_6$, 400.1 MHz, 298 K): δ 8.34 (1 H, br. s, NH), 7.20 (4 H, dd, ^3J = 8.7 Hz ^4J = 1.1 Hz, *o*-C$_6$H$_5$), 7.16 (4 H, m, *m*-C$_6$H$_5$ overlapping with solvent), 7.05 (2 H, d, ^3J = 7.4 Hz, *m*-C$_6$H$_3$Me$_2$), 6.88 (2 H, t, ^3J = 7.4 Hz, *p*-NC$_6$H$_5$), 6.75 (1 H, m, *p*-C$_6$H$_3$Me$_2$), 4.74 (2 H, sept., app. ^3J = 6.5 Hz, C<u>H</u>Me$_2$), 3.19 (2 H, m, ^{iPr}NC<u>H</u>$_2$), 3.00 (2 H, m, ^{iPr}NC<u>H</u>$_2$), 2.78 (2 H, m, ^{Me}NC<u>H</u>$_2$), 2.53 (2 H, m, ^{Me}NC<u>H</u>$_2$), 2.44 (6 H, s, C$_6$H$_3$<u>Me</u>$_2$), 2.12 (3 H, s, NMe), 0.99 (6 H, d, ^3J = 6.5 Hz, CH<u>Me</u>$_2$), 0.66 (6 H, d, ^3J = 6.5 Hz, CH<u>Me</u>$_2$) ppm. ^{13}C{^{1}H} NMR (C$_6$D$_6$, 100.6 MHz, 298 K): δ 153.4 (*i*-C$_6$H$_3$Me$_2$), 153.3 (*i*-C$_6$H$_5$), 129.3 (*m*-C$_6$H$_5$), 129.3 (*m*-C$_6$H$_3$Me$_2$),

125.4 (*o*-$C_6H_3Me_2$), 123.3 (*o*-C_6H_5), 121.9 (*p*-C_6H_5), 118.2 (*p*-$C_6H_3Me_2$), 57.8 ($\underline{C}HMe_2$), 56.5 ($^{Me}N\underline{C}H_2$), 46.9 ($^{iPr}N\underline{C}H_2$), 44.9 (NMe), 22.7 ($CH\underline{Me}_2$), 21.4 ($C_6H_3\underline{Me}_2$), 20.4 ($CH\underline{Me}_2$) ppm.

Common data: IR (NaCl plates, Nujol mull, cm^{-1}): 3260 (w, ν(N–H)), 1590 (m), 1313 (w), 1284 (w), 1256 (m), 1192 (m), 1174 (w), 1158 (w), 1097 (m), 1071 (m), 1026 (m), 993 (w), 915 (w), 859 (m), 822 (s), 763 (w), 750 (m), 700 (w). Anal. found (calcd. for $C_{31}H_{45}N_5Ti$): C, 69.33 (69.52); H, 8.26 (8.47); N, 12.92 (13.08)%.

Ti($N^{iPr}NH^{iPr}N^{Me}$)($NNPh_2$)(NPh_2) (7). To a stirred solution of Ti($N_2^{iPr}N^{Me}$)($NNPh_2$)(py) (**2.1**, 0.100 g, 0.197 mmol) in benzene (3 mL) was added a solution of diphenylamine (0.033 g, 0.197 mmol) in benzene (2 mL) all at RT. After 1 h the volatiles were removed under reduced pressure to afford **7** as a pale brown sticky solid which was then triturated with hexane (2 mL), filtered and the resultant pale brown powder dried *in vacuo*. Yield: 0.085 g (72 %). ^{1}H NMR (C_6D_6, 400.1 MHz, 298 K): δ 7.27-7.15 (8 H, overlapping 4 x m, *o*-$N(C_6H_5)_2$, *o*-$NN(C_6H_5)_2$, *m*-$N(C_6H_5)_2$ and *m*-$NN(C_6H_5)_2$), 6.88-6.77 (4 H, overlapping 2 x m, *p*-$N(C_6H_5)_2$ and *p*-$NN(C_6H_5)_2$), 4.42 (1 H, app. sept., app. ^3J = 6.5 Hz, $NC\underline{H}Me_2$), 3.63 (1 H, m, $^{iPr}NC\underline{H}_2CH_2N^{Me}$), 3.37 (1 H, d. sept., ^3J = 5.7 Hz, ^3J = 6.5 Hz, $NHC\underline{H}Me_2$), 3.05 (1 H, m, $^{iPr}NC\underline{H}_2CH_2N^{Me}$), 2.57 (1 H, m, $^{iPr}NCH_2C\underline{H}_2N^{Me}$), 2.52 (3 H, s, NMe), 2.43 (1 H, m, $^{iPr}NCH_2C\underline{H}_2N^{Me}$), 2.12 (1 H, m, NH), 1.95 (2 H, m, $^{iPr}NHC\underline{H}_2CH_2N^{Me}$), 1.80 (2 H, m, $^{iPr}NHCH_2C\underline{H}_2N^{Me}$), 1.32 (3 H, d, ^3J = 6.5 Hz, $NCH\underline{Me}_2$), 1.13 (3 H, d, ^3J = 6.5 Hz, $NCH\underline{Me}_2$), 0.71 (3 H, d, ^3J = 6.5 Hz, $NHCH\underline{Me}_2$), 0.59 (3 H, d, ^3J = 6.5 Hz, $NHCH\underline{Me}_2$) ppm. $^{13}C\{^1H\}$ NMR (C_6D_6, 100.6 MHz, 298 K): δ 156.9 (*i*-$N(C_6H_5)_2$), 146.9 (*i*-$NN(C_6H_5)_2$), 128.8 (*o*-$NN(C_6H_5)_2$), 128.5 (*o*-$N(C_6H_5)_2$), 121.6 (*m*-$NN(C_6H_5)_2$), 121.4 (*p*-$N(C_6H_5)_2$), 119.0 (*m*-$N(C_6H_5)_2$), 118.7 (*p*-$NN(C_6H_5)_2$), 60.4 ($^{iPr}NCH_2\underline{C}H_2N^{Me}$), 56.2 ($^{iPr}NHCH_2\underline{C}H_2N^{Me}$), 51.7 ($N\underline{C}HMe_2$), 49.3 ($NH\underline{C}HMe_2$), 47.6 (NMe), 44.3 ($^{iPr}N\underline{C}H_2CH_2N^{Me}$), 39.5 ($^{iPr}NH\underline{C}H_2CH_2N^{Me}$), 22.6 ($NCH\underline{Me}_2$), 22.5 ($NCH\underline{Me}_2$), 22.2 ($NHCH\underline{Me}_2$), 19.2 ($NHCH\underline{Me}_2$) ppm. IR (NaCl plates, Nujol mull, cm^{-1}): 3236 (w, ν(N–H)), 1583 (s), 1557 (w), 1543 (m), 1318 (w), 1261 (w), 1202 (m), 1152 (m), 1096 (s), 1024 (s), 998 (w), 849 (m), 801 (w), 746 (w), 668 (m). Satisfactory elemental analysis could not be obtained.

NMR tube scale synthesis of Ti($N^{iPr}NH^{iPr}N^{Me}$)($NNPh_2$)($NTol_2$) (8). To a solution of Ti($N_2^{iPr}N^{Me}$)($NNPh_2$)(py) (**2.1**, 0.02 g, 0.039 mmol) in C_6D_6 (0.3 mL) in an NMR tube equipped with a J. Young Teflon valve was added $HNTol_2$ (0.0078 mg, 0.067 mmol)

in C_6D_6 (0.3 mL) at RT. The reaction was monitored by ^{1}H NMR spectroscopy. After 1 h the volatiles were removed under reduced pressure and the resultant mixture dried *in vacuo* before being redissolved in C_6D_6 (0.6 mL). ^{1}H NMR spectroscopy showed Ti($N^{iPr}NH^{iPr}N^{Me}$)($NNPh_2$)($NTol_2$) (**8**) was the only product. Compound **8** was subsequently characterised by ^{1}H and ^{13}C NMR spectroscopy at RT. ^{1}H NMR (C_6D_6, 400.1 MHz, 298 K): δ 7.29 (4 H, d, ^3J = 8.1 Hz, *o*-C_6H_5), 7.23 (4 H, d, ^3J = 8.3 Hz, *o*-C_6H_4Me), 7.18 (4 H, m, *m*-C_6H_5), 7.01 (4 H, d, ^3J = 8.3 Hz, *m*-C_6H_4Me), 6.87 (2 H, t, ^3J = 7.3 Hz, *p*-C_6H_5), 4.43 (1 H, app. sept., app. ^3J = 6.4 Hz, NC<u>H</u>Me_2), 3.67 (1 H, m, $^{iPr}NC\underline{H}_2CH_2N^{Me}$), 3.42 (1 H, d. sept., ^3J = 5.8, 6.4 Hz, N<u>H</u>CHMe_2), 3.10 (1 H, m, $^{iPr}NC\underline{H}_2CH_2N^{Me}$), 2.59 (1 H, m, $^{iPr}NCH_2C\underline{H}_2N^{Me}$), 2.53 (3 H, s, NMe), 2.46 (1 H, m, $^{iPr}NCH_2C\underline{H}_2N^{Me}$), 2.19 (6 H, s, $C_6H_4\underline{Me}$), 2.13 (1 H, m, NH), 1.98 (2 H, m, $^{iPr}NHC\underline{H}_2CH_2N^{Me}$), 1.82 (2 H, m, $^{iPr}NHCH_2C\underline{H}_2N^{Me}$), 1.36 (3 H, d, ^3J = 6.4 Hz, NCH$\underline{Me}_2$), 1.17 (3 H, d, ^3J = 6.4 Hz, NCH$\underline{Me}_2$), 0.76 (3 H, d, ^3J = 6.4 Hz, NHCH$\underline{Me}_2$), 0.60 (3 H, d, ^3J = 6.4 Hz, NHCH$\underline{Me}_2$) ppm. $^{13}C\{^1H\}$ NMR (C_6D_6, 100.6 MHz, 298 K): δ 155.1 (*p*-C_6H_4Me), 147.4 (*i*-C_6H_5), 129.8 (*m*-C_6H_4Me), 128.9 (*m*-C_6H_5), 127.6 (*i*-C_6H_4Me), 121.9 (*o*-C_6H_4Me), 121.8 (*p*-C_6H_5), 119.4 (*o*-C_6H_5), 60.8 ($^{iPr}NCH_2\underline{C}H_2N^{Me}$), 55.6 ($^{iPr}NHCH_2\underline{C}H_2N^{Me}$), 52.2 (N<u>C</u>$HMe_2$), 49.7 (NH<u>C</u>$HMe_2$), 48.0 (NMe), 44.8 ($^{iPr}N\underline{C}H_2CH_2N^{Me}$), 40.0 ($^{iPr}NH\underline{C}H_2CH_2N^{Me}$), 23.0 (NCH$\underline{Me}_2$), 23.0 (NCH$\underline{Me}_2$), 22.6 (NHCH$\underline{Me}_2$), 20.8 (N($C_6H_4\underline{Me}$)$_2$), 19.7 (NHCH$\underline{Me}_2$) ppm.

Ti($N^{iPr}NH^{iPr}N^{Me}$)($NNPh_2$)(OC_6H_2-2,6-^{t}Bu-4-Me) (9). To a stirred solution of Ti($N_2^{iPr}N^{Me}$)($NNPh_2$)(py) (**2.1**, 0.155g, 0.304 mmol) in benzene (3 mL) was added a solution of butylated hydroxytoluene (0.067 g, 0.304 mmol) in benzene (2 mL) all at RT. After 1 h the volatiles were removed under reduced pressure to afford **9** as a dark red sticky solid which was then triturated with hexane (2 mL), filtered and the resultant red powder dried *in vacuo*. Yield: 0.098 g (49 %). Diffraction-quality crystals of **9** were grown from a saturated benzene solution at RT. ^{1}H NMR (C_6D_6, 400.1 MHz, 298 K): δ 7.45 (1 H, s, *m*-$C_6\underline{H}_2(CMe_3)_2Me$), 7.36-7.34 (5 H, overlapping 1 x m and 1 x s, *o*-C_6H_5 and *m*-$C_6\underline{H}_2(CMe_3)_2Me$), 7.02 (4 H, t, ^3J = 7.3 Hz, *m*-C_6H_5), 6.81 (2 H, t, ^3J = 6.7 Hz, *p*-C_6H_5), 5.77 (1 H, app. sept., app. ^3J = 6.5 Hz, NC<u>H</u>Me_2), 3.90 (1 H, app. sept., app. ^3J = 6.8 Hz, NHC<u>H</u>Me_2), 3.43 (1 H, m, $^{iPr}NC\underline{H}_2CH_2N^{Me}$), 2.84 (1 H, m, $^{iPr}NC\underline{H}_2CH_2N^{Me}$), 2.50 (3 H, s, $C_6H_2(CMe_3)_2\underline{Me}$), 2.25-1.94 (6 H overlapping 6 x m, $^{iPr}NCH_2C\underline{H}_2N^{Me}$, $^{iPr}NHC\underline{H}_2CH_2N^{Me}$, $^{iPr}NHCH_2C\underline{H}_2N^{Me}$ and N<u>H</u>CHMe_2), 2.16 (3 H, s, NMe), 1.74 (10 H, overlapping 1 x s and 1 x m, CMe_3 and

^{iPr}NHCH$_2$C$\underline{H}_2$N^{Me}), 1.57 (9 H, s, CMe$_3$), 1.33 (3 H, d, ^3J = 6.5 Hz, NCH$\underline{Me}_2$), 1.25 (3 H, d, ^3J = 6.5 Hz, NCH$\underline{Me}_2$), 0.92 (3 H, d, ^3J = 6.8 Hz, NHCH$\underline{Me}_2$), 0.71 (3 H, d, ^3J = 6.8 Hz, NHCH$\underline{Me}_2$) ppm. ^{13}C{^{1}H} NMR (C_6D_6, 100.6 MHz, 298 K): δ 164.5 (*i*-$\underline{C}_6H_2(CMe_3)_2Me$), 147.3 (*i*-$C_6H_5$), 138.3 (*o*-$\underline{C}_6H_2(CMe_3)_2Me$), 135.4 (*o*-$\underline{C}_6H_2(CMe_3)_2Me$), 128.7 (*m*-$C_6H_5$), 127.1 (*m*-$\underline{C}_6H_2(CMe_3)_2Me$), 126.2 (*m*-$\underline{C}_6H_2(CMe_3)_2Me$), 124.6 (*p*-$\underline{C}_6H_2(CMe_3)_2Me$), 122.0 (*p*-$C_6H_5$), 120.9 (*o*-$C_6H_5$), 62.2 (N$\underline{C}HMe_2$), 59.1 (^{iPr}NCH$_2\underline{C}H_2$N^{Me}), 56.2 (^{iPr}NHCH$_2\underline{C}$H$_2$N^{Me}), 53.3 (NH$\underline{C}$HMe$_2$), 45.2 (^{iPr}N$\underline{C}$H$_2$CH$_2$N^{Me}), 44.2 (NMe), 38.4 (^{iPr}NH$\underline{C}$H$_2$CH$_2$N^{Me}), 38.9 ($\underline{C}$Me$_3$), 35.5 ($\underline{C}$Me$_3$), 33.0 (C$\underline{Me}_3$), 32.3 (C$\underline{Me}_3$), 23.2 (NCH$\underline{Me}_2$), 21.7 (overlapping NCH$\underline{Me}_2$ and $C_6H_2(CMe_3)_2\underline{Me}$), 21.4 (NHCH$\underline{Me}_2$), 20.0 (NHCH$\underline{Me}_2$) ppm. IR (NaCl plates, Nujol mull, cm^{-1}): 3279 (w, ν(N–H)), 3246 (w, ν(N–H), 3246 (w), 1594 (s), 1583 (s), 1487 (s), 1413 (s), 1333 (w), 1294 (m), 1277 (m), 1243 (s), 1159 (s), 1080 (w), 1063 (m), 1014 (s), 993 (m), 831 (s), 808 (m), 745 (m). IR (NaCl cell, C_6H_6, cm^{-1}): 3250 (w, ν(N–H)). Anal. found (calcd. for $C_{38}H_{59}N_5OTi$): C, 70.01 (70.24); H, 9.26 (9.15); N, 10.53 (10.78)%.

NMR tube scale synthesis of Ti(N$_2$^{iPr}N^{Me}){N(Xyl)C(Me)C(4-C$_6$H$_4$F)} (10). To a solution of Ti(N$_2$^{iPr}N^{Me})(NXyl)(py) (**1**, 30.0 mg, 0.067 mmol) in C_6D_6 (0.3 mL) in an NMR tube equipped with a J. Young Teflon valve was added MeCC-4-C_6H_4F (9.1 mg, 0.067 mmol) in C_6D_6 (0.3 mL) at RT. The reaction was monitored by ^{1}H NMR spectroscopy. After 1 h the volatiles were removed under reduced pressure and the resultant mixture dried *in vacuo* before being redissolved in C_6D_6 (0.6 mL). ^{1}H NMR spectroscopy showed Ti(N$_2$^{iPr}N^{Me}){N(Xyl)C(Me)C(4-C$_6$H$_4$F)} (**10**) and **1** in 30:70% ratio. Compound **10** was subsequently characterised by ^{1}H, ^{19}F and ^{13}C NMR spectroscopy at RT. ^{1}H NMR (C_6D_6, 400.1 MHz, 298 K): δ 7.08-6.99 (7 H, overlapping 4 x m, *m*-$C_6H_3Me_2$, *p*-$C_6H_3Me_2$, *o*-C_6H_4F and *m*-C_6H_4F), 4.58 (2 H, app. sept., app. ^3J = 6.7 Hz, C$\underline{H}$Me$_2$), 3.02 (4 H, m, ^{iPr}NC$\underline{H}_2$), 2.62 (2 H, m, ^{Me}NC$\underline{H}_2$), 2.19 (2 H, m, ^{Me}NC$\underline{H}_2$), 2.16 (6 H, s, $C_6H_3\underline{Me}_2$), 1.96 (3 H, s, TiCC$\underline{Me}$), 1.73 (3 H, s, NMe), 1.15 (6 H, d, ^3J = 6.7 Hz, C$\underline{H}$Me$_2$), 1.13 (6 H, d, ^3J = 6.7 Hz, C$\underline{H}$Me$_2$) ppm. ^{13}C{^{1}H} NMR (C_6D_6, 100.6 MHz, 298 K): δ 203.9 (TiC), 167.8 (TiC$\underline{C}$), 149.4 (*i*-$C_6H_3Me_2$), 144.7 (d, $^4J_{C\text{-}F}$ = 3.2 Hz, *i*-C_6H_4F), 134.6 (*o*-$C_6H_3Me_2$), 133.6 (d, $^3J_{C\text{-}F}$ = 8.2 Hz, *o*-C_6H_4F), 128.1 (overlapping with solvent *m*-$C_6H_3Me_2$), 124.8 (*p*-$C_6H_3Me_2$), 115.7 (d, $^2J_{C\text{-}F}$ = 22.9 Hz, *m*-C_6H_4F), 56.3 (^{Me}N$\underline{C}$H$_2$), 52.7 ($\underline{C}$HMe$_2$), 46.6 (^{iPr}NC$\underline{H}_2$), 43.1 (NMe), 22.9 (CH$\underline{Me}_2$), 22.5 (CH$\underline{Me}_2$), 18.9 ($C_6H_3\underline{Me}_2$), 16.6 (TiCC$\underline{Me}$) ppm.

Resonances attributed to *p*-C_6H_4F were not observed. ^{19}F NMR (C_6D_6, 376.5 MHz, 298 K): δ -121.9 (1F) ppm.

NMR tube scale synthesis of Ti($N_2^{iPr}N^{Me}$){N(Xyl)C(Me)C(4-$C_6H_4CF_3$)} (11). To a solution of Ti($N_2^{iPr}N^{Me}$)(NXyl)(py) (**1**, 30.0 mg, 0.067 mmol) in C_6D_6 (0.3 mL) in an NMR tube equipped with a J. Young Teflon valve was added MeCC-4-$C_6H_4CF_3$ (12.4 mg, 0.067 mmol) in C_6D_6 (0.3 mL) at RT. The reaction was monitored by ^1H NMR spectroscopy. After 1 h the volatiles were removed under reduced pressure and the resultant mixture dried *in vacuo* before being redissolved in C_6D_6 (0.6 mL). This was repeated and ^1H NMR spectroscopy showed Ti($N_2^{iPr}N^{Me}$){N(2,6-$C_6H_3Me_2$)C(Me)C(4-$C_6H_4CF_3$)} (**11**) and **1** in 70:30% ratio. Compound **11** was subsequently characterised by ^1H, ^{19}F and ^{13}C NMR spectroscopy at RT. ^1H NMR (C_6D_6, 299.9 MHz, 298 K): δ 7.57 (2 H, d, ^3J = 8.5 Hz, *m*-$C_6H_4CF_3$), 7.14 (2 H, d, ^3J = 8.5 Hz, *o*-$C_6H_4CF_3$), 7.08-6.99 (3 H, overlapping 2 x m, *m*-$C_6H_3Me_2$ and *p*-$C_6H_3Me_2$), 4.58 (2 H, app. sept., app. ^3J = 6.3 Hz, C<u>H</u>Me_2), 2.99 (4 H, m, $^{iPr}NC\underline{H}_2$), 2.60 (4 H, m, $^{Me}NC\underline{H}_2$), 2.13 (6 H, s, $C_6H_3\underline{Me}_2$), 1.92 (3 H, s, TiCC<u>Me</u>), 1.69 (3 H, s, NMe), 1.12 (6 H, d, ^3J = 6.3 Hz, CH$\underline{Me}_2$), 1.09 (6 H, d, ^3J = 6.3 Hz, CH$\underline{Me}_2$) ppm. $^{13}C\{^1H\}$ NMR (C_6D_6, 75.4 MHz, 298 K): δ 201.3 (TiC), 167.8 (TiC<u>C</u>), 151.7 (*i*-$C_6H_4CF_3$), 148.8 (*i*-$C_6H_3Me_2$), 134.4 (*o*-$C_6H_3Me_2$), 126.4 (*p*-$C_6H_3Me_2$), 128.1 (overlapping with solvent *o*-$C_6H_4CF_3$), 128.1 (overlapping with solvent *m*-$C_6H_3Me_2$), 125.4 (q, $^3J_{C\text{-}F}$ = 3.8 Hz, *m*-$C_6H_4CF_3$), 118.9 (q, $^2J_{C\text{-}F}$ = 12.5 Hz, *p*-$C_6H_4CF_3$), 56.3 ($^{Me}N\underline{C}H_2$), 52.6 (<u>C</u>HMe_2), 46.5 ($^{iPr}N\underline{C}H_2$), 42.1 (NMe), 22.8 (CH$\underline{Me}_2$), 22.4 (CH$\underline{Me}_2$), 18.9 ($C_6H_3\underline{Me}_2$), 16.6 (TiCC<u>Me</u>) ppm. Resonances attributable to carbons directly bound to ^{19}F atoms were not observed. ^{19}F NMR (C_6D_6, 282.1 MHz, 298 K): δ -61.1 (3F) ppm.

NMR tube scale synthesis of Ti($N_2^{iPr}N^{Me}$){N(Xyl)C(Me)C(4-C_6H_4Me)} (12). To a solution of Ti($N_2^{iPr}N^{Me}$)(NXyl)(py) (**1**, 27.0 mg, 0.061 mmol) in C_6D_6 (0.3 mL) in an NMR tube equipped with a J. Young Teflon valve was added MeCC-4-C_6H_4Me (0.039 mL, 0.301 mmol) in C_6D_6 (0.3 mL) at RT. The reaction was monitored by ^1H NMR spectroscopy. After 2 h the volatiles were removed under reduced pressure and the resultant mixture dried *in vacuo* before being redissolved in C_6D_6 (0.6 mL). ^1H NMR spectroscopy showed Ti($N_2^{iPr}N^{Me}$){N(Xyl)C(Me)C(4-C_6H_4Me)} (**12**) and **1** in 55:45% ratio. Compound **12** was subsequently characterised by ^1H and ^{13}C NMR spectroscopy at RT. ^1H NMR (C_6D_6, 400.1 MHz, 298 K): δ 7.09-7.07 (4 H,

overlapping 2 x m, *m*-$C_6H_3Me_2$ and *m*-C_6H_4Me)), 7.01-6.96 (3 H, overlapping 2 x m, *p*-$C_6H_3Me_2$ and *o*-C_6H_4Me), 4.69 (2 H, app. sept., app. ^3J = 6.3 Hz, C$\underline{H}$$Me_2$), 3.05 (4 H, m, ^{iPr}NC$\underline{H}_2$), 2.64 (2 H, m, ^{Me}NC$\underline{H}_2$), 2.25 (3 H, s, $C_6H_4\underline{Me}$), 2.21 (2 H, m, ^{Me}NC$\underline{H}_2$), 2.19 (6 H, s, $C_6H_3\underline{Me}_2$), 2.07 (3 H, s, TiCC$\underline{Me}$), 1.76 (3 H, s, NMe), 1.18 (12 H, app. t, app. ^3J = 6.3 Hz, CH$\underline{Me}_2$) ppm. $^{13}C\{^1H\}$ NMR (C_6D_6, 100.6 MHz, 298 K): δ 206.1 (TiC), 167.4 (TiC$\underline{C}$), 149.0 (*i*-$C_6H_3Me_2$), 145.5 (*p*-C_6H_4Me), 134.3 (*o*-$C_6H_3Me_2$), 131.3 (*m*-C_6H_4Me), 128.8 (*p*-$C_6H_3Me_2$), 128.1 (overlapping with solvent *m*-$C_6H_3Me_2$), 124.3 (*o*-C_6H_4Me), 56.0 (^{Me}N$\underline{C}H_2$), 52.2 ($\underline{C}HMe_2$), 46.2 (^{iPr}N$\underline{C}H_2$), 41.8 (NMe), 22.5 (CH$\underline{Me}_2$), 22.2 (CH$\underline{Me}_2$), 20.9 ($C_6H_4\underline{Me}$), 18.6 ($C_6H_3\underline{Me}_2$), 16.4 (TiCC($\underline{Me}$)) ppm. The resonances attributable to *i*-C_6H_4Me was not observed.

NMR tube scale synthesis of Ti($N_2^{iPr}N^{Me}$){N(Xyl)C(Me)C(4-C_6H_4OMe)} (13). To a solution of Ti($N_2^{iPr}N^{Me}$)(NXyl)(py) (**1**, 30.0 mg, 0.067 mmol) in C_6D_6 (0.3 mL) in an NMR tube equipped with a J. Young Teflon valve was added MeCC-4-C_6H_4OMe (29.5 mg, 0.202 mmol) in C_6D_6 (0.3 mL) at RT. The reaction was monitored by ^1H NMR spectroscopy. After 2 h the volatiles were removed under reduced pressure and the resultant mixture dried *in vacuo* before being redissolved in C_6D_6 (0.6 mL). ^1H NMR spectroscopy showed Ti($N_2^{iPr}N^{Me}$){N(Xyl)C(Me)C(C_6H_4OMe)} (**13**) and **1** in 40:60% ratio. Compound **13** was subsequently characterised by ^1H and ^{13}C NMR spectroscopy at RT. ^1H NMR (C_6D_6, 400.1 MHz, 298 K): δ 7.18 (2 H, d, ^3J = 8.9 Hz, *o*-C_6H_4OMe), 7.09 (2 H, d, ^3J = 7.5 Hz, *m*-$C_6H_3Me_2$), 7.01 (1 H, m, *p*-$C_6H_3Me_2$), 6.99 (2 H, d, ^3J = 8.9 Hz, *m*-C_6H_4OMe), 4.67 (2 H, app. sept., app. ^3J = 6.3 Hz, C$\underline{H}$$Me_2$), 3.42 (3 H, s, OMe), 3.07 (4 H, m, ^{iPr}NC$\underline{H}_2$), 2.66 (2 H, m, ^{Me}NC$\underline{H}_2$), 2.19 (6 H, s, $C_6H_3\underline{Me}_2$), 2.13 (2 H, m, ^{Me}NC$\underline{H}_2$), 2.08 (3 H, s, TiCC$\underline{Me}$), 1.77 (3 H, s, NMe), 1.21 (6 H, d, ^3J = 6.3 Hz, CH$\underline{Me}_2$), 1.18 (6 H, d, ^3J = 6.3 Hz, CH$\underline{Me}_2$) ppm. $^{13}C\{^1H\}$ NMR (C_6D_6, 100.6 MHz, 298 K): δ 206.4 (TiC), 167.9 (TiC$\underline{C}$), 156.30 (*p*-C_6H_4OMe), 149.5 (*i*-$C_6H_3Me_2$), 141.6 (*i*-C_6H_4OMe), 134.7 (*o*-$C_6H_3Me_2$), 128.1 (overlapping with solvent *o*-C_6H_4OMe), 127.5 (*m*-$C_6H_3Me_2$), 124.6 (*p*-$C_6H_3Me_2$), 114.0 (*m*-C_6H_4OMe), 56.4 (^{Me}N$\underline{C}H_2$), 54.9 (OMe), 52.6 ($\underline{C}HMe_2$), 46.7 (^{iPr}N$\underline{C}H_2$), 42.2 (NMe), 23.0 (CH$\underline{Me}_2$), 22.6 (CH$\underline{Me}_2$), 19.0 ($C_6H_3\underline{Me}_2$), 16.8 (TiCC$\underline{Me}$) ppm.

NMR tube scale synthesis of Ti($N_2^{iPr}N^{Me}$){N(Xyl)C(Me)C(Ph)} (14). To a solution of Ti($N_2^{iPr}N^{Me}$)(NXyl)(py) (**1**, 30.0 mg, 0.067 mmol) in C_6D_6 (0.3 mL) in an NMR tube equipped with a J. Young Teflon valve was added MeCCPh (23.5 mg, 0.202 mmol) in C_6D_6 (0.3 mL) at RT. The reaction was monitored by ^1H NMR

spectroscopy. After 2 h the volatiles were removed under reduced pressure and the resultant mixture dried *in vacuo* before being redissolved in C_6D_6 (0.6 mL). ^{1}H NMR spectroscopy showed Ti($N_2^{iPr}N^{Me}$){N(Xyl)C(Me)C(Ph)} (**14**) and **1** in 40:60% ratio. Compound **14** was subsequently characterised by ^{1}H and ^{13}C NMR spectroscopy at RT. ^{1}H NMR (C_6D_6, 400.1 MHz, 298 K): δ 7.46 (1 H, dd, ^3J = 7.8, 1.7 Hz, *p*-C_6H_5), 7.38 (2 H, app. t, app. ^3J = 7.8 Hz, *m*-C_6H_5), 7.26 (2 H, dd, , ^3J = 7.8, 1.7 Hz, *o*-C_6H_5), 7.13 (2 H, m, *m*-$C_6H_3Me_2$), 7.07 (1 H, m, *p*-$C_6H_3Me_2$), 4.68 (2 H, app. sept., app. ^3J = 6.6 Hz, C$\underline{H}$$Me_2$), 3.04 (4 H, m, ^{iPr}NC$\underline{H}_2$), 2.64 (2 H, m, ^{Me}NC$\underline{H}_2$), 2.20 (2 H, m, ^{Me}NC$\underline{H}_2$), 2.18 (6 H, s, $C_6H_3\underline{Me}_2$), 2.04 (3 H, s, TiCC$\underline{Me}$), 1.75 (3 H, s, NMe), 1.17 (6 H, d, ^3J = 6.6 Hz, CH$\underline{Me}_2$), 1.16 (6 H, d, ^3J = 6.6 Hz, CH$\underline{Me}_2$) ppm. ^{13}C{^{1}H} NMR (C_6D_6, 100.6 MHz, 298 K): δ 205.8 (TiC), 167.6 (TiC$\underline{C}$), 149.3 (*i*-C_6H_5), 148.7 (*i*-$C_6H_3Me_2$), 134.6 (*o*-$C_6H_3Me_2$), 131.9 (*p*-C_6H_5), 126.6 (*o*-C_6H_5), 56.4 (^{Me}N$\underline{C}$$H_2$), 52.6 ($\underline{C}HMe_2$), 46.6 (^{iPr}N$\underline{C}$$H_2$), 42.2 (NMe), 22.9 (CH$\underline{Me}_2$), 22.6 (CH$\underline{Me}_2$), 18.9 ($C_6H_3\underline{Me}_2$), 16.8 (TiCC$\underline{Me}$) ppm. Resonances attributable to *m*-$\underline{C}_6H_3Me_2$, *p*-$\underline{C}_6H_3Me_2$ and *m*-C_6H_5 were not observed.

Ti($N_2^{iPr}N^{Me}$){N(Xyl)C(Me)C(H)C(C_6H_3F)} (15). To a stirred solution of Ti($N_2^{iPr}N^{Me}$)(NXyl)(py) (**1**, 0.119 g, 0.260 mmol) in benzene (3 mL) was added MeCC-4-C_6H_4F (0.036 g, 0.260 mmol) in benzene (3 mL). The solution was heated to 70 °C and left to react for 16 h. The volatiles were removed under reduced vacuum to yield a red sticky solid. **15** was obtained as a red powder following trituration with hexane which was then dried *in vacuo*. Yield 0.040 g (30 %). Diffraction-quality crystals were grown from a saturated hexane solution at RT. ^{1}H NMR (C_6D_6, 299.9 MHz, 298 K): δ 7.42 (1H, dd, *J* = 8.4, 2.8 Hz, TiCC(H)C(F)C($\underline{H}$)C(H)), 7.36 (1H, dd, *J* = 8.4, 5.0 Hz, TiCC(H)C(F)C(H)C($\underline{H}$)), 6.97-6.85 (4 H, overlapping 3 x m, *m*-$C_6\underline{H}_3Me_2$, *p*-$C_6H_3Me_2$, and TiCC($\underline{H}$)C(F)C(H)C(H)), 6.21 (1 H, s, TiN(Xyl)C(Me)C$\underline{H}$), 4.82 (2H, app. sept., app. ^3J = 6.8 Hz, C$\underline{H}$$Me_2$), 3.16 (2 H, m, ^{iPr}N$\underline{C}$$H_2$), 3.03 (2 H, m, ^{iPr}NCH_2), 2.70 (2 H, m, ^{Me}NCH_2), 2.15 (2 H, m, ^{Me}NCH_2), 2.06 (3 H, s, NMe), 2.01 (6 H, s, $C_6H_3\underline{Me}_2$), 1.81 (3 H, s, TiN(Xyl)C($\underline{Me}$)) 1.01 (6 H, d, ^3J = 6.8 Hz, CH$\underline{Me}_2$), 0.66 (6 H, d, ^3J = 6.8 Hz, CH$\underline{Me}_2$) ppm. ^{13}C{^{1}H} NMR (C_6D_6, 75.4 MHz, 298 K): δ 203.0 (Ti$\underline{C}$), 156.8 (d, $^1J_{C\text{-}F}$ = 249 Hz, CF), 149.9 (*i*-$\underline{C}_6H_3Me_2$), 142.6 (TiN(Xyl)$\underline{C}$(Me)C(H)), 140.6 (TiC(C_4F)$\underline{C}$C(H)), 133.5 (*o*-$\underline{C}_6H_3Me_2$), 131.4 (d, $^3J_{C\text{-}F}$ = 6.0 Hz, TiCC(H)C(F)C(H)$\underline{C}$(H)), 128.8 (*m*-$\underline{C}_6H_3Me_2$), 124.5 (*p*-$\underline{C}_6H_3Me_2$), 118.1 (d, $^2J_{C\text{-}F}$ = 16.6 Hz, TiCC(H)C(F)$\underline{C}$(H)C(H)), 114.0 (d, $^2J_{C\text{-}}$

$_F$ = 20.8 Hz, TiC<u>C</u>(H)C(F)C(H)C(H)), 111.0 (TiN(Xyl)C(Me)<u>C</u>H), 57.6 (^{Me}N<u>C</u>H$_2$), 51.8 (<u>C</u>HMe$_2$) 47.3 (^{iPr}N<u>C</u>H$_2$), 44.1 (NMe), 22.9 (TiN(Xyl)C(<u>Me</u>)C(H)), 21.7 (CH<u>Me</u>$_2$), 21.7 (CH<u>Me</u>$_2$), 19.6 (C$_6$H$_3$<u>Me</u>$_2$) ppm. ^{19}F NMR (C$_6$D$_6$, 282.1 MHz, 298 K): δ -124.3 (1F) ppm. IR (NaCl plates, Nujol mull, cm^{-1}): 1574 (w), 1344 (w), 1259 (m), 1211 (m), 1179 (w), 1161 (m), 1076 (m), 1021 (s), 997 (w), 873 (s), 799 (s), 762 (m). Anal. found (calcd. for C$_{28}$H$_{41}$FN$_4$Ti): C, 66.82 (67.19); H, 8.33 (8.26); N, 11.27 (11.19)%.

Ti(N$_2^{iPr}$N^{Me}){N(Xyl)C(Me)C(H)C(C$_6$H$_3$CF$_3$)} (16). To a stirred solution of Ti(N$_2^{iPr}$N^{Me})(NXyl)(py) (**1**, 0.200 g, 0.450 mmol) in benzene (3 mL) was added MeCC-4-C$_6$H$_3$CF$_3$ (0.082 g, 0.450 mmol) in benzene (3 mL). The solution was heated to 70 °C and left to react for 16 h. The volume of solution was then reduced by half and left at -80 °C for 2 hours, during which a red precipitate formed. The supernatant was decanted and the resulted red solid washed with a minimal amount of cold pentane (2 x 2 mL) to afford **16** as a red powder, which was dried *in vacuo.* Yield 0.074 g (30 %). The ^{1}H NMR spectrum indicated an approximately 90:10 mixture of the *trans* and *cis* isomers. Diffraction-quality crystals were grown from a saturated hexane solution at RT.

Major isomer (trans): ^{1}H NMR (C$_6$D$_6$, 299.9 MHz, 298 K): δ 8.04 (1 H, s, TiCC(<u>H</u>)C(CF$_3$)C(H)C(H)), 7.43 (1 H, d, ^3J = 8.5 Hz, TiCC(H)C(CF$_3$)C(<u>H</u>)C(H)), 7.37 (1 H, d, ^3J = 8.5, TiCC(H)C(CF$_3$)C(H)C(<u>H</u>)), 6.94-6.87 (3 H, overlapping 2 x m, *m*-C$_6$<u>H</u>$_3$Me$_2$ and *p*-C$_6$<u>H</u>$_3$Me$_2$), 6.22 (1 H, s, TiN(Xyl)C(Me)C<u>H</u>)), 4.77 (2 H, app. sept., app. ^3J = 6.7 Hz, C<u>H</u>Me$_2$), 3.15 (2 H, m, ^{iPr}NC<u>H</u>$_2$), 3.00 (2 H, m, ^{iPr}NC<u>H</u>$_2$), 2.70 (2 H, m, ^{Me}NC<u>H</u>$_2$), 2.17 (2 H, m, ^{Me}NC<u>H</u>$_2$), 2.11 (3 H, s, NMe), 1.96 (6 H, s, C$_6$H$_3$<u>Me</u>$_2$), 1.79 (3 H, s, TiN(Xyl)C(<u>Me</u>)), 1.00 (6 H, d, ^3J = 6.7 Hz, CH<u>Me</u>$_2$), 0.64 (6 H, d, ^3J = 6.7 Hz, CH<u>Me</u>$_2$) ppm. ^{13}C{^{1}H} NMR (C$_6$D$_6$, 75.4 MHz, 298 K): δ 200.2 (TiC), 149.4 (*i*-<u>C</u>$_6$H$_3$Me$_2$), 147.8 (TiC(C$_4$CF$_3$)<u>C</u>C(H)), 145.4 (TiN(Xyl)<u>C</u>(Me)), 133.5 (*o*-C$_6$H$_3$Me$_2$), 129.7 (TiCC(H)C(CF$_3$)C(H)<u>C</u>(H)), 129.2 (q, $^4J_{C\text{-}F}$ = 3.8 Hz, TiC<u>C</u>(H)C(CF$_3$)), 128.3 (*m*-C$_6$H$_3$Me$_2$), 124.8 (*p*-C$_6$H$_3$Me$_2$), 123.0 (q, $^4J_{C\text{-}F}$ = 3.9, TiCC(H)C(CF$_3$)<u>C</u>(H)C(H)), 119.4 (q, $^3J_{C\text{-}F}$ = 28.0 Hz, TiCC(H)<u>C</u>(CF$_3$)C(H)C(H)), 110.7 (TiN(Xyl)C(CH$_3$)<u>C</u>H)), 57.6 (^{Me}N<u>C</u>H$_2$), 51.9 (<u>C</u>HMe$_2$), 47.4 (^{iPr}N<u>C</u>H$_2$), 44.3 (NMe), 23.2 (TiN(C$_6$H$_3$Me$_2$)C(<u>C</u>H$_3$)CH)), 21.7 (CH<u>Me</u>$_2$), 21.5 (CH<u>Me</u>$_2$), 19.5 (TiN(C$_6$H$_3$<u>Me</u>$_2$) ppm. The resonance attributable to the carbon atom directly bound to

the ^{19}F atom was not observed. ^{19}F NMR (C_6D_6, 282.1 MHz, 298 K): δ -60.4 (3F) ppm.

Minor isomer (cis): ^{1}H NMR (C_6D_6, 299.9 MHz, 298 K): δ 7.78 (1 H, s, TiCC(H)C(CF_3)), 7.47-7.36 (2 H, overlapping 2 x m, TiCC(H)C(CF_3)C(H)C(H)) and TiCC(H)C(CF_3)C(H)C(H)) 6.94-6.87 (3 H, overlapping 2 x m, *m*-$C_6H_3Me_2$ and *p*-$C_6H_3Me_2$), 6.21 (1 H, s, TiN(Xyl)C(Me)C(H)C(H)), 4.57 (2 H, m, C$H$$Me_2$), 3.30 (2 H, m, NC$H_2$), 2.78 (2 H, m, NC$H_2$), 2.60 (2 H, m, NC$H_2$), 2.38 (2 H, m, NC$H_2$), 2.10 (6 H, s, $C_6H_3Me_2$), 1.75 (s, 3 H, TiN(Xyl)C(Me)), 1.62 (3 H, s, NMe), 0.77 (6 H, d, ^{3}J = 6.0 Hz, CHMe_2), 0.69 (6 H, d, ^{3}J = 6.0 Hz, CHMe_2) ppm. ^{19}F NMR (C_6D_6, 282.1 MHz, 298 K): δ -60.3 (3F) ppm.

Common data: IR (NaCl plates, Nujol mull, cm^{-1}): 1567 (w), 1317 (s), 1260 (m), 1158 (w), 1105 (m), 1068 (m), 1020 (w), 800 (w). Anal. found (calcd. for $C_{29}H_{41}N_4F_3Ti$): C, 63.13 (63.27); H, 7.68 (7.51); N, 9.95 (10.18)%.

Ti($N_2^{iPr}N^{Me}$){NC(Ph)N(Xyl)}(py) (17). To a stirred solution of Ti($N_2^{iPr}N^{Me}$)(NXyl)(py) (**1**, 0.132 g, 0.296 mmol) in benzene (5 mL) was added PhCN (0.031 mL, 0.296 mmol) at RT. The solution was left to stir for 1 hour at RT after which the volume was reduced by half resulting in precipitation of a yellow powder. The supernatant was decanted and the yellow solid washed with pentane (2 × 2 mL) and dried *in vacuo*. Yield: 0.085 g (52 %). On dissolving the yellow powder in C_6D_6 or CD_2Cl_2 ^{1}H NMR spectroscopy showed **1** was observed as well as **17** in approximately a 50:50% ratio, as well as 0.5 equivs of liberated PhCN. Diffraction-quality crystals were grown from the slow cooling of a saturated benzene solution. ^{1}H NMR (CD_2Cl_2, 499.9 MHz, 298 K): δ 8.38 (2 H, dd, ^{3}J = 7.7 Hz, ^{4}J = 1.8 Hz, *o*-C_6H_5), 8.07 (2 H, d, ^{3}J = 4.8 Hz, *o*-C_5H_5N), 7.68 (1 H, m, *p*-C_5H_5N), 7.35-7.21 (3 H, overlapping 2 x m, *m*-C_6H_5 and *p*-C_6H_5), 6.37 (2 H, d, ^{3}J = 7.1 Hz, *m*-$C_6H_3Me_2$), 6.20 (1 H, t, ^{3}J = 7.1 Hz, *p*-$C_6H_3Me_2$), 5.40 (2 H, app. sept., app. ^{3}J = 6.8 Hz, C$H$$Me_2$), 3.43 (2 H, m, ^{iPr}NCH_2), 3.19 (2 H, m, ^{iPr}NCH_2), 3.04 (2 H, m, ^{Me}NCH_2), 2.43 (2 H, m, ^{Me}NCH_2), 2.08 (6 H, s, $C_6H_3Me_2$), 1.40 (3 H, s, NMe), 1.10 (6 H, d, ^{3}J = 6.8 Hz, CHMe_2), 1.06 (6 H, d, ^{3}J = 6.8 Hz, CHMe_2) ppm. $^{13}C\{^{1}H\}$ NMR (CD_2Cl_2, 125.7 MHz, 298 K): δ 156.0 (*i*-C_6H_5), 152.3 (*i*-$C_6H_3Me_2$), 148.3 (*o*-C_5H_5N), 140.6 (TiNC(Ph)($NC_6H_3Me_2$), 138.2 (*p*-C_5H_5N), 129.3 (*o*-C_6H_5), 128.6 (*o*-$C_6H_3Me_2$), 128.3 (*p*-C_6H_5), 127.3 (*m*-C_6H_5), 126.6 (*m*-$C_6H_3Me_2$), 125.0 (*m*-C_5H_5N), 120.6 (*p*-$C_6H_3Me_2$), 59.7 (CHMe_2), 57.3 (^{Me}N$C$$H_2$), 45.7 (^{iPr}N$C$$H_2$), 43.1 (NMe), 22.9

(CH$\underline{Me}_2$), 21.9 (CH$\underline{Me}_2$), 18.4 ($C_6H_3\underline{Me}_2$) ppm. IR (NaCl plates, Nujol mull, cm^{-1}): 1602 (w), 1517 (m), 1348 (w), 1335 (w), 1296 (w), 1260 (m), 1089 (m), 1018 (m), 799 (m) 696 (w). Anal. found (calcd. for $C_{31}H_{44}N_6Ti$): C, 67.71 (67.87); H, 8.19 (8.08); N, 15.26 (15.32)%.

Ti($N_2^{iPr}N^{Me}$){NC(C_6F_5)N(Xyl)}(py) (18). To a stirred solution of Ti($N_2^{iPr}N^{Me}$)(NXyl)(py) (**1**, 0.100 g, 0.220 mmol) in benzene (5 mL) was added C_6F_5CN (0.028 mL, 0.220 mmol) at RT. Over the course of 30 mins a yellow precipitate formed. The supernatant was decanted and the yellow solid washed with pentane (2 × 2 mL) and dried *in vacuo* affording **18**. Yield 0.092 g (65 %). The ^{1}H NMR spectrum indicated approximately a 60:40 mixture of the *trans* and *cis* isomers.

Major isomer (trans): ^{1}H NMR (CD_2Cl_2, 499.9 MHz, 298 K): δ 8.08 (2 H, d, ^3J = 4.8 Hz, *o*-C_5H_5N)), 7.80 (1 H, t, ^3J = 7.6 Hz, *p*-C_5H_5N)), 7.29 (2 H, m, *m*-C_5H_5N)), 6.61 (2 H, d, ^3J = 7.2 Hz, *m*-$C_6H_3Me_2$), 6.51 (1 H, t, ^3J = 7.2 Hz, *p*-$C_6H_3Me_2$), 5.30 (2 H, app. sept., app. ^3J = 6.5 Hz, C$\underline{H}Me_2$), 3.27 (2 H, m, ^{iPr}NC$\underline{H}_2$), 3.13 (2 H, m, ^{iPr}NC$\underline{H}_2$), 2.97 (2 H, m, ^{Me}NC$\underline{H}_2$), 2.40 (2 H, m, ^{Me}NC$\underline{H}_2$), 2.10 (6 H, s, $C_6H_3\underline{Me}_2$), 1.48 (3 H, s, NMe), 1.04 (6 H, d, ^3J = 6.5 Hz, CH$\underline{Me}_2$), 0.91 (6 H, d, ^3J = 6.5 Hz, CH$\underline{Me}_2$) ppm. $^{13}C\{^1H\}$ NMR (CD_2Cl_2, 125.7 MHz, 298 K): δ 150.3 (*o*-$C_6H_3Me_2$), 148.8 (*o*-C_5H_5N), 146.1 (TiN$\underline{C}(C_6F_5)$), 144.0 (d, $^1J_{C\text{-}F}$ = 245.3 Hz, *o*-C_6F_5), 139.6 (d, $^1J_{C\text{-}F}$= 238.0 Hz, *p*-C_6F_5), 138.6 (*p*-C_5H_5N)), 137.7 (d, $^1J_{C\text{-}F}$= 253.4, *m*-C_6F_5), 129.1 (*i*-$C_6H_3Me_2$), 127.2 (*m*-$C_6H_3Me_2$), 125.1 (*m*-C_5H_5N)), 121.1 (*p*-$C_6H_3Me_2$), 119.2 (m, *i*-C_6F_5), 59.4 ($\underline{C}HMe_2$), 57.2 ($^{Me}N\underline{C}H_2$), 45.7 ($^{iPr}N\underline{C}H_2$), 43.4 (NMe), 22.7 (CH$\underline{Me}_2$), 21.6 (CH$\underline{Me}_2$), 18.5 ($C_6H_3\underline{Me}_2$) ppm. ^{19}F NMR (CD_2Cl_2, 282.1 MHz, 298 K): δ -143.8 (2F, m, *o*-C_6F_5), -162.0 (1F, m, *p*-C_6F_5), 164.9 (2F, m, *m*-C_6F_5) ppm.

Minor isomer (cis): ^{1}H NMR (CD_2Cl_2, 499.9 MHz, 298 K): δ 7.72 (2 H, d, ^3J = 4.8 Hz, *o*-C_5H_5N), 7.68 (1 H, t, ^3J = 7.6 Hz, *p*-C_5H_5N), 7.10 (2 H, m, *m*-C_5H_5N)), 7.06 (2 H, d, ^3J = 7.1 Hz, *m*-$C_6H_3Me_2$), 6.89 (1 H, t, ^3J = 7.1 Hz, *p*-$C_6H_3Me_2$), 3.72 (2 H, app. sept., app. ^3J = 6.5 Hz, C$\underline{H}Me_2$), 3.53 (2 H, m, ^{iPr}NC$\underline{H}_2$), 3.32 (2 H, m, ^{iPr}NC$\underline{H}_2$), 3.17 (2 H, m, ^{Me}NC$\underline{H}_2$), 2.56 (2 H, m, ^{Me}NC$\underline{H}_2$), 2.35 (6 H, s, $C_6H_3\underline{Me}_2$), 1.88 (3 H, s, NMe), 1.14 (6 H, d, ^3J = 6.5 Hz, CH$\underline{Me}_2$), 0.42 (6 H, d, ^3J = 6.5 Hz, CH$\underline{Me}_2$) ppm. $^{13}C\{^1H\}$ NMR (CD_2Cl_2, 125.7 MHz, 298 K): δ 152.2 (*o*-C_5H_5N) 151.3 (*o*-$C_6H_3Me_2$), 148.3 (TiN$\underline{C}(C_6F_5)$), 138.7 (*p*-C_5H_5N), 129.9 (d, $^1J_{C\text{-}F}$ = 240.0 Hz, *o*-C_6F_5) 130.5 (*i*-$C_6H_3Me_2$), 127.7 (*m*-$C_6H_3Me_2$), 124.4 (*m*-C_5H_5N), 121.3 (*p*-$C_6H_3Me_2$), 119.9 (m, *i*-C_6F_5), 59.8 ($^{Me}N\underline{C}H_2$), 50.8 ($\underline{C}HMe_2$), 45.9 ($^{iPr}N\underline{C}H_2$), 44.7 (NMe), 21.2 (CH$\underline{Me}_2$),

20.2 (CH$\underline{Me}_2$), 18.4 ($C_6H_3\underline{Me}_2$) ppm. ^{19}F NMR (CD_2Cl_2, 282.1 MHz, 298 K): δ -143.8 (2F, m, *o*-C_6F_5), -161.7 (1F, m, *p*-C_6F_5), -164.3 (2F, m, *p*-C_6F_5) ppm.

Common data : IR (NaCl plates, Nujol mull, cm^{-1}): 1525 (s), 1932 (w), 1364 (m), 1339 (w), 1294 (w), 1260 (w), 1108 (w), 983 (w). Anal. found (calcd. for $C_{31}H_{39}N_6F_5Ti$): C, 58.12 (58.30); H, 5.97 (6.16); N, 13.02 (13.16)%.

NMR tube scale synthesis of Ti($N_2^{iPr}N^{Me}$){NC(C_6F_5)N(Xyl)}(bipy) (19). To a solution of Ti($N_2^{iPr}N^{Me}$)(NXyl)(py) (**1**, 0.050 g, 0.112 mmol) in CD_2Cl_2 (0.3 mL) in an NMR tube equipped with a J. Young Teflon valve was added C_6F_5CN (0.0142 mL, 0.112 mmol) in CD_2Cl_2 (0.3 mL) at RT. The reaction was monitored by ^{1}H NMR spectroscopy. After 30 mins 2,2'-bipyridine (0.0175 mg, 0.112 mmol) was added at RT. After 6 hours the volatiles were removed under reduced pressure and the resultant mixture dried *in vacuo* before being redissolved in CD_2Cl_2 (0.6 mL). ^{1}H NMR spectroscopy indicated that **19** had formed quantitatively and was subsequently characterised by ^{1}H, ^{13}C and ^{19}F NMR spectroscopy. ^{1}H NMR (CD_2Cl_2, 499.9 MHz, 298 K): δ 9.15 (2 H, d, ^3J = 5.0 Hz, 3-NC_5H_4), 7.97 (2 H, t, ^3J = 8.1 Hz, 5-NC_5H_4), 7.92 (2 H, d, ^3J = 8.1 Hz, 6-NC_5H_4), 7.46 (2 H, t, ^3J = 5.0 Hz, 2-NC_5H_4), 6.60 (2 H, d, ^3J = 7.2 Hz, *m*-$C_6H_3Me_2$), 6.49 (1 H, t, ^3J = 7.2 Hz, *p*-$C_6H_3Me_2$), 4.86 (2 H, app. sept., app. ^3J = 6.5 Hz, C$\underline{H}Me_2$), 3.10 (4 H, m, $^{iPr}NC\underline{H}_2$), 2.64 (2 H, m, $^{Me}NC\underline{H}_2$), 2.08 (2 H, m, $^{Me}NC\underline{H}_2$), 1.91 (3 H, s, NMe), 1.11 (6 H, d, ^3J = 6.5 Hz, CH$\underline{Me}_2$), 0.94 (6 H, d, ^3J = 6.5 Hz, CH$\underline{Me}_2$) ppm. ^{13}C{^{1}H} NMR (CD_2Cl_2, 125.7 MHz, 298 K): δ 154.0 (6-NC_5H_4), 152.6 (1-NC_5H_4), 150.6 (*o*-$C_6H_3Me_2$), 139.2 (4-NC_5H_4), 129.1 (*i*-$C_6H_3Me_2$), 127.0 (*m*-$C_6H_3Me_2$), 125.4 (5-NC_5H_4), 120.9 (*p*-$C_6H_3Me_2$), 120.8 (3-NC_5H_4), 58.7 ($^{Me}N\underline{C}H_2$), 58.4 ($\underline{C}HMe_2$), 44.7 ($^{iPr}N\underline{C}H_2$), 43.9 (NMe), 22.7 (CH$\underline{Me}_2$), 21.7 (CH$\underline{Me}_2$), 18.4 ($C_6H_3\underline{Me}_2$) ppm. ^{19}F NMR (CD_2Cl_2, 282.1 MHz, 298 K): δ -143.8 (2F, m, *o*-C_6F_5), -163.2 (1F, m, *p*-C_6F_5), -164.9 (2F, m, *p*-C_6F_5) ppm.

Ti($N_2^{iPr}N^{Me}$){N(NPh_2)C(Ph)NC(Ph)N} (20). To a stirred solution of Ti($N_2^{iPr}N^{Me}$)($NNPh_2$)(py) (**2.1**, 0.300 g, 0.590 mmol) in benzene (5 mL) was added PhCN (0.121 mL, 1.18 mmol) at RT. The solution was then stirred at 70 °C for 3 hours. The volatiles were then removed under reduced pressure and the remaining sticky red solid was washed with a minimal amount of cold pentane (2 x 2 mL) yielding **20** as a dark red precipitate. Yield: 0.225 g (60 %). The ^{1}H NMR spectrum indicated an approximately 80:20% mixture of the *cis* and *trans* isomers. Diffraction-quality crystals were grown from a pentane solution at -30 °C.

Major isomer (cis): ^{1}H NMR (C_6D_6, 299.9 MHz, 298 K): δ 8.87 (2 H, d, ^{3}J = 7.8 Hz, TiNC(*o*-C_6H_5)), 7.27-7.22 (4 H, overlapping 2 x m, TiNC(*m*-C_6H_5) and TiNC(C_6H_5)NC(*o*-$C_6\underline{H}_5$), 7.18 (4 H, d, ^{3}J = 8.1 Hz, *o*-NN(C_6H_5)$_2$), 6.99 (4 H, m, *m*-NN(C_6H_5)$_2$), 6.92 (2 H, m, TiNC(C_6H_5)NC(*m*-$C_6\underline{H}_5$)), 6.83 (1 H, m, TiNC(*p*-C_6H_5)), 6.70-6.67 (3 H, overlapping 2 x m, *p*-NN(C_6H_5)$_2$ and TiNC(C_6H_5)NC(*p*-$C_6\underline{H}_5$)), 4.92 (2 H, app. sept., app. ^{3}J = 6.3 Hz, C$\underline{H}$Me$_2$), 3.18 (2 H, m, ^{iPr}NC$\underline{H}_2$), 2.94 (2 H, m, ^{iPr}NC$\underline{H}_2$), 2.64 (2 H, m, ^{Me}NC$\underline{H}_2$), 2.01 (3 H, s, NMe), 1.70 (2 H, m, ^{Me}NC$\underline{H}_2$), 1.36 (6 H, d, ^{3}J = 6.3 Hz, CH$\underline{Me}_2$), 1.08 (6 H, d, ^{3}J = 6.3 Hz, CH$\underline{Me}_2$) ppm. ^{13}C{^{1}H} NMR (C_6D_6, 75.4 MHz, 298 K): δ 177.0 (TiNC(C_6H_5)N$\underline{C}$(C_6H_5)), 164.2 (TiN$\underline{C}$(C_6H_5)NC(C_6H_5), 145.3 (*i*-NN(C_6H_5)$_2$), 140.8 (TiNC(*i*-C_6H_5)), 136.3 (TiNC(C_6H_5)NC(*i*-$\underline{C}_6H_5$)), 130.9 (TiNC(*m*-C_6H_5)), 129.9 (TiNC(*o*-C_6H_5)), 128.1 (*p*-NN(C_6H_5)$_2$), 128.1 (*o*-NN(C_6H_5)$_2$), 126.8 (TiNC(C_6H_5)NC(*m*-$\underline{C}_6H_5$)), 126.2 (TiNC(*p*-C_6H_5)), 120.8 (TiNC(C_6H_5)NC(*o*-$\underline{C}_6H_5$)), 120.2 (TiNC(C_6H_5)NC(*p*-$\underline{C}_6H_5$)), 118.4 (*o*-NN(C_6H_5)$_2$), 57.4 ($\underline{C}$HMe$_2$), 56.7 (^{Me}N$\underline{C}$H$_2$), 46.4 (^{iPr}N$\underline{C}$H$_2$), 43.6 (NMe), 24.4 (CH$\underline{Me}_2$), 21.4 (CH$\underline{Me}_2$) ppm.

Minor isomer (trans): ^{1}H NMR (C_6D_6, 299.9 MHz, 298 K): δ 8.75 (2 H, d, ^{3}J = 7.0 Hz, *o*-C$C_6\underline{H}_5$), 7.99 (2H, d, ^{3}J = 7.0 Hz, *o*-C$C_6\underline{H}_5$)), 7.24-6.69 (16 H, overlapping m, aromatic overlapping with major isomer), 4.57 (2 H, app. sept., app. ^{3}J = 6.4 Hz, C$\underline{H}$Me$_2$), 3.06 (4 H, m, ^{iPr}NC$\underline{H}_2$), 2.54 (2 H, m, ^{Me}NC$\underline{H}_2$), 2.21 (3 H, s, NMe), 2.18 (2 H, m, ^{Me}NC$\underline{H}_2$), 1.07 (6 H, d, ^{3}J = 6.3 Hz, CH$\underline{Me}_2$), 0.84 (6 H, d, ^{3}J = 6.3 Hz, CH$\underline{Me}_2$) ppm. ^{13}C{^{1}H} NMR (C_6D_6, 75.4 MHz, 298 K): δ 169.3 (N$\underline{C}$(C_6H_5)), 147.3 (*i*-NN(C_6H_5)$_2$), 141.1 (*i*-CC_6H_5), 137.2 (*i*-CC_6H_5)), 59.1 (^{Me}NC$\underline{H}_2$), 51.7 ($\underline{C}$HMe$_2$), 46.9 (^{iPr}NC$\underline{H}_2$), 42.4 (NMe), 22.3 (CH$\underline{Me}_2$), 20.6 (CH$\underline{Me}_2$) ppm. The remaining resonances were not observed.

Common data: IR (NaCl plates, Nujol mull, cm^{-1}): 1589 (m), 1518 (s), 1495 (s), 1260 (m), 1210 (w), 1155 (w), 1082 (w), 800 (m). Anal. found (calcd. for $C_{37}H_{45}N_7Ti$): C, 69.73 (69.91); H, 7.20 (7.14); N, 15.38 (15.42)%.

Ti($N_2^{iPr}N^{Me}$){N(NPh_2)C(Me)NC(Me)N} (21). To a stirred solution of Ti($N_2^{iPr}N^{Me}$)($NNPh_2$)(py) (**2.1**, 0.200 g, 0.390 mmol) in benzene (5 mL) was added MeCN (0.041 mL, 0.790 mmol) at RT. The solution was stirred at RT for 16 hours, filtered and the volatiles removed under reduced pressure to yield **21** as a dark brown powder. Yield: 0.151 g (75 %). The ^{1}H NMR spectrum indicated an approximately

80:20 mixture of the *cis* and *trans* isomers. Diffraction quality crystals were grown from a saturated ether solution at -30 °C.

Major isomer (cis): ^{1}H NMR (C_6D_6, 499.9 MHz, 298 K): δ 7.33 (4 H, app. dt, app. ^{3}J = 7.9 Hz, app. ^{4}J = 1.1 Hz, *o*-C_6H_5), 7.08 (4 H, t, ^{3}J = 7.2 Hz, *m*-C_6H_5), 6.75 (2 H, app. t, app. ^{3}J = 7.3 Hz, app. ^{4}J = 1.1 Hz, *p*-C_6H_5), 4.84 (2 H, app. sept., app. ^{3}J = 6.7 Hz, C<u>H</u>Me$_2$), 3.13 (2 H, m, ^{iPr}NC<u>H</u>$_2$), 2.89 (2 H, m, ^{iPr}NC<u>H</u>$_2$), 2.62 (2 H, m, ^{Me}NC<u>H</u>$_2$), 2.33 (3 H, s, TiNC(<u>Me</u>)), 2.16 (3H, s, TiN(NPh$_2$)C(<u>Me</u>)), 2.04 (3 H, s, NMe), 1.80 (2 H, m, ^{Me}NC<u>H</u>$_2$), 1.31 (6 H, d, ^{3}J = 6.7 Hz, CH<u>Me</u>$_2$), 1.12 (6 H, d, ^{3}J = 6.7 Hz, CH<u>Me</u>$_2$) ppm. ^{13}C{^{1}H} NMR (C_6D_6, 125.7 MHz, 298 K): δ 176.6 (TiN(NPh$_2$)<u>C</u>(Me)), 168.7 (TiN<u>C</u>(Me)), 144.9 (*i*-C_6H_5), 129.0 (*m*-C_6H_5), 120.9 (*p*-C_6H_5), 118.2 (*o*-C_6H_5), 57.5 (<u>C</u>HMe$_2$), 57.2 (^{Me}N<u>C</u>H$_2$), 46.7 (^{iPr}N<u>C</u>H$_2$), 44.0 (NMe), 24.4 (CH<u>Me</u>$_2$), 23.8 (TiNC(<u>Me</u>)), 22.7 (TiN(NPh$_2$)C(<u>Me</u>)), 22.1 (CH<u>Me</u>$_2$) ppm.

Minor isomer (trans): ^{1}H NMR (C_6D_6, 499.9 MHz, 298 K): δ 7.10-7.02 (6 H, overlapping 2 x m, *o*-C_6H_5 and *m*-C_6H_5), 6.82 (2 H, m, *p*-C_6H_5), 4.10 (2 H, app. sept., app. ^{3}J = 6.30 Hz, C<u>H</u>Me$_2$), 3.06 (2 H, m, ^{iPr}NC<u>H</u>$_2$), 2.86 (2 H, m, ^{iPr}NC<u>H</u>$_2$), 2.72 (3 H, s, TiN(NPh$_2$)C(<u>Me</u>)), 2.67 (2 H, m, ^{Me}NC<u>H</u>$_2$), 2.37 (3 H, s, TiNC(<u>Me</u>)), 2.17 (2 H, m, ^{Me}NC<u>H</u>$_2$), 2.04 (3 H, s, NMe), 1.09 (6 H, d, ^{3}J = 6.30 Hz, CH<u>Me</u>$_2$), 0.51 (6 H, d, ^{3}J = 6.30 Hz, CH<u>Me</u>$_2$) ppm. ^{13}C{^{1}H} NMR (C_6D_6, 125.7 MHz, 298 K): δ 171.3 (TiN(NPh$_2$)<u>C</u>(Me)), 168.3 (TiN<u>C</u>(Me)), 147.7 (*i*-C_6H_5), 129.1 (*o*-C_6H_5), 122.6 (*p*-C_6H_5), 121.9 (*m*-C_6H_5), 59.3 (^{Me}N<u>C</u>H$_2$), 51.6 (<u>C</u>HMe$_2$), 46.8 (^{iPr}N<u>C</u>H$_2$), 44.0 (NMe), 24.0 (Ti(NNPh$_2$)NC(<u>Me</u>), 23.4 (TiNC(<u>Me</u>)), 22.6 (CH<u>Me</u>$_2$), 20.9 (CH<u>Me</u>$_2$) ppm.

Common data: IR (NaCl plates, Nujol mull, cm^{-1}): 2175 (w), 1588 (m), 1260 (m), 1020 (m), 799 (m), 692 (w). Anal. found (calcd. for $C_{27}H_{41}N_7Ti$): C, 63.33 (63.40); H, 8.03 (8.08); N, 19.04 (19.17)%.

Ti(N$_2^{iPr}$N^{Me}){N(NPh$_2$)C(C$_6$F$_5$)NC(C$_6$F$_5$)N} (22). To a stirred solution of Ti(N$_2^{iPr}$N^{Me})(NNPh$_2$)(py) (**2.1**, 0.200 g, 0.390 mmol) in benzene (5 mL) was added C_6F_5CN (0.0193 mL, 0.790 mmol) at RT. The solution was stirred at RT for 1 hour, filtered and the volatiles removed under reduced pressure. The remaining sticky red solid was washed with a minimal amount of cold pentane (2 x 2 mL) yielding **22** as a dark brown powder. Yield: 0.120 g (38 %). The ^{1}H NMR spectrum indicated an approximately 80:20% mixture of the *cis* and *trans* isomers.

Major isomer (cis): ^{1}H NMR (C_6D_6, 499.9 MHz, 298 K): δ 7.12 (4 H, d, ^{3}J = 7.3 Hz, *o*-C_6H_5), 6.89 (4 H, app. t, app. ^{3}J = 7.3 Hz, *m*-C_6H_5), 6.72 (2 H, t, ^{3}J = 7.3 Hz, *p*-C_6H_5), 4.60 (2 H, app. sept., app. ^{3}J = 6.1 Hz, C<u>H</u>Me$_2$), 3.04 (2 H, m, ^{iPr}NC<u>H</u>$_2$), 2.94 (2 H, m, ^{iPr}NC<u>H</u>$_2$), 2.36 (2 H, m, ^{Me}NC<u>H</u>$_2$), 2.13 (2 H, m, ^{Me}NC<u>H</u>$_2$), 2.06 (3 H, s, NMe), 1.25 (6 H, d, ^{3}J = 6.1 Hz, CH<u>Me</u>$_2$), 0.97 (6 H, d, ^{3}J = 6.1 Hz, CH<u>Me</u>$_2$) ppm. ^{13}C{^{1}H} NMR (C_6D_6, 125.7 MHz, 298 K): δ 156.4 (<u>C</u>C$_6$F$_5$), 154.2 (<u>C</u>C$_6$F$_5$), 148.9 (*i*-C_6H_5), 144.2 (d, ^{1}J = 250.2 Hz, *o*$_b$-C_6F_5), 144.8 (d, ^{1}J = 246.6 Hz, *o*$_a$-C_6F_5), 140.9 (d, ^{1}J = 253.8 Hz, overlapping *p*$_a$-C_6F_5 and *p*$_b$-C_6F_5), 137.9 (d, ^{1}J = 250.2 Hz, overlapping *m*$_a$-C_6F_5 and *m*$_b$-C_6F_5), 128.8 (*m*-C_6H_5), 124.0 (*p*-C_6H_5), 123.3 (*o*-C_6H_5), 59.8 (^{Me}N<u>C</u>H$_2$), 52.9 (<u>C</u>HMe$_2$), 48.1 (^{iPr}N<u>C</u>H$_2$), 41.7 (NMe), 22.6 (CH<u>Me</u>$_2$), 21.2 (CH<u>Me</u>$_2$) ppm. Resonances attributed to *i*-<u>C</u>$_6$F$_5$ could not be identified. ^{19}F NMR (C_6D_6, 376.4 MHz, 298 K): δ -134.1 (2F, m, *o*$_a$-C_6F_5), -142.5 (2F, m, *o*$_b$-C_6F_5), -155.9 (1F, m, *p*$_a$-C_6F_5), -157.5 (1F, m, *p*$_b$-C_6F_5), -163.2 (2F, m, *m*$_a$-C_6F_5), -163.7 (2F, m, *m*$_b$-C_6F_5) ppm. Note: subscripts ″a″ and ″b″ refer to the inequivalent Ar^{F_5} environments.

Major isomer (trans): ^{1}H NMR (C_6D_6, 499.9 MHz, 298 K): δ 7.09 (4 H, m, *o*-C_6H_5), 6.93 (4 H, m, *m*-C_6H_5), 6.69 (2 H, m, *p*-C_6H_5), 5.07 (2H, app. sept., app. ^{3}J = 6.4 Hz, C<u>H</u>Me$_2$), 3.12 (2 H, m, ^{iPr}NC<u>H</u>$_2$), 2.85 (2 H, m, ^{iPr}NC<u>H</u>$_2$), 2.60 (2 H, m, ^{Me}NC<u>H</u>$_2$), 1.90 (3 H, s, NMe), 1.28 (6 H, d, ^{3}J = 6.4 Hz, CH<u>Me</u>$_2$), 1.17 (6 H, d, ^{3}J = 6.4 Hz, CH<u>Me</u>$_2$) ppm. ^{13}C{^{1}H} NMR (C_6D_6, 125.7 MHz, 298 K): δ 164.3 (<u>C</u>C$_6$F$_5$), 155.6 (<u>C</u>C$_6$F$_5$), 144.2 (*i*-C_6H_5), 128.4 (*m*-(C_6H_5), 121.9 (*p*-C_6H_5), 119.1 (*o*-C_6H_5), 58.1 (<u>C</u>HMe$_2$), 57.0 (^{Me}N<u>C</u>H$_2$), 47.1 (^{iPr}N<u>C</u>H$_2$), 44.3 (NMe), 24.2 (CH<u>Me</u>$_2$), 21.4 (CH<u>Me</u>$_2$) ppm. Resonances attributable to carbon atoms directly bound to ^{19}F atoms were not observed ppm. ^{19}F NMR (C_6D_6, 376.4 MHz, 298 K): δ -138.4 (*o*-C_6F_5), -142.9 (*o*-C_6F_5), -155.9 (*p*-C_6F_5), -157.3 (*p*-C_6F_5), -162.7 (*m*-C_6F_5), -163.7 (*m*-C_6F_5) ppm.

Common data: IR (NaCl plates, Nujol mull, cm^{-1}): 1589 (m), 1519 (m), 1496 (m), 1260 (m), 1082 (w), 1020 (w), 991 (w), 799 (w). Anal. found (calcd. for $C_{37}H_{35}F_{10}N_7Ti$): C, 54.37 (54.49); H, 4.29 (4.33); N, 11.87 (12.02)%.

5.6 Experimental details and characterising data for Chapter Three

Ti($H_2N_2^{iPr}N^{Me}$)(CCC_6F_5)$_2$(NXyl) (23). To a solution of Ti($N_2^{iPr}N^{Me}$)(NXyl)(py) (**1**, 0.200 g, 0.450 mmol) in benzene (2 mL) was added a solution of C_6F_5CCH (0.119 mL, 0.900 mmol) in benzene (2 mL). The solution was left to stir for 30 minutes at RT after which the volatiles were removed to yield a dark brown oil which was triturated in pentane (5 mL) and filtered. The resultant solid was washed with pentane (5 mL) to afford **23** as an off-white solid which was dried *in vacuo*. Yield: 0.150 mg (44 %). Diffraction-quality crystals were grown from a saturated toluene solution at -30 °C. ^{1}H NMR (C_6D_6, 299.9 MHz, 298 K): δ 7.06 (2 H, d, ^3J = 7.4 Hz, *m*-$C_6H_3Me_2$), 6.74 (1 H, t, ^3J = 7.4 Hz, *p*-$C_6H_3Me_2$), 3.84-3.66 (4 H, overlapping 2 x m, ^{Me}NC$\underline{H}_2$ and NH), 3.37 (2 H, d. sept., ^3J = 6.1, 6.2 Hz, C$\underline{H}$Me$_2$), 3.27 (6 H, s, $C_6H_3\underline{Me}_2$), 2.55 (2 H, app. qd, app. J = 13.3, 2.9 Hz, ^{iPr}NC$\underline{H}_2$), 2.28 (3 H, s, NMe), 2.24 (2 H, app. dt, app. J = 13.0 3.0 Hz, ^{iPr}NC$\underline{H}_2$), 1.73 (2 H, app. dd, app. J = 12.6 1.9 Hz, ^{Me}NC$\underline{H}_2$), 1.10 (6 H, d, ^3J = 6.5 Hz, CH$\underline{Me}_2$), 1.04 (6 H, d, ^3J = 6.5 Hz, CH$\underline{Me}_2$) ppm. ^{13}C{^{1}H} NMR (C_6D_6, 125.8 Hz, 298 K): δ 166.4, (d, $^4J_{C\text{-}F}$ = 3.9 Hz, Ti$\underline{C}_a$C), 164.0 (d, $^4J_{C\text{-}F}$ = 3.9 Hz, Ti$\underline{C}_b$C), 158.1 (*o*-$C_6H_3Me_2$), 147.4 (d, $^1J_{C\text{-}F}$ = 246.0 Hz, overlapping o_a-C_6F_5 and o_b-C_6F_5), 139.8 (d, $^1J_{C\text{-}F}$ = 254.0 Hz, *p*-C_6F_5), 139.4 (d, ^1J = 252 Hz, *p*-C_6F_5), 137.9 (d, $^1J_{C\text{-}F}$ = 248.0 Hz, overlapping m_a-C_6F_5 and m_b-C_6F_5), 135.5 (*i*-$C_6H_3Me_2$), 128.3 (*m*-$C_6H_3Me_2$), 121.2 (*p*-$C_6H_3Me_2$), 103.7 (td, $^2J_{C\text{-}F}$ = 19.3, $^3J_{C\text{-}F}$ = 4.2 Hz, *i*-C_6F_5) 103.4 (td, $^2J_{C\text{-}F}$ = 19.3 Hz, $^3J_{C\text{-}F}$ = 3.8 Hz, *i*-C_6F_5), 97.5 (d, $^3J_{C\text{-}F}$ = 3.2 Hz, TiC$\underline{C}_a$), 95.7 (d, $^3J_{C\text{-}F}$ = 3.2 Hz, TiC$\underline{C}_b$), 58.0 (^{Me}N$\underline{C}$H$_2$), 52.8 ($\underline{C}$HMe$_2$), 46.4 (NMe), 45.4 (^{i}PrN$\underline{C}$H$_2$), 22.6 (CH$\underline{Me}_2$), 21.8 (NC$_6$H$_3\underline{Me}_2$), 20.8 (CH$\underline{Me}_2$) ppm. ^{19}F NMR (C_6D_6, 282.1 MHz, 298 K): δ -140.2 (4F, m, overlapping o_a-C_6F_5 and o_b-C_6F_5), 158.1 (1F, t, ^3J = 21.0 Hz, p_b-C_6F_5), -159.6 (1F, ^3J = 21.0 Hz, p_a-C_6F_5), -163.5 (2H, m, m_b-C_6F_5), -164.3 (2H, m, m_a-C_6F_5) ppm. Note: subscripts ″a″ and ″b″ refer to the inequivalent CCC_6F_5 environments. IR (NaCl plates, Nujol mull, cm^{-1}): 3232 (w, ν(N-H), 2089 (w, ν(C≡C), 1585 (w), 1513 (s), 1494 (s), 1287 (m), 1260 (w), 1215 (w), 1163 (w), 1131 (w), 1095 (m), 1015 (w), 968 (s), 957 (s), 877 (w), 796 (m), 757 (m), 741 (w), 722 (w) 603 (w). EI-MS: *m/z* = 750 [M-H]$^+$ (1%). Anal. found (calcd. for $C_{35}H_{36}F_{10}N_4Ti$): C, 55.85 (56.01); H, 4.74 (4.83); N, 7.53 (7.46) %.

Ti($N_2^{iPr}N^{Me}$)(CCC_6F_5){N(Xyl)C(H)C(H)C_6F_5)} (24). To a stirred solution of Ti($N_2^{iPr}N^{Me}$)(NXyl)(py) (**1**, 0.400 g, 0.890 mmol) in benzene (7 mL) was added $HCCC_6F_5$ (0.238 mL, 1.78 mmol). The solution was heated to 70 °C and left to stir

for 12 hours during which a colour change to dark red was observed. The volatiles were then removed under reduced pressure to yield **24** as a red solid which was washed with minimal amount of cold pentane and then dried *in vacuo*. Yield: 0.467 mg (70%). Diffraction quality crystals were grown from a saturated toluene solution at -30 °C. ^{1}H NMR (C_6D_6, 299.9 MHz, 298K): δ 8.35 (1 H, d, ^{3}J = 13.5 Hz, TiNC(H)C(H)), 7.13-7.05 (3H, overlapping 2 x m, *p*- $C_6H_3Me_2$ and *m*-$C_6H_3Me_2$) 5.17 (2 H, app. sept., app. ^{3}J = 6.0 Hz, C$\underline{H}$Me$_2$), 4.64 (1 H, d, ^{3}J = 13.5 Hz, TiNC(H)C($\underline{H}$)), 3.39 (2 H, m, ^{iPr}NC$\underline{H}_2$), 3.05 (2 H, m, ^{iPr}NC$\underline{H}_2$), 2.75 (2 H, m, ^{Me}NC$\underline{H}_2$), 2.55 (6 H, s, $C_6H_3\underline{Me}_2$), 2.28 (2 H, m, ^{Me}NC$\underline{H}_2$), 2.27 (3 H, s, NMe), 1.33 (6 H, d, ^{3}J = 6.0 Hz, CH$\underline{Me}_2$) 0.95 (6 H, d, ^{3}J = 6.0 Hz, CH$\underline{Me}_2$) ppm. ^{13}C{^{1}H} NMR (C_6D_6, 125.8 MHz, 298 K): δ 165.0 (m, TiC), 147.9 (d, ^{1}J = 250.9 Hz, alkyne *o*-C_6F_5), 146.8 (t, ^{3}J = 7.4 Hz, TiN$\underline{C}$(H)C(H)), 143.8 (d, ^{1}J = 244.1 Hz, alkene *o*-C_6F_5), 142.6 (*i*-$C_6H_3Me_2$), 140.0 (d, ^{1}J = 264.6 Hz, alkyne *p*-C_6F_5), 138.1 (d, ^{1}J = 246.3 Hz, alkene *m*-C_6F_5), 137.8 (d, ^{1}J = 251.1Hz, alkyne *m*-C_6F_5), 137.2 (d, ^{1}J = 232.8 Hz, alkene *p*-C_6F_5), 134.8 (*o*-$C_6H_3Me_2$), 129.4 (*m*-$C_6H_3Me_2$), 126.8 (*p*-$C_6H_3Me_2$), 115.0 (t, ^{2}J = 15.0 Hz, alkene *i*-C_6F_5), 102.2 (t, ^{2}J = 18.2 Hz, alkyne *i*-C_6F_5), 83.7 (m, TiC$\underline{C}$), 82.9 (TiNC(H)$\underline{C}$(H)), 58.5 (^{Me}NCH$_2$), 53.5 ($\underline{C}$HMe$_2$), 47.7 (^{iPr}NCH$_2$), 44.7 (NMe), 21.3 (CH$\underline{Me}_2$), 19.8 ($C_6H_3Me_2$) 19.7 ($\underline{C}$HMe$_2$) ppm. ^{19}F NMR (C_6D_6, 282.1 MHz, 298 K): δ -138.7 (alkyne *o*-C_6F_5), -145.8 (alkene *o*-C_6F_5), -157.6 (alkyne *p*-C_6F_5), 163.7 (alkyne *m*-C_6F_5), -164.6 (alkene *p*-C_6F_5), -165.0 (alkene *p*-C_6F_5) ppm. IR (NaCl plates, Nujol mull, cm^{-1}): 1576 (m), 1515 (s), 1493 (s), 1308 (w), 1260 (m), 1225 (w), 1151 (m), 1087 (m), 1019 (s), 988 (w), 962 (m), 883 (m), 798 (s). EI-MS *m/z*: 750 $[M]^+$ (20%). Anal. found (calcd. for $C_{35}H_{36}F_{10}N_5Ti$): C, 55.84 (56.01); H, 4.93 (4.83); N 7.43 (7.46)%.

Low temperature NMR tube scale synthesis of Ti($H_2N_2^{iPr}N^{Me}$)(CC(3,5-$C_6H_3F_2$)(NXyl) (25). To a solution of Ti($N_2^{iPr}N^{Me}$)(NXyl)(py) (**1**, 0.040 g, 0.090 mmol) in toluene-d_8 (0.6 mL) precooled to -78 ^{0}C in an NMR tube equipped with a J. Young Teflon valve was added HCC-3,5-$C_6H_3F_2$ (0.021 mL, 0.180 mmol). The NMR probe was cooled to -70 ^{0}C and a blank toluene-d_8 sample added before being locked and shimmed. The experimental sample then replaced the blank sample and allowed to thermally equilibrate, the shimming was then checked. The sample was then gradually warmed to 0 ^{0}C, the ^{1}H NMR spectra indicated **25** was the only species present. Compound **25** was subsequently characterised by ^{1}H, ^{13}C and ^{19}F

spectroscopy at 0 ^{0}C. ^{1}H NMR (C_6D_5Br, 499.9 MHz, 273 K): δ 7.00 (2 H, d, ^4J = 5.9 Hz, *o*-$C_6H_3F_2$), 6.89 (2 H, d, ^4J = 5.9 Hz, *o*-$C_6H_3F_2$), 6.83 (2 H, d, ^3J = 7.4 Hz, *m*-$C_6H_3Me_2$), 6.55 (1H, t, ^3J = 7.4 Hz, *p*-$C_6H_3Me_2$), 6.46-6.38 (2 H, overlapping 2 x m, *p*-$C_6H_3F_2$ and *p*-$C_6H_3F_2$), 3.76-3.67 (4 H, overlapping 2 x m, $^{Me}NCH_2$ and NH), 3.23 (2 H, d. sept, ^3J = 6.0, 6.3 Hz, C<u>H</u>Me_2), 2.99 (6 H, s, C_6H_3<u>Me_2</u>), 2.55 (2 H, m, ^{iPr}NC<u>H_2</u>), 2.43 (2 H, m, ^{iPr}NC<u>H_2</u>), 1.93 (2 H, m, $^{Me}NCH_2$), 0.94 (6 H, d, ^3J = 6.4 Hz, CH<u>Me_2</u>), 0.93 (6 H, d, ^3J = 6.4 Hz, CH<u>Me_2</u>) ppm. ^{13}C NMR (C_6D_5Br, 125.7 MHz, 273 K): δ 157.6 (dd, $^1J_{C\text{-}F}$ = 249 Hz, $^3J_{C\text{-}F}$ = 14 Hz, overlapping *m*-$C_6H_3F_2$), 152.4 (*o*-$C_6H_3Me_2$), 148.7 (Ti<u>C</u>C), 144.5 (Ti<u>C</u>C), 125.6 (t, $^3J_{C\text{-}F}$ = 11.6 Hz, *i*-$C_6H_3F_2$), 125.2 (t, $^3J_{C\text{-}F}$ = 11.3 Hz, *i*-$C_6H_3F_2$), 122.4 (*o*-$C_6H_3Me_2$), 118.4 (*i*-$C_6H_3Me_2$), 115.0 (*p*-$C_6H_3Me_2$), 108.5 (dd, $^2J_{C\text{-}F}$ = 19.3 Hz, $^4J_{C\text{-}F}$ = 6.0 Hz, *o*-$C_6H_3F_2$), 108.2 (dd, $^2J_{C\text{-}F}$ = 18.4 Hz, $^4J_{C\text{-}F}$ = 5.5 Hz, *o*-$C_6H_3F_2$), 108.0 (t, $^4J_{C\text{-}F}$ = 3.2 Hz, Ti<u>C</u>C), 106.3 (t, $^4J_{C\text{-}F}$ = 3.2 Hz, Ti<u>C</u>C), 96.9 (t, $^2J_{C\text{-}F}$ = 25.2 Hz, *p*-$C_6H_3F_2$) 96.4 (t, $^2J_{C\text{-}F}$ = 24.8 Hz, *p*-$C_6H_3F_2$), 52.8 (^{Me}N<u>C</u>H_2), 47.3 (<u>C</u>HMe_2), 41.2 (NMe), 40.1 (^{iPr}N<u>C</u>H_2), 17.4 (CH<u>Me_2</u>), 16.3 (C_6H_3<u>Me_2</u>), 15.6 (CH<u>Me_2</u>) ppm. ^{19}F NMR (C_6D_5Br, 282.1 MHz, 273 K) δ -109.7 (2F, CF), -110.2 (2F, CF) ppm.

Low temperature NMR tube scale synthesis of Ti($H_2N_2^{iPr}N^{Me}$)(CC(4-$C_6H_4CF_3$)(NXyl) (26). To a solution of Ti($N_2^{iPr}N^{Me}$)(NXyl)(py) (**1**, 0.020 g, 0.045 mmol) in C_6H_5Br (0.6 mL) precooled to -78 ^{0}C in an NMR tube equipped with a J. Young Teflon valve was added HCC-4-$C_6H_4CF_3$ (0.015 mL, 0.090 mmol). The NMR probe was cooled to -20 ^{0}C and a blank C_6H_5Br sample added before being locked and shimmed. The experimental sample then replaced the blank sample and allowed to thermally equilibrate, the shimming was then checked. The sample was then warmed to -5 ^{0}C, the ^{1}H NMR spectra indicated **26** was the only species present after 40 mins at -5 ^{0}C. Compound **26** was subsequently characterised by ^{1}H, ^{13}C and ^{19}F spectroscopy at -5 ^{0}C. ^{1}H NMR (C_6D_5Br, 299.9 MHz, 298 K): δ 7.53 (2 H, d, ^3J = 7.4 Hz, *o*-$C_6H_4CF_3$), 7.44 (2 H, d, ^3J = 7.4 Hz, *o*-$C_6H_4CF_3$), 7.38 (2 H, m, *m*-$C_6H_4CF_3$), 6.92-6.86 (4 H, overlapping 2 x m, *m*-$C_6H_4CF_3$ and *m*-$C_6H_3Me_2$), 6.61 (1 H, t, ^3J = 7.16 Hz, *p*-$C_6H_3Me_2$), 3.96-3.84 (4 H, overlapping 2 x m, ^{Me}NC<u>H_2</u> and NH), 3.36 (2 H, d. sept., ^3J = 6.0, 6.2 Hz, C<u>H</u>Me_2), 3.11 (6 H, s, C_6H_3<u>Me_2</u>), 2.75 (2 H, m, ^{iPr}NC<u>H_2</u>), 2.50 (2 H, m, ^{iPr}NC<u>H_2</u>), 2.43 (3 H, s, NMe), 2.05 (2 H, m, ^{Me}NC<u>H_2</u>), 1.09 (12 H, app. t, app ^3J = 6.0 Hz, CH<u>Me_2</u>) ppm. ^{13}C{^{1}H} NMR (C_6D_5Br, 75.4 MHz, 268 K): δ 157.7 (Ti<u>C</u>C), 154.9 (Ti<u>C</u>C), 150.6 (*o*-$C_6H_3Me_2$), 135.2 (*i*-$C_6H_3Me_2$), 131.3 (*o*-$C_6H_4CF_3$),

130.9 (*o*-$C_6H_4CF_3$), 127.7 (*m*-$C_6H_4(CF_3)$), 125.3 (*m*-$C_6H_4(CF_3)$), 123.6 (*m*-$C_6H_3Me_2$), 120.3 (*p*-$C_6H_3Me_2$), 114.2 (TiC$\underline{C}$), 112.4 (TiC$\underline{C}$), 58.2 (^{Me}N$\underline{C}H_2$), 52.6 ($\underline{C}HMe_2$), 46.6 (NMe), 45.4 (^{i}PrN$\underline{C}H_2$), 22.8 ($CHMe_2$), 21.71 ($C_6H_3\underline{Me}_2$), 20.9 ($CH\underline{Me}_2$) ppm. The resonances attributable to CF_3, *p*-$\underline{C}_6H_4(CF_3)$ and *i*-$\underline{C}_6H_4(CF_3)$ were not observed. ^{19}F NMR (C_6D_6, 282.1 MHz, 268 K): δ -61.3 (3F, CF_3), -61.4 (3F, CF_3) ppm.

Low temperature NMR tube scale synthesis of Ti($H_2N_2^{iPr}N^{Me}$)(CC(3,5-$C_6H_3(CF_3)_2$)(NXyl) (27). To a solution of Ti($N_2^{iPr}N^{Me}$)(NXyl)(py) (**1**, 0.020 g, 0.045 mmol) in C_6D_5Br (0.6 mL) precooled to -78 ^{0}C in an NMR tube equipped with a J. Young Teflon valve was added HCC-3,5-$C_6H_3(CF_3)_2$ (0.016 mL, 0.90 mmol). The NMR probe was cooled to -30 ^{0}C and a blank C_6D_5Br sample added before being locked and shimmed. The experimental sample then replaced the blank sample and allowed to thermally equilibrate, the shimming was then checked. The sample was then warmed to 0 ^{0}C, the ^{1}H NMR spectra indicated **27** was the only species present. Compound **27** was subsequently characterised by ^{1}H, ^{13}C and ^{19}F spectroscopy at 0 ^{0}C. ^{1}H NMR (C_6D_5Br, 299.9 MHz, 273 K): δ 7.98 (2 H, s, *o*-$C_6H_3(CF_3)_2$), 7.86 (2 H, s, *o*-$C_6H_3(CF_3)_2$), 7.25 (1 H, s, *p*-$C_6H_3(CF_3)_2$) , 7.12 (1 H, s, *p*-$C_6H_3(CF_3)_2$), 6.88 (2 H, d, ^3J = 7.7 Hz, *m*-$C_6H_3Me_2$), 6.61 (1 H, t, ^3J = 7.7 Hz, *p*-$C_6H_3Me_2$), 3.85-3.77 (4 H, overlapping 2 x m, NH and ^{Me}NC$\underline{H}_2$), 3.36 (2 H, d. sept., ^3J = 5.9, 6.4 Hz, C$\underline{H}Me_2$), 3.10 (6 H, s, $C_6H_3\underline{Me}_2$), 2.64 (2 H, m, ^{iPr}NC$\underline{H}_2$), 2.35 (2 H, m, ^{iPr}NC$\underline{H}_2$), 2.33 (3 H, s, NMe), 1.98 (2 H, m, ^{Me}NCH_2), 1.04 (6 H, d, ^3J = 7.15 Hz, CH$\underline{Me}_2$), 1.02 (6 H, d, ^3J = 7.15 Hz, CH$\underline{Me}_2$) ppm.^{13}C{^{1}H} NMR (C_6D_6Br, 75.4 MHz, 273 K): δ 157.6 (Ti$\underline{C}$C), 155.7 (Ti$\underline{C}$C), 151.6 (*o*-$C_6H_3Me_2$), 135.0 (*i*-$C_6H_3Me_2$), 132.1 (Ar), 130.4 (Ar), 127.7 (Ar), 123.6 (*m*-$C_6H_3Me_2$), 122.0 (Ar), 120.6 (*p*-$C_6H_3Me_2$), 119.0 (m, *p*-$C_6H_3(CF_3)_2$), 118.7 (m, *p*-$C_6H_3(CF_3)_2$), 112.8 (TiC$\underline{C}$), 111.1 (TiC$\underline{C}$), 58.4 (^{Me}N$\underline{C}H_2$), 52.7 ($\underline{C}HMe_2$), 46.5 (NMe), 45.4 (^{i}PrN$\underline{C}H_2$), 22.8 ($CH\underline{Me}_2$), 21.5 ($C_6H_3\underline{Me}_2$), 20.9 ($CH\underline{Me}_2$) ppm. *o*-$C_6H_3(CF_3)_2$ and *m*-$C_6H_3(CF_3)_2$ aromatic resonances could not be distinguished. Resonances attributable to carbons directly bound to ^{19}F atoms were not observed. ^{19}F NMR (C_6D_5Br, 282.1 MHz, 283 K) δ -62.1 (12F, overlapping CF_3) ppm.

Ti($N_2^{iPr}N^{Me}$)(CC-3,5-$C_6H_3F_2$){N(Xyl)C(H)C(H)-3,5-$C_6H_3F_2$} (28). To a stirred solution of Ti($N_2^{iPr}N^{Me}$)(NXyl)(py) (**1**, 0.300 g, 0.670 mmol) in benzene (5 mL) was added HCC-3,5-$C_6H_3F_2$ (0.160 mL, 1.35 mmol). The solution was left to stir for 16 hours at RT. The volatiles were removed under reduced pressure to yield a red sticky

solid which was triturated in hexane and filtered yielding **28** as an orange powder which was washed with minimal amount of cold hexane and then dried *in vacuo*. Yield: 0.302 mg (70 %). ^{1}H NMR (C_6D_6, 299.9 MHz, 298 K): δ 8.11 (1 H, d, ^{3}J = 13.6 Hz, TiNC(H)C(H)), 7.19 (1 H, m, *p*-$C_6H_3Me_2$), 7.15 (2 H, m, *m*-$C_6H_3Me_2$), 7.07 (2 H, d, ^{3}J = 7.4 Hz, alkyne *o*-$C_6H_3F_2$), 6.58 (2 H, d, ^{3}J = 9.3 Hz, alkene *o*-$C_6H_3F_2$), 6.40-6.34 (2 H, overlapping 2 x m, alkyne *p*-$C_6H_3F_2$ and alkene *p*-$C_6H_3F_2$), 5.04 (2 H, app. sept., app. ^{3}J = 6.3 Hz, C$\underline{H}$Me$_2$), 4.72 (1 H, d, ^{3}J = 13.6 Hz, TiNC(H)C($\underline{H}$)), 3.32 (2 H, m, ^{iPr}NC$\underline{H}_2$), 2.97 (2 H, m, ^{iPr}NC$\underline{H}_2$), 2.75 (2 H, m, ^{Me}NC$\underline{H}_2$), 2.50 (6 H, s, $C_6H_3\underline{Me}_2$), 2.23 (2 H, m, ^{Me}NC$\underline{H}_2$), 2.14 (3 H, s, NMe), 1.21 (6 H, d, ^{3}J = 6.3 Hz, CH$\underline{Me}_2$), 0.86 (6 H, d, ^{3}J = 6.3 Hz, CH$\underline{Me}_2$) ppm. ^{13}C{^{1}H} NMR (C_6D_6, 75.4 MHz, 298 K): δ 162.4 (dd, $^{1}J_{C\text{-}F}$ = 244.6 Hz, $^{3}J_{C\text{-}F}$ = 14.0 Hz, alkene *m*-$C_6H_3F_2$), 161.7 (dd, $^{1}J_{C\text{-}F}$ = 248.9 Hz, $^{3}J_{C\text{-}F}$ = 13.5 Hz, alkyne *m*-$C_6H_3F_2$), 154.0 (Ti$\underline{C}$C), 144.2 (*i*-$C_6H_3Me_2$), 143.9 (t, $^{3}J_{C\text{-}F}$ = 10.0 Hz, alkene *i*-$C_6H_3F_2$), 142.3 (TiN$\underline{C}$(H)C(H)), 134.7 (*o*-$C_6H_3Me_2$), 129.3 (*m*-$C_6H_3Me_2$), 126.4 (*i*-$C_6H_3Me_2$), 114.4 (t, $^{3}J_{C\text{-}F}$ = 11.5 Hz, alkyne *i*-$C_6H_3F_2$), 114.1 (dd, $^{2}J_{C\text{-}F}$ = 17.2 Hz, $^{4}J_{C\text{-}F}$ =7.7 Hz, alkyne *o*-$C_6H_3F_2$), 107.2 (dd, $^{2}J_{C\text{-}F}$ = 17.4 Hz, $^{4}J_{C\text{-}F}$ = 7.7 Hz, alkene *o*-$C_6H_3F_2$), 102.8 (t, $^{2}J_{C\text{-}F}$ = 25.8 Hz, alkyne *p*-$C_6H_3F_2$), 99.0 (t, $^{2}J_{C\text{-}F}$ = 26.4 Hz, alkene *p*-$C_6H_3F_2$), 98.8 (t, $^{4}J_{C\text{-}F}$ = 3.4 Hz, TiC$\underline{C}$), 97.9 (t, TiNC(H)$\underline{C}$(H)), 58.4 (^{Me}N$\underline{C}$H$_2$), 53.3 ($\underline{C}$HMe$_2$), 47.4 (^{iPr}N$\underline{C}$H$_2$), 44.6 (NMe), 20.9 (CH$\underline{Me}_2$), 20.1 (CH$\underline{Me}_2$), 19.8 ($C_6H_3\underline{Me}_2$) ppm. ^{19}F NMR (C_6D_6, 282.1 MHz, 298 K): δ -110.4 (2F, CF), -111.4 (2F, CF) ppm. IR (NaCl plates, Nujol mull, cm^{-1}): 1611 (w), 1597 (s), 1260 (w), 1117 (m), 1019 (w), 858 (w), 799 (w). Anal. found (calcd. for $C_{35}H_{42}N_4F_4Ti$): C, 65.31 (65.42); H, 6.50 (6.59); N, 8.52 (8.72)%.

Ti($N_2^{iPr}N^{Me}$)(CC-4-$C_6H_4CF_3$)(N(Xyl)C(H)C(H)-4-$C_6H_4CF_3$) (29). To a stirred solution of Ti($N_2^{iPr}N^{Me}$)(NXyl)(py) (**1**, 0.080 g, 0.180 mmol) in benzene (3 mL) was added HCC-4-$C_6H_4CF_3$ (0.059 mL, 0.360 mmol). The solution was left to stir for 12 hours at RT. The volatiles were removed under reduced pressure to yield **29** as a red sticky solid. Yield: 0.110 mg (86 %). ^{1}H NMR (C_6D_6, 299.9 MHz, 298 K): δ 8.19 (1 H, d, ^{3}J = 13.5 Hz, TiNC($\underline{H}$)C(H)), 7.38 (2 H, d, ^{3}J = 8.1 Hz, alkyne *o*-$C_6H_4CF_3$), 7.32 (2 H, d, ^{3}J = 8.1 Hz, alkene *m*-$C_6H_4CF_3$), 7.24 (2 H, d, ^{3}J = 8.1 Hz, alkyne *m*-$C_6H_4CF_3$), 7.16-6.97 (3 H, overlapping 2 x m, *m*-NC$_6\underline{H}_3$Me$_2$ and *p*-NC$_6\underline{H}_3$Me$_2$), 6.99 (2 H, d, ^{3}J = 8.1 Hz, alkene *o*-$C_6H_4CF_3$), 5.09 (2 H, app. sept., app. ^{3}J = 6.3 Hz, C$\underline{H}$Me$_2$), 4.80 (1 H, d, ^{3}J = 13.5 Hz, TiNC(H)C($\underline{H}$)), 3.38 (2 H, m, ^{iPr}NC$\underline{H}_2$), 3.07 (2 H, m, ^{iPr}NC$\underline{H}_2$), 2.83 (2 H, m, ^{Me}NC$\underline{H}_2$), 2.54 (6 H, s, $C_6H_3\underline{Me}_2$), 2.31 (2 H, m,

$^{Me}NCH_2$), 2.24 (3 H, s, NMe), 1.27 (6 H, d, ^3J = 6.3 Hz, CHMe$_2$) , 0.89 (6 H, d, ^3J = 6.3 Hz, CHMe$_2$) ppm. $^{13}C\{^1H\}$ NMR (C_6D_6, 74.5 MHz, 298 K): δ 155.6 (TiC), 144.9 (*i*-$C_6H_3Me_2$), 144.5 (br. m, alkene *i*-$C_6H_4CF_3$), 143.0 (TiNC(H)C(H)), 135.3 (*o*-$C_6H_3Me_2$), 133.1 (alkyne *i*-$C_6H_4CF_3$), 132.3 (alkyne *o*-$C_6H_4CF_3$), 130.0 (*m*-$C_6H_3Me_2$), 127.0 (*p*-$C_6H_3Me_2$), 126.3 (m, alkene *m*-$C_6H_4CF_3$), 126.0 (m, alkyne *m*-C_6H_4(4-CF_3)), 125.3 (alkene *o*-$C_6H_4CF_3$), 100.1 (TiCC), 98.7 (TiNC(H)C(H)), 59.0 ($^{Me}NCH_2$), 54.0 (CHMe$_2$), 48.1 ($^{iPr}NCH_2$), 45.2 (NMe), 21.5 (CHMe$_2$), 20.7 (CHMe$_2$), 20.5 ($C_6H_3Me_2$) ppm. Resonances attributable to alkyne *p*-$C_6H_4CF_3$, alkene *p*-$C_6H_4CF_3$ and carbons directly bound to ^{19}F atoms were not observed. ^{19}F NMR (C_6D_6, 282.1 MHz, 298 K): δ -61.5 (alkene CF_3, 3F), -62.2 (alkyne CF_3, 3F) ppm. IR (NaCl plates, Nujol mull, cm^{-1}): 1595 (s), 1568 (w), 1321 (s), 1260 (m), 1163 (m), 1180 (m), 1124 (m), 1104 (s), 1084 (w), 1066 (s), 1016 (m), 924 (w), 840 (w), 799 (m). Anal. found (calcd. for $C_{37}H_{44}F_6N_4Ti$): C, 62.69 (62.89); H, 6.35 (6.28); N, 7.97 (7.93)%.

Ti($N_2^{iPr}N^{Me}$)(CC(3,5-$C_6H_3(CF_3)_2$)(N(Xyl)C(H)C(H)(3,5-$C_6H_3(CF_3)_2$) (30). To a stirred solution of Ti($N_2^{iPr}N^{Me}$)(NXyl)(py) (**1**, 0.300 g, 0.670 mmol) in benzene (5 mL) was added HCC-3,5-$C_6H_3(CF_3)_2$ (0.238 mL, 1.35 mmol). The solution was left to stir for 16 hours at RT. The volatiles were removed under reduced pressure to yield a red sticky solid which was triturated in hexane and filtered yielding **30** as an orange powder which was washed with minimal amount of cold hexane and then dried *in vacuo*. Yield: 0.320 mg (56 %). Diffraction-quality crystals were grown from a saturated hexane solution at -30 °C. The ^1H NMR spectrum indicated an approximately 90:10 mixture of the *cis* and *trans* isomers.

Major isomer (cis): ^1H NMR (C_6D_6, 299.9 MHz, 298 K): δ 8.21 (1 H, d, ^3J = 13.5 Hz, TiNC(H)C(H)), 7.91 (2 H, s, alkyne *o*-$C_6H_3(CF_3)_2$), 7.56 (1 H, s, alkene *p*-$C_6H_3(CF_3)_2$), 7.48 (1 H, s, alkyne *p*-$C_6H_3(CF_3)_2$), 7.45 (2 H, s, alkene *o*-$C_6H_3(CF_3)_2$), 7.09-7.18 (3 H, overlapping 2 x m, *m*-$C_6H_3Me_2$ and *p*-$C_6H_3Me_2$), 5.04 (2 H, app. sept., app. ^3J = 6.3 Hz, CHMe$_2$), 4.80 (1 H, d, ^3J = 13.5 Hz, TiNC(H)C(H)), 3.35 (2 H, m, $^{iPr}NCH_2$), 3.00 (2 H, m, $^{iPr}NCH_2$), 2.88 (2 H, m, $^{Me}NCH_2$), 2.50 (6 H, s, $C_6H_3Me_2$), 2.24 (2 H, m, $^{Me}NCH_2$), 2.14 (3 H, s, NMe), 1.23 (6 H, d, ^3J = 6.3 Hz, CHMe$_2$), 0.89 (6 H, d, ^3J = 6.3 Hz, CHMe$_2$) ppm. $^{13}C\{^1H\}$ NMR (C_6D_6, 74.5 MHz, 298 K): δ 155.2 (TiC), 144.0 (alkene *i*-$C_6H_3(CF_3)_2$), 143.1 (*i*-$C_6H_3Me_2$), 142.5 (TiNC(H)C(H)), 134.4 (*o*-$C_6H_3Me_2$), 132.1 (q, $^2J_{C\text{-}F}$ = 33.9 Hz, *m*-$C_6H_3(CF_3)_2$), 132.0 (q, $^2J_{C\text{-}F}$ = 32.8 Hz, *m*-$C_6H_3(CF_3)_2$), 131.1 (alkyne *o*-$C_6H_3(CF_3)_2$), 129.5 (*m*-$C_6H_3Me_2$), 126.7 (*p*-$C_6H_3Me_2$), 125.4 (q, $^1J_{C\text{-}F}$ = 272.6 Hz, CF_3), 124.2 (alkene *o*-$C_6H_3(CF_3)_2$), 123.8 (q, $^1J_{C\text{-}F}$ = 272.6 Hz, CF_3), 119.8 (m, alkyne *p*-$C_6H_3(CF_3)_2$), 116.9 (m,

alkene *p*-$C_6H_3(CF_3)_2$), 98.7 (TiC<u>C</u>), 96.9 (TiNC(H)<u>C</u>(H)), 58.3 (^{Me}N<u>C</u>H$_2$), 53.5 (<u>C</u>HMe$_2$), 47.5 (^{iPr}N<u>C</u>H$_2$), 44.5 (NMe), 20.8 (CH<u>Me</u>$_2$), 20.1 (CH<u>Me</u>$_2$), 19.8 (C_6H_3<u>Me</u>$_2$) ppm. The resonance attributable to alkyne *i*-$C_6H_3(CF_3)_2$ was not observed. ^{19}F NMR (C_6D_6, 282.1 MHz, 298 K): δ -62.8 (CF_3), -63.0 (CF_3) ppm.

Minor isomer (trans): ^{1}H NMR (C_6D_6, 299.9 MHz, 298 K): δ 8.72 (1 H, d, ^3J = 13.5 Hz, TiNC(<u>H</u>)C(H)), 4.94 (2 H, m, C<u>H</u>Me$_2$) 5.05 (1 H, d, ^3J = 13.5 Hz, TiNC(H)C(<u>H</u>) overlapping with C<u>H</u>Me$_2$ *cis* isomer), 1.13 (6 H, d, ^3J = 6.3 Hz, CH<u>Me</u>$_2$), 0.69 (6 H, d, ^3J = 6.3 Hz, CH<u>Me</u>$_2$) ppm. Remaining resonances were not observed. ^{19}F NMR (C_6D_6, 282.1 MHz, 298 K): δ -63.0 (CF_3), -63.2 (CF_3) ppm.

Common data: IR (NaCl plates, Nujol mull, cm^{-1}): 1594 (w), 1583 (m), 1299 (w), 1276 (s), 1241 (w), 1177 (s), 1138 (s), 1104 (w), 872 (m), 681 (w). EI-MS *m/z*: 842 $[M]^+$ (2%). Anal. found (calcd. for $C_{39}H_{42}F_{12}N_4Ti$): C, 55.48 (55.59); H, 4.96 (5.02); N, 6.78 (6.65)%.

Low temperature NMR tube scale synthesis of Ti(HN$_2^{iPr}$N^{Me})(CC$_6$F$_5$)(NXyl)(py) (31). To a solution of Ti(N$_2^{iPr}$N^{Me})(NXyl)(py) (**1**, 0.020 g, 0.045 mmol) in toluene-d_8 (0.6 mL) precooled to -78 °C in an NMR tube equipped with a J. Young Teflon valve was added HCCC$_6$F$_5$ (0.012 mL, 0.090 mmol). The NMR probe was cooled to -80 °C and a blank toluene-d_8 sample added before being locked and shimmed. The experimental sample then replaced the blank sample and allowed to thermally equilibrate, the shimming was then checked. The sample was then warmed to -60 °C, the ^{1}H NMR spectra indicated **31** was the only species present. Compound **31** was subsequently characterised by ^{1}H, ^{13}C and ^{19}F spectroscopy at -60 °C. ^{1}H NMR (toluene-d_8, 499.9 MHz, 213 K): δ 9.46 (2 H, br. m, *o*-C_5H_5N), 7.04 (2 H, d, ^3J = 7.2 Hz, *m*-$C_6H_3Me_2$), 6.77 (2 H, br. m, *m*-C_5H_5N), 6.70 (1 H, t, ^3J = 7.2 Hz, *p*-$C_6H_3Me_2$), 6.40 (1 H, br. t, ^3J = 5.9 Hz, *p*-C_5H_5N), 5.73 (1 H, br. m, NC<u>H</u>Me$_2$), 4.09 (1 H, m, ^{iPr}NHC<u>H</u>$_2$CH$_2$N^{Me}), 3.38 (1 H, br. m, NH), 2.97 (1 H, m, ^{iPr}NC<u>H</u>$_2$CH$_2$N^{Me}), 2.78 (1 H, m, ^{iPr}NC<u>H</u>$_2$CH$_2$N^{Me}), 2.64 (7 H, overlapping s and br. m, C_6H_3<u>Me</u>$_2$ and NHC<u>H</u>Me$_2$), 2.31-2.27 (3 H, overlapping 3 x m, ^{iPr}NCH$_2$C<u>H</u>$_2$N^{Me}, ^{iPr}NHC<u>H</u>$_2$CH$_2$N^{Me} and ^{iPr}NHCH$_2$C<u>H</u>$_2$N^{Me}), 2.17 (3 H, s, NMe), 1.92 (1 H, m, ^{iPr}NCH$_2$C<u>H</u>$_2$N^{Me}), 1.40-1.39 (6 H, overlapping 2 x br. m, NHCH<u>Me</u>$_2$ and NCH<u>Me</u>$_2$), 1.30 (1 H, m, ^{iPr}NHCH$_2$C<u>H</u>$_2$N^{Me}), 1.08 (3 H, d, ^3J = 4.9 Hz, NCH<u>Me</u>$_2$), 0.67 (3 H, d, ^3J = 4.9 Hz, NHCH<u>Me</u>$_2$) ppm. ^{13}C{^{1}H} NMR (toluene-d_8, 125.7 MHz, 213 K): δ 169.0 (Ti<u>C</u>C), 157.7 (*i*-$C_6H_3Me_2$), 153.6 (*o*-C_5H_5N), 147.5 (d, $^1J_{C\text{-}F}$ = 243 Hz, *o*-C_6F_5), 141.2 (d, $^1J_{C\text{-}F}$ = 259 Hz, *p*-C_6F_5), 137.9 (*p*-C_5H_5N), 136.9 (d, $^1J_{C\text{-}F}$ = 250 Hz, *m*-C_6F_5),

133.2 (*o*-C$_6$H$_3$Me$_2$), 124.0 (*m*-C$_5$H$_5$N), 117.6 (*p*-C$_6$H$_3$Me$_2$), 104.0 (t, $^2J_{C\text{-}F}$ = 19.4, *i*-C$_6$F$_5$), 93.1 (TiCC), 61.1 (NCHMe$_2$), 58.5 (^{iPr}NCH$_2$CH$_2$N^{Me}), 51.4 (^{iPr}NHCH$_2$CH$_2$N^{Me}), 49.4 (NHCHMe$_2$), 47.4 (NMe), 44.9 (^{iPr}NCH$_2$CH$_2$N^{Me}), 42.1 (^{iPr}NHCH$_2$CH$_2$N^{Me}), 25.1 (NCHMe$_2$), 22.1 (NCHMe$_2$), 21.1 (NHCHMe$_2$), 21.1 (NHCHMe$_2$), 20.5 (C$_6$H$_3$Me$_2$) ppm. ^{19}F NMR (toluene-d_8, 470.4 MHz, 213 K): δ -140.1 (2F, m, *o*-C$_6$F$_5$), -160.5 (1F, m, *p*-C$_6$F$_5$), -164.4 (2F, m, *m*-C$_6$F$_5$) ppm.

Low temperature NMR tube scale synthesis of Ti(HN$_2^{iPr}$N^{Me})(CC-3,5-C$_6$H$_3$F$_2$)(NXyl)(py) (32). To a solution of Ti(N$_2^{iPr}$N^{Me})(NXyl)(py) (**1**, 0.040 g, 0.090 mmol) in toluene-d_8 (0.6 mL) precooled to -78 ^{0}C in an NMR tube equipped with a J. Young Teflon valve was added HCC-3,5-C$_6$H$_3$F$_2$ (0.021 mL, 0.180 mmol). The NMR probe was cooled to -70 ^{0}C and a blank toluene-d_8 sample added before being locked and shimmed. The experimental sample then replaced the blank sample and allowed to thermally equilibrate, the shimming was then checked. The sample was then warmed to -40 ^{0}C, the ^{1}H NMR spectra indicated **32** was the only species present. Compound **32** was subsequently characterised by ^{1}H, ^{13}C and ^{19}F spectroscopy at -40 ^{0}C. ^{1}H NMR (toluene-d_8, 499.9 MHz, 233 K): δ 9.35 (2 H, br. m, *o*-C$_5$H$_5$N), 7.05 (2 H, d, ^4J = 6.3 Hz, *o*-C$_6$H$_3$F$_2$), 6.97 (2 H, d, ^3J = 7.4 Hz, *m*-C$_6$H$_3$Me$_2$), 6.65-6.62 (2 H, overlapping 2 x m, *p*-C$_6$H$_3$Me$_2$ and *p*-C$_5$H$_5$N), 6.53 (2 H, br. m, *m*-C$_5$H$_5$N), 5.74 (1 H, app. sept., ^3J = 6.2 Hz, NCHMe$_2$), 3.85 (1 H, m, ^{iPr}NHCH$_2$CH$_2$N^{Me}), 3.34 (1 H, br. m, NH), 3.03 (1 H, m, ^{iPr}NCH$_2$CH$_2$N^{Me}), 2.90-2.77 (2 H, overlapping 2 x m, NHCHMe$_2$ and ^{iPr}NCH$_2$CH$_2$N^{Me}), 2.55 (6 H, s, C$_6$H$_3$Me$_2$), 2.33 (1 H, m, ^{iPr}NHCH$_2$CH$_2$N^{Me}), 2.24-2.16 (2 H, overlapping 2 x m, ^{iPr}NHCH$_2$CH$_2$N^{Me} and ^{iPr}NCH$_2$CH$_2$N^{Me}), 2.09 (3 H, s, NMe), 2.00 (1 H, m, ^{iPr}NHCH$_2$CH$_2$N^{Me}), 1.41-1.36 (7 H, m, overlapping 3 x m ^{iPr}NCH$_2$CH$_2$N^{Me}, NHCHMe$_2$ and NCHMe$_2$), 1.10 (3 H, d, ^3J = 6.5 Hz, NHCHMe$_2$), 0.67 (3 H, d, ^3J = 6.2 Hz, NCHMe$_2$) ppm. ^{13}C{^{1}H} NMR (toluene-d_8, 125.7 MHz, 233 K): δ 163.3 (dd, $^1J_{C\text{-}F}$ = 246.6 Hz, $^3J_{C\text{-}F}$ = 13.7 Hz, *m*-C$_6$H$_3$F$_2$), 157.5 (*o*-C$_6$H$_3$Me$_2$), 154.6 (TiCC), 153.4 (*o*-C$_5$H$_5$N), 137.2 (*p*-C$_5$H$_5$N), 132.8 (*i*-C$_6$H$_3$Me$_2$), 131.7 (t, $^3J_{C\text{-}F}$ = 11.6 Hz, *i*-C$_6$H$_3$F$_2$), 128.1 (*m*-C$_6$H$_3$Me$_2$), 123.4 (*m*-C$_5$H$_5$N), 117.4 (*p*-C$_6$H$_3$Me$_2$), 113.4 (dd, $^2J_{C\text{-}F}$ = 19.6 Hz, $^4J_{C\text{-}F}$ = 5.2 Hz, *o*-C$_6$H$_3$F$_2$), 109.4 (m, TiCC), 101.0 (t, $^2J_{C\text{-}F}$ = 26.0 Hz, *p*-C$_6$H$_3$F$_2$), 61.0 (NCHMe$_2$), 58.8 (^{iPr}NHCH$_2$CH$_2$N^{Me}), 51.7 (^{iPr}NCH$_2$CH$_2$N^{Me}), 49.2 (NHCHMe$_2$), 47.7 (NMe), 45.0 (^{iPr}NCH$_2$CH$_2$N^{Me}), 41.9 (^{iPr}NHCH$_2$CH$_2$N^{Me}), 25.0 (NHCHMe$_2$), 21.9 (NCHMe$_2$), 21.0 (NCHMe$_2$), 20.8 (NHCHMe$_2$),

20.1($NC_6H_3\underline{Me}_2$) ppm. ^{19}F NMR (toluene-d^8, 376.4 MHz, 233 K): δ -111.1 (2F, CF) ppm.

Low temperature NMR tube scale synthesis of Ti($N_2^{iPr}N^{Me}$)(CC-4-$C_6H_4CF_3$)(NXyl)(py) (33). To a solution of Ti($N_2^{iPr}N^{Me}$)(NXyl)(py) (**1**, 0.040 g, 0.090 mmol) in toluene-d_8 (0.6 mL) precooled to -78 ^{0}C in an NMR tube equipped with a J. Young Teflon valve was added HCC-4-$C_6H_4CF_3$ (0.029 mL, 0.180 mmol). The NMR probe was cooled to -60 ^{0}C and a blank toluene-d_8 sample added before being locked and shimmed. The experimental sample then replaced the blank sample and allowed to thermally equilibrate, the shimming was then checked. The sample was then warmed to -40 ^{0}C, the ^{1}H NMR spectra indicated **33** was the only species present. Compound **33** was subsequently characterised by ^{1}H, ^{13}C and ^{19}F spectroscopy at -40 ^{0}C. ^{1}H NMR (toluene-d_8, 499.9 MHz, 233 K): δ 9.78 (2 H, br. m, *o*-C_5H_5N), 7.53 (2 H, d, ^3J = 8.2 Hz, *o*-$C_6H_4CF_3$), 7.35 (2 H, d, ^3J = 8.2 Hz, *m*-$C_6H_4CF_3$), 7.19 (2 H, d, ^3J = 7.3 Hz, *m*-$C_6H_3Me_2$), 6.84-6.81 (2 H, overlapping 2 x m, *p*-C_5H_5N and *p*-$C_6H_3Me_2$), 6.68 (2 H, br. m, *m*-C_5H_5N), 5.974 (1 H, app. sept., app ^3J = 6.1 Hz, $NC\underline{H}Me_2$), 4.08 (1 H, m, $^{iPr}NHC\underline{H}_2CH_2N^{Me}$), 3.23 (1 H, m, $^{iPr}NC\underline{H}_2CH_2N^{Me}$), 3.06-3.01 (2 H, overlapping 2 x m, $^{iPr}NC\underline{H}_2CH_2N^{Me}$ and $NHC\underline{H}Me_2$), 2.77 (6 H, s, $C_6H_3\underline{Me}_2$), 2.59-2.50 (2 H, overlapping 2 x m, $^{iPr}NHCH_2C\underline{H}_2N^{Me}$ and $^{iPr}NCH_2C\underline{H}_2N^{Me}$), 2.43 (1 H, m, $^{iPr}NHC\underline{H}_2CH_2N^{Me}$), 2.32 (3 H, s, NMe), 2.22 (1 H, m, $^{iPr}NHCH_2C\underline{H}_2N^{Me}$), 1.64 (1 H, m, $^{iPr}NCH_2C\underline{H}_2N^{Me}$), 1.58 (3 H, d, ^3J = 6.0 Hz, $NHCH\underline{Me}_2$), 1.55 (3 H, d, ^3J = 6.2 Hz, $NCH\underline{Me}_2$), 1.29 (3 H, d, ^3J = 6.2 Hz, $NCH\underline{Me}_2$), 0.87 (3 H, d, ^3J = 6.2 Hz, $NCH\underline{Me}_2$) ppm. $^{13}C\{^1H\}$ NMR (toluene-d_8, 125.7 MHz, 233 K): δ 157.6 (*o*-$NC_6H_3Me_2$), 155.3 (Ti$\underline{C}$C), 153.7 (*o*-C_5H_5N), 132.9 (*i*-$C_6H_3Me_2$) 132.4 (*p*-C_5H_5N), 131.2 (*o*-$C_6H_4CF_3$), 128.1 (*m*-$C_6H_3Me_2$), 125.9 (q, ^3J = 1.5 Hz, *m*-$C_6H_4CF_3$), 123.3 (*m*-C_5H_5N), 117.6 (*p*-$C_6H_3Me_2$), 110.4 (TiC$\underline{C}$), 61.2 (N$\underline{C}$HMe$_2$), 59.1 ($^{iPr}NHCH_2\underline{C}H_2N^{Me}$), 51.9 ($^{iPr}NCH_2\underline{C}H_2N^{Me}$), 49.3 (NH$\underline{C}HMe_2$), 47.9 (NMe), 45.2 ($^{iPr}N\underline{C}H_2CH_2N^{Me}$), 42.1 ($^{iPr}NH\underline{C}H_2CH_2N^{Me}$), 25.2 ($NHCH\underline{Me}_2$), 22.0 ($NCH\underline{Me}_2$), 21.2 ($NCH\underline{Me}_2$), 21.0 ($NHCH\underline{Me}_2$), 20.3 ($C_6H_3\underline{Me}_2$) ppm. The resonances attributable to CF_3, *p*-$\underline{C}_6H_4(CF_3)$ and *i*-$\underline{C}_6H_4(CF_3)$ were not observed. ^{19}F NMR (toluene-d_8, 470.1 MHz, 233 K): δ -61.4 (CF_3) ppm.

Low temperature NMR tube scale synthesis of Ti($HN_2^{iPr}N^{Me}$)(CC-3,5-$C_6H_3(CF_3)_2$)(NXyl)(py) (34). To a solution of Ti($N_2^{iPr}N^{Me}$)(NXyl)(py) (**1**, 0.030 g, 0.067 mmol) in toluene-d_8 (0.6 mL) precooled to -78 ^{0}C in an NMR tube equipped

with a J. Young Teflon valve was added HCC-3,5-$C_6H_3(CF_3)_2$ (0.024 mL, 0.134 mmol). The NMR probe was cooled to -60 ^{0}C and a blank toluene-d_8 sample added before being locked and shimmed. The experimental sample then replaced the blank sample and allowed to thermally equilibrate, the shimming was then checked. The sample was then warmed to -50 ^{0}C, the ^{1}H NMR spectra indicated **34** was the only species present. Compound **34** was subsequently characterised by ^{1}H, ^{13}C and ^{19}F spectroscopy at -50 ^{0}C. ^{1}H NMR (toluene-d_8, 499.9 MHz, 223 K): δ 9.28 (2 H, br. m, *o*-C_5H_5N), 7.94 (2 H, s, *o*-$C_6H_3(CF_3)_2$), 7.51 (1 H, s, *p*-$C_6H_3(CF_3)_2$), 6.96 (2 H, d, ^3J = 7.1 Hz, *m*-$C_6H_3Me_2$), 6.65-6.61 (2 H, overlapping 2 x m, *p*-$C_6H_3Me_2$ and *p*-C_5H_5N), 6.43 (2 H, br. m, *m*-C_5H_5N), 5.74 (1 H, app. sept., app. ^3J = 5.9 Hz, NC<u>H</u>Me_2), 3.85 (1 H, m, ^{iPr}NHC<u>H</u>$_2$CH$_2$N^{Me}), 3.27 (1 H, br. m, NH), 2.98 (1 H, m, ^{iPr}NC<u>H</u>$_2$CH$_2$N^{Me}), 2.81 (1 H, m, ^{iPr}NC<u>H</u>$_2$CH$_2$N^{Me}), 2.74 (1 H, br. m, NHC<u>H</u>Me_2), 2.55 (6 H, s, C_6H_3<u>Me_2</u>), 2.31 (1 H, m, ^{iPr}NCH$_2$C<u>H</u>$_2$N^{Me}), 2.20-2.13 (2 H, overlapping 2 x m, ^{iPr}NHC<u>H</u>$_2$CH$_2$N^{Me} and ^{iPr}NHCH$_2$C<u>H</u>$_2$N^{Me}), 2.00 (3 H, s, NMe), 1.96 (1 H, m, ^{iPr}NCH$_2$C<u>H</u>$_2$N^{Me}), 1.38 (3 H, d, ^3J = 5.2 Hz, NHCH<u>Me_2</u>), 1.35 (3 H, d, ^3J = 5.5 Hz, NHCH<u>Me_2</u>), 1.30 (1 H, m, ^{iPr}NHCH$_2$C<u>H</u>$_2$N^{Me}), 1.08 (3 H, d, ^3J = 5.5 Hz, NHCH<u>Me_2</u>), 0.64 (3 H, d, ^3J = 5.2 Hz, NHCH<u>Me_2</u>) ppm. ^{13}C{^{1}H} NMR (toluene-d_8, 125.8 MHz, 223 K): δ 157.5 (*i*-$C_6H_3Me_2$), 153.4 (*o*-C_5H_5N), 132.8 (*o*-$C_6H_3Me_2$), 131.4 (q, $^2J_{C\text{-}F}$ = 32.4 Hz, *m*-$C_6H_3(CF_3)_2$), 130.6 (*o*-$C_6H_3(CF_3)_2$), 127.8 (*m*-$C_6H_3Me_2$), 124.4 (*i*-$C_6H_3(CF_3)_2$), 123.4 (q, $^1J_{C\text{-}F}$ = 275.0 Hz, CF_3), 118.0 (*p*-$C_6H_3(CF_3)_2$), 117.7 (*p*-$C_6H_3Me_2$), 109.1 (TiC<u>C</u>), 61.3 (N<u>C</u>HMe_2), 58.9 (^{iPr}NCH$_2$<u>C</u>H$_2$N^{Me}), 51.5 (^{Pr}NHCH$_2$<u>C</u>H$_2$N^{Me}), 49.2 (NH<u>C</u>HMe_2), 47.7 (NMe), 45.1 (^{iPr}N<u>C</u>H$_2$CH$_2$N^{Me}), 42.0 (^{iPr}NH<u>C</u>H$_2$CH$_2$N^{Me}), 25.3 (NHCH<u>Me_2</u>), 21.9 (NCH<u>Me_2</u>), 21.1 (NCH<u>Me_2</u>), 20.9 (NHCH<u>Me_2</u>), 20.2 (C_6H_3<u>Me_2</u>) ppm. ^{19}F NMR (toluene-d_8, 470.1 MHz, 223 K): δ -62.4 (6F, CF_3) ppm.

Kinetic measurements for the isomerisation of Ti($H_2N_2^{iPr}N^{Me}$)(CCC_6F_5)$_2$(NXyl) (23) to Ti($N_2^{iPr}N^{Me}$){N(Xyl)C(H)C(H)C_6F_5}(C_6F_5) (24). The general procedure is as follows. In a dry-box, **23** (10 mg, 13.3 μmol) was weighed into a vial and dissolved in toluene-d_8 (0.5 mL). The vial was agitated and the solution transferred to a J. Young NMR tube. A blank toluene-d_8 sample was added to the NMR probe at RT, locked and shimmed, heated to 70 °C (other reaction temperatures were also used as noted in the main text), and the sample shimmed again. The experimental sample then replaced the blank sample (and allowed to thermally equilibrate where necessary) the shimming checked and an array set up recording a spectrum of 4 scans every 120 s.

The decay of **23** was calculated by measuring the integral of the $NC_6H_3\underline{Me_2}$. First order rate constants were obtained from linear plots of -ln([Ti]/[Ti]$_0$) *vs.* time.

Kinetic measurements for reaction of Ti($H_2N_2^{iPr}N^{Me}$)(CCC_6F_5)$_2$(NXyl) (23) with Ti($N_2^{iPr}N^{Me}$)($NNPh_2$)(py) (2.1). The general procedure is as follows. In a dry-box, compound **23** (10 mg, 13.3 μmol) was weighed into a vial and dissolved in toluene-d_8 (0.25 mL). In a separate vial, **2.1** (6.7 mg, 13.3 μmol) was dissolved in toluene-d_8 (0.25 mL). The two vials were then combined, agitated quickly and transferred to a J. Young NMR tube. A blank toluene-d_8 sample was added to the NMR probe at RT, locked and shimmed, heated to 31 °C (other reaction temperatures were also used as noted in the main text), and the sample shimmed again. The experimental sample then replaced the blank sample (and allowed to thermally equilibrate where necessary) the shimming checked and an array set up recording a spectrum of 4 scans every 120 s. The decay of **23** was calculated by measuring the integral of the $^{iPr}NC\underline{H_2}$. First order rate constants were obtained from linear plots of -ln([Ti]/[Ti]$_0$) *vs.* time.

Ti($N_2^{iPr}N^{Me}$)(CCC_6F_5)(N(Xyl)C(H)C(H)($C_6H_4CF_3$) (35). To a stirred solution of Ti($H_2N_2^{iPr}N^{Me}$)(CCC_6F_5)$_2$(NXyl) (**23**, 0.497 g, 0.670 mmol, made *in situ*) in benzene (5 mL) was added HCC-4-$C_6H_4CF_3$ (0.220 mL, 1.35 mmol). The solution was left to stir for 15 hours at RT then heated at 70 °C for 3 hours. The volatiles were removed under reduced pressure to yield a dark red oil which was triturated in hexane and filtered to yield **35** as a bright red powder which was dried *in vacuo*. Yield: 0.170 g (35%). Diffraction-quality crystals were grown from a saturated benzene solution at 4 ^{0}C. ^{1}H NMR (C_6D_6, 299.9 MHz, 298 K): δ 8.18 (1 H, d, ^3J = 13.6 Hz, TiNC($\underline{H}$)C(H)), 7.31 (2 H, d, ^3J = 8.3 Hz, *m*-$C_6H_4CF_3$), 7.16-7.11 (3 H, overlapping 2 x m, overlapping *m*-$C_6H_3Me_2$ and *p*-$C_6H_3Me_2$), 6.95 (2 H, d, ^3J = 8.3 Hz, *o*-$C_6H_4CF_3$), 5.13 (2 H, app. sept., app. ^3J = 6.2 Hz, C$\underline{H}Me_2$), 4.82 (1 H, d, ^3J = 13.6 Hz, TiNC(H)C($\underline{H}$)), 3.35 (2 H, m, $^{iPr}NC\underline{H_2}$), 3.01 (2H, m, $^{iPr}NC\underline{H_2}$), 2.72 (2 H, m, $^{Me}NC\underline{H_2}$), 2.53 (6 H, s, $C_6H_3\underline{Me_2}$), 2.21 (2 H, m, $^{Me}NC\underline{H_2}$), 2.16 (3 H, s, NMe), 1.34 (6 H, d, ^3J = 6.2 Hz, CH$\underline{Me_2}$), 0.87 (6 H, d, ^3J = 6.2 Hz, CH$\underline{Me_2}$) ppm. ^{13}C{^{1}H} NMR (C_6D_6, 75.4 MHz, 298 K): δ 164.8 (TiC), 147.9 (d, $^1J_{C\text{-}F}$ = 257.0, *o*-C_6F_5) 143.97 (*i*-$C_6H_3Me_2$), 143.7 (*p*-$C_6H_4CF_3$), 142.10 (TiN$\underline{C}$(H)C(H)), 140.0 (d, $^1J_{C\text{-}F}$= 259.4 Hz, *p*-C_6F_5), 141.2 (d, $^1J_{C\text{-}F}$ = 251.5 Hz, *m*-C_6F_5), 134.7 (*o*-$C_6H_3Me_2$), 129.4 (*m*-$C_6H_3Me_2$), 126.6 (*p*-$C_6H_3Me_2$), 125.8 (m, *m*-$C_6H_4CF_3$), 124.9 (*o*-$C_6H_4CF_3$), 102.3 (t, $^2J_{C\text{-}F}$ = 20.5 Hz, *i*-C_6F_5), 101.3 (*i*-$C_6H_4CF_3$), 98.6 (TiNC(H)$\underline{C}$(H)), 84.4 (TiC$\underline{C}$), 58.4 ($^{Me}N\underline{C}H_2$), 53.2 ($\underline{C}HMe_2$), 47.5

($^{iPr}NCH_2$), 44.6 (NMe), 21.2 ($CHMe_2$), 20.1 ($CHMe_2$), 19.9 ($C_6H_3Me_2$) ppm. The resonance attributable to CF_3 was not observed. ^{19}F NMR (C_6D_6, 282.1 MHz, 298 K): δ -61.5 (3F, CF_3), -138.8 (m, *o*-C_6F_5), -157.7 (t, ^3J = 20.1 Hz, *p*-C_6F_5), -163.8 (m, *m*-C_6F_5) ppm. IR (NaCl plates, Nujol mull, cm^{-1}): 1596 (m), 1513 (m), 1260 (s), 1067 (s), 1019 (m), 961 (w), 800 (m). EI-MS: *m/z* = 728 $[M]^+$ (2%). Anal. found (calcd. for $C_{36}H_{40}N_4F_8Ti$): C, 59.28 (59.35); H, 5.39 (5.53); N, 7.71 (7.69)%.

Ti($N_2^{iPr}N^{Me}$)(CCC_6F_5)(N(2,6-$C_6H_3Me_2$)C(H)C(H)C_6H_4Me) (36). To a stirred solution of Ti($H_2N_2^{iPr}N^{Me}$)(CCC_6F_5)(NXyl) (**23**, 0.100 g, 0.133 mmol, made *in situ*) in benzene (3 mL) was added HCC-4-C_6H_4Me (0.169 mL, 1.33 mmol). The solution was left to stir for 7 days at RT. The volatiles were removed under reduced pressure yielding **36** as a dark red sticky solid to which was dried *in vacuo.* Yield: 0.085 g (95%).^1H NMR (C_6D_6, 500.3 MHz, 298 K): δ 8.24 (1 H, d, ^3J = 13.8 Hz, TiNC(H)C(H)), 7.18 (2 H, d, ^3J = 7.5 Hz, *m*-$C_6H_3Me_2$), 7.14-7.01 (3 H, overlapping 2 x m, *p*-$C_6H_3Me_2$ and *o*-C_6H_4Me), 6.95 (2 H, d, ^3J = 8.0 Hz, *m*-C_6H_4Me), 5.14 (2 H, app. sept., app. ^3J = 6.3 Hz, $CHMe_2$), 4.96 (1 H, d, ^3J = 13.8 Hz, TiNC(H)C(H)), 3.36 (2 H, m, $^{iPr}NCH_2$), 3.03 (2 H, m, $^{iPr}NCH_2$), 2.72 (2 H, m, $^{Me}NCH_2$), 2.57 (6 H, s, $C_6H_3Me_2$), 2.23 (2 H, m, $^{Me}NCH_2$), 2.19 (3 H, s, NMe), 2.11 (3 H, s, C_6H_4Me), 1.35 (6 H, d, ^3J = 6.3 Hz, $CHMe_2$), 0.93 (6 H, d, ^3J = 6.3 Hz, $CHMe_2$) ppm. $^{13}C\{^1H\}$ NMR (C_6D_6, 125.8 MHz, 298 K): δ 165.1 (m, TiC), 148.0 (d, $^1J_{C\text{-}F}$ = 250.8 Hz, *o*-C_6F_5), 144.4 (*i*-$C_6H_3Me_2$), 139.9 (d, $^1J_{C\text{-}F}$ = 250.7 Hz, *p*-C_6F_5), 139.2 (TiNC(H)C(H)), 137.9 (d, $^1J_{C\text{-}F}$ = 248.0 Hz, *m*-C_6F_5), 136.8 (*i*-C_6H_4Me), 134.9 (*o*-$C_6H_3Me_2$), 133.9 (*p*-C_6H_4Me), 129.6 (*m*-C_6H_4Me), 129.2 (*m*-$C_6H_3Me_2$), 126.3 (*p*-$C_6H_3Me_2$), 125.5 (*o*-C_6H_4Me), 102.5 (t, $^1J_{C\text{-}F}$ = 19.1 Hz, *o*-C_6F_5), 100.3 (TiNC(H)C(H)), 84.8 (m, TiCC), 58.4 ($^{Me}NCH_2$), 53.0 ($CHMe_2$), 47.3 ($^{iPr}NCH_2$), 44.7 (NMe), 21.2 ($CHMe_2$), 21.1 (C_6H_4Me), 20.1 ($C_6H_3Me_2$), 20.1 ($CHMe_2$) ppm. ^{19}F NMR (C_6D_6, 376.5 MHz, 298 K): δ -138.7 (2F, *o*-C_6F_5), -158.3 (1F, *p*-C_6F_5), -164.0 (2F, *m*-C_6F_5) ppm. IR (NaCl plates, Nujol mull, cm^{-1}): 1648 (M), 1601 (m), 1512 (m), 1494 (m), 1260 (w), 1158 (w), 1084 (w), 1021 (w), 990)m), 960 (m), 797 (m), 765 (w), 722 (m). EI-MS *m/z*: 674 $[M]^+$ (10%). Anal. found (calcd. for $C_{36}H_{43}F_5N_4Ti$): C,64.12 (64.09); H, 6.32 (6.42); N, 8.46 (8.31)%.

NMR tube scale synthesis of Ti($H_2N_2^{iPr}N^{Me}$)(CCC_6F_5)$_2$($NNPh_2$) (2.1_Int3-C_6F_5). To a solution of Ti($N_2^{iPr}N^{Me}$)($NNPh_2$)(py) (**2.1**, 0.020 mg, 0.039 mmol) in C_6D_6 (0.3 mL) in an NMR tube equipped with a J. Young Teflon valve was added $HCCC_6F_5$

(0.015 mg, 0.079 mmol) in C_6D_6 (0.3 mL) at RT. An immediate colour change from brown to red was observed. Five minutes after mixing the ^{1}H NMR spectrum showed Ti($H_2N_2^{iPr}N^{Me}$)(CCC_6F_5)$_2$($NNPh_2$) (**2.1_Int3-C_6F_5**) and **3.5** in a 15:85% ratio. **2.1_Int3-C_6F_5** was characterised by ^{1}H and ^{19}F NMR spectroscopy.^{1}H NMR (C_6D_6, 500.3 MHz, 298 K): δ 8.22-2.21 (4 H, m, *o*-C_6H_5 overlapping with **3.5**), 7.36 (4 H, app. t, app. ^3J = 7.9 Hz, *o*-C_6H_5), 6.94 (2 H, t, ^3J = 7.4 Hz, *p*-C_6H_5), 3.69-3.61 (4 H, overlapping 2 x m, overlapping NH and ^{Me}NC$\underline{H}_2$), 3.26 (2H, d of sept., ^3J = 6.3, 6.2 Hz, HNC$\underline{H}$Me$_2$), 2.51 (2 H, m, ^{iPr}NC$\underline{H}_2$), 2.26 (2 H, m, ^{iPr}NC$\underline{H}_2$), 2.24 (3 H, s, NMe) 1.67 (2 H, m, ^{Me}NC$\underline{H}_2$), 1.03 (12 H, overlapping 2 x d, ^3J = 6.3 Hz, CH$\underline{Me}_2$) ppm. ^{19}F NMR (C_6D_6, 376.5 MHz, 298 K): δ -140.3 (4F, o_a-C_6F_5 and o_b-C_6F_5), -158.3 (1F, p_a-C_6F_5), -159.7 (1F, p_b-C_6F_5), -163.5 (2F, m_a-C_6F_5), -164.3 (2F, m_b-C_6F_5) ppm.

NMR tube scale synthesis of Ti($N_2^{iPr}N^{Me}$){N(NPh_2)C(H)C(H)-4-$C_6H_4CF_3$)}(CCC_6F_5) (37). To a solution of Ti($N_2^{iPr}N^{Me}$)($NNPh_2$)(py) (**2.1**, 0.020 mg, 0.039 mmol) in C_6D_6 (0.3 mL) in an NMR tube equipped with a J. Young Teflon valve was added a premixed solution of $HCCC_6F_5$ (0.0076 mg, 0.039 mmol) and HCC-4-$C_6H_4CF_3$ (0.0067 mg, 0.039 mmol) in C_6D_6 (0.3 mL) at RT. An immediate colour change from brown to red was observed. The ^{1}H NMR spectrum showed Ti($N_2^{iPr}N^{Me}$){N(NPh_2)C(H)C(H)$C_6H_4CF_3$)}(CCC_6F_5) (**37**), **3.3** and **3.5** in a 75:16:9% ratio. **37** was characterised by ^{1}H, ^{13}C and ^{19}F NMR spectroscopy. ^{1}H NMR (C_6D_6, 299.9 MHz, 298 K): δ 8.02 (1 H, d, ^3J = 13.9 Hz, TiNC($\underline{H}$)C(H)), 7.63 (4 H, d, ^3J = 7.8 Hz, *o*-C_6H_5), 7.23 (H, d, ^3J = 8.3 Hz, *m*-$C_6H_4CF_3$), 7.15 (4 H, m, *m*-C_6H_5), 6.97 (2 H, d, ^3J = 8.3 Hz, *o*-$C_6H_4CF_3$), 6.79 (2 H, t, ^3J = 6.8 Hz, *p*-C_6H_5), 5.70 (1 H, d, ^3J = 13.9 Hz, TiNC(H)C($\underline{H}$)), 5.59 (2 H, app. sept., app. ^3J = 6.4 Hz, C$\underline{H}$Me$_2$), 3.34 (2 H, m, ^{iPr}NCH$_2$), 2.96 (2 H, m, ^{iPr}NCH$_2$), 2.77 (2 H, m, ^{Me}NCH$_2$), 2.11 (2 H, m, ^{Me}NCH$_2$), 1.94 (3 H, s, NMe), 1.39 (6 H, d, ^3J = 6.4 Hz, CH$\underline{Me}_2$), 0.87 (6 H, d, ^3J = 6.4 Hz, CH$\underline{Me}_2$) ppm. ^{13}C{^{1}H} NMR (C_6D_6, 125.7 MHz, 298 K): δ 164.7 (TiC), 147.5 (d, $^1J_{C\text{-}F}$ = 244.9 Hz, *o*-C_6F_5), 146.5 (*i*-C_6H_5), 142.6 (*p*-$C_6H_4CF_3$), 142.4 (*i*-$C_6H_4CF_3$), 142.2 (TiN$\underline{C}$(H)C(H)), 139.6 (d, $^1J_{C\text{-}F}$ = 251.7 Hz, *p*-C_6F_5), 137.5 (d, $^1J_{C\text{-}F}$ = 251.7 Hz, *m*-C_6F_5), 128.5 (*m*-C_6H_5), 125.3 (q, $^3J_{C\text{-}F}$ = 3.8 Hz, *m*-$C_6H_4CF_3$), 124.5 (*o*-$C_6H_4CF_3$), 122.5 (*p*-C_6H_5), 120.5 (*o*-C_6H_5), 102.2 (t, $^2J_{C\text{-}F}$ = 18.6 Hz, *i*-C_6F_5), 101.4 (TiNC(H)$\underline{C}$(H)), 83.9 (m, TiC$\underline{C}$), 57.7 (^{Me}N$\underline{C}$H$_2$), 53.4 ($\underline{C}$HMe$_2$), 47.3 (^{iPr}N$\underline{C}$H$_2$), 44.4 (NMe), 20.9 (CH$\underline{Me}_2$), 20.6 (CH$\underline{Me}_2$) ppm. ^{19}F NMR (C_6D_6, 282.1 MHz, 298 K): -61.7 (3F, CF_3), -138.7 (2F, *o*-C_6F_5), -157.8 (1F, *p*-C_6F_5), -163.9 (2F, *m*-C_6F_5) ppm.

NMR tube scale synthesis of Ti($N^{iPr}N^{Me}NCMe_2C(H)CC_6H_4CF_3$))(N(Xyl)C(H)C(H)$C_6H_4CF_3$) (39). To a solution of Ti($N_2{}^{iPr}N^{Me}$)(NXyl)(py) (**1**, 0.020 mg, 0.045 mmol) in C_6D_6 (0.3 mL) in an NMR tube equipped with a J. Young Teflon valve was added HCC-4-$C_6H_4CF_3$ (0.015 μL, 0.089 mmol) in C_6D_6 (0.3 mL) at RT. The solution was heated at 70 °C for 40 mins. A colour change from dark brown to red was observed. ^{1}H NMR showed Ti($N^{iPr}N^{Me}NCMe_2C(H)CC_6H_4CF_3$))(N(Xyl)C(H)C(H)$C_6H_4CF_3$) (**39**) and **29** in a 45:55% ratio. **39** was subsequently characterised by ^{1}H, ^{13}C and ^{19}F NMR spectroscopy. ^{1}H NMR (C_6D_6, 500.3 MHz, 298 K): δ 8.50 (1 H, d, ^3J = 13.0 Hz, TiN(Xyl)C(H)C(H)), 7.61 (2 H, d, ^3J = 8.1 Hz, TiC(*m*-$C_6H_4CF_3$)), 7.47 (2 H, d, ^3J = 8.3 Hz, TiN(Xyl)C(H)C(H)-*m*-$C_6H_4CF_3$), 7.31-7.20 (3 H, overlapping 2 x m, *m*-$C_6H_3Me_2$ and *p*-$C_6H_3Me_2$), 7.15 (2 H, d, ^3J = 8.1 Hz, TiC(*o*-$C_6H_4CF_3$)), 7.12 (2 H, d, ^3J = 8.3 Hz, TiN(Xyl)C(H)C(H)-*o*-$C_6H_4CF_3$), 6.70 (1 H, s, TiC($C_6H_4CF_3$)C(H)), 5.04 (1 H, d, ^3J = 13.0 Hz, TiN(Xyl)C(H)C(H)), 4.64 (1 H, app. sept., app. ^3J = 6.3 Hz, CHMe$_2$), 3.83 (1 H, m, ^{CMe_2}NCH$_2$CH$_2$N^{Me}), 3.62 (1 H, m, ^{iPr}NCH$_2$CH$_2$N^{Me}), 3.21-3.13 (2 H, overlapping 2 x m, ^{CMe_2}NCH$_2$CH$_2$N^{Me} and ^{iPr}NCH$_2$CH$_2$N^{Me}), 3.07 (1 H, m, ^{iPr}NCH$_2$CH$_2$N^{Me}), 3.03 (1 H, m, ^{CMe_2}NCH$_2$CH$_2$N^{Me}), 2.52 (3 H, s, $C_6H_3Me_2$), 2.52 (1 H, m, ^{CMe_2}NCH$_2$CH$_2$N^{Me}), 2.39 (3 H, s, $C_6H_3Me_2$), 2.04 (1 H, m, ^{iPr}NCH$_2$CH$_2$N^{Me}) 2.0 (3 H, s, NMe), 1.52 (3 H, s, CMe$_2$), 1.27 (3 H, s, CMe$_2$), 1.05 (3 H, d, ^3J = 6.3 Hz, CHMe$_2$), 0.73 (3 H, d, ^3J = 6.3 Hz, CHMe$_2$) ppm. ^{13}C{^{1}H} NMR (C_6D_6, 125.8 MHz, 298 K): δ 198.1 (TiC), 154.3 (TiC(*i*-$C_6H_4CF_3$), 152.9 (TiC($C_6H_4CF_3$)C(H)), 144.8 (*i*-$C_6H_3Me_2$), 144.4 (TiN(Xyl)C(H)C(H)-*i*-$C_6H_4CF_3$), 142.9 (TiN(Xyl)C(H)C(H)), 135.1 (*o*-$C_6H_3Me_2$), 134.7 (*o*-$C_6H_3Me_2$), 129.3 (*m*-$C_6H_3Me_2$), 129.2 (*m*-$C_6H_3Me_2$), 126.4 (TiC(*o*-$C_6H_4CF_3$), 126.2 (*p*-$C_6H_3Me_2$), 125.8 (m, TiN(Xyl)C(H)C(H)-*m*-$C_6H_4CF_3$), 124.8 (m, TiC(*m*-$C_6H_4CF_3$)), 123.9 (TiN(Xyl)C(H)C(H)-*o*-$C_6H_4CF_3$), 98.2 (TiN(Xyl)C(H)C(H)), 67.1 (CMe$_2$), 59.7 (^{CMe_2}NCH$_2$CH$_2$N^{Me}), 54.1 (^{iPr}NCH$_2$CH$_2$N^{Me}), 50.7 (^{CMe_2}NCH$_2$CH$_2$N^{Me}), 50.0 (CHMe$_2$), 45.5 (^{iPr}NCH$_2$CH$_2$N^{Me}), 44.0 (NMe), 28.9 (CMe$_2$), 25.0 (CMe$_2$), 22.8 (CHMe$_2$), 20.4 (CHMe$_2$), 20.4 ($C_6H_3Me_2$), 19.5 ($C_6H_3Me_2$) ppm. Resonances attributable to carbon atoms directly bound to ^{19}F atoms, TiN(Xyl)C(H)C(H)-*p*-$C_6H_4CF_3$ and TiC(*p*-$C_6H_4CF_3$) were not observed. ^{19}F NMR (C_6D_6, 282.1 MHz, 298 K): δ -61.34 (TiC($C_6H_4CF_3$), 3F), -61.49 (N($C_6H_3Me_2$)C(H)C(H)$C_6H_4CF_3$, 3F) ppm.

Ti($H_2N_2^{iPr}N^{Me}$)(CCC_6F_5)$_2$(NDipp) (40). To a stirred solution of Ti($N_2^{iPr}N^{Me}$)(NDipp)(py) (**3**, 0.080 g, 0.160 mmol) in benzene (1 mL) was added $HCCC_6F_5$ (0.043 mL, 0.320 mmol) all at RT. The solution was left to stir for 30 minutes at RT after which the volatiles were removed to yield a dark brown oil which was triturated in pentane (2 mL) and filtered. The resultant solid was washed with pentane cold (2 mL) to afford **40** as an off-white solid which was dried *in vacuo*. Yield 0.102 mg (78 %). ^{1}H NMR (C_6D_6, 400.1 MHz, 298 K): δ 7.09 (2 H, d, ^3J = 7.5 Hz, *m*-$C_6H_3(CHMe_2)_2$), 6.87 (1 H, t, ^3J = 7.5 Hz, *p*-$C_6H_3(CHMe_2)_2$), 5.51 (2 H, br. m, $C_6H_3(C\underline{H}Me_2)_2$), 3.80-3.71 (4H, overlapping 2 x m, N$\underline{H}$ and $^{Me}NC\underline{H}_2$), 3.43 (2 H, d. sept., ^3J = 6.1, 6.2 Hz, C$\underline{H}Me_2$), 2.60 (2 H, app. q, app. ^3J = 11.6 Hz, $^{iPr}NC\underline{H}_2$), 2.29 (2 H, app. d, app. ^3J = 13.0 Hz, $^{iPr}NC\underline{H}_2$), 2.24 (3 H, s, NMe), 1.76 (2 H, app. d, app. ^3J = 11.7 Hz, $^{Me}NC\underline{H}_2$), 1.50 (12 H, d, ^3J = 6.6 Hz, $C_6H_3(CH\underline{Me}_2)_2$), 1.14 (6 H, d, ^3J = 6.4 Hz, CH$\underline{Me}_2$), 1.11 (6 H, d, ^3J = 6.4 Hz, CH$\underline{Me}_2$) ppm. $^{13}C\{^1H\}$ NMR (C_6D_6, 100.6 MHz, 298 K): δ 166.0 (m, TiCC), 163.6 (m, TiCC), 154.5 (*o*-$C_6H_3(CHMe_2)_2$), 146.8 (d, $^1J_{C\text{-}F}$ = 242.6 Hz, overlapping o_a-C_6F_5 and o_b-C_6F_5), 146.4 (*i*-$C_6H_3(CHMe_2)_2$), 139.3 (d, $^1J_{C\text{-}F}$ = 253.0 Hz, p_a-C_6F_5), 139.0 (d, $^1J_{C\text{-}F}$ = 253.0 Hz, p_b-C_6F_5), 137.7 (d, $^1J_{C\text{-}F}$ = 148.9 Hz, overlapping m_a-C_6F_5 and m_b-C_6F_5), 122.5 (*m*-$C_6H_3(CHMe_2)_2$), 121.7 (*p*-$C_6H_3(CHMe_2)_2$), 103.4 (app. t, app. $^2J_{C\text{-}F}$ = 18.8 Hz, i_a-C_6F_5), 103.9 (app. t, app. $^2J_{C\text{-}F}$ = 18.8 Hz, i_b-C_6F_5), 96.0 (m, TiC$\underline{C}$), 94.5 (TiC$\underline{C}$), 57.7 ($^{Me}N\underline{C}H_2$), 52.3 ($\underline{C}HMe_2$), 46.2 (NMe), 44.9 ($^{iPr}N\underline{C}H_2$), 27.0 ($C_6H_3(C\underline{H}Me_2)_2$), 24.7 ($C_6H_3(CH\underline{Me}_2)_2$), 22.3 (CH$\underline{Me}_2$), 20.4 (CH$\underline{Me}_2$) ppm. ^{19}F NMR ($C_6D_6$, 376.4 MHz, 298 K): δ -140.3 (4F, m, overlapping o_a-C_6F_5 and o_b-C_6F_5), -158.1 (1F, p_a-C_6F_5), -159.5 (1F, p_b-C_6F_5), -163.3 (2F, m_a-C_6F_5), -164.1 (2F, m_b-C_6F_5) ppm. Note: subscripts ″a″ and ″b″ refer to the inequivalent CCC_6F_5 environments. IR (NaCl plates, Nujol mull, cm^{-1}): 3231 (w), 2084 (w), 1627 (w), 1513 (m), 1462 (m), 1331.2 (w), 1271 (m), 1095 (m), 1095 (m), 1055 (w), 988 (s), 957 (s), 805 (m), 754 (m). Anal. found (calcd. for $C_{39}H_{43}F_{10}N_4Ti$): C, 57.94 (58.14); H, 5.48 (5.38); N, 7.04 (6.95)%.

Ti($N_2^{iPr}N^{Me}$)(CCC_6F_5){N(Dipp)C(H)C(H)C_6F_5} (41). To a stirred solution of Ti($N_2^{iPr}N^{Me}$)(NDipp)(py) (**3**, 0.080 g, 0.160 mmol) in benzene (1 mL) was added C_6F_5CCH (0.043 mL, 0.320 mmol) all at RT. The solution was heated to 70 °C and left to stir for 24 hours during which a colour change to dark red was observed. The volatiles were then removed under reduced pressure to yield **41** as a red solid which was washed with minimal amount of cold pentane and then dried *in vacuo*. Yield 0.85

mg (66%). The ^{1}H NMR spectrum indicated an approximately 50:50% mixture of the *cis* and *trans* isomers.

Cis isomer: ^{1}H NMR (C_6D_6, 500.3 MHz, 298 K): δ 8.43 (1 H, d, ^{3}J = 13.8 Hz, TiNC(H)C(H)), 7.29-7.22 (3 H, overlapping 2 x m, *m*-$C_6H_3(CHMe_2)_2$ and *p*-$C_6H_3(CHMe_2)_2$), 5.32 (2 H, app. sept., app. ^{3}J = 6.3 Hz, $CHMe_2$), 4.59 (1 H, d, ^{3}J = 13.8 Hz, (TiNC(H)C(H)), 3.75 (2 H, br. m, $C_6H_3(CHMe_2)_2$), 3.35 (2 H, m, $^{iPr}NCH_2$), 3.01 (2 H, m, $^{iPr}NCH_2$), 2.79 (2 H, m, $^{Me}NCH_2$), 2.35 (3 H, s, NMe), 2.31 (2 H, m, $^{Me}NCH_2$), 1.38 (6 H, d, ^{3}J = 6.5 Hz, $C_6H_3(CHMe_2)_2$), 1.35 (6H, d, ^{3}J = 6.3 Hz, $CHMe_2$), 1.34 (6 H, d, ^{3}J = 6.5 Hz, $C_6H_3(CHMe_2)_2$), 0.76 (6 H, d, ^{3}J = 6.3 Hz, $CHMe_2$) ppm. $^{13}C\{^{1}H\}$ NMR (C_6D_6, 125.8 MHz, 298 K): δ 164.0 (TiC), 148.1 (TiNC(H)C(H)), 147.8 (d, $^{1}J_{C\text{-}F}$ = 250.6 Hz, overlapping alkyne *o*-C_6F_5 and alkene *o*-C_6F_5), 144.3 (*o*-$C_6H_3(CHMe_2)_2$), 143.9 (d, $^{1}J_{C\text{-}F}$ = 247.4 Hz, overlapping alkyne *p*-C_6F_5 and alkene *p*-C_6F_5), 142.5 (*i*-$C_6H_3(CHMe_2)_2$), 137.9 (d, $^{1}J_{C\text{-}F}$ = 251.6 Hz, overlapping alkyne *m*-C_6F_5 and alkene *m*-C_6F_5), 127.2 (*p*-$C_6H_3(CHMe_2)_2$), 124.9 (*p*-$C_6H_3(CHMe_2)_2$), 114.7 (alkyne *i*-C_6F_5), 102.5 (t, $^{2}J_{C\text{-}F}$ = 18.5 Hz, alkene *i*-C_6F_5), 86.5 (TiNC(H)C(H)), 85.0 (TiCC), 58.2 ($CHMe_2$), 53.6 ($^{Me}NCH_2$), 47.2 ($^{iPr}NCH_2$), 44.7 (NMe), 28.3 ($C_6H_3(CHMe_2)_2$), 26.9 ($C_6H_3(CHMe_2)_2$), 24.4 ($C_6H_3(CHMe_2)_2$), 20.9 ($CHMe_2$), 19.3 ($CHMe_2$) ppm. ^{19}F NMR (C_6D_6, 376.4 MHz, 298 K): δ -138.7 (alkyne *o*-C_6F_5), -145.6 (alkene *o*-C_6F_5), -157.1 (alkyne *p*-C_6F_5), 163.5 (alkyne *m*-C_6F_5), -164.2 (alkene *p*-C_6F_5), -164.9 (alkene *p*-C_6F_5) ppm.

Trans isomer: ^{1}H NMR (C_6D_6, 500.3 MHz, 298 K): δ 9.03 (1H, d, ^{3}J = 13.9 Hz, TiNC(H)C(H)), 5.05 (1H, d, ^{3}J = 13.9 Hz, TiNC(H)C(H)) ppm. $^{13}C\{^{1}H\}$ NMR (C_6D_6, 126 MHz, 298 K): δ 159.1 (TiC), 88.9 (TiNC(H)C(H)), 87.6 (TiCC) ppm. Remaining resonances were not observed.

Common data: IR (NaCl plates, Nujol mull, cm^{-1}): 1633(s), 1592 (s), 1515 (s), 1494 (s), 1362 (w), 1334 (m), 1318 (m), 1256 (m), 1216 (w), 1178 (w), 1151 (w), 1123 (w), 1090 (w), 1075 (w), 1029 (m), 1009 (m), 991 (m), 961 (s), 889 (m), 878 (m), 823 (w), 803 (w), 789 (m), 754 (w). EI-MS: *m/z* = 806 $[M]^{+}$ (10%). Anal. found (calcd. for $C_{39}H_{44}F_{10}N_4Ti$): C, 57.89 (58.07); H, 5.41 (5.50); N, 6.97 (6.95)%.

Ti($N_2^{iPr}N^{Me}$){N(Dipp)C(H)C(4-C_6H_4Me)} (42). To a stirred solution of Ti($N_2^{iPr}N^{Me}$)(NDipp)(py) (**3**, 0.050 g, 0.09 mmol) in benzene (1 mL) was added TolCCH (0.013 mL, 0.09 mmol) all at RT. The solution was left to stir for 5 hours at RT after which the volatiles were removed to afford **42** as a dark red oil. Yield 0.040 mg (75 %). ^{1}H NMR (C_6D_6, 400.1 MHz, 298 K): δ 10.13 (1 H, s, TiCC(H), 7.46 (2 H,

d, ^{3}J = 7.8 Hz, *o*-C_6H_4Me), 7.19 (3 H, overlapping 2 x m, overlapping *m*-$C_6H_3(CHMe_2)_2$ and *p*-$C_6H_3(CHMe_2)_2$), 7.15 (2 H, m, *m*-C_6H_4Me overlapping with solvent), 4.75 (2 H, app. sept., app. ^{3}J = 6.8 Hz, C<u>H</u>Me_2), 3.41 (2 H, sept., ^{3}J = 7.0 Hz, $C_6H_3(C\underline{H}Me_2)_2$), 3.15 (2 H, m, $^{Me}NC\underline{H}_2$), 3.00 (2 H, m, $^{Me}NC\underline{H}_2$), 2.74 (2 H, m, $^{iPr}NC\underline{H}_2$), 2.26 (2 H, m, $^{iPr}NC\underline{H}_2$), 2.19 (3 H, s, $C_6H_4\underline{Me}$), 1.84 (3 H, s, NMe), 1.25 (6 H, d, ^{3}J = 6.8 Hz, C<u>H</u>Me_2), 1.20 (12 H, d, ^{3}J = 7.0 Hz, $C_6H_3(C\underline{H}Me_2)_2$), 1.04 (6 H, d, ^{3}J = 6.8 Hz, C<u>H</u>Me_2) ppm. $^{13}C\{^{1}H\}$ NMR (C_6D_6, 100.6 MHz, 298 K): δ 200.1 (Ti<u>C</u>C), 161.5 (TiC<u>C</u>), 149.4 (*i*-$C_6H_3(CHMe_2)_2$), 144.5 (*o*-$C_6H_3(CHMe_2)_2$), 142.8 (*i*-C_6H_4Me), 132.3 (*p*-C_6H_4Me), 129.4 (*m*-C_6H_4Me), 125.8 (*o*-C_6H_4Me), 125.4 (*p*-$C_6H_3(CHMe_2)_2$), 123.2 (*m*-$C_6H_3(CHMe_2)_2$), 56.0 ($^{Me}N\underline{C}H_2$), 52.3 (<u>C</u>HMe_2), 46.5 ($^{iPr}N\underline{C}H_2$), 42.4 (NMe), 27.3 ($C_6H_3(\underline{C}HMe_2)_2$), 25.6 ($C_6H_3(CH\underline{Me}_2)_2$) 22.8 (CH<u>Me</u>$_2$), 21.9 (CH<u>Me</u>$_2$), 20.8 ($C_6H_4\underline{Me}$) ppm. IR (NaCl plates, Nujol mull, cm^{-1}): 2725 (w), 2078 (w), 1647 (w), 1600 (s), 1504 (m), 1418 (w), 1335 (m), 1280 (w), 1259 (m), 1212 (w), 1157 (m), 1100 (m), 1086 (s), 1072 (w), 1041 (w), 918 (w), 817 (m), 800 (s), 759 (s), 674 (s). Anal. found (calcd. for $C_{32}H_{50}N_4Ti$): C, 72.91 (73.16); H, 9.27 (9.36); N, 10.35 (10.40)%.

5.7 Experimental details and characterising data for Chapter Four

Ti($N_2^{iPr}N^{Me}$){N(H)SiH_2Ph}(NPh_2) (43). To a stirred solution of Ti($N_2^{iPr}N^{Me}$)($NNPh_2$)(py) (**2.1**, 0.364g, 0.716 mmol) in benzene (5 mL) was added $PhSiH_3$ (0.089 mL, 0.716 mmol) at RT. After 12 h the volatiles were removed under reduced pressure to afford **43** as a dark red sticky solid. Yield: 0.364 g (90%). The ^{1}H NMR spectrum indicated approximately 60:40% mixture of the *cis* and *trans* isomers.

Major isomer (cis): ^{1}H NMR (C_6D_6, 400.1 MHz, 298 K): δ 7.39 (2 H, m, *o*-SiC_6H_5), 7.25-7.15 (9 H, overlapping 3 x m, *p*-SiC_6H_5, *o*-NC_6H_5 and *m*-NC_6H_5, and overlapping with minor isomer), 6.94-6.79 (4 H, overlapping 2 x m, *m*-SiC_6H_5 and *p*-NC_6H_5 and overlapping with minor isomer), 5.65 (1 H, br. s, NH), 5.22 (2 H, d, ^{3}J = 4.6 Hz, SiH_2), 5.10 (2 H, app. sept., app. ^{3}J = 6.7 Hz, C<u>H</u>Me_2), 3.32 (2 H, m, $^{iPr}NC\underline{H}_2$), 3.05 (2 H, m, $^{iPr}NC\underline{H}_2$), 2.89 (2 H, m, $^{Me}NC\underline{H}_2$), 2.31 (2 H, m, $^{Me}NC\underline{H}_2$), 2.01 (3 H, s, NMe), 1.13 (6 H, d, ^{3}J = 6.7 Hz, CH<u>Me</u>$_2$), 0.85 (6 H, d, ^{3}J = 6.7 Hz, CH<u>Me</u>$_2$) ppm. $^{13}C\{^{1}H\}$ NMR (C_6D_6, 100.6 MHz, 298 K): δ 156.4 (*i*-NC_6H_5), 137.8 (*i*-SiC_6H_5), 134.6 (*o*-SiC_6H_5), 129.6 (*p*-SiC_6H_5), 128.8 (*m*-NC_6H_5), 123.3 (*o*-NC_6H_5), 121.8 (*p*-NC_6H_5), 118.2 (*m*-NC_6H_5), 57.5 ($^{Me}N\underline{C}H_2$), 55.4 (<u>C</u>HMe_2), 47.4 ($^{iPr}N\underline{C}H_2$),

46.0 (NMe), 22.5 (CH$\underline{Me}_2$), 22.2 (CH$\underline{Me}_2$) ppm. ^{29}Si NMR (HMBC ^{1}H-observed, C_6D_6, 499.9 MHz, 298 K): δ -32.0 ($^1J_{Si\text{-}H}$ = 203 Hz, SiH_2Ph) ppm.

Minor isomer (trans): ^{1}H NMR (C_6D_6, 400.1 MHz, 298 K): δ 7.49 (2 H, dd, ^3J = 7.6 Hz ^4J = 1.8 Hz, *o*-SiC_6H_5), 7.31 (4 H, d, ^3J = 7.5 Hz, *o*-NC_6H_5), 7.25-7.15 (7 H, overlapping 3 x m, *m*-NC_6H_5, *p*-SiC_6H_5, *m*-SiC_6H_5 and overlapping with major isomer), 6.86 (2 H, m, *p*-NC_6H_5 overlapping with major isomer), 5.88 (1 H, br. s, NH), 5.51 (2 H, d, ^3J = 4.6 Hz, SiH_2), 5.09 (2 H, app. sept., app. ^3J = 6.7 Hz C$\underline{H}Me_2$), 3.04 (2 H, m, ^{iPr}NC$\underline{H}_2$), 2.96 (2 H, m, ^{iPr}NC$\underline{H}_2$), 2.56 (2 H, m, ^{Me}NC$\underline{H}_2$), 2.06 (2 H, m, ^{Me}NC$\underline{H}_2$), 2.05 (3 H, s, NMe), 1.08 (6 H, d, ^3J = 6.7 Hz, CH$\underline{Me}_2$), 1.04 (6 H, d, ^3J = 6.7 Hz, CH$\underline{Me}_2$) ppm. ^{13}C{^{1}H} NMR (C_6D_6, 100.6 MHz, 298 K): δ 154.2 (*i*-NC_6H_5), 138.6 (*i*-SiC_6H_5), 134.7 (*o*-SiC_6H_5), 129.6 (*p*-SiC_6H_5), 129.0 (*m*-NC_6H_5), 123.2 (*o*-NC_6H_5), 121.3 (*p*-NC_6H_5), 121.2 (*m*-SiC_6H_5), 59.9 ($\underline{C}HMe_2$), 55.8 (^{Me}N$\underline{C}H_2$), 46.8 (^{iPr}N$\underline{C}H_2$), 43.4 (NMe), 22.8 (CH$\underline{Me}_2$), 20.7 (CH$\underline{Me}_2$) ppm. ^{29}Si NMR (HMBC ^{1}H-observed, C_6D_6, 499.9 MHz, 298 K): δ -32.5 ($^1J_{Si\text{-}H}$ = 202 Hz, SiH_2Ph) ppm.

Common data: IR (NaCl plates, Nujol mull, cm^{-1}): 3394 (w, ν(N–H)), 2724 (w), 2103 (m, ν(Si-H)), 1593 (s), 1309 (m), 1255 (m), 1193 (w), 1156 (m), 1113 (w), 992 (m), 941 (w), 848 (m), 745 (m), 697 (m). Anal. found (calcd. for $C_{29}H_{43}N_5SiTi$): C, 64.65 (64.79); H, 7.82 (8.06); N, 12.94 (13.03)%.

Ti($N_2^{iPr}N^{Me}$){N(D)SiD_2Ph}(NPh_2) (43-*d*$_3$). To a stirred solution of Ti($N_2^{iPr}N^{Me}$)($NNPh_2$)(py) (**2.1**, 0.050g, 0.098 mmol) in benzene (2 mL) was added $PhSiD_3$ (0.011 g, 0.098 mmol) at RT. After 12 h the volatiles were removed under reduced pressure to afford **43-*d*$_3$** as a dark red sticky solid. ^{2}H NMR (C_6H_6, 76.7 MHz, 298 K): 5.85 (br. s, ***trans*-43-*d*$_3$**, ND), 5.72 (br. s, ***cis*-43-*d*$_3$**, ND), 5.49 (br. s, ***trans*-43-*d*$_3$**, SiD_2) 5.21 (br. s, ***cis*-43-*d*$_3$**, SiD_2) ppm. IR (NaCl plates, Nujol mull, cm^{-1}): 2359 (m, ν(N–D)), 1593 (s), 1499 (m, ν(Si–D)), 1457 (m), 1371 (w), 1355(m), 1311 (m), 1257 (s), 1156 (s), 1112 (m), 1073 (m), 993 (m), 918 (m), 856 (w), 823 (w).

Ti($N_2^{iPr}N^{Me}$){N(H)SiH_2-3,5-$C_6H_3(CF_3)_2$}(NPh_2) (44). To a stirred solution of Ti($N_2^{iPr}N^{Me}$)($NNPh_2$)(py) (**2.1**, 0.115g, 0.226 mmol) in benzene (5 mL) was added (3,5-$C_6H_3(CF_3)_2$)SiH_3 (0.055 g, 0.226 mmol) all at RT. A colour change from brown to dark red was observed. After 4 h the volatiles were removed under reduced pressure to afford **44** as a dark red solid. Yield: 0.080 g (60%). The ^{1}H NMR spectrum indicated an approximately 65:35% mixture of the *trans* and *cis* isomers.

Major isomer (trans): ^{1}H NMR (C_6D_6, 400.1 MHz, 298 K): δ 7.77 (2 H, s, *o*-$C_6H_3(CF_3)_2$), 7.74 (1 H, s, *p*-$C_6H_3(CF_3)_2$), 7.16-7.08 (8 H, overlapping 2 x m, *o*-C_6H_5 and *m*-C_6H_5), 6.84 (2 H, m, *p*-$N(C_6H_5)_2$ overlapping with *cis* isomer), 5.33 (1 H, br. t, ^3J = 5.0 Hz, NH), 5.24 (2 H, d, ^3J = 5.0 Hz, SiH_2), 5.01 (2 H, app. sept., ^3J = 6.5 Hz, C<u>H</u>Me_2), 3.04 (2 H, m, ^{iPr}NC<u>H</u>$_2$), 2.90 (2 H, m, ^{iPr}NC<u>H</u>$_2$), 2.53 (2 H, m, ^{Me}NC<u>H</u>$_2$), 2.00 (2 H, m, ^{Me}NC<u>H</u>$_2$), 1.97 (3 H, s, NMe), 1.08 (12 H, overlapping 2 x d, ^3J = 6.3 Hz, CH<u>Me</u>$_2$) ppm. ^{13}C{^{1}H} NMR (C_6D_6, 100.6 MHz, 298 K): δ 152.4 (*i*-C_6H_5), 142.4 (*i*-$C_6H_3(CF_3)_2$), 133.0 (*o*-$C_6H_3(CF_3)_2$), 129.4 (q, $^2J_{C\text{-}F}$ = 257.3 Hz, *m*-$C_6H_3(CF_3)_2$), 127.7 (*o*-C_6H_5), 121.8 (overlapping *m*-C_6H_5 and *p*-$C_6H_3(CF_3)_2$), 121.0 (*p*-C_6H_5), 58.9 (<u>C</u>HMe_2), 54.4 (^{Me}N<u>C</u>H$_2$), 45.6 (^{iPr}N<u>C</u>H$_2$), 42.1 (NMe), 21.5 (CH<u>Me</u>$_2$), 19.4 (CH<u>Me</u>$_2$) ppm. Resonances attributable to carbons directly bound to ^{19}F atoms were not observed. ^{19}F NMR (C_6D_6, 376.5 MHz, 298 K): δ -62.4 (6F) ppm. ^{29}Si NMR (HMBC ^{1}H-observed, C_6D_6, 499.9 MHz, 298 K): δ -34.7 ($^1J_{Si\text{-}H}$ = 208 Hz, ($C_6H_3(CF_3)_2$)SiH_2 ppm.

Minor isomer (cis): ^{1}H NMR (C_6D_6, 400.1 MHz, 298 K): δ 7.77 (2 H, s, *o*-$C_6H_3(CF_3)_2$), 7.74 (1 H, s, *p*-$C_6H_3(CF_3)_2$), 7.15 (4 H, m, *o*-C_6H_5 overlapping with *trans* isomer), 6.91-6.78 (6 H, overlapping 2 x m, *m*-C_6H_5 and *p*-C_6H_5 and overlapping with *trans* isomer), 5.08 (2 H, app. sept., app. ^3J = 6.0 Hz, C<u>H</u>Me_2), 5.04 (1 H, br. m, NH overlapping with *trans* isomer), 4.94 (2 H, d, ^3J = 4.5 Hz, SiH_2), 3.31 (2 H, m, ^{iPr}NC<u>H</u>$_2$), 3.29 (2 H, m, ^{iPr}NC<u>H</u>$_2$), 2.89 (2 H, m, ^{Me}NC<u>H</u>$_2$), 2.25 (2 H, m, ^{Me}NC<u>H</u>$_2$), 1.94 (3 H, s, NMe), 1.11 (6 H, d, ^3J = 6.0 Hz, CH<u>Me</u>$_2$), 0.84 (6 H, d, ^3J = 6.0 Hz, CH<u>Me</u>$_2$) ppm. ^{13}C{^{1}H} NMR (C_6D_6, 100.6 MHz, 298 K): δ 154.7 (*i*-C_6H_5), 141.5 (*i*-$C_6H_3(CF_3)_2$), 133.1 (*o*-$C_6H_3(CF_3)_2$), 129.7 (q, $^2J_{C\text{-}F}$ = 257.3 Hz, *m*-$C_6H_3(CF_3)_2$), 128.3 (*o*-C_6H_5), 121.8 (*p*-$C_6H_3(CF_3)_2$), 120.0 (*p*-C_6H_5), 117.0 (*m*-C_6H_5), 56.0 (^{Me}N<u>C</u>H$_2$), 54.7 (<u>C</u>HMe_2), 46.2 (^{iPr}N<u>C</u>H$_2$), 44.8 (NMe), 21.3 (CH<u>Me</u>$_2$), 21.0 (CH<u>Me</u>$_2$) ppm. Resonances attributable to carbons directly bound to ^{19}F atoms were not observed. ^{19}F NMR (C_6D_6, 376.5 MHz, 298 K): δ -62.5 (6F) ppm. ^{29}Si NMR

(HMBC ^{1}H-observed, C_6D_6, 499.9 MHz, 298 K): δ -34.7 ($^{1}J_{Si-H}$ = 208 Hz, $(C_6H_3(CF_3)_2)SiH_2$) ppm.

Common data: IR (NaCl plates, Nujol mull, cm^{-1}): 3395 (w, ν(N–H), 2667 (w), 2111 (s, ν(Si-H)), 1593 (s), 1416 (w), 1310(w), 1278 (m), 1135 (m), 1096 (w), 1027 (w), 869 (w), 746 (w), 695 (w). Anal. found (calcd. for $C_{31}H_{41}F_6N_5SiTi$): C, 55.12 (55.19); H, 6.12 (6.28); N, 10.41 (10.38)%.

Ti($N_2^{iPr}N^{Me}$){N(H)SiH_2-4-C_6H_4OMe)}(NPh_2) (45). To a stirred solution of Ti($N_2^{iPr}N^{Me}$)($NNPh_2$)(py) (**2.1**, 0.110g, 0.216 mmol) in benzene (5 mL) was added H_3Si-4-C_6H_4OMe (0.029 g, 0.216 mmol) all at RT. A colour change from brown to dark red was observed. After 4 h the volatiles were removed under reduced pressure to afford **45** as a dark red solid. Yield: 0.120 g (98%). The ^{1}H NMR spectrum indicated an approximately 60:40% mixture of the *cis* and *trans* isomers.

Major isomer (cis): ^{1}H NMR (C_6D_6, 400.1 MHz, 298 K): δ 7.35 (2H, d, ^{3}J = 7.6 Hz, *o*-C_6H_4OMe), 7.27-7.23 (6 H, overlapping 2 x m, *o*-C_6H_5 and *m*-C_6H_4OMe), 6.93 (4 H, app. t, app. ^{3}J = 7.7 Hz, *m*-C_6H_5), 6.83 (2 H, m, *p*-C_6H_5), 5.74 (1 H, br. m, NH), 5.26 (2 H, d, ^{3}J = 4.5 Hz, SiH_2), 5.14 (2 H, app. sept., app. ^{3}J = 6.2 Hz, C<u>H</u>Me_2), 3.35 (2 H, m, ^{iPr}NC<u>H_2</u>), 3.30 (3 H, s, C_6H_4O<u>Me</u>), 3.05 (2 H, m, ^{iPr}NC<u>H_2</u>), 2.91 (2 H, m, ^{Me}NC<u>H_2</u>), 2.35 (2 H, m, ^{Me}NC<u>H_2</u>), 2.05 (3 H, s, NMe), 1.16 (6 H, d, ^{3}J = 6.2 Hz, CH<u>Me_2</u>), 0.86 (6 H, d, ^{3}J = 6.2 Hz, CH<u>Me_2</u>) ppm. $^{13}C\{^{1}H\}$ NMR (C_6D_6, 100.6 MHz, 298 K): δ 161.4 (*p*-C_6H_4OMe), 156.5 (*i*-C_6H_5), 143.6 (*i*-C_6H_4OMe), 136.2 (*o*-C_6H_4OMe), 128.8 (*m*-C_6H_4OMe), 123.3 (*o*-C_6H_5), 121.2 (*m*-C_6H_5), 114.1 (*p*-C_6H_5), 57.5 (^{Me}N<u>C</u>H_2), 55.4 (<u>C</u>HMe_2), 54.6 (C_6H_4O<u>Me</u>), 47.4 (^{iPr}N<u>C</u>H_2), 46.0 (NMe), 22.5 (CH<u>Me_2</u>), 22.2 (CH<u>Me_2</u>) ppm. ^{29}Si NMR (HMBC ^{1}H-observed, C_6D_6,499.9 MHz, 298 K): δ -32.4 ($^{1}J_{Si-H}$ = 204 Hz, $(C_6H_4OMe)SiH_2$) ppm.

Minor isomer (trans): ^{1}H NMR (C_6D_6, 400.1 MHz, 298 K): δ 7.43 (2 H, d, ^{3}J = 8.7 Hz, *o*-C_6H_4OMe), 7.33 (4 H, d, ^{3}J = 7.4 Hz, *o*-C_6H_5), 7.10 (2 H, d, ^{3}J = 8.7 Hz, *m*-C_6H_4OMe), 6.92 (4 H, m, *m*-C_6H_5 overlapping with *cis* isomer), 6.83 (2 H, m, *p*-C_6H_5 overlapping with *cis* isomer), 5.96 (1 H, br. t, ^{3}J = 4.4 Hz, NH), 5.54 (2 H, d, ^{3}J = 4.4 Hz, SiH_2), 5.13 (2 H, app. sept., app. ^{3}J = 6.7 Hz, C<u>H</u>Me_2), 3.27 (3 H, s, C_6H_4O<u>Me</u>), 3.03 (4 H, m, ^{iPr}NC<u>H_2</u>), 2.56 (2 H, m, ^{Me}NC<u>H_2</u>), 2.07 (2 H, m, ^{Me}NC<u>H_2</u>), 2.06 (3 H, s, NMe), 1.10 (6 H, d, ^{3}J = 6.7 Hz, CH<u>Me_2</u>), 1.06 (6 H, d, ^{3}J = 6.7 Hz, CH<u>Me_2</u>) ppm. $^{13}C\{^{1}H\}$ NMR (C_6D_6, 100.6 MHz, 298 K): δ 161.2 (*p*-C_6H_4OMe), 154.3 (*i*-C_6H_5),

143.6 (*i*-C_6H_4OMe), 136.2 (*o*-C_6H_4OMe), 129.0 (*m*-C_6H_4OMe), 123.2 (*o*-C_6H_5), 121.7 (*m*-C_6H_5), 114.0 (*p*-C_6H_5), 59.9 ($\underline{C}HMe_2$), 55.8 ($^{Me}N\underline{C}H_2$), 55.5 ($C_6H_4O\underline{Me}$), 46.8 ($^{iPr}N\underline{C}H_2$), 43.4 (NMe), 22.8 ($CH\underline{Me}_2$), 20.8 ($CH\underline{Me}_2$) ppm. ^{29}Si NMR (HMBC ^{1}H-observed, C_6D_6, 499.9 MHz, 298 K): δ -32.7 ($^1J_{Si\text{-}H}$ = 204 Hz, $C_6H_4OMeSiH_2$) ppm.

Common data: IR (NaCl plates, Nujol mull, cm^{-1}): 3390 (m, ν(N–H)), 3054 (m) 2665 (w), 2101 (s, ν(Si-H)), 1539 (s), 1565 (w), 1483 (s), 1354 (w), 1335 (w), 1309 (w), 1279 (w), 1256 (m), 1178 (m), 1157 (m), 1131 (m), 1112 (w), 1073 (m), 1028 (m), 993 (m), 940 (w), 864 (w), 823 (m), 745 (m), 692 (w). Anal. found (calcd. for $C_{30}H_{45}N_5OSiTi$): C, 63.44 (63.47);H, 7.93 (7.99);N, 12.17 (12.34)%.

Ti($N_2^{iPr}N^{Me}$){N(H)SiHPh$_2$}(NPh$_2$) (46). To a stirred solution of Ti($N_2^{iPr}N^{Me}$)(NNPh$_2$)(py) (**2.1**, 0.200g, 0.393 mmol) in benzene (5 mL) was added Ph_2SiH_2 (0.073 mL, 0.393 mmol) at RT. After 12 h the volatiles were removed under reduced pressure to afford **46** as a dark orange sticky solid which was then triturated with hexane (2 mL), filtered and the resultant pale orange powder dried *in vacuo*. Yield: 0.094 g (40%). The ^{1}H NMR spectrum indicated an approximately 50:50% mixture of the *cis* and *trans* isomers. Diffraction-quality crystals were grown from a saturated benzene solution at RT.

Cis isomer: ^{1}H NMR (C_6D_6, 400.1 MHz, 298 K): δ 7.40 (4 H, m, *o*-SiC_6H_5), 7.20-7.13 (14 H, overlapping 4 x m, *m*-SiC_6H_5, *p*-SiC_6H_5, *m*-NC_6H_5 and *o*-NC_6H_5 and overlapping with *trans* isomer), 6.85 (2 H, m, *p*-NC_6H_5), 6.13 (1 H, d, ^3J = 7.1 Hz, NH), 5.75 (1 H, d, ^3J = 7.1 Hz, SiH), 5.11 (2 H, app. sept., app. ^3J = 6.5 Hz, $C\underline{H}Me_2$), 3.30 (2 H, m, $^{iPr}NC\underline{H}_2$), 3.06 (2 H, m, $^{iPr}NC\underline{H}_2$), 2.87 (2 H, m, $^{Me}NC\underline{H}_2$), 2.25 (2 H, m, $^{Me}NC\underline{H}_2$), 1.95 (3 H, s, NMe), 1.12 (6 H, d, ^3J = 6.5 Hz, $CH\underline{Me}_2$), 0.82 (6 H, d, ^3J = 6.5 Hz, $CH\underline{Me}_2$) ppm. $^{13}C\{^1H\}$ NMR (C_6D_6, 100.6 MHz, 298 K): δ 156.6 (*i*-NC_6H_5), 139.1 (*i*-SiC_6H_5), 134.9 (*o*-SiC_6H_5), 129.4 (Ar), 128.9 (Ar), 128.5 (Ar), 123.2 (*o*-NC_6H_5), 121.2 (*p*-NC_6H_5), 59.7 ($\underline{C}HMe_2$), 57.8 ($^{Me}N\underline{C}H_2$), 47.6 ($^{iPr}N\underline{C}H_2$), 45.6 (NMe), 22.3 ($CH\underline{Me}_2$), 21.9 ($CH\underline{Me}_2$) ppm. *m*-SiC_6H_5, *p*-SiC_6H_5 and *m*-NC_6H_5 aromatic resonances could not be distinguished. ^{29}Si NMR (HMBC ^{1}H-observed, C_6D_6, 499.9 MHz, 298 K): δ -20.3 ($^1J_{Si\text{-}H}$ = 200 Hz, $SiHPh_2$) ppm.

Trans isomer: ^{1}H NMR (C_6D_6, 400.1 MHz, 298 K): δ 7.54 (4 H, dd, ^3J = 7.3 Hz ^4J = 2.0 Hz, *o*-SiC_6H_5), 7.27 (4 H, dd, ^3J = 8.6 Hz ^4J = 1.0 Hz, *o*-NC_6H_5), 7.15 (10 H,

overlapping 3 x m, *m*-NC_6H_5, *m*-SiC_6H_5 and *p*-SiC_6H_5 and overlapping with *cis* isomer), 6.90 (2 H, t, ^3J = 7.2 Hz, *p*-NC_6H_5), 6.30 (1 H, d, ^3J = 7.7 Hz, NH), 5.95 (1 H, d, ^3J = 7.7 Hz, SiH), 5.13 (2 H, app. sept., app. ^3J = 6.5 Hz, C<u>H</u>Me_2), 3.03 (2 H, m, ^{iPr}NC<u>H_2</u>), 2.95 (2 H, m, ^{iPr}NC<u>H_2</u>), 2.56 (2 H, m, ^{Me}NC<u>H_2</u>), 2.01 (3H, s, NMe), 2.04 (2 H, m, ^{Me}NC<u>H_2</u>), 1.09 (6 H, d, ^3J = 6.5 Hz, CH<u>Me_2</u>), 0.98 (6 H, d, ^3J = 6.5 Hz, CH<u>Me_2</u>) ppm. $^{13}C\{^1H\}$ NMR (C_6D_6, 100.6 MHz, 298 K): δ 154.2 (*i*-NC_6H_5), 139.6 (*i*-SiC_6H_5), 135.0 (*o*-SiC_6H_5), 130.2 (Ar), 129.2 (Ar), 128.8 (Ar), 123.2 (*o*-NC_6H_5), 121.7 (*p*-NC_6H_5), 55.8 (^{Me}N<u>C</u>H_2), 55.2 (<u>C</u>HMe_2), 46.7 (^{iPr}N<u>C</u>H_2), 43.4 (NMe), 22.7 (CH<u>Me_2</u>), 20.5 (CH<u>Me_2</u>) ppm. *m*-SiC_6H_5, *p*-SiC_6H_5 and *m*-NC_6H_5 aromatic resonances could not be distinguished. ^{29}Si NMR (HMBC ^{1}H-observed, C_6D_6, 499.9 MHz, 298 K): δ -19.9 ($^1J_{Si\text{-}H}$ = 201 Hz, $SiHPh_2$) ppm.

Common data: IR (NaCl plates, Nujol mull, cm^{-1}): 3317 (w, ν(N–H)), 2089 (m, ν(Si–H)), 1591 (s), 1427 (m), 1317 (m), 1255 (m), 1196 (w), 1183(w), 1170 (m), 1114 (w), 1032 (w), 1018 (m), 992 (w), 865 (w), 849 (m), 822 (w), 694 (w). Anal. found (calcd. for $C_{35}H_{47}N_5SiTi$): C, 68.34 (68.49); H, 7.60 (7.72); N, 11.35 (11.41)%.

Kinetic isotope effect measurements for the reaction of Ti($N_2^{iPr}N^{Me}$)($NNPh_2$)(py) (2.1) with $PhSiH_3$.

Competition reaction. In a glovebox Ti($N_2^{iPr}N^{Me}$)($NNPh_2$)(py) (**2.1**) (0.015 g, 0.0295 mmol) was weighed into a vial and dissolved in toluene-d_8 (0.3 mL) and cooled to -45 °C. In separate vials $PhSiH_3$ (0.0159 g, 0.1475 mmol) and $PhSiD_3$ (0.0164 g, 0.1475 mmol) were weighed out and then dissolved in toluene-d_8 (0.3 mL) which was then cooled to -45 °C. After 2 h at -45 °C the two vials were placed on a pre-cooled tile and the solutions combined using a pre-cooled pipette, agitated quickly and transferred to a pre-cooled J. Young NMR tube. The sealed NMR tube was taken out of the glovebox and placed in a dry ice/acetone cold bath. The NMR probe was cooled to -40 °C and a blank toluene-d_8 sample added before being locked and shimmed. The experimental sample then replaced the blank sample and allowed to thermally equilibrate, the shimming was then checked and a ^{1}H NMR spectrum indicated that the reaction had proceeded 15 %. The sample was then warmed to -10 °C and an array set up recording a spectrum of 4 scans every 10 mins. The reaction had reached completion after 12 h at -10 °C and the ratio of **43** and **43-*d*$_3$** was

calculated by comparing the integration of the $Si\underline{H}_2$ resonances to the $C\underline{H}Me_2$ resonances.

Initial rates method. To a solution of $PhSiH_3$ or $PhSiD_3$ (0.0295 mmol) in C_6D_6 (0.3 mL) was added $Ti(N_2^{iPr}N)(NNPh_2)(py)$ (**2.1**, 0.015g, 0.0295 mmol) in C_6D_6 (0.3 mL), all at RT, before being transferred to an NMR tube equipped with a J. Young Teflon valve. The reaction was monitored by ^1H NMR spectroscopy using an array which recorded spectra (nt = 4 scans) every 120 seconds. Initial rate constants were obtained from plots of **43** *vs.* time using *Origin*.

$Ti(N_2^{iPr}N^{Me})(NNPh_2)$(DMAP) (47). To a stirred solution of $Ti(N_2^{iPr}N^{Me})(NNPh_2)(py)$ (**2.1**, 0.200 g, 0.393 mmol) in benzene (5 mL) was added a solution of dimethylaminopyridine (0.048 g, 0.393 mmol) in benzene (2 mL) at RT. The solution was left for 1 hour at RT after which the volatiles were removed under reduced pressure to yield a sticky orange solid which was then triturated with hexane (3 mL) and washed twice with hexane (1 mL) yielding **47** as a bright orange powder. Yield: 0.130 mg (60%). The ^1H NMR spectrum indicated an approximately 70:30% mixture of the *trans* and *cis* isomers.

Major isomer (trans): ^1H NMR (C_6D_6, 400.1 MHz, 298 K): δ 8.26 (2 H, br. m, *o*-$NC_5H_4NMe_2$), 7.66 (4 H, d, ^3J = 7.8 Hz, *o*-NC_6H_5), 7.16 (4 H, m, *m*-NC_6H_5), 6.82 (2 H, t, ^3J = 7.4 Hz, *p*-NC_6H_5), 5.76 (2 H, br. m, *m*-$NC_5H_4NMe_2$), 5.35 (2 H, app. sept., app. ^3J = 6.2 Hz, $C\underline{H}Me_2$), 3.52 (2 H, m, $^{iPr}NC\underline{H}_2$), 3.34 (2 H, m, $^{iPr}NC\underline{H}_2$), 2.89 (2 H, m, $^{Me}NC\underline{H}_2$), 2.29 (2 H, m, $^{Me}NC\underline{H}_2$), 2.08 (6 H, br. s, $NC_5H_4N\underline{Me}_2$), 1.62 (3 H, s, NMe), 1.53 (6 H, d, ^3J = 6.2 Hz, $CH\underline{Me}_2$), 1.41 (6 H, d, ^3J = 6.2 Hz, $CH\underline{Me}_2$) ppm. $^{13}C\{^1H\}$ NMR (C_6D_6, 125.7 MHz, 298 K): δ 154.3 (*p*-$NC_5H_4NMe_2$), 149.0 (*o*-$NC_5H_4NMe_2$), 148.0 (*i*-NC_6H_5), 128.4 (*m*-NC_6H_5), 119.9 (*p*-NC_6H_5), 118.9 (*o*-NC_6H_5), 106.3 (*m*-$NC_5H_4NMe_2$), 60.0 ($\underline{C}HMe_2$), 57.4 ($MeN\underline{C}H_2$), 46.9 ($iPrN\underline{C}H_2$), 43.5 (NMe), 38.3 ($NC5H4N\underline{Me}_2$), 23.8 ($CH\underline{Me}_2$), 23.2 ($CH\underline{Me}_2$) ppm.

Minor isomer (cis): ^1H NMR (C_6D_6, 400.1 MHz, 298 K): δ 8.64 (2 H, d, ^3J = 5.4 Hz, *o*-$NC_5H_4NMe_2$), 8.00 (4 H, d, ^3J = 7.5 Hz, *o*-NC_6H_5), 7.30 (4 H, m, *m*-NC_6H_5), 6.90 (2 H, m, *p*-NC_6H_5), 5.75 (2 H, d, ^3J = 5.4 Hz, *m*-$NC_5H_4NMe_2$), 3.90 (2 H, app. sept., app. ^3J = 6.2 Hz, $C\underline{H}Me_2$), 3.60 (2 H, m, $iPrNC\underline{H}_2$), 3.39 (2 H, m, $iPrNC\underline{H}_2$), 3.12 (2 H, m, $MeNC\underline{H}_2$), 2.67 (2 H, m, $MeNC\underline{H}_2$), 2.62 (3 H, s, NMe), 2.08 (6 H, s, $NC_5H_4N\underline{Me}_2$), 1.43 (6 H, d, ^3J = 6.2 Hz, $CH\underline{Me}_2$), 1.10 (6 H, d, ^3J = 6.2 Hz, $CH\underline{Me}_2$)

ppm. $^{13}C\{^{1}H\}$ NMR (C_6D_6, 125.7 MHz, 298 K): δ 154.3 (*p*-$NC_5H_4NMe_2$), 152.2 (*o*-$NC_5H_4NMe_2$), 147.3 (*i*-NC_6H_5), 128.5 (*m*-NC_6H_5), 120.6 (*p*-NC_6H_5), 118.6 (*o*-NC_6H_5), 105.6 (*m*-$NC_5H_4NMe_2$), 58.6 ($MeN\underline{C}H_2$), 51.3 ($\underline{C}HMe_2$), 47.3 (NMe), 45.2 ($iPrN\underline{C}H_2$), 38.3 ($NC_5H_4N\underline{Me}_2$), 22.6 ($CH\underline{Me}_2$), 22.6 ($CH\underline{Me}_2$) ppm.

Common data: IR (NaCl plates, Nujol mull, cm-1): 1610 (s), 1594 (m), 1581 (m), 1531 (m), 1347 (w), 1260 (m), 1225 (w), 1168 (w), 1016 (w), 808 (w), 691 (w). Satisfactory elemental analysis could not be obtained.

Ti($N_2^{iPr}N^{Me}$){N(H)$SiH_2{}^{n}$Bu)}(NPh_2) (48). To a stirred solution of Ti($N_2^{iPr}N^{Me}$)($NNPh_2$)(py) (**2.1**, 0.350g, 0.688 mmol) in benzene (10mL) was added $^{n}BuSiH_3$ (0.466 mL, 3.44 mmol) all at RT. A colour change from brown to dark red was observed. After 3 h the volatiles were removed under reduced pressure to afford **48** as a dark red waxy solid. Yield: 0.348 g (97%). The ^{1}H NMR spectrum indicated an approximately 60:40 mixture of the *cis* and *trans* isomers.

Major isomer (cis): ^{1}H NMR (C_6D_6, 400.1 MHz, 298 K): δ 7.31 (4 H, d, ^{3}J =7.8 Hz, *o*-C_6H_5), 7.24 (4 H, m, *m*-C_6H_5 overlapping with *trans* isomer), 6.90 (1 H, m, *p*-C_6H_5 overlapping with *trans* isomer), 5.69 (1 H, br. t, ^{3}J = 4.3 Hz, NH), 5.08 (2 H, app. sept., app. ^{3}J = 6.5 Hz, $C\underline{H}Me_2$), 4.71 (2 H, dt, ^{3}J = 4.3, 3.2 Hz, SiH_2), 3.34 (2 H, m, $^{iPr}NC\underline{H}_2$), 3.04 (2 H, m, $^{iPr}NC\underline{H}_2$), 2.91 (2 H, m, $^{Me}NC\underline{H}_2$), 2.35 (2 H, m, $^{Me}NC\underline{H}_2$), 2.06 (3 H, s, NMe), 1.33-1.21 (4 H, overlapping 2 x m, $SiCH_2C\underline{H}_2CH_2CH_3$ and $SiCH_2CH_2C\underline{H}_2CH_3$), 1.17 (6 H, d, ^{3}J = 6.5 Hz, $CH\underline{Me}_2$), 0.90-0.86 (9 H, overlapping 1 x d and 1 x m, $CH\underline{Me}_2$ and $SiCH_2CH_2CH_2C\underline{H}_3$), 0.40 (2 H, m, $SiC\underline{H}_2CH_2CH_2CH_3$) ppm. $^{13}C\{^{1}H\}$ NMR (C_6D_6, 100.6 MHz, 298 K): δ 156.1 (*i*-C_6H_5), 128.4 (*m*-C_6H_5), 122.8 (*o*-C_6H_5), 121.2 (*p*-C_6H_5), 57.1 ($^{Me}NC\underline{H}_2$), 54.8 ($\underline{C}HMe_2$), 46.9 ($^{iPr}N\underline{C}H_2$), 45.7 (NMe), 26.1 ($SiCH_2\underline{C}H_2CH_2CH_3$), 25.9 ($SiCH_2CH_2\underline{C}H_2CH_3$), 22.1 ($CH\underline{Me}_2$), 21.7 ($CH\underline{Me}_2$), 14.5 ($Si\underline{C}H_2CH_2CH_2CH_3$), 13.7 ($SiCH_2CH_2CH_2\underline{C}H_3$) ppm. ^{29}Si NMR (HMBC ^{1}H-observed, C_6D_6, 499.9 MHz, 298 K): δ -26.1 ($^{1}J_{Si\text{-}H}$ = 196 Hz, $^{n}BuSiH_2$) ppm.

Minor isomer (trans): ^{1}H NMR (C_6D_6, 400.1 MHz, 298 K): δ 7.25 (4 H, m, *m*-C_6H_5 overlapping with *cis* isomer), 7.16 (4 H, m, *o*-NC_6H_5 overlapping with solvent), 6.84 (2 H, m, *p*-$N(C_6H_5)_2$ overlapping with *cis* isomer), 5.97 (1 H, br. t, ^{3}J = 4.4 Hz, NH), 5.08 (2 H, app. sept., app. ^{3}J = 6.5 Hz, $C\underline{H}Me_2$), 4.99 (2 H, dt, ^{3}J = 4.4 Hz, ^{3}J = 3.0 Hz, $Si\underline{H}_2$), 2.94 (4 H, m, $^{iPr}NC\underline{H}_2$), 2.54 (2 H, m, $^{Me}NC\underline{H}_2$), 2.03 (3 H, s, NMe), 2.01

(2 H, m, $^{Me}NCH_2$), 1.33-1.21 (4 H, overlapping 2 x m, $SiCH_2CH_2CH_2CH_3$ and $SiCH_2CH_2CH_2CH_3$), 1.15 (6 H, d, ^3J = 6.5 Hz, $CHMe_2$), 1.10 (6 H, d, ^3J = 6.5 Hz, $CHMe_2$), 0.89 (2 H, m, $SiCH_2CH_2CH_2CH_3$), 0.53 (2 H, m, $SiCH_2CH_2CH_2CH_3$) ppm. $^{13}C\{^1H\}$ NMR (C_6D_6, 100.6 MHz, 298 K): δ 153.9 (*i*-C_6H_5), 128.5 (*m*-C_6H_5), 122.7 (*o*-C_6H_5), 120.8 (*p*-C_6H_5), 59.7 ($CHMe_2$), 55.3 ($^{Me}NCH_2$), 46.4 ($^{iPr}NCH_2$), 42.9 (NMe), 26.3 ($SiCH_2CH_2CH_2CH_3$), 26.0 ($SiCH_2CH_2CH_2CH_3$), 22.4 ($CHMe_2$), 20.4 ($CHMe_2$), 15.1 ($SiCH_2CH_2CH_2CH_3$), 13.8 ($SiCH_2CH_2CH_2CH_3$) ppm. ^{29}Si NMR (HMBC ^1H-observed, C_6D_6, 499.9 MHz, 298 K): δ -26.6 ($^1J_{Si\text{-}H}$ = 194 Hz, $^n BuSiH_2$) ppm.

Common data: IR (NaCl plates, Nujol mull, cm^{-1}): 3317 (w, ν(N–H)), 3056 (w), 2665 (w), 2092 (m, ν(Si–H)), 1593 (s), 1484 (s), 1414 (w), 1335 (m), 1310 (w), 1257 (w), 1193 (w), 1171 (w), 1157 (m), 1073 (m), 1028 (s), 993 (m), 941 (m), 896 (w), 865 (w), 843 (w), 823 (m), 746 (m), 695 (m), 668 (w). Anal. found (calcd. for $C_{27}H_{47}N_5SiTi$): C, 62.51 (62.65);H, 8.89 (9.15);N, 13.55 (13.53)%.

$Ti_2(N_2^{iPr}N^{Me})_2(\mu\text{-}NNPh_2)(\mu\text{-}NSiH_2{}^n Bu)$ (49). To a stirred solution of $Ti(N_2^{iPr}N^{Me})(NNPh_2)(py)$ (**2.1**, 0.150 g, 0.295 mmol) in benzene (5 mL) was added $^n BuH_3Si$ (0.191 mL, 1.48 mmol) all at RT. After 3 h the volatiles were removed under reduced pressure and the sticky solid redissolved in benzene (5 mL). $Ti(N_2^{iPr}N^{Me})(NNPh_2)(py)$ (**2.1**, 0.150g, 0.295 mmol) in benzene (5 mL) was added and the solution left to stir at RT for 14 days. The volatiles were then removed under reduced pressure and the remaining sticky solid extracted into benzene (5 mL). The volatiles were again removed and resultant solid washed with hexane (2 x 1 mL) at -78 °C to yield **49** as a dark brown powder. Yield: 0.130 g (56%). ^1H NMR (C_6D_6, 400.1 MHz, 298 K): δ 7.85 (4 H, d, ^3J = 7.8 Hz, *o*-C_6H_5), 7.17 (4 H, app. t, app. ^3J = 8.1 Hz, *m*-C_6H_5 overlapping with solvent), 6.79 (2 H, t, ^3J = 7.1 Hz, *p*-C_6H_5), 5.50 (4 H, app. sept., app. ^3J = 6.4 Hz, $CHMe_2$), 5.25 (2 H, t, ^3J = 3.9 Hz, SiH_2), 3.14 (8 H, m, $^{iPr}NCH_2$), 2.52 (4 H, m, $^{Me}NCH_2$), 1.85 (6 H, s, NMe), 1.69 (4 H, m, $^{Me}NCH_2$), 1.65-1.52 (4 H, overlapping 2 x m, $SiCH_2CH_2CH_2CH_3$ and $SiCH_2CH_2CH_2CH_3$), 1.49 (12 H, d, ^3J = 6.4 Hz, $CHMe_2$), 1.39 (12 H, d, ^3J = 6.4 Hz, $CHMe_2$), 1.19 (2 H, m, $SiCH_2CH_2CH_2CH_3$), 0.97 (3 H, t, ^3J = 7.2 Hz, $SiCH_2CH_2CH_2CH_3$) ppm. $^{13}C\{^1H\}$ NMR (C_6D_6, 100.6 MHz, 298 K): δ 146.0 (*i*-C_6H_5), 127.8 (*m*-C_6H_5 overlapping with solvent), 120.1 (*p*-C_6H_5), 117.7 (*o*-C_6H_5), 55.5 ($^{Me}NCH_2$), 55.3 ($CHMe_2$), 45.3 ($^{iPr}NCH_2$), 42.7 (NMe), 26.2 ($SiCH_2CH_2CH_2CH_3$), 26.1 ($SiCH_2CH_2CH_2CH_3$), 23.5

(CH$\underline{Me}_2$), 22.7 (CH$\underline{Me}_2$), 15.7 (Si$\underline{C}H_2CH_2CH_2CH_3$), 13.8 ($SiCH_2CH_2CH_2\underline{C}H_3$) ppm. ^{29}Si NMR (HMBC ^{1}H-observed, C_6D_6, 499.9 MHz, 298 K): δ -44.5 ($^1J_{Si\text{-}H}$ = 193 Hz, ^{n}BuSiH_2) ppm. IR (NaCl plates, Nujol mull, cm^{-1}): 2110 (m, ν(Si–H)), 2082 (m, ν(Si–H)), 1583 (m), 1542 (s), 1337 (w), 1290 (w), 1153 (w), 1077 (s), 1026 (m), 991 (w), 938 (w), 871 (w), 743 (w), 720 (w). Anal. found (calcd. for $C_{38}H_{71}N_9SiTi_2$): C, 58.55 (58.68); H, 9.32 (9.20); N, 16.14 (16.21)%.

Ti($N_2^{iPr}N^{Me}$){N(H)BC_8H_{14}}(NPh_2) (50). To a stirred solution of Ti($N_2^{iPr}N^{Me}$)($NNPh_2$)(py) (**2.1**, 0.400 g, 0.787 mmol) in benzene (10 mL) was added 9-BBN dimer (0.194 g, 0.787 mmol) at RT. A color change from dark brown to light orange was observed. After 12 h the volatiles were removed under reduced pressure to afford **50** and py·HBC_8H_{14} quantitatively as a pale brown sticky solid. Repeated recrystallisation from benzene yielded analytically pure **50** as orange crystals. Yield: 0.040 g (10%). The ^{1}H NMR spectrum indicated an approximately 75:25 mixture of the *cis* and *trans* isomers. Diffraction-quality crystals of **50** were grown from a saturated hexane solution at RT.

Major isomer (cis): ^{1}H NMR (C_6D_6, 499.9 MHz, 298 K): δ 7.30 (1 H, br.s, NH), 7.22 (4 H, d, ^3J = 8.3 Hz, *o*-NC_6H_5), 7.11 (4 H, d, ^3J = 7.7 Hz, *m*-NC_6H_5), 6.90 (2 H, t, ^3J = 8.3 Hz, *p*-NC_6H_5), 5.13 (2 H, app. sept., app. ^3J = 6.5 Hz, C$\underline{H}Me_2$), 3.36 (2 H, m, $^{iPr}NC\underline{H}_2$), 2.99 (2 H, m, $^{iPr}NC\underline{H}_2$), 2.94 (2 H, m, $^{Me}NC\underline{H}_2$), 2.42 (2 H, m, $^{Me}NC\underline{H}_2$), 2.00 (3 H, s, NMe), 1.96 (8 H, m, BCC$\underline{H}$), 1.73 (4 H, br. m, BCCC$\underline{H}$), 1.52 (2 H, m, BC$\underline{H}$), 1.12 (6 H, d, ^3J = 6.5 Hz, CH$\underline{Me}_2$), 0.87 (6 H, d, ^3J = 6.5 Hz, CH$\underline{Me}_2$) ppm. ^{13}C{^{1}H} NMR (C_6D_6, 125.7 MHz, 298 K): δ 155.5 (*i*-NC_6H_5), 128.9 (*o*-NC_6H_5), 122.9 (*m*-NC_6H_5), 122.0 (*p*-NC_6H_5), 56.3 ($\underline{C}HMe_2$), 56.0 ($^{Me}N\underline{C}H_2$), 47.2 ($^{iPr}N\underline{C}H_2$), 46.9 (NMe), 34.2 (BC$\underline{C}$), 24.2 (BCC$\underline{C}$), 22.8 (CH$\underline{Me}_2$), 21.7 (CH$\underline{Me}_2$) ppm. The resonance attributable to the carbon atom directly bound to the ^{11}B atom was not observed. ^{11}B{^{1}H} NMR (C_6D_6, 160.4 MHz 298 K): δ 54.4 Hz (BC_8H_{14}) ppm.

Minor isomer (trans): ^{1}H NMR (C_6D_6, 499.9 MHz, 298 K): δ 7.68 (1 H, br. s, NH), 7.27 (4 H, d, ^3J = 7.5 Hz, *o*-NC_6H_5), 7.20 (4 H, m, *m*-$N(C_6H_5)_2$), 7.15 (2 H, t, ^3J = 8.3 Hz, *p*-NC_6H_5, overlapping with solvent peak), 5.16 (2 H, app. sept., app. ^3J = 6.5 Hz, C$\underline{H}Me_2$), 3.08 (2 H, m, $^{iPr}NC\underline{H}_2$), 3.00 (2 H, m, $^{iPr}NC\underline{H}_2$), 2.59 (2 H, m, $^{Me}NC\underline{H}_2$), 2.09 (2 H, m, $^{Me}NC\underline{H}_2$), 2.10 (3 H, s, NMe), 1.92 (4 H, br. m, BCCC$\underline{H}$), 1.52 (2 H, m, BC$\underline{H}$), 1.42 (8 H, m, BCC$\underline{H}$), 1.13 (6 H, d, ^3J = 6.5 Hz, CH$\underline{Me}_2$), 0.96 (6 H, d, ^3J =

6.5 Hz, CH$\underline{Me}_2$) ppm. $^{13}C\{^1H\}$ NMR (C_6D_6, 125.7 MHz, 298 K): δ 153.6 (*i*-NC_6H_5), 129.0 (*o*-NC_6H_5), 123.4 (*m*-NC_6H_5), 122.8 (*p*-NC_6H_5), 58.9 ($\underline{C}HMe_2$), 56.2 ($^{Me}N\underline{C}H_2$), 46.9 ($^{iPr}N\underline{C}H_2$), 46.9 (NMe), 34.2 (BC$\underline{C}$), 24.3 (BCC$\underline{C}$), 22.3 (CH$\underline{Me}_2$), 20.5 (CH$\underline{Me}_2$) ppm. The resonance attributable to the carbon atom directly bound to ^{11}B atom was not observed. $^{11}B\{^1H\}$ NMR (C_6D_6, 160.4 MHz 298 K): δ 54.4 Hz (BC_8H_{14}) ppm.

Common data : IR (NaCl plates, Nujol mull, cm^{-1}): 3583 (w), 3187 (w, ν(N–H)), 2293 (w), 1509 (s), 1493 (s), 1336 (m), 1313(m), 1260 (s), 1097 (s), 1021 (s), 923 (w), 807 (m), 766 (s), 747 (m), 694 (m). EI-MS: *m/z* = 551 $[M]^+$ (3%). Anal. found (calcd. for $C_{31}H_{50}BN_5Ti$): C, 67.41 (67.52); H, 8.98 (9.14); N, 12.78 (12.70)%.

Ti($N_2^{iPr}N^{Me}$){N(H)BMes_2}(NPh_2) (51). To a stirred solution of Ti($N_2^{iPr}N^{Me}$)($NNPh_2$)(py) (**2.1**, 0.151 g, 0.297 mmol) in benzene (5 mL) was added Mes_2BH (0.150 g, 0.594 mmol) all at RT. An immediate colour change from dark brown to bright red was observed. After 1 h the volatiles were removed under reduced pressure to afford **51** and py.$HBMes_2$ quantitatively as a red sticky solid. The resultant solid was then washed with hexane (2 x 1 mL) filtered and dried *in vacuo* yielding **51** exclusively as a bright red powder. Yield: 0.080 g (40%). The ^1H NMR spectrum indicated an approximately 85:15% mixture of the *cis* and *trans* isomers. Diffraction-quality crystals were grown from a saturated benzene solution at RT.

Major isomer (cis): ^1H NMR (C_6D_6, 499.9 MHz, 298 K): δ 7.09 (4 H, app. t, app. ^3J = 8.2 Hz, *o*-C_6H_5), 7.03 (2 H, br. m, *m*-$C_6H_2Me_3$), 6.81-6.78 (6 H, overlapping 2 x m, *m*-C_6H_5 and *p*-C_6H_5), 5.11 (2 H, app. sept., app. ^3J = 6.3 Hz, C$\underline{H}Me_2$), 3.30 (2 H, m, $^{iPr}NC\underline{H}_2$), 3.00 (2 H, m, $^{iPr}NC\underline{H}_2$), 2.78 (2 H, br.m, $^{Me}NC\underline{H}_2$), 2.33 (12 H, br.s, $\underline{2}$,4,$\underline{6}$-$C_6H_2\underline{Me}_3$), 2.26-2.18 (6 H, br.s, 2,$\underline{4}$,6-$C_6H_2\underline{Me}_3$), 2.12-2.10 (2 H, m, $^{Me}NC\underline{H}_2$), 1.99 (3 H, s, NMe), 1.14 (6 H, d, ^3J = 6.3 Hz, C$\underline{H}Me_2$), 0.94 (6 H, d, ^3J = 6.3 Hz, C$\underline{H}Me_2$) ppm. The resonance attributable to N-H was not observed. $^{13}C\{^1H\}$ NMR (C_6D_6, 125.7 MHz, 298 K): δ 154.1 (*i*-C_6H_5), 142.2 (*p*-$C_6H_2Me_3$), 140.1 (*o*-$C_6H_2Me_3$), 128.6 (*m*-C_6H_5), 128.0 (*o*-C_6H_5), 123.3 (br. *m*-$C_6H_2Me_3$), 121.8 (*p*-C_6H_5), 56.4 ($\underline{C}HMe_2$), 55.0 ($^{Me}N\underline{C}H_2$), 46.6 ($^{iPr}N\underline{C}H_2$), 44.9 (NMe), 23.7 (br. $C_6H_2\underline{Me}_3$), 23.1 (CH$\underline{Me}_2$), 21.6 (CH$\underline{Me}_2$), 20.9 ($C_6H_2\underline{Me}_3$) ppm. The resonance attributable to the carbon directly bound to ^{11}B was not observed. $^{11}B\{^1H\}$ NMR (C_6D_6, 128.4 MHz, 298 K): δ 48.7 ($B(C_6H_2Me_3)_2$) ppm.

Minor isomer (trans): ^{1}H NMR (C_6D_6, 499.9 MHz, 298 K): δ 5.20 (2 H, m, C<u>H</u>Me$_2$), 3.12 (2 H, m, ^{iPr}NC<u>H</u>$_2$), 2.90 (2 H, m, ^{iPr}NC<u>H</u>$_2$), 0.98 (6 H, d, ^{3}J = 6.3 Hz, CH<u>Me</u>$_2$), 0.62 (6 H, d, ^{3}J = 6.3 Hz, CH<u>Me</u>$_2$) ppm. Remaining resonances were not observed.

Common data: IR (NaCl plates, Nujol mull, cm^{-1}): 3726(w), 3702 (w), 3626 (w, ν(N–H)), 2724 (w), 1606 (m), 1586 (m), 1458 (m), 1317 (w), 1290 (w), 1281 (w), 1255 (m), 1156 (m), 1072 (s), 1026 (s), 850 (m). EI-MS: *m/z* = 679 [M]$^{+}$ (1%). Anal. found (calcd. for $C_{41}H_{55}BN_6Ti$): C, 72.27 (72.46); H, 8.51 (8.60); N, 9.99 (10.30)%.

Kinetic measurements for reaction of Ti(N$_2^{iPr}$N^{Me})(NNPh$_2$)(py) (2.1) with 9-BBN at room temperature. To a solution of 9-BBN in C_6D_6 (0.3 mL) was added Ti(N$_2^{iPr}$N)(NNPh$_2$)(py) (**1**, 0.015g, 0.0295 mmol) in C_6D_6 (0.3 mL), all at RT, before being transferred to an NMR tube equipped with a J. Young Teflon valve. The reaction was monitored by ^{1}H NMR spectroscopy using an array which recorded spectra (nt = 4 scans) every 120 seconds. Initial rate constants were obtained from plots of **50** *vs.* time using *Origin*.

NMR tube scale synthesis of Ti(N$_2^{iPr}$N^{Me}){N(H)SiH$_2$Ph)}(NTol$_2$) (52). To a solution of Ti(N$_2^{iPr}$N^{Me})(NNPh$_2$)(py) (**2.1**, 0.020 g, 0.039 mmol) in C_6D_6 (0.3 mL) in an NMR tube equipped with a J. Young Teflon valve was added $SiPhH_3$ (4.80 μL, 0.039 mmol). The reaction was monitored by ^{1}H NMR spectroscopy. After 4 h, the volatiles were removed under reduced pressure and the resultant mixture dried *in vacuo* before being redissolved in C_6D_6 (0.3 mL) and Tol_2NH (0.0078 g, 0.039 mmol) in C_6D_6 (0.3 mL) was added. The solution was heated at 70 °C for 15 hours after which Ti(N$_2^{iPr}$N^{Me}){N(H)SiH$_2$Ph)}(NTol$_2$) (**52**) and **43** were observed in an approximately 50:50% ratio as determined by ^{1}H NMR spectroscopy. The ^{1}H NMR spectrum indicated an approximately 50:50% mixture of the *cis* and *trans* isomers. **52-*cis*** and **52-*trans*** were subsequently characterised by ^{1}H, ^{13}C and ^{29}Si NMR spectroscopy

Cis isomer: ^{1}H NMR (C_6D_6, 499.9 MHz, 298 K): δ 5.55 (1 H, br. m, NH), 5.27 (2 H, d, ^{3}J = 4.6 Hz, SiH$_2$Ph), 3.36 (2 H, m, ^{iPr}NC<u>H</u>$_2$), 3.05 (2 H, m, ^{iPr}NC<u>H</u>$_2$), 2.90 (2 H, m, ^{Me}NC<u>H</u>$_2$), 2.35 (2 H, m, ^{iPr}NC<u>H</u>$_2$), 2.04 (3 H, s, NMe) ppm. ^{13}C{^{1}H} NMR (C_6D_6, 125.7 MHz, 298 K): δ 57.4 (^{Me}N<u>C</u>H$_2$), 47.4 (^{iPr}N<u>C</u>H$_2$), 45.9 (NMe) ppm.

Trans isomer: ^{1}H NMR (C_6D_6, 499.9 MHz, 298 K): δ 5.83 (1H, br. t, ^{3}J = 4.8 Hz, NH), 5.54 (2H, d, ^{3}J = 4.8 Hz, SiH$_2$Ph), 2.97 (4 H, m, ^{iPr}NC<u>H</u>$_2$), 2.55 (4 H, m,

$^{Me}NC\underline{H}_2$), 2.09 (3 H, s, NMe) ppm. $^{13}C\{^1H\}$ NMR (C_6D_6, 125.7 MHz, 298 K): δ 55.6 ($^{Me}N\underline{C}H_2$), 46.7 ($^{iPr}N\underline{C}H_2$), 43.4 (NMe) ppm.

Common data: ^1H NMR (C_6D_6, 499.9 MHz, 298 K): δ 7.49 (1 H, d.t, ^3J = 8.0 Hz, ^4J = 1.6 Hz, *o*-SiC_6H_5), 7.26 (2 H, d, ^3J = 7.9 Hz, *m*-C_6H_4Me), 7.23-7.14 (aromatic), 7.11-7.03 (aromatic), 6.85-6.80 (aromatic), 5.13 (2 H, m, $C\underline{H}Me_2$), 2.22 (3 H, s, $C_6H_4\underline{Me}$), 2.20 (3H, s, $C_6H_4\underline{Me}$), 1.17 (6 H, d, ^3J = 6.7 Hz, $CH\underline{Me}_2$), 1.10 (6 H, d, ^3J = 6.7 Hz, $CH\underline{Me}_2$), 1.09 (6 H, d, ^3J = 6.7 Hz, $CH\underline{Me}_2$), 0.99 (6 H, d, ^3J = 6.7 Hz, $CH\underline{Me}_2$) ppm. $^{13}C\{^1H\}$ NMR (C_6D_6, 125.7 MHz, 298 K): δ 154.1 (*i*-$C_6H_4Me_2$), 152.0 (*i*-C_6H_4Me), 138.8 (*i*-SiC_6H_5), 137.9 (*i*-SiC_6H_5), 134.7 (*o*-SiC_6H_5), 134.6 (*o*-SiC_6H_5), 129.9 (*o*-C_6H_4Me), 129.5 (*o*-C_6H_4Me), 129.3 (*p*-SiC_6H_5), 129.2 (*p*-SiC_6H_5), 123.3 (aromatic), 123.2 (aromatic), 121.7 (aromatic), 121.3 (aromatic), 59.7 ($\underline{C}HMe_2$), 55.8 ($\underline{C}HMe_2$), 22.8 ($CH\underline{Me}_2$), 22.6 ($CH\underline{Me}_2$), 22.3 ($CH\underline{Me}_2$), 21.0 ($C_6H_4\underline{Me}$), 20.9 ($C_6H_4\underline{Me}$), 20.8 ($CH\underline{Me}_2$) ppm. ^{29}Si NMR (HMBC ^1H-observed, C_6D_6, 499.9 MHz, 298 K): δ -32.8 ($^1J_{Si\text{-}H}$ = 202 Hz, SiH_2Ph) ppm.

Kinetic measurements for reaction of Ti($N_2^{iPr}N^{Me}$){N(H)SiH_2Ph}(NPh_2) (43) with $H_3Si(3,5\text{-}C_6H_3(CF_3)_2$ at room temperature. The general procedure is as follows. In a glove box, compound **2.1** (0.015 g, 0.0295 mmol) was weighed into a vial and dissolved in C_6D_6 (0.3 mL), in a separate vial $PhSiH_3$ (0.0032 g, 29.5 μmol) (or $PhSiD_3$) were dissolved in C_6D_6 (0.3 mL) and the solutions combined, agitated quickly and transferred to a J. Young NMR tube. When the formation of **43** had reached completion, as determined by ^1H NMR spectroscopy, the solvent was removed *in vacuo*. The J. Young NMR tube was then opened in the glovebox and $H_3Si(3,5\text{-}C_6H_3(CF_3)_2$ (0.072 g, 0.295 mmol) was added as a solution in C_6D_6 (0.6 mL). The NMR tube was taken out of the dry-box and placed in the NMR probe at RT before being locked and shimmed and an array set up recording a spectrum of 4 scans every 120 seconds. The decay of **43** was calculated by measuring the integral of the $CH\underline{Me}_2$. First order rate constants were obtained from linear plots of -ln([Ti]/$[Ti]_0$) *vs.* time.

Kinetic measurements for reaction of Ti($N_2^{iPr}N^{Me}$){N(D)SiHDPh}(NPh_2) with $H_3Si(3,5\text{-}C_6H_3(CF_3)_2$ at room temperature. In a glove box, compound **2.1** (0.015 g, 0.0295 mmol) was weighed into a vial and dissolved in C_6D_6 (0.3 mL), in a separate vial $PhSiD_3$ (0.0033 mg, 0.0295 mmol) were dissolved in C_6D_6 (0.3 mL) and the solutions combined, agitated quickly and transferred to a J. Young NMR tube. When

the formation of **43** had reached completion, as determined by ^{1}H NMR spectroscopy, the solvent was removed *in vacuo*. The J. Young NMR tube was then opened in the glovebox and $PhSiH_3$ (0.0032 mg, 0.0295 mmol) was added as a solution in C_6D_6 (0.6 mL) and was left to stand at RT for 24 hours. After which time the SiH_2 positions had reached approximately 50 % protonation and the ND position remained deuterated. The solvent and remaining D/H_3SiPh was removed under reduced pressure and the kinetic analysis was carried out as is described for $Ti(N_2^{iPr}N^{Me})\{N(H)SiH_2Ph\}(NPh_2)$.

$Ti(N_2^{iPr}N^{Me})\{(\mu\text{-}H)_2BC_8H_{14}\}(NPh_2)$ (53). To a stirred solution of $Ti(N_2^{iPr}N^{Me})(NNPh_2)(py)$ (**2.1**, 0.450 g, 0.885 mmol) in benzene (6 mL) was added $PhSiH_3$ (0.109 mL, 0.885 mmol) at RT. The solution was left to stir at RT for 12 h after which the volatiles were removed under reduced pressure. The resulting sticky solid was redissolved in benzene (6 mL) and a benzene solution (3 mL) of 9-BBN dimer (0.216 g, 0.885 mmol) was added at RT and stirred for 14 h. The volatiles were then removed under reduced pressure to afford **53** and **54** in a 1:1 ratio. The red sticky solid was washed with pentane (2 x 2 ml) and dried in vacuo yielding exclusively **53** as a bright red solid. Yield: 0.220 g (46%). The ^{1}H NMR spectrum indicated an approximately 50:50 mixture of the *cis* and *trans* isomers. Diffraction-quality crystals were grown from a saturated benzene solution at RT.

Trans isomer: ^{1}H NMR (C_6D_6, 400.1 MHz, 298 K) δ 7.21-7.06 (6 H, overlapping 2 x m, *o*-NC_6H_5 and *p*-NC_6H_5 and overlapping with *cis* isomer), 6.98 (4 H, m, *m*-NC_6H_5 overlapping with *cis* isomer), 5.18 (2 H, app. sept., app. ^{3}J = 6.6 Hz, C<u>H</u>Me_2), 3.11-2.94 (6 H, 3 x m, $^{iPr}NC\underline{H}_2$, $^{Me}NC\underline{H}_2$ and $^{Me}NC\underline{H}_2$ and overlapping with *cis* isomer $^{iPr}NC\underline{H}_2$), 2.56 (2 H, m, $^{Me}NC\underline{H}_2$), 2.01 (3 H, s, NMe) 1.02 (6 H, d, ^{3}J = 6.6 Hz, CH<u>Me</u>$_2$), 0.65 (6 H, d, ^{3}J = 6.6 Hz, CH<u>Me</u>$_2$) ppm. $^{13}C\{^{1}H\}$ NMR (C_6D_6, 100.6 MHz, 298 K): δ 158.0 (*i*-NC_6H_5), 128.7 (*o*-NC_6H_5), 128.2 (*p*-NC_6H_5 overlapping with solvent), 122.2 (*m*-NC_6H_5), 60.5 (<u>C</u>HMe_2), 56.0 ($^{Me}N\underline{C}H_2$), 47.3 ($^{iPr}N\underline{C}H_2$), 43.9 (NMe), 23.1 (CH<u>Me</u>$_2$), 21.7 (CH<u>Me</u>$_2$) ppm.

Cis isomer: ^{1}H NMR (C_6D_6, 400.1 MHz, 298 K): δ 7.21-7.06 (10 H, overlapping 3 x m, *o*-$N(C_6H_5)_2$, *m*-$N(C_6H_5)_2$ and *p*-$N(C_6H_5)_2$ and overlapping with *trans* isomer), 5.28 (2 H, app. sept., app. ^{3}J = 6.7 Hz, C<u>H</u>Me_2), 3.33 (2 H, m, $^{iPr}NC\underline{H}_2$), 3.10 (2 H, m, $^{iPr}NC\underline{H}_2$), 3.02 (2 H, m, $^{Me}NC\underline{H}_2$), 2.35 (2 H, m, $^{Me}NC\underline{H}_2$), 2.20 (3 H, s, NMe), 1.19 (6 H, d, ^{3}J = 6.7 Hz, CH<u>Me</u>$_2$), 1.12 (6 H, d, ^{3}J = 6.7 Hz, CH<u>Me</u>$_2$) ppm. $^{13}C\{^{1}H\}$ NMR (C_6D_6, 100.6 MHz, 298 K): δ 153.7 (*i*-NC_6H_5), 128.3 (*o*-NC_6H_5 overlapping with

solvent), 128.1 (*p*-NC_6H_5 overlapping with solvent), 123.0 (*m*-NC_6H_5), 57.9 ($^{Me}NCH_2$), 56.5 ($CHMe_2$), 49.5 ($^{iPr}NCH_2$), 47.5 (NMe), 23.2 ($CHMe_2$), 21.0 ($CHMe_2$) ppm.

Common data: ^{1}H NMR (C_6D_6, 400.1 MHz, 298 K): δ 1.98-1.55 (28 H, overlapping 6 x m, overlapping BCH, BCCH and BCCCH *trans* and *cis* isomers) ppm. $^1H\{^{11}B\}$ NMR (C_6D_6, 400.1 MHz, 298 K) δ 2.32 (1 H, br.s, BH_2), 0.40 (1 H, br.s, BH_2) ppm. $^{13}C\{^1H\}$ NMR (C_6D_6, 100.6 MHz, 298 K): δ 33.4 (BCC), 30.0 (BCC), 25.1 (BCCC), 24.6 (BCCC) ppm. Resonances attributed to carbons directly bound to ^{11}B atoms were not observed. ^{11}B NMR (C_6D_6, 128.4 MHz, 298 K): δ 15.3 (BH_2), 18.4 (BH_2) ppm. IR (NaCl plates, Nujol mull, cm^{-1}): 2726 (w), 2089 (w), 1593 (w, ν(B–H)),), 1337 (w), 1311 (w), 1259 (m), 1149 (w), 1072 (w), 1020 (w), 899 (w), 801 (w), 693 (w), 668 (w). Anal. found (calcd. for $C_{31}H_{51}BN_4Ti$): C, 68.82 (69.15);H, 9.40 (9.55);N, 10.28 (10.41)%.

$PhH_2SiN(H)BC_8H_{14}$ (54). To a solution of $Ti(N_2^{iPr}N^{Me})(NNPh_2)(py)$ (**2.1**, 0.450 g, 0.885 mmol) in benzene (6 mL) was added $PhSiH_3$ (0.109 mL, 0.885 mmo) all at RT. The solution was left to stir at RT for 12 h after which the volatiles were removed under reduced pressure. The resulting sticky solid was redissolved in benzene (6 mL) and a benzene solution (3 mL) of 9-BBN dimer (0.216 g, 0.885 mmol) was added at RT and stirred for 14 h. The volatiles were then removed under reduced pressure to afford **54** and **56** in a 1:1 ratio. The red sticky solid was extracted into pentane (5 mL) and the volatiles removed under reduced pressure. The resultant oil was sublimed (45-50°C, 8 x 10^{-2} mbar, 3 h) onto a dry ice/acetone cold finger affording **54** as a white solid. Yield: 0.032 g (15%).

^{1}H NMR (C_6D_6, 400.1 MHz, 298 K): δ 7.53 (2 H, m, *o*-C_6H_5), 7.17 (2 H, d, ^3J = 2.6 Hz, *m*-C_6H_5), 7.07 (1 H, t, ^3J = 4.3 Hz, *p*-C_6H_5), 5.05 (2 H, d, ^3J = 3.5 Hz, SiH_2), 3.34 (1 H, br.s, NH), 1.92-1.58 (13 H, overlapping 4 x m, BCH, BCCH, BCCH and BCCCH), 1.00-0.98 (1 H, m, BCH) ppm. $^{13}C\{^1H\}$ NMR (C_6D_6, 100.6 MHz, 298 K): δ 134.7 (*o*-C_6H_5), 134.4 (*i*-C_6H_5), 130.4 (*p*-C_6H_5), 128.4 (*m*-C_6H_5), 33.9 (BCC), 33.3 (BCC), 29.0 (BC), 23.8 (2 x BCCC), 20.4 (BC) ppm. $^{11}B\{1H\}$ NMR (C_6D_6, 128.4 MHz, 298 K): δ 56.4 (BC_8H_{14}) ppm. ^{29}Si NMR (HMBC ^{1}H-observed, C_6D_6, 499.9 MHz, 298 K): δ -35.4 ($^1J_{Si\text{-}H}$ = 209 Hz, SiH_2Ph) ppm. IR (NaCl plates, Nujol mull, cm^{-1}): 3376 (w, ν(N–H)), 2149 (s, ν(Si–H)), 1594 (s), 1407 (s), 1337 (m), 949 (m), 877 (m). EI-HRMS: *m/z* found (calcd. for $C_{14}H_{22}NSiB$, $[M]^+$) 243.1622 (243.1615).

Kinetic measurements for reaction of Ti($N_2^{iPr}N^{Me}$){N(H)SiH_2Ph}(NPh_2) (43) with 9-BBN at room temperature. The general procedure is as follows. In a glove box, compound **2.1** (0.015 g, 0.0295 mmol) was weighed into a vial and dissolved in C_6D_6 (0.3 mL), in a separate vial $PhSiH_3$ (0.0032 mg, 0.0295 mmol) (or $PhSiD_3$) was dissolved in C_6D_6 (0.3 mL) and the solutions combined, agitated quickly and transferred to a J. Young NMR tube. When the formation of **43** had reached completion, as determined by ^{1}H NMR spectroscopy, the solvent was removed *in vacuo*. The J. Young NMR tube was then opened in the glovebox and 9-BBN (0.072 g, 0.295 mmol) was added as a solution in C_6D_6 (0.6 mL). The NMR tube was taken out of the dry-box and placed in the NMR probe at RT before being locked and shimmed and an array set up recording a spectrum of 4 scans every 120 seconds. The decay of **43** was calculated by measuring the integral of the C<u>H</u>Me_2. First order rate constants were obtained from linear plots of -ln([Ti]/[Ti]$_0$) *vs.* time.

Ti{N(Me)($CH_2CH_2N^iPr$)($CH_2CH_2N(^iPr)B(H)NNPh_2$)}{$OC(Me)_2C(Me_2)O$} (55). To a stirred solution of Ti($N_2^{iPr}N^{Me}$)($NNPh_2$)(py) (**2.1**, 0.113g, 0.222 mmol) in benzene (5 mL) was added pinacolborane (0.033 μL, 0.222 mmol) all at RT. An immediate colour change from dark brown to light brown was observed. After 1 h the volatiles were removed under reduced pressure to afford **55** as a pale brown sticky solid. Yield: 0.080 g (65%). Diffraction-quality crystals were grown from a saturated benzene solution. ^{1}H NMR (C_6D_6, 400.1 MHz, 298 K): δ 7.80 (2 H, d, ^3J = 7.6 Hz, o_a-C_6H_5), 7.48 (2 H, d, ^3J = 7.6 Hz, o_b-C_6H_5), 7.20 (2 H, app. t, app. ^3J = 8.0 Hz, m_a-C_6H_5), 7.05 (2 H, app. t, app. ^3J = 8.0 Hz, m_b-C_6H_5), 6.99 (1 H, t, ^3J = 7.2 Hz, p_a-C_6H_5), 6.83 (1 H, t, ^3J = 7.6 Hz, p_b-C_6H_5), 4.92 (1 H, app. sept., app. ^3J = 6.7 Hz, C<u>H</u>Me_2), 4.23 (1 H, m, B(H)^{iPr}NC<u>H</u>$_2$), 3.45 (1 H, m, ^{Me}NC<u>H</u>$_2$), 3.32 (1 H, app. sept., app. ^3J = 6.7 Hz, B(H)NC<u>H</u>Me_2), 3.13 (1 H, m, ^{iPr}NC<u>H</u>$_2$), 2.84 (1 H, m, ^{iPr}NC<u>H</u>$_2$), 2.54-2.43 (3 H, overlapping 2 x m, B(H)^{iPr}NC<u>H</u>$_2$ and B(H)^{iPr}NCH_2C<u>H</u>$_2$N^{Me}), 2.52 (3 H, s, NMe), 2.19 (1 H, m, ^{Me}NC<u>H</u>$_2$), 1.68 (3 H, s, OC<u>Me</u>), 1.23 (3 H, s, OC<u>Me</u>), 1.20 (3 H, d, ^3J = 6.7 Hz, CH<u>Me</u>$_2$), 1.16 (3 H, s, OC<u>Me</u>), 0.99 (3 H, d, ^3J = 6.7 Hz, B(H)NCH<u>Me</u>$_2$), 0.92 (3 H, d, ^3J = 6.7 Hz, B(H)NCH<u>Me</u>$_2$), 0.88 (3 H, s, OC<u>Me</u>), 0.84 (3 H, d, ^3J = 6.7 Hz, CH<u>Me</u>$_2$) ppm. ^{1}H{^{11}B} NMR (C_6D_6, 499.9 MHz, 298K): δ 4.79 (1H, br.s, BH) ppm. ^{11}B{^{1}H} NMR (C_6D_6, 160.4 MHz, 298 K): δ 30.0 Hz (BH) ppm. ^{13}C{^{1}H} NMR (C_6D_6, 100.6 MHz, 298 K): δ 154.3 (i_a-C_6H_5), 150.6 (i_b-C_6H_5), 128.4 (m_a-C_6H_5, overlapping with solvent), 128.2 (m_b-C_6H_5, overlapping with solvent),

126.6 (o_b-C_6H_5), 124.7 (p_b-C_6H_5), 123.6 (p_a-C_6H_5), 123.4 (o_a-C_6H_5), 95.3 (O<u>C</u>Me), 94.4 (O<u>C</u>Me), 67.5 (B(H)^{iPr}NCH$_2$<u>C</u>H$_2$N^{Me}), 60.1 (^{Me}N<u>C</u>H$_2$), 57.2 (<u>C</u>HMe$_2$), 53.4 (B(H)N<u>C</u>HMe$_2$), 47.3 (NMe), 44.8 (^{iPr}N<u>C</u>H$_2$), 43.0 (B(H)^{iPr}N<u>C</u>H$_2$), 29.3 (OC<u>Me</u>), 28.9 (OC<u>Me</u>), 27.9 (OC<u>Me</u>), 26.3 (OC<u>Me</u>), 24.0 (B(H)NCH<u>Me</u>$_2$), 23.5 (B(H)NCH<u>Me</u>$_2$), 22.2 (CH<u>Me</u>$_2$), 20.9 (CH<u>Me</u>$_2$) ppm. Note: subscripts ″a″ and ″b″ refer to the inequivalent Ph environments. IR (NaCl plates, Nujol mull, cm^{-1}): 3061 (w), 2726 (w), 2667 (w), 2483 (m), 1590 (s,), 1490 (s), 1354 (m), 1354 (m), 1308 (w), 1260 (m), 1150 (s), 1072 (w), 968 (s), 887 (s), 720 (s). EI-MS: *m/z* = 557 [M]$^+$ (1%). Anal. found (calcd. for $C_{29}H_{48}BN_5O_2Ti$): C, 62.43 (62.49); H, 8.79 (8.68); N, 12.39 (12.56)%.

Ti{N(Me)(CH$_2$CH$_2$N^{i}Pr)(CH$_2$CH$_2$N(^{i}Pr)B(H)NNPh$_2$)}{O$_2$C$_6$H$_4$} (56). To a stirred solution of Ti($N_2^{iPr}N^{Me}$)($NNPh_2$)(py) (**2.1**, 0.146g, 0.287 mmol) in benzene (5 mL) was added catecholborane (0.035 g, 0.287 mmol) all at RT. An immediate colour change from dark brown to light brown was observed. After 1 h the volatiles were removed under reduced pressure to afford **56** as a pale brown sticky solid. Yield: 0.141 g (90%). ^{1}H NMR (C_6D_6, 400.1 MHz, 298 K): δ 7.32 (2 H, d, ^3J = 7.5 Hz, *o*-C_6H_5), 7.20 (2 H, d, ^3J = 7.5 Hz, *o*-C_6H_5), 6.95-6.92 (6 H, br. m, overlapping 4 x m, *p*-C_6H_5 and Ti$O_2C_6H_4$), 6.88 (4 H, br.m, *m*-C_6H_5), 5.15 (1 H, app. sept., app. ^3J = 6.9 Hz, C<u>H</u>Me$_2$), 3.90 (1 H, m, B(H)^{iPr}NC<u>H</u>$_2$), 3.32-3.21 (2 H, overlapping 2 x m, B(H)NC<u>H</u>Me$_2$ and ^{Me}NC<u>H</u>$_2$), 2.73-2.70 (3 H, overlapping 2 x m, overlapping B(H)^{iPr}NCH$_2$C<u>H</u>$_2$N^{Me} and B(H)^{iPr}NC<u>H</u>$_2$), 2.59 (1 H, m, ^{iPr}NC<u>H</u>$_2$), 2.40 (1 H, m, ^{iPr}NC<u>H</u>$_2$), 2.32 (3 H, s, NMe), 0.92 (3 H, d, ^3J = 6.9 Hz, CH<u>Me</u>$_2$), 0.90 (3 H, d, ^3J = 6.8 Hz, B(H)NCH<u>Me</u>$_2$), 0.86 (3 H, d, ^3J = 6.8 Hz, B(H)NCH<u>Me</u>$_2$), 0.45 (3 H, d, ^3J = 6.9 Hz, CH<u>Me</u>$_2$) ppm. The resonance attributable to the proton directly bound to ^{11}B was not observed in the ^{1}H{^{11}B} NMR spectrum. ^{11}B{^{1}H} NMR (C_6D_6, 160.4 MHz 298 K): δ 30.3 ppm. ^{13}C{^{1}H} NMR (C_6D_6, 100.6 MHz, 298 K): δ 152.2 (i_a-C_6H_5), 147.2 (i_a-C_6H_5), 124.8 (overlapping m_a-C_6H_5 and m_b-C_6H_5), 123.6 (o_a-C_6H_5), 123.2 (o_b-C_6H_5), 119.9 (p_a-C_6H_5), 118.4 (p_b-C_6H_5), 112.0 (TiO_2<u>C</u>$_6$H$_4$), 108.7 (TiO_2<u>C</u>$_6$H$_4$), 68.5 (B(H)^{iPr}NCH$_2$<u>C</u>H$_2$N^{Me}), 58.5 (^{Me}N<u>C</u>H$_2$), 58.4 (C<u>H</u>Me$_2$), 53.0 (B(H)N<u>C</u>HMe$_2$), 46.1 (NMe), 44.2 (^{iPr}N<u>C</u>H$_2$), 42.3 (B(H)^{iPr}N<u>C</u>H$_2$), 23.0 (B(H)NCH<u>Me</u>$_2$), 23.0 (B(H)NCH<u>Me</u>$_2$), 21.2 (CH<u>Me</u>$_2$), 20.4 (CH<u>Me</u>$_2$) ppm. Note: subscripts ″a″ and ″b″ refer to the inequivalent Ph environments. IR (NaCl plates, Nujol mull, cm^{-1}): 2726 (w), 1586 (m), 1259 (s), 1094 (m), 1019 (m), 801 (s). EI-MS: *m/z* = 549 [M]$^+$ (1%).

Anal. found (calcd. for $C_{29}H_{40}BN_5O_2Ti$): C, 63.12 (63.41); H, 7.36 (7.51); N, 12.69 (12.73)%.

Ti{N_2N^{py}-(HBC_8H_{14})}($NNPh_2$) (57). To a stirred solution of Ti(N_2N^{py})($NNPh_2$)(py) (**1.75**, 0.157 g, 0.254 mmol) in benzene (5 mL) was added 9-BBN dimer (0.062 g, 0.254 mmol) all at RT. After 12 h the volatiles were removed under reduced pressure to afford **57** and py.HBC_8H_{14} quantitatively as a pale brown sticky solid. The resultant solid was then triturated with hexane (2 mL), filtered to yield a pale green solid which was then washed with hexane (2 x 1 mL) filtered and dried *in vacuo*. Yield: 0.046 g (27%). Diffraction-quality crystals were grown from a saturated benzene solution at RT. ^{1}H NMR (C_6D_6, 400.1 MHz, 298 K): δ 8.99 (1 H, d, ^3J = 5.3 Hz, py-H^6), 7.83 (4 H, d, ^3J = 7.0 Hz, *o*-C_6H_5), 7.25 (4 H, app.t, app. ^3J = 7.0 Hz, *m*-C_6H_5), 6.93-6.87 (3 H, overlapping 2 x m, *p*-C_6H_5 and py-H^4), 6.69 (1 H, d, ^3J = 7.8 Hz, py-H^3), 6.38 (1 H, ddd, ^3J = 6.2, 7.7 Hz ^4J = 1.0 Hz, py-H^6), 3.62 (1 H, d, ^3J = 12.7 Hz, C$\underline{H_2}$NSiMe$_3$), 3.10 (1 H, d, ^3J = 12.7 Hz, C$\underline{H_2}$NSiMe$_3$), 3.04 (1 H, d, ^3J = 13.8 Hz, C$\underline{H_2}$N(HBC_8H_{14})SiMe$_3$), 2.89 (1 H, m, BCCH), 2.74 (1 H, d, ^3J = 13.8 Hz, C$\underline{H_2}$N(HBC_8H_{14})SiMe$_3$), 2.29-1.76 (11 H, overlapping 11 x br.m, BCH, BCCH and BCCH), 1.37 (1 H, m, BCCCH), 1.01 (1 H, m, BCH), 0.85 (3 H, s, $CH_2C\underline{Me}$), 0.24 (9 H, s, SiMe$_3$), -0.47 (3 H, s, N(HBC_8H_{14})Si$\underline{Me_3}$) ppm. ^{1}H{^{11}B} NMR (C_6D_6, 499.9 MHz, 298K): δ 3.96 (1H, br.s, BH) ppm. ^{13}C{^{1}H} NMR (C_6D_6, 100.6 MHz, 298 K): δ 160.9 (py-C^2), 150.6 (py-C^6), 145.9 (*i*-C_6H_5), 139.3 (py-C^4), 127.9 (*m*-C_6H_5), 121.1 (*p*-C_6H_5), 121.0 (py-C^5), 120.5 (py-C^3), 118.2 (*o*-C_6H_5), 63.3 ($\underline{C}H_2$NSiMe$_3$), 56.1 ($\underline{C}H_2$N(HBC_8H_{14})SiMe$_3$), 44.8 ($\underline{C}$Me), 36.8 (BC$\underline{C}$), 36.6 (BC$\underline{C}$), 29.5 (BC$\underline{C}$), 29.3 (BC$\underline{C}$), 23.8 (BCC$\underline{C}$), 23.3 (C$\underline{Me}$), 20.0 (BCC$\underline{C}$), 0.22 (N(HBC_8H_{14})Si$\underline{Me_3}$), 0.16 (SiMe$_3$) ppm. Resonances attributable to carbons directly bound to ^{11}B atoms were not observed. ^{11}B{^{1}H} NMR (C_6D_6, 160.4 MHz 298 K): δ 1.25 (BC_8H_{14}) ppm. ^{29}Si NMR (HMBC ^{1}H-observed, C_6D_6, 499.9 MHz, 298 K) δ 10.7 (N(HBC_8H_{14})$\underline{Si}$Me$_3$), 1.61 (SiMe$_3$) ppm. IR (NaCl plates, Nujol mull, cm^{-1}): 2727 (w), 2152 (w), 1764 (w), 1594 (m), 1586 (m), 1487 (m), 1310 (w), 1259 (m), 1245 (m), 1210 (w), 1044 (m), 916 (m), 841 (m), 780 (w), 745 (m), 693 (m). Anal. found (calcd. for $C_{35}H_{54}BN_5Si_2Ti$): C, 63.54 (63.72); H, 8.32 (8.25); N, 10.51 (10.62)%.

Si($N_2^{iPr}N^{Me}$)(H)(Ph) (58) and MeN{$CH_2CH_2N(^iPr)(SiH_2Ph)$}$_2$ (59). To stirred solution of $Li_2N_2^{iPr}N^{Me}$ (0.080 g, 0.375 mmol) in toluene (2 mL) cooled to -78 °C was added $PhClSiH_2$ (0.107 g, 0.750 mmol) and the reaction allowed to warm to RT. After 2 hours the volatiles were removed under reduced pressure and the sticky white solid was extracted into hexane (3 x 2 mL). The volatiles were removed under reduced pressure and the resultant oil dried *in vacuo*. Yield: 0.044 g. The ^{1}H NMR spectra indicated an approximately 50:50% mixture of **58** and **59**.

Si($N_2^{iPr}N^{Me}$)(H)(Ph) (58). ^{1}H NMR (C_6D_6, 400.1 MHz, 298 K): δ 7.51 (2 H, dd, ^3J = 7.7 Hz ^4J = 1.6 Hz, *o*-C_6H_5), 7.34 (2 H, t, ^3J = 7.6 Hz, *m*-C_6H_5) 7.17 (1 H, br. m, *p*-C_6H_5 overlapping with **59**), 5.03 (1 H, br. s, SiH), 4.06 (2 H, sept., d, ^3J = 6.7 Hz, ^4J =1.4 Hz, C$\underline{H}$Me$_2$), 2.69 (4 H, m, ^{iPr}NC$\underline{H}_2$), 2.17 (2 H, m, ^{Me}NC$\underline{H}_2$), 1.95 (2 H, m, ^{Me}NC$\underline{H}_2$), 1.28 (6 H, d, ^3J = 6.5 Hz, CH$\underline{Me}_2$), 1.21 (3 H, s, NMe), 1.18 (6 H, d, ^3J = 6.5 Hz, CH$\underline{Me}_2$) ppm. ^{13}C{^{1}H} NMR (C_6D_6, 100.6 MHz, 298 K): δ 147.0 (*i*-C_6H_5), 131.8 (*o*-C_6H_5), 127.3 (*m*-C_6H_5), 126.5 (*p*-C_6H_5), 51.9 (^{Me}N$\underline{C}$H$_2$), 47.4 ($\underline{C}$HMe$_2$), 42.7 (NMe), 36.3 (^{iPr}N$\underline{C}$H$_2$), 22.1 (CH$\underline{Me}_2$), 21.4 (CH$\underline{Me}_2$) ppm. ^{29}Si NMR (HMBC ^{1}H-observed, C_6D_6, 499.9 MHz, 298 K): δ -54.2 ($^1J_{Si-H}$ = 171 Hz, SiH). EI-MS: *m/z* 305 $[M]^+$ (50%).

MeN{$CH_2CH_2N(^iPr)(SiH_2Ph)$}$_2$ (59). ^{1}H NMR (C_6D_6, 400.1 MHz, 298 K): δ 7.71 (4 H, m, *o*-C_6H_5), 7.35-7.32 (2H, br. m, *p*-C_6H_5 overlapping with **58**), 7.21 (4 H, br. m, *m*-C_6H_5), 5.18 (4 H, s, SiH_2), 3.11 (2 H, sept., ^3J = 6.6 Hz, C$\underline{H}$Me$_2$), 2.91 (4 H, t, ^3J = 7.0 Hz, ^{iPr}NC$\underline{H}_2$), 2.38 (4 H, t, ^3J = 7.0 Hz, ^{Me}NC$\underline{H}_2$), 1.97 (3 H, s, NMe), 1.05 (12 H, d, ^3J = 6.6 Hz, CH$\underline{Me}_2$) ppm. ^{13}C{^{1}H} NMR (C_6D_6, 100.6 MHz, 298 K): δ 136.5 (*i*-C_6H_5), 134.6 (*o*-C_6H_5), 130.4 (*p*-C_6H_5), 129.5 (*m*-C_6H_5), 59.4 (^{Me}N$\underline{C}$H$_2$), 50.0 ($\underline{C}$HMe$_2$), 44.5 (^{iPr}N$\underline{C}$H$_2$), 41.8 (NMe), 22.0 (CH$\underline{Me}_2$) ppm. ^{29}Si NMR (HMBC ^{1}H-observed, C_6D_6, 499.9 MHz, 298 K): δ -29.9 ($^1J_{Si-H}$ = 206 Hz, SiH_2). EI-MS: *m/z* 427 $[M]^+$ (1%).

Common data: IR (NaCl plates, Nujol mull, cm^{-1}): 3067 (w), 3051 (w), 2151 (s, ν(Si–H)), 2023 (w, ν(Si–H)), 1988 (w), 1938 (w), 1591 (w), 1428 (m), 1358 (m), 1321 (m), 1289 (w), 1259 (m), 1206 (m), 1171 (w), 1123 (m), 1103 (m), 1082 (m), 1063 (w), 1027 (m), 949 (m), 736 (m), 696 (m).

5.8 References

1. A. B. Pangborn, M. A. Giardello, R. H. Grubbs, R. K. Rosen and F. J. Timmers, *Organometallics*, 1996, **15**, 1518.
2. T. B. Parsons, N. Hazari, A. R. Cowley, J. C. Green and P. Mountford, *Inorg. Chem.*, 2005, **44**, 8442.
3. J.-L. Fauré, H. Gornitzka, R. Réau, D. Stalke and G. Bertrand, *Eur. J. Inorg. Chem.*, 1999, 2295.
4. A. D. Schwarz, C. S. Onn and P. Mountford, *Angew. Chem. Int. Ed.*, 2012, **51**, 12298.
5. A. J. Blake, P. E. Collier, S. C. Dunn, W.-S. Li, P. Mountford and O. V. Shishkin., *J. Chem. Soc., Dalton Trans.*, 1997, 1549.
6. A. Pelter, K. Smith and H. C. Brown, *Borane Reagents*, Academic Press, New York, 1988.
7. C. Chiappe, G. Imperato, D. Lenoir and E. Napolitano, *Tet. Letts.*, 2006, **47**, 8893.
8. N. R. Neale and T. D. Tilley, *J. Am. Chem. Soc.*, 2002, **124**, 3802.
9. C. Klein, H. Nöth, M. Tacke and M. Thomann, *Angew. Chem., Int. Ed. Engl.*, 1993, **32**, 886.
10. T. Nishikawa, A. Ino and M. Isobe, *Tetrahedron*, 1994, **50**, 1449.
11. Y. Zhang and J. Wen, *J. Fluorine Chem.*, 1990, **47**, 533.
12. X. Li, T. Vogel, C. D. Incarvito and R. H. Crabtree, *Organometallics*, 2005, **24**, 62.
13. J. Braddock-Wilking, M. Schieser, L. Brammer, J. Huhmann and R. Shaltout, *J. Organomet. Chem.*, 1995, **499**, 89.
14. Z. Otwinowski and W. Minor, *Processing of X-ray Diffraction Data Collected in Oscillation Mode*, Academic press, New York, 1997.
15. *Journal*, 2011.
16. A. Altomare, G. Cascarano, G. Giacovazzo, A. Guagliardi, M. C. Burla, G. Polidori and M. Camalli, *J. Appl. Crystallogr.*, 1994, **27**, 435.
17. L. Palatinus and G. Chapuis, *J. Appl. Cryst.*, 2007, **40**, 786.
18. P. W. Betteridge, J. R. Cooper, R. I. Cooper, K. Prout and D. J. Watkin, *J. Appl. Cryst.*, 2003, **36**, 1487.
19. M. J. Frisch, G. W. Trucks, H. B. Schlegel, G. E. Scuseria, M. A. Robb, J. R. Cheeseman, G. Scalmani, V. Barone, B. Mennucci, G. A. Petersson, H.

Nakatsuji, M. Caricato, X. Li, H. P. Hratchian, A. F. Izmaylov, J. Bloino, G. Zheng, J. L. Sonnenberg, M. Hada, M. Ehara, K. Toyota, R. Fukuda, J. Hasegawa, M. Ishida, T. Nakajima, Y. Honda, O. Kitao, H. Nakai, T. Vreven, J. A. Montgomery, J. E. Peralta, F. Ogliaro, M. Bearpark, J. J. Heyd, E. Brothers, K. N. Kudin, V. N. Staroverov, R. Kobayashi, J. Normand, K. Raghavachari, A. Rendell, J. C. Burant, S. S. Iyengar, J. Tomasi, M. Cossi, N. Rega, J. M. Millam, M. Klene, J. E. Knox, J. B. Cross, V. Bakken, C. Adamo, J. Jaramillo, R. Gomperts, R. E. Stratmann, O. Yazyev, A. J. Austin, R. Cammi, C. Pomelli, J. W. Ochterski, R. L. Martin, K. Morokuma, V. G. Zakrzewski, G. A. Voth, P. Salvador, J. J. Dannenberg, S. Dapprich, A. D. Daniels, Ö. Farkas, J. B. Foresman, J. V. Ortiz, J. Cioslowski and D. J. Fox, *Journal*, 2009.

20. A. D. Becke, *J. Chem. Phys.*, 1993, **98**, 5648.
21. J. P. Perdew and Y. Wang, *Phys. Rev. B*, 1992, **45**, 13.
22. S. Grimme, S. Ehrlich and L. Goerigk, *J. Comput. Chem.*, 2011, **32**, 1456.
23. S. Grimme, J. Antony, S. Ehrlich and H. Krieg, *J. Chem. Phys.*, 2010, **132**, 154104.
24. D. Andrae, U. Haussermann, M. Dolg, H. Stoll and H. Preuss, *Theor. Chim. Acta*, 1990, **77**, 123.
25. A. W. Ehlers, M. Bohme, S. Dapprich, A. Gobbi, A. Hollwarth, V. Jonas, K. F. Kohler, R. Stegmann, A. Veldkamp and G. Frenking, *Chem. Phys. Lett.*, 1993, **208**, 111.
26. A. Schäfer, H. Horn and R. Ahlrichs, *J. Chem. Phys.*, 1992, **97**, 2571.
27. A. V. Marenich, C. J. Cramer and D. G. Truhlar, *J. Phys. Chem. B*, 2009, **2009**, 6378.
28. F. Weigend and R. Ahlrichs, *Phys. Chem. Chem. Phys.*, 2005, **7**, 3297.
29. **NBO 6.0.** E. D. Glendening, J. K. Badenhoop, A. E. Reed, J. Carpenter, J. A. Bohmann, C. M. Morales, C. R. Landis and F. Weinhold, Theoretical Chemistry Institute, University of Wisconsin, Madison (2013)

Appendix

Figure A1. Decay of Ti($H_2N_2^{iPr}N^{Me}$)(CCC_6F_5)$_2$(NXyl) (**23**, blue) and growth of Ti($N_2^{iPr}N^{Me}$){N(Xyl)C(H)C(H)(C_6F_5)}(CCC_6F_5) (**24**, red) at 75 ^oC in toluene-d_8.

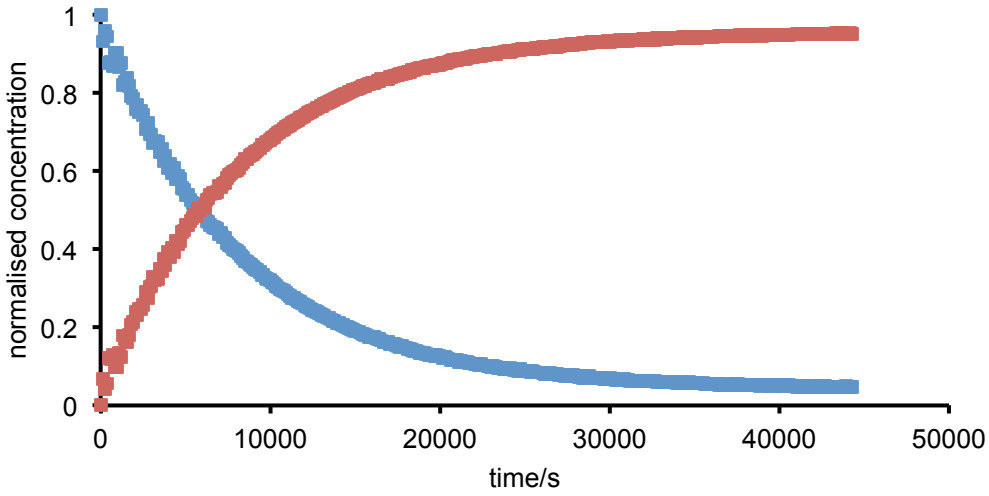


Table A1. Rate constants obtained for the isomerisation of $Ti(H_2N_2^{iPr}N^{Me})(CCC_6F_5)_2(NXyl)$ (**23**) to $Ti(N_2^{iPr}N^{Me})\{N(Xyl)C(H)C(H)C_6F_5\}(CCC_6F_5)$ (**24**), described in Chapter Three.

Temperature K	Notes	k_{obs} x 10^{-5} s^{-1}
333		1.23(1)
333		0.99(1)
338		1.76(1)
341		4.86(1)
343		6.18(1)
343		6.16(1)
343	**23** made *in situ*	6.44(1)
343	**23-*d*$_3$**	4.17(1)
343	+ 2 equivs of alkyne	6.15(1)
343	+ 6 equivs of alkyne	5.99(2)
348		9.33(2)
348	**23-*d*$_3$**	7.05(1)
348	**23-*d*$_3$** made *in situ*	6.90(2)
348	Double [**23**]	11.45(2)
348	Triple [**23**]	10.52(2)
353		14.88(5)
356		19.45(14)
356		19.69(8)
356	**23-*d*$_3$**	13.56(5)

Unless otherwise stated, $[\mathbf{23}]_0 = 0.027$ mol dm^{-3}

Table A2. Rate constants obtained for the reaction of $Ti(H_2N_2^{iPr}N^{Me})(CCC_6F_5)_2(NXyl)$ (**23**) with $Ti(N_2^{iPr}N^{Me})(NNPh_2)(py)$ (**2.1**), described in Chapter Three.

Temperature K	Notes	k_{obs} x 10^{-5} s^{-1}
298		23.8(2)
298	**23-*d*$_3$**	6.99(3)
298	+ 1 equiv py	31.3(2)
298	+ 3 equivs py	35.2(3)
298	+ 6 equivs py	35.1(3)
298	Double [**2.1**]	22.64(7)
301		30.7(2)
301		29.6(1)
304		40.33(5)
307		48.3(2)
310		73.7(4)

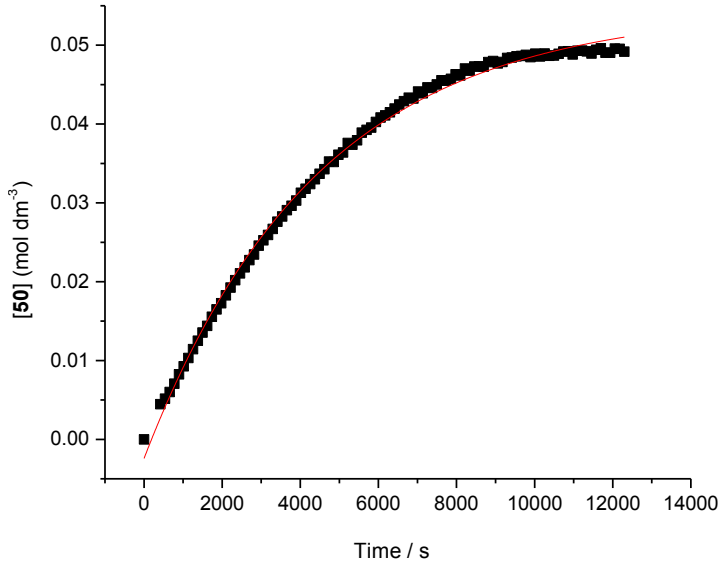
Unless otherwise stated, $[\mathbf{23}]_0 = [\mathbf{2.1}]_0 = 0.027$ mol dm^{-3}

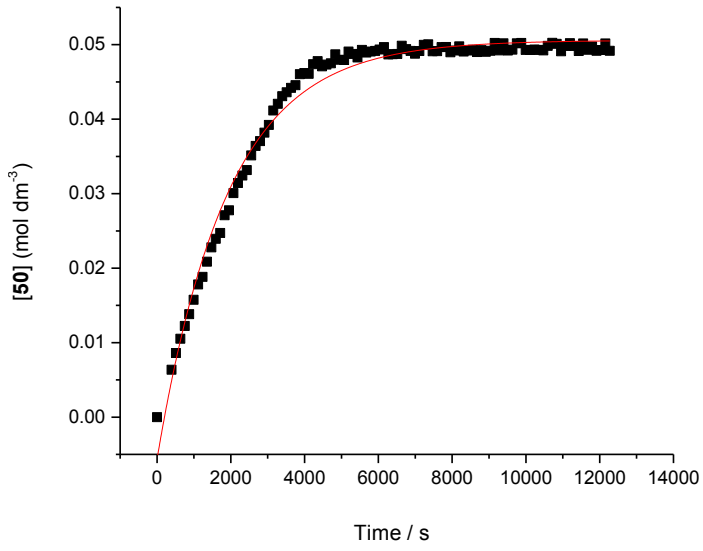
Table A3. Initial rates obtained for the reaction of $Ti(N_2^{iPr}N^{Me})(NNPh_2)(py)$ (**2.1**) with one equivalent of $PhSiH_3$, described in Chapter Four.

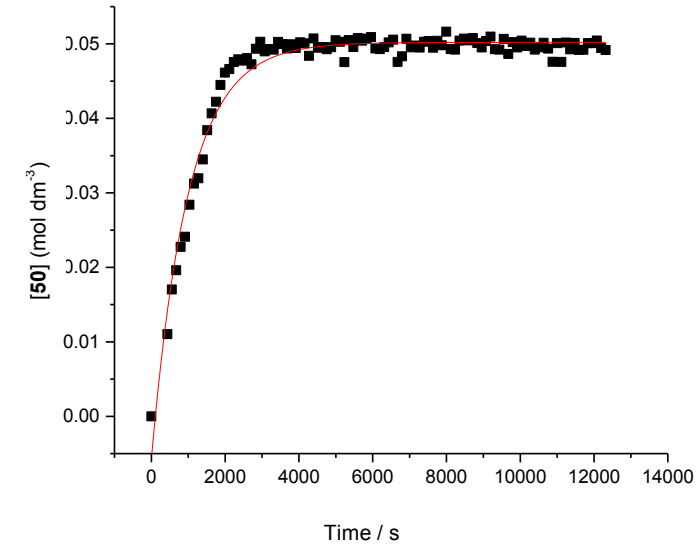
Temperature K	Notes	Initial rate x 10^{-5} mol dm^{-3} s^{-1}
298		12.44(5)
298		12.44(1)
298	$PhSiD_3$	8.80(1)
298	$PhSiD_3$	9.26(3)

$[\mathbf{2.1}]_0 = 0.049$ mol dm^{-3}

Figure A2. Plots of [Ti($N_2^{iPr}N^{Me}$){N(H)SiH_2Ph}(NPh_2)] ([**50**]) *vs.* time plotted in Origin. Top: one equivalent of 9-BBN dimer, the best-fit line (r^2 = 0.9964) shown gave A_1 = -0.0569(3) and B_1 = 4421(86) giving an initial rate of 1.28(3) x 10^{-5} mol dm^{-3} s^{-1}. Second: two equivalents of 9-BBN dimer, the best-fit line (r^2 = 0.9853) shown gave A_1 = -0.0562(8) and B_1 = 1903(49), giving an initial rate of 2.9(1) x 10^{-5} mol dm^{-3} s^{-1}. Third: three equivalents of 9-BBN dimer, the best-fit line (r^2 = 0.9707) shown gave A_1 = -0.056(13) and B_1 = 989(30), giving an initial rate of 5.7(2) x 10^{-4} mol dm^{-3} s^{-1}. Fourth: four equivalents of 9-BBN dimer, the best-fit line (r^2 = 0.9579) shown gave A_1 = -0.059(18) and B_1 = 839(36), giving an initial rate of 7.1(4) x 10^{-4} mol dm^{-3} s^{-1}.






[50] (mol dm-3)
0.05
0.04
0.03
0.02
0.01
0.00
0
2000
4000
6000
8000
10000
12000
14000
Time / s

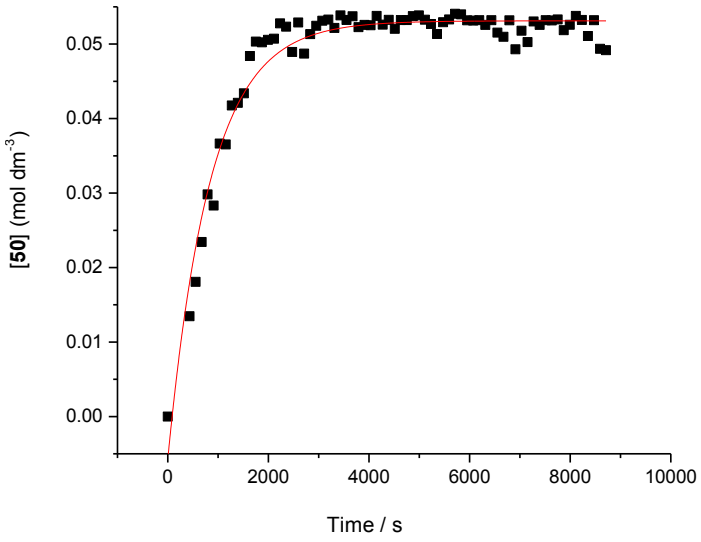

[50] (mol dm-3)
0.05
0.04
0.03
0.02
0.01
0.00
0
2000
4000
6000
8000
10000
Time / s

Table A4. Initial rates obtained for the reaction of $Ti(N_2^{iPr}N^{Me})(NNPh_2)(py)$ (**2.1**) with 9-BBN, described in Chapter Four.

Temperature	Equivs of 9-BBN dimer	Initial rate x 10^{-5} mol dm^{-3} s^{-}
298	1	1.28(3)
298	2	2.9(1)
298	3	5.7(2)
298	4	7.1(4)
298	1 (double [**2.1**])	1.09(1)
298	1 (with **47**)	1.01(1)

Unless otherwise stated $[\mathbf{2.1}]_0 = 0.049$ mol dm^{-3}

Figure A3. Full derivation of Equations 4.11 - 4.13 described in Chapter Four. This derivation differs from what is published in the literature in that two equivalents of 9-BBN monomer are consumed for every one equivalent of [**2.1**]. This is discussed in the main text.

$$\frac{d[\mathbf{50}]}{dt} = k_2[\mathbf{2.1}][\text{9-BBN}]$$

$$\frac{d[\text{9-BBN}]}{dt} = k_1[\text{9-BBN dimer}] - k_{-1}[\text{9-BBN}]^2 - k_2[\mathbf{2.1}][\text{9-BBN}] = 0$$

$$[\text{9-BBN}] = \frac{k_1[\text{9-BBN dimer}]}{k_{-1}[\text{9-BBN}] + k_2[\mathbf{2.1}]}$$

$$\text{Rate} = \frac{k_1 k_2[\mathbf{2.1}][\text{9-BBN dimer}]}{k_{-1}[\text{9-BBN}] + k_2[\mathbf{2.1}]} \tag{4.11}$$

if $k_{-1}[\text{9-BBN}] << k_2[\mathbf{2.1}]$

$$\text{Rate} = k_1[\text{9-BBN dimer}] \tag{4.12}$$

if $k_{-1}[\text{9-BBN}] >> k_2[\mathbf{2.1}]$

$$K_{eq} = \frac{k_1}{k_{-1}} = \frac{[\text{9-BBN}]^2}{[\text{9-BBN dimer}]}$$

$$[\text{9-BBN}] = \left[\frac{k_1}{k_{-1}}\right]^{1/2}[\text{9-BBN dimer}]^{1/2}$$

$$\text{Rate} = \left[\frac{k_1}{k_{-1}}\right]^{1/2} k_2[\mathbf{2.1}][\text{9-BBN dimer}]^{1/2} \tag{4.13}$$

Table A5. Rate constants obtained for the reaction of $Ti(N_2^{iPr}N^{Me})\{N(H)SiH_2Ph\}(NPh_2)(py)$ (**43**) with $3,5\text{-}C_6H_3(CF_3)_2SiH_3$, described in Chapter Four.

Temperature K	Equivs of $3,5\text{-}C_6H_3(CF_3)_2SiH_3$	k_{obs} x 10^{-5} s^{-1}
298	10	12.5(1)
298	20	12.7(1)
298	10 (**43-*d*$_3$**)	2.24(1)
298	10 (**43-*d*$_1$**)	2.30(1)

$[\mathbf{43}]_0 = 0.049$ mol dm^{-3}

Table A6. Rate constants obtained for the reaction of $Ti(N_2^{iPr}N^{Me})\{N(H)SiH_2Ph\}(NPh_2)(py)$ (**43**) with 10 equivalents of 9-BBN dimer, described in Chapter Four.

Temperature K	Notes	k_{obs} x 10^{-5} s^{-1}
298		36.8(1)
298	**43-*d*$_3$**	30.9(6)

$[\mathbf{43}]_0 = 0.049$ mol dm^{-3}